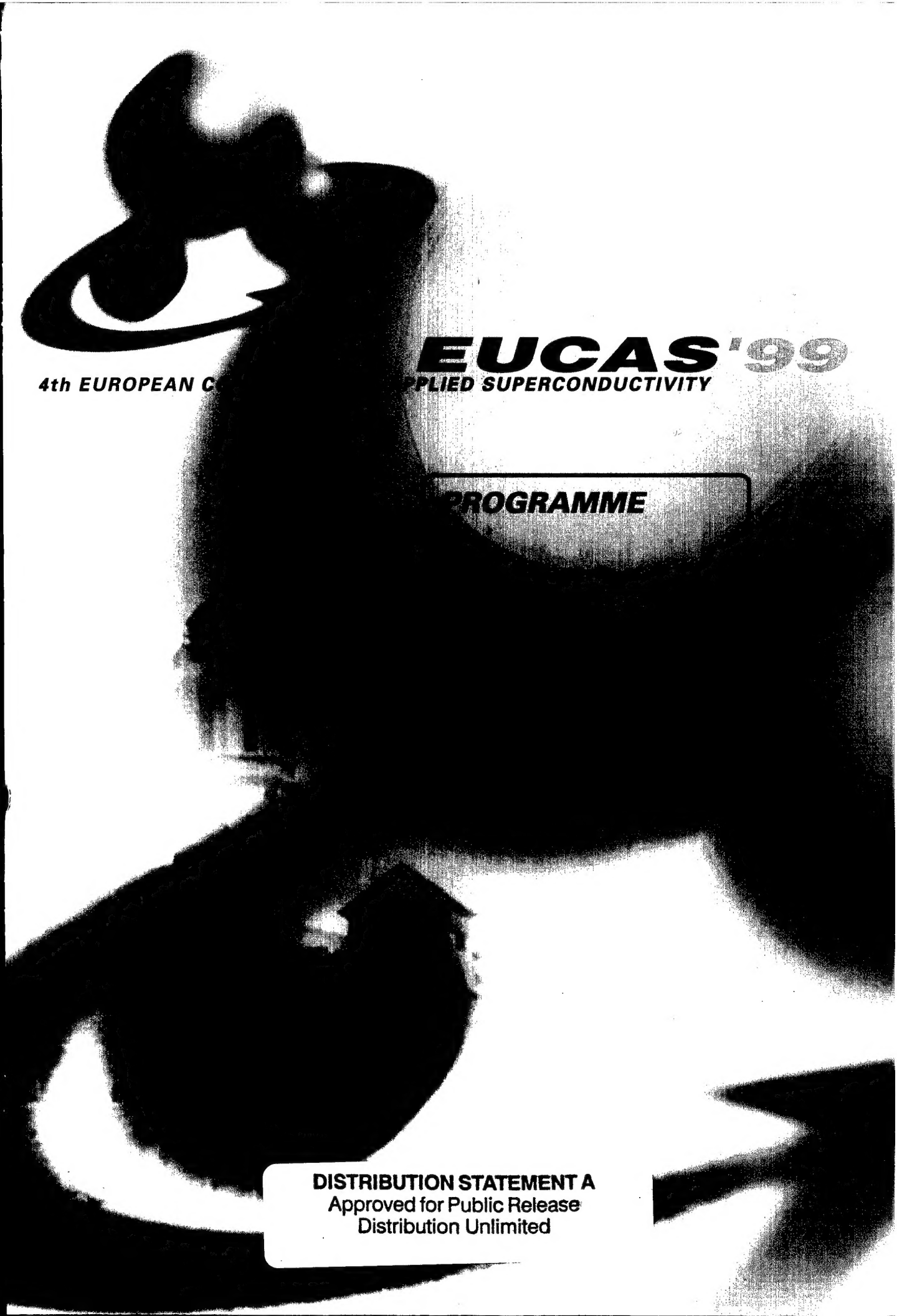

REPORT DOCUMENTATION PAGE

Form Approved OMB No. 0704-0188

1. AGENCY USE ONLY (Leave blank)	2. REPORT DATE	3. REPORT TYPE AND DATES COVERED
	8 November 1999	Conference Proceedings

4. TITLE AND SUBTITLE

4th European Conference on Applied Superconductivity

5. FUNDING NUMBERS

F61775-99-WF055

6. AUTHOR(S)

Conference Committee

7. PERFORMING ORGANIZATION NAME(S) AND ADDRESS(ES)

Univesitat Autonoma de Barcelona
Bellaterra
Barcelona 08293
Spain

8. PERFORMING ORGANIZATION REPORT NUMBER

N/A

9. SPONSORING/MONITORING AGENCY NAME(S) AND ADDRESS(ES)

EOARD
PSC 802 BOX 14
FPO 09499-0200

10. SPONSORING/MONITORING AGENCY REPORT NUMBER

CSP 99-5055

11. SUPPLEMENTARY NOTES

12a. DISTRIBUTION/AVAILABILITY STATEMENT

Approved for public release; distribution is unlimited.

12b. DISTRIBUTION CODE

A

13. ABSTRACT (Maximum 200 words)

The Final Proceedings for 4th European Conference on Applied Superconductivity, 14 September 1999 - 17 September 1999

This is an interdisciplinary conference consisting of all aspects in applied superconductivity from a scientific point of view and an industrial perspective. Topics include: Superconductivity gap, Superconductivity Technology for power applications, application to bulk superconductors, and recent advances in superconducting electronic technology in USA

14. SUBJECT TERMS

EOARD, Power, Superconductivity

15. NUMBER OF PAGES

261

16. PRICE CODE

N/A

17. SECURITY CLASSIFICATION OF REPORT	18. SECURITY CLASSIFICATION OF THIS PAGE	19. SECURITY CLASSIFICATION OF ABSTRACT	20. LIMITATION OF ABSTRACT
UNCLASSIFIED	UNCLASSIFIED	UNCLASSIFIED	UL

EUCAS'99

4th European Conference on Applied Superconductivity

SITGES 14-17 SEPTEMBER

PROGRAMME

Technical sessions

Exhibition

abstracts

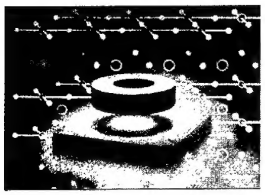

Aventis
Research & Technologies

Aventis Research and Technologies (Formally Hoechst Corporate Research and Technology) has been manufacturing HTS materials and developing HTS applications for over 12 years.

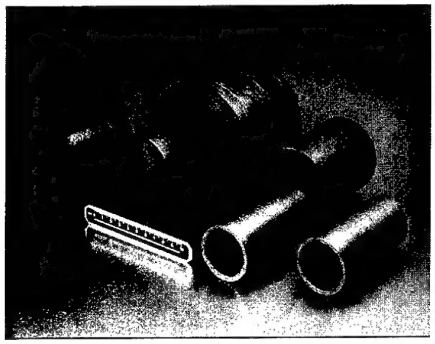

The Aventis proprietary Melt Cast Process is used to manufacture Bi-2212 bulk parts for

- Current leads
- Levitators
- Fault Current Limiters
- Transformers
- Power Transmission Links

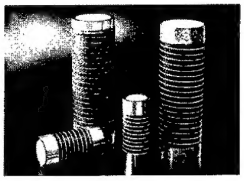

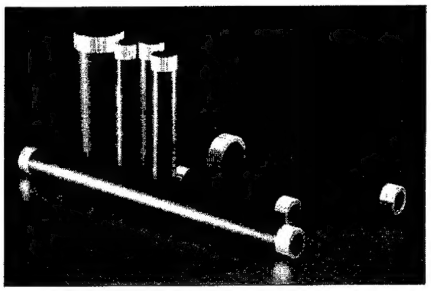

Aventis Bi 2212 current leads offer a major advantages over both conventional all metal current leads and HTS leads based on other materials. Reduction by more than a factor of 10 in the heat load to the 4K stage ensures a significant reduction in refrigeration costs and enables the application of new

Other features include:

- Transport Currents of > 15 kA (AC and DC)
- Thermal conductivity of < 1 W/mK (77K)
- Fully integrated, low thermal conductivity shunts
- Current contact resistance in the micro-ohm range
- Parts up to 800 mm in length and diameter

High quality Bi,Pb-2223 and Bi-2212 precursors for the manufacture of high performance tapes are prepared to customer specification.

Aventis offers phase pure Y-123 powder and powder mixtures. Presintered parts for

- sputter targets
- MTG processes
- High trapped fields

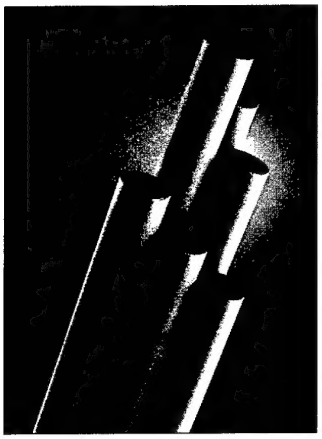

Aventis' unique pressed precursor rods improve and significantly simplify the OPIT wire production process.

- Ready for rapid and easy insertion in to the appropriate silver or silver alloy sheath
- Eliminate need for powder containment during billet packing
- Reduction in possible contamination from atmospheric absorption of carbon and similar gasses
- Associated improvement in current carrying

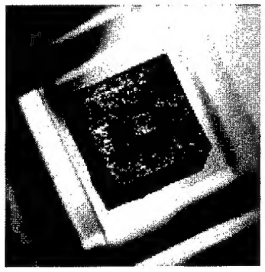

For further information please contact:
Dr. Lisa Cowey
Aventis Research and Technologies
High Temperature Superconductors
Chemiepark Knapsack
D-50351 Huerth
Germany
Tel: +49 2233 486491
Fax: +49 2233 486847
e-mail: cowey@msmiuk.hoechst.com

HTS Products for Power Engineering

CONTENTS

ACKNOWLEDGMENTS

We wish to thank the following companies and organisations for their contribution to the success of this conference :

SPONSORING

- **Aventis Research Technologies**, Huerth, Germany
- **BICC General Superconductors**, Wrexham, United Kingdom
- **CIRIT , Generalitat de Catalunya**, Barcelona, Spain
- **Consejo Superior de Investigaciones Cientificas**, Spain
- **Crystec**, Berlin, Germany
- **European Office of Aerospace Research and Development, Air Force Office of Scientific Research, United States Air Force Research Laboratory**
- **INTAS,** Brussels, Belgium
- **Ministerio de Educación y Cultura**, Spain
- **NST Nordic Superconductor Technologies**, Brondby, Denmark
- **SCENET**, European Commission
- **Universitat de Barcelona,** Barcelona, Spain

SUPPORTING

- **Alcatel - Cables & Components Sector**, Paris, France
- **Australian Superconductors**, Eveleigh, Australia
- **EURUS Technologies Inc.** , Tallahassee, USA
- **Everson Electric Company**, Bethlehem, USA
- **MERCK KgaA - Darmstadt**, Gernsheim, Germany
- **Stirling Cryogenics & Refrigeration,** Eindhoven, The Netherlands
- **THEVA Thin Film Technology,** Eching-Dietersheim, Germany
- **Universitat Autonoma de Barcelona**, Bellaterra, Spain

WELCOME

On behalf of the organizing committee of EUCAS´99 and, more widely, on the Spanish superconductivity community, I would like to welcome all of you to Sitges.

We hope, first of all, that you will have the opportunity to feel that Sitges is a warm village which manages with finesse the cosmopolitan character and the Mediterranean tradition of Catalonia. This village has an important cultural tradition generated by several artists and writers who during the Modernist period, at the end of the last century, settled down in Sitges. They enjoyed its peaceful atmosphere which stimulated the creation of new ideas and artistic trends. Nowadays, Sitges is not only a modern and dynamic cultural center but also the place of multiple Congresses and Festivals all over the year.

The proximity to Barcelona, an open and generous city which has ever been a meeting place for cultures and people, has certainly helped to promote the charm of this year-round active village. Now, in the edge of XXI century, Sitges is fully integrated in a metropolitan Mediterranean area where a wealthy and sustainable growth is being promoted by knowledge-based technologies. Therefore, the scientific progress encompasses the traditional cultural radiance.

We wish that the traditional warm atmosphere of Sitges impregnates the scientific discussions which will be held during the conference and so we will have a very fruitful meeting.

EUCAS´99 is the 4th of a series of successful conferences previously held in Göttingen (1993), Edinburgh (1995) and Twente (1997) which have contributed to consolidate the European dimension of the research community in the field of Superconductivity and its Applications. Additionally, EUCAS has been a point of reference in promoting interaction and cooperation among scientists and engineers from Universities , Research Laboratories and Industrial Companies.

The stimulus of SCENET (Superconductor European Network), under the auspices of the European Community, has also been remarkable and now, with the creation of the European Society of Applied Superconductivity, ESAS, an additional sign of maturity of the field is reached. The first general meeting of ESAS will be held this week in Sitges. We would like to express our personal wish for a flourishing future to this new Society which will promote Superconductivity and its Applications throughout Europe.

I have the feeling that the progress in developing applications based on High Temperature Superconductors is being impressive. In EUCAS´99 we will have the opportunity to perceive that the path to the market is being elapsed at a very vigorous pace. We hope that this conference will help to promote a larger widespread acceptance of Superconductivity in our Society.

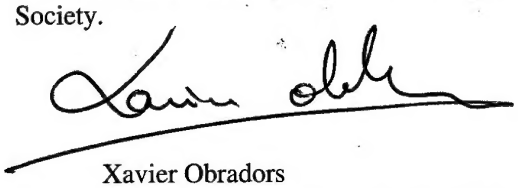

Xavier Obradors
Conference Chairman of EUCAS´99

EUCAS´99 ORGANISATION COMMITTEES

EUCAS´99 is the fourth of this conference series , after those celebrated in Göttingen, Germany in 1993, Edinburgh, Scotland in 1995 and Enschede, The Netherlands in 1997. The Institut of Materials Science of Barcelona, from the Spanish National Research Council, has assumed the responsability to organize EUCAS´99, with the collaboration of three catalan Universities (Barcelona, Autònoma de Barcelona and Politècnica de Catalunya) and the Institut of Materials Science of Zaragoza.

All these institutions leaded, together with other spanish Universities, a national Program instaured after the discovery of High Temperature Superconductivity (MIDAS program) which allowed a fast progress of Superconductivity Research in Spain in spite of the previous low tradition for this discipline. At present, the organizing laboratories remain very active in Superconductivity research mainly focused on materials processing of high current superconductors and development of enabling technologies though with broad interest and close feedback in fundamental and applied research.

LOCAL ORGANIZING COMMITTEE

Prof. Dr.Xavier Obradors	Conference Chairman
Dr. Josep Fontcuberta	Vicechairman , Treasurer
Dr. Felip Sandiumenge	Abstracts and publications
Dr. Benjamin Martínez	Local arrangements and sponsors
Dra. Teresa Puig	General Programme
Dr. Carles Frontera	Abstracts book
Dr. Enrico Varesi	Industrial Exhibition
Dr. Vicente Gomis	Technical arrangements
Dr. Dave Blank	ESAS representative
Dr. Alvar Sánchez	WWW , Publications
Dr. Joan O´Callaghan	Sponsors, Publications
Dr. Rafael Navarro	Sponsors , Publications
Dr. Xavier Granados	Posters and sponsors
Dr. Salvador Piñol	Publications
Dr. Manuel Varela	Publications
Dr. Luis Angurel	Publications
Dr. Conrado Rillo	Publications
Dra. Lourdes Fábrega	Publications
Dr. Lluïs Balcells	Posters
Dr. Ricard Bosch	Sponsors
Dr. José Luis García	Publications
Ing. Joan Figuerola	WWW
Ing. Susana Garelik	Sponsors
Pilar Massaguer	Secretary

NATIONAL ADVISORY BOARD

Prof. M.A.Alario	Universidad Complutense de Madrid
Dr. L. García – Tabarés	CEDEX - Madrid
Ing. V. González	Red Eléctrica España
Prof. J. Tejada	Universitat de Barcelona
Prof. A. Cardama	Universitat Politècnica de Catalunya
Prof. R. Pascual	Universitat Autònoma de Barcelona
Prof. M.Vallet	Universidad Complutense de Madrid
Prof. J.L.Vicent	Universidad Complutense de Madrid
Prof. F. Vidal	Universidad Santiago de Compostela
Prof. F. Yndurain	CIEMAT - Madrid

EUCAS INTERNATIONAL ADVISORY BOARD

Dr. H.Akoh	ETL Tsukuba , Japan
Prof. A.Barone	Department de Scienze Fisiche Napoli , Italy
Prof. A.Braginski	Institut für Schicht und Ionentechnik Jülich , Germany
Prof. Y.Bruynserade	Laboratorium Vaste Stoffysika Leuven , Belgium
Prof. A. Campbell	IRC on Superconductivity Cambridge , UK
Prof. T.D.Claesson	Department of Physics Goteborg , Sweden
Prof. Dr.F.da Silva	Centro de Fisica da Universidade do Porto , Portugal
Prof. G.Donaldson	University of Strathclyde Glasgow , UK
Prof. J.T. Eriksson	Tampere University of Technology, Finland
Prof. R.Flükiger	University of Geneva , Switzerland
Prof. K.Fossheim	Department of Physics Trondheim , Norway
Dr.T.Freltoft	NKT Research Center Bridby , Denmark
Prof. H.C.Freyhardt	University of Göttingen , Germany
Dr.L. Gherardi	Pirelli Cavi Spa Milano , Italy
Prof.C.Gough	University of Birmingham , UK
Dr. K.H.Gundlach	Institut de Radio Astronomie Millimetrique Grenoble , France
Prof. H.Hayakawa	Dept. of Electronics Nagoya , Japan
Dr. P. Herrmann	Alcatel Alstrom Recherche, France
Dr. H.Koch	PTB Berlin , Germany
Dr. R.Koch	IBM Yorktown Heights New York , USA
Prof. P.Komarek	KFK Institut für Technische Physisk Kalsruhe , Germany
Prof. D.Larbalestier	University of Wisconsin Madison , USA
Dr. A Lauder	Dupont Exp. Station Wilmington , USA
Dr.J.Mannhart	University of Augsburg , Germany
Dr. I McDougall	Oxford Instruments Oxon , UK
Prof. M. Marezio	MASPEC-CNR, Italy
Prof. R. Navarro	ICMA-CSIC Zaragoza , Spain
Dr. H.W. Neumüller	Siemens , Germany
Prof. X.Obradors	ICMAB-CSIC Barcelona , Spain
Dr.Ing. G.Papst	American Superconductor Europe , Germany
Prof. N.F.Pedersen	Technical University of Denmark , Lyngby , Denmark
Prof.H.Piel	University of Wuppertal , Germany
Dr. P.Regnier	SRMP/CEREM Gif sur Yvette , France
Prof. C.Rizzuto	Consorzio Interuniversity Genova , Italy
Prof. H.Rogalla	University of Twente , The Netherlands
Dr. J.M.Rowell	Northwestern University, USA
Dr. K.Sato	Sumitomo Electric Ind.Ltd.Osaka , Japan
Prof. S.Tanaka	Superconducting Laboratories ISTEC , Tokyo , Japan
Prof. O. Toennesen	Technical University of Denmark. Denmark
Prof. R. Tournier	Laboratoire EPM-Matformag, Grenoble, France

ICMAB

CSIC

Xarxa temàtica
Aplicacions de la superconductivitat i el magnetisme
II Pla de Recerca de Catalunya 1997/2000

GENERAL INFORMATION

VENUE AND LOCATION

The Conference will be held at Melia Gran Sitges Hotel located in Sitges, a seaside ressort 35 Km southern Barcelona. The Hotel is located in the Aiguadolç area, very near to several nice beaches. The Hotel is at a walking distance from the center of the town where you will find also many restaurants, bars, recreation facilities and the railway station. The mild climate in September in Sitges will allow to the delegates to practice many outdoor recreation activities, like jogging, walking, beach volley-ball, swimmimng, etc. Some information concerning the touristic potential of Sitges will be provided to the delegates in their Conference bags.

SESSIONS

All plenary sessions will take place in the Auditorio (abbreviation: A).
The parallel oral sessions thereafter will take place in the Auditorio (A), Tramontana 1 (B), Tramontana 2 (C) and the Tramontana 3 (D).
Please, refer to the programme for the allocated room for each session. All lecture rooms will be clearly signposted at the conference site.
The poster sessions will be located in Llevant hall and the Industrial Exhibition will be located in the Garbi and Mestral halls.

SESSIONS NUMBERING

The sessions are numbered in the following way:

For oral: **2A-4**, means the second session (Monday 10:30 – 11:45 hours) in Auditorio (A), the fourth presentation.

For poster: **10-12**, means tenth session (Tuesday 15:30 – 17:30 hours), poster number 12 (all poster sessions will take place in "Llevant" rooms).

Abstracts received after the deadline are indicated with letter P (e.g. **16-79P1** is a late poster).

Invited talks are marked with an asterisk in the Scientific Programme.

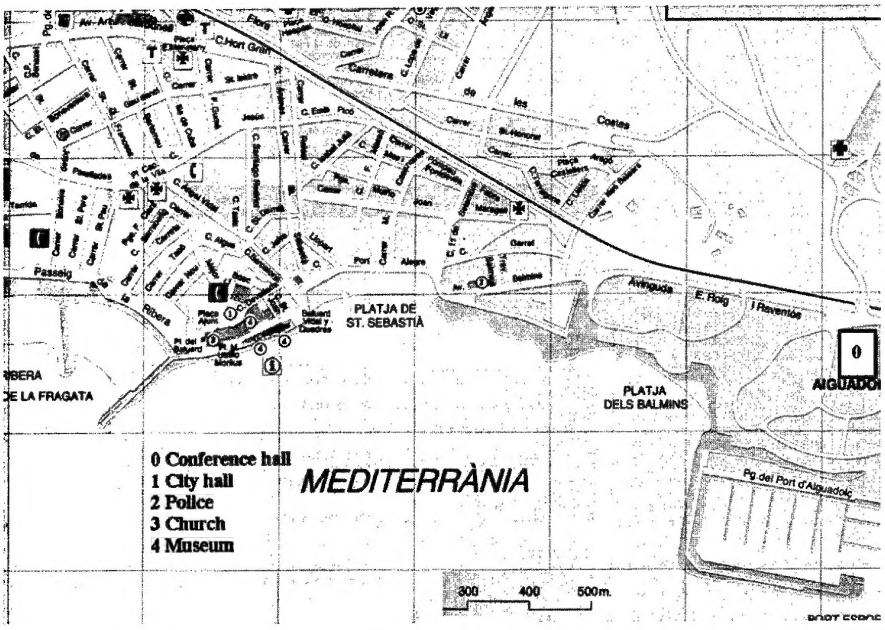

Map of Sitges

REGISTRATION / INFORMATION DESK

On Monday 13th and Tuesday 14th morning the Conference Registration / Information Desk will be situated at the main entrance, in the first floor of the Congress Center at Gran Sitges Hotel. Thereafter, the desk will be located in the lobby of the ground floor near the Tramuntana Halls. The Registartion / Information Desk will be open at the following times :

- Monday, September 13th 14.00h - 20.00h
- Tuesday, September 14th 07.30h - 19.00h
- Wednesday, September 15th 08.00h - 19.00h
- Thursday, September 16th 08.00h - 19.00h
- Friday September 17th 08.00h - 13.00h

CONFERENCE SECRETARIAT AND PUBLICATIONS OFFICE

The Conference Secretariat and the Publications Office are located in room "Catalunya" on the first floor of the Gran Sitges Hotel. Reception of publications is planed for :

Tuesday September 14th 8.00-20.00h
Wednesday September 15th 8.00-10:30h
Manuscript deadline is Wednesday September 15th 10:30h.

To submit a paper, please, don't forget:

1) One original and two copies of each paper.
2) A filled and signed copyright form.
3) A filled and signed reprint order form.
4) An author's checklist.

The refereed papers will be published in a special issue of the Institute of Physics Conference Series. For further information about the proceedings contact Kathryn Cantley, IOP Publishing Ltd, e-mail: kathryn.cantley@ioppublishing.co.uk.

A selection of the Plenary and Invited papers will assembled for a special issue of Superconductor Science and Technology. The scheduled length and format is the same that in the IOP Proceedings.

REFEREEES

The referees will be able to pick up the manuscripts for review in the Manuscript Office after Wednesday 15th September at 15.00h.

BADGES

Name badges will be issued to all delegates upon registration. These must be worn at all times. Please note that the badges will be color coded as follows :

Blue : Delegates
Red : Organisation Committee
Green : Exhibitors
White : Accompanying Persons

Access to all the scientific sessions of the Conference will require the wearing of the badge.

MEALS

Restaurants and bars may be found in the Aiguadolç area near by the Melia Gran Sitges Hotel (Marina Port area), at the Melia Hotel itself and in the town center of Sitges. You can walk all around the beaches and the Maritime Boulevard and also within the small streets of the old part of the town. Lunch time will be long enough (2.45h), accordingly to spanish style, to have time to be served at the restaurants and to encourage social relationship.

You will find a list of restaurants in the documentation included in your Conference bag.

MESSAGES

A message board will be available in the lobby where the Registration/Information Desk will be installed during the Conference. Any messages or faxes for the delegates will be displayed there. The telephone, Fax and e-mail of Melia Sitges Gran Hotel are :
Tel. 34-938110811 , Fax 24-938949037 , E-Mail : melia.gran.sitges@solmelia.es

TRANSPORT TO BARCELONA AND AIRPORT

Train
There is a regular train service from Barcelona to Sitges and viceversa. The first service is at 5.40h and the last one at 22.20h. The journey takes about 30 minutes and there is a train every 10 minutes. The same train may be used to go to the Barcelona airport. In that case you need to change the train at El Prat de Llobregat where there are trains to the airport every 30 minutes.

Shuttle buses
The conference will arrange buses from Barcelona airport to Sitges on Monday 13th September. There will be a coach service every hour on the hour. On Friday 17th afternoon there will be also a coach shuttle service from Melia Gran Sitges Hotel to the airport. The service will start at 14.00h. Those delegates interested in using this service are required to communicate it in advance to the Information Desk (before Thursday 16th at 17.00h)

Taxi
An average journey by taxi from the Barcelona Airport to Sitges should take 20 minutes, depending on traffic and weather. The cost of the ride should be around 6.000 Ptas with the motorway tolls and baggage included.

SOCIAL PROGRAMME

WELCOME RECEPTION
Monday 13th September, 19.30h

A welcome reception will be held at the gardens of the Melia Gran Sitges Hotel, very near to the Registration Desk

EVENING DRINKS
Tuesday 14th and Wednesday 15th September, 20.00h

Some drinks and snacks will be distributed to the delegates in the Poster/Exhibition Area within the Gran Sitges Hotel

CONFERENCE DINNER
Thursday 16th September, 21.00 - 24.00h

The Conference Dinner will be held at the Drassanes Reials in Barcelona. The Drassanes Reials is the world's single most important secular Gothic monument. Originally the shipyard of the royal fleet, since the 13th century it has served the city in one capacity or another, and now offers itself as an exceptional public forum and is the home to one of the world's great Maritime Museums. The cost of the banquet is included in the registration fee for delegates. The cost for acompanying persons is 10.000 Ptas (to be paid in advance at the Registration Desk before 15th September 17.00h). The dinner will include at the end a popular Catalan "cremat" and a touch of fisherman's songs (Habaneres). Buses will be available to transport all delegates from Melia Gran Sitges Hotel to the Drassanes Reials and viceversa.

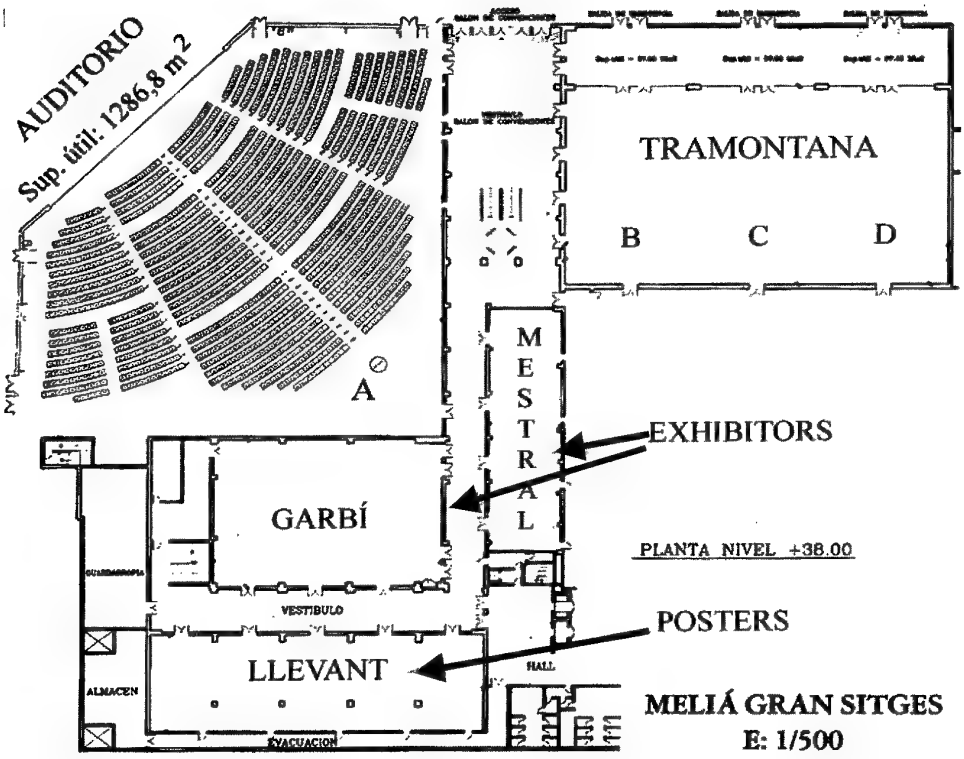

GROUND FLOOR

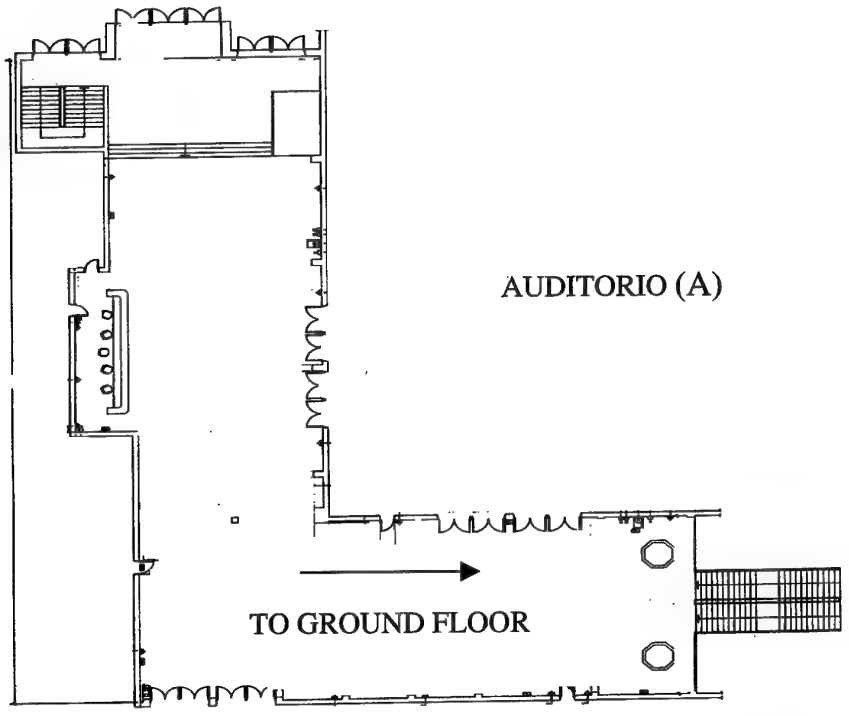

FIRST FLOOR

Scientific Programme

EUCAS'99

8.30/10.00	**Welcome & Opening PLENARY SESSION 1 2 × 40 MIN**				**PLENARY SESSION 7 2 × 45 MIN**				**PLENARY SESSION 13 2 × 45 MIN**			**PLENARY SESSION 18 4 × 30 MIN**
	Coffee Break											
10.30/11.45	**Session 2-A** *Bulk Materials I*	**Session 2-B** *System Aspects*	**Session 2-C** *Materials Electronic I*	**Session 2-D** *Passive Devices I*	**Session 8-A** *Wires and Tapes I - BSCCO*	**Session 8-B** *Motors, bearings, levitation*	**Session 8-C** *Josephson Junctions I*	**Session 8-D** *Oscillators and Volt-Standards*	**Session 14-A** *Wires and tapes II*	**Session 14-B** *Fault Current Limiters*	**Session 14-C** *SQUIDS II*	**Session 14-D** *AC Losses I*
11.45/12.45	**Session 3-A** *Bulk Materials I*	**Session 3-B** *System Aspects*	**Session 3-C** *Materials Electronic I*	**Session 3-D** *Systems Electronic*	**Session 9-A** *Wires and Tapes II - BSCCO*	**Session 9-B** *Motors, bearings, levitation*	**Session 9-C** *Josephson Junctions I*	**Session 9-D** *Bulk Materials II*	**Session 15-A** *Wires and Tapes II*	**Session 15-B** *Fault Current Limiters*	**Session 15-C** *SQUIDS II*	**Session 15-D** *Digital Applications*
Lunch												
15.30/17.30	**Session 4 POSTERS COFFEE/TEA**				**Session 10 POSTERS COFFEE/TEA**				**Session 16 POSTERS COFFEE/TEA**			
17.30/19.00	**Session 5-A** *Coated Conduct I*	**Session 5-B** *Flux Pinning I*	**Session 5-C** *SQUIDS I*	**Session 5-D** *Mixers and Detectors*	**Session 11-A** *Coated Conduct II*	**Session 11-B** *Cables and Transform.*	**Session 11-C** *Passive Devices II*	**Session 11-D** *Flux Pinning II*	**Session 17-A** *AC losses II*	**Session 17-B** *Fusion and SMES*	**Session 17-C** *Materials Electron II*	**Session 17-D** *Josephson Junctions II*
19.00/21.00	**Session 6 POSTERS DRINKS**				**Session 12 POSTERS DRINKS**				**BREAK ESAS MEETING**			
21.00/23.00	**FREE DINNER**				**FREE DINNER**				**CONFERENCE DINNER**			

PLENARY SESSION 19

1 x 45 MIN
3 x 30 MIN
CLOSING

INFORMATION FOR SCIENTIFIC PROGRAMME

ORAL PRESENTATION

The oral presentations are scheduled for 15 minutes, the invited speakers for 30 minutes and the Plenary speakers, either 30 minutes or 45 minutes, depending on the session. Audio-visual equipment will include an overhead projector, slide projector, screen, pointer and a label microphone. A slide preview Room will be available. Those speakers requiring the use of the slide projector are requested to contact the responsible of the preview room in advance of the scheduled time for the corresponding session. All speakers are requested to check in with the session chairman at the session room before the start of the session.

POSTER PRESENTATION

The Poster sessions will take place in the Llevant Hall. Posterboards measure 0.9 meter wide by 1.3 meters high. Posters should be fixed by adhesive tape or similar but not with tacks.

At least one author per poster should be available to answer questions during the poster session. Any poster not displayed during the relevant poster session will not be eligible for publication in the proceedings. The poster session timetable is the following :

Poster Sessions 4, 10 and 16 :	Mounting between 11.00 and 15.30h
	Dismounting between 17.30 and 18.00h
Poster Sessions 6 and 12 :	Mounting between 18.00 and 19.00h
	Dismounting between 21.00 and 21.30h

EXHIBITION

The conference is accompanied by a full Trade Exhibition.
The exhibition areas are located in the Garbi and Mestral halls.

The exhibition opening hours are as following:

Tuesday	14th September	14:30 - 21:00 hours
Wednesday	15th September	09:00 - 21:00 hours
Thursday	16th September	09:00 - 17:30 hours

LIST OF EXHIBITORS

The following Companies and Organisations will exhibit at EUCAS'99 Conference.
Refer to the exhibition plan for each company's booth location.

Company	Booth No.
Alcatel - Secteur Cables & Composants, Paris, France	G 15
Alstom Industrie - MSA Unit, Belfort, France	G 21
Antec, Portugalete, Spain	M 9 – M 10
Australian Superconductors, Eveleigh, Australia	G 23
Aventis Research Technologies, Huerth, Germany	G 17 – G 18
BICCGeneral Superconductors, Wrexham, United Kingdom	G 8
CAN SUPERCONDUCTORS, Praha, Czech Republic	G 6
Cryogenic Ltd., London, United Kingdom	G 5
Cryophysics SA, Geneva, Switzerland	G 10
Crystal GmbH, Berlin, Germany	G 9
CrysTec, Berlin, Germany	M 2
DANFYSIK S/A, Jyllinge, Denmark	G 16
DIOPMA, Barcelona, Spain	G 7
Elsevier Science, Amsterdam, The Netherlands	M 1
EPION Corporation, Billerica, USA	G 4
ESCETE, Enshede, The Netherlands	G 3
EUS Tecnologías S.A. (EURUS), Madrid, Spain	G 12
Everson Electric Company, Bethlehem, USA	G 24
Forschungszentrum Jülich, Julich, Germany	M 7 – M 8
FZK GmbH INFP, Karlsruhe, Germany	M 5 – M 6
MERCK KGaA, Gernsheim, Germany	G 19 – G 20
NST Nordic Superconductor Technologies, Brondby, Denmark	G 1 – G 2
Oxford Instruments, Oxfordshire, United Kingdom	G 13 – G 14
Primatec, Erding, Germany	G 22
Stirling Cryogenics & Refrigeration BV, Eindhoven, The Netherlands	G 11
THEVA Thin Film Technology, Eching-Dietersheim, Germany	M 3 – M 4

Connecting Tomorrow's World

ECONEXO™

Cryobicc™

With over 10 years experience in High Temperature Superconductivity we are providing superconducting tapes and current leads. Our products are engineered to your individual requirements for specific products and projects.

To ensure the highest possible quality standard we have an ISO 9000 accredited Quality System for R&D, production and marketing of our products and services.

For more further information please contact us:

Current Leads

Specially designed to help reduce your refrigeration costs by minimising the heat leak to your magnet system.

Key characteristics include:

- Manufactured with Bi-2223 Tapes with a reduced thermal conductivity matrix
- Specific robust design for cryogen-free or vapour-cooled magnets
- Current rating $\geq$ 10 Amps
- Operating temperature range 77 - 4 K
- Advice offered on low contact resistance connections

Bi-2223 Tapes

Tapes can be supplied in lengths up to 1.2 km and free test samples will be supplied on request. A range of sheath materials and dimensions, including new and innovative conductor configurations, are available to meet your requirements.

Typical applications for our tapes include current leads, cables, transformers, magnets, motors and energy storage systems.

BICCGeneral
Superconductors

BICCGeneral Superconductors, Oak Road, Wrexham LL13 9XP, United Kingdom
Tel: +44 (0) 1978 662594 ***Fax: +44 (0) 1978 662464***
Email: biccsc@bicc.co.uk http://www.bicc-sc.com

ISO 9001 FM24689

EXHIBITION HALLS

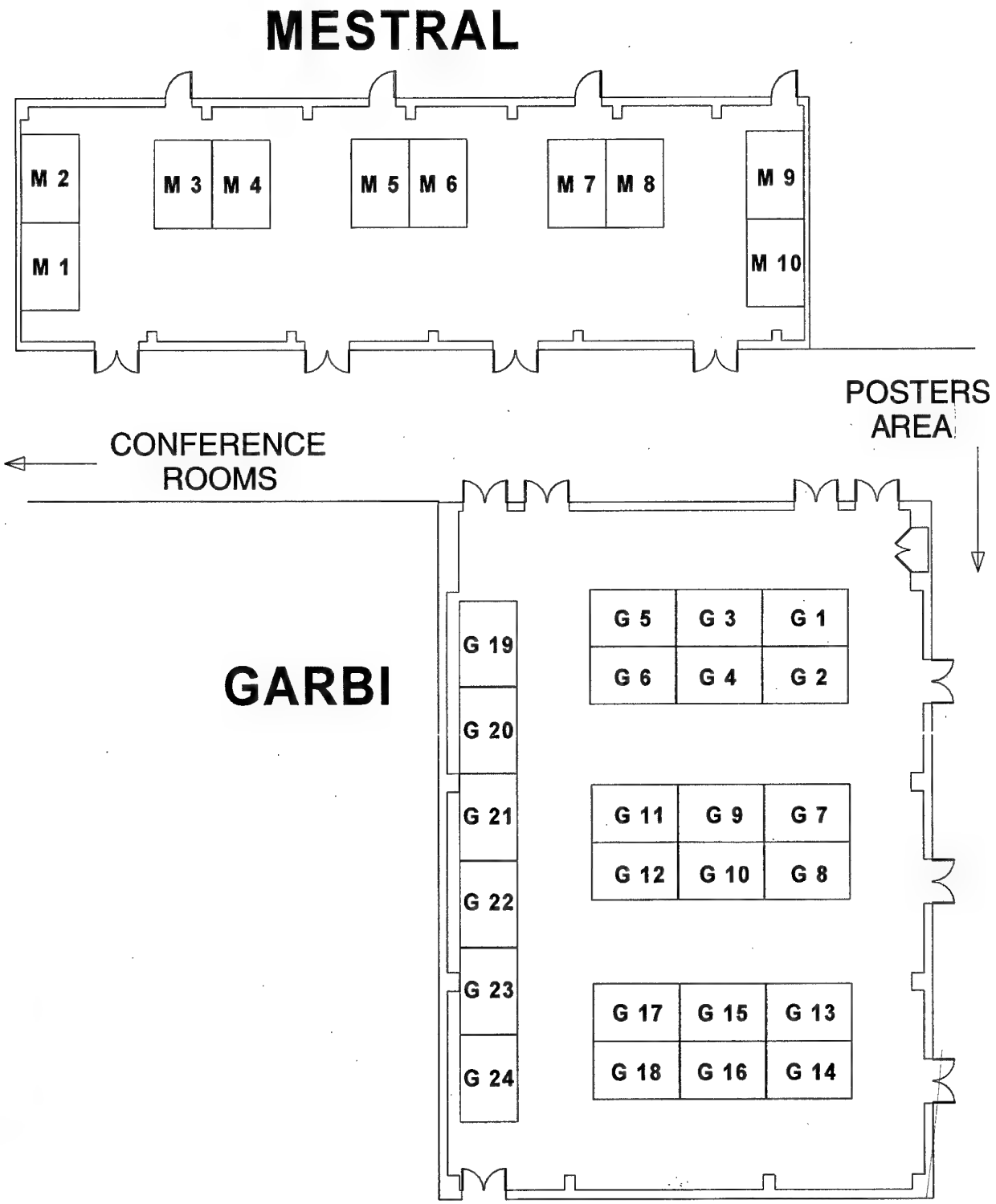

Booth: G 15 **Alcatel - Cables & Components Sector** 54, rue de La Boetie 75411 Paris Cedex 08, France Contact: Yves Parasie Phone: +33-0-1-40-762896 Fax: +33-0-1-40-761040 e-mail: yves.parasie@accyd.alcatel.fr *Superconducting Wire*	Booth: G 21 **Alstom Industrie - MSA Unit** 3, aveneue des Trois Chênes 90018 Belfort Cedex, France Contact: Claude Kohler Phone: +33-3-84-55-32-26 Fax: +33-3-84-55-16-15 e-mail: claude.kohler@energy.alstom.com *Superconducting Wires and Cables*
Booth: M 9 - M 10 **Antec** Ramón y Cajal, 74 48920 Portugalete, Spain Contact: Rafael Iturbe Phone: +34-94-4965011 Fax: +34-94-4965337 e-mail: antec@sarenet.es *Electromagnetic Devices*	Booth: G 23 **Australian Superconductors** P.O Box 21 Gloucester Boulevard Port Kembla NSW 2505, Australia Contact: Miles Apperley Phone: +61-2-42235331 Fax: +61-2-42751347 e-mail: milesa@ozemail.com.au *HTS Wire, Tape and Components*
Booth: G 17 - G 18 **Aventis Research and Technologies** Chemiepark Knapsack Building 2703 D-50351-Huerth, Germany Contact: Lisa Cowey Phone: +49-22-33-486491 Fax: +49-22-33-486847 e-mail: cowey@msmiuk.hoechst.com *HTS Bulk Parts and Precursors*	Booth: G 8 **BICCGeneral Superconductors** Oak Road Wrexham LL13 9XP, United Kingdom Contact: Wolfgang Blendl Phone: +44-0-1978-662594 Fax: +44-0-1978-662464 e-mail: biccsc@bicc.co.uk *HTS Current Leads & Tapes*
Booth: G 6 **CAN SUPERCONDUCTORS** Cukrovarnicka, 10 16200 Praha 6, Czech Republic Contact: Jan Plechacek Phone: +420-2-24315705 Fax: +420-2-22254329 e-mail: janpl@can.cz *HTS Superconducting current leads, magnetic shields, levitators, powders*	Booth: G 5 **Cryogenic Ltd.** Unit 30 Acton Park, Ind. Estate The Vale London W3 7QE, United Kingdom Contact: Zakiya Omar / Nick Corps Phone: +44-181-743-6049 Fax: +44-181-749-5315 e-mail: sales@cryogenic.co.uk *Cryogenic Systems and Current Leads*
Booth: G 10 **Cryophysics SA** 39, rue Rothschild CH-1202 Geneva, Switzerland Contact: Rene Koch Phone: +41-22-732 9520 Fax: +41-22-738-5246 e-mail: CryophysicsCH@compuserve.com *Full Range in Cryogenics & Magnetic Properties*	Booth: G 9 **Crystal GmbH** Ostendstrasse, 1-14 D-12459 Berlin, Germany Contact: Steffen Sandner Phone: +49-30-53881713 Fax: +49-30-5350436 e-mail: crystal@t-online.de *Substrates, Wafers*

Booth: M 2 **CrysTec** Köpenicker Str. 325 D-12555 Berlin, Germany Contact: Knut Peters Phone: +49-30-65762806 Fax: +49-30-65762808 e-mail: CrysTec@aol.com *Substrates for Thin Film Deposition*	Booth: G 16 **DANFYSIK A/S** Mollehaven 31 DK-4040 Jyllinge, Denmark Contact: Erik Steinmann Phone: +45-46-788150 Fax: +45-46-73-1551 e-mail: sales@danfysik.dk *Accelerators and Components for Accelerators*
Booth: G 7 **DIOPMA** Llacuna 162-166 08018 Barcelona, Spain Contact: Alberto Calleja Phone: +34-93-4021316 Fax: +34-93-4021291 e-mail: calleja@icmab.es *Superconducting Powders and Materials*	Booth: M 1 **Elsevier Science** P.O. Box 211 NL 1000 AE Amsterdam, The Netherlands Contact: Customer Support Department Phone: +31-20-4853757 Fax: +31-20-4853432 e-mail: nl.info-f@elsevier.nl *Scientific books, journals and electronic products*
Booth: G 4 **EPION Corporation** 37 Manning Road Billerica, MA 01821, USA Contact: Wesley J. Skinner Phone: +1-978-6701910 Fax: +1-978-6709119 e-mail: wskinner@epion.com *Gas Cluster Ion Beam, PVD, DLC*	Booth: G 3 **ESCETE** P.O. Box 3896 NL 7547 DW Enschede, The Netherlands Contact: Peter Droste Phone: +31-53-4356146 Fax: +31-53-4352134 e-mail: escete@escete.com *Crystals, Substrates, Pucks, Powders*
Booth: G 12 **EURUS Technologies Inc.** 2031 East Paul Dirac Drive, Innovation Park Tallahassee, FL 32310, USA Contact: Michael Tomsic / John Romans Phone: +1-850-574-1800 Fax: +1-850-574-2998 e-mail: info@TeamEURUS.com *HTS Current Lead Systems, HTS Tape, Ni_3Al, Ni_3Sn, Special Magnet*	Booth: G 24 **Everson Electric Company** 2000 City Line Rd Bethlehem, PA 18017, USA Contact: Leong Ying Phone: +1-610-2663218 Fax: +1-610-2641040 e-mail: leongying@eversonelec.com *Superconducting Magnets and Cryogenics*
Booth: M 7 - M 8 **Forschungszentrum Jülich** Leo Brandstrasse 52478 Julich, Germany Contact: Watter Wolf Phone: +49-2461-61-3200 Fax: +49-2661-61-2630 e-mail: w.wolf@fz-juelich.de *HTS Devices*	Booth: M 5 - M 6 **FZK GmbH INFP** Postfach 3640 D-76021 Karlsruhe, Germany Contact: Gerd Krafft Phone: +49-7247-822940 Fax: +49-7247-824624 e-mail: edith.maass@infp.fzk.de *Bulk and Thin Film high-Tc Superconductors (YBCO), Magnetic Bearings*

Booth: G 19 – G 20 **MERCK KGaA, Darmstadt** Mainzer Strasse, 41 D-64579 Gernsheim, Germany Contact: Michael Gerards Phone: +49-6258-12565 Fax: +49-6258-12567 e-mail: michael.gerards@merck.de *HTSC Precursor Powders*	Booth: G 1 - G2 **NST Nordic Superconductor Technologies** Priorparken 685 2605 - Brøndby, Denmark Contact: Juan Farré Phone: +45-43-482500 Fax: +45-43-482501 e-mail: j.farre@nst.com *HTS- BSCCO 2223 tapes*
Booth: G 13 - G 14 **Oxford Instruments** Tubney Woods Abingdon Oxfordshire, OX13 5QX, United Kingdom Contact: Pam Cox Phone: +44-0-1865-393200 Fax: +44-0-1865-393333 e-mail: info.ri@oxinst.co.uk *Cryofree Magnet*	Booth: G 22 **Primatec GmbH** Schlossallee, 28 D-85435 Erding, Germany Contact: Harith Rassam Phone: +49-81-22-5385 Fax: +49-81-22-53-26 e-mail: primatec@t-online.de *YBCO Thin Film, Thermal Evaporation Systems*
Booth: G 11 **Stirling Cryogenics & Refrigeration BV** Achtseweg Noord 5, P.O.Box 218, Building AQ 5600 MD Eindhoven, Holland Contact: Francesco Dioguardi Phone: +31-40-2766087 Fax: +31-40-2766144 e-mail: dioguardi@scr.nl *65 K Refrigeration Systems / Cryogenic Engineering*	Booth: M 3 - M 4 **THEVA Thin Film Technology** Hauptstrasse 1b D-85386 Eching-Dietersheim, Germany Contact: Werner Prusseit Phone: +49-89-32929176 Fax: +49-89-32929177 e-mail: prusseit@theva.com *YBCO-films, Evaporation Systems*

Scientific Programme

Tuesday, September 14th

WELCOME AND OPENING

Tuesday Morning, September 14th, 8:30-8:40

PLENARY SESSION 1

Tuesday Morning, September 14th, 8:40-10:00

8:40 **1–1 Materials: the path to applications.** *J.E. Evetts* and *B.A.Glowacki*. Interdisciplinary Research Center in Superconductivity and Department of Materials Science, University of Cambridge Premboke Street, Cambridge, CB2 3QZ UK.

9:20 **1–2 Superconducting gaps and pseudogaps: STM spectroscopy** *Ø. Fischer*. Université de Genève, Departement de Physique de la Matière Condensée, 1211 Genève 4, Switzerland.

ORAL SESSION 2A+3A: Bulk Materials and Materials Aspects I

Tuesday Morning, September 14th, 10:30-12:45

10:30 ***2A–1 Fabrication and Microstructural Features of Large Grain Nd-Ba-Cu-O Composites.** *N. Hari Babu*[1], *W. Lo*[1,2], *D. A. Cardwell*[1] and *Y.H. Shi*[1]. [1]IRC in Superconductivity, University of Cambridge, Cambridge, CB3OHE, UK. [2]Texas Center for Superconductivity, University of Houston, Houston, TX77204-5932, USA.

11:00 **2A–2 Growth of large $YBa_2Cu_3O_{7-\delta}$ mono domains with improved characteristics for current limiting applications.** *D.Isfort*, *X.Chaud*, *E. Beaugnon*, *D.Bourgault* and *R.Tournier*. CNRS/CRETA/Matformag Grenoble Isère 38000 France.

11:15 **2A–3 Massive YBCO material for rotating electric machines.** *W. Gawalek*[1], *T. Habisreuther*[1], *D. Litzkendorf*[1], *M. Zeisberger*[1], *T. Strasser*[2], *J. Best*[2], *B. Oswald*[2], *K. V. Ilushin*[3], *L. K. Kovalev*[3] and *H. J. Gutt*[4]. [1]Institut fuer Physikalische Hochtechnologie e.V., Helmholtzweg 4, D-07743 Jena, Germany. [2]OSWALD Elektromotoren GmbH, Benzstr. 12, D-63897 Miltenberg, Germany. [3]Moscow State Aviation Institute, Volokolamskoe shosse, 125871 Moscow, Russia. [4] Institut fuer Elektrische Maschinen und Antriebe, Universitaet Stuttgart, Pfaffenwaldring 47, D-70569 Stuttgart, Germany.

11:30 **2A–4 Top Seeded Growth and Joining of Bulk YBCO.** *H. Zheng*, *B. W. Veal*, *A. Paulikas*, *R. Nikolova*, *U. Welp*, *H. Claus* and *G. W. Crabtree*. Argonne National Laboratory, Argonne, IL, USA, 60439.

11:45 **3A–1 Tailoring of critical currents of melt textured $YBa_2Cu_3O_7$ / Y_2BaCuO_5 composites by high oxygen pressure.** *J. Plain*[1,3], *T. Puig*[1], *F. Sandiumenge*[1], *X. Obradors*[1], *J.A. Alonso*[2] and *J. Rabier*[3]. [1] Institut de Ciència de Materials de Barcelona, Consejo Superior de Investigaciones Científicas, Campus de la UAB, 08193 Bellaterra, Spain. [2] Instituto de Ciencia de Materiales de Madrid, Consejo Superior de Investigaciones Científicas, Cantoblanco, 28049 Madrid, Spain. [3] Laboratoire de Métallurgie physique, UMR 6630-CNRS Université de Poitiers - UFR Sciences, SP2MI, BP 179 86960 Futuroscope Cedex, France.

12:00 **3A–2 Reproducible production of large YBCO - monoliths with peak -effect.** *G. Krabbes*[1], *P. Schaetzle*[1], *G. Stoever*[1], *J.W. Park*[2], *S. Gruss*[1] and *G. Fuchs*[1]. [1] Institute of Solid Sate and Material Research Dresden, P.O. Box 270016, D-01171 Dresden,. [2]Solvay Barium Strontium GmbH, Hans- Böckler Allee 20, D-30173 Hannover.

12:15 **3A–3 High critical currents in Ce/Sn doped YBCO pellets grown by top seeding method.** *C. Leblond*, *S. Marinel*, *I. Monot*, *G. Desgardin* and *B. Raveau*. CRISMAT laboratory-CNRS UMR 6508, 6 Bd. Du Marechal Juin, 14050 Caen CEDEX. France.

12:30 **3A–4 Crystal defects in melt grown Re-Ba-Cu-O.** *P. Diko*. Institute of Experimental Physics, Watsonova 47, 04 353 Košice.

ORAL SESSION 2B+3B: System Aspects and High Fields

Tuesday Morning, September 14th, 10:30-12:45

10:30 ***2B–1 Recent R&D Status on 70MW class Superconducting Generators in Super-GM Projec.** T.Hirao[1], M.Shibuya[1], S.Shimada[1], H.Kusafuka[1], R.Shiobara[2], K.Suzuki[3] and K.Miyaike[4]. [1]Engineering Research Association for Superconductive Generation Equipment and Materials(Super-GM), Osaka,530-0047,Japan. [2]Hitachi Ltd., Hitachi, Ibaragi, 317-8511, Japan. [3]Mitsubishi Electric Corp., Kobe, Hyogo, 652-8555, Japan. [4]Toshiba Corp., Yokohama, Kanagawa, 230-0045, Japan.

11:00 **2B–2 An HTS Magnet for Whole-body MRI.** A.F. Byrne[1], F.J. Davies[1], C. Raynor[1], W. Stautner[1], F. Steinmeyer[2], C. Albrecht[2], P. Kummeth[2], P. Massek[2], H.-W. Neumüller[2] and M. Wilson[3]. [1] Oxford Magnet Technology Ltd, Eynsham, UK. [2] Siemens AG, Corporate Technology, ZT EN 4, Erlangen, Germany. [3] Oxford Instruments Research Instruments, Tubney Woods, UK.

11:15 **2B–3 Applications of HTS Technologies in the Danish Utilities.** P. Jorgensen and J.J. Oestergaard. DEFU, P.O. Box 259, 2800 Lyngby, Denmark.

11:30 **2B–4 Compact iron screened HTS dedicated magnet for osteoporosis.** A. Matrone[1], M. Ariante[1], V. Cavaliere[1], M. Mariani[1], A. Sotgiu[2] and V. Varoli[3]. [1]ANSALDO-CRIS,via Nuova delle Brecce n. 260, I-80147 Napoli, Italy. [2]Università dell'Aquila - Dip. Scienze e Tecnologie Biomediche, via Vetoio, I-67100 Coppito - L'Aquila, Italy. [3]Politecnico di Milano, via Ponzio n. 34, I-20133 Milano, Italy.

11:45 **3B–1 600 A HTc Current Leads based on BSCCO 2212 Rods for LHC Magnets.** L. García-Tabarés[1], J. Calero[1], P. Abramian[2], F. Toral[2], L.A. Angurel[3], C. Diez[3], R. Iturbe[4], J. Etxeandia[4], A. Ballarino[5] and J.C. Perez[5]. [1]Centro de Estudios y Experimentación de Obras Publicas CEDEX. Alfonso XII, 3 28014 Madrid. Spain. [2]Centro de Investigaciones Energeticas MedioAmbientales y Tecnologicas CIEMAT. AV. Complutense 22. 28040 Madrid.Spain. [3]Departamento de Ciencia y Tecnologia de Materiales y Fluidos. ICMA. CSIC. Universidad de Zaragoza. Maria de Luna 3. 50015 Zaragoza.Spain. [4]ANTEC. Ramon y Cajal 74. 48920. Portugalete. Spain. [5]CERN. Geneva. Switzerland.

12:00 **3B–2 13000 amp current lead with 1W heat load at 4.5K for the large hadron collider at CERN.** J. A. Good[1], M. Allitt[1] and L. Martini[2]. [1]Cryogenic Ltd, Unit 30 Acton Park Industrial Estate, The Vale, London W3 7QE, United Kingdom. [2]ENEL S.p.A, Struttura Ricerca, Via Volta, 20093 Cologne (MI), Italy.

12:15 **3B–3 Development of high field insert coils using high temperature superconductors.** D. Ryan[1], H. Jones[2], K. Marken[3], M. Newson[2] and M.N. Wilson[1]. [1]Oxford Instruments, Tubney Woods, Abingdon, OX13 5QX, UK. [2]University of Oxford, Clarendon Laboratory, Parks Rd, Oxford, OX1 3PU, UK. [3]Oxford Superconducting Technology, 600 Milik St, PO Box 429, Carteret NJ07008-0429 USA.

12:30 **3B–4 Development and testing of a 3 T Class Bi-2212 Insert Coil.** H.W. Weijers[1], Q.Y. Hu[1], Y. Viouchkov[1], E. Celik[1], Y.S. Hascicek[1], J. Schwartz[1], K. Marken[2] and J. Parrell[2]. [1]National High Magnetic Field Laboratory, Tallahassee, Florida, 32310, USA. [2]Oxford Superconducting Technology, Carteret, New Jersey,07008, USA.

ORAL SESSION 2C+3C: Materials Related to Electronic Applications

Tuesday Morning, September 14th, 10:30-12:45

10:30 ***2C–1 Interval pulsed laser deposition of REBaCuO.** D.H.A. Blank, G.J.H.M. Rijnders and H. Rogalla. University of Twente, Department of Applied Physics, Low Temperature Division, The Netherlands.

11:00 **2C–2 Microwave and DC Field-Dependent Surface Impedance of YBaCuO Epitaxial Thin Films.** A. V. Velichko[1,2], A. Porch[1], A. P. Kharel[1], M. J. Lancaster[1] and R. G. Humphreys[3]. [1]School of Electronic and Electrical Engineering, University of Birmingham, Birmingham B15 2TT, UK. [2]Institute of Radiophysics and Electronics, NAS of Ukraine, Kharkov 310085, Ukraine. [3]KF 1209, DERA, Malvern WR14 3PS, UK.

15:00 **2C–3 The Study of Thermal Fatigue Behavior of YBCO High-Temperature Superconductor Thin Films.** F.Yang[1], K.H.Wu[1] and G.Larkins[2]. [1]Department of Mechanical Engineering, Florida International University, Miami, FL 33199, U.S.A. [2] Department of Electrical Engineering, Florida International University, Miami, FL 33199, U.S.A.

11:30 **2C–4 New method for fabricating ribbon-like thin films of Bi-2212 on Ag substrates and their superconducting properties.** *S. Arisawa*[1,2], *H. Miao*[2], *H. Fuji*[1,2], *A. Ishii*[1], *S. Labat*[1], *T. Hatano*[1] and *K. Togano*[1,2]. [1]Natinal Research Institute for Metals, 1-2-1, Sengen, Tsukuba, Ibaraki 305-0047, Japan. [2]CREST, Japan Science and Technology, 2-1-6, Sengen, Tsukuba, Ibaraki 305-0047, Japan.

11:45 **3C–1 $SrTiO_3$ as a substrate for the electrodeposition of HTSC films.** *M.S. Martín-González, E. Moran* and *M.A. Alario-Franco*. Laboratorio de Química del Estado Sólido, Departamento de Química Inorgánica, Facultad de Ciencias Químicas, Universidad Complutense, 28040-Madrid Spain (EU).

12:00 **3C–2 Structure and properties of (Sr,Ca)CuO_2 - $BaCuO_2$ superlattices grown by layer-by-layer PLD.** *K. Verbist*[1], *G. Van Tendeloo*[1], *G. Koster*[2], *G. Rijders*[2], *D.H.A. Blank*[2] and *H. Rogalla*[2]. [1]EMAT, University of Antwerp (RUCA), Antwerp, Belgium. [2]Low Temperature Physics, Applied Physics, University of Twente, Enschede, Netherlands.

12:15 **3C–3 $Bi_2Sr_2CaCu_2O_{8+x}$ epitaxial thin films on silicon substrates.** *J. C. Martínez*[1], *S. Ingebrandt*[1], *M. Basset*[1], *M. Mauer*[1], *M. Mayer*[1], *H. Adrian*[1], *S. Linzen*[2] and *P. Seidel*[2]. [1]Johannes Gutenberg – Universität Mainz, Institut für Physik, D-55099 Mainz; Germany. [2]Friedrich-Schiller-Universität Jena, Institut für Festkörperphysik, Helmholzweg 5, D-07743 Jena, Germany.

12:30 **3C–4 defects in YBCO films on CeO_2 buffered sapphire and $LaAlO_3$ and their effect on the microwave properties.** *J. Einfeld*[1], *P. Lahl*[1], *R. Kutzner*[1], *R. Wördenweber*[1] and *G. Kaestner*[2]. [1]ISI, Forschungszentrum Juelich, 52425 Juelich, Germany. [2]MPI fuer Mikrostrukturphysik, 06120 Halle, Germany.

ORAL SESSION 2D: Passive Devices I

Tuesday Morning, September 14th, 10:30-11:45

10:30 ***2D–1 Cryogenic dielectric resonators for future microwave communication.** *M. Winter, D. Schemion, I.S. Ghosh* and *N. Klein*. Forschungszentrum Jülich GmbH Institut of Solid State Research 52425 Jülich Germany.

11:00 **2D–2 Low Field MRI System with HTS Receive Coils.** *N.McN. Alford*[1], *S.J. Penn*[1], *A.A. Esmail*[1], *D. Bracanovic*[1], *T.W. Button*[2], *C. Nicholls*[3] and *S. F. Keevil*[4]. [1]South Bank University, London, SE1 0AA, UK. [2]Birmingham University, B15 2TT, UK. [3]SMIS Ltd, Guildford, GU2 5YF, UK. [4]Guy's Hospital, London Bridge, London, SE1 9ET.

11:15 **2D–3 Demonstration of a Power Handling of 0.5kW at 0.5GHz in a Stripline of YBCO on a 3" $LaAlO_3$ Wafer.** *N. Levy*[1], *G. Koren*[1], *E. Polturak*[1] and *Y. Koral*[2]. [1]Technion, Physics Dept., Haifa 32000 Israel. [2]Elisra electronic systems ltd. , Bney Brak 51203 Israel.

11:30 **2D–4 Characterisation of the superconducting and microwave properties of YBCO films simultaneously sputtered on both sides of sapphire wafers.** *A.G. Zaitsev*[1], *R. Schneider*[1], *J. Geerk*[1], *G. Linker*[1], *F. Ratzel*[1], *R. Smithey*[1], *S. Kolesov*[2] and *T. Kaiser*[2]. [1]Institut fuer Nuleare Festkoerperphysik, Forschungszentrum Karlsruhe, P.O.Box 3640, D-76021 Karlsruhe, Germany. [2]Universitaet Wuppertal, D-42119 Wuppertal, Germany.

ORAL SESSION 3D: System Aspects Related to Electronic Applications

Tuesday Morning, September 14th, 11:45-12:45

11:45 ***3D–1 Cryogenic packageing of superconducting electronic systems: A crucial, enabling technology.** *M. Nisenoff*. M. Nisenoff Associates Post Office Box 2748 Kensington MD 20896-2748 USA.

12:15 **3D–2 A 4-pixel YBCO mid-infrared bolometer array with associated cryogenic CMOS circuit.** *F. Voisin*[1], *G. Klisnick*[1], *Y. Hu*[1], *M. Redon*[1], *J. Delerue*[2], *A. Gaugue*[2] and *A. Kreisler*[2]. [1]Laboratoire des Instruments et Systemes - Universite P. et M. Curie (Paris 6) BP 252, T12-13 E2 4 place jussieu 75252 Paris cedex 05 - France. [2]Laboratoire de Genie Electrique de Paris - UMR 8507 CNRS - Universités Paris 6 et Paris 11 SUPELEC - Plateau de Moulon 91192 Gif Sur Yvette Cedex - France.

12:30 **3D–3 The Defense Advanced Research Projects Agency (DARPA) Program on Applied Superconductivity.** *S. A. Wolf*[1,2] and *F. W. Patten*[2]. [1]Naval Research Laboratory, Washington DC 20375. [2]Defense Advanced research Projects Agency, 3701 N. Fairfax Dr. Arlington VA 22203.

POSTER SESSION 4

Tuesday Afternoon, September 14th, 15:30-17:30

Session Bulk materials and materials aspects

4–1 A new fast and non-destructive method for evaluating the superconducting properties of bulk materials. *Ph. Vanderbemden*[1], *H.W. Vanderschueren*[1], *Z. Aouina*[2], *R. Cloots*[3] and *M. Ausloos*[4]. [1]University of Liège, S.U.P.R.A.S., Montefiore Electricity Institute B28, Sart-Tilman, B-4000 Liège, Belgium. [2]Institut Supérieur Industriel Liégeois Rennequin Sualem Quai Gloesener, 6 B-4020 Liège, Belgium. [3]University of Liège, S.U.P.R.A.S., Chemistry Institute B6, Sart-Tilman, B-4000 Liège, Belgium. [4]University of Liège, S.U.P.R.A.S., Physics Institute B5, Sart-Tilman, B-4000 Liège, Belgium.

4–2 Bulk textured Bi2212/MgO with high critical currrent densities at low temperatures. *S. Pavard*[1], *D. Bourgault*[1], *C. Villard*[2], *R. Tournier*[1], *S. Rivoirard*[1] and *J.L. Soubeyroux*[1]. [1] Laboratoire de Cristallographie/CRETA - CNRS 38042 Grenoble France. [2]CRTBT/CRETA - CNRS 38042 Grenoble France.

4–3 Preparation and Properties of Bi-2212/(Sr,Ca)SnO_3 Superconducting Composites. *P.E. Kazin*[1], *R.A. Shuba*[1], *V.V. Lennikov*[1], *Yu.D. Tretyakov*[1] and *M. Jansen*[2]. [1]Chemistry Department, Moscow State University, 119899 Moscow, Russian Federation. [2]Max-Plank-Institut fuer Festkoerperforschung, D-70569 Stuttgart, Germany.

4–4 Electrical, mechanical and thermal characterisation of LFZ Bi-2212 textured thin rods. *E. Natividad*[1], *J.C. Díez*[1], *L.A. Angurel*[1], *M. Castro*[1], *R. Burriel*[1], *R. Navarro*[1], *J.Y. Pastor*[2], *P. Poza*[2], *J. Llorca*[2], *J. Calero*[3], *L. García-Tabarés*[3] and *P. Abramian*[4] [1]Instituto de Ciencia de Materiales de Aragón (C.S.I.C.-Universidad de Zaragoza), María de Luna, 3, 50015 Zaragoza (Spain). [2]Departamento de Ciencia de Materiales, E.T.S. Ingenieros de Caminos, U.P.M., Ciudad Universitaria, 28040 Madrid (Spain). [3]CEDEX AlfonsoXII, 3, 28014 Madrid (Spain). [4]CIEMAT Av Complutense 22, 28040 Madrid (Spain).

4–6 Scale-up and production of ~1000A current elements from MgO fibre textured Bi-2212. *K.A. Kursumovic*[1], *B.A. Glowacki*[1], *J.E. Evetts*[1], *M.A. Henson*[2], *M.P. Hills*[2] and *R.M. Henson*[2]. [1]IRC in Superconductivity and Department of Materials Science and Metallurgy, University of Cambridge, Cambridge CB2 3QZ, UK. [2]Advanced Ceramics Limited, Castle Works, Stafford ST16 2ET, UK.

4–7 An Analysis for Finding a Suitable Design Condition to Improve J_C of a Bi-System by SRPM Method. *H. Nakane*[1], *S. Haseyama*[2], *S. Yamazaki*[1], *H. Miyairi*[1] and *S. Yoshizawa*[3]. [1]Kogakuin Univ., Shinjuku-ku, Tokyo 163-8677, Japan. [2]Dowa Mining Co. Ltd., Hachioji-shi, Tokyo 192-0001, Japan. [3]Meisei Univ., Hino-Shi, Tokyo 191-8506, Japan.

4–8 HTSC bulk materials - shielding elements and their properties. *H. Altenburg*[1], *J. Plewa*[2], *W. Jasczcuk*[1] and *N. Munser*[1]. [1]Fachhochschule Münster - University of Applied Sciences Stegerwaldstraße 39 48565 Steinfurt Germany. [2]SIMa - Steinfurter Initiative für Materialforschung e.V. Uhlandstraße 17 48565 Steinfurt Germany.

4–9 Holes Control Superconductivity and Critical Current Densitiy in $Bi_2Sr_2(Ca_{1-x}Y_x)Cu_2O_{8+\delta}$. *R. S. Liu*[1], *I. J. Hsu*[1], *J. M. Chen*[2] and *L. Y. Jang*[2]. [1]Department of Chemistry, National Taiwan University, Taipei, Taiwan, R.O.C. [2]Synchrotron Radiation Research Center, Hsinchu, Taiwan, R.O.C.

4–10 Large area deposition of high quality YBCO films by pulsed injection CVD. *A. Teiserkis*[1], *A. Abrutis*[1], *V. Kubilius*[1], *Z. Saltyte*[1], *J.P. Senateur*[2] and *F. Weiss*[2]. [1] Vilnius University, Dept. of General and Inorganic Chemistry, LT-2006 Vilnius, Lithuania. [2]LMPG-ENSPG, CNRS UMR 5628, BP 46, 38402 St Martin D'Heres, France.

4–12 The Influence of Elevated Magnetic Fields on the Texture Formation of Melt-Processed Bi-2212. *E. Cecchetti*, *P.J. Ferreira* and *J.B.V. Sande*. Massachusetts Institute of Technology (MIT) Department of Materials Science and Engineering Cambridge, MA, 02139, USA.

4–13 Numerical stability analysis for a solenoidal HTS coil. *J. Lehtonen*, *R. Mikkonen* and *J. Paasi*. Laboratory of Electromagnetics, Tampere University of Technology P.O.Box 692, 33101 Tampere, Finland.

4–14 Copper Oxides Superconductors Containing Phosphate Group. *J. C. Gonzalez*[1], *A. Bustamante*[1], *D. Landinez*[2] and *J. Albino*[2]. [1]Laboratorio de Superconductividad, Facultad de Ciencias Fisicas, Universidad Nacional Mayor de San Marcos, Apartado Postal 14-0149, Lima 14 - Peru. [2]Departamento de Fisica, Universidad Federal de Pernambuco, 50670-901 Recife PE, Brazil.

4–15 Improving thermal and electrical conductivity of cylindrical superconducting YBCO magnetron targets. *I. Van Driessche*[1], *F. Persyn*[1], *R. Mouton*[1], *G. De Mey*[2] and *S. Hoste*[1]. [1]University Gent, Department Inorganic and Physical Chemistry, Gent, 9000, Belgium. [2]University Gent, Department of Electronics and Information Systems, Gent,9000, Belgium.

4–16 Development of cylindrical superconducting magnetron targets by flame spraying and atmospheric plasma spraying. *I. Van Driessche*[1], *R. Mouton*[1], *F. Persyn*[1], *E. Georgiopoulos*[2], *A. Tsetsekou*[2] and *S. Hoste*[1]. [1]University Gent, Department Inorganic and Physical Chemistry, Gent, 9000, Belgium. [2]Ceramics and refractories technological development company, CERECO S. A., Chalkida, Evia, 34100, Greece.

4–17 Low Pressure Plasma Spraying of Superconducting Powders. *E. Georgiopoulos*[1] and *A. Tsetsekou*[2]. [1]CERECO S.A, P.O Box 146, Chalkida, Greece. [2]CERECO S.A, P.O Box 146, Chalkida, Greece.

4–18 Quantitative Phase Analysis of HTSC-Multifilamentary-Tapes by X-ray Diffraction using the Rietveld Method. *A. Risch*, *P.O.G. Gaeberlein*, *J. Neubauer* and *M. Goebbels*. Department of Mineralogy, Friedrich-Alexander University Erlangen-Nuernberg, Schloßgarten 5a, 91054 Erlangen, Germany.

4–19 AC Susceptibility measurements and simulation of magnetic percolation effect in Bi2223 composites with MgO. *E. Bruneel*[1], *A.J. Ramirez-Cuesta*[2], *R. Mouton*[1], *F. Persyn*[1] and *S. Hoste*[1]. [1]Department of Inorganic and Physical Chemistry, Solid State and Superconducting Materials Division, University of Gent, 9000 Gent, Belgium. [2] Department of Chemistry, University of Reading Whiteknights, PO Box 224 Reading RG6 AD, United Kingdom.

4–20 Quantitative Rietveld Phase Analysis of BPSCCO-2223 Precursor Powders using XRD. *P.O.G. Gaeberlein*, *A. Risch*, *J. Neubauer* and *M. Goebbels*. Department of Mineralogy, Friedrich Alexander University, Schlossgarten 5a, 91054 Erlangen, Germany.

4–21 Preparation of Bi-2223/Ag multilayered sintered bulk. *S. Yoshizawa*[1], *S. Nemoto*[1], *I. Tezuka*[1] and *S. Haseyama*[2]. [1]Meisei University, Advanced Materials R & D center, Hino, Tokyo, 191-850, Japan. [2]Dowa Mining Co., Ltd., Tobuki, Hachioji, Tokyo, 192-0001 Japan.

4–22 Effect of CaF2 additions on the formation of the (Bi,Pb)2Sr2Ca2Cu3Oy phase. *J.-C. Grivel*[1,2]. [1]Nordic Superconductor Technologies A/S, Priorparken 685, DK-2605 Broendby, Denmark. [2]Materials Department, Risoe National Laboratory, DK-4000 Roskilde, Denmark.

Session Motors, bearings and levitation

4–23 Parasitic Resonances in Contactless Bearings. *A.A. Kordyuk*, *E.A. Laptev* and *V.V. Nemoshkalenko*. Institute of Metal Physics, Kyiv 252680, Ukraine.

4–24 Characterization of melt-textured YBCO for Superconducting Magnetic Bearings. *U. Sutter*, *M. Adam*, *R. Wagner*, *R. Koch*, *M. Kläser* and *M. Sander*. Forschungszentrum Karlsruhe GmbH, INFP, P. O. Box 3640, D-76021 Karlsruhe.

4–25 Numerical analysis of a rotating superconducting magnetic bearing. *E. Portabella*, *R. Palka*, *H. May* and *W.R. Canders*. Institut für Elektrische Maschinen, Antreibe und Bahnen. Technische Universität Braunschweig. Braunschweig, 38106, Germany.

4–26 Stability and stiffness of superconducting bearings. *R.J. Storey*, *T.A. Coombs*, *A.M. Campbell* and *R.A. Weller*. IRC in Superconductivity, University of Cambridge, Cambridge CB3 0HE, UK.

4–27 Application of High Performance Bulk Sm-Ba-Cu-O to Superconducting Magnetic Bearings. *T. Otani*, *M. Tomita* and *M. Murakami*. ISTEC, Superconductivity Research Laboratory, 1-16-25 Shibaura, Minato-ku, Tokyo 105-0023, Japan.

4–28 Numerical Simulation of Reluctance Motors Containing Bulk High Temperature Superconducting Materials in the Rotor. *G.J. Barnes*, *M.D. McCulloch* and *D. Dew-Hughes*. Dept. Engineering Science, University of Oxford, Parks Road, Oxford OX1 3PJ, U.K.

4–29 6-DOF superconducting magnetic bearing with high accuracy of the rotor positioning. *A.V. Filatov*, *O.L. Poluschenko* and *N.A. Nigelskiy*. Moscow N.E. Bauman State Technical University, Moscow, 107005, Russia.

4–31 Construction and Experiments of a Superconducting Cylindrical Linear Induction Motor with AC Superconducting Primary Windings. *M. Tomita*, *T. Kikuma*, *M. Tsuda* and *A.I. Ishiyama*. Dept. of EECE, Waseda University, Shinjuku-ku, Tokyo 169-8555, Japan.

4–32 Superconducting Magnetic Bearing based on the Magnetic Gradient Levitation Concept. *H. Ohsaki*, *N. Nozawa* and *Y. Fukasawa*. The University of Tokyo, Bunkyo-ku, Tokyo, 113-8656, Japan.

4–33 The principles of construction and computer simulation of superconducting graviinertial sensors. *G.E. Shunin*, *S.A. Kostryukov* and *V.V. Peshkov*. Voronezh State Technical University, Voronezh, RU, 394026, Russia.

4–34 Finite Element Simulation of Autostable Superconducting Magnet Rails. *G.C. da Costa*[1], *A.S. Pereira*[2], *L. Landau*[1] and *R. Nicolsky*[2]. [1] LAMCE - Laboratório de Métodos Computacionais em Engenharia, PEC/COPPE/UFRJ Cx.P. 68552, Rio de Janeiro 21949-900, Brazil; e-mail: gian@lamce.ufrj.br. [2]LASUP - Laboratório de Aplicações de Supercondutores, IF/UFRJ Cx.P. 68528, Rio de Janeiro 21945-970, Brazil; e-mail: agnaldo@if.ufrj.br.

4–35 Hybrid superconducting/electromagnetic bearing for induction machines. *R. de Andrade, Jr.*[1], *A.S. Pereira*[2], *D.F.B. David*[3,4], *J.A. Santisteban*[5], *A. Ripper*[4], *R.M. Stephan*[1,6] and *R. Nicolsky*[2]. [1]LASUP, DEE/EE/UFRJ, Cx.P. 68515, Rio de Janeiro 21945-970, Brazil. [2]LASUP, IF/UFRJ, Cx.P. 68528, Rio de Janeiro 21945-970, Brazil. [3]TEM/UFF, Niteroi 24210-240, Brazil. [4]LASUP, PEM/COPPE/UFRJ, Rio de Janeiro 21945-970, Brazil. [5]DEE/UFF, Niteroi 24210-240, Brazil. [6]LASUP, PEE/COPPE/UFRJ, Rio de Janeiro 21945-970, Brazil.

4–36 Thickness effects in the levitation of superconducting cylinders and disks. *C. Navau* and *A. Sanchez*. Departament de Fisica, Universitat Autonoma de Barcelona, 08193 Bellaterra, Barcelona, Spain.

Session Wires, tapes and coated conductors

4–37 Preparation of Bi 2223 Multifilamentary Tapes by Two-Step Heat Treatment Process. *S.K.Xia*[1], *A.Polasek*[1], *M.B.Lisboa*[1], *E.T.Serra*[1] and *F.Rizzo*[2]. [1]CEPEL-Electric Power Research Center, Rio de Janeiro, RJ, 21944-970 Rio de Janeiro, RJ, Brazil. [2]Pontifícia Universidade Católica - PUC-Rio, Rua Marques de Sao Vicente, 225 22453-900 Rio de Janeiro, RJ, Brazil.

4–38 A new type of superconductor/ferromagnet heterostructures for high-current applications. *Yu.A.Genenko*[1,2], *A.Usoskin*[1], *A.Snezhko*[2,3] and *H.C.Freyhardt*[1,4]. [1]Zentrum für Funktionswerkstoffe gGmbH, 37073 Göttingen, Germany. [2]Donetsk Physical and Technical Institute NAS Ukraine, 340114 Donetsk, Ukraine. [3]Charles University, 180 00 Prague 8, Czech Republik. [4]Institut für Materialphysik, Universität Göttingen, 37073 Göttingen, Germany.

4–39 Influence of irradiation on the superconducting properties of uranium-doped $Bi_2Sr_2Ca_2Cu_3O_x$-tapes. *S. Tönies*[1], *C. Klein*[1], *H.W. Weber*[1], *B. Zeimetz*[2], *Y.C. Guo*[2], *S.X. Dou*[2], *R. Sawh*[3], *Y. Ren*[3] and *R. Weinstein*[3]. [1]Atomic Institute of the Austrian Universities, Vienna, A-1100,Vienna, Austria. [2]Institute of Superconducting and Electronic Materials, University of Wollongong, Wollongong NSW 2522, Australia. [3]Institute for Beam Particle Dynamics, University of Houston, Houston, TX 77204-5506, USA .

4–40 Assembled conductors of Bi2223/Ag-tapes for AC-applications. *J. Rieger*, *M.P. Oomen*, *P. Kummeth*, *W. Herkert*, *R. Nanke* and *M. Leghissa*. Siemens AG, Corporate Technology, P.O.Box 3220, D-91050 Erlangen, Germany.

4–41 Design of HTS pancake coil by the optimization of tape width. *S.S. Oh*, *H.B. Jin*, *H.S. Ha*, *D.W. Ha*, *D. Y. Jeong* and *K.S. Ryu*. Applied Superconductivity Lab., Korea Electrotechnology Research Institute, Changwon 641-120, Korea.

4–42 Quench characteristics of Ag sheathed Bi-2223 superconducting tapes with different Ag/SC ratio. *S.S. Oh*[1], *H.M. Jang*[1], *H.S. Ha*[1], *D.W. Ha*[1], *K.S. Ryu*[1] and *S.H. Kim*[2]. [1]Applied Superconductivity Lab., Korea Electrotechnology Research Institute, Changwon 641-120, Korea. [2]Gyeongsang National University, Chinju 660-701, Korea.

4–43 Thermal and Electrical Properties of Bi-2223 tape conductors. *A.K. Shikov*[1], *N.I. Kozlenkova*[1], *I.I. Akimov*[1], *P.A. Kuznetsov*[1], *D.N. Rakov*[1], *F.V. Popov*[1], *I.V. Bogdanov*[2], *S.S. Kozub*[2], *A.A. Olunin*[2] and *P.A. Sherbakov*[2]. [1]SSC RF Bochvar's All – Russia Seientific Research Institute of Inorganic Materials, Moscow, Rogova St., 123060, Russia. [2]SSC RF Institute for High Energy Physics, Protvino, Moscow region, Russia.

4–44 Optimization of deformation processing for Bi-2223 composite superconductors. *A.D. Nikulin*, *A.K. Shikov*, *A.E. Vorobieva*, *I.I. Akimov*, *F.V. Popov*, *A.V. Rekudanov*, *D.B. Gusakov*, *M.I. Medvedev* and *O.I. Lomov*. SSC RF Bochvar's All – Russia Seientific Research Institute of Inorganic Materials,Moscow, Rogova St. 5a, 123060, Russia.

4–45 Cooling studies of BSCCO/Ag Tapes in 8% Oxygen. *L. G. Andersen*[1], *Y.L. Liu*[1], *J.-C. Grivel*[1,2], *H.F. Poulsen*[1] and *W.G. Wang*[2]. [1]Materials Research Department, Risø National Laboratory, DK-4000 Roskilde, Denmark. [2]Nordic Superconductor Technologies, Priorparken 878, DK-2605 Brøndby, Denmark.

4–46 Current carrying capacity and the anisotropy of Bi-2212/Ag ROSATwire. *M. Okada*[1], *K. Tanaka*[1], *K. Ohata*[2], *J. Sato*[2], *H. Kitaguchi*[3], *H. Kumakura*[3], *K. Togano*[3], *T. Kiyoshi*[3] and *H. Wada*[3]. [1]Hitachi Research Laboratory, Hitachi, Ltd., Hitachi, Ibaraki 319-1292, Japan. [2]Advanced Research Center, Hitachi Cable, Ltd., Tsuchiura, Ibaraki 300-0026, Japan. [3]National Research Institute for Metals, Tsukuba, Ibaraki 305-0047, Japan.

4–47 Improving the Mechanical Properties of Multifilament Ag/Bi-2223 Tape. *M.H.Apperley*, *R. Zhao*, *F. Darmann*, *G.D. McCaughey* and *T.P. Beales*. Australian Superconductors Pty. Ltd., Eveleigh, NSW, 1430, Australia.

4–48 Estimation of the upper limit of the critical currents of Bi(2223)Ag tapes with various orientation of filaments. *J. Pitel*, *P. Kovac* and *I. Husek*. Institute of Electrical Engineering Slovak Academy of Sciences Dubravska 9 842 39 Bratislava Slovakia.

4–49 The effective resistance between superconducting filaments in tapes. *S. Takács*[1], *K. Funaki*[2] and *M. Iwakuma*[2]. [1]Instiute of Electrical Engineering, Slovak Academy of Sciences, 842 39 Bratislava, Slovakia. [2]Research Institute of Superconductivity, Graduate School of Information Science and Electrical Engineering, Kyushu University, 6-10-1 Hakozaki, Higashi-ku, Fukuoka 812-8581, Japan.

4–50 Mechanical Properties and Fracture of Ag-BSCCO Tapes. *N.McN. Alford*[1], *O.O. Oduleye*[2] and *S.J. Penn*[3]. [1]South Bank University, London, SE1 0AA UK. [2]Clarendon Laboratory, Oxford, OX1 3PU, UK. [3]South Bank University, London, SE1 0AA UK.

4–51 Detection of Pores and Cracks in Bi-2223/Ag Multifilamentary Tapes. *A. Kasztler*[1], *M. Polak*[2] and *H. Kirchmayr*[1]. [1] Institute for Experimental Physics, University of Technology Vienna, Austria Austria. [2]Institute of Electrical Engineering, Slovak Academy of Sciences, Bratislava, Slovak Republic.

4–52 Influence of Ge addition on phase formation and electromagnetic properties in internal tin processed Nb_3Sn wires. *D.W. Ha*[1], *S.S. Oh*[1], *H.S. Ha*[1], *N.J. Lee*[1], *K.S. Ryu*[1] and *H.K. Baek*[2]. [1]Applied Superconductivity Lab., Korea Electrotechnology Research Institute, Changwon 641-120, Korea. [2]Department of Metallurgical Engineering, Yonsei University, Seoul 120-749, Korea.

4–53 The temperature dependence of the critical currents in commercial Nb_3Sn superconductors with respect to applied field and strain. *A. Godeke*, *H.J.G. Krooshoop*, *B. ten Haken* and *H.H.J. ten Kate*. University of Twente, Faculty of Applied Physics, P.O. Box 217, 7500 AE Enschede, The Netherlands.

4–54 The effect of strain on the critical current density of Nb_3Sn wires. *D. P. Hampshire*, *N. Cheggour* and *S. A. Keys*. Superconductivity Group, Dept of Physics, Durham University, South Road, Durham DH1 3LE England.

4–55 Direct study of transport characteristics in YBCO coated-conductors. *S.B. Kim*[1], *Y. Takahashi*[1], *K. Matsumoto*[1], *T. Takagi*[2], *T. Machi*[2], *N. Koshizuka*[2], *A.I. Ishiyama*[3] and *I. Hirabayashi*[1]. [1]Superconductivity Research Laboratory ISTEC, Nagoya, 456-8587, Japan. [2]Superconductivity Research Laboratory ISTEC, Tokyo, 135-0062, Japan. [3]Department of EEC Engineering Waseda University, Tokyo, 169-8555, Japan.

4–56 Fabrication of biaxially textured substrates and buffer layer architectures for Tl-1223 thick films. *T.A. Gladstone*, *J.C. Moore*, *A.J. Wilkinson* and *C.R.M. Grovenor*. Department of Materials, University of Oxford, Oxford, UK.

4–57 Variations of superconducting properties with F content in F-dopped Tl-1223/Ag tapes. *D. Y. Jeong*[1], *H. K. Kim*[1], *H. Y. Lee*[1], *H. S. Ha*[1], *S. S. Oh*[1], *J. H. Lee*[2], *B. J. Kim*[2] and *Y. C. Kim*[2]. [1]Korea Electrotechnology Research Institute, Changwon 641-120, Korea. [2]Pusan National University, Pusan 609-735, Korea.

4–58 Comparative study of microstructures in Tl-1223/Ag tapes with different chemical compositions and J_c's. *D. Y. Jeong*[1], *H. K. Kim*[1], *H. Y. Lee*[1], *H. S. Ha*[1], *S. S. Oh*[1], *S. Horiuchi*[2], *Y. Matsui*[2], *J. H. Lee*[3], *B. J. Kim*[3] and *Y. C. Kim*[3]. [1]Korea Electrotechnology Research Institute, Changwon 641-120, Korea. [2]National Institute for Reseach in Inorganic Materials, Tsukuba, Ibaraki 305-0044, Japan. [3]Pusan National University, Pusan 609-735, Korea.

4–59 Texturation of YBCO films deposited by an electrophoretic technique. *E. Meunier*[1], *F. Weiss*[2], *C. Chabaud-Villard*[3], *J.W. Park*[4] and *F. Hardinghaus*[5]. [1]CRETA - BP 166 - 38042 Grenoble CEDEX 09 - France. [2]LMGP - Domaine Universitaire BP 46 - 38402 ST Martin d'Heres CEDEX - France. [3]CRTBT - BP 166 - 38042 Grenoble CEDEX 09 - France. [4]Solvay Barium Strontium GmBH, Hans-Bockler Allee 20, 53557-Bad Honningen, Germany. [5]Solvay Barium Strontium GmBH, Am Guterbacker Hof, 53557-Bad Honningen, Germany.

4–60 Processing of YBCO Thick Films on Ag Substrates in Low $p(O_2)$ Environments. *T.C.Shields*[1], *J.S.Abell*[1], *T.W.Button*[2], *W.Haessler*[3], *J.Eickemeyer*[3] and *L.Schultz*[3]. [1]School of Metallurgy and Materials, University of Birmingham, Birmingham, B15 2TT, UK. [2]IRC in Materials for High Performance Applications, University of Birmingham, Birmingham, B15 2TT, UK. [3]IFW Dresden Institute of Solid State and Materials Research, D-01171 Dresden, Germany.

4–61 Texture development of YBCO thick films by directional solidification on metallic substrates. *M. Najib*[1], *S. Piñol*[1], *T. Puig*[1], *J.M. Chimenos*[2], *E. Varesi*[1] and *X. Obradors*[1]. [1]Institut de Ciencia de Materials de Barcelona. Consejo Superior de Investigaciones Cientificas. Campus de la UAB. Bellaterra. Barcelona. 08193 Spain. [2]Departament d'Enginyeria Química i Metal·lúrgia, Facultat de Química, Universitat de Barcelona, Diagonal 647, E-08028, Barcelona, Spain.

4–62 Epitaxial growth of Re-123 (Re: Gd, Nd) superconducting phases on pure Ag single crystals. *M. Schindl*[1], *E. Koller*[1], *J.-Y. Genoud*[1], *E. Walker*[1], *G. Triscone*[1], *H. Suo*[1,2], *Ø. Fischer*[1] and *R. Flükiger*[1]. [1]DPMC, University of Geneva, 24 quai E.-Ansermet, 1211 Geneva 4, Switzerland. [2]Beijing Polytechnic University, 100022 Beijing, China.

4–63 Preparation of (100) and (110) textured Ag tapes for superconducting biaxially aligned coated tapes. *H. Suo*[1,2], *J.-Y. Genoud*[1], *E. Walker*[1], *G. Triscone*[1], *M. Schindl*[1], *E. Koller*[1], *Ø. Fischer*[1] and *R. Flükiger*[1]. [1]DPMC, University of Geneva, 24 quai E.-Ansermet, 1211 Geneva 4, Switzerland. [2]Beijing Polytechnic University, 100022 Beijing, China.

4–64 Pulsed laser deposition of oxide layers onto metallic substrates for coated conductor applications. *A.P. Bramley*[1], *N.A. Rutter*[1], *G. Gibson*[1], *B.A. Glowacki*[1], *E. Maher*[2], *Z.H. Barber*[1] and *J. E. Evetts*[1]. [1]Department of Materials Science and IRC in Superconductivity, University of Cambridge, Pembroke Street, Cambridge, CB2 3QZ. [2]Oxford Instruments plc, Eynsham, Witney, Oxon, OX8 1TL.

4–65 Development of a deposition system for continuous production of YBCO coated conductor. *J. Denul*[1], *G. De Winter*[2], *R. De Gryse*[1] and *H. te Lintelo*[3]. [1]Centre for Vacuum and Materials Sciences, Gent, B-9000, Belgium. [2]University of Gent, Gent, B-9000, Belgium. [3]Innovative Sputtering Technology, Zulte, B-9870, Belgium.

Session Josephson Junctions

4–66 Efficient Multi-Josephson Junction Oscillator using a Cavity. *G.Filatrella*[1], *N.F. Pedersen*[2] and *K. Wiesenfeld*[3]. [1]INFM Unit Salerno and Science Faculty, University of Sannio,. [2]Department of Electric Power Engineering Building 325, Technical University of Denmark DK-2800 Lyngby, Denmark [3]School of Physics, Georgia Institute of Technology, Atlanta.

4–67 Induced ferroelectric state and the intrinsic Josephson effect in cuprate superconductors. *S. Shafranjuk.* RIEC, Tohoku University, 2-1-1 Katahira, Aoba-ku, Sendai 983.

4–68 Quantum fluctuations of current in superconducting tunnel junctions. *G.I.Urushadze* and *Z.Z.Toklikashvili.* Tbilisi State University, Tbilisi, 380028, Georgia.

4–69 Analysis of a hot-spot response of a long Josephson junction in the flux-flow regime. *M. V. Fistul* and *A. V. Ustinov.* Erlangen-Nürnberg Universität, Erlangen, D-91058, Germany.

4–70 The possibility of sound wave amplification in Josephson junctions (JJ). *G.I.Urushadze.* Tbilisi State University, Tbilisi, 380028, Georgia.

4–71 Supercurrent enhancement by coherent tunneling in double-barrier Nb/Al-AlO_x-Al-AlO_x-Nb devices. *I. P. Nevirkovets*[1] and *J. B. Ketterson*[2]. [1]Northwestern University, Department of Physics and Astronomy, Evanston, Illinois 60208 Permanent address: Institute for Metal Physics, National Academy of Sciences of the Ukraine, 36 Vernadsky Blvd., UA-252680 Kyïv-142, Ukraine. [2]Northwestern University, Department of Physics and Astronomy, Evanston, Illinois 60208.

4–72 The influence nonharmonisity of current-phase relation on $I-V$ curve of Josephson junction. *I.N. Askerzade.* Institute of Physics, Azerbaijan Academy of Sciences, H. Cavid ave. 33, 370143, Baku, Azerbaijan.

4–73 Fabrication and Dynamical Analysis of Etching Process on $SrTiO_3$ Step Substrates for Step-edge YBCO Josephson Junctions. *QianSheng Yang, GengHua Chen, Jin Wang, Shiping Zhao* and *FengZhi Xu.*

4–74 Transition properties of $YBa_2Cu_3O_7$ step-edge junctions with various step orientations. *S.G. Lee*[1], *Y. Hwang*[2] and *J.T. Kim*[3]. [1]Korea University, Jochiwon, Chungnam, 339-800, Republic of Korea. [2]Korea University, Seoul, 136-701, Republic of Korea. [3]Korea Research Institute of Standards and Science, Taejon 305-600, Republic of Korea.

4–76 Characteristics of step-edge $YBa_2Cu_3O_y$ junctions on various step-angle substrates. *S.Y. Yang*[1], *C.H. Chen*[1], *J.T. Jeng*[1], *H.E. Horng*[1] and *H.C. Yang*[2]. [1]Department of Physics, National Taiwan Normal University, Taipei 117, Taiwan. [2]Department of Physics, National Taiwan University, Taipei 106, Taiwan.

4–77 On the Combination of $YBa_2Cu_3O_{7-\delta}$ (YBCO) and Niobium Technology: Material and Electrical Interface Characterization. *H.J.H. Smilde, D.H.A. Blank, G.J. Gerritsma* and *H. Rogalla.* University of Twente, Low Temperature Division, P.O.Box 217, 7500 AE Enschede, The Netherlands.

4–78 Anomalous resistance peaks in highly transmissive ScS contacts with microwave irradiation. *K. Hamasaki*[1], *A. Saito*[1] and *Z. Wang*[2]. [1]Department of Electrical Engineering, Nagaoka University of Technology, Nagaoka, Niigata 940-2188, Japan. [2]KARC, Communication Research Laboratory, M.P.T. 588-2, Iwaoka-chou, Nishi-ku, Kobe, 651-2401, Japan.

4–80 Effects of He^+ irradiation on electromagnetic properties of $YBa_2Cu_3O_{7-\delta}$ grain boundary Josephson junctions. *M. A. Navacerrada, M. L. Lucia* and *F. Sanchez-Quesada.* Departamento de Fisica Aplicada III, Facultad de Ciencias Fisicas, Universdidad Complutense, 28040 Madrid, Spain.

4–81 Zero-crossing Steps in Over-damped Josephson Junctions. *A.Takada*[1], *A.Chiba*[1] and *T.Noguchi*[2]. [1]Hakodate National College of Technology,Hakodate,042-8501,Japan. [2]Nobeyama Radio Observatory,Nobeyama,Nagano,384-1305,Japan.

4–82 Preparation and characterization of a-axis oriented $NdBa_2Cu_3O_{7-\delta}$ / doped $PrBa_2Cu_3O_{7-\delta}$ / $NdBa_2Cu_3O_{7-\delta}$ trilayers. *M. Sato, G.A. Alvarez, F. Wang, T. Utagawa, K. Tanabe* and *T. Morishita.* International Superconductivity Technology Center, Koto-Ku, Tokyo, 135-0062, Japan.

4–83 Electrical characteristics of all-NbCN Josephson junctions with TiN films as barriers. *H.Yamamori, S.Kohjiro, H.Sasaki* and *A.Shoji.* Electrotechnical Laboratory, 1-1-4, Umezono, Tsukuba, 305-8568, Japan.

4–84 Effects of Post Ion-milling, Pre-annealing, and Post-annealing on the Characteristics of High-T_c Ramp-edge Junctions. *G.Y. Sung*[1], *C.H. Choi*[1], *K.Y. Kang*[1], *M.C. Lee*[2] and *S.G. Lee*[3]. [1]Electronics and Telecommunications Research Institute, Taejon, 305-350, Rep. of Korea. [2]Dept. of Physics, Korea University, Seoul, 136-701, Rep. of Korea. [3]Dept. of Physics, Korea University, Jochiwon, Chungnam, 339-800, Rep. of Korea.

4–85 Dynamics of Josephson vortices in intrinsic Josephson junctions in $Bi_2Sr_2CaCu_2O_y$ single crystal mesas. *A. Irie*[1,2] and *G. Oya*[1,2,3]. [1]Department of Electrical and Electronic Engineering, Utsunomiya University 7-1-2, Yoto, Utsunomiya 321-8585, Japan. [2]Crest (Core Reserch for Evolutional Science and Technology) of Japan Science and Technology Corporation (JST). [3]Department of Energy and Environmental Science, Utsunomiya University 7-1-2, Yoto, Utsunomiya 321-8585, Japan.

4–86 On the phase difference in Josephson equations. *D.-X. Chen*[1], *J. J. Moreno*[1], *A. Hernando*[1] and *A. Sanchez*[2]. [1]Instituto Magnetismo Aplicado, RENFE-UCM, P.O.Box 155, 28230 Las Rozas, Madrid, Spain. [2]Grup d'Electromagnetisme, Departament de Fisica, UAB, 08193 Bellaterra, Barcelona, Spain.

4–87 Cross-section TEM characterization on measured microbridges of artificial grain boundary Josephson Junctions. *K. Verbist*[1], *G. Van Tendeloo*[1], *F. Tafuri*[2], *F. Miletto Granozio*[2] and *H. Bender*[3]. [1]EMAT, University of Antwerp (RUCA), Antwerp, Belgium. [2] INFM-Dipt. Scienze Fisiche, University of Napels "Fed. II", Napels, Italy. [3]IMEC, Leuven,Belgium.

4–88 Fabrication and Properties of Sr_2AlTaO_6/YBCO Interface-treated Junctions. *G.Y. Sung*, *C.H. Choi*, *S.K. Han*, *J.D. Suh* and *K.Y. Kang*. Electronics and Telecommunications Research Institute, Taejon, 305-350, Rep. of Korea.

4–89 Characteristics of ramp-type $YBa_2Cu_3O_{7-\delta}$ / $SrRuO_3$ / $YBa_2Cu_3O_{7-\delta}$ junctions prepared with interfaces grown in situ. *L. M. Wang*[1], *H. H. Sung*[1] and *J. H. Chen*[2]. [1]Department of Electronic Engineering, Da-Yeh University, Changhua 515, Taiwan, R. O. C. [2]Department of Physics, National Taiwan University, Taipei 106, Taiwan, R. O. C.

4–90 Fiske Resonance in YBCO/PBCO/YBCO Ramp-type Josephson Junctions. *H. H. Sung*[1], *L. M. Wang*[1] and *C. H. Chen*[2]. [1]Department of Electrical Engineering, Da-Yeh University, Changhua, 51542, Taiwan. [2]Department of Physics, National Taiwan University, Taipei, 10660, Taiwan.

4–91 Superconducting structures on tilted $NdGaO_3$ substrates. *P.V. Komissinski*[1,2], *G.A. Ovsyannikov*[2], *Z.G. Ivanov*[1], *I.M. Kotelyanskii*[2] and *T. Claeson*[1]. [1]Chalmers University of Technology and Gothenburg University, Gothenburg, S412-96, Sweden. [2]Institute of Radio Engineering and Electronics RAS, Moscow,103907, Russia.

Session Passive Devices

4–93 TBCCO based HTS Channel Combiners for Digital Cellular Communications. *A.P. Jenkins*[1], *D.M.C. Hyland*[2], *D. Dew-Hughes*[1], *D.J. Edwards*[1] and *C.R.M. Grovenor*[2]. [1]Department of Engineering Science, University of Oxford. [2]Department of Materials, University of Oxford.

4–94 Thermal breakdown of HTS devices based on S/N transition. *E. Loskot*, *M. Sitnikova* and *V. Kondratiev*. St.-Petersburg Electrotechnical University, St.-Petersburg, 197376, Russia.

4–95 HTS switchable diplexer. *V. Kondratiev*, *A. Svishchev* and *I. Vendik*. St.-Petersburg Electrotechnical University, St.-Petersburg, 197376, Russia.

4–96 Optical Modulator with Superconducting Resonant Electrodes for Subcarrier Optical Transmission. *K. Yoshida*[1], *H. Morita*[1], *H. Kanaya*[1], *Y. Kanda*[2], *T. Uchida*[3], *H. Shimakage*[3] and *Z. Wang*[3]. [1] Graduate School of Information Science and Electrical Engineering, Kyushu University, Fukuoka 812-8581, Japan. [2] Fuculty of Engineering, Fukuoka Institute of Technology, Fukuoka 811-0295, Japan. [3] KARC Communications Research Laboratory, Kobe 651-2401, Japan.

4–97 $YBa_2Cu_3O_{7-\delta}$ thin films grown by RF sputtering on buffered $LiNbO_3$ substrates. *L. Fàbrega*[1], *R. Rubí*[1], *F. Sandiumenge*[1], *J. Fontcuberta*[1], *C. Collado*[2] and *J.M. O'Callaghan*[2]. [1]Institut de Ciència de Materials de Barcelona (C.S.I.C.), Campus de la U.A.B., 08193 Bellaterra (SPAIN). [2]Dpt. Teoria del Senyal i Comunicacions, Campus Nord UPC, Jordi Girona 1-3, 08034 Barcelona (SPAIN).

4–98 Tl-2212-Films for Microwave Devices. *H.Schneidewind*[1], *M.Zeisberger*[1], *H.Bruchlos*[1], *M.Manzel*[1] and *T.Kaiser*[2]. [1]Institut für Physikalische Hochtechnologie, Jena, Thuringia, D-07743, Germany. [2]Bergische Universität Gesamthochschule Wuppertal, Wuppertal, Nordrhein-Westfalen, D-42097, Germany.

4–99 High temperature superconducting microwave filtrs for space applications. *J.P.Shivhare, D.Balasubrnayam, O.P.Kaushik, A.D.Dadve* and *Dr.H.O.Gautam.* Space Applications Centre ,India Space Research Organisation,Govt of India.

4–100 Spectral-domain Modelling of Superconducting Microstrip Structures. *Z. D. Genchev*[1], *A. P. Jenkins*[2] and *D. Dew-Hughes*[2]. [1]Institute of Electronics, Bulg. Ac. Sci.,1784 Sofia,Bulgaria. [2]Department of Engineering Science, Parks Road, Oxford OX1 3PJ, UK.

4–101 Large-area and Double-sided PLD YBCO:Ag Thin Films for Microwave Applications. *M.A. Lorenz*[1], *H. Hochmuth*[1], *D. Natusch*[1], *K. Kreher*[1], *T. Kaiser*[2], *M. A. Hein*[2], *R. Schwab*[3] and *R. Heidinger*[3]. [1]Universität Leipzig, Fakultät für Physik und Geowissenschaften, D-04103 Leipzig, Germany. [2]Bergische Universität Wuppertal, Fachbereich Physik, D-42097 Wuppertal, Germany. [3]Forschungszentrum Karlsruhe, Institut für Materialforschung I, D-76021 Karlsruhe, Germany.

4–102 Voltage Tunable $YBa_2Cu_3O_7$ -$BaTiO_3$ - Microwave Ring Resonator Processing and Characterization. *A.I. Lacambra, J.C. Blanco, G. Dimarco, D.D. Dixon, F.A. Leon, M. Rossman, Yu.A. Vlasov* and *G.L. Larkins,Jr.*. Florida International University (CEAS 3850) 10555 W. Flagler Street Miami, Florida 33174, USA.

4–103 Characteristics of Electrically Tunable Phase Shifter Using YBCO/Ferroelectric Thin Films. *S. K. Han, S. J. Lee, S. D. Jung* and *K. Y. Kang.* Telecomm. Basic Research Lab., ETRI, Taejon 305-350, South Korea.

4–104 Modeling and Fabrication of a Microelectromechanical Switch for H-Tc Superconductive Applications. *I.O. Hilerio*[1], *J.R. Reid*[2], *J.S. Derov*[2], *T.M. Babij*[1] and *G. Larkins*[1]. [1]Florida International Univeristy, Miami, FL, 33199, USA. [2]Air Force Research Laboratory / SNHA, Hanscom AFB, MA, 01731, USA.

4–105 Fabrication of YBCO films and its application to microwave devices. *S. Ohshima, M. Mukaida, M. Kusunoki, T. Tomiyama, Y. Takano, K. Chiba* and *T. Kinpara.* Yamagata University, Yonezawa, Yamagata, 992-8510, Japan.

4–107 Planar electrooptical phase modulators: An intermediate step towards superconducting Mach-Zehnder integrated modulators. *E. Rozan, C. Collado, J. Prat* and *J.M. O'Callaghan.* Campus Nord UPC, D3 Barcelona 08034 Spain.

4–108 Experimental determination of nonlinear parameters in HTSC transmission line using a multiport harmonic balance algorithm. *J. Mateu*[1], *C. Collado*[1], *L.M. Rodriguez*[2] and *J.M. O'Callaghan*[1]. [1]Universitat Politecnica de Catalunya (UPC) Campus Nord UPC-D3 Barcelona 08034, Spain. [2]Centro de Investigacion Cientifica y de Educacion Superior de Ensenada (CICESE) Km 107 Carretera Tijuana-Ensenada Ensenada, B.C. Mexico 22860.

4–109 Computer simulation of the non-linear response of superconducting devices using the Multiport Harmonic Balance algorithm. *C. Collado, J. Mateu* and *J.M. O'Callaghan.* Universitat Politecnica de Catalunya (UPC) Campus Nord UPC-D3 Barcelona 08034 Spain.

4–110 Modelling the Nonlinear Microwave Surface Impedance of a Superconducting Weak Link. *A. V. Velichko*[1,2] and *A. Porch*[1]. [1]School of Electronic and Electrical Engineering, University of Birmingham, Birmingham B15 2TT, UK. [2]Institute of Radiophysics and Electronics, NAS of Ukraine, Kharkov 310085, Ukraine.

4–111 Weakly Coupled Grain Model for High Tc Superconducting Thin Films Taking Account of Anisotropic Complex Conductivities. *K. Yoshida*[1], *H. Takeyoshi*[1], *H. Morita*[1], *H. Kanaya*[1], *T. Uchida*[2], *H. Shimakage*[2] and *Z. Wang*[2]. [1] Graduate School of Information Science and Electrical Engineering, Kyushu University, Fukuoka 812-8581, Japan. [2]KARK Communications Research Laboratory, Kobe, 651-2401, Japan.

ORAL SESSION 5A: Coated Conductors I

Tuesday Afternoon, September 14th, 17:30-19:00

17:30 ***5A–1 Low-cost YBCO coated conductor technology.** *A.P. Malozemoff*[1], *S. Annavarapu*[1], *L. Fritzemeier*[1], *Q. Li*[1], *V. Prunier*[1], *M. Rupich*[1], *C. Thieme*[1], *W. Zhang*[1], *A. Goyal*[2], *M. Paranthaman*[2] and *D.F. Lee*[1] [1]American Superconductor Corporation 2 Technology Dr., Westborough MA 01581 USA. [2]Oak Ridge National Laboratory, Oak Ridge TN 37831 USA.

18:00 **5A–2 In-plane Aligned YBCO Thick Films on Ag and $LaAlO_3$ Substrates by Ultrasonic Mist Pyrolysis.** *J.J. Wells*[1], *A.L. Crossley*[1], *M.J. Vallet-Regi*[2] and *J.L. MacManus-Driscoll*[1]. [1]Department of Materials, Imperial College of Science Technology and Medicine, Prince Consort Road, London SW7 2BP, England. [2]Dep. De Quimica Inorganica, Facultad de Farmacia, Universidad Complutense, 28040 Madrid, Spain.

18:15 **5A–3 Sol-gel technique applied to buffer deposition on textured flexible substrates for YBCO coated conductor.** *S.Lesca*[1], *P.Caracino*[2], *P.Scardi*[3] and *R.Scotti*[4]. [1]INFM, UdR di Milano, Università Statale - Dipartimento di Scienza dei Materiali, Via Cozzi, 53, 20126 Milan, Italy. [2]PIRELLI CAVI & SISTEMI SpA, viale Sarca 222, 20126, Milan, Italy. [3]Università di Trento, Dipartimento di Ingegneria dei Materiali, 38050 Mesiano TN Italy. [4]Universita' Statale di Milano -Dipartimento di Scienza dei Material, Via Cozzi, 53, 20126 Milan, Italy.

18:30 **5A–4 Superconducting Thick Films of $YBa_2Cu_3O_{7-\delta}$ with Y_2O_3 Additions on Ag Substrates.** *W. Hässler*[1], *P. Schätzle*[1], *L. Schultz*[1], *T.C. Shields*[2], *T.W. Button*[2] and *J.S. Abell*[2]. [1]Institut of Solid State and Materials Research Dresden, PF 270016, D-01171 Dresden, Germany. [2]School of Metallurgy and Materials, The University of Birmingham, Edgbaston Birmingham, B152TT, UK.

18:45 **5A–5 Development of Cube Textured Nickel-Alloys as Substrate for Superconducting Tapes.** *N. Reger*, *B. de Boer*, *B. Holzapfel*, *J. Eickemeyer*, *R. Opitz* and *L. Schultz*. Institute of Solid State and Materials Research Dresden, Institute of Metallic Materials PO-Box 270016, D-01171 Dresden, Germany.

ORAL SESSION 5B: Flux Pinning I

Tuesday Afternoon, September 14th, 17:30-19:00

17:30 ***5B–1 New Method to Induce Periodic Pinning in 3D Vortex Structures: High and Low Temperature Superconductors** *F. de la Cruz*. Centro atómico de Bariloche, 8400 S.C. de Bariloche, Rio Negro, Argentina

18:00 **5B–2 Flux pinning in thick $YBa_2Cu_3O_7$ films by the BaF_2 process.** *L.-J. Wu*, *V. F. Solovyov*, *H. J. Wiesmann* and *M. Suenaga*. Brookhaven National Laboratory, Upton, New York, 11793 USA.

18:15 **5B–3 Irreversibility line in $HgBa_2CuO_{4+\delta}$ single crystal.** *D. Stamopoulos*[1], *M. Pissas*[1], *D. Niarchos*[1] and *M. Charalambous*[2]. [1]Institute of Materials Science National Center for Scientific Research "Demokritos" 153-10, Aghia Paraskevi, Athens GREECE. [2]Centre de Recherches sur les Tres Basses Temperatures, CNRS, BP166X,38042 Grenoble FRANCE.

18:30 **5B–4 Geometry, vortex pinning, and surface-barrier effects in platelet and "prism" shaped BSCCO single crystals.** *T.B. Doyle*[1], *R. Labusch*[2] and *R.A. Doyle*[3]. [1]School of Pure and Applied Physics, University of Natal, Durban, 4001, South Africa. [2]Institut fuer Angewandte Physik, Technischen Universitat Clausthal, Clausthal-Zellerfeld 3992, Germany. [3]c/0 Interdisciplinary Research Centre in Superconductivity, University of Cambridge, Cambridge CB3 OHE, UK.

18:45 **5B–5 Interlayer metallization and plastic deformation: two ways to improve flux pinning in Hg-based superconductors?.** *L. Fàbrega*[1], *A. Sin*[1], *A. Calleja*[1], *S. Piñol*[1], *J. Fontcuberta*[1], *D. Eyidi*[2] and *J. Rabier*[2]. [1]Institut de Ciència de Materials de Barcelona (C.S.I.C.), Campus de la U.A.B., 08193 Bellaterra (SPAIN). [2]Laboratoire de Métallurgie Physique, UMR 6630 CNRS, Université de Poitiers, SP2MI, BP 179, 86960 Futuroscope Cedex (FRANCE).

ORAL SESSION 5C: SQUIDS and SQUIDS Applications

Tuesday Afternoon, September 14th, 17:30-19:00

17:30 ***5C–1 High-T_c SQUIDs: Gradiometers and Microscopes.** *J. Clarke*. Department of Physics, University of California, Berkeley, CA 94720-7300 and Materials Sciences Division, Lawrence Berkeley National Laboratory, Berkeley, CA 94720.

18:00 **5C–2 HTS SQUID current comparator for ion beam measurements.** *L. Hao*[1], *J.C. Gallop*[1], *J.C. Macfarlane*[2] and *C. Carr*[2]. [1]Centre for Basic and Thermal Metrology, National Physical Laboratory, Teddington, TW11 0LW, UK. [2]Dept. of Physics and Applied Physics, Strathclyde University, Glasgow G4 0NG, UK.

18:15 **5C–3 An HTS SQUID Magnetometer Using Coplanar Resonator with Vector Reference for Operation in Unshielded Environment.** *Y. Zhang*[1], *G. Panaitov*[1], *N. Wolters*[1], *L.H. Zhang*[2], *R. Otto*[1], *J. Schubert*[1], *W. Zander*[1], *M. Bick*[1], *H.-J. Krause*[1] and *H. Bousack*[1]. [1]Institut für Schicht- und Ionentechnik (ISI), Forschungszentrum Juelich (FZJ), D 52425 Juelich, Germany. [2]Institute of Physics Chinese Academy of Sciences, Beijing 100080, China.

18:30 **5C–4 A Second Order Electronic Gradiometer for Nondestructive Evaluation.** *C. Carr*, *E.J. Romans*, *A.J. Millar*, *A. Eulenburg*, *C.M. Pegrum* and *G.B. Donaldson*. Physics and Applied Physics, University of Strathclyde 107 Rottenrow Glasgow G4 0NG United Kingdom.

18:45 **5C–5 HTS RF SQUID Gradiometer With Long Baseline For the Inspection of Aircraft Wheels.** *M. Maus*, *H.-J. Krause*, *Y. Zhang*, *H. Bousack*, *M. Vaupel*, *R. Kutzner* and *R. Wördenweber*. Institute of Thin Film and Ion Technology, Research Centre Juelich, 52425 Juelich, Germany.

ORAL SESSION 5D: Mixers and Detectors

Tuesday Afternoon, September 14th, 17:30-19:00

17:30 ***5D–1 The role of the geometry in superconducting tunnel junctions detectors.** *R. Cristiano*. Istituto di Cibernetica del CNR Arco Felice, Napoli, I-80072 Italy.

18:00 **5D–2 Superconducting YBCO nanobridges for submillimeter-wave detectors.** *A. Gaugue*[1], *C. Ulysse*[1], *A. Sentz*[2], *C. Gunther*[3], *D. Robbes*[3], *J. Gierak*[4], *C. Vieu*[4], *G. Beaudin*[5], *M. Fourrier*[2] and *A. Kreisler*[1]. [1]LGEP - UMR8507 CNRS, Universités Paris 6 & Paris 11; Supélec plateau de moulon; GIF sur YVETTE 91192 France. [2]LDIM, EA 253 MENRT, Tour 12, Université Paris 6; 4 place de jussieu; PARIS 75252 France. [3]GREYC, URA 1526 CNRS, ISMRa et Université de Caen; 6 Bd du Marechal Juin; CAEN 14050 France. [4]L2M, UPR 20 CNRS; 196 Av. Henri Ravera; BAGNEUX 92225 France. [5]DEMIRM Observatoire de Paris; 61 Av de l'Observatoire; Paris 75014 Paris.

18:15 **5D–3 Methods of submillimeter wave Josephson spectroscopy.** *M. Tarasov*[1,3], *E. Stepantsov*[1,2], *A. Shul'man*[3], *E. Kosarev*[4], *O. Polyansky*[3], *D. Golubev*[1,5], *M. Darula*[6], *O. Harnack*[6], *A. Vystavkin*[3] and *Z.G. Ivanov*[1]. [1]Chalmers University of Technology and University of Gothenburg, S-41296, Sweden. [2]Institute of Crystallography of the RAS, Moscow, RU-117333, Russia. [3]Institute of Radio Engineering and Electronics of the RAS, Moscow, RU-103907, Russia. [4]P.L.Kapitza Institute for Physical Problems of the RAS, Mo cow, RU-117973, Russi. [5]P.N.Lebedev Physical Institute of the RAS, Moscow, RU-117810, Russia. [6]Institut fur Schicht und Ionentechnik, Research Center Juelich GmbH, Juelich, D-52425Germany.

18:30 **5D–4 Single photon imaging spectrometers using superconducting tunnel junctions.** *L. Frunzio*, *K. Segall*, *C. Wilson*, *L. Li*, *M. C. Gaidis* and *D. E. Prober*. Department of Applied Physics, Yale University, New Haven, CT 06520-8284, USA.

18:45 **5D–5 Cryogenic microcalorimeters for high resolution energy dispersive x-ray spectroscopy.** *J. Höhne*[1], *M. Altmann*[2], *G. Angloher*[2], *M. Bühler*[1], *F. v. Feilitzsch*[2], *P. Hettl*[2], *T. Hertrich*[1], *J. Jochum*[2], *S. Pfnür*[2] and *J. Schnagl*[2]. [1]CSP Cryogenic Spectrometers GmbH, Bahnhofstr. 18a, D-85737 Ismaning, Germany. [2]Technische Universität München, Physik Department E15, D-85747 Garching, Germany.

POSTER SESSION 6

Tuesday Evening, September 14th, 19:00-21:00

Session Bulk materials and materials aspects

6–1 Inhomogeneous Magnetic Properties of Melt-Textured YBCO. *T. Habisreuther*, *D. Litzkendorf*, *M. Zeisberger* and *W. Gawalek*. IPHT, Jena, 07702, Germany.

6–2 Multi seeded YBCO - bars for cryogenic applications. *G. Krabbes*, *P. Schaetzle*, *G. Stoever*, *N. Mattern*, *D. Stephan*, *D. Schlaefer* and *G. Fuchs*. Institute of Solid Sate and Material Research Dresden, P.O. Box 270016, D-01171 Dresden,.

6–3 The effect of the addition of gold on secondary phase formation in RE-Ba-Cu-O (RE = Nd, Y, La). *P.J. Smith*, *N. Hari Babu*, *D.A. Cardwell* and *Y.H. Shi*. I.R.C. in Superconductivity, University of Cambridge, Madingley Road, Cambridge, CB3 0HE, England.

6–4 Fabrication of 100mm-diameter Y-Ba-Cu-O bulk QMG Superconductors with Larger Levitation Forces. *T. Fujimoto*, *M. Morita*, *N. Masahashi* and *T. Kaneko*. Advanced Technology Research Laboratories, Nippon Steel Corporation.

6–5 Magnetooptic Imaging System for Studies of Magnetic Flux and Current Flow in Superconductors. *A. Polyanskii*[1], *L. Dorosinskii*[2] and *H. Bocuk*[2]. [1]Applied Superconductivity Center, University of Wisconsin-Madison, WI 53706, USA. [2]National Metrology Institute,P.K.21, 41470 Gebze-Kocaeli, Turkey.

6–6 Top seeding growth and microstructure of large grain Nd123/422 superconductors. *M.Gombos*[1], *A.E.Carrillo*[1], *V.Gomis*[1], *X.Obradors*[1], *S.Pace*[2] and *A.Vecchione*[2]. [1]Institut de Ciència de Materials de Barcelona (CSIC). Campus UAB, 08193 Bellaterra (SPAIN). [2]Istituto Nazionale di Fisica della Materia, unità di Salerno e Dipartamento di Fisica, Università di Salerno, Via S.Allende, Baronissi (Salerno), Italia.

6–7 Magnetic field dependences of rf absorption in HTS ceramics as a way to grains quality evaluation. *G.V. Golubnichaya*, *A.Ya. Kirichenko*, *I.G. Maximchuk* and *N.T. Cherpak*. Usikov Institute of Radiophysics and Electronics of National Academy of Sciences, Kharkov, 310085, Ukraine.

6–8 Persistent current in melt-processed YBCO-rings. *N.A. Nijelskiy*[1], *O.L. Poluschenko*[1], *A.V. Kalinov*[2], *I.F. Voloshin*[2] and *S.V. Shavkin*[3]. [1]Moscow N.E.Bauman State Technical University, 5 2nd Baumanskaya str, Moscow 107005, Russia. [2]All-Russian Electrical Engineering Institute, 12 Krasnokazarmennaya str, 111250 Moscow, Russia. [3]RRC "Kurchatov institute", Kurchatov sq, 123182 Moscow, Russia.

6–9 Preparation of Melt-Textured YBCO with optimized shape for Cryomagnetic Applications. *D. Litzkendorf*, *T. Habisreuther*, *M. Zeisberger* and *W. Gawalek*. Institut fuer Physikalische Hochtechnologie e. V., Helmholtzweg 4, PF 100239, D-07702 Jena, Germany.

6–10 An Approach to Homogeneity in YBCO Melt Texturing. *F.N. Werfel*[1], *U. Flögel - Delor*[1], *L. Woodell*[2], *S. Remke*[2] and *M. Gerards*[2]. [1]Adelwitz Technologiezentrum GmbH, D-04886 Adelwitz, Germany. [2]MERCK KGaA,Darmstadt, Germany.

6–11 Processing of superconducting Y-123 cylindrical bars. *A. Calleja*[1], *M. Segarra*[1], *I. García*[2], *J.M. Chimenos*[1], *M.A. Fernández*[2], *F. Espiell*[2], *E. Mendoza*[3], *T. Puig*[3], *S. Piñol*[3] and *X. Obradors*[3]. [1]DIOPMA, Llacuna 162-166, Barcelona, E-08018, Spain. [2]Departament d'Enginyeria Química i Metal.lúrgia, Facultat de Quimica, Martí i Franques 1, E-08028, Barcelona, Spain. [3]Institut de Ciència de Materials de Barcelona-C.S.I.C., Campus de la UAB, Bellaterra, Barcelona, E-08193, Spain.

6–12 Homogeneity of Top-Seeded Single-Grained (RE)BCO Superconductors. *I.-G. Chen*[1], *S.-H. Hsu*[1], *S.-Y. Chen*[1] and *M.K. Wu*[2]. [1]Dept. of Materials Sci. & Eng., National Cheng Kung Univ., #1 Ta-Hsueh Rd., 70101, Tainan, Taiwan, R.O.C. [2]Materials Science Center, National Tsing Hua Univ., Hsinchu, 30043, TAIWAN, R.O.C.

6–13 Improvement of the mechanical properties of bulk-superconductors by impregnation of epoxy resins. *M. Tomita* and *M. Murakami*. Superconductivity Research Laboratory,1-16-25 Shibaura, Minato-ku, Tokyo 105-0023, Japan.

6–14 Fabrication of Large Single-Domained Y-Ba-Cu-O Superconductor by Multiseeding in Top-Seeded Melt Growth. *Y.A. Jee*, *G.W. Hong* and *C.J. Kim*. Functional Materials Lab, Korea Atomic Energy Research Institute, PO Box 105, Yusong, Taejon 305-600, South Korea.

6–15 Different limitations of trapped fields in melt-textured YBCO. *G.Fuchs*[1], *C.Wenger*[2], *A.Gladun*[2], *S.Gruss*[1], *P.Schaetzle*[1], *G.Krabbes*[1], *J.Fink*[1], *K.-H.Müller*[1] and *L.Schultz*[1]. [1]Institute of Solid State and Materials Research Dresden, D-01171 Dresden, Germany. [2]Technical University Dresden, D-01062 Dresden, Germany.

6–16 Trapped fields up to 9 T in bulk $YBa_2Cu_3O_{7-\delta}$ material. *S. Gruss, G. Fuchs, P. Schaetzle, G. Krabbes, J. Fink, K.-H. Müller* and *L. Schultz.* Institute of Solid State and Materials Research Dresden, P.O. Box 27 00 16, 01171 Dresden, Germany.

6–17 YBaCuO monoliths of complex shapes processed by welding and optimized by infiltration. *H. Walter*[1], *M.P. Delamare*[2], *B. Bringmann*[2], *A. Leenders*[1,2] and *H.C. Freyhardt*[1,2]. [1]Zentrum für Funktionwerkstoffe Göttingen gGmbH, Windausweg 2, 37073 Göttingen, Germany Zentrum für Funktionwerkstoffe Göttingen gGmbH, Windausweg 2, 37073 Göttingen, Germany. [2]Institut für Materialphysik, Universität Göttingen, Hospitalstrasse 3-7, 37073 Göttingen, Germany.

6–18 $BaZrO_3$ and $YBa_2ZrO_{5.5}$ additions in melt textured $YBa_2Cu_3O_{7-\delta}$: influence on the microstructure and physical properties. *A. E. Carrillo, T. Puig, V. Gomis, S. Piñol, J. Plain, F. Sandiumenge* and *X. Obradors.* Institut de Ciència de Materials de Barcelona, Campus UAB, 08193 Bellaterra, Barcelona, Spain.

6–19 Top seeding growth and superconducting properties of bulk YBCO - Ag composites. *E. Mendoza*[1], *M. Carrera*[2], *E. Varesi*[1], *A.E. Carrillo*[1], *T. Puig*[1], *J. Amorós*[3], *X. Granados*[1] and *X. Obradors*[1]. [1] Institut de Ciencia de Materials de Barcelona Consejo Superior de Investigaciones Cientificas Campus de la UAB Bellaterra 08193 Barcelona Spain. [2]DMACS. Universitat de Lleida Jaume II, 69 Lleida 25001 Spain. [3]Departament de Matematica Aplicada Universitat Politecnica de Catalunya Diagonal 647 08028 Barcelona Spain.

Session Wires tapes and coated conductors

6–20 Magnetic field of bent BSCCO tapes carrying magnetisation currents. *J. Kvitkovic* and *M. Polak.* Institute of Electrical Engineering, Slovak Academy of Sciences, Bratislava, 842 39, Slovak Republic.

6–21 Some aspects of Bi(2223)/Ag tapes with resistive barriers. *P. Kovac*[1], *I. Husek*[1], *F. Gömöry*[1], *L. Cesnak*[1], *T. Melisek*[1] and *W. Pachla*[6]. [1]Institute of Electrical Engineering of Slovak Academy of Science, Bratislava, 842 39, Slovakia. [2] High Pressure Research Center of Polish Academy of Science, Warszawa, 01 142, Poland.

6–22 Quality measurement of Bi(2223)/Ag tapes by Hall probe array. *P. Kovac, V. Cambel* and *J. Pitel.* Institute of Electrical Engineering of Slovak Academy of Sciences, Bratislava, 842 39, Slovakia.

6–23 Transport current and texture of Bi-2223 grains in multicore Ag sheathed tapes. *P. Kovac*[1], *T. Melisek*[1], *A. Kasztler*[2], *W. Pachla*[3], *J. Pitel*[1], *R. Diduszko*[4] and *H. Kirchmayr*[5]. [1]Institute of Electrical Engineering of Slovak Academy of Sciences, Bratislava, 842 39, Slovakia. [2]Institute of Experimental Physics of Technical University, Wien, A-1030, Austria. [3]High Pressure Research Center of Polish Academy of Sciences, Warszawa, 01 142, Poland. [4]Institute of Vacuum Technology, Warszawa, 00 241, Poland. [5]Institute of Experimental Physics of Technical University, Wien, A-1030, Austria.

6–24 Stoichiometric variations in Bi-2212 thick film conductors: electrical and microstructural characterisation. *B.R. Balmer*[1], *G.W. Grime*[1], *C.J. Salter*[1], *R. Riddle*[2] and *C.R.M. Grovenor*[1]. [1]Dept. of Materials Science, University of Oxford, Oxford OX1 3PH, U.K. [2]Merck Research and Development UK, University of Southampton, Highfield SO17 1BJ.

6–25 Vortex pinning and anisotropy in Ag/Bi(Pb)SrCaCuO-2223 tapes by means of surface columnar defects. *R.Gerbaldo*[1], *G.Ghigo*[1], *L.Gozzelino*[1], *E.Mezzetti*[1], *B.Minetti*[1], *L.Martini*[2] and *G.Cuttone*[3]. [1]I.N.F.M. UdR Torino Politecnico; I.N.F.N. Sez. di Torino; Dipartimento di Fisica, Politecnico di Torino, Torino, Italy. [2]ENEL-SRI, Segrate (Milano), Italy. [3]I.N.F.N. Laboratorio Nazionale del Sud, Catania.

6–26 Filament by filament mapping of BISCCO2212-2223 conversion in multifilamentary tapes. *J. Tundidor, R. Dudley, E. Young, Y. Yang* and *C. Beduz.* Institute of Cryogenics, University of Southampton, Southampton SO17 1BJ, UK.

6–27 Normal-zone Propagation Properties in BSCCO Silver Sheathed Tapes. *S. Shimizu*[1], *A.I. Ishiyama*[1] and *S.B. Kim*[2]. [1]Dept. of EECE, Waseda Univ., Shinjuku-ku, Tokyo 169-8555, Japan. [2]SRL, ISTEC, Atsuta-ku, Nagoya 456-8287, Japan.

6–28 A Systematic Comparison of the Phase Development in Powders from the PBSCCO 2223 System, considered in PIT Processing, prepared by Solid State Processing, Co-Precipitation, Citrate Gel and Spray Pyrolysis. *Y.W. Hsueh*[1], *R.S. Liu*[1], *L. Woodall*[2] and *M. Gerards*[2]. [1]Department of Chemistry, National Taiwan University, Taipei, Taiwan, R.O.C. [2]Merck KGaA Darmstadt, D-64271 Darmstadt, Germany.

6–29 Quantitative Phase Analysis of PBSCCO 2223 Phase Mixtures used in PIT Processing. *S. Raeth*[1], *W.W. Schmahl*[1], *L. Woodall*[2] and *M. Gerards*[2]. [1]Institut für Mineralogie, Ruhr Universität, D-44780 Bochum, germany. [2]Merck KGaA Darmstadt, D-64271 Darmstadt, Germany.

6–30 Prospects of Utilization of HTSC Having High Critical Currents due to Nuclear Fission Fragment Tracks. *I.N.Goncharov*. Joint Institute for Nuclear Research, Dubna, 141980, Russia.

6–31 Influence of the precursor powder properties on phase formation and critical current density of (Bi,Pb)-2223-tapes. *F. Schwaigerer*, *B. Sailer*, *A. Trautner*, *W. Wischert*, *H. J. Meyer* and *S. Kemmler-Sack*. Universität Tübingen, Institut für Anorganische Chemie, Auf der Morgenstelle 18, D-72076 Tübingen, Deutschland.

6–32 Lattice constant differentiation and texture distribution within the monocore (Bi,Pb)-2223/Ag tapes. *W. Pachla*[1], *R. Diduszko*[2], *P. Kovac*[3] and *I. Husek*[3]. [1]High Pressure Research Center, Polish Academy of Sciences, ul. Sokolowska 29, 01-142 Warszawa, Poland. [2]Institute of Vacuum Technology, ul. D[3]uga 44/50, 00-241 Warszawa, Poland. [3]nstitute of Electrical Engineering, Slovak Academy of Sciences, Dubravska cesta 9, 842-39 Bratislava, Slovak Republ.

6–33 An XRD Rietveld Analysis of the Phase Assemblage in PBSSCO PIT Precursor Powders. *W.W. Schmahl*[1], *S. Raeth*[1], *B. Seipel*[1], *L. Woodall*[2], *M. Bartels*[2] and *M. Gerards*[2]. [1]Ruhr Universität - Bochum and Tübingen Universität, Germany. [2]Merck KGaA Darmstadt, D-64271 Darmstadt, Germany.

6–34 Preparation of Bi(2223) tape conductors with resistive matrix components and new composite structures. *W.Goldacker*, *R.Nast*, *H.Eckelmann* and *J.Krelaus*. Forschungszentrum Karlsruhe-Institut für Technische Physik, Eggenstein-Leopoldshafen, Baden-Württemberg, 76344, Germany.

6–35 Thermal Quenches in Monolayer Bi-2223 Coil. *F. Chovanec*[1], *P. Usak*[1], *L. Jansak*[1], *A. Kasztler*[2], *H. Kirchmayr*[2] and *M. Polak*[1]. [1]Institute of Electrical Engineering, Slovak Academy of Sciences,Bratislava,Sk 84239, Slovakia. [2]Institut fur Experimentalphysik, Technische Universitat Wien, Austria.

6–36 Bi,Pb(2212) grain growth and relationship between the initial and final texture in Ag-sheathed Bi,Pb(2223) tapes. *J.-C. Grivel*[1,2], *Y.L. Liu*[1], *H.P. Poulsen*[1], *L.G. Andersen*[1], *T. Frello*[1], *N.H. Andersen*[1] and *W.G. Wang*[2]. [1]Risø National Laboratory, DK-4000 Roskilde, Denmark. [2]Nordic Superconductor Technologies, Priorparken 685, DK-2605 Bröndby, Denmark.

6–37 YBCO Coated Tapes Fabricated by Magnetron Deposition. *K.H. Müller*, *N. Savvides*, *S. Gnanarajan*, *A. Katsaros*, *A. Thorley*, *J. Herrmann* and *R. Clissold*. CSIRO Telecom. and Industrial Physics, Lindfield, NSW 2070, Australia.

6–38 Characterisation of substrates and buffer layers for next-generation HTS coated conductor tapes. *C. Prouteau*[1], *J. S. Abell*[1], *T. W. Button*[1], *E. Maher*[2], *K. Marken*[3] and *B.A. Glowacki*[4]. [1]School of Metallurgy, University of Birmingham, Edgbaston, Birmingham B15 2TT. [2]Oxford Instruments plc, Old Station Way, Eynsham, Witney, Oxford, OX8 1TL. [3]Oxford Superconducting Technology, 600 Milik Street, PO Box 429, Carteret, New Jersey, 07008 0429, USA. [4]Dept. of Materials Science and Metallur y, University of Cambridge, Pembroke Street, Cambridge CB3 OH.

6–39 YBCO - deposition on metal tape substrates. *J. Egly*[1], *R. Nemetschek*[1], *W. Prusseit*[1], *B. Holzapfel*[2] and *W. Goldacker*[3]. [1]THEVA Thin Film Technology GmbH, 85386 Eching, Germany. [2]IFW Dresden, 00171 Dresden, Germany. [3]FZ Karlsruhe, 76021 Karlsruhe, Germany.

6–40 LPE Growth of REBCO Thick Films. *X. Qi*, *J.J. Wells* and *J.L. MacManus-Driscoll*. Dept of Materials, Imperial College, London SW7 2BP.

6–41 Study of the recrystallisation of nickel and Ni-based alloy substrates for YBCO coated conductors. *B. Lehndorff*[1], *M. Hortig*[1], *B. Mönter*[1], *H. Piel*[1], *J. Pouryamout*[1], *N. Pupeter*[1] and *E. Bischoff*[2]. [1]Cryoelectra GmbH, Wettinerstr. 6h, D-42287 Wuppertal, Germany. [2]MPI für Metallforschung, Seestr. 92, D-70174 Stuttgart, Germany.

6–42 Biaxially textured Ni and CuNi alloy substrate tapes for HTS coated conductor applications. *A.Tuissi*[1], *R.Corti*[1], *A.P.Bramley*[2], *M.E.Vickers*[2] and *J.E.Evetts*[2]. [1]Istituto per la Tecnologia dei Materiali e dei Processi Energetici del Consiglio Nazionale delle Ricerche - CNR TEMPE, C.so P.Sposi 29, 23900 Lecco, Italy. [2]University of Cambridge, Department of Materials Science and Metallurgy, Pembroke Street, Cambridge,CB2 3QZ, U.K.

6–43 Texture Development in Pd and Ag Layers on Ni-based Substrates for Coated Conductor Applications. *N.A. Rutter*[1,2], *M.E. Vickers*[1], *Z.H. Barber*[1,2], *A.P. Bramley*[1], *B.A. Glowacki*[1,2], *J.E. Evetts*[1,2] and *E. Maher*[3]. [1]Department of Materials Science and Metallurgy, University of Cambridge, Pembroke Street, Cambridge, CB2 3QZ, U.K. [2]IRC in Superconductivity, Madingley Road, Cambridge CB3 0HE, U.K. [3]Oxford Instruments plc, Old Station Way, Eynsham, Witney, OX8 1TL, U.K.

6–44 Formation of native cube textured oxide on a flexible Ni-alloy tape substrate for coated conductor applications. *N.A. Rutter*[1,2], *B.A. Glowacki*[1,2], *J.E. Evetts*[1,2], *H. te Lintelo*[3], *R. De Gryse*[4] and *J. Denul*[4]. [1]Department of Materials Science and Metallurgy, University of Cambridge, Pembroke Street, Cambridge, CB2 3QZ, U.K. [2]IRC in Superconductivity, Madingley Road, Cambridge CB3 0HE, U.K. [3]Innovative Sputtering Technology, Karreweg 18, B-9870 Zulte, Belgium. [4]Centrum voor Vacuum en Materiaalwetenschappen (CVM), Krijgslaan 281 / S1, B-9000 Gent, Belgium.

6–45 Recrystallization Kinetics of Biaxially Textured Ni Substrates for YBCO Coated Conductors. *R. Nast*[1], *W. Goldacker*[1], *B. Obst*[1] and *G. Linker*[2]. [1]Forschungszentrum Karlsruhe, Institut für Technische Physik, Karlsruhe, D-76021, Germany. [2]Forschungszentrum Karlsruhe, Institut für Nukleare Festkörperphysik, Karlsruhe, D-76021, Germany.

6–46 Raman and X-ray Characterisation of Structural Disorder in YBCO Thick Films Grown at High Rates for IBAD Conductors. *G. Gibson*[1], *S. R. Foltyn*[2], *N. Malde*[3], *L.F. Cohen*[3], *P.N. Arendt*[2], *E.J. Peterson*[2], *D.E. Peterson*[2] and *J.L. MacManus-Driscoll*[3]. [1]Dept. of Materials Science and Metallurgy, Cambridge University, Pembroke St., Cambridge, CB2 3QZ. [2]Superconductivity Technology Center, Los Alamos National Laboratory, Los Alamos, New Mexico 87545, U.S.A. [3]Centre for High Temperature Superconductivity, Imperial College of Science Technology and Medicine, Prince Consort Road, London SW7 2AZ, U.K.

6–47 Heteroepitaxial growth of oxide buffer layers by pulsed laser deposition on biaxially oriented Ni and Ni-alloy tapes. *B. Holzapfel*[1], *L. Fernandez*[1], *M. Arranz*[2], *N. Reger*[1], *B. de Boer*[1], *J. Eickemeyer*[1] and *L. Schultz*[1]. [1]IFW Dresden, Institute of Metallic Materials, D-01171 Dresden, Germany. [2]Departamento de Fisica Aplicada, Facultad de Ciencias Quimicas, UCLM, 13071 Ciudad Real, Spain.

6–48 Effects of impurities on texturing of Ni tapes and the properties of YBCO films. *S.H. Oh*, *J.E. Yoo*, *K.C. Chung*, *H.S. Kim*, *B.S. Lee*, *K.H. Lee*, *J.S. Lee*, *H.K. Lee* and *D. Youm*. KAIST, 373-1, Kusong-dong, Yusong-gu, Taejon, 305-701 Korea.

6–49 High J_c YBCO Thick Films on Biaxially Textured Ni-V Substrate with CeO_2/NiO Intermediate Layers. *V. Boffa*[1], *T. Petrisor*[1,2], *F. Fabbri*[1,3], *C. Annino*[1], *D. Bettinelli*[1,3], *G. Celentano*[1], *L. Ciontea*[1,2], *U. Gambardella*[1,4], *G. Grimaldi*[1] and *A. Mancini*[1]. [1]ENEA-Centro Ricerche Frascati. [2]Technical University of Cluj, 3400 Cluj-Napoca, Romania. [3]Under PIRELLI-ENEA contract. [4]INFN-LNF, 00044 Frascati, Rome, Italy.

6–50 Deposition of Buffer and YBCO-Layers on Textured Metal Tapes Using RF and DC Sputtering Techniques. *S. Kreiskott*[1], *M. Getta*[1,2], *B. Lehndorff*[1,2], *B. Mönter*[1,2], *G. Müller*[2], *B. Skriba*[1], *R. Wagner*[1,2] and *E. Bischoff*[3]. [1]Cryoelectra GmbH, Wettinerstr. 6H, D-42287 Wuppertal. [2]Bergische Universität Wuppertal, Gaußstr. 20, D-42097 Wuppertal. [3]MPI f. Metallforschung, Seestr. 92, D-70174 Stuttgart.

6–51 Non magnetic $Ni_{100-x}V_x$ Biaxially Textured Substrates for YBCO Tape Fabrication. *T. Petrisor*[1,5], *V. Boffa*[1], *S. Ceresara*[2], *C. Annino*[1], *D. Bettinelli*[1,6], *F. Fabbri*[1,6], *U. Gambardella*[1,7], *G. Celentano*[1], *P. Scardi*[3] and *P. Caracino*[4]. [1]ENEA-Centro Ricerche Frascati. [2]CNR-TEMPE, C.so Promessi Sposi, 29, 22053 Lecco, Italy. [3]Università di Trento, Dipartimento di Ingegneria dei Materiali, 38050 Mesiano, Trento, Italy. [4]PIRELLI CAVI&SISTEMI, viale Sarca 222, 20126 Milan, Italy. [5]Technical University of Cluj, 3400 Cluj-Napoca, Romania. [6]Under PI ELLI-ENEA contract. [7]INFN-LNF, 00044 Frascati, Rome, Italy.

6–52 Influence of external strains on YBCO films deposited on thin buffered technical substrates. *F. García-Moreno*[1,2], *A. Usoskin*[1], *H.C. Freyhardt*[1,2], *J. Wiesmann*[2], *J. Dzick*[2] and *J. Hoffmann*[2]. [1]Zentrum fuer Funktionswerkstoffe Goettingen gGmbH, Windausweg 2, D-37073 Goettingen, Germany. [2]Institut fuer Materialphysik, Universitaet Goettingen, Windausweg 2, D-37073 Goettingen, Germany.

6–53 YBCO Tape Coating by Thermal Reactive Co-Evaporation. *U.Schmatz*, *Ch.Hoffmann*, *R.Metzger*, *M.Bauer*, *P.Berberich* and *H.Kinder*. Physikdepartment E10, Technische Universität München, 85747 Garching, Germany.

6–53P1 Evidence for the Influence of the Grain Structure of Textured Nickel Substrates on the YBCO Layer in Coated Conductors. *D.M. Feldmann*, *J.L. Reeves*, *A. Polyanskii*, *S.E. Babcock* and *D.C. Larbalestier*. Applied Superconductivity Center University of Wisconsin - Madison 1500 Engineering Drive Madison, WI 53706 USA.

Session Cables, transformers and generators

6–54 Discussion of the current leads for AC magnet. *K. Kaiho*[1], *H. Yamaguchi*[1], *K. Arai*[1], *T. Saitoh*[2], *S. Sadakata*[2], *H. Fuji*[2] and *M. Yamaguchi*[3]. [1]Electrotechnical Laboratory, Tsukuba, Ibaraki, 305-8568, Japan. [2]Fujikura Co.Ltd., Koto-ku, Tokyo, 135-0042. Japan. [3]Niigata Univ., Niigata-shi, Niigata, 950-2102, Japan.

6–55 The magnetic field distribution in a transmission superconducting cables. *V.E. Sytnikov*, *G.G. Svalov*, *P.I. Dolgosheev* and *N.V.Polyakova*. JSC"VNIIKP", Moscow, 111024, Russia.

6–56 The study of additional losses in multilayer transmission cable. *G.G. Svalov*, *V.E. Sytnikov*, *P.I. Dolgosheev* and *N.V. Polyakova*. JSC"VNIIKP", Moscow, 111024, Russia.

6–57 Transport AC losses in a coaxial cylindrical cable. *F. Gömöry*. Institute of Electrical Engineering, Slovak Academy of Sciences, Dubravska 9, 84239 Bratislava, Slovak Republic.

6–58 Influence of spread in tape properties on DC critical current of a superconducting cable. *F. Gömöry* and *L. Frolek*. Institute of Electrical Engineering, Slovak Academy of Sciences, Dubravska 9, 84239 Bratislava, Slovak Republic.

6–59 A 10-20 kVA Single Phase High Temperature Superconducting Demonstrator Transformer. *M.K. Al-Mosawi*[1], *C. Beduz*[1], *M. Webb*[1] and *A. Power*[2]. [1]Institute of Cryogenics, University of Southampton, Southampton SO17 1BJ, UK. [2]The National Grid Company plc, UK.

6–60 A model for the current distribution and ac losses in superconducting multi-layer power cables. *M. Däumling*. NKT Research Center, DK-2605 Brøndby, Denmark.

6–61 Electrically and Thermally Insulated Connection for Liquid Nitrogen Transfer. *C.N. Rasmussen* and *J.T. Holboell*. Technical University of Denmark Department of Electric Power Engineering Lyngby DK-2800 Denmark.

6–62 Bending test of a 3 meter long, 2 kArms HTS cable conductor. *C.N. Rasmussen*[1], *S. Hutchinson*[1], *M. Däumling*[1], *D.W.A. Willén*[1], *Martin Andersen*[2], *K. Høj Jensen*[3], *C. Træholt*[3] and *O. Tønnesen*[3]. [1]NKT Research Center, Priorparken 878, DK-2605 Brøndby, Denmark. [2]NKT Cables, Priorparken 510, DK-2605 Brøndby, Denmark. [3]Technical University of Denmark, Department of Electric Power Engineering, Bldg. 325, DK-2800 Lyngby, Denmark.

6–63 Theoretical and experimental investigation of the effect of the gap between tapes on the critical current in a cable-like environment. *A. Bentien*, *M. Däumling* and *D. W. A. Willén*. NKT Research Center, Priorparken 878, 2605 Brondby, Denmark.

6–64 BSCCO/Ag Resonator Coil with an Air - Gap Iron Yoke. *O. A. Shevchenko*[1], *A. Godeke*[1], *J. J. Rabbers*[1], *H. J. G. Krooshoop*[1], *G.C. Damstra*[2], *C. J. G. Spoorenberg*[3], *B. ten Haken*[1] and *H. H. J. ten Kate*[1]. [1]Faculty of Applied Physics, University of Twente, Enschede, The Netherlands. [2]University of Eindhoven, Eindhoven, The Netherlands. [3]Smit Transformatoren, B.V.,Postbus 9107,6500 HJ, Nijmegen, The Netherlands.

6–64P1 Theoretical geometric considerations about design of coreless superconducting transformers. *A. Alvarez*, *P. Suarez* and *D. Caceres*. Universidad de Extremadura Escuela de Ingenierías Industriales Avda. de Elvas s/n. Apdo de correo, 382 06071 Badajoz (Spain).

Session Materials related to electronic applications

6–65 Even and Odd Hall Effects in YBCO Thin Films. *V.Shapiro*, *A.Verdyan*, *I.Lapsker* and *J.Asoulay*. Center for Technological Education Holon affiliated with Tel-Aviv University.

6–66 High pressure behavior of ferroelectric-superconducting composites $Pb_2(ScTa)O_6$-$YBa_2Cu_3O_{7-\delta}$. *J. Marfaing*[1], *C. Caranoni*[1], *M. Krupski*[2], *J. Stankowski*[2], *S. Przybyl*[2], *B. Andrzejewski*[2], *A. Kaczmarek*[2] and *B. Hilczer*[2]. [1]Lab. MATOP-CNRS, Case 151, F-13397 Marseille Cedex 20. [2]Inst. of Molecular Physics, Pol; Aca. Sci., Pl-60179 Poznan.

6–67 Peculiarities of Noise Behavior of YBCO Films Showing Strong Pinning. *I.A Khrebtov*[1], *A.D. Tkachenko*[1], *A.V. Bobyl*[2], *F.C. Klaassen*[3], *J.M. Huijbregtse*[3] and *B. Dam*[3]. [1]S.I. Vavilov State Optical Institute, St. Petersburg, 199034, Russia. [2]St. Petersburg State Technical University, 195251, Russia. [3]Vrije Univers., De Boelelaan 1081, 1081HV Amsterdam, Netherlands.

6–68 Surface resistance of YBCO thin films at THz-frequencies. *I.Wilke*[1], *C.Rieck*[1], *C.Jaekel*[2] and *H.Kurz*[2]. [1]Universität Hamburg, Jungiusstrasse 11, D-20355 Hamburg, Germany. [2]Institut für Halbleitertechnik II, RWTH Aachen, Sommerfeldstrasse 24, D-52056 Aachen, Germany.

6–69 Development of Tl-2212 Films for Device Applications. *D.M.C. Hyland*[1], *O.S. Chana*[2], *A.P. Jenkins*[1], *P.A. Leigh*[1], *P.A. Warburton*[2], *C.R.M. Grovenor*[3] and *D. Dew-Hughes*[1]. [1]Department of Engineering Science, University of Oxford, Parks Road, Oxford, OX1 3PJ, UK. [2]Department of Electronic Engineering, King's College London, Strand, London, WC2R 2LS, UK. [3]Department of Materials, University of Oxford, Parks Road, Oxford, OX1 3PH, UK.

6–70 Plasma sprayed superconducting YBCO and Dy-substituted YBCO coatings. *R. Enikov*, *T. Koutzarova*, *D. Oliver* and *I. Nedkov*. Institute of Electronics, Bulg. Acad. Sci., Sofia, 1784, Bulgaria.

6–71 Microwave Properties of Screen-Printd Bi2223 Thick Films on $Ba(Sn,Mg,Ta)O_3$ Dielectric Ceramics. *Y. Kintaka*[1], *T. Tatekawa*[1], *N. Matsui*[1], *H. Tamura*[1], *Y. Ishikawa*[1] and *A. Oota*[2]. [1] Murata MFG Co.Ltd.,Nagaokakyo,Kyoto,617-8555,Japan. [2] Toyohashi University of Technology,Toyohashi,Aichi,441-8580,Japan.

Session SQUIDs, and SQUIDs applications

6–72 Direct measurement of vortex motion in Nb variable-thickness-bridges. *S. Hirano*[1], *S. Kuriki*[1], *M. Matsuda*[2], *T. Morooka*[3] and *S. Nakayama*[3]. [1]Research Institute for Electronic Sciences, Hokkaido University, Sapporo, 060-0812, Japan. [2]Muroran Institute of Technology, Muroran, 050-8585, Japan. [3]Seiko Instruments Inc., Matsudo, Chiba, 270-2222, Japan.

6–73 Thermal Noise in Digital DC SQUID. *G.H. Chen*, *H. Du* and *Q.S. Yang*. Institute of Physics,Chinese Academy of Sciences,Beijing 100080,China.

6–75 The simulation and design of HTS RSQUID noise thermometers. *L. Hao*[1], *J.C. Gallop*[1], *J.C. Macfarlane*[2], *D.A. Peden*[2] and *C.M. Pegrum*[2]. [1]Centre for Basic and Thermal Metrology, National Physical Laboratory, Teddington, TW11 0LW, UK. [2]Dept. of Physics and Applied Physics, Strathclyde University, Glasgow G4 0NG, UK.

6–76 Integrated resistors in $YBa_2Cu_3O_{7-\delta}$ thin films suitable for superconducting quantum interference devices with resistively shunted inductance. *F. Kahlmann*[1], *W.E. Booij*[1], *M.G. Blamire*[1], *P.F. McBrien*[1], *N.H. Peng*[2], *C. Jeynes*[2] and *E.J. Tarte*[1]. [1]IRC in Superconductivity, University of Cambridge, Madingley Road, Cambridge CB3 0HE, United Kingdom. [2]urrey Centre for Research into Ion Beam Applications, School of Electronic Engineering, Information Technology and Mathematics, University of Surrey, Guildford GU2 5XH, United Kingdom.

6–77 Effect of the thermally activated phase slippage on characterizations of step-edge YBCO SQUIDs. *H.E. Horng*[1], *S.Y. Yang*[1], *C.H. Chen*[1], *J.T. Jeng*[1] and *H.C. Yang*[2]. [1]Department of Physics, National Taiwan Normal University, Taipei 117, Taiwan. [2]Department of Physics, National Taiwan University, Taipei 106, Taiwan.

6–78 $YBa_2Cu_3O_{7-\delta}$ dc SQUID array magnetometers and multichannel flip-chip current sensors. *J. Ramos*, *R. IJsselsteijn*, *R. Stolz*, *V. Zakosarenko*, *V. Schultze*, *A. Chwala*, *H.-G. Meyer* and *H. E. Hoenig*. Institute for Physical High Technology, Dept. of Cryoelectronics, P. O. Box 100239, D-07702 Jena, Germany.

6–79 Smart DROS Sensor with Digital Readout. *M. Podt*, *D. Keizer*, *J. Flokstra* and *H. Rogalla*. Low Temperature Division, Department of Applied Physics, University of Twente, P.O. Box 217, 7500 AE Enschede, The Netherlands.

6–80 Low-noise S-band DC SQUID Amplifier. *G.V. Prokopenko*[1], *S.V. Shitov*[1], *D.V. Balashov*[1], *V.P. Koshelets*[1] and *J. Mygind*[2]. [1]Institute of Radio Engineering and Electronics RAS, Moscow, Russia. [2]Department of Physics, Technical University of Denmark, Lyngby, Denmark.

6–81 Noises study of high-T_c $YBa_2Cu_3O_y$ SQUIDs magnetometers under microwave irradiation. *H.C. Yang*[1], *M.P.H. Chang*[1], *J.H. Chen*[1], *H.W. Yu*[1], *H.E. Horng*[2], *J.T. Jeng*[2] and *S.Y. Yang*[2]. [1]Department of Physics, National Taiwan University, Taipei 106, Taiwan. [2]Department of Physics, National Taiwan Normal Unversiy, Taipei 117, Taiwan.

6–82 HTS-DC-SQUID Flux-Locked-Loop based on a cooled integrated electronics. *J. Kunert*[1], *V. Zakosarenko*[1], *V. Schultze*[1], *R. Gross*[2], *F. Nitsche*[2] and *H.-G. Meyer*[1]. [1]Institut fuer Physikalische Hochtechnologie, Abteilung Kryoelektronik, PF 100 239, D - 07702 Jena, Germany. [2]MAZeT GmbH, In den Weiden 7, D - 99099 Erfurt, Germany.

6–83 Radio Frequency Amplifier Based on a Niobium dc SQUID with Microstrip Input Coupling. *M.Mueck*[1,2], *M.-O. Andre*[1], *J.Clarke*[1], *J.Gail*[2], *C.Heiden*[2] and *C.Hagmann*[3]. [1]Department of Physics University of California at Berkeley Berkeley, CA 94720, U.S.A. [2]Institut fuer Angewandte Physik Justus-Liebig-Universitaet Giessen 35392 Giessen, Germany. [3]MS 414, Lawrence Livermore National Laboratory Livermore, CA 94550, U.S.A.

6–84 HTS dc SQUID behavior under the influence of external fields. *V. Schultze*, *A. Chwala*, *R. IJsselsteijn*, *J. Ramos*, *R. Stolz*, *V. Zakosarenko* and *H.-G. Meyer*. Institute for Physical High Technology Jena Dept. of Cryoelectronics P.O.Box 100239 D-07702 Jena Germany.

6–85 Alternative structures in washer-type high-T_c dc SQUIDs. *A.B. Jansman*[1], *P.G. Jeurink*[1], *A.I. Gómez-Corona*[2], *M. Izquierdo*[2], *J. Flokstra*[1] and *H. Rogalla*[1]. [1]Low Temperature Division Department of Applied Physics University of Twente P.O. Box 217 Enschede 7500 AE Netherlands. [2]On leave from Low Temperature Division Department of Applied Physics University of Twente P.O. Box 217 Enschede 7500 AE Netherlands.

6–86 Superconductive and traditional electromagnetic probes in eddy current nondestructive testing of conductive materials. *M. Valentino*[1,2], *A. Ruosi*[1], *G. Pepe*[1] and *G. Peluso*[1]. [1] Istituto Nazionale per la Fisica della Materia (INFM), Unita' di Napoli Università di Napoli "Federico II", Piazzale Tecchio 80, 80125 Napoli, Italy. [2] Dipartimento di Ingegneria dei Materiali per la Produzione Università di Napoli "Federico II", Piazzale Tecchio 80, 80125 Napoli, Italy.

6–87 HTS dc-SQUID with a gradiometric multilayer flux transformer. *M.I.Faley*[1], *U.Poppe*[1], *K.Urban*[1], *D.N.Paulson*[2], *T.N.Starr*[2] and *R.L.Fagaly*[2]. [1]Institut fuer Festkoerperforschung, FZ-Juelich GmbH D-52425 Juelich, Germany. [2]Tristan Technologies inc., San Diego, CA 92121 USA.

6–88 Field-Cooled Noise Characteristics in the SQUID Magnetometers with Holes. *J.T.Jeng*[1], *Y.C. Liu*[1], *S.Y. Yang*[1], *J.R. Chiou*[2], *H.E. Horng*[1], *J.H. Chen*[2] and *H.C. Yang*[2]. [1]Department of Physics, National Taiwan Normal University, Taipei 117, Taiwan. [2]Department of Physics, National Taiwan University, Taipei 106, Taiwan.

Session Mixers/Detectors

6–89 Realisation of a flux-flow dc-transformer using high temperature superconductors. *S.Berger*, *K.Bouzehouane*, *D.Crete* and *J.P.Contour*. Unite Mixte de Pysique CNRS / Thomson, Domaine de Corbeville, 91404 Orsay Cedex, France.

6–91 Far-Infrared Hilbert-Transform Spectrometer based on Stirling Linear Cooler. *O.Y. Volkov*[1], *V.V. Pavlovskii*[1], *Y.Y. Divin*[2] and *U. Poppe*[2]. [1]Institute of Radioengineering & Electronics of RAS, Moscow 103907, Russian Federation. [2]Institut fuer Festkoerperforschung, Forschungszentrum Juelich GmbH, 52425 Juelich, Germany.

6–92 Development and Characterization of NbN Phonon Cooled Hot Electron Bolometer Mixers at 810 GHz. *C. Rösch*, *F. Mattiocco* and *K.F. Schuster*. Institut de Radio Astronomie (IRAM) 300, rue de la piscine Domaine Universitaire de Grenoble 38406 St. Martin d'Heres France.

6–93 Current Tunable IF-Phase Using High-Tc Superconducting 100GHz Mixer. *K. Suzuki*, *K. Kashiwagi* and *Y. Enomoto*. Superconductivity Research Laboratory, ISTEC 1-16-25, Shibaura, Minato-ku, Tokyo, 105-0023, Japan.

6–94 Relaxation Times and Noise in Sub-Micron Long HTS Hot-Electron Mixers. *O. Harnack*[1,2], *B. S. Karasik*[1], *W. R. McGrath*[1], *A. W. Kleinsasser*[1] and *J. B. Barner*[1]. [1]Center for Space Microelectronics Technology, Jet Propulsion Laboratory, California Institute of Technology, 4800 Oak Grove Drive, MS 168-314, Pasadena, CA 91109, USA. [2]Institute of Thin Film and Ion Technology, Research Center Juelich, 52425 Juelich, Germany.

6–95 Heterodyne type response in SIS direct detector. *A. Karpov*[1], *J. Blondel*[1], *P.N. Dmitriev*[2] and *V.P. Koshelets*[2]. [1]Institut de Radioastronomie Millimétrique, St. Martin d'Hères, France. [2]Institute of Radio Electronics and Engineering, Moscow, Russia.

6–96 Metal - High Tc Superconductor Point Contact Responce to Millimeter Wave Radiation. *A. Laurinavicius*, *K. Repsas*, *R. A. Vaskevicius* and *A. Deksnys*. Semiconductor Physics Institute, Vilnius, A. Gostauto 11, 2600 Vilnius, Lithuania.

6–97 Performance of Inhomogeneous Distributed Junction Arrays. *M.Takeda*[1] and *T.Noguchi*[2]. [1]The Graduated University for Advanced Studies, Nobeyama, Minamisaku, Nagano, 384-1305 Japan. [2]Nobeyama Radio Observatory, Nobeyama, Minamisaku, Nagano, 384-1305 Japan.

6–98 Ka-Band High-T_c Superconductor and III-V Semiconductor Hybrid Balanced Mixer. *S. K. Han*, *J. D. Suh*, *G. Y. Sung* and *K. Y. Kang*. Telecomm. Basic Research Lab., ETRI, Taejon 305-350, South Korea.

6–99 HTSC-Bolometer for IR-Spectrometer -Processing and Operation-. *K.-S. Roever*[1], *T. Heidenblut*[1], *B. Schwierzi*[1], *T. Eick*[2], *W. Michalke*[2] and *E. Steinbeiss*[2]. [1]Institut fuer Halbleitertechnologie UNI-Hannover, Appelstrasse 11A, Hannover, Niedersachsen, 30167, Germany. [2]Institut fuer Physikalische Hochtechnologie e.V., Helmholtzweg 4, Jena, Thueringen, 07743, Germany.

6–100 A superconducting integrated receiver with phase-lock loop. *S.V. Shitov*[1], *V.P. Koshelets*[1], *L.V. Filippenko*[1], *P.N. Dmitriev*[1], *A.M. Baryshev*[2], *V.L. Vaks*[3], *W. Luinge*[2], *J.-R. Gao*[2,4] and *N.D. Whyborn*[2]. [1]Institute of Radio Engineering and Electronics (IREE), Moscow 103907, Russia. [2]Space Research Organization of the Netherlands (SRON), Groningen 9700 AV, the Netherlands. [3]Institute for Physics of Microstructure (IPM), Nizhny Novgorod 603600, Russia. [4]Department of Applied Physics and Materials Science Center, University of Groningen, the Netherlands.

6–101 Numerical Simulation based on a Five-Port Model of the Parallel SIS Junction Array Mixer. *M.-H. Chung* and *M. Salez*. DEMIRM, Observatoire de Paris, 61 avenue de l'Observatoire, 75014 Paris, France.

6–102 The Characterization of Radiation Beam Pattern and Fabrication of Superconducting Hot Electron Bolometer Mixer. *C.C. Chin*[1], *P.Z.Y. Pan*[2], *C.C. Chi*[2], *S.F. Horng*[3], *Y.S. Yang*[1], *S.S. Shen*[1] and *R. Hu*[1]. [1] Institute of Astronomy and Astrophysics, Academia Sinica, Nankang, Taipei, Taiwan. [2] Center for Material Science and Department of Physics, Tsing Hwa University, Hsin Chu, Taiwan. [3] Department of Electrical Engineering, Tsing Hwa University, Hsin Chu, Taiwan.

6–103 Surface Resistance of NbN and NbC_x N_{1-x} Films in the Frequency Range of 0.5-1.5THz. *S. Kohjiro* and *A. Shoji*. Electrotechnical Laboratory, Tsukuba, Ibaraki, 305-8568, Japan.

6–105 Fabrication and Testing of Microcalorimeter for X-ray spectroscopy. *M. Ukibe*, *F. Hirayama*, *M. Koyanagi*, *M. Ohkubo* and *N. Kobayashi*. Electrotechnical Laboratory, 1-1-4, Umezono, Tsukuba-shi, Ibaraki, 305-8568, Japan.

6–106 A Compact High-resolution X-ray Detector System using STJ and SQUID Amplifier. *T. Ikeda*[1], *H. Kato*[1], *K. Kawai*[1], *H. Miyasaka*[1], *T. Oku*[1], *W. Ootani*[1], *C. Otani*[1], *H. Sato*[1], *Y. Takizawa*[1], *H. M. Shimizu*[1], *H. Watanabe*[1], *H. Nakagawa*[2], *H. Akoh*[2], *M. Aoyagi*[2] and *T. Taino*[3]. [1] The Institute of Physical and Chemical Research (RIKEN), 2-1 Hirosawa, Wako, Saitama 351-0198, Japan. [2] Electrotechnical Laboratory (ETL), 1-1-4 Umezono, Tsukuba, Ibaraki 305-8568, Japan. [3] Department of Nuclear Engineering, Kyushu University, Hakozaki, Fukuoka 812-8581, Japan.

6–107 Sensitivity of a NbN phonon-cooled hot-electron mixer in the frequency range from 0.7 THz to 5.2 THz. *A.D. Semenov*[1], *J. Schubert*[2], *G.N. Gol'tsman*[1], *H.-W. Huebers*[2], *G. Schwaab*[3], *E.M. Gershenzon*[1] and *B.M. Voronov*[1]. [1]Physical Department, State Pedagogical University of Moscow, M.Pirogovskaya 29, 119435 Moscow, Russia. [2]DLR Institute of Space Sensor Technology, D-12489 Berlin, Germany. [3]Physical Chemistry II, Ruhr-University Bochum, D-44801 Bochum, Germany.

6–108 Fabrication of Diffusion-cooled Nb Hot-Electron-Bolometer Mixer for Terahertz Applications. *M. Frommberger, P. Sabon, M. Schicke, K.H. Gundlach* and *K.F. Schuster*. IRAM, 300 Rue de la Piscine, 38406 St. Martin d'Heres, France.

6–109 Anodic oxidation for NbN film thickness measurements. *M. Schicke*[1], *K. H. Gundlach*[1] and *K. Mizuno*[2]. [1]Institut de Radioastronomie Millimétrique, 300 rue de la piscine, Saint Martin d'Hères, 38406, France. [2]Central Research Laboratories, Matsushita Electric Industrial Co. Ltd., 3-4 Hikaridai, Seika-Cho, Soraku-Gun, Kyoto, 619-02, Japan.

6–110 Conductivity and Kinetic-Inductance Response of the YBaCuO Bicrystal Josephson Junctions Array. *A.P. Lipatov*[1], *D.V. Meledin*[1], *A.S. Kalabukhov*[2], *A.N. Zherikhin*[3], *G.N. Goltsman*[1] and *O.V. Snigirev*[2]. [1]Moscow State Pedagogical University, Moscow,119435 Russia. [2]Moscow State University, Moscow, 119899, Russia. [3]Scientific Research Center for Technological Lasers, Toitzk, Moscow region,142092 Russia.

6–111 A Superconducting Tunnel Junction with Superconducting Microstrip Coil for X-ray Detector. *T.Taino*[1,2], *H.Nakagawa*[1], *M.Aoyagi*[1], *H.Akoh*[1], *K.Maehata*[2], *K.Ishibashi*[2], *H.Satoh*[3], *T.Ikeda*[3], *T.Oku*[3], *C.Otani*[3], *W.Otani*[3], *H.Kato*[3], *K.Kawai*[3], *H.Miyasaka*[3], *H.M.Shimizu*[3], *H.Takizawa*[3] and *H.Watanabe*[3]. [1]Electrotechnical Laboratory (ETL), Tsukuba, Ibaraki, 305-8568, Japan. [2]Kyushu University, Fukuoka, Fukuoka, 812-8581, Japan. [3]The Institute of Physical and Chemical Research (RIKEN), Wako, Saitama, 351-0198, Japan.

6–112 Mm and submm wave mixing and selective detection by YBCO bicrystal Josephson junctions on sapphire. *K. Y. Constantinian*[1], *G. A. Ovsyannikov*[1], *A. D. Mashtakov*[1], *N. G. Pogosyan*[2], *A. A. Hakhoumian*[2], *J. Mygind*[3] and *N. F. Pedersen*[3]. [1]Institute of Radio Engineering and Electronics RAS, 103907, Moscow, Russia. [2]Institute of Radiophysics and Electronics Armenian National Academy of Sciences, 378410, Ashtarak-2, Armenia. [3]Department of Physics, Technical University of Denmark, DK-2400, Lyngby, Denmark.

6–113 Investigation of quasiparticles diffusion to the edge process in superconducting tunnel junction detectors. *E. Esposito*[1,3], *R.Cristiano*[1], *L.Frunzio*[1], *M.Lisitski*[1], *C.Nappi*[1], *G.Ammendola*[2], *L.Parlato*[2,3], *G.Pepe*[2], *H.Kraus*[4] and *P.Valko*[4]. [1]Istituto di Cibernetica del C.N.R., Arco Felice, Napoli, I-80072, Italy. [2]INFM-Dipartimento di Scienze Fisiche dell'Università di Napoli Federico II, Napoli, Italy. [3]Osservatorio Astronomico di Capodimonte, Napoli, I-80131 Ital. [4]Dept. of Physics, Particle and Nuclear Physics, University of Oxford, Oxford OX1 3RH, UK.

6–114 Development of Superconducting Tunnel Junctions with Al Trapping Layers for X-ray Detectors. *H. Sato*[1], *K. Kawai*[1], *H. Miyasaka*[1], *T. Oku*[1], *W. Ootani*[1], *C. Otani*[1], *H.M. Shimizu*[1], *H. Watanabe*[1], *H. Nakagawa*[2], *T. Taino*[3], *T. Ikeda*[1], *H. Kato*[1] and *M. Aoyagi*[2]. [1]The Institute of Physical and Chemical Research (RIKEN), 2-1 Hirosawa, Wako, Saitama 351-0198, Japan. [2]Electrotechnical Laboratory (ETL), 1-1-4 Umezono, Tsukuba, Ibaraki 305-8568, Japan. [3]Department of Nuclear Engineering, Kyushu University, Hakozaki, Fukuoka 812-8581, Japan.

6–116 Performance of NbN hot electron bolometric mixers at terahertz frequencies. *P. Yagoubov*[1], *M. Kroug*[1], *H. Merkel*[1], *E. Kollberg*[1], *J. Schubert*[2] and *H.-W. Hubers*[2]. [1]Department of Microelectronics, Chalmers University of Technology, S-412 96 Gothenburg, Sweden. [2]DLR Institute of Space Sensor Technology, D-12489 Berlin, Germany.

6–117 Particle Detection with Geometrically-Metastable Type-I Superconductors. *M.R. Gomes*[1], *T.A. Girard*[1], *C. Oliveira*[2] and *V. Jeudy*[3]. [1]Centro de Fisica Nuclear, Universidade de Lisboa, Lisboa 1649-003 Portugal. [2]Departamento da Fisica, Instituto Tecnologico e Nuclear, Sacavem 2685, Portugal. [3]Groupe de Phsysique des Solides (CNRS UMR 75-88), Universites de Paris 7/6, Paris 75251, France.

6–118 $(YBCO/STO)_n$ mutilayers : a way to avoid substrate micromachining of microbolometers ?. *N.Cheenne*[1,2], *D.Robbes*[1], *J.P.Maneval*[3], *S.Flament*[1], *B.Mercey*[2], *J.F.Hamet*[2] and *L.Mechin*[1]. [1]GREYC-Instru - UPRES-A 6072, CAEN, 14050, France. [2]CRISMAT - UMR 6508, CAEN, 14050, France. [3]Ecole Normale Superieure, PARIS, 75231, France.

6–119 A Self-Consistent Hot Spot Mixer Model for NbN Phonon-Cooled Hot Electron Bolometer. *H. F. Merkel, P. Khosropanah, P. Yagoubov, M. Kroug* and *E. Kollberg*. Department of Microwave Electronics, Chalmers University of Technology, S 412 96 Göteborg, Sweden.

6–120 Investigation of the far-infrared absorption processes in high temperature superconductors for construction fast infrared radiation detectors. *E. A. Kafadaryan.* Institute for Physical Research National Academy of Scienses, Ashtarak-2,378410,Armenia.

6–121 Disordered suspensions of metastable superconducting microgranules. *A. Peñaranda, C.E. Auguet* and *L. Ramírez-Piscina.* Departamento de Física Aplicada, E.U.P.B., Universidad Politècnica de Catalunya, c/ Dr. Marañón, 44, 08028 Barcelona.

Wednesday, September 15th

PLENARY SESSION 7

Wednesday Morning, September 15th, 8:30-10:00

8:30 **7–1 Advances in large scale applications of superconductors** *P. Komarek*. Forschungszentrum Karlsruhe GmbH Institute for Technical Physics D76021 Karlsruhe, P.O. Box 3640.

9:15 **7–2 Materials for Superconducting Electronics.** *H. Rogalla*. University of Twente, Low Temperature Division, 7500AE Enschede, the Netherlands.

ORAL SESSION 8A+9A: Wires and Tapes- BSCCO I

Wednesday Morning, September 15th, 10:30-12:45

10:30 ***8A–1 Thermal Equilibrium and Texturing in Ag/Bi,Pb(2223) and Ag/RE(123) Tapes.** *R. Flükiger, E. Giannini, F. Marti, R. Passerini, M. Schindl, H. L. Suo, E. Koller* and *J.-Y. Genoud*. Département de Physique de la Matière Condensée Université de Genève 24, quai Ernest Ansermet CH-1211 Genève 4, Switzerland.

11:00 ***8A–2 Long Length PIT Conductors Realized by Rectangular deformation Route.** *P. F. Herrmann*[1], *G. Duperray*[1], *D. Legat*[1], *A. Leriche*[1], *C-E. Bruzek*[2], *Y. Parasie*[3] and *J. Bock*[4]. [1]Alcatel, F-91461 Marcoussis, France. [2]Alcatel, F-59460 Jeumont, France. [3]Alcatel, 75411 Paris, France. [4]Aventis Research & Technologies, D-50351 Hürth, Germany.

11:30 **8A–3 Performance at 10-50K of Bi-2212/Ag multilayer tapes fabricated by using PAIR process.** *H. Kitaguchi*[1], *K. Itoh*[1], *T. Takeuchi*[1], *H. Kumakura*[1], *H. Miao*[1,2], *K. Togano*[1,2], *T. Hasegawa*[3] and *T. Koizumi*[3]. [1]National Research Institute for Metals. [2]CREST, Japan Science and Technology Corporation. [3]Showa Electric Wire & Cable Co. Ltd.

11:45 **9A–1 Advanced rolling techniques for Bi(2223)/Ag wires and tapes.** *P. Kovac*[1], *I. Husek*[1] and *L. Kopera*[1]. [1]Institute of Electrical Engineering of Slovak Academy of Sciences, Bratislava, 842 39, Slovakia.

12:00 **9A–2 High critical current and defect free km long Bi-2223 alloyed multifilament tapes.** *W.G. Wang, M.D. Bentzon, J. Goul, A. Barkani, M.B. Jensen, P. Skov-Hansen, Z. Han* and *P. Vase*. Nordic Superconductor Technologies A/S, Priorparken 685, DK-2605 Broendy, Denmark.

12:15 **9A–3 Bi-2223 tape processing.** *B. Fischer*[1], *T. Arndt*[1], *J. Gierl*[1], *H. Krauth*[1], *M. Munz*[1], *A. Szulczyk*[1], *M. Leghissa*[2] and *H.-W. Neumüller*[2]. [1]Vacuumschmelze GmbH, 63450 Hanau, Germany. [2]Siemens AG, 91050 Erlangen, Germany.

12:30 **9A–4 Novel, internally stranded "Ring Bundled Barrier" Bi-2223 tapes for low AC loss applications.** *J. Krelaus, R. Nast, H. Eckelmann* and *W. Goldacker*. Forschungszentrum Karlsruhe - ITP, P.O.Box 3640, D-76344 Karlsruhe, Germany.

ORAL SESSION 8B+9B: Motors, Bearings and Levitation

Wednesday Morning, September 15th, 10:30-12:45

10:30 ***8B–1 Electric Machines With the Bulk HTS Rotor Elements. Recent Results and Future Development.** *L.K. Kovalev*[1], *K.V. Ilushin*[1], *S.M.A. Koneev*[1], *V.T. Penkin*[1], *V.N. Poltavets*[1], *W. Gawalek*[2], *T. Habisreuther*[2], *B. Oswald*[3] and *T. Strasser*[3]. [1]Moscow State Aviation Institute (Technical University). [2]Institut fur Physikalische Hochtechnologie (IPHT), Jena, Ger. [3]Oswald Elektromotoren GmbH, Miltenberg, Germany.

11:00 **8B–2 High - Speed Rotor Systems with HTS Bearings.** *F. N. Werfel, R. Rothfeld, D. Wippich* and *U. Flögel - Delor*. Adelwitz Technologiezentrum GmbH, Adelwitz, D-04886, Germany.

11:15 **8B–3 Stability of magnetic HTSC bearings under axial vibrations.** *E. Portabella, R. Palka, H. May* and *W.R. Canders*. Institut für Elektrische Maschinen, Antreibe und Bahnen. Technische Universität Braunschweig. Braunschweig, 38106, Germany.

11:30 **8B–4 Superconducting Motors with HTS Bulk Material for Medium Power Range.** *B. Oswald*[1], *T. Strasser*[1], *M. Krone*[1], *M Soell*[2], *J. Oswald*[1] and *K.J. Best*[1]. [1]OSWALD Elektromotoren GmbH, D-63897 Miltenberg, Germany. [2]Fachhochschule Landshut, Germany.

11:45 **9B–1 Levitated Liquid Hydrogen Cryotank For Automotive Applications.** *J. Bock*[1], *M. Baecker*[1], *G. Brommer*[1], *L. Cowey*[1], *M. Kesten*[2], *H. Fieseler*[2], *W. R. Canders*[3], *H. May*[3], *H. C. Freyhardt*[4] and *A. Leenders*[4]. [1]Aventis Research & Technologies, D-50351 Huerth, Germany. [2]Messer, D-47805 Krefeld, Germany. [3]University of Braunschweig IMAB, D-38023 Braunschweig, Germany. [4] 4ZFW gGmbH, D-37073 Goettingen, Germany.

12:00 **9B–2 Superconducting Thrust Bearings.** *T.A. Coombs* and *A.M. Campbell*. IRC in Superconductivity, Cambridge University, Madingley Road, Cambridge CB4 0HE United Kingdom.

12:15 **9B–3 Development and Test of a 300Wh/10kW Flywheel Energy Storage System.** *R. Koch*[1], *R. Wagner*[1], *U. Sutter*[1], *M. Sander*[1] and *H. J. Gutt*[2]. [1]Forschungszentrum Karlsruhe GmbH, INFP, P. O. Box 3640, D-76021 Karlsruhe. [2]Universität Stuttgart, IEMA, Pfaffenwaldring 47, D-70569 Stuttgart .

12:30 **9B–4 1 kW Bearingless Superconducting Motor with Axial Field Exitation.** *J. Pallarés*[1,2], *X. Granados*[1], *R. Bosch*[2] and *X. Obradors*[1]. [1]Institut de Ciència de Materials de Barcelona, Bellaterra, Barcelona, 08193, Spain. [2]Escola Tècnica Superior d'Enginyers Industrials de Barcelona (UPC), Barcelona, 08028, Spain.

ORAL SESSION 8C+9C: Josephson Junctions I

Wednesday Morning, September 15th, 10:30-12:45

10:30 ***8C–1 Intrinsic josepson junctions and grain boundary π-junctions in high temperature superconductors** *A. Yurgens, V. Krasnov, Z. Ivanov, T. Claeson*. Physics and Engineering Physics, Chalmers, SE-41296 Göteborg, Sweden.

11:00 ***8C–2 C-axis Microbridge Junctions for HTS Single Flux Quantum Circuits.** *R.G.Humphreys, P.J.Hirst, J.S.Satchell, I.L.Atkin* and *M.J.Wooliscroft*. DERA, Malvern, Worcestershire WR14 3PS, UK.

11:30 **8C–3 Mechanisms controlling the electric field effect in High-T_c Josephson Junctions.** *C.W. Schneider, A. Schmehl, B. Goetz, H. Bielefeldt, R.R. Schulz, H. Hilgenkamp* and *J. Mannhart*. Experimentalphysik VI, Center for Electronic Correlations and Magnetism,Institute of Physics, Augsburg University, 86135 Augsburg, Germany.

11:45 **9C–1 Current-Phase Relation in High-T_c YBCO Josephson Junctions.** *E.Il'ichev, V. Zakosarenko, R.P.J. Ijsselsteijn, H.E. Hoenig, V. Schultze* and *H.-G. Meyer*. Institute for Physical High Technology, Dept. of Cryoelectronics, P.O. Box 100239, D-07702 Jena, Germany.

12:00 **9C–2 Meandering of resistive states in two-dimensional arrays of underdamped Josephson tunnel junctions.** *D.Abraimov*[1], *P.Caputo*[1], *G.Yu.Logvenov*[2], *M.V.Fistul*[1], *A.V.Ustinov*[1] and *G.Filatrella*[3]. [1]Physikalisches Institut III, Universitaet Erlangen-Nuernberg Erwin-Rommel-Str. 1, D-91058 Erlangen, Germany. [2]OXXEL oxide electronics technology Fahrenheitstrasse 9 D-28359 Bremen Germany. [3]INFM Unit and Physics Department University of Salerno, I-84081 Baronissi, Italy.

12:15 **9C–3 A high sensitivity directly coupled Josephson-Fraunhofer-Meissner magnetometer.** *E.Sassier, Y.Montfort, C.Gunther* and *D.Robbes*. GREYC, UPRES-A 6072, ISMRA Universite de Caen, Caen, 14050, FRANCE.

12:30 **9C–4 Spatially inhomogeneous temperature effects in Josephson tunnel junctions.** *D. Abraimov*[1], *M. V. Fistul*[1], *P. Caputo*[1], *A. V. Ustinov*[1] and *G. Yu. Logvenov*[2]. [1]Physikalisches Institut III, Erlangen-Nürnberg Universität, Erwin-Rommel-Str.1, D-91058 Germany. [2]OXXEL GmbH, Technologiepark Universität, Fahrenheitstraße 9, D-28359, Bremen, Germany.

ORAL SESSION 8D: Oscillators and Volt Standards

Wednesday Morning, September 15th, 10:30-11:45

10:30 ***8D–1 Josephson Arrays for DC and AC Voltage Metrology.** *J. Niemeyer*. Physikalisch-Technische Bundesanstalt Bundesallee 100 D-38116.

11:00 **8D–2 Externally Phase Locked Sub-MM Flux Flow Oscillator for Integrated Receiver.** *V.P. Koshelets*[1], *A.M. Baryshev*[1,2], *J. Mygind*[3], *V.L. Vaks*[4], *S.V. Shitov*[1], *L.V. Filippenko*[1], *P.N. Dmitriev*[1], *W. Luinge*[2] and *N. Whyborn*[2]. [1]Institute of Radio Engineering and Electronics, Mokhovaya 11, 103907, Moscow, Russia. [2]SRON-Groningen, P.O.Box 800, 9747 AV Groningen, the Netherlands. [3]Department of Physics, Technical University of Denmark, B309, DK-2800 Lyngby, Denmark. [4]Institute for Physics of Microstructure, GSP-105, 603600 Nizhny Novgorod, Russia.

11:15 **8D–3 Microwave Circuts with High-T_c Josephson Junctions for Programmable Voltage Standard and Voltage Calibrator.** *A.M. Klushin*[1,2], *C. Weber*[1], *Kh.A. Ainitdinov*[2], *S.I. Borovitskii*[2], *V.D. Gelikonova*[2], *A.V. Komkov*[2] and *R. Semerad*[3]. [1]Institut fuer Schicht- und Ionentechnik, Forschungszentrum Juelich GmbH, Juelich, 52425, Germany. [2]Institute of Electronic Measurements "KVARZ", Nizhny Novgorod, 603009, Russia. [3]Technical University of Munich, Physic Dept. E10, Garching, 85748, Germany.

11:30 **8D–4 MM wave Josephson radiation in High-Tc bicrystal junction arrays.** *K. Y. Constantinian*[1], *A. D. Mashtakov*[1], *G. A. Ovsyannikov*[1], *V.K. Kornev*[2], *N.A. Shcherbakov*[2], *M. Darula*[3], *J. Mygind*[4] and *N. F. Pedersen*[4]. [1]Institute of Radio Engineering and Electronics RAS, 103907, Moscow, Russia. [2]Moscow State University, Moscow, Russia. [3]Research Centre Juelish, Juelish, Germany. [4] Department of Physics, Technical University of Denmark, DK-2400, Lyngby, Denmark.

ORAL SESSION 9D: Bulk Materials and Materials Aspects II

Wednesday Morning, September 15th, 11:45-12:45

11:45 **9D–1 A Model for Texture Development in BSCCO High-Tc Superconductors.** *E. Cecchetti*, *P.J. Ferreira* and *J.B.V. Sande*. Massachusetts Institute of Technology (MIT) Department of Materials Science and Engineering Cambridge, MA, 02139, USA.

12:00 **9D–2 Synthesis and densification of Hg- and Hg(Re)-1223 superconductors.** *A. Tampieri*[1], *G. Celotti*[1], *D. Martínez*[2], *S. Piñol*[2], *A. Calleja*[3], *T. Puig*[2], *A. Sin*[2] and *X. Obradors*[2]. [1]IRTEC-CNR, via Granarolo,64-48018 Faenza, ITALY. [2]ICMAB-CSIC, campus de la UAB-E08193 Bellaterra, SPAIN. [3]DIOPMA. Llacuna 162-166 Barcelona, E-08018, Spain.

12:15 **9D–3 Effect of Fluorine substitution in HTCS: new structures in Bi-based superconductor.** *E. Bellingeri*[1], *G. Grasso*[1,2], *R. Gladyshevskii*[1,3], *E. Giannini*[1], *F. Marti*[1], *M. Dhallé*[1] and *R. Flükiger*. [1]DPMC, Université de Genève 24, Quai Ernest Ansermet CH-1211 Genève 4, Switzerland. [2]Present address: INFM Unità di Genova, Via Dodecaneso 33, Genova, Italy. [3]Present address: Department of Inorganic Chemistry, L'viv State University, Ukraine.

12:30 **9D–4 Magneto-optic characterisation of artificial grain boundaries in melt textured YBCO.** *G.J. French*[1], *S.A.L. Foulds*[1], *J.S. Abell*[1], *W.Lo*[2], *A. Bradley*[2], *R.A. Doyle*[2] and *D.A. Cardwell*[2]. [1]School of Metallurgy and Materials, University of Birmingham , Birmingham B15 2TT. [2]IRC in superconductivity, University of Cambridge, Cambridge CB3)he.

POSTER SESSION 10

Wednesday Afternoon, September 15th, 15:30-17:30

Session Bulk materials and materials aspects

10–1 Scaling of the critical current density vs specific contact resistance in ceramic $Y_1Ba_2Cu_3O_{7-\delta}$ superconductors. *S.R. Currás*, *J.A. Veira*, *J. Maza* and *F. Vidal*. Laboratorio de Bajas Temperaturas y Superconductividad, Universidad de Santiago de Compostela Santiago de Compostela, E-15706, Spain.

10–2 Current-Voltage characteristics in granular superconductors at very low magnetic field. *M.T. González, S.R. Currás,* *J. Maza* and *F. Vidal.* Laboratorio de Bajas Temperaturas y Superconductividad, Universidad de Santiago de Compostela Santiago de Compostela, E-15706, Spain.

10–3 Determination of inter- and intragrain critical current densities of YBCO ceramics in high fields by Hall magnetometry. *H.Varahram*[1], *M.Reissner*[1], *W.Steiner*[1] and *H.Hauser*[2]. [1]Institut für Angewandte und Technische Physik, Technische Universität Wien, A-1040, Austria. [2]Institut für Werkstoffe der Elektrotechnik, Technische Univresität Wien, A-1040, Austria.

10–4 Non-contact Measurements of Resistivity of HTS materials. *W. Nawrocki*[1], *J. Pajakowski*[1], *P. Seidel*[2] and *K-U. Barholz*[2]. [1] Poznan University of Technology Institute of Electronics and Telecom. ul. Piotrowo 3A, PL-60965 Poznan Poland. [2] Friedrich Schiller University Institute of Solide State Physics Helmholtzweg 5, D-07743 Jena Germany.

10–5 The Upper Critical Field and Irreversibility Field of the Chevrel Phase Superconductor Tin-Molybdenum-Sulphide Doped with Europium. *N. R. Leigh, I. J. Daniel* and *D. P. Hampshire.* Superconductivity Group, University of Durham, Department of Physics, South Road, Durham, DH1 3LE. U.K.

10–6 Modelling of Current Transfer in Current Contacts to Superconducting Devices. *R. P. Baranowski*[1,2], *K. A. Kursumovic*[1,2] and *J. E. Evetts*[1,2]. [1]IRC in Superconductivity, Madingley Road, Cambridge, CB3 OHE, UK. [2]Department of Materials Science, University of Cambridge, Cambridge CB2 2QZ, UK.

10–7 Preparation and characterization of electrical contacts to bulk high-temperature superconductors. *J.G. Noudem, M. Tarka* and *G.J. Schmitz.* ACCESS e.V., Intzestr. 5, D-52072 Aachen, Germany.

10–8 Spin dynamics effects on the resistivity and the magnetoresistance of the $La_{1.85}Sr_{0.15}(Cu_{1-x},Li_x)O_4$ system with $0.0 < x < 0.15$. *S. García*[1], *J. E. Musa*[2] and *E. M. Baggio-Saitovitch*[2]. [1]Centro Brasileiro de Pesquisas Físicas (CBPF-DME). rua Dr. Xavier Sigaud 150, Urca, Rio de Janeiro 22290-180, RJ, Brazil. Permanent address: Laboratorio de Superconductividad, Facultad de Física-IMRE, Universidad de La Habana, San Lázaro y L, 10400, Ciudad de La Habana, Cuba. [2]Centro Brasileiro de Pesquisas Físicas (CBPF-DME). rua Dr. Xavier Sigaud 150, Urca, Rio de Janeiro 22290-180, RJ, Brazil.

10–9 Moessbauer characterization of the prospective Pr1.9Ba1.1Cu3O7+y substrate material. *A.V.Kravchenko, I.S.Bezverkhy, E.A.Goodilin* and *Yu.D.Tretyakov.* Moscow State University, Chemistry Faculty, Inorganic Chemistry Divison, Lenin Hills, 119899, Moscow, Russia.

10–10 Routine method for determination of stoichiometric ratios of elements in high temperature superconductors. *D. Geilenberg*[1], *J.A.C. Broekaert*[2] and *M. Gerards*[3]. [1]University of Dortmund Department of Chemistry-Analytical Chemistry D-44227 Dortmund Germany. [2]University of Leipzig Institute for Analytical Chemistry D-04103 Leipzig Germany. [3]Merck KGaA, Darmstadt Werk Gernsheim D-64579 Gernsheim Germany.

10–11 Local Studies of high-Tc Superconductors using a Cryogenic Microwave Near-Field Microscopy. *A.F. Lann*[1], *M. Abu-Tair*[1], *M. Golosovsky*[1], *D. Davidov*[1], *A. Frenkel*[2], *S. Djordjevic*[3], *N. Bontemps*[3] and *L.F. Cohen*[4]. [1]Racah Institute of Physics, Hebrew University of Jerusalem, Jerusalem 91904,Israel. [2]M.S.I. Engineering Software Ltd., Tel-Aviv, Israel. [3]Ecole Normale Superieure,rue Lhomond 24, Paris, France. [4]Imperial College, London, UK.

10–12 Local magnetic-field-modulated microwave reflection - a new tool contactless technique for detection of superconductivity. *M. Abu-Tair*[1], *A.F. Lann*[1], *M.Golosovsky*[1], *D.Davidov*[1], *A.Goldgirsh*[2] and *V.Beilin*[2]. [1]Hebrew University of Jerusalem, Racah Institute of Physics. [2]Hebrew University of Jerusalem, Applied Physics Department.

10–13 Surface resistance $R_S(T,f)$ of YBCO and its quantification below $0.8T_C$ by weak links. *A. Dierlamm, E. Keskin, R. Schwab* and *J. Halbritter.* Forschungszentrum Karlsruhe, Institut für Materialforschung I P.O.Box 3640, D-76021 Karlsruhe, Germany.

Session Flux pinning and ac losses

10–14 Electrical transport properties of high temperature superconductors at intense current densities. *W. Goeb*[1], *W. Lang*[1], *R. Roessler*[2], *J.D. Pedarnig*[2] and *D. Baeuerle*[2]. [1]Institut fuer Materialphysik der Universitaet Wien, Kopernikusgasse 15, A-1060 Vienna, Austria [2]Angewandte Physik, Johannes-Kepler-Universitaet Linz, A-4040 Linz, Austria.

10–15 Non-Destructive Critical Currents Determination in Large Grain HTS Bulks. *A.A. Kordyuk*[1], *V.V. Nemoshkalenko*[1], *R.V. Viznichenko*[1], *W. Gawalek*[2] and *T. Habisreuther*[2]. [1]Institute of Metal Physics, Kyiv 252680, Ukraine. [2]Institut für Physikalische Hochtechnologie, Jena D-07743, Germany.

10–16 Experimental and theoretical study of heating of bulk HTSC samples due to AC losses. *V. Sokolovsky*, *V. Meerovich* and *M. Gladstein*. Ben-Gurion University, Beer-Sheva, 84105, Israel.

10–17 The extended critical state model for a nonuniform Type II superconductor. *A.Y. Galkin*[1], *B.A. Ivanov*[2] and *V. Kambersky*[3]. [1] Institute for Metal Physics, Vernadsky 36, 252142 Kiev, Ukraine. [2] Institute of Magnetism, Vernadsky 36b, 252142 Kiev, Ukraine. [3] Institute of Physics, Na Slovance 2, 18040, Prague8, the Czech Republic.

10–18 Real Time Dynamics of Flux Expulsion from Type-I Superconducting Strips. *G. Jung*[1,5], *V. Jeudy*[2], *D. Limagne*[2], *G. Waysand*[2], *T.A. Girard*[3], *M.J. Gomes*[3] and *B.Y. Shapiro*[4]. [1] Department of Physics, Ben Gurion University of the Negev, P.O.Box 653, 84105 Beer Sheva, Israel. [2] Groupe de Physique des Solides Universite Paris VII, 75251 Paris Cedex 05, France. [3] Centro de Fisica Nuclear Universidade de Lisboa, 1649-003 Lisboa, Portugal. [4] Department of Physics, Bar-Ilan University, Ramat-Gan, 52900, Israel. [5]Instytut Fizyki PAN, 02668 Warszawa, Poland.

10–19 Effets of columnar defects on flux lines pinning in $Bi_2Sr_2Ca_{1-x}Y_xCu_2O_8$ single crystals. *L.Ammor*[1], *R.De Sousa*[1], *J.C. Soret*[1], *V. Ta Phuoc*[1], *G. Villard*[2], *A. Ruyter*[1], *A. Wahl*[2] and *E. Olive*[1]. [1]Laboratoire LEMA Université F.Rabelais UFR Sciences 37200 Tours France. [2]Laboratoire CRISMAT,ISMRA 6 Bd Marechal juin 14050 Caen France.

10–21 Pinning of grain-boundary vortices by neighboring Abrikosov vortices in the nearby grains. *D.H. Kim*[1], *M.B. Field*[2], *D.J. Miller*[2], *K.E. Gray*[2], *Y.H. Kim*[3] and *T.S. Hahn*[3]. [1]Yeungnam University, Kyungsan, 712-749, S. Korea. [2]Argonne National Laboratory, Argonne, IL 60439, USA. [3]Korea Institute of Science of Technology, Seoul, 136-791, S.Korea.

10–22 Twin planes pinning in the ab-planes of large YBCO monodomain samples. *A. Sulpice*[1], *S. Sanfilippo*[2], *D. Bourgault*[2], *O. Laborde*[1], *X. Chaud*[3] and *R. Tournier*[2]. [1]Centre de Recherches sur les Tres Basses Temperatures, CNRS, Grenoble, BP 166, 38042 Grenoble CEDEX 9 France. [2]Laboratoire de Cristallographie, CNRS, Grenoble, BP 166, 38042 Grenoble CEDEX 9 France. [3]Centre de Recherches et d'Etudes Techniques Avancees, CNRS, Grenoble, BP 166, 38042 Grenoble CEDEX 9 France.

10–23 Direct evidence for a transition from elastic to plastic regimes in the vortex phase diagram of $YBa_2Cu_3O_{7-\delta}$. *S. Kokkaliaris*[1], *A. A. Zhukov*[1,2], *P. A. J. de Groot*[1], *R. Gagnon*[3], *L. Taillefer*[3] and *T. Wolf*[4]. [1]Department of Physics and Astronomy, University of Southampton, Southampton, SO17 1BJ, UK. [2]Physics Department, Moscow State University, Moscow 117234, Russia. [3]Department of Physics, McGill University, Montreal, Quebec, H3A 2T8, Canada. [4]Forschungszentrum Karlsruhe, Institut für Technische Physik, Postfach 3640,D-76021 Karlsruhe, Germany.

10–24 Study of Collective Flux Creep in Directionally Solidified YBCO. *R. A. Ribeiro*[1], *O. F. de Lima*[1], *X. Obradors*[2], *B. Martínez*[2] and *T. Puig*[2]. [1]Instituto de Fisica "Gleb Wataghin", UNICAMP, Brasil. [2]Institut de Ciencia de Materials de Barcelona, CSIC, Spain.

10–25 Anisotropic pinning defects in melt textured $YBa_2Cu_3O_7$ / Y_2BaCuO_5 composites by cold isostatic pressing. *J.Figueras*[1], *T.Puig*[1], *F.Sandiumenge*[1], *X.Obradors*[1] and *J.Rabier*[2]. [1]Institut de Ciència de Materials de Barcelona (ICMAB-CSIC), Bellaterra, Barcelona, 08193, Catalunya, Spain. [2]Laboratoire de Métallurgie Physique, UMR 6630 CNRS, Université de Poitiers, 86960 Futuroscope Cedex, France.

10–26 Microwave surface resistance measurements in YBCO/Au bilayer films and observation of proximity effect. *V. M. Pan*[1], *V. F. Tarasov*[1], *M.A. Lorenz*[2], *A. Y. Ivaniuta*[3] and *G. A. Melkov*[3]. [1]Institute for Metal Physics, Kiev 252142, Ukraine. [2] Institute of Experimental Physics II, University of Leipzig,Leipzig D-04103, Germany. [3] Department of Cryo- Taras Shevchenko University of Ukraine at Kiev, Kiev 252030, Ukraine.

10–27 Grain Boundary Magnetic Flux Pinning in High-T_C Superonductors. *A. Tuohimaa*[1], *J. Paasi*[1] and *T. Di Matteo*[2]. [1]Tampere University of Technology, Tampere, FIN-33720, Finland. [2]University of Salerno, Baroniss i,(Salerno), I-84081, Italy.

10–28 Effect of Inhomogeneous Distribution of Flux Pinning Strength on Critical Current Characteristics in Bi-2212 Tapes Prepared by PAIR Process. *M. Kiuchi*[1], *A. Yamasaki*[2], *T. Kiss*[1], *T. Matsushita*[1,2], *M. Takeo*[1] and *H. Kumakura*[3]. [1]Graduate School of Information Science and Electrical Engineering, Kyushu University, 6-10-1 Hakozaki, Higashi-ku Fukuoka 812-8581, Japan. [2]Department of Computer Science and Electronics, Kyushu Institute of Technology, 680-4 Kawazu, Iizuka 820-8502, Japan. [3]National Research Institute for Metals, 1-2-1 Sengen, Tsukuba 305-0047, Japan.

10–29 Magnetically investigated E-J characteristics of Bi-2212/Ag tape conductors. *H. Kumakura*, *H. Kitaguchi*, *T. Mochiku* and *K. Togano*. National Research Institute for Metals Tsukuba, Ibaraki 305-0047 Japan.

10–30 Dynamic flux patterns of multifilamentary Ag/Bi2Sr2Ca2Cu3010-d tapes at 8K-77K temperatures. *B.A.Glowacki*[1,2], *K. Van der Beek*[3] and *M.Konczykowski*[3]. [1] Department of Materials Science and Metallurgy University of Cambridge, Pembroke Street, Cambridge CB2 3QZ, U. K. [2]IRC in Superconductivity, University of Cambridge, Madingley Road, Cambridge CB3 OHE,U.K. [3]Laboratoire des Solides Irradies, Ecole Politechnique, 91128 Plalaiseau, France.

10–31 Surface nanostructuring and optimization of the vortex confinement in melt textured YBCO. *L.Gozzelino*[1], *R.Gerbaldo*[1], *G.Ghigo*[1], *E.Mezzetti*[1], *B.Minetti*[1], *P.Schätzle*[2], *G.Krabbes*[2], *E.Carlino*[3] and *A.Rovelli*[4]. [1]I.N.F.M. UdR Torino Politecnico; I.N.F.N. Sez. di Torino; Dipartimento di Fisica, Politecnico di Torino, Torino, Italy. [2]Institute of Solid State and Materials Research Dresden(IFW), Dresden, Germany. [3]C.N.R.S.M - PA.S.T.I.S., Brindisi, Italy. [4]I.N.F.N. Laboratorio Nazionale del Sud, Catania. [5].

10–32 Influence of the grain size on I-V curves and critical current density in granular superconductors in the self-field approximation. *A. Kilic*[1], *K. Kilic*[1] and *S. Senoussi*[2]. [1]Abant Izzet Baysal University Department of Physics, Bolu/Turkey. [2] Laboratoire de Physique des Solides (associé au C.N.R.S, URA, 0002) Université Paris Sud, 91405 Orsay Cedex, France.

10–33 The ab-plane and c-axis studies of vortex pinning in $Y_{0.4}Ho_{0.6}Ba_2Cu_3O_{7-\delta}$ high-T_C superconductor crystal. *Y.S. Chen*[1], *W.K. Chu*[1], *C.C. Lam*[1], *X. Jin*[2], *L.J. Shen*[1], *J.Q. Li*[1] and *J. Feng*[1]. [1]Department of Physic and Materials Science, City University of Hong Kong, Kowloon, Hong Kong. [2]National Laboratory of Solid State Microstructures and Department of Physics, Nanjing University, Nanjing 210008, P.R. China.

10–34 Chemical Introduction of flux pinning centres in Bi-2212 and YBCO. *A.V. Berenov*[1], *A.L. Crossley*[1], *A.D. Caplin*[2] and *J.L. MacManus-Driscoll*[1]. [1]Department of Materials, Imperial College, London, SW7 2BP. [2]Department of Physics, Imperial College, London, SW7 2BP.

10–35 The role of the LRE-rich phase in the formation of the peak effect in LRE-123 superconductors. *M. R. Koblischka*[1], *M. Muralidhar*[1], *T. Higuchi*[1], *K.Waki*[1], *N. Chikumoto*[1], *M. Murakami*[1] and *T. Wolf*[2]. [1]SRL/ISTEC, Div.3, 1-16-25 Shibaura, Minato-ku, Tokyo 105, Japan. [2]Institut fuer Technische Physik, Forschungszentrum Karlsruhe, D-76023 Karlsruhe, Germany.

10–36 Current-Voltage Characteristics and Flux Creep in Melt-Textured YBCO Strips. *H. Yamasaki* and *Y. Mawatari*. Electrotechnical Laboratory, Tsukuba, 1-1-4 Umezono, Ibaraki, 305-8568, Japan.

10–37 Characterisation of the magnetization hysteresis in RE-123 superconductors by exponentially decaying functions. *M. Jirsa*[1], *M. R. Koblischka*[2], *T. Higuchi*[2] and *M. Murakami*[2]. [1]Institute of Physics, ASCR, Na Slovance 2, CZ-182 21 Praha 8, Czech Republic. [2]SRL/ISTEC, Div. 3, 1-16-25 Shibaura, Minato-ku, Tokyo 105, Japan.

10–38 Distribution of vortex lattice melting obtained from electrical resistivity. *M. Pekala*[1] and *M. Ausloos*[2]. [1]Department of Chemistry, University of Warsaw, Al. Zwirki i Wigury 101, PL-02-089 Warsaw, Poland. [2]SUPRAS, Institut de Physique, Universite de Liege, Liege, B-4000 Sart Tilman, Belgium.

10–39 Anisotropic current transport property and its scaling in a YBCO film under the magnetic fields up to 27T. *T. Kiss*[1], *M. Inoue*[1], *M. Kiuchi*[1], *M. Takeo*[1], *T. Matsushita*[1,2], *S. Awaji*[3] and *K. Watanabe*[3]. [1]Dept. of Electrical and Electronic Systems Engineering, Kyushu University, Fukuoka 812-8581, Japan. [2]Kyushu Institute of Technology, Iizuka 820-8502, Japan. [3]Institute for Material Research, Tohoku University, Sendai 980-8577, Japan.

10–40 Neutron irradiation and annealing effects in single crystalline Y-123. *F. M. Sauerzopf*[1], *M. Zehetmayer*[1], *H. W. Weber*[1] and *M.A. Kirk*[2]. [1]Atomic Institute of the Austrian Universities, Vienna, A-1020, Austria. [2]Argonne National Laboratory, Argonne, IL 60439, USA.

10–41 Magnetic relaxation measurements in a thin disk of $YBa_2Cu_3O_{7-\delta}$ superconductor. *E. Moraitakis*, *M. Pissas*, *G. Kallias* and *D. Niarchos*. Institute of Materials Science, NCSR "Demokritos", 15310 Ag. Paraskevi, Athens,Greece.

10–44 He Irradiation and oxygen disorder in epitaxial $YBa_2Cu_3O_{7-\delta}$ thin films. *D. Arias*[1], *Z. Sefrioui*[1], *M. Varela*[2], *C. Leon*[1], *G. D. Loos*[1] and *J. Santamaria*[1]. [1]Departamento de Física Aplicada III, Universidad Complutense de Madrid, 28040- Madrid, Spain. [2]Departamento de Física, Universidad Carlos III de Madrid, Leganés 28911- Madrid, Spain.

10–45 The influence of the propagation of the critical state in the Ag-(Bi,Pb)2Sr2Ca2Cu3Ox sequentially pressed tape conductor on V-I characteristic. *B.A.Glowacki*[1,2]. [1]IRC in Superconductivity, University of Cambridge, Madingley Road, Cambridge CB3 OHE,U.K. [2]Department of Materials Science and Metallurgy University of Cambridge, Pembroke Street, Cambridge CB2 3QZ, U. K.

10–46 Surface resistance measurements on HTS films with a high- power niobium-shielded sapphire resonator. *T. Kaiser*[1], *M. A. Hein*[2] and *G. Müller*[2]. [1]Cryoelectra GmbH, Wettinerstr. 6H, D-42287 Wuppertal, Germany. [2]Bergische Universität Wuppertal, Fachbereich Physik, Gaußstr. 20, D-42097 Wuppertal, Germany.

10–47 Low frequencies method to estimate the Labusch parameter and the depinning current in thin YBCO films. *M.Pannetier*[1], *P.Bernstein*[1,2], *Ph.Lecoeur*[1,2], *T.D.Doan*[2] and *J.F.Hamet*[2]. [1]LUSAC-EIC (EA-2607) Site Universitaire de Cherbourg F50130 Octeville France. [2]CRISMAT-ISMRA (UMR-CNRS 6508) F14050 Caen France.

10–48 Crossover from 3D to pure 2D vortex-glass transition in deoxygenated $YBa_2Cu_3O_{7-\delta}$ thin films. *Z. Sefrioui*[1], *D. Arias*[1], *M. Varela*[2], *M. A. Lopez de la Torre*[3], *C. Leon*[1], *G. D. Loos*[1] and *J. Santamaria*[1]. [1]Departamento de Física Aplicada III, Universidad Complutense de Madrid, 28040- Madrid, Spain. [2]Departamento de Física, Universidad Carlos III de Madrid, Leganés 28911- Madrid, Spain. [3]Departamento de Física Aplicada, Universidad de Castilla-La Mancha, 13071 Ciudad Real, Spain.

10–48P1 Comparative study of Ca-doped and undoped $YBa_2Cu_3O_{7-\delta}$ thin film bicrystals lying in the low angle to high angle crossover regime. *G.A. Daniels*[1], *A. Gurevich* and *D.C. Larbalestier*. University of Wisconsin - Applied Superconductivity Center 1500 Engineering Drive, Madison, WI 53706 USA.

Session Josephson Junctions

10–49 Josephson effects and anisotropy in Tl-2212 thin films. *O.S. Chana*[1], *D.M.C. Hyland*[2], *R.J. Kinsey*[3], *W.E. Booij*[3], *M.G. Blamire*[3], *C.R.M. Grovenor*[4], *D. Dew-Hughes*[2] and *P.A. Warburton*[1]. [1]Department of Electronic Engineering, King's College London, Strand, London, WC2R 2LS, UK. [2]Department of Engineering Science, University of Oxford, Parks Road, Oxford, OX1 3PJ, UK. [3]Department of Materials Science, University of Cambridge, Pembroke Street, Cambridge, CB2 3QZ, UK. [4]Department of Materials, University of Oxford, Park Road, Oxford, OX1 3PH, UK.

10–50 Structure modification and superconducting properties of La- and Nd-substituted Bi-2201 crystals. *K.K. Uk*[1], *T.E. Os'kina*[2], *Yu.D. Tretyakov*[2], *V.F. Kozlovsii*[2], *A. Krapf*[3], *M.A. Lorenz*[4] and *Ya.G. Ponomarev*[5]. [1] M.V. Lomonosov Moscow State University, Faculty of Physics, 119 899 Moscow, Russia. [2] M.V. Lomonosov Moscow State University, Faculty of Chemistry, 119 899 Moscow, Russia. [3] Humboldt-Universität zu Berlin, Institut für Physik, Invalidenstr. 110, D-10 115 Berlin, Germany. [4] Bergische Universität Wuppertal, Fachbereich Physik, Gaußstr. 20, D-42 097 Wuppertal, Germany. [5] M.V. Lomonosov Moscow State University, Faculty of Physics, 119 899 Moscow, Russia.

10–51 Dependence of the gap parameter on the number of CuO_2 layers in a unit cell of the optimally doped BSCCOO, TBCCO and HBCCO. *Ya.G. Ponomarev*[1], *N.Z. Timergaleev*[1], *K.K. Uk*[1], *M.A. Lorenz*[2], *C. Janowitz*[3], *A. Krapf*[3] and *R. Manzke*[3]. [1] M.V. Lomonosov Moscow State University, Faculty of Physics, 119 899 Moscow, Russia. [2] Bergische Universität Wuppertal, Fachbereich Physik, Gaußstr. 20, D-42 097 Wuppertal, Germany. [3] Humboldt-Universität zu Berlin, Institut für Physik, Invalidenstr. 110, D-10 115 Berlin, Germany.

10–52 Three-dimensional Josephson junction networks: general properties and possible applications. *R. De Luca*. INFM - Dept. of Physics - University of Salerno - Baronissi (SA) 84081 ITALY.

10–53 Current transport mechanism in YBCO bicrystal junction on sapphire. *G. A. Ovsyannikov*, *A. D. Mashtakov*, *I.V. Borisenko* and *K. Y. Constantinian*. Institute of Radio Engineering and Electronics RAS, 103907, Moscow, Russia.

10–54 Observation of subharmonic gap structures in NbN/AlN/NbN tunnel junctions. *Z. Wang*[1], *A. Saito*[2] and *K. Hamasaki*[2]. [1]Kansai Advanced Research Center, Communications Research Laboratory 588-2 Iwaoka, Iwaoka-cho Nishi-ku, Kobe, 651-2401 Japan. [2]Nagaoka University of Technology 1603-1 Kamitomioka-cho, Nagaoka, 940-2188 Japan.

10–55 Effect of trapped Abrikosov vortices on the critical current of YBCO step-edge junctions. *K.H. Müller*, *E.E. Mitchell*, *C. Andrikidis* and *C.P. Foley*. CSIRO, Telecommunications and Industrial Physics, Sydney 2070, Australia.

10–56 A high-T_c multilayer ramp-edge junction process for digital circuit applications. *I.H. Song*[1], *E.H. Lee*[1], *S.Y. Yoon*[1] and *G. Park*[2]. [1]Samsung Advanced Institute of Technology, P.O.Box 111, Suwon 440-600, Korea. [2]Sogang University, C.P.O.Box 1142, Seoul 100-611, Korea.

10–57 Fabrication of YBCO step-edge Josephson junctions. *M.J. Chen*[1], *H.W.Yu*[1], *J.R. Chiou*[1], *J.H. Chen*[1], *H.C. Yang*[1], *H.E. Horng*[2], *S.Y. Yang*[2], *J.T. Jeng*[2], *C.H. Chen*[2] and *Y.C. Liu*[2]. [1]Department of Physics, National Taiwan University, Taipei 106, Taiwan. [2]Department of Physics, National Taiwan Normal Unversiy, Taipei 117, Taiwan.

10–58 Influence of the passive region on zero field steps for window junctions. *A. Benabdallah*[1], *J. G. Caputo*[2] and *N. Flytzanis*[3]. [1]Laboratoire de Matématiques Institut National de Sciences Appliquées and Unité C.N.R.S. 6085, B. P. 8, 76131 Mont-Saint-Aignan Cedex France. [2]Laboratoire de Physique Mathématique et Théorique Université de Montpellier II and Unité C.N.R.S. 5095 34095 Montpellier cedex 05 France. [3]Physics Dept. University of Crete POB 2208 710 03 Heraklion Greece.

10–59 Laminar phase flow for an exponentially tapered Josephson oscillator. *A. Benabdallah*[1], *J. G. Caputo*[2] and *A. C. Scott*[3]. [1]Laboratoire de Matématiques Institut National de Sciences Appliquées and Unité C.N.R.S. 6085, B. P. 8, 76131 Mont-Saint-Aignan Cedex France. [2]Laboratoire de Physique Mathématique et Théorique Université de Montpellier II and Unité C.N.R.S. 5095 34095 Montpellier cedex 05 France. [3]Department of Mathematics, University of Arizona, Tucson, AZ, 85721, U.S.A. Department of Mathematical Modeling, Technical University of Denmark, Lyngby, Dk.

10–60 Characterisation of ramp-edge Josephson junctions and junction arrays with Ga-doped $PrBa_2Ga_xCu_{3-x}O_7$ and $SrTiO_3$-barrier. *H. Burkhardt*, *A. Rauther* and *M. Schilling*. Institut fuer Angewandte Physik und Zentrum fuer Mikrostrukturforschung der Universitaet Hamburg, Jungiusstrasse 11, 20355 Hamburg, Germany.

10–61 Flux flow properties of $Bi_2Sr_2Ca_1Cu_2\ O_{8+y}$ Intrinsic Josephson junctions fabricated by Si ion implantation. *K. Nakajima*[1,3], *S. Sudo*[1], *T. Tachiki*[1] and *T. Yamashita*[2,3]. [1]Research Institute of Electrical Communication, Tohoku University, Sendai, Japan. [2]New Industry Creation Hatchery Center, Tohoku University, Sendai, Japan. [3]CREST, Japan Science & Technology Cooporation, Japan.

10–62 SNS Ramp Type Josephson Junctions for Highly Integrated Superconducting Circuit Applications. *R. Pöpel*, *D. Hagedorn*, *F.-Im. Buchholz* and *J. Niemeyer*. Physikalisch-Technische Bundesanstalt, Bundesallee 100, D-38116 Braunschweig, Germany.

10–63 Effect of pressure on the c-axis critical current of Bi-2212 intrinsic Josephson junctions. *A. Yurgens*, *D. Winkler* and *T. Claeson*. Department of Microelectronics and Nanoscience, Chalmers University of Technology, S-41296, Gothenburg, Sweden.

10–64 Vortex dynamics and Cherenkov radiation of linear waves in long narrow Josephson junction connected with wide stripline. *A.V. Chiguinev*[1] and *V.V. Kurin*[2]. [1]IPM RAS, Nizhny Novgorod, 603600, Russia. [2]IPM RAS, Nizhny Novgorod, 603600, Russia.

10–65 Josephson Current along the c-axis of the Mesa-structured $Bi_2Sr_2CaCu_2O_{8+\delta}$. *K. Hirata* and *T. Mochiku*. [1]National Research Institute for Metals, 1-2-1 Sengen, Tsukuba,Ibaraki, 305-0047, JAPAN. [2]1-2-1 Sengen, Tsukuba,Ibaraki, 305-0047, JAPAN.

10–66 Effects induced by microwaves on S-I-N-I-S junctions. *G. Carapella*, *G. Costabile* and *R. Latempa*. Dipartimento di Fisica and Unita' INFM, Baronissi 84081, Italy.

10–67 Submicron $YBa_2Cu_3O_{7-\delta}$ Step-Edge Josephson Junctions For A Scanning SQUID Microscope Sensor. *P.Larsson*[1], *A.Tzalenchuk*[1,2], *Z.G.Ivanov*[1] and *T.Claeson*[1]. [1]Department of Physics, Chalmers University of Technology and University of Göteborg, S-412 96 Göteborg, Sweden. [2]Institute of crystallography RAS, 117333 Moscow, Russia.

10–68 Calculation of flux focusing efficiency of grain-boundary Josephson junctions electrodes. *C.Cordier*, *S.Flament*, *C.Dubuc* and *E.Sassier*. GREYC - ISMRA , 6 Bd Marechal Juin F-14050 CAEN Cedex, France.

10–69 Highly localised light ion irradiation of $YBa_2Cu_3O_{7-\delta}$ using metal masks. *W.E. Booij*[1], *N.H. Peng*[2], *F. Kahlmann*[1], *R. Webb*[2], *E.J. Tarte*[1], *D.F. Moore*[1], *C. Jeynes*[2] and *M.G. Blamire*[1]. [1]IRC in Superconductivity, University of Cambridge, Cambridge, CB3 0HE, United Kingdom. [2]Surrey Centre for Research into Ion Beam Applications, School of Electronic Engineering, Information Technology and Mathematics, University of Surrey, Guildford, GU2 5XH, United Kingdom.

10–70 Two-dimensional arrays of tunnel junctions: transport properties and phase transitions. *I. Wooldridge*[1], *B. Camarota*[2] and *P. Delsing*[1]. [1]Chalmers University of Technology and Göteborg University, 412 96 Göteborg, Sweden. [2]CNRS-CRTBT, BP166, 38042 GRENOBLE CEDEX 9, France.

10–71 Statistical analysis of the size dependence of *c*-axis critical currents in Bi2212 mesas. *V.M. Krasnov*[1,2]. [1]Department of Microelectronics and Nanoscience, Chalmers University of Technology, S-41296 Göteborg, Sweden. [2]Institute of Solid State Physics, 142432 Chernogolovka, Russia.

10–72 Influence of the passive region on zero field steps for window junctions. *A. Benabdallah*[1], *J. G. Caputo*[2] and *N. Flytzanis*[3]. [1]Laboratoire de Matématiques Institut National de Sciences Appliquées and Unité C.N.R.S. 6085 B. P. 8, 76131 Mont-Saint-Aignan cedex, France. Place Emile Blondel, B.P. 08 76131, Mont Saint Aignan France. [2]Laboratoire de Physique Mathématique et Théorique, Université de Montpellier II and Unité C.N.R.S. 5095 34095 Montpellier cedex 05, France. [3]Department of Physics University of Crete POB 2208 710 03 Heraklion, Greece.

10–73 Laminar phase flow for an exponentially tapered Josephson oscillator. *A. Benabdallah*[1], *J. G. Caputo*[2] and *A. C. Scott*[3]. [1]Laboratoire de Matématiques Institut National de Sciences Appliquées and Unité C.N.R.S. 6085 B. P. 8, 76131 Mont-Saint-Aignan cedex, France. Place Emile Blondel, B.P. 08 76131, Mont Saint Aignan France. [2]Laboratoire de Physique Mathématique et Théorique, Université de Montpellier II and Unité C.N.R.S. 5095 34095 Montpellier cedex 05, France. [3]Department of Mathematics, University of Arizona, Tucson, AZ, 85721, U.S.A. Department of Mathematical Modeling, Technical University of Denmark, Lyngby, Dk.

Session Passive Devices

10–75 Frequency dispersion of tunability and losses in ferrite/superconducting structures. *A. Kuzhakhmetov*[1], *A. Jenkins*[1], *D.M.C. Hyland*[1], *M. Koledintseva*[2] and *D. Dew-Hughes*[1]. [1] Department of Engineering Science, University of Oxford Department of Engineering Science, University of Oxford, Parks Road, Oxford OX1 3PJ, UK. [2]Department of Radio Engineering, Moscow Power Engineering Institute, Moscow 111250, Russia.

10–76 Comparative study of YBaCuO thin film microwave surface resistance measurement methods. *A. Dégardin*[1], *A. Gensbittel*[1], *P. Crozat*[2], *M.S. Boutboul*[3], *M. Achani*[4], *Y. Roelens*[4], *S. Sautrot*[3], *J-C. Carru*[4], *M. Fourrier*[3] and *A. Kreisler*[1]. [1]LGEP - UMR 8507 CNRS - Universités Paris 6 & Paris 11 - Supélec, Plateau de Moulon, 91190 Gif-sur-Yvette, France. [2]IEF - UMR 8622 CNRS - Université Paris 11 - Bâtiment 220, 91405 Orsay, France. [3]DIM - Université Paris 6 - Tour 12, 4 Place Jussieu, 7 005 Paris, France. [4]IEMN - UMR 8520 - Université Lille 1 - Avenue Poincaré, BP 69 - 59652 Villeneuve d'Ascq, France.

10–77 Ion milled YBaCuO films for microwave applications. *R. Monaco*[1], *U. Gambardella*[2], *C. Beneduce*[3], *F. Bobba*[3], *M. Boffa*[3], *A.M. Cucolo*[3] and *M.C. Cucolo*[3]. [1]Istituto di Cibernetica del C.N.R., Arco Felice (Na), Italy. [2]Centro Ricerche ENEA, Frascati, Italy. [3]Dipartimento di Fisica, Universita' di Salerno, Baronissi (Sa), Italy.

10–78 Development of superconductive microwave filters for UMTS mobile communications. *B.Marcilhac*, *Y.Lemaitre*, *D.Mansart* and *J.C. Mage*. U.M.R.137 Thomson-CSF LCR / CNRS, Orsay,France.

10–79 Calculation of RF spurious in planar superconducting structures. *J. Parrón*, *C. Collado*, *J. Mateu*, *E. Úbeda*, *J. M. O'Callaghan* and *J. M. Rius*. Universitat Politécnica de Catalunya Campus Nord UPC, D3 Barcelona 08034 Spain.

10–80 Full wave analysis of YBCO Coplanar transmission lines on Lithium Niobate Substrates. *E. Rozan*[1], *J.M. O'Callaghan*[1], *J. Byun*[2] and *F.J. Harackiewicz*[2]. [1]Universitat Politècnica de Catalunya Campus Nord, Modulo D3 Jordi Girona 1-3 08034 Barcelona Spain. [2]Southern Illinois University Dpt of Electrical Engineering 62901 Carbondale, Il USA.

10–81 Simulation of Global Heating Effects on Non-linear Resonance Curves at Microwave Frequencies. *A. Cowie*[1], *S. Thiess*[1], *N. Lindop*[2], *J.C. Gallop*[3] and *L.F. Cohen*[1]. [1]Blackett Laboratory, Imperial College Prince Consort Rd, London SW7 2BZ. [2]Dept. of Biological Sciences, University of Warwick, CV4 2AL. [3]National Physical Laboratory, Queens Rd, Teddington, Middlesex.

10–82 Forward coupled superconducting filters for DCS1800 mobile phone base stations. *M. Salluzzo*[1], *A. Andreone*[1], *M. Iavarone*[1], *F. Palomba*[1], *G. Pica*[1], *R. Vaglio*[1], *G. Panariello*[2], *R. Monaco*[3], *A. Guidarelli Mattioli*[4] and *E. Petrillo*[5]. [1]INFM Unita' di Napoli and Universita' di Napoli "Federico II", Napoli, Italy. [2]Dip. di Ingegneria Elettronica, Universita' di Napoli "Federico II", Napoli, Italy. [3]INFM Unita' di Salerno and Universita' di Salerno, Salerno, Italy. [4]Omnitel Pronto Italia, Ivrea, Italy. [5]Ansaldo C.R.I.S., Napoli, Italy.

10–83 Varactor switchable/tunable HTS-notch filter for the mobile communication system. *B.A.Aminov*[1], *H.Chaloupka*[1], *S.Kolesov*[1], *H.Piel*[1], *J.Bohult*[2], *H.Medelius*[2] and *A.Rogachev*[3]. [1]Cryoelectra GmbH, Wettinerstr. 6h, D-42287 Wuppertal, Germany. [2]Ericsson Radio Access AB, Gullfossgatan 6, S-16493 Stockholm, Sweden. [3]Bergische Universitat, Fachbereich Elektrotechnik, D-42097, Wuppertal, Germany.

10–84 Superconductor Band-Pass Analog-to-Digital Converter. *V.K. Semenov*[1] and *E.B. Wikborg*[2]. [1]Department of Physics, SUNY, Stony Brook, NY 11794, USA. [2]Ericsson Components AB, Kista-Stockholm, SE 164 81, Sweden.

10–85 Performance of passive microwave devices made from thin films of $YBa_2Cu_3O_{7-\delta}$ superconductor. *E. Moraitakis*, *M. Pissas* and *D. Niarchos*. Institute of Materials Science, NCSR "Demokritos", 15310 Ag. Paraskevi,Athens,Greece.

10–86 Third-order local nonlinear microwave response of $YBa_2Cu_3O_7$ thin films. *R.K.Belov*, *V.V.Kurin*, *Yu.N.Nozdrin* and *E.E.Pestov*. Institute for Physics of Microstructures(RAS),Nizhny Novgorod,603600,Russia.

10–87 Study of the tunability of superconducting passive microwave components by laser light. *M. S. Boutboul*[1], *S. Sautrot*[1], *A. Dégardin*[2], *H. Kokabi*[1], *A. Kreisler*[2], *M. Pyée*[1] and *M. Fourrier*[1]. [1]LDIM - University Pierre and Marie Curie 4, place Jussieu - 75252 Paris - France. [2]LGEP - Supelec plateau Moulon - 91190 Gif sur Yvette - France.

10–88 Surface Wave High Temperature Superconducting Resonators. *G.A. Melkov*[1], *Y.V. Egorov*[1], *A.N. Ivanyuta*[1], *V.Y. Malysh*[1] and *A.M. Klushin*[2,3]. [1]Kiev Taras Shevchenko University, Kiev, 252017, Ukraine. [2]Institut fuer Schicht - und Ionentechnik, Forschungszentrum Juelich GmbH, Juelich, 52425, Germany. [3]Institute of Electronic Measurements "KVARZ", Nizhny Novgorod, 603009, Russia.

10–89 Microwave power handling capabilities and intermodulation distortion in sputtered YBCO films on sapphire and $LaAlO_3$. *P. Lahl*, *J. Einfeld* and *R. Wördenweber*. Institut fuer Schicht- und Ionentechnik (ISI), Forschungszentrum Juelich, 52425 Juelich, Germany.

Session Materials related to electronic applications

10–90 Undestructive Microwave Characterization of Large-Area Single Crystal Dielectric Substrates and Ferroelectric Thin Films. *N.T.Cherpak*[1], *Yu.G.Makeev*[1], *A.P.Motornenko*[1], *I.N.Chukanova*[2] and *E.V.Izhyk*[1]. [1] Usikov Institute of Radiophysics and Electronics, National Academy of Sciences, Kharkov, 310085, Ukraine. [2] Institute of Single Crystales , National Academy of Sciences, Kharkov, 310001, Ukraine.

10–91 Ferroelectric polarisation charging in $YBa_2Cu_3O_{7-\delta}/SrTiO_3/Pb(Zr_{0.54}Ti_{0.46})O_3/Au$ heterostructures. *R. Aidam*, *D. Fuchs* and *R. Schneider*. Forschungszentrum Karlsruhe, Institut für Nukleare Festkorperphysik, P.O.B. 3640, D-76021 Karlsruhe, Germany.

10–92 Mosaic structure of epitaxial films (001) $YBa_2Cu_3O_{7-\delta}$ (10.2)Al_2O_3 and microwave properties of microstrip resonators. *O.D. Poustylnik*. SRC "Phonon" Kiev KPI-3240 Ukraine.

10–93 Plasma Optical Emission Studies during HTSC Thin Film Deposition Process Optimisation. *V.N. Tsaneva*[1,3], *C. Christou*[1], *J.H. Durrell*[1,2], *G. Gibson*[1,2], *F. Kahlmann*[2], *E.J. Tarte*[2], *Z.H. Barber*[1,2], *M.G. Blamire*[1,2] and *J.E. Evetts*[1,2]. [1]Cambridge University, Dept. of Materials Sci., Cambridge CB2 3QZ, UK. [2]IRC in Superconductivity, Cambridge University, Cambridge CB3 0HE, UK. [3]Institute of Electronics, Bulg. Acad. Sci., Sofia 1784, Bulgaria.

10–94 New Prospects for Using Layered Superconductors in Electronics. *A.Lykov*. P.N.Lebedev Physical Institute of RAS, 117924, Moscow, Russia.

10–95 Dynamic electrical response of YBaCuO thin films as a function of substrate crystallinity for electronic applications. *A. De Luca*, *A. Dégardin*, *É. Caristan*, *G. Klimek*, *A. Gaugue*, *J. Baixeras* and *A. Kreisler*. LGEP - UMR 8507 CNRS - Universités Paris 6 & Paris 11 - Supélec, Plateau du Moulon, Gif-sur-Yvette, 91190, France.

10–96 Protective layers for the encapsulation of YBCO - thin film devices. *W. Prusseit*. THEVA Thin Film Technology GmbH, 85386 Eching, Germany.

10–97 Fabrication of Low Microwave Surface Resistance $YBa_2Cu_3O_y$ Films on MgO Substrate by Self-template Method. *M. Kusunoki*, *Y. Takano*, *M. Mukaida* and *S. Ohshima*. Yamagata University, Yonezawa, Yamagata, 992-8510, Japan.

10–98 Atomic force microscopy with conducting tips: an original and efficient way to probe superconducting film surface. *O. Schneegans*, *A. Dégardin*, *É. Caristan*, *P. Chrétien*, *F. Houzé*, *A. De Luca*, *L. Boyer* and *A. Kreisler*. LGEP - UMR 8507 CNRS - Universités Paris 6 & Paris 11 - Supélec, Plateau du Moulon, Gif-sur-Yvette, 91190, France.

10–99 Columnar defects as a tool to investigate vortex confinement mechanisms in YBCO films. *G.Ghigo*[1], *C.Camerlingo*[2], *G.Cuttone*[3], *R.Gerbaldo*[1], *L.Gozzelino*[1], *E.Mezzetti*[1], *B.Minetti*[1] and *A.Rovelli*[3]. [1]I.N.F.M. UdR Torino Politecnico; I.N.F.N. Sez. di Torino; Dipartimento di Fisica, Politecnico di Torino, Torino, Italy. [2]Istituto di Cibernetica del C.N.R., Arco Felice (NA), Italy. [3]I.N.F.N. Laboratorio Nazionale del Sud, Catania, Italy.

Session SQUIDs, and SQUIDs applications

10–100 Optimization of Inductance for the Directly-coupled SQUID Gradiometer. *J.T. Jeng*[1], *Y.C. Liu*[1], *S. Y. Yang*[1], *H.E. Horng*[1], *J.H. Chen*[2] and *H.C. Yang*[2]. [1]Department of Physics, National Taiwan Normal University, Taipei 117, Taiwan. [2]Department of Physics, National Taiwan University, Taipei 106, Taiwan.

10–101 Detection of Internal Defects using HTS-SQUID for Non-destructive Evaluation. *Y.H Hatsukade*[1,2], *N.K. Kasai*[2], *F.K. Kojima*[3], *H.T. Takashima*[2] and *A.I. Ishiyama*[1]. [1]Waseda Univ.,3-4-1 Ohkubo,Shinjuku-ku,Tokyo,169-8555,Japan. [2]Electrotechnical Laboratory,1-1-4 Umezono,Tsukuba-shi,Ibaraki,305-8568,Japan. [3]Kobe Univ.,1-1 Rokkodai-cho,Nada-ku,Kobe,657-8501,Japan.

10–102 Development of an HTS Cryogenic Current Comparator. *M. D. Early*[1] and *M. A. van Dam*[1,2]. [1] Meaurement Standards Laboratory, Industrial Research Limited, P O Box 31-310, Lower Hutt,6009, New Zealand. [2]Present Address: School of Engineering, University of Canturbury, Private Bag 4800, Christchurch, New Zealand.

10–103 Development of HTS Resistive SQUIDs for Noise Thermometry. *D.A. Peden*[1], *J.C. Macfarlane*[1], *L. Hao*[2], *R.P. Reed*[2] and *J.C. Gallop*[2]. [1]Department of Physics and Applied Physics, University of Strathclyde, Glasgow G4 0NG, UK. [2]Centre for Basic and Thermal Metrology, National Physical Laboratory, Teddington, TW11 0LW, UK.

10–104 Application of SQUID based position detectors for testing the Weak Equivalence Principle at the Drop Tower Bremen. *W. Vodel*, *S. Nietzsche*, *H. Koch*, *J.v. Zameck Glyscinski* and *R. Neubert*. Friedrich Schiller University Jena, Institute of Solid State Physics, Helmholtzweg 5, 07743 Jena, Germany.

10–105 High Temperature SQUID Magnetometers for Nondestructive Evaluation. *J.T. Jeng*[1], *J.H. Chen*[2], *H.C. Yang*[1] and *H.E. Horng*[2]. [1]National Taiwan Normal University Department of Physics 88 Section 4, Ting-Chou Road Taipei,117-18 Taiwan. [2]National Taiwan University Department of Physics One Section 4, Roosevelt Road Taipei,106-17 Taiwan.

10–106 Effect of asymmetric junction configurations on the voltage to magnetic flux transfer function in resistively shunted dc SQUIDs. *G. Testa*[1,2], *E. Sarnelli*[1], *S. Pagano*[1] and *M. Russo*[1]. [1]Istituto di Cibernetica - CNR, Arco Felice, I-80072, Italy. [2]Istituto Nazionale di Fisica della Materia, Unita di Napoli, Italy.

10–107 Radiofrequency dc SQUID Amplifier with Microstrip Inpit Coil: Simulations and Experiment. *M.A. Tarasov*[1], *A.S. Kalabukhov*[2], *S.I. Krasnosvobodtsev*[3], *O.V. Snigirev*[2], *Z.G. Ivanov*[4] and *A. Kovalenko*[1]. [1]Insitute of Radioelectronics and Engeneering, Moscow,103907 Russia. [2]Moscow State University, Moscow, 119899, Russia. [3]Lebedev Institute of Physics, Russian Academy of Sciencies, Moscow,117924, Russia. [4]Department of Physics, Chalmers University of Technology and University of Geteborg, Geteborg, Sweden.

10–108 Noise Characteristics of a Two Stage dc SQUID-based Amplifier. *D.E. Kirichenko*[1], *A.B. Pavolotskij*[2], *I.G. Prokhorova*[1], *O.V. Snigirev*[1], *R. Mezzena*[3], *S. Vitale*[3], *Y.V. Maslennikov*[4] and *V.Y. Slobodtchikov*[4]. [1]Department of Physics, Moscow State University, 119899 Moscow, Russia. [2]Nuclear Physics Institute, Moscow State University, 119899 Moscow, Russia. [3]Department of Physics, University of Trento, 38050 Trento, Italy. [4]Cryoton Co. Ltd., 142092 Troitsk, Moscow Region, Russia.

10–109 A scanning SQUID microscopy of the HTS thin-film specimens at 77 K. *S.A. Gudoshnikov*[1], *M.I. Koshelev*[2], *A.S. Kalabukhov*[2], *O.V. Snigirev*[2], *L.V. Matveets*[1], *M. Muck*[3], *J. Dechert*[3] and *C. Heiden*[3]. [1]Institute of Terrestrial Magnetism, Ionosphere and Radio Wave Propagation, Russian Academy of Sciences, (IZMI-RAN), Troitsk, Moscow region 142092, Russia. [2]Moscow State University, Moscow, 119899, Russia. [3]Institut fur Angewandte Physik Justus Liebig Universitat Giessen, 35392 Giessen, Germany.

10–110 Low-field NMR and MRI of room temperature samples detected with a high-T_c SQUID. *K. Schlenga*[1], *R.E. de Souza*[2], *A. Wong-Foy*[2], *R. McDermott*[1], *A. Pines*[2] and *J. Clarke*[1]. [1]Department of Physics, UC Berkeley and LBNL, Berkeley, CA 94720 USA. [2]Department of Chemistry, UC Berkeley and LBNL, Berkeley, CA 94720 USA.

10–111 A 40-channel double relaxation oscillation SQUID system for biomagnetic multichannel applications. *Y. H. Lee, H. C. Kwon, J. M. Kim, Y. K. Park* and *J.-C. Park.* Korea Research Institute of Standards and Science, P.O. Box 102, Yusong, Taejon, 305-600, Republic of Korea

ORAL SESSION 11A: Coated Conductors II

Wednesday Afternoon, September 15th, 17:30-19:00

17:30 ***11A–1 Prospects of YBCO coated conductors for applications** *H.C. Freyhardt*[1,2], *F. García-Moreno*[2,1], *J. Hoffmann*[1], *J. Dzick*[1], *S. Sievers*[1], *A. Usoskin*[2] and *C. Jooss*[1]. [1]Institut fuer Materialphysik,Universitaet Goettingen,D-37073 Goettingen. [2]Zentrum fuer Funktionswerkstoffe gGmbH,D-37073 Goettingen.

18:00 **11A–2 Microstructure in $YBa_2Cu_3O_{7-\delta}$ Coated Conductors and Their Buffer Layers.** *S.E. Babcock*[1], *Chau-Yun Yang*[1], *Yuehong Wu*[1], *D.M. Feldman*[1], *A. Polyanskii*[1], *A. Ichinose*[1], *D.C. Larbalestier*[1], *A. Goyal*[2] and *S.R. Foltyn*[3]. [1]University of Wisconsin, Madison Wisconsin, USA. [2]Oak Ridge National Laboratory, Oak Ridge Tennessee, USA. [3]Los Alamos National Laboratory, Los Alamos New Mexico, USA.

18:15 **11A–3 Multi-functional flexible high temperature superconducting tape (MUST).** *J. Denul*[1], *I. Van Driessche*[2], *H.T. Lintelo*[3], *R. De Gryse*[1], *A. Testsekou*[4], *E. Georgiopoulos*[4], *S. Hoste*[2], *B.A. Glowacki*[5], *R. Garre*[6] and *E. Maher*[7]. [1]Centre for Vacuum and Materials Sciences, Gent, B-9000, Belgium. [2]University of Gent, Gent, B-9000, Belgium. [3]Innovative Sputtering Technology, Zulte, B-9870, Belgium. [4]Cereco, Chalkida, 34100, Greece. [5]University of Cambridge, Cambridge, CB2 3QZ, United Kingdom. [6]Europa Metalli, Fornace di Barga, 55052, Italy. [7]Oxford Instruments, Eynsham, Witney, OX8 1TL, United Kingdom. [8]Cryogenic, London, W3 7QE, United Kingdom. [9]KTH, Stockholm, S-10044, Sweden. [10]GAIKER, Zamudio, 48170, Spain.

90 **11A–4 Laser deposition of biaxially aligned MgO buffer layers.** *R. Huehne*[1], *B. Holzapfel*[2], *C.-G. Oertel*[1], *L. Schultz*[2] and *W. Skrotzki*[1]. [1]Institut fuer Kristallographie und Festkoerperphysik, Technische Universitaet Dresden, 01062 Dresden, Germany. [2]Institut fuer Metallische Werkstoffe, Institut fuer Festkoerper- und Werkstofforschung, PF 270016, 01171 Dresden, Germany.

45 **11A–5 Fabrication and Characterization of Textured YBCO Superconductor Thick Films on Oxide/Cu Sheets.** *M. Jin*[1], *E. Kim*[1], *T.H. Sung*[2], *S.C. Han*[2] and *K. No*[1]. [1] Electronic and Optical Materials Laboratory, Dep. of Mat. Sci.& Eng., Korea Advanced Institute of Science and Technology 373-1, KuSung-dong, YuSung-gu, TaeJon, Korea 305-701,. [2]Materials and Corrosion Research Laboratory, Korea Electric Power Research Institute 103-16 Munji-dong, Yusong-gu, Taejon, Korea 305-380.

ORAL SESSION 11B: Cables, Transformers ans Generators

Wednesday Afternoon, September 15th, 17:30-19:00

90 ***11B–1 Development and test of a 100 kVA superconducting transformer operated at 77 K.** *P. Kummeth*[1], *R. Schlosser*[2], *P. Massek*[1], *H. Schmidt*[2], *C. Albrecht*[1], *D. Breitfelder*[2] and *H.-W. Neumüller*[1]. [1]Siemens AG, Corporate Technology, Erlangen, D-91052, Germany. [2]Siemens AG, Power Transmission and Distribution, Nuremberg, D-90027, Germany.

90 ***11B–2 Power applications for superconducting cables.** *O. Tønnesen*. Department of Electric Power Engineering, Technical University of Denmark, Building 325, DK-2800 Lyngby, Denmark.

90 **11B–3 Short-Circuit Test of a Bi-2223 Model Winding for a High-Voltage-Type HTS Transformer.** *K. Funaki*[1], *M. Iwakuma*[1], *K. Kajikawa*[1], *T. Bohno*[2], *S. Nose*[2], *M. Konno*[3], *J. Kuwayama*[3], *H. Maruyama*[4], *T. Ogata*[4] and *K. Tsutsumi*[5]. [1]Kyushu University, 6-10-1 Hakozaki, Higashi-Ku, Fukuoka 812-8581, Japan. [2]Fuji Electric Corporate Research & Development, Ltd., Ichihara, Chiba 290-8511, Japan. [3]Fuji Electric Co., Ltd., Shinagawa, Tokyo 141-0032, Japan. [4]Kyushu Transformer Co. Ltd., Fukuma-Cho, Munakata 811-32, Japan. [5]Kyushu Electric Power Co., 2-1-47 Shiobaru, Minami-Ku, Fukuoka 815-8520, Japan.

45 **11B–4 Manufacture and Testing of a HTS Prototype Cable for Power Transmission.** *G. Pasztor*[1], *A. Anghel*[1], *B. Jakob*[1], *A.M. Fuchs*[1], *D. Trajkovic*[1], *R. Wesche*[1], *G. Vécsey*[1] and *R. Schindler*[2]. [1]Centre de Recherches en Physique des Plasmas, Technologie de la Fusion Ecole Polytechnique Fédérale de Lausanne, CH-5232 Villigen PSI, Switzerland CH-5232 Villigen. [2]Brugg Kabel AG, CH-5201 Brugg, Switzerland.

ORAL SESSION 11C: Passive Devices II

Wednesday Afternoon, September 15th, 17:30-19:00

90 **11C–1 Investigations on the unloaded quality factor of planar resonators with respect to substrate materials and packaging.** *A. Baumfalk*, *M. Reppel*, *H. Chaloupka* and *S. Kolesov*. University of Wuppertal FB13, Wuppertal, 42119, Germany.

45 **11C–2 Progress towards superconducting optoelectronic modulators.** *J.M. O'Callaghan*[1], *J. Fontcuberta*[2], *L. Torner*[1], *R. Pous*[1] and *A. Cardama*[1]. [1]Universitat Politecnica de Catalunya (UPC) Campus Nord UPC-D3 Barcelona 08034 Spain. [2]ICMAB-CSIC, Campus UAB Bellaterra 08193 Spain.

90 **11C–3 Applications of coupled dielectric resonators using HTS coated SrTiO3 pucks: tuneable resonators and novel thermometry.** *J.C. Gallop* and *L. Hao*. National Physical Laboratory, Teddington, TW11 0LW, UK.

15 **11C–4 Bandpass filter on a parallel array of coupled coplanar waveguides.** *A. Deleniv*[1], *V. Kondratiev*[1], *P.K. Petrov*[2] and *I. Vendik*[1]. [1] St.-Petersburg Electrotechnical University, St.-Petersburg, 197376, Russia. [2] Chalmers University of Technology, Goteborg, S-412 96, Sweden.

18:30 **11C–5 High - temperature superconducting microwave circuits with ferrimagnetic or ferroelectric tuning.** *D. Schemion, M. Winter, R. Ott* and *N. Klein*. Forschungszentrum Jülich GmbH Institut of Solid State Research 52425 Jülich Germany.

18:45 **11C–6 Progress in superconducting preselect filters for mobile communications base stations.** *J.S. Hong*[1], *M.J. Lancaster*[1], *D. Jedamzik*[2], *R.B. Greed*[2] and *J.C. Mage*[3]. [1]SEEE, Univ. of Birmingham, Edgbaston, Birmingham B15 2TT, UK. [2]Marconi Res.Cen.,Great Baddow,Chelmsford Essex,CM2 8HN, UK. [3]Thomson-CSF/CNRS,UMR137,Domaine de Corbeville F-91404,France.

ORAL SESSION 11D: Flux Pinning II

Wednesday Afternoon, September 15th, 17:30-19:00

17:30 ***11D–1 Flux pinning in textured high temperature superconductors by artificial defects.** *H.W. Weber*. Atominstitut der Österreichischen Universitäten, A-1020 Wien, Austria.

18:00 **11D–2 Pinning force diagram of the ternary superconductor (Nd,Eu,Gd)-123 with secondary phase additions.** *M. R. Koblischka, M. Muralidhar* and *M. Murakami*. SRL/ISTEC, Div.3, 1-16-25 Shibaura, Minato-ku, Tokyo 105, Japan.

18:15 **11D–3 Vortex pinning dynamics anisotropy for perfect YBCO films with $J_c\,(77K) > 3\,MA/cm^2$ studied by direct transport measurements of $J_c(H,T,\theta)$.** *V.M. Pan*[1], *V.A. Komashko*[1], *A.L. Kasatkin*[1], *V. L. Svetchnikov*[1], *A. G. Popov*[1], *A. V. Pronin*[1], *A. Yu. Galkin*[1], *C.L. Snead*[2], *M. Suenaga*[2] and *H.W. Zandbergen*[3]. [1]Institute for Metal Physics, Kiev 252142, Ukraine. [2]Brookhaven National Laboratory, Upton, NY 11973, USA. [3] National Centre for HREM, TU Delft, Rotterdamseweg,34, AL Delft 2628, The Netherlands.

18:30 **11D–4 Surface columnar defects as a tool to tune the static and dynamic superconducting properties of HTS bulks without any damage.** *E.Mezzetti, R.Gerbaldo, G.Ghigo, L.Gozzelino* and *B.Minetti*. I.N.F.M. UdR Torino Politecnico; I.N.F.N. Sez. di Torino; Dipartimento di Fisica, Politecnico di Torino, Torino, Italy.

18:45 **11D–5 Flux pinning forces in irradiated a-axis oriented $EuBa_2Cu_3O_7$ films.** *J. I. Martin*[1], *E. M. Gonzalez*[1], *W. K. Kwok*[2] and *J. L. Vicent*[1]. [1]Dpto. Fisica Materiales, Universidad Complutense, 28040 Madrid (SPAIN). [2]Materials Science Division, Argonne National Laboratory, IL. 60439 (USA).

POSTER SESSION 12

Wednesday Evening, September 15th, 19:00-21:00

Session Bulk materials and materials aspects

12–1 Melt processing and flux pinning behaviors of (Nd, Sm)-Ba-Cu-O superconductors. *A.M. Hu, G. Krabbes, P. Schätzle* and *W. Bieger*. Insitute of solid state and materials researchs Dresden, P.O. Box: 270016, D-01171 Dresden, Germany.

12–2 Decomposition of the supersaturated $Nd_{1+x}Ba_{2-x}Cu_3O_z$ solid solution as a way to superconductors with strong vortex pinning. *E.A.Goodilin, A.P.Soloshenko, V.V.Lennikov, A.V.Knot'ko* and *Yu.D.Tretyakov*. Moscow State University, Chemistry Faculty, Inorganic Chemistry Divison, Lenin Hills, 119899, Moscow, Russia.

12–3 Thermodynamics of the $RE_1Ba_2Cu_3O_{7-x}$ (REBCO) Phases. *J.A.G. Nelstrop* and *J.L. MacManus-Driscoll*. Departement of Materials, Royal School of Mines, Prince Consort Road, London SW7 2BP, England.

12–4 Effects of Nd partial substitution on the Y123/Y211 composites. *R. Cabré*[1], *Jna. Gavaldà*[2], *R. Solé*[2], *J. Massons*[2], *M. Aguiló*[2] and *F. Díaz*[2]. [1]Dept. d'Enginyeria Electrònica, Elèctrica i Automàtica, Univ. Rovira i Virgili, 43005 Tarragona, Spain. [2]Lab. de Física Aplicada i Cristal.lografia, Univ. Rovira i Virgili, 43005 Tarragona, Spain.

12–5 Peculiarities of high pressure-high temperature processing of MeBCO (Me=Y, Nd). *T. Prikhna*[1], *W. Gawalek*[2], *V. Moshchil*[1], *V. Melnikov*[3], *F. Sandiumenge*[4], *P. Nagorny*[1], *T. Habisreuther*[2], *P. Shaetzle*[5], *Ch. Wende*[2] and *S. Dub*[1]. [1]Institute for Superhard Materials, Kiev, 254074, Ukraine. [2]Institut fuer Physikalische Hochtechnologie, Jena, D-07743,. [3]Institute of Geochemistry, Mineralogy and Ore-Formation, Kie. [4]Instituto de Cincia de Materiales de Barcelona, Bellaterra,. [5]Institut fuer Festkrper- und Werkstofforschung, Dresden, D-0.

12–6 Directional solidification in air of NdBaCuO bulk superconductor. *A. Vecchione*[1,2], *P. Tedesco*[1], *M. Gombos*[1,2], *M. Polichetti*[1,2] and *S. Pace*[1,2]. [1]Dipartimento di Fisica Università di Salerno Via Salvador Allende, Baronissi (SA), I-84081 Italia. [2] Istituto Nazionale per la Fisica della Materia Unità di Salerno Via Salvador Allende, Baronissi (SA), I-84081 Italia.

12–7 Microstructure development in thick YBCO films grown by liquid phase epitaxy. *K.A. Kursumovic*[1,2], *Y.S. Cheng*[1,2], *A.P. Bramley*[1], *B.A. Glowacki*[1,2] and *J.E. Evetts*[1,2]. [1]Department of Materials Science and Metallurgy, University of Cambridge, Pembroke Street, Cambridge CB2 3QZ, UK. [2]IRC in Superconductivity, Cavendish Laboratory, Madingley Road, University of Cambridge, Cambridge CB3 0HE, UK.

12–8 Statistical Thermodynamics of Point Defects, Dopant Segration, and Carrier Densities Near Dislocations, Grain Boundaries, and Other Interfaces in $YBa_2Cu_3O_x$. *D. O. Welch*. Department of Applied Science, Brookhaven National Laboratory, Upton, New York 11973-5000 USA.

12–9 Rf field dependencies of the surface impedance of YBCO: A new analysis of the ratio $r = dX_s/dR_s$. *K. Numssen*[1], *E. Gaganidze*[2] and *J. Halbritter*[2]. [1]TU Muenchen, James-Frank Str. 1, D-85747 Garching, Germany. [2]Forschungszentrum Karlsruhe, IMF 1, Postfach 3640, D-76021 Karlsruhe, Germany.

12–10 Gold-Doped YBCO Superconducting Samples. *A. Marino*, *M. Sanchez*, *D. Riano* and *H. Sanchez*. Department of Physics, Universidad Nacional de Colombia, Bogota, Colombia.

12–11 Enrichment of NdBCO Superconducting Powders by Electromagnetic Separation. *E.Broide*[1], *G.E.Shter*[2] and *G.S.Grader*[2]. [1]Separator Ltd.,Kiryat Weizmann Science Park,Ness-Ziona,70400,Israel. [2]Chemichal Engineering Dept.,Technion,Haifa,32000,Israel.

12–12 Superconducting Properties of Textured $YBa_2Cu_3O_{7-\delta}/Y_2BaCuO_5$ Grown with Addition of Nanoparticles. *Z.H. He*[1,2], *O.B. Surzhenko*[1], *T. Habisreuther*[1] and *W. Gawalek*[1]. [1]Institut für Physikalische Hochtechnologie e.V., Postfach 100239, D-07702, Jena, Germany. [2]Department of Physics, Zhongshan University, Guangzhou, 510275, P.R. China.

12–13 Exploring the ternary superconductors of the type (Nd,Eu,Gd)-123. *M. Muralidhar*, *M. R. Koblischka* and *M. Murakami*. SRL/ISTEC, Div.3, Tokyo 105, Japan.

12–14 High transport critical current of Y123 zone melted samples processed in a microwave cavity. *S. Marinel*[1], *D. Bourgault*[2], *O. Belmont*[3], *A. Sotelo*[1], *G. Desgardin*[1] and *B. Raveau*[1]. [1]CRISMAT laboratory-CNRS UMR 6508, 6 Bd. Du Marechal Juin, 14050 Caen cedex. France. [2]Laboratoire de Cristallographie-CRETA, 25 Avenue des Martyrs, 38042 Grenoble Cedex 9, France. [3] Centre de Recherches sur les Très Basses Températures Centre National de La Recherche Scientifique 25 Avenue des Martyrs, 38042 Grenoble Cedex 9, France.

Session Flux pinning and ac losses

12–15 Surface effect on the M-H diagram of the current-carrying superconductor in a parallel field. *Yu.A.Genenko*[1,2] and *H.C.Freyhardt*[1,3]. [1]Zentrum für Funktionswerkstoffe gGmbH, 37073 Göttingen, Germany. [2]Donetsk Physical and Technical Institute NAS Ukraine, 340114 Donetsk, Ukraine. [3]Institute für Materialphysik, Universität Göttingen, 37073 Germany.

12–16 AC transport losses in self fields for superconducting parallel-conductors cables. *A. Oota*[1], *R. Inada*[1] and *T. Fukunaga*[2]. [1]Toyohashi University of Technology, Tempaku-cho, Toyohashi, Aichi 441-8 580, Japan. [2]Gifu National College of Technology, Shinsei-cho, Motosu-gun, Gifu 501-0495, Japan. .

12–17 AC Losses in BiPbSrCaCuO/Ag 19-filaments tape in form of a helix measured by different potential taps. *M.Majoros*[1,2], *B.A.Glowacki*[1,3], *A.M.Campbell*[1], *Z. Han*[4] and *P. Vase*[4]. [1]IRC in Superconductivity,University of Cambridge,Cambridge,CB3 OHE,U.K. [2]Institute of Electrical Engineering,SAS,Bratislava,842 39,Slovak Republic. [3]Department of Materials Science and Metallurgy,University of Cambridge,Cambridge,CB2 3QZ,U.K. [4]Nordic Superconductor Technology,Brondby,DK-2605,Denmark.

12–18 Influence of matrix resistivity on transport ac losses and current-voltage characteristics of BiPbSrCaCuO-2223/Ag multifilamentary tapes. *M.Majoros*[1,2], *B.A.Glowacki*[1,3], *A.M.Campbell*[1], *Z. Han*[4] and *P. Vase*[4]. [1]IRC in Superconductivity,University of Cambridge,Cambridge,CB3 OHE,U.K. [2]Institute of Electrical Engineering,SAS,Bratislava,842 39,Slovak Republic. [3]Department of Materials Science and Metallurgy,University of Cambridge,Cambridge,CB2 3QZ,U.K. [4]Nordic Superconductor Technology,Brondby,DK-2605,Denmark.

12–19 Influence of defects on transport ac losses and current-voltage characteristics of BiPbSrCaCuO-2223/Ag multifilamentary tapes. *M.Majoros*[1,2], *B.A.Glowacki*[1,3], *A.M.Campbell*[1], *Z. Han*[4] and *P. Vase*[4]. [1]IRC in Superconductivity,University of Cambridge,Cambridge,CB3 OHE,U.K. [2]Institute of Electrical Engineering,SAS,Bratislava,842 39,Slovak Republic. [3]Department of Materials Science and Metallurgy,University of Cambridge,Cambridge,CB2 3QZ,U.K. [4]Nordic Superconductor Technology,Brondby,DK-2605,Denmark.

12–20 Time constants and coupling losses in superconducting cables and in magnetic systems. *S. Takács*. Institute of Electrical Engineering, Slovak Academy of Sciences, 842 39 Bratislava, Slovakia.

12–21 Voltage and Losses in Hard Superconductors Carrying Alternating Transport Current. *A.N.Ulyanov*. Donetsk Physico-Technical Institute Ukrainian Academy of Sciences, 340114 Donetsk-114, Ulyanov.

12–22 Numerical modeling of the Critical State and calculation of AC losses and current profiles in multifilamentary Bi-2223 tapes. *Y. Yang*, *E. Martínez* and *C. Beduz*. Institute of Cryogenics, University of Southampton, Southampton, United Kingdom.

12–23 Temperature Dependence of AC Losses in High-Temperature Superconductors. *N. Magnusson*[1], *N. Schönborg*[1] and *S. Hörnfeldt*[2]. [1]Royal Institute of Technology, Electric Power Engineering, SE-100 44 Stockholm, Sweden. [2]ABB Corporate Research, SE-721 78 Västerås, Sweden.

12–24 Transport ac losses and current-voltage characteristics of BiPbSrCaCuO-2223/Ag multifilamentary tapes with Ag and AgMg sheaths. *M.Majoros*[1,2], *B.A.Glowacki*[1,3], *A.M.Campbell*[1], *M.Leghissa*[4], *B.Fischer*[5] and *T.Arndt*[5]. [1]IRC in Superconductivity,University of Cambridge,Cambridge,CB3 OHE,U.K. [2]Institute of Electrical Engineering,Slovak Academy of Sciences,Bratislava,842 39,Slovak Republic. [3]Department of Materials Science and Metallurgy,University of Cambridge,Cambridge,CB2 3QZ,U.K. [4]Siemens AG, ZT EN 4,Erlangen,D-91050,Germany. [5]Vacuumschmelze GmbH,HT-SE,Hanau,D-63450,Germany.

12–25 Superconductor modelling : an useful tool for ac losses. *E. Vinot*[1], *P. Tixador*[1], *G. Meunier*[2] and *G. Donnier-Valentin*[1]. [1]CNRS-CRTBT/LEG, Grenoble, 38042, France. [2]LEG - CNRS/INPG-UJF, Saint Martin d'Heres, 38402, France.

12–26 Magnetization and transport loss of Bi-2223 tapes in alternating magnetic field. *M.P. Oomen*[1], *J. Rieger*[1], *M. Leghissa*[1], *J.J. Rabbers*[2] and *B. ten Haken*[2]. [1]Siemens AG, Corporate Technology, PO Box 3220, 91050 Erlangen, Germany. [2]Low Temperature Division, Faculty of Applied Physics, University of Twente, PO Box 217, 7500 AE Enschede, The Netherlands.

12–27 Scanning Hall Probe Imaging of Multifilamenary HTS Conductors: Implications for AC Losses. *G.K. Perkins*, *J.E. Everett* and *A.D. Caplin*. Centre for High Temperature Super-conductivity, Blackett Lab., Imperial College London SW7 2BZ, UK.

12–28 Self-field losses and I-V curves of Bi-2223 tape without silver sheath. *M. Polak* and *L. Jansak*. Institute of Electrical Engineering, Slovak Academy of Sciences Bratislava, 842 39 Slovakia.

12–29 Weak AC Magnetic Field Influence on Nonlinear Flux Diffusion in the Mixed State of Superconductors. *A.L. Kasatkin*, *V. V. Vysotskii* and *V. M. Pan*. Superconductivity Dept., Institute of Metal Physics, 36 Vernadsky str., Kiev 252142, Ukraine.

12–30 What causes the steep increase of the critical current density below 20 K in Bi-based superconductors?. *M. R. Koblischka* and *M. Murakami*. SRL/ISTEC, Div.3, 1-16-25 Shibaura, Minato-ku, Tokyo 105, Japan.

12–31 Alternative approach to the hysteresis of transport current in Bi-based tapes. *P. Nalevka*[1], *M. Jirsa*[1], *M. R. Koblischka*[2] and *D. Dew-Hughes*[3]. [1]Institute of Physics AV CR, Na Slovance 2, 182 21 Praha 8, Czech Republic. [2]SRL/ISTEC, Div. 3 1-16-25 Shibaura, Minato-ku Tokyo 105 [3]Department of Engineering Science, University of Oxford, Oxford OX1 3PJ, UK.

12–32 Transport AC losses in (Bi,Pb)SrCaCuO-2223/Ag (6+1) multifilamentary tapes with different architecture. *M.Majoros*[1,2], *B.A.Glowacki*[1,3], *A.M.Campbell*[1], *M.Apperley*[4] and *F.Darmann*[4]. [1] IRC in Superconductivity, University of Cambridge, Madingley Road, Cambridge CB3 OHE,U.K. [2]Institute of Electrical Engineering, SAS, Bratislava, Slovak Republic. [3]Department of Materials Science and Metallurgy University of Cambridge, Pembroke Street, Cambridge CB2 3QZ, U. K. [4]Metal Manufactures Ltd., Australian Technology Park, Eveligh, 1430, Australia.

12–33 Introduction of Flux-Pinning Defects in Bi-2212 Superconducting Tapes. *T. Haugan, W. Wong-Ng, L. P. Cook, H. J. Brown* and *L. Schwartzendruber*. National Institute of Standards and Technology Gaithersburg, MD 20899 U.S.A.

12–34 Transport Properties of $Bi_2Sr_2CuO_{6+\delta}/CaCuO_2$ Multilayers Obtained by Molecular Beam Epitaxy. *S.L. Prischepa*[1], *M. Salvato*[2], *C. Attanasio*[2], *G. Carbone*[2] and *L. Maritato*[2]. [1] State University of Informatics and RadioElectronics, State University of Informatics and RadioElectronics, Minsk, 220600, Belarus. [2]INFM and Dipartimento di Fisica Università di Salerno, Baronissi, Salerno,84081,Italy.

12–35 Influence of collective interaction of turns on transverse-field losses in superconducting multifilamentary wires. *K. Kajikawa, A. Takenaka, M. Iwakuma* and *K. Funaki*. Kyushu University, Fukuoka, 812-8581, Japan.

12–36 AC Losses in Bi-2223 Multifilamentary Tapes. *F. Sumiyoshi*[1], *K. Fukushige*[1], *M. Nakagami*[1] and *H. Hayashi*[2]. [1]Kagoshima University, Kagoshima, 890-0065, Japan. [2]Kyushu Electric Power Co. Inc., Fukuoka, 812-0053, Japan.

12–37 AC losses in filamentary YBCO/hastelloy superconducting tapes. *K.H. Müller, N. Savvides* and *J. Herrmann*. CSIRO, Telecommunications and Industrial Physics, Sydney 2070, Australia.

12–38 Magnetic AC Loss Measurements using Hall Sensor Magnetometry. *M.P. Staines*[1], *S. Rupp*[1], *A.D. Caplin*[2] and *S. Fleshler*[3]. [1]Industrial Research Ltd, Lower Hutt, New Zealand. [2]Imperial College, London SW7 2BZ, UK. [3]American Superconductor Corporation, Westborough, MA 01581, USA.

Session Fault current limiters and related materials

12–39 Current Limiting Properties of YBCO-Films on Sapphire Substrates. *A. Heinrich*[1], *R. Semerad*[1], *H. Kinder*[1], *H. Mosebach*[2] and *M. Lindmayer*[2]. [1]Technical University of Munich, Physics Department E10, 85748 Garching, Germany. [2]Technical University of Braunschweig, Institut für Hochspannungstechnik, D-38023 Braunschweig, Germany.

12–40 Shaping and Assembling of HTS Bulk Materials for High-Current Applications. *J. Reichert, R. Ochs, M. Kläser* and *M. Sander*. Forschungszentrum Karlsruhe GmbH, INFP, P. O. Box 3640, D-76021 Karlsruhe.

12–41 Ceramic Substrates for Bi-2212 Partial Melt Processing. *S. Köbel, D. Schneider, R. Nussbaumer* and *L.J. Gauckler*. Swiss Federal Institute of Technology, CH-8092 Zürich, Switzerland.

12–42 Critical Current Densities in Bi-2212+Ag / MgO Thick Films. *S. Köbel, D. Schneider, L. Fall, P. Sütterlin* and *L.J. Gauckler*. Swiss Federal Institute of Technology, CH-8092 Zürich, Switzerland.

12–43 Non-Uniformities In Multifilament Superconductors - Influence On Quench Currents Under Fast Current Change. *V.S. Vysotsky*[1,2], *Y.A. Ilyin*[1,2], *K. Funaki*[1], *M. Takeo*[1], *K. Shimohata*[3], *S. Nakamura*[3], *T. Kaito*[4], *K. Hasegawa*[4] and *A.L. Rakhmanov*[5]. [1]Kyushu University, Fukuoka, 812-8581, Japan. [2]Visiting scientists from Kurchatov Institute, Moscow, Russia. [3]AT R& D Center, Mitsubishi Electric Co, Japan. [4]TRC, Kansai Electric Power Company, Japan. [5]SCAPE, Russian Academy of Science, Moscow, Russia.

12–44 Non-Uniformities In Multifilament Superconductors - Influence On Quench Development Under Fast Current Change. *V.S. Vysotsky*[1,2], *Y.A. Ilyin*[1,2], *K. Funaki*[1], *M. Takeo*[1], *K. Shimohata*[3], *S. Nakamura*[3], *T. Kaito*[4], *K. Hasegawa*[4] and *A.L. Rakhmanov*[5]. [1]Kyushu University, Fukuoka, 812-8581, Japan. [2]Visiting scientists from Kurchatov Institute, Moscow, Russia. [3]AT R& D Center, Mitsubishi Electric Co, Japan. [4]TRC, Kansai Electric Power Company, Japan. [5]SCAPE, Russian Academy of Science, Moscow, Russia.

12–45 Quench behaviour of high temperature superconducting bulk material in resistive fault current limiters. *M. Noe*[1], *K.-P. Juengst*[1], *F. N. Werfel*[2], *M. Baecker*[3], *J. Bock*[3] and *S. Elschner*[4]. [1] Forschungszentrum Karlsruhe, Institut fuer Technische Physik, Eggenstein-Leopoldshafen, 76344, Germany. [2] Adelwitz Technologiezentrum GmbH, Adelwitz, 04886, Germany. [3] Aventis Research & Technologies, Hürth, 50351, Germany. [4] Fachhochschule Mannheim, Mannheim, 68157, Germany.

12–46 Computer Modelling of Superconducting Fault Current Limiters. *R.A.Weller*, *A.M.Campbell*, *T.A.Coombs* and *R.J.Storey*. IRC in Superconductivity, Madingley Road, Cambridge CB3 0HE, UK.

12–47 Characteristics of Bulk Superconducting Cylinder for Magnetic Shielding Type Superconducting Fault Current Limiter. *S.N. Noguchi*, *A.I. Ishiyama* and *H.U. Ueda*. Dept. of EECE, Waseda University, 3-4-1 Ohkubo, Shinjuku-ku, Tokyo 169-8555, Japan.

12–48 Utility Survey of Requirements for a HTS Fault Current Limiter. *J.N. Nielsen*[1], *P. Joergensen*[1], *J.J. Oestergaard*[1] and *O. Toennesen*[2]. [1]DEFU Research Institute of Danish Electric Utilities, P.O. Box 259, 2800 Lyngby, Denmark. [2]Department of Electric Power Engineering, Technical University of Denmark, 2800 Lyngby, Denmark.

12–49 Resistive current limiter with Bulk Bi:2223. *J.G. Noudem*[1,2], *J. M. Barbut*[2], *O. Belmont*[2], *D. Bourgault*[1], *J. Sanchez*[2], *P. Tixador*[3] and *R. Tournier*[1]. [1]CRETA, CNRS, B.P. 166, 38042 Grenoble cedex 09, France. [2]SCHNEIDER ELECTRIC S.A, A3, rue Volta,38050 Grenoble cedex 09, France. [3]CRTBT/LEG, CNRS, B.P. 166, 38042 Grenoble cedex 09, France.

12–50 Key Design Issues of YBCO Current Leads: Low Resistance Contacts. *U.F. Delor*, *R. Rothfeld*, *D. Wippich* and *F.N. Werfel*. Adelwitz Technologiezentrum GmbH, Adelwitz, D-04886, Germany.

12–51 Quench transition in high current bulk YBCO elements for Fault Current Limiters. *E. Mendoza*[1], *X. Granados*[1], *T. Puig*[1], *E. Varesi*[1], *L. García-Tabarés*[2] and *X. Obradors*[1]. [1]Institut de Ciència de Materials de Barcelona, CSIC, Campus UAB, 08193 Bellaterra, Spain. [2]Centro de Estudios de Técnicas Aplicadas, CEDEX, Alfonso XII, 6, 28040 Madrid, Spain.

12–52 Large - Area YBCO-Sputter Deposition for Fault Current Limiters. *W. Klein*[1], *U. Pyritz*[2], *R. Wördenweber*[1], *B. Holländer*[1], *R. Kutzner*[1], *H. Schiewe*[2], *J. Einfeld*[1], *S. Bunte*[1] and *U. Krüger*[2]. [1]Forschungszentrum Jülich, ISI, D-52425 Jülich, Germany. [2]Siemens AG, ZT MF5, Siemensdamm 50, D-13629 Berlin, Germany.

12–53 Thermal characterization of an inductive fault current limiter*. *L.G. Sanz*, *M.R. Osorio*, *S.R. Currás*, *J.A. Veira*, *J. Maza* and *F. Vidal*. Laboratorio de Bajas Temperaturas y Superconductividad, Universidad de Santiago de Compostela Santiago de Compostela, E-15706, Spain.

12–54 Current limitation by YBCO single domains. *P. Tixador*[1], *J.M. Duval*[1], *D. Bourgault*[2], *R. Tournier*[2] and *D. Isfort*[2]. [1]CNRS-CRTBT/LEG, Grenoble, 38042, France. [2]CNRS-Laboratoire de Cristallographie, Grenoble, 38042, France.

12–55 Rectifier Type Fault Current Limiter by Use of Micro SMES. *T.Ise*, *T.Oka*, *N.H.Nguyen* and *S.Kumagai*. Department of Electrical Engineering, Graduate School of Engineering, Osaka University, 2-1, Yamada-oka, Suita, Osaka, 565-0871, JAPAN.

12–56 The Effect of Jc and Magnetic Shielding Capacity on the Performance of Superconducting Screening Fault Current Limiter. *I.-G. Chen* and *J.-M. Lin*. Dept. of Materials Sci. & Eng., National Cheng Kung Univ., 1 Ta-Hsueh Rd., Tainan, Taiwan, R.O.C.

12–57 Current Induced Transition into a Highly Dissipative State: Implication for the Fault Current Limiter. *L. Antognazza*[1], *M. Decroux*[1], *N. Musolino*[1], *J.-M. Triscone*[1], *W. Paul*[2], *M. Chen*[2] and *Ø. Fischer*[1]. [1]Department of Condensed Matter Physics, University of Geneva, 24 Ernest Ansermet, 1211 Genève 4, Switzerland. [2]ABB Corporate Research, 5405 Baden, Switzerland.

12–58 A Small Scale Test Model for an AC-Fault Current Limiter. *B.A.Aminov*[1] and *H.Piel*[1,2]. [1]Cryoelectra GmbH, Wettinerstr. 6H, 42287 Wuppertal, Germany. [2]Bergische Universitaet, Gaussstr. 20, 42096 Wuppertal, Germany.

12–59 Properties of the quench release in current-carrying thin film HTS. *B. Heismann*. B. Heismann, Siemens AG Erlangen, ZT EN 4, Paul-Gossen-Str. 100, 91050 Erlangen, Germany.

12–60 Current Limiting Characteristics of Inductive Fault Current Limiter Using YBCO Bulk Superconducting Ring. *D. Ito*, *S. Harada* and *O. Miura*. Tokyo Metropolitan University, Hachioji, Tokyo, 192-0397, Japan.

12–61 Preparation of switching elements for a resistive type HTS fault current limiter. *R. Nies*[1], *W. Schmidt*[1], *B. Seebacher*[2], *B. Utz*[1] and *H.-W. Neumüller*[1]. [1]Siemens AG, Corporate Technology, 91052 Erlangen, Germany. [2]Siemens AG, Corporate Technology, 81730 Munich, Germany.

12–62 Study of MCP BSCCO 2212 bulk material with respect to application in resistive current limiters. *S. Elschner*[1], *J. Bock*[2], *G. Brommer*[2] and *L. Cowey*[2]. [1]FH Mannheim, University of Applied Sciences, D-68163 Mannheim, Germany. [2]Aventis Research & Technologies, D-50351 Huerth, Germany.

12–63 Transport Critical Current Measurements in a Pressurised Liquid Nitrogen Vessel. *B. Zeimetz*[1], *B. A. Glowacki*[1], *Y. S. Cheng*[1], *K.A. Kursumovic*[1], *E. Mendoza*[2], *X. Obradors*[2], *S. X. Dou*[3], *J. E. Evetts*[1] and *T. Puig*[2]. [1]Department of Materials Science, Cambridge University, Cambridge CB2 3QZ, UK. [2]ICMAB-CSIC, Campus de la Universitat Autonoma de Barcelona, 08193 Bellaterra, Spain. [3]ISEM, University of Wollongong, NSW 2522, Australia.

Session Wires tapes and coated conductors

12–64 Weak Link Path Model and E - J Characterisitcs in Ag/Bi2223 Tapes. *K. Osamura*[1], *K. Ogawa*[1], *T. Thamizhavel*[1] and *A. Sakai*[2]. [1]Department of Materials Science and Engineering, Kyoto University, Sakyo-ku, Kyoto 606-8501, Japan. [2]Mesoscopic Materials Research Center, Kyoto University, Sakyo-ku, Kyoto 606-8501, Japan.

12–65 Effect of intermediate treatment on the structure of monocore Bi-2223/Ag tapes made by two-axial and eccentric rolling. *W. Pachla*[1], *R. Diduszko*[2], *P. Kovac*[3] and *I. Husek*[3]. [1]High Pressure Research Center, Polish Academy of Sciences, ul. Sokolowska 29, 01-142 Warszawa, Poland. [2]Institute of Vacuum Technology, ul. Długa 44/50, 00-241 Warszawa, Poland. [3]Institute of Electrical Engineering, Slovak Academy of Sciences, Dubravska cesta 9, 842-39 Bratislava, Slovak Republic.

12–66 Relating the Magnetic Field Response to the Transport Properties of BSCCO/Ag Superconducting Tapes. *W.F.A. Klein Zeggelink*[1], *J.J. Rabbers*[1], *B. ten Haken*[1], *H.H.J. ten Kate*[1], *M.D. Bentzon*[2] and *P. Vase*[2]. [1]Faculty of Applied Physics, University of Twente, P.O. Box 217, 7500 AE Enschede, The Netherlands. [2]Nordic Superconductor Technologies, Priorparken 878, 2605 Brøndby, Denmark.

12–67 The Investigation of the Formation of Bi-2223 in Bi-2223/ Ag-Tapes by in situ XRD. *T. Fahr*, *K. Fischer*, *W. Pitschke* and *H.-P. Trinks*. IFW Dresden, Dresden, D-01069, Germany.

12–68 Magneto Optical and Electromagnetic Investigations of Multifilamentary Ag/BSCCO-2223 Tapes. *A. Polyanskii*[1], *D.M. Feldmann*[1], *X.Y. Cai*[1], *L. Schwartzkopf*[1], *J. Jiang*[1], *D. Apodaca*[1], *Y. Wu*[1], *S. E. Babcock*[1], *D. C. Larbalestier*[1], *Q. Li*[2], *R.D. Parrella*[2], *M.W. Rupich*[2] and *G.N. Riley, Jr.*[2]. [1]University of Wisconsin, Applied Superconductivity Center, 1500 Engineering Dr., Madison, WI 53705 USA. [2]American Superconductor Corporation, Two Technology Dr., Westborough, MA 01581 USA.

12–69 Reactivity of electrically isolating barrier layers in Bi(Pb)-2223/Ag tapes with coated filaments. *H. Caudevilla*, *G.F. De la Fuente*, *L.A. Angurel* and *R. Navarro*. Instituto de Ciencia de Materiales de Aragón, CSIC-Universidad de Zaragoza, CPS, María de Luna 3, 50015 Zaragoza (Spain).

12–70 Efficiency of filament decoupling in Bi(Pb)-2223/Ag tapes with electrically isolating barrier layers. *H. Caudevilla*, *J.A. Gómez*, *L.A. Angurel* and *R. Navarro*. Instituto de Ciencia de Materiales de Aragón, CSIC-Universidad de Zaragoza, CPS, María de Luna 3, 50015 Zaragoza (Spain).

12–71 Bi,Pb(2223) phase formation in Ag-sheathed tapes: direct in-situ observations by high-temperature neutron- and synchrotron X-ray diffraction. *E. Giannini*, *E. Bellingeri*, *R. Passerini*, *F. Marti*, *M. Dhallé*, *M. Ivancevic* and *R. Flükiger*. Département de Physique de la Matière Condensée Université de Genève 24, quai Ernest-Ansermet CH-1211 Genève 4 Switzerland.

12–72 Study of microstructure homogeneity in Bi2223 multifilamentary tapes. *Y. B. Huang*, *D.M. Spiller*, *J. Jutson*, *S. Mills*, *I. Ferguson*, *R. Prowse*, *C. Groombridge* and *W.W. Blendl*. BICC Superconductors, Oak Road, Wrexham LL13 9XP, United Kingdom.

12–73 Critical current anisotropy in longitudinaly strained Bi(2223) tapes: probing the connectivity. *R. Passerini*, *F. Marti*, *L. Porcar*, *M. Dhallé*, *G. Witz*, *B. Seeber* and *R. Flükiger*. Département de Physique de la Matière Condensée, Université de Genève, CH-1211 Genève 4, Switzerland.

12–74 Flux penetration into the system of superconducting filaments in normal conducting matrix. *S. Takács* and *F. Gömöry*. Institute of Electrical Engineering, Slovak Academy of Sciences, 842 39 Bratislava, Slovakia.

12–75 Flat rolling of round and square superconducting multifilaments for HTS tapes. *M.Eriksen*[1], *J.I.Bech*[1], *N.Bay*[1] and *P.Skov-Hansen*[2]. [1]Institut for Manufacturing Engineering, Technical University of Denmark, 2800 Lyngby, Denmark. [2]Nordic Superconductor Technologies A/S Priorparken 685, DK-2605 Brondby, Denmark.

12–76 Influence of geometry and overpressure processing on Bi-2212/Ag multifilamentary tapes. *B. Lehndorff*[1], *J. L. Reeves*[2], *A. Polyanskii*[2], *M. Rikel*[2], *E. E. Hellstrom*[2] and *D. C. Larbalestier*[2]. [1]Bergische Universität-GH Wuppertal, FB Physik, Institut für Materialwissenschaften, Gaußstr. 20, D-42097 Wuppertal, Germany. [2]Appl. Supercond. Center, University of Wisconsin-Madison, 1500 Engineering Dr., Madison, WI 53706, U.S.A.

12–77 Intermediate mechanical deformation processes in the OPIT fabrication of HTS Bi-2223 tapes. *P. Skov-Hansen*[1], *Z. Han*[1], *H. Wu*[1], *A. Polyanskii*[2], *D. M. Feldmann*[2], *X. Y. Cai*[2], *D. C. Larbalestier*[2], *P. Kovac*[3], *F. Marti*[4] and *R. Flükiger*[4]. [1]Nordic Superconductor Technologies A/S, Priorparken 685, DK-2605 Brondby, Denmark. [2]Applied Superconductivity Center, University of Wisconsin-Madison, 1500 Engineering drive, Madison, Wisconsin 53706, USA. [3] Institute of Electrical Engineering, Slovak Academy of Sciences, Dubravska cesta 9, 842 39 Bratislava, Slovakia. [4]University of Geneva, Dept. Phys. Mat. Cond., 24, quai Ernest Ansermet, 1211 Geneva, Switzerland.

12–78 AC-losses vs temperature and frequency in multifilamentary Ag-sheated bscco−2223. *R. Tebano*[1], *F. Gömöry*[2], *R. Mele*[3] and *A. Melini*[3,4]. [1]Dipartimento di Scienza dei Materiali, Universita' degli Studi di Milano, via Cozzi, 53,Milano, 20126, Italy. [2]Institute of Electrical Engineering, Slovak Academy of Science, Dubravska 9, 842 39, Bratislava, Slovak Republic. [3]Pirelli Cavi & Sistemi S.p. A., v.le Sarca 222, Milano, 20126, Italy. [4]Dipartimento di Fisica, Universita' degli Studi di Milano, via Celoria, 16, Milano, 20133, Italy.

12–79 Phase formation in Bi2223 tapes at different cooling rates and oxygen partial pressure. *E. Young*[1], *Y. Yang*[1], *C. Beduz*[1], *Y. Huang*[2] and *C.M. Friend*[2]. [1]Institute of Cryogenics, Unversity of Southampton, Southampton SO17 1BJ, UK. [2]BICC Superconductors, Oak Rd., Wrexham. LL13 9XP UK.

Session Materials related to electronic applications

12–80 Comparison of structural and compositional properties of YBaCuO thin films for microwave applications. *A. Dégardin*[1], *S. Bourg*[1], *X. Castel*[2], *C. Bodin*[1], *J. Berthon*[3], *C. Dolin*[4], *É. Caristan*[1], *F. Pontiggia*[1], *A. Perrin*[2] and *A. Kreisler*[1]. [1]LGEP - UMR 8507 CNRS - Universités Paris 6 & Paris 11 - Supélec, Plateau du Moulon, 91190 Gif-sur-Yvette, France. [2]LCSIM - UMR 6511 CNRS - Université Rennes 1 - Avenue du Général Leclerc, 35042 Rennes, France. [3]LCS - URA 446 CNRS - Université Paris 11 - Bâtiment 414, 91405 Orsay, France. [4]Unité Mixte de Physique CNRS - Thomson-CSF - Domaine de Corbeville, 91404 Orsay, France.

12–81 Non-destructive characterisation of HTSC wafer homogeneity by mm-wave surface resistance measurements. *R. Heidinger* and *R. Schwab*. Forschungszentrum Karlsruhe, Institut für Materialforschung I Postfach 3640, D-76021 Karlsruhe, Germany.

12–82 Temporal response of high-temperature superconductor thin-film using femtosecond pulses. *V. Garces-Chavez*[1], *A. De Luca*[2], *A. Gaugue*[2], *P. Georges*[1], *A. Kreisler*[2] and *A. Brun*[1]. [1]Laboratoire Charles Fabry de l'Institut d'Optique, Orsay, Essonne, 91403, France. [2]LGEP-SUPELEC, Gif sur Yvette, Essonne, 91192, France.

12–84 Growth and Superconducting Properties of $YBa_2Cu_3O_{7-\delta}$ / $Nd_{0.7}Sr_{0.3}MnO_3$ Multilayers. *L. M. Wang*[1], *H. H. Sung*[1], *J. H. Chen*[2], *H. C. Yang*[2] and *H. E. Horng*[3]. [1]Department of Electronic Engineering, Da-Yeh University, Changhua 515, Taiwan, R. O. C. [2]Department of Physics, National Taiwan University, Taipei 106, Taiwan, R. O. C. [3]Department of Physics, National Taiwan Normal University, Taipei 106, Taiwan, R. O. C.

12–85 Ferromagnetic and superconducting oxide heterostructures for spin injection devices. *L. Fàbrega*[1], *R. Rubí*[1], *J. Fontcuberta*[1], *V. Trtík*[2], *F. Sànchez*[2], *C. Ferrater*[2] and *M. Varela*[2]. [1]Institut de Ciència de Materials de Barcelona (C.S.I.C.), Campus de la U.A.B., 08193 Bellaterra (SPAIN). [2]Departament de Física Aplicada i Òptica, Universitat de Barcelona, Diagonal 648, 08028 Barcelona (SPAIN).

12–86 Effect of $YBa_2Cu_3O_{7-\delta}$ electrodes on the strain and lattice distortion in multilayered $SrTiO_3$ films. *P.K. Petrov*[1], *S.S. Gevorgian*[1] and *Z.G. Ivanov*[2]. [1]Dept. of Microelectronics, Chalmers University of Technology, 412-96 Gothenburg, Sweden. [2]Dept. of Physics, Chalmers University of Technology and Gothenburg University, 412-96 Gothenburg, Sweden.

12–87 Raman Spectroscopy as a characterisation tool for FIB damage of HTS thin films. *N. Malde*[1], *L. F. Cohen*[1] and *M. W. Denhoff*[2]. [1]Blackett Laboratory, Imperial College, Prince Consort Rd, London SW7 2BZ. [2]Institute for Microstructural Sciences, National Research Council, Canada.

12–88 Transport and High Frequency Behaviour of c-Axis $REBa_2Cu_3O_{7-x}$. *W. Schmitt*, *R. Aidam*, *J. Geerk*, *G. Linker* and *R. Schneider*. Forschungszentrum Karlsruhe, INFP, P.O.B. 3640, D-76021 Karlsruhe, Germany.

12–89 Nb_3Sn-films on sapphire for passive device applications. *M. Perpeet*, *A. Cassinese*, *M.A. Hein*, *G. Müller* and *H. Piel*. Universität Wuppertal, Fachbereich Physik, Gaußstr. 20, D-42097 Wuppertal, Germany.

Session SQUIDs, and SQUIDs applications

12–90 $YBa_2Cu_3O_7$ step-edge dc SQUID magnetometers. *I.S. Kim*, *J.M. Kim*, *H.C. Kwon*, *Y.H. Lee* and *Y.K. Park*. Korea Research Institute of Standards and Science, Yusong PO Box 102, Taejon 305-600, Republic of Korea.

12–91 Study of the magnetic recording media using a scanning dc SQUID microscope. *S.A. Gudoshnikov*[1], *M.I. Koshelev*[2], *O.V. Snigirev*[2] and *A.M. Tishin*[2]. [1]Institute of Terrestrial Magnetism, Ionosphere and Radio Wave Propagation, Russian Academy of Sciences, (IZMIRAN), Troitsk, Moscow region 142092, Russia. [2]Department of Physics, Moscow State University, Moscow 119899 GSP, Russia.

12–92 Magnetic Detection of Mechanical Degradation of Low Alloy Steel by SQUID-NDE system. *N.K. Kasai*[1], *S. Nakayama*[2], *Y. Hatsukade*[1,3] and *M. Uesaka*[4]. [1]Electrotechnical Laboratory, Tsukuba, Ibaraki, 305-8568, Japan. [2]Seiko Insturuments Inc., Matsudo, Chiba, 270-2222, Japan. [3]Waseda university, Shinjyuku, Tokyo, 169-0072, Japan. [4]University of Tokyo, Tokai, Ibaraki, 319-1106, Japan.

12–93 Design Aspects of the FHARMON Fetal Heart Monitor. *A.P. Rijpma*, *H.J.M. ter Brake*, *J. Borgmann*, *H.J.G. Krooshoop* and *H. Rogalla*. Low Temperature Division, Department of Applied Physics, University of Twente, PO Box 217, 7500 AE Enschede, The Netherlands.

12–94 Direct coupled HTS magnetometers. *P.R.E. Petersen*[1,2], *Y.Q. Shen*[1], *M.P. Sager*[1,2], *T. Holst*[1] and *J.B. Hansen*[2]. [1]NKT Research Center, Priorparken 878, DK-2605 Brøndby, Denmark. [2]Department of Physics, Technical University of Denmark, DK-2800 Lyngby, Denmark.

12–95 Low Temperature Scanning SQUID. *B. C. Yao*, *M. J. Wang*, *C. C. Hung*, *C. C. Chi* and *M. K. Wu*. Material Science Center & Department of Physics, Tsing Hua University, Hsinchu, Taiwan, R.O.C.

12–96 HTS Single Layer Gradiometers with a Large Baseline and Electronically Improved Balance. *A. Eulenburg*, *E.J. Romans*, *C. Carr*, *A.J. Millar*, *C.M. Pegrum* and *G.B. Donaldson*. Dept of Physics and Applied Physics, University of Strathclyde, Glasgow, G4 0NG, UK.

12–97 Operation of integrated HTS dc-SQUID magnetometers in unshielded environment. *K.O. Subke*, *C. Hinnrichs*, *S. Krey*, *H.-J. Barthelmeß*, *C. Pels* and *M. Schilling*. Institut für Angewandte Physik und Zentrum für Mikrostrukturforschung, Universität Hamburg, Jungiusstraße 11, D-20355 Hamburg, Germany.

12–98 Technique for compensation of background magnetic field for HTS dc SQUID systems operating in unshielded environment. *S.A. Gudoshnikov*[1], *L.V. Matveets*[1], *A.A. Khorev*[2], *O.V. Snigirev*[2], *L. Dörrer*[3], *R. Weidl*[3] and *P. Seidel*[3]. [1]Institute of Terrestrial Magnetism, Ionosphere and Radio Wave Propagation, Russian Academy of Sciences, (IZMIRAN), Troitsk, Moscow region 142092, Russia. [2]Moscow State University, Moscow, 119899, Russia. [3]Institut fur Festkorperphysik, Friedrich-Schiller-Universitat Jena, Germany.

12–99 Scanning SQUID Microscopy of Superconducting and Magnetic Films. *A.Tzalenchuk*[1,2], *Z.G.Ivanov*[1], *A.Lõhmus*[3] and *T.Claeson*[1]. [1]Department of Physics, Chalmers University of Technology and University of Göteborg, S-412 96 Göteborg, Sweden. [2]Institute of crystallography RAS, 117333 Moscow, Russia. [3]Institute of Physics, University of Tartu, Riia 142, EE2400 Tartu, Estonia.

12–100 Noise measurements in a dc SQUID based Cryogenic Current Comparator. *J. Sesé*[1], *A. Camón*[1], *C. Rillo*[1], *E. Bartolomé*[2], *J. Flokstra*[2] and *G. Ritveld*[3]. [1]ICMA, CSIC-University of Zaragoza, 50009 Zaragoza, Spain. [2]University of Twente, P.O.Box 217, 7500 AE Enschede, The Netherlands. [3]NMi Van Swinden Laboratorium, P.O.Box 654, 2600 AR Delft, The Netherlands.

12–101 Characteristics of High-T_c $YBa_2Cu_3O_{7-\delta}$ SQUIDs with Shunted Resistance. *J.H. Chen*[1], *M.J. Chen*[1], *H.C. Yang*[1], *H.E. Horng*[2], *C.H. Chen*[2], *S.Y. Yang*[2] and *J.T. Jeng*[2]. [1]National Taiwan University Department of Physics One Section 4, Roosevelt Road Taipei,106-17 Taiwan. [2]National Taiwan Normal University Department of Physics 88 Section 4, Ting-Chou Road Taipei,117-18 Taiwan.

12–102 Characterization of biepitaxial YBCO dc-SQUIDs based on c-axis misaligned grain boundary junctions. *E. Sarnelli*[1], *G. Testa*[1,2], *F. Tafuri*[2,3], *F. Carillo*[2], *F. Lombardi*[2], *F. Miletto Granozio*[2] and *U. Scotti di Uccio*[2]. [1]Istituto di Cibernetica - CNR, Arco Felice, Napoli, 80072 Italy. [2]INFM- Dipartimento di Scienze Fisiche, Universita' di Napoli "Federico II", Napoli, 80125 Italy. [3]Dipartimento di Ingegneria dell'Informazione, Seconda Universita' di Napoli, Aversa, Italy.

12–103 The system to operate cryogenics calorimeters with superconducting phase transition thermometers. *V. Khanin*[2], *V.Y. Slobodchikov*[2] and *S. Uchaikin*[1]. [1]Max Planck Institute fuer Physik, Munich, 80805, Germany. [2]Cryoton Ltd, Troizk, Moscow region, 142092, Russia.

12–104 Measurement System for Magnetorelaxometry with Planar and Axial SQUID Gradiometer. *J. Schambach*, *L. Warzemann* and *P. Weber*. Friedrich-Schiller-University Jena Max-Wien-Platz 1 D-07743 Jena Germany.

12–105 A SQUID Switch for Non Invasive Measurements in a Macroscopic Quantum Coherence experiment. *C. Cosmelli*[1,2], *P. Carelli*[3,2], *M.G. Castellano*[4,2], *F. Chiarello*[1,2], *R. Leoni*[4,2] and *G. Torrioli*[4,2]. [1]Dipartimento di Fisica, Universita' La Sapienza, Roma, 00185, Italy. [2]Istituto Nazionale di Fisica Nucleare, Roma, 00185, Italy. [3]Dip. Di Energia Elettrica, Fac. di Ingegneria, Monteluco di Roio, L'Aquila, 67040, Italy. [4]Istituto di Elettronica dello Stato Solido - CNR, 00156, Italy.

12–106 16-channel operation of high Tc SQUID magnetometers for magnetocardiogram. *H.C. Kwon*, *I.S. Kim*, *Y.H. Lee*, *J.M. Kim* and *Y.K. Park*. Korea Research Institute of Standards and Science Taejon 305-600 Korea.

12–107 A new general purpose low-T_c multiloop SQUID family. *D. Drung*, *S. Knappe*, *C. Aßmann*, *M. Peters*, *K. Wenzel* and *Th. Schurig*. Physikalisch-Technische Bundesanstalt, D-10587 Berlin, Germany.

12–108 Read-out electronics for a 9-channel High-T_c dc SQUID system. *S. Bechstein*, *D. Drung*, *M. Scheiner*, *F. Ludwig* and *Th. Schurig*. Physikalisch-Technische Bundesanstalt, D-10587 Berlin, Germany.

12–109 Noise Characteristics of Asymmetric Multi-Junction HTSC rf-SQUID Magnetometer and Gradiometer on Bi-crystal Substrates. *M. Fardmanesh*, *K. Barthel*, *J. Schubert*, *H. Bousack* and *A. Braginski*. Institute of Thin Film and Ion Technology, Research Center Juelich, Germany.

12–110 Step-Edge Structure Dependence of 1/f Noise in rf-SQUIDs and The Effect of IBE Parameters. *M. Fardmanesh*, *J. Schubert*, *Y. Zhang*, *H. Bousack* and *A. Braginski*. Institute of Thin Film and Ion Technology, Research Center Juelich, Germany.

Thursday, September 16th

PLENARY SESSION 13

Thursday Morning, September 16th, 8:30-10:00

8:30 **13–1 Progress in the applications of bulk high temperature superconductors.** *M. Murakami*. ISTEC, Superconductivity Research Laboratory 1-16-25, Shibaura, Minato-ku, Tokyo, 105-0023 Japan.

9:15 **13–2 Challenges in the Realization of SFQ Digital Circuits.** *T. Van Duzer* Department of Electrical Engineering and the Electronics Research Laboratory, University of California, Berkeley, CA 94720-1770, USA.

ORAL SESSION 14A+15A: Wires and Tapes II

Thursday Morning, September 16th, 10:30-12:45

10:30 ***14A–1 Current Limiting Mechanisms in BSCCO-2223 Tapes.** *D. C. Larbalestier*. Applied Superconductivity Center, University of Wisconsin, Madison University of Wisconsin, Madison, WI USA.

11:00 **14A–2 Enhanced Critical Current Density in Overdoped $YBa_2Cu_3O_{7-\delta}$ - Grain Boundaries.** *R.R. Schulz, H. Bielefeldt, B. Goetz, H. Hilgenkamp, A. Schmehl, C.W. Schneider* and *J. Mannhart.* Experimentalphysik VI, Center for Electronic Correlations an Magnetism, Institute of Physics, Augsburg University, D-86135 Augsburg, Germany.

11:15 **14A–3 Preparation of (100) and (110) textured Ag tapes for superconducting biaxially aligned coated tapes.** *H. Suo*[1,2], *J.-Y. Genoud*[1], *E. Walker*[1], *G. Triscone*[1], *M. Schindl*[1], *E. Koller*[1], *Ø. Fischer*[1] and *R. Flükiger*[1]. [1]DPMC, University of Geneva, 24 quai E.-Ansermet, 1211 Geneva 4, Switzerland. [2]Beijing Polytechnic University, 100022 Beijing, China.

11:30 **14A–4 Microstructure and properties of Bi2212/Ag tapes grown in high magnetic fields.** *W.P. Chen*[1,2], *H. Maeda*[1,2], *K. Kakimoto*[1], *P.X. Zhang*[1], *K. Watanabe*[1,2], *M. Motokawa*[1,2], *H. Kitaguchi*[3] and *H. Kumakura*[3]. [1]Institute for Materials Research, Tohoku University, Sendai 980-8577, Japan. [2]CREST, Japan Science and Technology Corporation, Tsukuba 305-0047, Japan. [3]National Research Institute for Metals, Tsukuba 305-0047, Japan.

11:45 **15A–1 Processing of Tl-1223(F) thick films for HTS power applications.** *J.C. Moore*[1], *T.A. Gladstone*[1], *X. Zhou*[1], *M.D. McCulloch*[2] and *C.R.M. Grovenor*[1]. [1]Dept. of Materials, University of Oxford, Oxford, U.K. [2]Dept. of Engineering, University of Oxford, Oxford, U.K.

12:00 **15A–2 Progress on Fabrication and Procesing of $(Hg,X)_1Ba_2Ca_2Cu_3O_y$ Superconductor on Ceramic and Metallic Substrates.** *J. Schwartz*[1,2] and *P.V.P.S.S. Sastry*[1]. [1]National High Magnetic Field Laboratory, Florida State University, Tallahassee, Florida, 32310, USA. [2]Department of Mechanical Engineering, Florida State University, Tallahassee, Florida, 32310, USA.

12:15 **15A–3 Improved Critical Current Density of Rapidly Heated/Quenched Processed $Nb_3(Al,Mg)$ and $Nb_3(Al,Ge)$ Multifilamentary Wires.** *A. Kikuchi, Y. Iijima* and *K. Inoue*. National Research Institute for Metals.

12:30 **15A–4 Effect of Uranium Doping and Neutron Irradiation on the Properties of Bi-2223/Ag Superconducting Tapes.** *Y.C. Guo*[1], *J. Horvat*[1], *J.W. Boldeman*[1], *S.X. Dou*[1], *A. Gandini*[2], *Y. Ren*[2], *R. Sawh*[2], *R. Weinstein*[2], *S. Tönies*[3], *C. Klein*[3] and *H.W. Weber*[3]. [1]Institute for Superconducting and Electronic Materials, University of Wollongong, Northfields Av., Wollongong, New South Wales 2522, Australia. [2]Institute for Beam Particle Dynamics, University of Houston, Houston, TX 77204-5506, USA. [3]Atomic Institute of the Austrian Universities, Stadionallee 2, A-1020 Vienna, Austria.

ORAL SESSION 14B+15B: Fault Current Limiters and Related Materials

Thursday Morning, September 16th, 10:30-12:45

10:30 ***14B–1 Development of resistive current limiters with YBCO films.** *B. Gromoll*[1], *H.-P. Krämer*[1], *G. Ries*[1], *W. Schmidt*[1], *B. Heismann*[1], *H.-W. Neumüller*[1], *R. R. Volkmar*[2] and *S. Fischer*[2]. [1]Siemens AG, Corporate Technology, 91050 Erlangen, Germany. [2]Siemens AG, Power Transmission and Distribution, 13623 Berlin, Germany.

11:00 ***14B–2 European project on a self-limiting superconducting power link.** *T. Verhaege*[1], *P.F. Herrmann*[1], *J. Bock*[2], *L. Cowey*[2], *G. Moulaert*[3], *H.C. Freyhardt*[4,5], *A. Usoskin*[4] and *J. Paasi*[6]. [1]Alcatel CIT, F-91460 Marcoussis, France. [2]Aventis, D-50351 Hürth, Germany. [3]Laborelec, B-1630 Linkebeek, Belgium. [4]ZFW gGmbH, D-37073 Göttingen, Germany. [5]Universität Göttingen, D-37073 Germany. [6]TUT, FI-33101 Tampere, Finland.

11:30 ***14B–3 Quench in bulk HTS materials: Application to the Fault Current Limiter.** *P. Tixador*[1], *X. Obradors*[2], *R. Tournier*[1], *T. Puig*[2], *D. Bourgault*[1], *X. Granados*[2], *X. Chaud*[1], *E. Mendoza*[2], *E. Beaugnon*[1], *D. Isfort*[1], *J.M. Duval*[1] and *E. Varesi*[2]. [1]CNRS, CRETA, 38000 Grenoble , France. [2]ICMAB, CSIC , Campus UAB, 08193 Bellaterra, Spain.

12:00 **15B–1 Quenching in BSCCO hollow cylinders employed in an inductive fault current limiter.** *V. Meerovich*, *V. Sokolovsky*, *G. Jung* and *S. Goren*. Ben-Gurion University, Beer-Sheva, 84105, Israel.

12:15 **15B–2 One DC Reactor Type Fault Current Limiter for Three-phase Power System.** *M. Yamaguchi*, *S. Fukui*, *K. Usui*, *T. Horikawa* and *T. Satoh*. Graduate School of Science and Technology, Niigata University, Niigata 8050, Japan .

12:30 **15B–3 Operation of an HTS Fault Current Limiter in an Asymmetrical Three Phase System.** *V. Sokolvsky*[1], *V. Meerovich*[1], *I. Vajda*[2], *T. Porjesz*[3] and *A. Szalay*[4]. [1]Physics Dept, Ben Gurion University, Beer Sheva, Israel. [2]Dept. of Electrical Machines and Drives, TU Budapest, Budapest, Hungary. [3]Dept. of General Physics, Eotvos University, Budapest, Hungary. [4]S-Metalltech ltd, Budapest, Hungary.

ORAL SESSION 14C+15C: SQUIDS and SQUIDS Applications II

Thursday Morning, September 16th, 10:30-12:45

10:30 ***14C–1 SQUID-NDE of semiconductor samples with high spatial resolution.** *J.Beyer*[1], *Th.Schurig*[1], *A.Luedge*[2] and *H.Riemann*[2]. [1]Physikalisch-Technische Bundesanstalt Berlin, D-10587 Berlin, Germany . [2]Institut fuer Kristallzuechtung Berlin, D-12489 Berlin, Germany.

11:00 ***14C–2 Superconducting sensors for weak magnetic signals in combination with BiCMOS electronics at 77 K.** *P. Seidel*[1], *L. Dörrer*[1], *F. Schmidl*[1], *N. Ukhansky*[1,2], *R. Neubert*[1], *D. Hieronymus*[1], *S. Wunderlich*[1], *R. Gross*[3], *F. Nitsche*[3] and *S. Linzen*[1]. [1]Institut für Festkörperphysik, Friedrich-Schiller-Universität Jena, Jena, D-07743, Germany. [2]Institute of Terrestrial Magnetism, Ionosphere and Radio Wave Propagation, Troitsk, 142092, Russia. [3]MAZeT GmbH, Erfurt, D-99099 Erfurt.

11:30 **14C–3 Practical Low Noise dc SQUIDs for a Cryogenic Current Comparator.** *E. Bartolomé*, *J. Flokstra* and *H. Rogalla*. University of Twente, P.O.Box 217, 7500 AE Enschede, The Netherlands.

11:45 **14C–4 High-T_c SQUID magnetometers in $YBa_2Cu_3O_{7-\delta}$ thin films with resistively shunted inductances.** *F. Kahlmann*[1], *W.E. Booij*[1], *M.G. Blamire*[1], *P.F. McBrien*[1], *N.H. Peng*[2], *C. Jeynes*[2] and *E.J. Tarte*[1]. [1]IRC in Superconductivity, University of Cambridge, Madingley Road, Cambridge CB3 0HE, United Kingdom. [2]urrey Centre for Research into Ion Beam Applications, School of Electronic Engineering, Information Technology and Mathematics University of Surrey, Guildford GU2 5XH, United Kingdom.

12:00 **15C–1 HTS SQUIDs and cryogenically operated magnetoresistive sensors - an open competition?.** *C. Dolabdjian*[1], *S. Saez*[1], *D. Robbes*[1], *C. Bettner*[2], *U. Loreit*[2], *F. Dettmann*[2], *G. Kaiser*[3] and *A. Binneberg*[3]. [1]GREYC-CNRS, UPRES-A 6072,ISMRA et Université de Caen 6, Bd. du Maréchal Juin 14050 Caen Cedex, France. [2]Institut fuer Mikrostrukturtechnologie und Optoelektronik Im Amtmann 6 D-35578, Wetzlar, Germany. [3]Institut fuer Luft- und Kaeltetechnik Bertolt-Brecht-Allee 20 D-01309, Dresden, Germany.

12:15 **15C–2 The spatial distribution of flux lines in YBCO dc SQUIDs and the correlation with their low-frequency noise properties.** *R. Straub*[1], *S. Keil*[1], *D. Koelle*[2], *K. Barthel*[3], *R. Gross*[2] and *R.P. Huebener*[1]. [1]Physikalisches Institut, Lehrstuhl für Experimentalphysik II, Universität Tübingen, 72076, Germany. [2]II. Physikalisches Institut, Lehrstuhl für Angewandte Physik, Universität zu Köln, 50937, Germany. [3]Institut für Schicht- und Ionentechnik (ISI), Forschungszentrum Jülich, 52428, Germany.

12:30 **15C–3 High T_C dc SQUIDs operated in the presence of large thermal fluctuations.** *K. Barthel*[1], *D. Koelle*[1,2], *R. Kleiner*[3], *R. Gross*[2] and *A. Braginski*[1]. [1]Institut für Schicht und Ionentechnik, Forschungszentrum Jülich, D-52425 Jülich, Germany. [2]II. Physikalisches Institut, Lehrstuhl für Angewandte Physik, Universität zu Köln, D-50937 Köln, Germany. [3]Physikalisches Institut III, Universität Erlangen-Nürnberg, D-91058 Erlangen, Germany.

ORAL SESSION 14D: AC Losses I

Thursday Morning, September 16th, 10:30-11:45

10:30 ***14D–1 Transport AC losses in Bi-2223 multifilamentary tapes - conductor materials aspect.** *B.A.Glowacki*[1,2] and *M.Majoros*[1,3]. [1] IRC in Superconductivity, University of Cambridge, Madingley Road, Cambridge CB3 OHE,U.K. [2]Department of Materials Science and Metallurgy University of Cambridge, Pembroke Street, Cambridge CB2 3QZ, U. K. [3]Institute of Electrical Engineering, SAS, Bratislava, Slovak Republic.

11:00 **14D–2 The self-field ac losses of twisted Bi-2223 conductors.** *C.M. Friend*, *Y.B. Huang* and *D.M. Spiller*. BICC Supercondcutors, Oak Road, Wrexham LL13 9XP, UK.

11:15 **14D–3 Aspect Ratio Modified Effective Transverse Matrix Resistivity in Multifilamentary HTSC/Ag Strands.** *E.W. Collings* and *M.D. Sumption*. Materials Science and Engineering, the Ohio State University.

11:30 **14D–4 Critical current densities and magnetic losses in Bi-2223 tapes determined from experiments in perpendicular AC magnetic field.** *F. Gömöry*, *F. Strycek*, *E. Seiler*, *P. Kovac* and *S. Takács*. Institute of Electrical Engineering, Slovak Academy of Sciences, Bratislava, 842 39, Slovak Republic.

ORAL SESSION 15D: Digital Applications

Thursday Morning, September 16th, 11:45-12:45

11:45 ***15D–1 Applications of Josephson electronics to digital systems.** *J.X. Przybysz*. Northrop Grumman Science & Technology Center Linthicum, MD, 21090 USA.

12:15 **15D–2 Digital-to-Analog Converter Concept with RSFQ Circuits.** *R. Koch*, *P. Ostertag* and *W. Jutzi*. Institut fuer Elektrotechnische Grundlagen der Informatik, University of Karlsruhe, Hertzstr. 16, D-76187 Karlsruhe, Germany.

12:30 **15D–3 Hybrid Analog-to-Digital Converter based on a Delta Sigma Modulator in HTS Technology.** *B. Ruck*, *R. Dittmann* and *M. Siegel*. Institut fuer Schicht- und Ionentechnik, Forschungszentrum Juelich GmbH, 52425 Juelich, Germany.

POSTER SESSION 16

Thursday Afternoon, September 16th, 15:30-17:30

Session Bulk materials and materials aspects

16–1 Dependency of physical properties on F content in $Tl_{0.8}Pb_{0.2}Bi_{0.2}Sr_{1.8}Ba_{0.2}Ca_{2.2}Cu_3O_{(9+\delta)}F_x$ ($0 \leq x \leq 2$) polycrystalline bulk. *J. H. Lee*[1], *B. J. Kim*[1], *Y. C. Kim*[1], *D. Y. Jeong*[2], *H. K. Kim*[2] and *H. Y. Lee*[2]. [1]Pusan National University, Pusan 609-735, Korea. [2]Korea Electrotechnology Research Institute, Changwon 641-120, Korea.

16–2 Hg and Tl HTS thin films by high gas pressure treatment with DTA controlled process. *A.Morawski*[1], *A.Paszewin*[1], *T.Lada*[1], *A.Presz*[1], *H.Marciniak*[1], *R.Gatt*[2], *L.-G.Johansson*[3], *M. Valkeapää*[3] and *K.Przybylski*[4]. [1]High Pressure Research Centre, Polish Academy of Sciences, ul. Sokolowska 29/37, 01-142 Warsaw,Poland. [2]Physics Department, University of Wisconsin, 1150 University Avenue, Madison, WI 53706, U.S.A. [3]Department of Inorganic Chemistry, University of Göteborg, 41296, Göteborg, Sweden. [4]Department of Solid State Chemistry, University of Mining and Metallurgy, Al. Mickiewicza 30, 30-059 Cracow, Poland.

16–3 Optimal Tc in the mercury double layer system Hg-2212 by Pb doping. *P. Toulemonde*[1], *P. Bordet*[1], *J.J. Capponi*[1], *P. Odier*[1] and *J.L. Tholence*[2]. [1]Laboratoire de Cristallographie - CNRS Grenoble. [2]LEPES - CNRS Grenoble.

16–4 Toward new low anisotropy materials in superconducting artificial multilayers $(BaCuO_2)_2/(CaCuO_2)_n$. *V. Braccini*[1], *D. Marrè*[2], *M. Putti*[1] and *A.S. Siri*[1]. [1]University of Genoa, Physics Department, Via Dodecaneso 33, 16146 Genoa - Italy. [2]I.N.F.M., Research Unity of Genoa, Physics Department, Via Dodecaneso 33, 16146 Genoa - Italy.

16–5 Copper Oxides Superconductors of Composite $Y_{1-x}Ca_xBa_2Cu_4O_8$. *A. Diaz*[1], *A. Bustamante*[1], *D. Sanchez*[2] and *D. Tellez*[3]. [1]Laboratorio de Superconductividad, Facultad de Ciencias Fisicas, Universidad Nacional Mayor de San Marcos, Apartado Postal 14-0149, Lima 14 - Peru. [2]Centro Brasileiro de Pesquisas Fisicas, Rua Xavier Sigaud 150, CEP 22290-180, Rio de Janeiro, Brazil. [3]Departamento de Fisica, Universidad Federal de Pernambuco, 50670-901 Recife PE, Brazil.

16–6 Processing and superconducting properties of $Hg_{1-x}Re_xBa_2Ca_2Cu_3O_{8+\delta}$. *A.Sin*[1], *S.Piñol*[2], *A.G.Cunha*[3], *M.T.D.Orlando*[3] and *P.Odier*[1]. [1]Laboratoire de Cristallographie-CNRS, 25 Av. Des Martyrs, Bp166, F38042 Grenoble CEDEX09, France. [2]Institut de Ciència de Materials de Barcelona (CSIC), Campus de la UAB, Bellaterra E-08193, Barcelona, Spain. [3]Departamento de Física, Universidade Federal do Espírito Santo, 29060-900 Vitória-ES, Brazil.

16–7 In-situ pressure measurements and synthesis parameters in Hg-cuprate superconductors. *A.Sin*[1], *A.G.Cunha*[2], *M.T.D.Orlando*[2], *S.Piñol*[3] and *P.Odier*[1]. [1]Laboratoire de Cristallographie-CNRS, 25 Av. des Martyrs, Bp166, F38042 Grenoble Cedex09, France. [2]Departamento de Física, Universidade Federal do Espírito Santo, 29060-900 Vitória-ES, Brazil. [3]Institut de Ciència de Materials de Barcelona (CSIC), Campus de la UAB, Bellaterra E-08193, Barcelona, Spain.

16–8 Pressure effects in $Hg_{0.82}Re_{0.18}Ba_{(2-y)}Sr_yCa_2Cu_3O_{8+\delta}$. *A.Sin*[1], *M.T.D.Orlando*[2], *M.Nunez-Regueiro*[3], *A.G.Cunha*[2] and *P.Odier*[1]. [1]Laboratoire de Cristallographie-CNRS, 25 Av. des Martyrs, Bp166, F38042 Grenoble Cedex09, France. [2]Departamento de Física, Universidade Federal do Espírito Santo, 29060-900 Vitória-ES, Brazil. [3]Centre de Reserche sur les Tres Basses Temperatures-CNRS, 25 Av. des Martyrs, Bp166, F38042 Grenoble Cedex09, France.

16–9 Bi-epitaxial YBaCuO films grown on eutetic substrates. *J. Santiso*[1], *L.A. Angurel*[2], *V. Laukhin*[1,3], *R.I. Merino*[2], *M. Doudkowsky*[1], *G. García*[1], *J.I. Peña*[2], *M.L. Sanjuán*[2], *A. Figueras*[1] and *V. M. Orera*[2]. [1]Institut de Ciència de Materials de Barcelona (C.S.I.C.), Campus de la Universitat Autònoma de Barcelona, 08193 Bellaterra (Spain). [2]Instituto de Ciencia de Materiales de Aragón (C.S.I.C.-Universidad de Zaragoza), Facultad de Ciencias, Pza San Francisco, 50009 Zaragoza (Spain). [3]Permanent address:Institute of Problems of Chemical Physics, RAS, Chernogolovka, MD 142432 Russia.

16–10 The Influence of Preparative Sequence on the Intergrain Coupling of Tl-1223 HTS-Ceramics. *Chr. L. Teske*. Institut f. Anorganische Chemie CAU Kiel, D-24098, Germany.

16–11 DTA High Pressure System for in-situ Identification of Phase Transformation during Hg and Tl HTS Crystallization Process. *T. Lada*[1], *A.Paszewin*[1], *A.Morawski*[1], *A.Presz*[1], *S.Gierlotka*[1], *K.Przybylski*[2] and *R.Gatt*[3]. [1]High Pressure Research Centre, Polish Academy of Sciences, ul. Sokolowska 29/37, 01-142 Warszawa, Poland. [2]Department of Solid State Chemistry, University of Mining and Metallurgy, Al. Mickiewicza 30, 30-059 Cracow, Poland. [3]Physics Department, University of Wisconsin, 1150 University Avenue, Madison, WI 53706, U.S.A.

16–12 Percolation effects of the $YBa_2Cu_3O_x$ phase in the Y_2BaCuO_5 green phase. *G.A.Costa*[1,2], *P.Mele*[1,2] and *A.Ubaldini*[1,2]. [1]INFM, Via Dodecaneso 33, I-16146 Genova, Italy. [2]Dipartimento di Chimica e Chimica Industriale, Universita' di Genova, Via Dodecaneso 31, I-16146 Genova, Italy.

16–13 Dynamic Compaction for the Fabrication of HTS Ceramic Components. *A. G. Mamalis*[1], *A. Szalay*[2], *B. Raveau*[3], *G. Desgardin*[3], *L. Chubraeva*[4], *I. Vajda*[5], *N. Gobl*[2], *T. Porjesz*[6] and *I. Kotsis*[7]. [1]NTUA, Athens, Greece. [2]S-Metalltech ltd, Budapest, Hungary. [3]CRISMAT-ISMRA, Caen, France. [4]VNII El. Mach, St-Petersburg, Russia. [5]TU Budapest, Budapest, Hungary. [6]Eotvos University, Budapest, Hungary. [7]University of Veszprem, Veszprem, Hungary.

Session Wires tapes and coated conductors

16–14 Development of ion assisted sputter deposition of biaxially aligned YSZ layers. *G. De Winter*[1], *J. Denul*[2] and *R. De Gryse*[1]. [1]University of Gent, Gent, B-9000, Belgium. [2]Centre for Vacuum and Materials Sciences, Gent, B-9000, Belgium.

16–15 Electrical, magnetic and AC loss properties of Bi-2223/Ag(alloy) tapes subjected to bending strain. *L. Bigoni*[1], *F. Barberis*[1], *E. Cereda*[1], *F. Curcio*[1], *P. La Cascia*[2], *L. Martini*[1] and *V. Ottoboni*[1]. [1]ENEL-SRI, Segrate, Milan, 20090, Italy. [2]Univerity of Bologna, 40126, Italy.

16–16 Preparation of Tl-based superconducting tapes by electrochemical deposition. *E. Bellingeri, H. Suo, J.-Y. Genoud, M. Schindl, E. Walker* and *R. Flükiger*. DPMC, Université de Genève 24, Quai Ernest Ansermet CH-1211 Genève 4, Switzerland.

16–17 Optimum geometry of ceramic cores in multifilamentary Ag/BSCCO tapes. *J.I. Bech*[1], *M. Eriksen*[1], *B. Seifi*[1], *N. Bay*[1], *P. Skov-Hansen*[2] and *B. Kindl*[3]. [1]Department of Manufacturing Engineering (IPT), Technical University of Denmark (DTU), Lyngby, 2800, Denmark. [2]Nordic Superconductor Technologies A/S(NST)Brøndby, 2605, Denmark. [3]Materials Research Department, Risø, Roskilde, 4000, Danmaark.

16–18 Step Sintering and Jc Behavior in Multifilamentary Bi-2223 Tapes. *D.A. Esparza* and *M.T.Malachevsky*. Centro Atomico Bariloche - Comision Nacional de Energia Atomica - 8400 S.C. de Bariloche - Argentina.

16–19 Manufacturing and Characterisation of a Novel Geometry for (Pb,Bi)2223 Superconducting wires. *D.M. Spiller, C.M. Friend, Y.B. Huang, I.G. Ferguson* and *W.W. Blendl*. BICC Superconductors, Oak Road, Wrexham LL13 9XP. UK.

16–20 Temperature dependence of filament coupling in multyfilament Bi-2223 tapes: Magneto-optical study. *T. H. Johansen*[1], *Y. M. Galperin*[1,2], *M. Bazilievich*[1], *A. V. Bobyl*[2] and *D. V. Shantsev*[1,2]. [1]Department of Physics, University of Oslo, P. O. Box 1048, Blindern, 0316 Oslo, Norway. [2]A. F. Ioffe Physico-Technical Institute, Polytechnicheskaya 26, St.Petersburg 194021, Russia.

16–21 Magneto-optical study of multyfilament Bi-2223 tapes in current-carrying state: Visualisation of individual filaments. *T. H. Johansen*[1], *Y. M. Galperin*[1,2], *M. Bazilievich*[1], *A. V. Bobyl*[2], *D. V. Shantsev*[1,2] and *M. E. Gaevski*[2,3]. [1]Department of Physics, University of Oslo, P. O. Box 1048, Blindern, 0316 Oslo, Norway. [2]A. F. Ioffe Physico-Technical Institute, Polytechnicheskaya 26, St.Petersburg 194021, Russia. [3]Department of Materials Science, Uppsala University, P O Box 534, SE-751 21 Uppsala, Sweden.

16–22 Ageing effect on ac losses of BSCCO−2223 tapes with different geometrical structures. *P. Caracino*[1], *G. Grasso*[2], *P. Guasconi*[2] and *D. Uglietti*[3]. [1]Pirelli Cavi e Sistemi - Viale Sarca, 222 20126 Milano Italy. [2]INFM UdR di Genova - Via Dodecaneso, 33 146 Genova Italy. [3]INFM UdR di Milano - Via Cozzi, 53 20126 Milano Italy.

16–23 Performance Characteristics of Bi-2212 Multifilament Round Wire and Cable Designs. *L. R. Motowidlo*[1], *R. S. Sokolowski*[1], *T. Hasegawa*[2], *D. R. Dietderich*[3] and *R. M. Scanlan*[3]. [1]IGC Advanced Superconductors, Waterbury, CT 06704, USA. [2]Showa Electric Wire & Cable, 2-1-1, Kawasaki, Kanagawa 210,Japan. [3]SC Magnet Group,Lawrence Berkeley National Lab.,Berkeley,CA 94707,USA.

16–24 Single source MOCVD systems for YBCO deposition onto moved tapes. *O. Stadel*[1], *J. Schmidt*[1], *G. Wahl*[1], *C. Jimenez*[2], *F. Weiss*[2], *M. Krellmann*[3], *D. Selbmann*[3], *S.V. Samoilenkov*[4], *O.Yu. Gorbenko*[4] and *A.R. Kaul*[4]. [1]Institut für Oberflächentechnik und Plasmatechnische Werkstoffentwicklung (IOPW), Technische Universität Braunschweig, Bienroder Weg 53, 38108 Braunschweig, Germany. [2]Laboratoire des Materiaux et du GeniePhysique (LMGP), ENSPG, Rue de La Houille Blanche, Domaine Universitaire BP46, F-38402 Saint Martin D'Heres Cedex, France. [3]Institut für Festkörper und Werkstofforschung Dresden (IFW), Postfach 270016, D-01171 Dresden, Germany. [4]Department of Chemistry, Moscow State University, 119899 Moscow, Russia.

16–25 Evidence for anisotropic texturing in silver sheathed Bi(2223) tapes through magnetic measurements. *C. Ferdeghini*[1], *M.R. Cimberle*[2], *G. Grasso*[1] and *I. Pallecchi*[3]. [1]INFM-Research Unit of Genoa, Via Dodecaneso 33, 16146 Genoa, Italy. [2]CNR-CFSBT, Via Dodecaneso 33, 16146 Genoa, Italy. [3]Università di Genova, Dipartimento di Fisica, Via Dodecaneso 33, 16146 Genoa, Italy.

16–26 YSZ buffer layers on large metallic and ceramic substrates. *J. Dzick*[1,3], *J. Hoffmann*[1], *S. Sievers*[1,3], *K. Thiele*[1], *J. Wiesmann*[1], *F. García-Moreno*[1,2], *A. Usoskin*[2], *C. Jooss*[1] and *H. C. Freyhardt*[1,2]. [1]Institut fuer Materialphysik, Universitaet Goettingen, Windausweg 2, 37073 Goettingen, Germany. [2]Zentrum fuer Funktionswerkstoffe, Windausweg 2, 37073 Goettingen, Germany. [3]kabelmetal electro GmbH, Kabelkamp 20, 30179 Hannover, Germany.

16–27 How important is the precursor powder quality for bringing Bi-tapes to market ?. *M. Gerards*[1] and *R. Riddle*[2]. [1]Merck KGaA, Darmstadt Werk Gernsheim D-64579 Gernsheim Germany. [2]Merck Ltd. Poole BH15 1TD England.

16–28 Large-area HTS conductors obtained by novel PLD technique on metallic substrates. *A. Usoskin*[1], *F. García-Moreno*[1,2], *S. Sievers*[2,3], *J. Knoke*[1], *H. C. Freyhardt*[1,2], *J. Dzick*[2,3] and *J. Wiesmann*[2]. [1]Zentrum fuer Funktionswerkstoffe gGmbH Goettingen, Windausweg 2, D-37073 Goettingen, Germany. [2]Institut fuer Materialphysik, Windausweg 2, D-37073 Goettingen, Germany. [3]kabelmetal electro GmbH, Kabelkamp 20, D-30179 Hannover, Germany.

16–29 Magneto-optic investigation of bent Bi-2223 multifilamentary tapes. *M.R. Koblischka*[1], *T. H. Johansen*[1] and *P. Vase*[2]. [1]University of oslo, Department of Physics, Oslo, N-0316, Norway. [2]NST A/S, Brondby, DK-2605, Denmark.

16–30 Slow cooling effect on transport and structural properties of Ag-sheathed Bi(2223) tapes. *G. Grasso*, *F. Grilli* and *P. Guasconi*. INFM-Research Unit of Genoa, Via Dodecaneso 33, 16146 Genoa, Italy.

16–31 Deformation-induced defects in a ceramic core and their healing with thermal processing the Ag/BiSCCO superconducting tapes. *V. Beilin*[1], *A. Goldgirsh*[1], *E. Yashchin*[1], *M. Roth*[1] and *A. Verdyan*[2]. [1] School of Applied Science, the Hebrew University of Jerusalem, Jerusalem, 91904 Israel. [2]Center for Technological Education Holon, affiliated with Tel-Aviv University, P.O.B. 305, Holon, 5812, Israel.

16–32 Phase decomposition and transformation during final process of Ag/Bi-2223 tapes. *H.K. Liu*, *R. Zeng*, *X.K. Fu* and *S.X. Dou*. Institute for Superconducting and Electronic Materials University of Wollongong, Wollongong, NSW 2522 Australia.

16–33 Mechanical properties of superconducting Bi-2223/Ag composite tapes. *Z. Han*, *H. Wu*, *P. Skov-Hansen* and *P. Vase*. Nordic Superconductor Technologies A/S, Priorparken 685, DK-2605 Brondby, Denmark

16–34 Measurements on long Silver/BSCCO tapes by a contact-less method. *M.D. Bentzon* and *P. Vase*. Nordic Superconductor Technologies A/S Priorparken 685 DK-2605 Broendby Denmark.

16–35 Mono and multifilamentary Bi(Pb)-2223 tapes with Ag-Cu-Ti alloyed sheaths. *M. Artigas*, *J.A. Gómez*, *J.M. Pérez* and *R. Navarro*. Instituto de Ciencia de Materiales de Aragón, CSIC-Universidad de Zaragoza Centro Politécnico Superior, María de Luna 3, 50015 Zaragoza, SPAIN.

16–36 Critical Currents of Bi-2223 tapes in extremely non-uniform local magnetic fields perpendicular to the axis of grain alignment. *F.A.Darmann*, *G.D.McCaughey*, *M.H.Apperley* and *T.P.Beales*. Australian Superconductors, Australian Technology Park, Eveleigh NSW 1430.

Session Flux pinning and ac losses

16–37 Total AC loss of BSCCO/Ag tape in different orientations of the external AC magnetic field. *J. J. Rabbers*, *B. ten Haken*, *O. A. Shevchenko* and *H. H. J. ten Kate*. University of Twente, Low Temperature Division, P.O. Box 217, 7500 AE Enschede, The Netherlands.

16–38 Development of Bi,Pb(2223) multifilamentary tapes with oxide barriers. *G. Witz*[1], *Y.B. Huang*[1,2], *R. Passerini*[1], *F. Marti*[1], *M. Dhallé*[1], *L. Porcar*[1], *E. Giannini*[1], *M. Leghissa*[3], *K. Kwasnitza*[4] and *R. Flükiger*[1]. [1]DPMC, Université de Genève, Geneva, CH-1211, Switzerland. [2]Presently at BICC Superconductors, Great Britain. [3]Siemens AG, Erlangen, Germany. [4]PSI, Villigen, Switzerland.

16–39 On 50 Hz magnetic field losses of superconducting High-T_c multifilament Bi(2223)/Ag tapes with high-resistive barriers. *K.Kwasnitza* and *S.Clerc*. Paul Scherrer Institute, CH-5232 Villigen, Switzerland.

16–40 AC Losses in HTS multilayer cable conductor. *S. Redaelli*[1,2], *F. Gömöry*[3] and *R. Mele*[1]. [1]Pirelli Cavi & Sistemi, Viale Sarca 222, MIlano, 20126, Italy. [2]Dipartimento di Fisica, Universita' degli studi di Milano, Milano, 20133, Italy. [3]Institute of Electrical Engineering, Slovak Academy of Science, Dubravska 9, 842 39 Bratislava, Slovak Republik.

16–41 Global Properties of HTS Tape Model using Field-Dependent Power-Law in Finite Element Calculations. *N. Nibbio*, *M. Sjöström* and *B. Dutoit*. EPFL-CIRC, 1015 Lausanne, Switzerland.

16–42 Losses in HTS Tapes due to External AC Magnetic Field and AC Transport Current. *N. Nibbio*, *M. Sjöström* and *B. Dutoit*. EPFL-CIRC, 1015 Lausanne, Switzerland.

16–43 Field distribution evolution on Bi(2223) tapes by dynamic Hall probe array measurements. *B. Dutoit*, *M. Sjöström* and *N. Nibbio*. Swiss Federal Institute of Technology, Lausanne, 1015, Switzerland.

16–45 Angle Dependency of AC losses in a BSCCO/Ag Tape – Simulation and Experiment: a Comparison. *O. A. Shevchenko*, *J. J. Rabbers*, *H. J. G. Krooshoop*, *B. ten Haken* and *H. H. J. ten Kate*. Faculty of Applied Physics, University of Twente, P.O. Box 217, 7500AE Enschede, The Netherlands.

16–46 Measurements of losses in bulk Bi-2223 plate carrying dc transport currents exposed to an alternating field. *T. Hardono*[1], *C.D. Cook*[1], *X.K. Fu*[2], *J.X. Jin*[2], *S.X. Dou*[2], *F. Darmann*[3] and *M.H. Apperley*[3]. [1]School of Electrical, Computer & Telecommunications Engineering, University of Wollongong, NSW 2522 Australia;. [2]Institute for Superconducting and Electronic Materials, University of Wollongong, NSW 2522 Australia;. [3]Australian Superconductors, Eveleigh NSW 1430 Australia;.

16–47 Shielding currents in orthorhombic superconductors. *A. Sanchez* and *C. Navau*. Departament de Fisica, Universitat Autonoma de Barcelona, 08193 Bellaterra, Barcelona, Spain.

16–48 Voltage noise of $YBa_2Cu_3O_{7-\delta}$ thin films in the vortex glass phase. *A. Taoufik*[1], *A. Tirbiyine*[1], *S. Senoussi*[2], *E. Aassif*[3] and *A. Ramzi*[1]. [1]Equipe des Matériaux Supraconducteurs à Haute Température Critique, Département de Physique, Faculté des Sciences, Université Ibn Zohr, B. P:28/S, 80000 Agadir, Morocco. [2]Laboratoire de Physique des Solides (associé au CNRS. URA. 0002), Université Paris Sud, 91405 Orsay Cedex, France. [3]Laboratoire d'Instrumentation et de Mesure, Département de Physique, Faculté des Sciences, Université Ibn Zohr, B. P:28/S, 80000 Agadir.

16–49 Modelling current distribution in granular superconductors: transport, inductive and simultaneous measurements on YBCO samples. *J.L. Giordano*[1], *L.A. Angurel*[1], *F. Lera*[1], *A. Badía*[1] and *C. López*[2]. [1]Instituto de Ciencia de Materiales de Aragón (C.S.I.C.–Universidad de Zaragoza), CPS, María de Luna 3, Zaragoza, E - 50 015, Spain. [2]Departamento de Matemática, CPS, María de Luna 3, Zaragoza, E - 50 015, Spain.

16–50 The 1/f noise of high-temperature superconductor$YBa_2Cu_3O_{7-\delta}$ thin films. *A. Tirbiyine*[1], *A. Taoufik*[1], *S. Senoussi*[2], *E. Aassif*[2,3] and *A. Ramzi*[1]. [1]Equipe des Matériaux Supraconducteurs à Haute Température Critique, Département de Physique, Faculté des Sciences, Université Ibn Zohr, B. P:28/S, 80000 Agadir, Morocco. [2]Laboratoire de Physique des Solides (associé au CNRS. URA. 0002), Université Paris Sud, 91405 Orsay Cedex, France [3]Laboratoire d'Instrumentation et de Mesure, Département de Physique, Faculté des Sciences, Université Ibn Zohr, B. P:28/S, 80000 Agadir.

Session Fusion, SMES, detectors and accelerators

16–51 Laboratory-Scale SMES Device with Liquid Nitrogen Cooled HTS Coil. *A. Friedman*[1], *N. Shaked*[1], *E. Perel*[1], *M. Sinvani*[1], *Y. Wolfus*[1], *E. Yogev*[2], *O.Kugel*[2], *G. Meiron*[2] and *Y. Yeshurun*[1]. [1]Institute for Superconductivity, Department of Physics, Bar-Ilan University, Ramat-Gan, 52900, Israel,. [2]Israel Electric Company, Haifa, PB10, 31000, Israel.

16–52 RF magnetron sputtering target for Nb_3Al made by powder metallurgy. *K. Agatsuma*[1], *H. Tateishi*[1], *K. Arai*[1], *T. Saitoh*[2] and *N. Futaki*[2]. [1]Electrotechnical Laboratory, Tsukuba, Ibaraki, 305-8568 Japan. [2]Fujikura Ltd., Koutou-ku, Tokyo, 135-8512 Japan.

16–53 Studies of decay and snapback effects on LHC dipole magnets. *L. Bottura*[1], *M. Haverkamp*[2] and *M. Schneider*[3]. [1]Cern, division LHC-MTA, CH-1211 Geneva 23, Switzerland. [2]University of Twente, The Netherlands. [3]TU, Technische Universität, Vienna, Austria.

16–54 Direct Measurements of Temperature and Electric Field Distribution Inside the LHD Helical Conductor. *V.S. Vysotsky*[1,3], *Y.A. Ilyin*[1,3], *N. Yanagi*[2], *M. Takeo*[1], *S. Sato*[1], *A.V. Gavrilin*[2], *S. Imagawa*[2], *A. Iwamoto*[2], *S. Hamaguchi*[2], *T. Mito*[2], *T.Satow*[2], *S.Satoh*[2] and *O.Motojima*[2]. [1]Kyushu University, Fukuoka, 812-8582, Japan. [2]National Institute for Fusion Sciences, Toki, Gifu, 509-5292, Japan. [3]Visiting scientist from Kurchatov Institute, 123182, Moscow, Russia.

16–56 Electromagnetic analysis of current distribution in multistrand superconducting cables. *L.Bottura*[2], *M. Breschi*[1], *F. Negrini*[1] and *P.L. Ribani*[1]. [1]Department of Electrical Engineering - University of Bologna - Bologna - 40136 - Italy. [2]LHC Division - CERN - 1211 Geneva 23 - Switzerland.

16–57 Design and Fabrication of a Superconducting Trim Quadrupole for the LHC. *F. Toral*[1], *L. García-Tabarés*[2], *A. Ijspeert*[3], *J. Salminen*[3], *J. Etxeandia*[4] and *F. López-Mantaras*[1]. [1]CIEMAT, Madrid, 28040, Spain. [2]CEDEX, Madrid, 28014, Spain. [3]CERN, Geneva, 1211, Switzerland. [4]ANTEC, Portugalete, Vizcaya, 48920, Spain.

16–58 The Design, Construction and Test of a Gradient Solenoid for the High Powered RF Cavity Experiment for the Muon Collider. *M. A. Green*[1] and *S. T. Wang*[2]. [1]Lawrence Berkeley National Laboratory, Berkeley CA 94720, USA. [2]Wang NMR, Livermore CA 94550, USA.

16–59 A Design for a Combined Function Superconducting Dipole for a Muon Collider FFAG Accelerator. *M. A. Green*. Lawrence Berkeley National Laboratory, Berkeley CA 94720, USA.

16–60 Stability and quench propagation in a long length NbTi CICC. *E. Balsamo*, *A. Catitti*, *S. Chiarelli*, *M. Ciotti*, *A. Della Corte*, *E. Di Ferdinando*, *P. Gislon*, *C. Mastacchini*, *M.V. Ricci* and *M. Spadoni*. Associazione EURATOM-ENEA sulla Fusione, C.E. Frascati Frascati (Rome), 00044, Italy.

16–61 Transient Behaviour of a Resistive Joint in the ATLAS Toroids during the Magnet Ramp-up and Discharge. *G. Volpini*[1] and *E. Acerbi*[1,2]. [1]INFN sez. di Milano, lab. LASA, via f.lli Cervi 201, 20090 Segrate (MI) Italy. [2]Universita' degli Studi di Milano, dipartimento di Fisica, lab. LASA, via f.lli Cervi 201, 20090 Segrate (MI) Italy.

16–62 Progress in the Construction of the B0 Model of the ATLAS Barrel Toroid Magnet. *E. Acerbi*[1,2], *F. Alessandria*[1], *G. Ambrosio*[1], *G. Baccaglioni*[1], *F. Broggi*[1], *L. Rossi*[1], *M. Sorbi*[1] and *G. Volpini*[1]. [1]INFN, sez. di Milano, LASA lab., via f.lli Cervi 201, 20090 SEGRATE Italy. [2]Universita' degli studi di Milano, dip. di Fisica, LASA lab., via f.lli Cervi 201, 20090 SEGRATE Italy.

Session System aspects and high fields

16–63 Confocal Open Resonators Based on Superconducting Film Structures. *A.B. Kazarov*. Institute of Radio Engineering and Electronics of the Russia.

16–64 Stressed state of conductors in solenoidal windings. *E.A. Deviatkin*. Institute of Problems in Mechanics of Russian Academy of Sciences, Moscow 117526, Russia.

16–66 Induced currents and AC losses in superconducting cables due to changing fields at the and portions of magnets. *S. Takács*. Institute of Electrical Engineering, Slovak Academy of Sciences, 842 39 Bratislava, Slovakia.

16–67 Sensitive usage of proton-MR in forensic medicine. *U. Onbasli*[3], *T.O. Eruygun*[1] and *A. Dincer*[2]. [1]University of Istanbul Institute of forensic medicine, Istanbul,Uskudar, 81130, Turkey. [2]Radyomar MR imaging center, Istanbul, Bakirkoy, Turkey. [3]University of Marmara, dept. of phys., Ridvanpasa cad., 2.SOK., 85/12, Göztepe, Istanbul, 81080, Turkey.

16–68 Development of cryocooled Bi-2212/Ag solenoid magnet system generating 8T in 50mm room temperature bore. *H. Kitaguchi*[1], *H. Kumakura*[1], *K. Togano*[1], *M. Okada*[2] and *J. Sato*[3]. [1]National Research Institute for Metals. [2]Hitachi Ltd. [3]Hitachi Cable Ltd.

16–69 Scaling for the Quench Development in HTSC Devices - Theory. *A.L. Rakhmanov*[1], *V.S. Vysotsky*[2,3], *Y.A. Ilyin*[2,3], *T. Kiss*[2] and *M. Takeo*[2]. [1]SCAPE, Russian Academy of Sciences, Moscow, Russia. [2]Kyushu University, Fukuoka, 812-8581, Japan. [3]Visiting scientist from Kurchatov Institute, 123182, Moscow, Russia.

16–70 Scaling For The Quench Development In HTSC Devices - Comparison With The Experiment. *V.S. Vysotsky*[1,2], *Y.A. Ilyin*[1,2], *T. Kiss*[1], *M. Takeo*[1] and *A.L. Rakhmanov*[3]. [1]Kyushu University, Fukuoka, 812-8581, Japan. [2]Visiting scientist from Kurchatov Institute, 123182, Moscow, Russia. [3]SCAPE, Russian Academy of Sciences, Moscow, Russia.

16–71 An influence of the number of Bi(2223)Ag pancake coils on the critical currents of the assembled magnet systems and the energy stored. *J. Pitel*[1], *P. Kovac*[1], *T. Melisek*[1], *H. Kirchmayr*[2] and *A. Katzler*[2]. [1]Institute of Electrical Engineering Slovak Academy of Sciences Dúbravská 9 842 39 Bratislava Slovakia. [2]Institut fur Experimentalphysik Technische Universität Wien Wiedner Hauptstrasse 8 1040 Wien Austria.

16–72 High Magnetic Field Critical Behavior in Dy Substituted YBCO. *I. Nedkov*[1], *T. Koutzarova*[1], *V. Lovchinov*[2] and *T. Mydlarz*[3]. [1]Institute of Electronics, Bulg.Acad.Sci., Sofia, 1784, Bulgaria. [2]Institute Solid State Physics, Bulg.Acad.Sci., Sofia, 1784, Bulgaria. [3]International Laboratory of High Magnetic Fields and Low Temperatures, Wroclaw, 53-529, Poland.

16–73 Anomalies of Homological row of a Superconductings metaloxides. *V.A.Demchenko*. Institute of Thermoelectricity, General Post Chernovtsy 274000, Box 86, Ukraine.

16–74 Quench protection of 13 kA HTS prototype leads for the LHC. *A.Ballarino*, *F.Rodriguez-Mateos* and *O.Wendling*. CERN,CH-1211 Geneve 23, Switzerland.

16–75 Development of Current Leads Using Electrolycally Deposited BSCCO 2212 Tapes. Manufacturing and Testing of Prototype Leads. *J. Le Bars* and *T. Dechambre*. CEA/SACLAY DSM/DAPNIA/STCM Bât 123 91191 GIF-SUR-YVETTE CEDEX.

16–76 A Variable Temperature Test Facility with Variable Field Orientation. *D. Ryan*[1], *M.N. Wilson*[1], *J. van Beersum*[2], *P.F. Herrmann*[4] and *K. Marken*[3]. [1]Oxford Instruments, Tubney Woods, Abingdon, OX13 5QX, UK. [2]University of Twente, Faculty of Physics (Low temperature division), PO Box 217, 7500 Enschede Netherlands. [3]Oxford Superconducting Technology, 600 Milik St, PO Box 429, Carteret NJ07008-0429 USA. [4] Alcatel, Route de Nozay, F-91460 MARCOUSSIS, France.

16–77 Characterization of Bi-2223 conductor for high field insert coils. *H.W. Weijers*[1], *Y.Viouchkov*[1], *M.D. Bentzon*[2] and *J. Schwartz*[1]. [1]National High Magnetic Field laboratory, Tallahassee, Florida, 32310, USA. [2]Nordic Superconductor technologies A/S, Brondy, DK-2605, Denmark.

16–78 Current distribution in a 1T cryocooler-cooled pulse coil wound with a Bi2223 interlayer-transposed 4-strand parallel conductor. *M.Iwakuma*[1], *K.Funaki*[1], *H.Tanaka*[1], *K.Kajikawa*[1], *H.Hayashi*[2], *K.Tsutsumi*[2], *A.Tomioka*[3], *M.Konno*[3] and *S.Nose*[3]. [1]Research Inst. of Supercond., Kyushu University, Fukuoka 812-8581, Japan. [2]Kyushu Electric Power Co.,Inc., Fukuoka 815-8520, Japan. [3]Fuji Electric Co.,Ltd., Kawasaki 210-8530, Japan.

16–79 Preliminary design of 5 T - Bi2223/Ag - magnet at 30 K. *G. Masullo*[1], *A. Matrone*[1], *R. Quarantiello*[1], *L. Bigoni*[2], *L. Martini*[2], *G. Grasso*[3] and *A.S. Siri*[3]. [1] CRIS - Consorzio Ricerche Innovative per il Sud via Nuova delle Brecce n. 260 80147 Napoli - Italy. [2] ENEL/SRI - Nucleo Materiali e Rivestimenti Innovativi Via R. Emilia 39, 20090 Segrate (MI) , Italy. [3] INFM - Unità di Genova, Via Dodecaneso 33, 16146 Genova , Italy.

16–79P1 Cryostatic stabilization of a large supercoducting coil in pressurized superfluid helium. *H. Kobayshi*, *J. Osakabe*, *T. Tanifuji* and *M. Tomita*. Nihon University, 1-8 Kanda Surugadai Chiyodaku, Tokyo.

Session Materials related to electronic applications

16–80 Significant Improvements in the Surface Smoothness of dc Magnetron-sputtered $YBa_2Cu_3O_{7-\delta}$ Films on r-cut Sapphire Substrates With rf Magnetron-sputtered CeO_2 Buffer Layers. *J.H. Lee*[1], *V.A. Komashko*[2], *W.I. Yang*[1], *H.J. Kwon*[1] and *S.Y. Lee*[1]. [1] Department of Physics and Center for Advanced Materials and Devices, Konkuk University, Seoul, 143-701, Korea. [2]Institute for Metal Physics of Ukranian Academy of Sciences, Kiev, 252680, Ukraine.

16–81 Thin film deposition of superconducting borocarbides: a preliminary study for in situ realization of devices. *G. Grassano*, *M.R. Cimberle*, *C. Ferdeghini*, *I. Pallecchi*, *M. Putti* and *A.S. Siri*. INFM/CNR Dipartimento di Fisica, Via Dodecanneso 33, 16146 Genova, Italia.

16–82 Development of a radiation heater for large-area double-sided HTS deposition by high-pressure DC-sputtering. *M. Getta*[1,2], *G. Müller*[1], *J. Pouryamout*[1,2] and *R. Wagner*[1,2]. [1]Bergische Universität Wuppertal, Wuppertal, NRW, 42097, Germany. [2]Cryoelectra GmbH, Wuppertal, NRW, 42287, Germany.

16–83 Microwave properties of $DyBa_2Cu_3O_7$ films on AO–,LAO–,YAO–substrates and measurements in dielectric resonators. *K. Irgmaier*, *S. Drexl*, *R. Semerad* and *H. Kinder*. Technische Universitaet Muenchen, Physik–Department E10, James–Frank–Str. 1, 85748 Garching, Germany.

16–84 Nd/Ba substitutions in $NdBa_2Cu_3O_y$ thin films. *P.B. Mozhaev*[1,2], *P. Larsen*[1], *G.A. Ovsyannikov*[2], *Z.G. Ivanov*[1] and *T. Claeson*[1]. [1]Department of Physics, Chalmers University of Technology, Göteborg, S-41296, Sweden. [2]Institute of Radio Engineering and Electronics RAS, Moscow, 103907, Russia.

16–85 $YBa_2Cu_3O_x$ superconducting thin films on (130) $NdGaO_3$ substrate. *A.D. Mashtakov*[1], *I.K. Bdikin*[2], *I.M. Kotelyanskii*[1], *P.B. Mozhaev*[1], *G.A. Ovsyannikov*[1] and *E.I. Raksha*[1]. [1]Institute of Radio Engineering and Electronics RAS, Moscow, 103907, Russia. [2]Institute of Solid State Physics, Chernogolovka, Moscow dist. 142432, Russia.

16–86 Phase relations in thin RBCO (R=Lu,Ho,Gd,Nd) epitaxial films prepared by MOCVD. *S.V. Samoilenkov*[1], *O.Yu. Gorbenko*[1], *S.V. Papucha*[1], *N.A. Mirin*[1], *I.E.Graboy*[1], *A.R.Kaul*[1], *O. Stadel*[2], *G. Wahl*[2] and *H.W. Zandbergen*[3]. [1]Chemistry Department, Moscow State University, 119899 Moscow, Russia. [2]IOPW, TU Braunschweig, Bienroder Weg 53, 38108 Braunschweig, Germany. [3]National Centre for HREM, Delft TU, Rotterdamseweg 137, 2628 AL Delft, The Netherlands.

16–87 The effect of laser beam intensity homogenisation on the smoothness of YBCO films obtained by laser ablation. *R.A.Chakalov*[1,2], *F.Wellhofer*[1,3], *S.Corner*[2], *M.Allsworth*[2] and *C.M.Muirhead*[2]. [1]Interdisciplinary Laser Deposition Facility, The University of Birmingham, Edgbaston, Birmingham B15 2TT, United Kingdom. [2]School of Physics and Astronomy, The University of Birmingham, Edgbaston, Birmingham B15 2TT, United Kingdom. [3]School of Metallurgy and Materials, The University of Birmingham, Edgbaston, Birmingham B15 2TT, United Kingdom.

16–88 Ag/YBCO thin film growth by single resistive evaporation. *A. Verdyan*, *I. Lapsker* and *J. Azoulay*. Center for Technological Education Holon affiliated with Tel-Aviv University.

16–89 Importance of the interface effects in Au-$YBa_2Cu_3O_{7-\delta}$ sintered composites at low temperature. *C. Lambert-Mauriat*, *J.M. Debierre* and *J. Marfaing*. Lab. MATOP-CNRS, case 151,Fac. des Sc. et Techn. de Saint-Jérôme, Avenue Normandie-Niemens,F-13397 Marseille cedex 20.

16–89P1 Gas sensitivity of the cuprate oxides. *O.J. Bomk*, *V.V. Il'chenko*, *G.V. Kuznetsov*, *A.M. Pinshuk*, *V.V. Skursky* and *A.I. Tsiganova*. Kiev University, Kiev, Volodimirska, 64, 252033, Ukraine.

Session System Aspects related to electronic applications

16–90 On-orbit status of the high temperature superconductivity space experiment (htsse-ii). *M. Nisenoff*. US Naval Research Laboratory Code 6850.1 4555 Overlook Avenue SW Washington DC 20375-5347 USA.

16–91 Transformation of Heat Energy to Electric Energy in a System of Mesoscopic Superconducting Rings. *A.V.Nikulov*. Institute of Microelectronics Technology and High Purity Materials, Russian Academy of Sciences.

16–92 RF Magnetic Shielding Effect of an HTS Cylinder. *M. Itoh*[1], *K. Mori*[2], *K. Itoh*[1] and *Y. Horikawa*[1]. [1]Deptartment of Electronic Engineering, Kinki University, Japan. [2]Division of System Science, Kobe University, Japan.

16–93 Estimation of Magnetic Field within High Effective Magnetic Shielding Vessel. *M. Itoh*[1], *K. Mori*[2], *Y. Horikawa*[1] and *T. Minemoto*[2]. [1]Deptartment of Electronic Engineering, Kinki University, Japan. [2]Division of System Science, Kobe University, Japan.

16–94 Low noise hybrid TlBaCaCuO / GaAs 5.4 GHz transponders. *K.C.Huang*[1], *A.Jenkins*[1], *D.J.Edwards*[1] and *D.Dew-Hughes*[1]. [1] Department of Engineering Science, University of Oxford, Parks Road, Oxford, OX1 3PJ, UK.

16–95 HTS filters and cooled electronics for communications - system performance and cooling needs. *R.B.Greed*[1] and *J.Tilsley*[2]. [1]1 Marconi Research Centre, Great Baddow, Chelmsford, Essex, CM2 8HN, England. [2]2 Marconi Infra-Red, Southampton, Hampshire, SO15 0EG, England.

16–96 Jena Superconductive Electronics Foundry (JeSEF). *H.-G. Meyer, L. Fritzsch, R.P.J. Ijsselsteijn, J. Ramos, H. Elsner, W. Morgenroth, J. Kunert, G.Wende, M. Schubert* and *R. Stolz*. Institute for Physical High Technology Dept. of Cryoelectronics P.O.Box 100239 D-07702 Jena Germany.

16–97 Thermoelectric Generator with the Passive Superconducting branch. *V.A.Demchenko*. Institute of Thermoelectricity, General Post Chernovtsy 274000, Box 86, Ukraine.

16–98 Numerical analyses of superconductive electronic structures at high frequencies. *H.Toepfer, T.Lingel* and *F.H.Uhlmann*. Technical University of Ilmenau Department of Fundamentals and Theory of Electrical Engineering P.O.Box 100565 D-98684 Ilmenau Germany.

Session Digital Applications

16–99 SQUID Applications for SFQ Logic Circuits. *Y.Harada*. Kokushikan University, Faculty of Engineering 4-28-1 Setaga.

16–100 Digital Superconducting Gauges of Temperature. *V.A.Demchenko*. Institute of Thermoelectricity, General Post Chernovtsy 274000, Box 86, Ukraine.

16–101 Basic RSFQ circuits and digital SQUIDs realised in standard Nb/Al-Al_2O_3/Nb technology. *M. Khabipov*[1,2], *L. Fritzsch*[1], *S. Lange*[3], *R. Stolz*[1], *H.Uhlmann*[3] and *H.-G. Meyer*[1]. [1]Institute for Physical High Technology, Department of Cryoelectronics, Jena, P.O. Box 100239, D-07702, Germany. [2]Permanent address: IREE Russian Academy of Sciences, Mokhovaya St. 11, Moscow, 103907 Russia. [3]Technical University of Ilmenau, Ilmenau,P.O. Box 100565, D-98684, Germany.

16–102 Ramp Edge Junctions on a Ground Plane for RSFQ Applications. *A.H. Sonnenberg, G.J. Gerritsma* and *H. Rogalla*. Low Temperature Division, Faculty of Applied Physics, University of Twente P.O. box 217, 7500 AE, Enschede, The Netherlands.

16–103 RSFQ-Based D/A Converter for Precise-Measurement Applications. *F. Hirayama, H. Sasaki, S. Kiryu, M. Maezawa, T. Kikuchi* and *A. Shoji*. Electrotechnical Laboratory, Tsukuba, Ibaraki, 305-8568 Japan.

16–104 Measurements of a High Tc RSFQ 4-Stage Shift Register and the Inductance of the Shift Register Cell. *Y. H. Kim*[1], *J. H. Park*[1], *J. H. Kang*[2], *T. S. Hahn*[1], *C. H. Kim*[1], *J. M. Lee*[1] and *S. S. Choi*[1]. [1]Korea Institute of Science and Technology, Seoul 130-650, Korea. [2]University of Inchon, Inchon 402-749, Korea.

16–105 Comparators for HTS ADCs based on the tri-crystal Josephson junctions. *A.Yu. Kidiyarova-Shevchenko*[1,2], *F. Komissinsky*[3], *E.A. Stepancov*[4], *Z.G. Ivanov*[1], *D.E. Kirichenko*[5], *M.M. Khapaev, Jr.*[6], *M. Jacobson*[1] and *T. Claeson*[1]. [1]Chalmers University of Technology, Gothenburg, Sweden. [2]Nuclear Physics Institute, Moscow State University, Moscow, Russia. [3]Institute of Radio Engineering and Electronic RAS, Moscow, Russia. [4]Institute of Crystallography RAS, Moscow, Russia. [5]Physics Dep., Moscow State University, Moscow, Russia. [6]Computer Science Dep., Moscow State University, Moscow, Russia.

16–106 Universal NAND Gate Based on Single Flux Quantum Logic. *H. Myoren, S. Ono* and *S. Takada*. Faculty of Engineering, Saitama University, 255 Shimo-Okubo, Urawa, Saitama 338-8570, Japan.

16–107 HTS implementation of Analogue to Digital Converters. *J. S. Satchell* and *I. L. Atkin*. DERA (Malvern), Malvern, Worcs, WR14 3PS, United Kingdom.

16–108 Matching of Rapid Single Flux Quantum Digital Circuits and Superconductive Microstrip Lines. *N.A. Joukov*[1], *A.Yu. Kidiyarova-Shevchenko*[2,3], *D.E. Kirichenko*[1], *A.B. Pavolotskij*[3] and *M.Y. Kuprianov*[3]. [1]Department of Physics, Moscow State University, 119899 Moscow, Russia. [2]Department of Physics and Engineering Physics, Chalmers University of Technology, S-41296 Gothenburg, Sweden. [3]Nuclear Physics Institute, Moscow State University, 199899 Moscow, Russia.

Session Oscillators and Volt standards

16–110 High Temperature Superconducting Low Noise Oscillator. *T.A. Koetser*[1] and *R.B. Greed*[2]. [1]T.A. Koetser Marconi Research Centre West Hanningfield Road Great Baddow Chelmsford Essex CM2 8HN. [2]R.B. Greed Marconi Research Centre West Hanningfield Road Great Baddow Chelmsford Essex CM2 8HN.

16–111 Subharmonic Gap Structures in Josephson Flux Flow Oscillators. *M.A. Nordahn*[1], *M.H. Manscher*[1], *J. Mygind*[1] and *L.V. Filippenko*[2]. [1]Department of Physics, Technical University of Denmark, B309, DK-2800 Lyngby, Denmar. [2]Institute of Radio Engineering and Electronics RAS, Mokhovaya 11, Moscow 103907, Russia.

16–112 Josephson-Junction Arrays with Lumped and Distributed Coupling Circuits. *V.K. Kornev*, *A. V. Arzumanov* and *N. A. Shcherbakov*. Physics Department, Moscow State University, Moscow, 119899, Russia Department of Physics, Moscow State University, Moscow, 119899, Russia;

16–113 Linewidth Measurement of Josephson Array Oscillators with Microstrip Resonators. *A. Kawakami*, *Y. Uzawa* and *Z. Wang*. Kansai Advanced Research Center, Communications Research Laboratory, 588-2 Iwaoka, Iwaoka-cho, Nishi-ku, Kobe, Hyogo, 651-2401, Japan.

16–114 Microwave properties of SINIS Josephson junction series arrays. *H. Schulze*[1], *R. Behr*[1], *J. Kohlmann*[1], *F. Mueller*[1], *I.Ya. Krasnopolin*[2] and *J. Niemeyer*[1]. [1]Physikalisch-Technische Bundesanstalt, 38116 Braunschweig, Germany. [2]Russian Research Institute for Metrological Service, Moscow, 117965 GSP-1, Russia.

16–115 Influence of the phase-whirling states on the fluxon motion in two inductively coupled long Josephson junctions. *E. Goldobin*[1], *A. Wallraff*[2] and *A.V. Ustinov*[2]. [1]Institute of Thin Film and Ion technology, Research Center Juelich GmbH, 52425, Juelich, Germany. [2]Physics Institute III, University of Erlangen-Nuernberg, 91054, Erlangen, Germany.

16–116 Two-stacks of parallel arrays of long Josephson junctions. *G. Carapella*[1,2], *G. Costabile*[1,2], *G. Filatrella*[2,3] and *R. Latempa*[1,2]. [1]Dipartimento di Fisica, Baronissi 84081, Italy. [2]UdR INFM dell'Universita' di Salerno, Baronissi 84081, Italy. [3]Universita' del Sannio, Benevento 82100, Italy.

16–117 Optical functions of cuprate superconductors. *N.P.Netesova*. M.V.Lomonosov Moscow State University.Department of Physics.Lab.Cryoelectronics,C60a Moscow.119899 Russia.

16–118 Programmable Josephson voltage standards using SINIS junctions. *J. Kohlmann*, *H. Schulze*, *R. Behr*, *F. Mueller* and *J. Niemeyer*. PTB, Bundesallee 100, D-38116 Braunschweig, Germany.

ORAL SESSION 17A: AC Losses II

Thursday Afternoon, September 16th, 17:30-19:00

17:30 **17A–1 AC loss of YBCO tape in AC back ground field.** *O.Tsukamoto*[1], *M.Ciszek*[1], *D.Miyagi*[1], *J.Ogawa*[1], *O.Kasuu*[2], *H.Ii*[2], *K.Takeda*[2] and *M.Shibuya*[2]. [1]Yokohama National University. Japan. [2]Engineering Research Association for Superconductive Generation Equipment and Materials (Super-GM), Japan.

17:45 **17A–2 The Calorimetric Measurement of AC Losses in HTS Conductors in Combinations of Applied Magnetic Fields and Transport Currents.** *S.P.Ashworth* and *M.Suenaga*. Materials Science Division Brookhaven National Laboratory PO Box 5000 Upton New York NY -11973 USA.

18:00 **17A–3 AC losses of multifilamentary Bi(2223) tapes in external magnetic field with different internal resistive barrier structures between the filaments.** *H. Eckelmann*, *J. Krelaus*, *R. Nast* and *W. Goldacker*. Forschungszentrum Karlsruhe, Institut für Technische Physik, Karlsruhe, D-76021, Germany.

18:15 **17A–4 AC losses of twisted multifilamentary Bi-2223 tapes under AC perpendicular fields.** *E. Martínez*[1], *Y. Yang*[1], *C. Beduz*[1], *Y. Huang*[2] and *C.M. Friend*[2]. [1]Institute of Cryogenics, University of Southampton, Southampton, United Kingdom. [2]BICC Cables Ltd. Technology Center, Wrexham LL13 9XP, United Kingdom.

18:30 **17A–5 Measurements of Losses in a High-Temperature Superconductor Exposed to Both AC and DC Magnetic Fields and Transport Currents.** *N. Schönborg*[1], *N. Magnusson*[2] and *S. Hörnfeldt*[3]. [1]Royal Institute of Technology, Department of Electric Power Engineering SE-100 44 Stockholm Sweden. [2]Royal Institute of Technology, Department of Electric Power Engineering SE-100 44 Stockholm Sweden. [3]ABB Corporate ResearchSE-721 78 Västerås Sweden.

18:45 **17A–6 A simple HTS-cable model to study the effect of the geometrical arrangement of the tapes on AC losses.** *R. Tebano*[1], *D. Uglietti*[2], *G. Coletta*[3], *L. Gherardi*[3], *F. Gömöry*[4] and *R. Mele*[3]. [1]Dipartimento di Scienza dei Materiali, Universita' degli Studi di Milano, Via Cozzi 53, Milano, 20126, Italy. [2]INFM, UdR di Milano, Dipartimento di Scienza dei Materiali, Universita' degli Studi di Milano, Via Cozzi 53, Milano, 20126, Italy. [3]Pirelli Cavi & Sistemi S. p. A. , Viale Sarca 222, Milano, 20126, Italy. [4]Institute of Electrical Engineering, Slovak Academy of Science, Dubravska 9, 842 39 Bratislava, Slovak Republik.

ORAL SESSION 17B: Fusion, SMES, detectors, accelerators

Thursday Afternoon, September 16th, 17:30-19:00

17:30 ***17B–1 The superconducting magnet system for the WENDELSTEIN 7-X Stellarator.** *J. Sapper* and W7-X team. Max-Planck -Institut für Plasmaphysik, EURATOM Association, D-85748 Garching, Germany.

18:00 **17B–2 AC loss measurements of the 100kWh SMES model coil.** *N. Hirano*[1], *K. Shinoda*[1], *S. Hanai*[2], *T. Hamajima*[2], *M. Kyoto*[2], *N. Martovetsky*[3], *J. Zbasnik*[3], *M. Yamamoto*[4], *T. Himeno*[4] and *T. Satow*[5]. [1]Chubu Electric Power Co., Inc., 20-1 Ohdaka-cho, Midori-ku, Nagoya, 459-8522, Japan. [2]Toshiba Corporation, 2-4 Suehiro-cho, Tsurumi-ku, Yokohama 230-0045, JAPAN. [3]Lawrence Livermore National Laboratory, L-641, 7000 East Ave., Livermore, CA 94550, USA. [4]International Superconductivity Technology Center, 5-34-3 Shinbashi, Minato-ku, Tokyo 105-0004, JAPAN. [5]National Institute for Fusion Science, 322-6 Oroshi, Toki, Gifu 509-5292, JAPAN.

18:15 **17B–3 High Field Solenoids for Muon Cooling.** *M. A. Green*[1], *Y. Eyssa*[2], *S. Kenny*[2], *J. R. Miller*[2] and *S. Prestemon*[2]. [1]Lawrence Berkeley National Laboratory, Berkeley CA 94720, USA. [2]National High Magnetic Field Laboratory, Tallahassee FL 32310, USA.

18:30 **17B–4 Test Results of Compensation for Load Fluctuation by Using 1kWh/1MW Module-Type SMES.** *H. Hayashi*[1], *T. Sannomiya*[1], *K. Tsutsumi*[1], *F. Irie*[1], *T. Ishii*[2] and *R. Ikeda*[3]. [1]Kyushu Electric Power Co.,Inc..2-1-45,Shiobaru,Minami-ku,Fukuoka,815-8520,Japan. [2]West Japan Engineering Consultants,Inc.1-7-11,Chuo-ku,Fukuoka,810-0003,Japan. [3]Fukuoka Denki Keiki Co.,Inc.4-18-15,Minami-ku,Fukuoka,815-0031,Japan.

18:45 **17B–5 Comparison of HTS and LTS μ-SMES Concepts.** *R. Mikkonen*, *J. Lehtonen* and *J. Paasi*. Tampere University of Technology, Laboratory of Electromagnetics, P.O. Box 692, FIN-33101 Tampere, Finland.

ORAL SESSION 17C: Materials Related to Electronic Applications

Thursday Afternoon, September 16th, 17:30-19:00

17:30 ***17C–1 Series production of large area YBCO - films for microwave and electrical power applications.** *W. Prusseit*, *S. Furtner* and *R. Nemetschek*. THEVA Thin Film Technology, 85386 Eching, Germany.

18:00 **17C–2 Epitaxial (101) YBa2Cu3O7 thin-fims on (103) NdGaO3 substrates.** *Y.Y. Divin*[1], *U. Poppe*[1], *C.L. Jia*[1], *J.W. Seo*[2,3] and *V. Glyantsev*[4]. [1]Institut für Festkoerperforschung, Forschungszentrum Juelich GmbH, D-52425 Juelich, Germany. [2]Institute de Physique Universite de Neuchatel,CH-2000, Switzerland. [3]IBM -Zuerich Research Laboratory, CH-8803 Rueschlikon, Switzerland. [4]Conductus Inc., Sunnyvale, CA 94086, USA.

18:15 **17C–3 Electrostatic modulation of superconductivity in ultrathin epitaxial $GdBa_2Cu_3O_{7-x}$ films.** *C.H. Ahn*, *S. Gariglio*, *P. Paruch*, *T. Tybell*, *L. Antognazza* and *J.-M. Triscone* Département de Physique de la Matière Condensée, Université de Genève, 24 quai Ernest-Ansermet, 1211 Genève 4, Switzerland

18:30 **17C–4 Spatial variation of the non-linear surface impedance of HTS films.** *L. Hao* and *J.C. Gallop*. National Physical Laboratory, Teddington, TW11 0LW, UK.

18:45 **17C–5 Optimization of Microwave Losses of Ferromagnetic Perovskite Thin Films for Magnetically Tunable Microwave Superconducting Filters.** *J. Wosik*[1], *M. Strikovski*[1], *L.-M. Xie*[1], *P. Przyslupski*[2], *M. Kamel*[1] and *S. A. Long*[1]. [1]Electrical and Computer Engineering Department and Texas Center for Superconductivity, University of Houston, 4800 Calhoun Rd., Houston, TX 77204-5932, USA. [2]Institute of Physics, Polish Academy of Sciences, Al. Lotnikow 32/36, PL-02 668 Warszawa, Polan.

ORAL SESSION 17D: Josephson Junctions II

Thursday Afternoon, September 16th, 17:30-19:00

17:30 ***17D–1 Investigation of microstructure of ramp-type $YBa_2Cu_3O_{7-d}$ structures.** *H. Sato*, *F.J.G. Roesthuis*, *A.H. Sonnenberg*, *A.J.H.M. Rijnders*, *D.H.A. Blank* and *H. Rogalla*. University of Twente, 7500 AE, Enschede, Netherland.

18:00 **17D–2 Josephson phenomenology and microstructure in $YBa_2Cu_3O_{7-\delta}$ artificial grain boundaries characterized by misalignment of the c-axes.** *F. Tafuri*[1,2], *F. Miletto Granozio*[2], *F. Carillo*[2], *F. Lombardi*[2], *U. Scotti di Uccio*[2], *K. Verbist*[3] and *G. Van Tendeloo*[3]. [1] Dipartimento di Ingegneria, Seconda Università di Napoli, Aversa (CE) , Italy. [2]INFM-Dipartimento di Scienze Fisiche- Università di Napoli "Federico II",Napoli, Italy. [3]EMAT, University of Antwerp (RUCA), Groenenborgerlaan 171, B-2020 Antwerp, Belgium.

18:15 **17D–3 Interval deposition: growth manipulation for use in fabrication of planar $ReBa_2Cu_3O_{7-\delta}$ junctions.** *A.J.H.M. Rijnders*, *G. Koster*, *D. H.A. Blank* and *H. Rogalla*. Univ. of Twente, Dept. of Applied Physics, Low Temperature Division, P.O.Box 217, 7500 AE, Enschede, The Netherlands.

18:30 **17D–4 Microwave responses of $Bi_2Sr_2Ca_1Cu_2O_{8+y}$ Intrinsic Josephson junctions.** *K. Nakajima*[1,3], *Y. Aruga*[1], *H.B. Wang*[3], *T. Tachiki*[1], *Y. Mizugaki*[1,3], *J. Chen*[1,3], *T. Yamashita*[2,3] and *P.H. Wu*[4]. [1]Research Institute of Electrical Communication, Tohoku University, Sendai, Japan. [2]New Industry Creation Hatchery Center, Tohoku University, Sendai, Japan. [3]CREST, Japan Science & Technology Cooporation, Japan. [4]Department of Electronic Science & Engneering, University of Nanjing, Nanjing 210093, China.

18:45 **17D–5 Experiments on Energy Level Quantization in Underdamped Josephson Junctions.** *E.Esposito*[1,2], *C.Granata*[1,3], *M. Russo*[1,2], *B.Ruggiero*[1,2] and *P.Silvestrini*[1,2]. [1] Istituto di Cibernetica del CNR, I-80072, Arco Felice (Napoli), Italy. [2] Macroscopic Quantum Coherence Group, Istituto Nazionale Fisica Nucleare, I-80126 Napoli, Italy. [3]AtB, Advanced Technologies Biomagnetics, I-66013 Chieti Scalo, Italy.

Friday, September 17th

PLENARY SESSION 18

Friday Morning, September 17th, 8:30-10:30

30 **18–1 Strategies for Tailoring New High T_c Superconductors.** *M. Marezio* and *F. Licci*. Istituto MASPEC-CNR, Fontanini-PARMA, 43010, Italy.

90 **18–2 Roadmap of Superconducting Elecronics.** *C.E.Gough*. Superconductivity Research Group, University of Birmingham, School of Physics and Astronmy, B15 2TT, UK.

30 **18–3 Research and Developments of High-Tc Superconductivity in Japan.** *S. Tanaka*. Superconductivity Research Laboratory / ISTEC, 1-10-13 Shinonome Koto-ku, Tokyo, JAPAN

90 **18–4 Superconductivity in the US.** *H. Weinstock*. Air Force Office of Scientific Research Arlington, VA 22203-1977 USA.

PLENARY SESSION 19

Friday Morning, September 17th, 11:00-13:15

90 **19–1 Status of superconducting power applications.** *H.-W. Neumüller*. Siemens AG Corporate Technology D-91050 Erlangen, P.O.Box 3220.

45 **19–2 HTS Prototype for power transmission cables: recent results and future programs** *M. Nassi*. Pirelli Cavi & Sistemi, Milano, Italy.

15 **19–3 Status for business development of HTS SQUID applications.** *T. Freltoft* and *Y.Q. Shen*. NKT Research Center A/S Priorparken 878 DK-2605 Brøndby Denmark.

45 **19–4 Superconductors and Cryogenics for Future Communication Technology.** *M. Klauda*[1], *T. Kässer*[1], *B. Mayer*[1], *C. Schrempp*[1], *C. Neumann*[2], *N. Klein*[3] and *H. Chaloupka*[4]. [1]Bosch Telecom GmbH; Space Communication Systems; D-71520 Backnang; Germany. [2]Robert Bosch GmbH; Corporate Research and Development; D-70049 Stuttgart; Germany. [3]Forschungszentrum Jülich; D-52425 Jülich; Germany. [4]Universität Wuppertal; Fachbereich Elektrotechnik; D-42097 Wuppertal; Germany.

CLOSING

Friday Morning, September 17th, 13:15-13:45

Abstracts

EUCAS'99

4th European Conference on Applied Superconductivity

SITGES 14-17 SEPTEMBER

PLENARY SESSION 1

Tuesday Morning, September 14th, 8:40-10:00

8:40 1–1

Materials: the path to applications.

J.E. Evetts and *B.A.Glowacki*. Interdisciplinary Research Center in Superconductivity and Department of Materials Science, University of Cambridge Premboke Street, Cambridge, CB2 3QZ UK.

As the application of high temperature superconductivity gradually becomes a reality it is clear that painstaking incremental progress in the development of materials is the key to success. Although there are parallels with the development of low temperature superconducting metallic materials; the short coherence length, extreme anisotropy and uncompromising mechanical properties of the oxide superconductors bring challenges of a new order. An overview will first be given of the current status of materials processing with emphasis on fundamental issues and limitations. A detailed assessment will be given of some of the problems in the development and specification of materials for particular applications. In summary the scope for significant innovation will be discussed and likely trends in materials performance assessed.

9:20 1–2

Superconducting gaps and pseudogaps: STM spectroscopy

Ø. Fischer. Université de Genève, Departement de Physique de la Matière Condensée, 1211 Genève 4, Switzerland.

High temperature superconductors display a behaviour very different from classical BCS superconductors. The gaps are exceptionally large with $2\Delta/k_BT_c$ values as high as 12 and above. Furthermore, as doping is reduced and T_c decreases as one enters the underdoped region, it is found that the gaps on the contrary continue to increase. Related to this is the existence of a pseudogap in the quasiparticle excitation spectrum observed above the critical temperature. These features which have now been deduced from measurements with many different techniques can be very directly observed in scanning tunneling spectroscopy, which measures the local density of states just beneath the tip. With this technique one can also observe vortices and the electronic structure of the vortex cores. The spectroscopy of the vortex cores reveal again very unusual behaviour. While a BCS d-wave superconductor is expected to show a zero bias anomaly due to extended states associated with the vortex core, we find either one localized state ($Yba_2Cu_3O_7$) or no visible states at all ($Bi_2Sr_2CaCu_2O_{8+\delta}$). In the latter compound the vortex core show a spectrum basically identical to the pseudogap spectrum observed above T_c. All these observations contribute to confirm the non-BCS behaviour of these superconductors and put strong constraints on possible future theoretical explanations of their properties.

This work has been done in collaboration with Ch. Renner, I. Maggio-Aprile, B. Hoogenboom, and M. Kugler.

ORAL SESSION 2A+3A: Bulk Materials and Materials Aspects I

Tuesday Morning, September 14th, 10:30-12:45

10:30 *2A–1

Fabrication and Microstructural Features of Large Grain Nd-Ba-Cu-O Composites.

N. Hari Babu[1], *W. Lo*[1,2], *D. A. Cardwell*[1] and *Y.H. Shi*[1]. [1]IRC in Superconductivity, University of Cambridge, Cambridge, CB3OHE, UK. [2]Texas Center for Superconductivity, University of Houston, Houston, TX77204-5932, USA.

Large, single grain Nd-Ba-Cu-O (NdBCO) composite consisting of $NdBa_2Cu_3O_{7-\delta}$ (Nd123) containing various amounts of non-superconducting $Nd_4Ba_2Cu_2O_{10}$(Nd422) phase inclusions have been successfully fabricated using a top-seeded melt growth method in reduced oxygen partial pressure. These large grains are shown to have high irreversibilty field values over wide temperature range, indicating that these composites have high potential for bulk engineering applications. In this paper we report the processing rate in the specific temperature range in which a seeded grain can grow without being hindered by the subsidiary nucleations, the variation in microstructural features such as the size, morphology, and spacial distribution of Nd422 phase inclusions in Nd123 matrix with the Nd422 phase inclusion concentration. The influence of Nd422 phase particles on the growth rate, the pores and macro cracks have also been discussed.

11:00 2A–2

Growth of large $YBa_2Cu_3O_{7-\delta}$ mono domains with improved characteristics for current limiting applications.

D.Isfort, *X.Chaud*, *E. Beaugnon*, *D.Bourgault* and *R.Tournier*. CNRS/CRETA/Matformag Grenoble Isère 38000 France.

The use of $YBa_2Cu_3O_{7-\delta}$ mono domains for resistive current limitation implies new requirements of the material since homogeneous long conductors have to be cut in them. Large size and quality optimised $YBa_2Cu_3O_{7-\delta}$ mono domains have been developped and produced by controlling the following parameters : 1) The reaction at the pellet/substrate interface is the governing factor for the mono-domain size in the c-direction which is often blocked by grains nucleated at the substrate or by reactions of the liquid phase with the substrate; 2) A carefull adjustement of the thermal treatment with the help of in situ video recording of the growth enabled us to enlarge the mono-domain size in a- and b-direction, despite of a very narrow growth window. 3) The choice of the granulometry of the precursor powder helps to reduce the porosity and especially to avoid large pores in the mm range. As a result of the optimisation work, YBCO mono-domains with 45mm diameter and 15mm height can be produced in a standardised process and show high superconducting properties $J_c > 10^5 A/cm^2$ at 77K and 20 000 A/cm^2 at 89K, levitation force 80N with a 22 mm diameter NdFeB magnet). The only remaining macro-defects are cracks parallel to the ab-plane and a certain but small porosity that should not affect the homogeneity of the transport properties in the ab planes. Shaping, joining and testing of the current limiting elements will also be

presented.

11:15 2A–3
Massive YBCO material for rotating electric machines.
W. Gawalek[1], *T. Habisreuther*[1], *D. Litzkendorf*[1], *M. Zeisberger*[1], *T. Strasser*[2], *J. Best*[2], *B. Oswald*[2], *K. V. Ilushin*[3], *L. K. Kovalev*[3] and *H. J. Gutt*[4]. [1]Institut fuer Physikalische Hochtechnologie e.V., Helmholtzweg 4, D-07743 Jena, Germany. [2]OSWALD Elektromotoren GmbH, Benzstr. 12, D-63897 Miltenberg, Germany. [3]Moscow State Aviation Institute, Volokolamskoe shosse, 125871 Moscow, Russia. [4] Institut fuer Elektrische Maschinen und Antriebe, Universitaet Stuttgart, Pfaffenwaldring 47, D-70569 Stuttgart, Germany.

Single domain bulk blocks of melt textured YBCO, cylindrically shaped with 30 mm and 45 mm in diameter and cuboid shaped with 35 mm lenght (all 17 mm in thickness) are prepared in a batch process with 30 or 16 samples, respectively, in one run. In small samples critical current densities up to $6 \cdot 10^4$ A/cm^2 are measured by vibration sample magnetometry. But there are indications of reduced critical current densities over full sample diameter, caused by misoriented subgrains. Bulk cryomagnetic elements for HTS motors as cylinders, bars, and plates are assembled by cutting and bonding parts of single domain blocks. These elements are used in rotors for hysteresis and reluctance motors. In order to increase the interaction between the rotating stator field and the anisotropic superconducting material, the optimal orientation of the material in the rotors is considered. The material quality is given by the current load, the product of critical current density and diameter of superconducting current loop. In practise the magnetic quality of single blocks is controlled by zero field cooled levitation force measurement of every sample and field mapping. In rotor elements the quality can be controlled also by field mapping. The function principles of hysteresis and reluctance motors are quite different. In hysteresis motors the pinned stator field is essential, in reluctance motors the shielding efficiency of material. This has to be considered with the constuction of the rotor elements. With bulk superconductor rotors series of hysteresis and reluctance machines with rotation speeds up to 24000 rpm and output powers larger 10 kW are constructed and tested successfully in OSWALD Electromotor Company Miltenberg, Moscow State Aviation Institute and Institute for Electrical Machines and Drives Stuttgart.
Work Supported by the German BMBF under contract 13N6854

11:30 2A–4
Top Seeded Growth and Joining of Bulk YBCO.
H. Zheng, *B. W. Veal*, *A. Paulikas*, *R. Nikolova*, *U. Welp*, *H. Claus* and *G. W. Crabtree*. Argonne National Laboratory, Argonne, IL, USA, 60439.

We report (i) systematic studies of the growth rate for melt textured YBCO, (ii) top seeding growth techniques to determine a minimum seed size, and (iii) joining techniques for melt textured YBCO enabling the fabrication of large single domain structures of arbitrary shape. Seeded growth of YBCO occurs in a narrow temperature window about 20 C below the peritectic decomposition temperature. Successful top seeding depends on the size of the NdBCO seed crystal. Small seeds are eventually dissolved in the melt before nucleation occurs, while large seeds regularly produce single domain monoliths. Joining techniques based on seeding of low melting point Tm123/Y211 filler material by neighboring YBCO will be described. Magneto-optical images of the YBCO/TmBCO/YBCO assembly show no detectable penetration of magnetic field at the joints. Using this joining technique, large single domain objects of arbitrary shape for motors, fault current limiters, and trapped field magnets may be produced. This work was supported by the US Department of Energy, Office of Basic Energy Sciences-Materials Sciences, under contract #W-31-ENG-38 (BWV, AP, RN, UW, HC, GWC) and the NSF Science and Technology Center for Superconductivity under contract #DMR91-20000 (HZ).

11:45 3A–1
Tailoring of critical currents of melt textured $YBa_2Cu_3O_7$ / Y_2BaCuO_5 composites by high oxygen pressure.
J. Plain[1,3], *T. Puig*[1], *F. Sandiumenge*[1], *X. Obradors*[1], *J.A. Alonso*[2] and *J. Rabier*[3]. [1] Institut de Ciència de Materials de Barcelona, Consejo Superior de Investigaciones Científicas, Campus de la UAB, 08193 Bellaterra, Spain. [2] Instituto de Ciencia de Materiales de Madrid, Consejo Superior de Investigaciones Científicas, Cantoblanco, 28049 Madrid, Spain. [3] Laboratoire de Métallurgie physique, UMR 6630-CNRS Université de Poitiers - UFR Sciences, SP2MI, BP 179 86960 Futuroscope Cedex, France.

High oxygen pressure (HPO_2) post-processing treatments are presented as a very efficient and scalable technique for critical current enhancement of melt-textured Y123/211 composites. Jc improvements up to 100% between 5 and 77 K have been obtained by oxygenating the Y123/211 composites at 100 bar at 450 °C. Samples were prepared by top seeding growth and oxygenated at 450 °C at 1 bar for 120 hours. Afterwards, they were submitted to different oxygen pressures (from 100 to 200 bar) at several temperatures (from 350 to 600 °C) for 12 hours. TEM analysis show that HPO_2 treatments induces the growth of large stacking faults and partial dislocations and, that by properly choosing the temperature and pressure conditions, it is possible to tailor their growth. The relationship between microstructure and physical properties is analysed. Magnetisation measurements show that HPO_2 treatments increase the critical currents in all the temperature range analysed. However, an aging process is induced by HPO_2 treatments at 600 °C, which consequently decreases the irreversibility line. The overall analysis suggest that there is a competing effect between dislocations and stacking faults. While the former act as vortex flux pinning centres, the latter induces an aging effect. An optimisation of the process has been performed. Financial support from the EU-TMR network Supercurrents, EBR 4061PL97-0281, is acknowledged.

12:00 3A–2

Reproducible production of large YBCO - monoliths with peak -effect.

G. Krabbes[1], *P. Schaetzle*[1], *G. Stoever*[1], *J.W. Park*[2], *S. Gruss*[1] and *G. Fuchs*[1]. [1] Institute of Solid Sate and Material Research Dresden, P.O. Box 270016, D-01171 Dresden,. [2]Solvay Barium Strontium GmbH, Hans- Böckler Allee 20, D-30173 Hannover.

Well known from high quality Y-123 single crystals a peak effect in the J_C curve versus an applied external magnetic field is established by an deficient oxygen content resulting in oxygen clusters. Such a peak effect is also typical in NdBaCuO melt processed materials which is attributed to an substitution of Nd on Ba sites. In the present investigations large YBCO - monoliths (d = 25 - 35 mm) were reproducible produced by the modified melt crystallization process (MCP) starting from an Y-123 precursor which was doped by an increasing amount of metallic cations. The J_C vs. $H_{ext.}$ curves represents an peak effect at about 3 T (J_C = 3 x 10^4 A/cm^2) and high J_C values above 1 x 10^4 A/cm^2 between 1 and 5 T at 75K. The trapped magnetic fields and levitation forces were found to be between $B_0 \approx$ 0.7 T (d = 25 mm) and $F_N \approx$ 60 N. The normalized pinning force versus the reduced field is in the order of b_0 = 0.4 and similar to the published values of the NdBaCuO material. T_C and low temperature magnetization measurements were performed to investigate the occurrence of the peak effect on this high quality YBCO - monolithic material.

12:15 3A–3

High critical currents in Ce/Sn doped YBCO pellets grown by top seeding method.

C. Leblond, *S. Marinel*, *I. Monot*, *G. Desgardin* and *B. Raveau*. CRISMAT laboratory-CNRS UMR 6508, 6 Bd. Du Marechal Juin, 14050 Caen CEDEX. France.

YBCO superconductor has been shown to be a good candidate owing to its flux pinning characteristics under field. We investigated different compositions and processing conditions for growing large sizes and high quality single grain YBCO pellets, obtained by Top Seeding Melt Texturing process in isothermal box furnace with a SmBaCuO melt textured seed. $YBa_2Cu_3O_{7-\delta}$ / Y_2BaCuO_5 system with SnO_2 and/or CeO_2 doping were shown to exhibit very high inductive critical current densities at 77K, between 0 and 2 teslas (80000 A/cm^2 in self field, 50000 A/cm^2 under 1 T and 35000 A/cm^2 under 2 T). Thus, we studied the adequate thermal cycle which is closely related to the material system characteristics (precursor powders, granulometry, green density, composition...). The seeding techniques need to know accurately the solidification window where this additional driving force of the texture formation, provided by the seed, can take place in an effective way. It has been shown that SnO_2 and CeO_2 dopants do not only modify the microstructure and the critical current densities but also the growth rates along ab planes. By controlling all these parameters, we succeeded in producing highly textured monolithic pellets, as confirmed by X-ray four circle pole and field mapping. The top seeding method allows to produce a material with high performances at centimeter scale, in a reproducible way.

12:30 3A–4

Crystal defects in melt grown Re-Ba-Cu-O.

P. Diko. Institute of Experimental Physics, Watsonova 47, 04 353 Košice.

The crystal defect formation mechanisms are summarized in the contribution. On the base of extended microstructural studies it is shown that defects as porosity, shape change of the sample, subgrains, 211 particle inhomogeneity and secondary phases can be related to the solidification process. The defects as are macrocracks, a-b microcracks, residual dilatation stresses and twins are directly influenced by the size and volume fraction of 211 particles. The role of some of these crystal defects in oxygenation process will be pointed out.

This work has been supported by the Slovak Grant Agency

ORAL SESSION 2B+3B: System Aspects and High Fields

Tuesday Morning, September 14th, 10:30-12:45

10:30 *2B–1

Recent R&D Status on 70MW class Superconducting Generators in Super-GM Projec.

T.Hirao[1], *M.Shibuya*[1], *S.Shimada*[1], *H.Kusafuka*[1], *R.Shiobara*[2], *K.Suzuki*[3] and *K.Miyaike*[4]. [1]Engineering Research Association for Superconductive Generation Equipment and Materials(Super-GM), Osaka,530-0047,Japan. [2]Hitachi Ltd., Hitachi, Ibaragi, 317-8511, Japan. [3]Mitsubishi Electric Corp., Kobe, Hyogo, 652-8555, Japan. [4]Toshiba Corp., Yokohama, Kanagawa, 230-0045, Japan.

Super-GM in Japan has been vigorously promoting R&D on application of superconductive technology to electric power apparatuses. On the development of 70MW class superconducting model generators to verify the basic technologies for a 200MW class pilot machine, series of on-site verification tests for two slow-response-excitation-type generators have completed successfully by September in 1998. Through the tests, the world highest output of 79.7MW, the world longest continuous operation of 1500Hr as a superconducting generator were recorded, and the other excellent outcomes were achieved so far. On the other hand, series of on-site verification tests for a quick-response-excitation-type generator was started in December,1998. Recent R&D status focusing on the 70MW class superconducting generators will be presented together with the latest test results. In addition, recent research activities on the superconductors in the Super-GM project are given.

This work has been performed as a part of "R&D on superconducting technology for electric power apparatuses" under the New Sunshine Program of Agency of Industrial Science and Technology, MITI, being consigned by NEDO in Japan.

11:00 2B–2

An HTS Magnet for Whole-body MRI.

A.F. Byrne[1], *F.J. Davies*[1], *C. Raynor*[1], *W. Stautner*[1], *F. Steinmeyer*[2], *C. Albrecht*[2], *P. Kummeth*[2], *P. Massek*[2], *H.-W. Neumüller*[2] and *M. Wilson*[3]. [1] Oxford Magnet Technology Ltd, Eynsham, UK. [2] Siemens AG, Corporate Technology, ZT EN 4, Erlangen, Germany. [3] Oxford Instruments Research Instruments, Tubney Woods, UK.

In a collaboration between the parties listed above, we have developed and successfully tested the first MRI electromagnet that uses high temperature superconductor (HTS) coils. The system comprises a C-shaped iron yoke and two pole pieces, each energised by an HTS coil. The flux density in the 46cm patient gap is 0.19T and in the windings is 1T. The coils were manufactured separately in Erlangen (Siemens ZT) and Oxford (OIRI) as a stack of pancake coils 80cm in inner diameter. Each coil used BSCCO-2223 tape produced by Vakuumschmelze (for Siemens ZT) and Nordic Superconductor Technologies (for OIRI) of total lengths 1.7km and 2.5km respectively. The engineering current density achieved in each coil was approximately 50A/mm2 in the operating field of 1T and at the operating temperature of 20K. This temperature was maintained in each case by a separate single stage Gifford-McMahon Leybold RGS 120T refrigerator and a stainless steel vacuum vessel. The experiment demonstrated a large-scale application of the use of HTS tapes and gives a clear insight into where future HTS research will benefit the MRI industry.

11:15 2B–3

Applications of HTS Technologies in the Danish Utilities.

P. Jorgensen and *J.J. Oestergaard*. DEFU, P.O. Box 259, 2800 Lyngby, Denmark.

In Denmark as well as in many other countries a number of research are dealing with different aspects of using HTS technologies. In many ways we can still talk about a technology push more than a demand-pull, since HTS is still a relatively new technology, and the customers for instance at the utilities are not demanding cables, generators, motors, SMES and fault current limiters with HTS technologies. Five years ago a survey was performed based on a simple literature study in order to point out which types of applications we could imagine that could be reasonable in the Danish electric system. This survey showed that a transmission cable could be reasonable to focus on, as a first step to applied HTS technology in the Danish electric system. The purpose of this paper is to discuss different possibilities of using HST technologies at the utilities in Denmark today. Here we should bear in mind that Denmark is a relatively small country with only 5 million inhabitants, and has a relatively large cable manufacturer, which are dealing with developing of a HTS cable.

11:30 2B–4

Compact iron screened HTS dedicated magnet for osteoporosis.

A. Matrone[1], *M. Ariante*[1], *V. Cavaliere*[1], *M. Mariani*[1], *A. Sotgiu*[2] and *V. Varoli*[3]. [1]ANSALDO-CRIS,via Nuova delle Brecce n. 260, I-80147 Napoli, Italy. [2]Università dell'Aquila - Dip. Scienze e Tecnologie Biomediche, via Vetoio, I-67100 Coppito - L'Aquila, Italy. [3]Politecnico di Milano, via Ponzio n. 34, I-20133 Milano, Italy.

It has been recently shown that the state of osteoporosis can be studied by determining the structure and interconnession of calcaneous trabecular bones by means oh high resolution MRI images. Feasibility of a compact 2T HTS superconducting magnet, dedicated to MRI of the calcaneous with higher sensitivity and resolution of a general purpose high field commercial unit, has been investigated. The magnet is an iron screened solenoid in which the field is generated by four pairs of independently powered Bi-2223/Ag symmetric pancakes. The magnet has a cylindrical shape of 50 cm in length and 44 cm in diameter. The room temperature bore has a diameter of 21 cm and allows an easy access of the foot. The preliminary simulations, which have been carried on using standard programs of field computation, have allowed to determine the positions, dimensions, intensities of the coils to achieve a uniform field of 2T in a cilindrical region of 10 cm in size. The presence of four remotely controlled power supply will allow an a posteriori optimization tecnique that has been used successfully in similar problems.

11:45 3B–1

600 A HTc Current Leads based on BSCCO 2212 Rods for LHC Magnets.

L. García-Tabarés[1], *J. Calero*[1], *P. Abramian*[2], *F. Toral*[2], *L.A. Angurel*[3], *C. Diez*[3], *R. Iturbe*[4], *J. Etxeandia*[4], *A. Ballarino*[5] and *J.C. Perez*[5]. [1]Centro de Estudios y Experimentación de Obras Publicas CEDEX. Alfonso XII, 3 28014 Madrid. Spain. [2]Centro de Investigaciones Energeticas MedioAmbientales y Tecnologicas CIEMAT. AV. Complutense 22. 28040 Madrid.Spain. [3]Departamento de Ciencia y Tecnologia de Materiales y Fluidos. ICMA. CSIC. Universidad de Zaragoza. Maria de Luna 3. 50015 Zaragoza.Spain. [4]ANTEC. Ramon y Cajal 74. 48920. Portugalete. Spain. [5]CERN. Geneva. Switzerland.

This paper describes the design, test and construction of four prototypes of 600A current leads based on BSCCO 2212 laser grown rods, to feed the LHC superconducting correction magnets that will be installed at the CERN´s Large Hadron Collider. These leads are gas cooled units working from room temperature to 4.2 K and are divided into two sections: A classical resistive part from 300 K down to 50 K, approximately, and a HTc superconducting element from 50 K to 4.2 K. This element uses four BSCCO rods manufactured using the LFZ (Laser Floating Zone) technique, which are assembled around a glass fiber cylinder containing, also, the shunt to protect the lead in the event of a quench. This configuration provides a high mechanical strength, with low thermal and Joule losses. The resistive part is cooled from its lower side using a fixed 20 K helium gas massic flow, that allows to maintain the temperature at the cold end bellow 50 K. The paper describes the design and fabrication of the leads, as well as some final measurements, including the description of an experimental facility, which has been developed to optimise the efficiency of the resistive part.

12:00 3B–2

13000 amp current lead with 1W heat load at 4.5K for the large hadron collider at CERN.

J. A. Good[1], *M. Allitt*[1] and *L. Martini*[2]. [1]Cryogenic Ltd, Unit 30 Acton Park Industrial Estate, The Vale, London W3 7QE, United Kingdom. [2]ENEL S.p.A, Struttura Ricerca, Via Volta, 20093 Cologne (MI), Italy.

Cryogenic Ltd. and ENEL S.p.A. have collaborated on the design and construction of prototype 13 kA current leads for the Large Hadron Collider project at CERN. This project requires that a nominal operating current of 13 kA is delivered into the 4.5K helium bath with a total heat load (dissipation plus conduction) of less than 1.5W, dropping to no more than 1W in standby operation. This is achieved by using hybrid conventional or high temperature superconductor (HTS) current leads, which are comprised of a resistive heat exchanger operating between 300K and 50K and a novel design of HTS BSCCO tape to carry the current from 50K to 4.5K. The resistive section is cooled by heat exchange with helium gas at a temperature of 20K that is introduced at the top of the HTS section. A maximum of 1 gs^{-1} mass flow of this 20K gas is available, which cannot leak back into the vapour space above the 4.5K bath. Finally, the lead must have an electrical resistance of at least 1GΩ to ground with 3.5kV between the current carrying part and ground in a helium atmosphere. An overview of the lead design is presented along with the results obtained during acceptance tests at CERN.

12:15 3B–3

Development of high field insert coils using high temperature superconductors.

D. Ryan[1], *H. Jones*[2], *K. Marken*[3], *M. Newson*[2] and *M.N. Wilson*[1]. [1]Oxford Instruments, Tubney Woods, Abingdon, OX13 5QX, UK. [2]University of Oxford, Clarendon Laboratory, Parks Rd, Oxford, OX1 3PU, UK. [3]Oxford Superconducting Technology, 600 Milik St, PO Box 429, Carteret NJ07008-0429 USA.

The manufacture of insert coils to boost the magnetic fields generated by superconducting magnets wound from low temperature superconducting materials is an application in which high temperature superconducting materials (HTS) can be economic today, due to their high critical current densities in magnetic fields above 20 T at liquid helium temperatures. The magnetic field generated by an insert coil of a given size is proportional to the engineering current density in the winding. Sufficient current density can now be obtained in BSCCO conductors but the manufacture of coils with high engineering current density remains difficult. We discuss two approaches for the production of coils from long lengths (several tens of metres) of HTS conductors: pancake coils manufactured from dip coated tapes using a wind, react and tighten (WRAT) process and layer wound solenoids using powder-in-tube conductor. Part of this work is supported by the SHIFT project, EC Brite Euram contract BE 96 3638.

12:30 3B–4

Development and testing of a 3 T Class Bi-2212 Insert Coil.

H.W. Weijers[1], *Q.Y. Hu*[1], *Y. Viouchkov*[1], *E. Celik*[1], *Y.S. Hascicek*[1], *J. Schwartz*[1], *K. Marken*[2] and *J. Parrell*[2]. [1]National High Magnetic Field Laboratory, Tallahassee, Florida, 32310, USA. [2]Oxford Superconducting Technology, Carteret, New Jersey,07008, USA.

This paper describes the development and testing of a 3 T Class Bi-2212 insert magnet. The magnet consists of 3 sections, each built by stacking double pancakes using Powder-In-Tube conductor and the Wind&React approach. Conductor with a pure Ag matrix was used for the inner stack and conductor with a mixed Ag and AgMg matrix was used for the outer 2 stacks. Elements of the design, conductor characterization, heat treatment optimization, construction and testing are presented. Both the successes and some of the problems are discussed. Research supported in part by the NSF and the State of Florida under cooperative grant DMR 9527035

ORAL SESSION 2C+3C: Materials Related to Electronic Applications

Tuesday Morning, September 14th, 10:30-12:45

10:30 *2C–1

Interval pulsed laser deposition of REBaCuO.

D.H.A. Blank, *G.J.H.M. Rijnders* and *H. Rogalla*. University of Twente, Department of Applied Physics, Low Temperature Division, The Netherlands.

With the introduction of the possibility to use Reflective High Energy Electron Diffraction (RHEED) at standard Pulsed Laser Deposition (PLD) pressures, it became possible to study the growth of oxide materials under different oxygen and temperature conditions. In this contribution we applied this technique to study the growth of the high temperature superconductor, using modified etch treated single terminated $SrTiO_3$ single crystal substrates.
In addition to the RHEED oscillations another phenomenon is observed, typical for PLD. The pulsed way of deposition leads to discontinuities in the intensity of the diffracted pattern. This is caused by the mobility of the deposited material from a disordered distribution till an ordered one and leads to a characteristic exponential slope with characteristic relaxation time constants. These time constants give extra information about relaxation, crystallization, and nucleation of the deposited material during growth.
From these results (intensity oscillations as well as relaxations), a new approach to deposit these complex oxide materials will be introduced. The basic idea of this so-called interval deposition is to deposit an equivalent of one unit cell of material in such a short time that no coalescence in larger islands can occur, followed by a relaxation time before the next unit cell layer is deposited. This interval deposition leads to an imposed layer by layer growth. The latest results on the infinite layer structure as well as REBaCuO-superconductors will be presented.

11:00 2C–2

Microwave and DC Field-Dependent Surface Impedance of YBaCuO Epitaxial Thin Films.

A. V. Velichko[1,2], *A. Porch*[1], *A. P. Kharel*[1], *M. J. Lancaster*[1] and *R. G. Humphreys*[3]. [1]School of Electronic and Electrical Engineering, University of Birmingham, Birmingham B15 2TT, UK. [2]Institute of Radiophysics and Electronics, NAS of Ukraine, Kharkov 310085, Ukraine. [3]KF 1209, DERA, Malvern WR14 3PS, UK.

We report on the non-linear microwave surface impedance, $Z_s = R_s + jX_s$, of YBaCuO thin films studied with the help of coplanar resonators at 8 GHz in external dc fields up to 12 mT applied parallel to the c-axis. For some of the samples, both the surface resistance, R_s, and the surface reactance, X_s, were found to decrease with increased microwave field, H_{rf}. A similar decrease in R_s and X_s is observed with increased dc field, H_{dc}, both in low-power (linear) and high-power (nonlinear) regimes. Another anomalous feature observed is an oscillatory behavior of R_s and X_s as a function of both H_{dc} and H_{rf}, which is more cleary seen in the DC field-dependences. Here, the decrease in R_s and X_s is the most pronounced at low temperature, T ($\sim$ 15 K), whereas the oscillatory behavior becomes dominant with increased T. Suggestions are made about possible mechanisms responsible for the unusual behavior observed.

15:00 2C–3

The Study of Thermal Fatigue Behavior of YBCO High-Temperature Superconductor Thin Films.

F. Yang[1], *K.H. Wu*[1] and *G.Larkins*[2]. [1]Department of Mechanical Engineering, Florida International University, Miami, FL 33199, U.S.A. [2] Department of Electrical Engineering, Florida International University, Miami, FL 33199, U.S.A.

Thermal cycling behavior on YBCO high-temperature superconductor (HTS) thin films on the different substrates including $LaAlO_3$, Al_2O_3, and Si-MgO was systematically studied. These HTS assemblies underwent thermal cycling from 77K to room temperature, and their thermal fatigue reliability was evaluated by the initiation and propagation of their thermal fatigue cracks by using SEM measurements. It was found that samples with lower CTE mismatch between the YBCO thin films and the substrates generally demonstrated a better resistance to crack initiation and propagation. The number of cycles for crack initiating significantly decreases with the increasing film thickness or the thermal cycling temperature range. Furthermore, a TEM study indicates that the orientation of the buffer layers has strong effects on the thermal fatigue life of YBCO thin films. Based on the experimental results, a two-dimensional model is proposed to describe the thermal stress and thermal cycling life of YBCO thin films. The implications of these results on electronic applications and thermal durability will also be discussed in this paper.

11:30 2C–4

New method for fabricating ribbon-like thin films of Bi-2212 on Ag substrates and their superconducting properties.

S. Arisawa[1,2], *H. Miao*[2], *H. Fuji*[1,2], *A. Ishii*[1], *S. Labat*[1], *T. Hatano*[1] and *K. Togano*[1,2]. [1]Natinal Research Institute for Metals, 1-2-1, Sengen, Tsukuba, Ibaraki 305-0047, Japan. [2]CREST, Japan Science and Technology, 2-1-6, Sengen, Tsukuba, Ibaraki 305-0047, Japan.

Since the discovery of the Bi-based superconductors a variety of methods have been proposed for synthesizing films of the material. The common techniques to synthesize Bi-based superconductor films are vapor processes which require highly sophisticated vacuum apparatus and particular single crystalline ceramic substrates. In this paper we demonstrate that ribbon-like single crystalline films of Bi-2212 can be grown on Ag substrates by a very simple process. Small pellets of the Bi-2212 were put on silver substrates with the area of 10mm x 10mm and the thickness of 50-200 m. The samples were then heated up to 905C in a furnace and were kept at the temperature for 10 minutes. They were then gradually cooled down to 860 C and kept for 6 hours followed by furnace cooling. The heat treatment was performed under 1 atm of oxygen. By this simple method, very thin ribbon-like films of Bi-2212 crystals grew on the Ag substrates. Each ribbon was elongated to several hundred of microns with a couple of tens of microns in width. The thicknesses of the ribbons were the order of submicrons. The ribbon-like films showed

the superconducting transition with the onset temperature of 70-80K.

11:45 3C–1

$SrTiO_3$ as a substrate for the electrodeposition of HTSC films.

M.S. Martín-González, *E. Moran* and *M.A. Alario-Franco*. Laboratorio de Química del Estado Sólido, Departamento de Química Inorgánica, Facultad de Ciencias Químicas, Universidad Complutense, 28040-Madrid Spain (EU).

At the present time the research on superconductivity has been focused on three main streams: explanation of the superconducting properties, search of materials with higher T_c and development of techniques suitable for the application of the HTSC materials to commercial devices. In this last subject, one of the most promising techniques comes from electrochemical science: the well-known cathodic electrodeposition. Preparation of HTSC thick films via electrodeposition techniques provides a low-cost and fast procedure, which is widely employed in industry. In summary, the process requires the deposition of the constituent elements of the superconductor from the adequate electrolyte on a conducting substrate, followed by an oxidative heating. One of the most interesting substrates $SrTiO_3$ is insulating, therefore, by now, for using it in electrodeposition a conducting layer (Ag in most of cases) had to be previously deposited by using other methods. In this work, the obtaining of $YBa_2Cu_3O_{7-\delta}$ thick films on $SrTiO_3$ without using the conducting layer is reported. The process consists, basically, in reducing the substrate at high temperature, so that it becomes conducting and then is followed by the simultaneous co-deposition of the cations. The precursor film is heat-treated at 900°C in oxygen in order to obtain the superconducting phase, the substrate becoming insulating again. In this way it is possible to obtain a superconducting film on an insulating substrate by electrodeposition. The superconducting properties of these films are (T_c=92 K and $J_c \approx 2000$ A/cm^2).

12:00 3C–2

Structure and properties of (Sr,Ca)CuO_2 - $BaCuO_2$ superlattices grown by layer-by-layer PLD.

K. Verbist[1], *G. Van Tendeloo*[1], *G. Koster*[2], *G. Rijders*[2], *D.H.A. Blank*[2] and *H. Rogalla*[2]. [1]EMAT, University of Antwerp (RUCA), Antwerp, Belgium. [2]Low Temperature Physics, Applied Physics, University of Twente, Enschede, Netherlands.

We report on the growth and characterization of (Sr,Ca)CuO_2 -$BaCuO_2$ superlattices. The structures have been grown by PLD on surface treated $SrTiO_3$ substrates ensuring a single terminated surface, i.e., TiO_2. The surface termination was changed by deposition of SrO. To impose a true layer-by-layer growth mode, the interval deposition technique has been used, resulting in high quality superlattice structures.
Samples with growth sequences of [(Sr_{1-x},$Ca_x$$CuO_2$)a -($BaCuO_2$)b]n and n=20;a=b=4, n=20;a=2;b=3 and n=20;a=b=2 have been investigated by HREM. To our knowledge, this is the first report on characterization of artificial layered infinite layer compound by HREM. These materials suffer considerably from radiation damage during ion milling and HREM observations. Nevertheless with precautions these structures could be observed in HREM. The superlattice period has been deduced from electron diffraction patterns.
The local superlattice period has been analyzed from computer diffractograms obtained from HREM images. Locally steps in the layers can be found resulting in deviations from the average superlattice period. Under certain deposition conditions and thickness of the individual Ba containing layers in the sequence it was observed that the $BaCuO_2$ material is converted to Ba_2CuO_4. Image simulations to interpret the HREM contrast are performed. In this way step-rich regions in the superlattice could be correlated with deviations in the substrate surface termination.
K. Verbist is a postdoctoral fellow of the FWO Flanders.

12:15 3C–3

$Bi_2Sr_2CaCu_2O_{8+x}$ epitaxial thin films on silicon substrates.

J. C. Martínez[1], *S. Ingebrandt*[1], *M. Basset*[1], *M. Mauer*[1], *M. Mayer*[1], *H. Adrian*[1], *S. Linzen*[2] and *P. Seidel*[2]. [1]Johannes Gutenberg – Universität Mainz, Institut für Physik, D-55099 Mainz; Germany. [2]Friedrich-Schiller-Universität Jena, Institut für Festkörperphysik, Helmholzweg 5, D-07743 Jena, Germany.

Most of the high temperature superconducting cuprates show superconducting properties in temperature ranges where classical Si-based devices can still operate. The enormous potential of this marriage inspired a number of groups to work on the deposition of $YBa_2Cu_3O_{7-\delta}$ (Y:123) thin films on Si substrates [E.M.Ajimine, *et al.* Appl.Phys.Lett. **59** 2889 (1991); R.Haakenaasen, *et al.* Appl.Phys.Lett. **64** 1573 (1994); Y.A.Boikov, *et al.* J.Appl.Phys. **78** 4591 (1995); L.Méchin, *et al.* Physica C **269** 124 (1996)]. Three years ago, the feasibility of Josephson Junctions and Superconducting Quantum Interference Devices (SQUID) on Si substrates was demonstrated [P.Seidel, *et al.* Journal de Physique IV C3 **361** (1996)]. In this work we describe our results on the deposition of $Bi_2Sr_2CaCu_2O_{8+x}$ (Bi2212) on Si substrates. By using a YSZ/CeO_2 buffer layer it was possible to obtain epitaxial films of Bi2212 with T_C(R=R_n/2)=88.7 K.

12:30 3C–4

defects in YBCO films on CeO_2 buffered sapphire and $LaAlO_3$ and their effect on the microwave properties.

J. Einfeld[1], *P. Lahl*[1], *R. Kutzner*[1], *R. Wördenweber*[1] and *G. Kaestner*[2]. [1]ISI, Forschungszentrum Juelich, 52425 Juelich, Germany. [2]MPI fuer Mikrostrukturphysik, 06120 Halle, Germany.

HTS microwave applications require the preparation of high-quality thick YBCO films on large-area technical substrates with low microwave losses. Previously we demonstrated, that crack-free YBCO films with thickness up to 700nm can be deposited on 2 inch sapphire substrates (despite of the large lattice mismatch) with low surface resistance (R_s(77K)=1.4mΩ; R_s(4.2K)=110μΩ at 19GHz) and excellent power handling capability (B_{HF}(77K)=17.5mT; B_{HF}(4.2K)>54mT at 19GHz). The improvement of the

critical film thickness was achieved by introducing structural defects into the films. In this contribution we examine the influence of different defects upon microwave surface resistance R_s and power handling capability for these YBCO films on CeO_2 buffered sapphire and, for comparison, on CeO_2 (0 to 25nm thick) buffered $LaAlO_3$, deposited with the same process. The structural properties of the YBCO films strongly vary with the thickness of the buffer layer. TEM experiments reveal small Y_2O_3-precipitates which cause the development of micropores in YBCO on sapphire. The temperature dependence of R_s and power handling is investigated in ambient dc magnetic field. In contrast to the literature, all films show an exponential temperature dependence. Thus, the temperature dependence of R_s seems to be a fingerprint of the deposition process rather than the HTS-substrate mismatch.

ORAL SESSION 2D: Passive Devices I

Tuesday Morning, September 14th, 10:30-11:45

10:30 *2D–1

Cryogenic dielectric resonators for future microwave communication.

M. Winter, *D. Schemion*, *I.S. Ghosh* and *N. Klein*. Forschungszentrum Jülich GmbH Institut of Solid State Research 52425 Jülich Germany.

A whispering gallery sapphire resonator with Q-values of 2×10^6 at T = 77 K has been employed to build a low phase noise oscillator at 23 GHz for satellite communication in collaboration with Bosch Telecom GmbH. In order to set the oscillator frequency accurately, we have investigated the performance of mechanical and piezomechanical tuning. The mechanical tuning range without reducing the resonator Q by more than 10% was found to be about 40 MHz. In order to achieve the more precise frequency tuning, we have implemented a piezoelectric transducer providing an electrical tuning range of 40 kHz. The complete oscillator is incorporated on a commercial Stirling-type miniature cooler (AEG SL200 ; max. cooling power at 77 K = 3 W), which we have mechanically de-coupled from the cold finger of the Stirling cooler via stranded copper wires. According to Leesons Model and the measured 1/f noise of the integrated two staged HEMT Amplifier, we expect a phase noise value of about -130 dBc/Hz at 1 kHz offset from the carrier. As a second application of cryogenic dielectric resonators we have developed a sapphire/rutile composite whispering gallery resonator for secondary frequency standard applications. This composite resonator incorporates both sapphire and rutile single crystal elements to achieve a turning point in the temperature dependence of the resonator frequency at about 60 K with Q-values above 10^7. A Pound stabilisation technique also has been used to reduce the effect of drifting in the room temperature circuits elements. First experimental results will be shown.

11:00 2D–2

Low Field MRI System with HTS Receive Coils.

N.McN. Alford[1], *S.J. Penn*[1], *A.A. Esmail*[1], *D. Bracanovic*[1], *T.W. Button*[2], *C. Nicholls*[3] and *S. F. Keevil*[4]. [1]South Bank University, London, SE1 0AA, UK. [2]Birmingham University, B15 2TT, UK. [3]SMIS Ltd, Guildford, GU2 5YF, UK. [4]Guy's Hospital, London Bridge, London, SE1 9ET.

Magnetic Resonance Imaging (MRI) is a powerful technique which forms anatomical details in multiple planes and provides information of tissue characterisation. One of the key factors in achieving useful clinical images is obtaining good Signal-to-Noise Ratio (SNR). At low frequencies < 0.1T coil noise is the dominant source of loss. However, by using lower fields signal is also compromised. To retrieve SNR at low fields we have used superconducting YBaCuO7-x receive coils on 100mm square YSZ substrates. In this study we compare the performance and sensitivity of copper, silver and YBCO coils of similar dimension and design. The assessment of SNR has been carried out using measurements made of reconstructed multi-spin echo (SE) phantom images using a 6.1MHz (0.15T) MR Imager. Far lower field imag-

ing of 400kHz (0.01T)will also be reported. It was found that the YBCO coil showed excellent improvement in SNR over all other coils. SNR measurements under similar condition suggest that the YBCO receive coil has a factor of 3 improvement at 6.1MHz. Such good SNR suggests high spatial resolution and is evident in clinical right-wrist and knee images using a standard multi-SE technique. Similar images in axial and coronal planes have been taken and compared. It was found that clinical images obtained using the YBCO coil are far superior. Scout scans of only 17s duration taken using the YBCO coil provide useful information normally not seen. This suggests further development in rapid acquisition imaging and may be particularly useful when imaging children.

11:15 2D–3

Demonstration of a Power Handling of 0.5kW at 0.5GHz in a Stripline of YBCO on a 3" $LaAlO_3$ Wafer.

N. Levy[1], *G. Koren*[1], *E. Polturak*[1] and *Y. Koral*[2]. [1]Technion, Physics Dept., Haifa 32000 Israel. [2]Elisra electronic systems ltd. , Bney Brak 51203 Israel.

We developed a system for the Preparation of YBCO striplines on 3" $LaAlO_3$ wafers for use in passive microwave devices in the 0.5GHz regime. We used a Laser ablation deposition system utilizing the third harmonic of a Nd:YAG laser to prepare the YBCO films. In order to achieve good thickness uniformity of the films we scanned the heater over the plume. The stripline was patterned on the film using photolithography and wet etching in dilute HCl acid. Gold was evaporated onto the two ends of the stripline to form contacts, and then the wafer was annealed in an oxygen atmosphere to improve the Au contacts and replenish the oxygen in the YBCO film. RF testing of the stripline was done at 77K in liquid nitrogen, and the films withstood a cw power of ~0.5kW at 0.5GHz for more than an hour (striplines on 2" wafers withstood ~1kW). Two modes of failure were observed, the first consisted of contact heating, (which was solved by thickening the Au pads and using more gold leads), and in the second mode the strip itself failed which indicates the limits of the present quality of the films.

11:30 2D–4

Characterisation of the superconducting and microwave properties of YBCO films simultaneously sputtered on both sides of sapphire wafers.

A.G. Zaitsev[1], *R. Schneider*[1], *J. Geerk*[1], *G. Linker*[1], *F. Ratzel*[1], *R. Smithey*[1], *S. Kolesov*[2] and *T. Kaiser*[2]. [1]Institut fuer Nuleare Festkoerperphysik, Forschungszentrum Karlsruhe, P.O.Box 3640, D-76021 Karlsruhe, Germany. [2]Universitaet Wuppertal, D-42119 Wuppertal, Germany.

Implementation of HTSC microwave filters requires the preparation of the double-sided YBaCuO films on large-area sapphire substrates as well as fast, reliable and non-destructive characterisation of the superconducting and microwave properties of these films. YBaCuO films simultaneously sputtered on both sides of the 3 inch in diam. CeO2 buffered r-cut sapphire wafers were routinely examined. Spatially and side resolved measurements of Tc and Jc were performed inductively using the third-harmonic response. Jc(77K) values of 3-4 MA/cm2 were obtained homogeneously on each side of the samples. The microwave surface resistance was characterised on both sides of the samples using them as the disk resonators. One side of the samples was patterned as a circle of 67 mm in diam., yielding the resonant frequency of the TM010 mode of 1.72 GHz. The quality factor of the resonators was determined by the one-port vector reflection measurements, which allowed to simplify substantially the cooling and measurement system. For the YBCO films with Rs(77K, 10GHz) = 0.6 mOhm an unloaded Q as high as 77000 was reached at 77 K. The contribution will concentrate on the details of the measurements and the correlations between the measured parameters.

ORAL SESSION 3D: System Aspects Related to Electronic Applications

Tuesday Morning, September 14th, 11:45-12:45

11:45 *3D–1

Cryogenic packageing of superconducting electronic systems: A crucial, enabling technology.

M. Nisenoff. M. Nisenoff Associates Post Office Box 2748 Kensington MD 20896-2748 USA.

After superconducting electronic applications have been demonstrated in the laboratory, commercialization of the circuit or component may be attempted. If superconducting electronic applications are to reach the market place, it must be integrated into a compact, lightweight cryogenic packages which makes the superconducting and cryogenic nature of the electronic component "transparent" to the end user. The packaged superconducting component should resemble, as close as feasible, the size, weight and electrical input power of the conventional equipment that the superconducting system is intended to replace. In this talk, the issues associated with the thermal design of a cryogenic electronic system will be reviewed and the progress achieved to date for packaging both LTS and HTS components will be described. Packaging areas where additional development activity would be beneficial will be outlined. If superconductivity is to become a viable electronic technology, the commercial availability of physica lly small, lightweight, high reliability, and energy efficient cryogenic refrigerators is also extremely crucial.

12:15 3D–2

A 4-pixel YBCO mid-infrared bolometer array with associated cryogenic CMOS circuit.

F. Voisin[1], *G. Klisnick*[1], *Y. Hu*[1], *M. Redon*[1], *J. Delerue*[2], *A. Gaugue*[2] and *A. Kreisler*[2]. [1]Laboratoire des Instruments et Systemes - Universite P. et M. Curie (Paris 6) BP 252, T12-13 E2 4 place jussieu 75252 Paris cedex 05 - France. [2]Laboratoire de Genie Electrique de Paris - UMR 8507 CNRS - Universités Paris 6 et Paris 11 SUPELEC - Plateau de Moulon 91192 Gif Sur Yvette Cedex - France.

The design of a high Tc superconducting bolometer geometry and its readout electronics for applications to mid-infrared imaging arrays are discussed. The sensor part consists of an YBCO thin film patterned into meander line shape. An YBCO thin film can be chosen as a practical candidate for bolometric detection in the mid-infrared because it acts as both a radiation absorber and a sensitive thermometer. To obtain a matrix of 2x2 pixels we have used four meander lines in a bridge connection. Detection experiments, performed with the 10 μm radiation from a CO2 gas laser, will be described. The low-level signal delivered by the sensor is often degraded if processed out of the cryostat. By processing directly the signal from the sensor in the cryostat, an improvement of the overall noise level of the detector can be achieved. We have conceived a low noise CMOS amplifier which works from room temperature down to 77K with a thermal noise of 0.5nV/sqrt(Hz) at 77K. In order to form an integrated system, the realized cryogenic CMOS ASIC contains all the readout circuits (low noise amplifiers and buffers) and the programmable bias current sources that are needed to drive the bolometer array.

12:30 3D–3

The Defense Advanced Research Projects Agency (DARPA) Program on Applied Superconductivity.

S. A. Wolf[1,2] and *F. W. Patten*[2]. [1]Naval Research Laboratory, Washington DC 20375. [2]Defense Advanced research Projects Agency, 3701 N. Fairfax Dr. Arlington VA 22203.

DARPA has had a project on applied superconductivity for the past 12 years and has spent well over $300M to develop superconducting technology. This project has recently focused on the development of a host of rf and microwave devices, circuits, and subsystems for communications, surveillance and remote sensing. In addition, recently several new efforts have been started the first combines frequency agile materials like ferroelectrics, ferrites and MEMs to superconducting filters to add tuneability and the second is a modeling that has the goal of understadning the deposition of superconducting films by MOCVD and IBAD. In this talk I will review the status of these efforts and give my prospects for the future.

POSTER SESSION 4

Tuesday Afternoon, September 14th, 15:30-17:30

Session Bulk materials and materials aspects

4–1

A new fast and non-destructive method for evaluating the superconducting properties of bulk materials.

Ph. Vanderbemden[1], *H.W. Vanderschueren*[1], *Z. Aouina*[2], *R. Cloots*[3] and *M. Ausloos*[4]. [1]University of Liège, S.U.P.R.A.S., Montefiore Electricity Institute B28, Sart-Tilman, B-4000 Liège, Belgium. [2]Institut Supérieur Industriel Liégeois Rennequin Sualem Quai Gloesener, 6 B-4020 Liège, Belgium. [3]University of Liège, S.U.P.R.A.S., Chemistry Institute B6, Sart-Tilman, B-4000 Liège, Belgium. [4]University of Liège, S.U.P.R.A.S., Physics Institute B5, Sart-Tilman, B-4000 Liège, Belgium.

A new, simple and low-cost experimental setup has been constructed in order to rapidly investigate the electrical properties of bulk superconducting monoliths. This system allows superconductivity to be checked on large disk-shaped samples. The main advantage resides in the fact that properties of circular pellets can be studied without cutting them. The principle follows that of an induction motor. Two neighbouring and 90° out-of-phase AC magnetic fields are applied perpendicularly to the disk to be measured. This causes the material to experience an electromagnetic couple which is function of its electrical properties. Hence a measurement of either (i) the couple developed or (ii) the rotation speed of the disk leads information about its electrical resistance. In this communication experimental details of the system are described and illustrative measurements on BSSCO-2223 ceramics as well as (RE)BCO-123 large grain high-Tc superconductors are included.

4–2

Bulk textured Bi2212/MgO with high critical current densities at low temperatures.

S. Pavard[1], *D. Bourgault*[1], *C. Villard*[2], *R. Tournier*[1], *S. Rivoirard*[1] and *J.L. Soubeyroux*[1]. [1] Laboratoire de Cristallographie/CRETA - CNRS 38042 Grenoble France. [2]CRTBT/CRETA - CNRS 38042 Grenoble France.

High critical current densities at low temperatures are obtained in bulk Bi2212 materials added with MgO and textured by solidification in a high magnetic field (MMP: Magnetic Melt Processing) followed or not by forging. The texturation induced by MMP is demonstrated using superconducting and microstructural characterizations, including neutron diffraction: the c axis tends to be parallel to the processing field direction in the whole volume of the bulk. Adding MgO induces the precipitation of submicronic MgO-rich inclusions. These particles increase bulk vortex pinning. Consequently, transport Jc withstands higher magnetic fields and its self-field value is increased by a factor 2.5 at 77 K. Irreversibility fields are twice higher at variable temperatures. Transport and magnetic properties are slightly improved by forging following MMP. The transport Jc (self-field, 77 K) of bulk textured Bi2212/MgO material reaches 1900 A/cm^2 for a 5 mm^2 section bar (Ic = 90 A) after annealing in air and then in argon. For lower temperatures, transport Jc of about 10 kA/cm^2 is reached at 40 K. At 4 K, Jc values higher than 160 kA/cm^2 are magnetically measured with a record value of 165 kA/cm^2 for bulk Bi2212.

4–3

Preparation and Properties of Bi-2212/(Sr,Ca)SnO_3 Superconducting Composites.

P.E. Kazin[1], *R.A. Shuba*[1], *V.V. Lennikov*[1], *Yu.D. Tretyakov*[1] and *M. Jansen*[2]. [1]Chemistry Department, Moscow State University, 119899 Moscow, Russian Federation. [2]Max-Plank-Institut fuer Festkoerperforschung, D-70569 Stuttgart, Germany.

Melt-processed superconductor composites were obtained which consisted of Bi-2212 matrix and submicron (Sr,Ca)SnO_3 inclusions. The specimens were prepared using different routes: (i) formation from the homogeneous sol-gel precursor containing all the components, (ii) formation from the mixtures of nanocrystalline strontium calcium stannates and the precursors of the BSCCO system. It was shown that Bi-2212 was compatible with $Sr_1 - xCa_xSnO_3$ (x=0.1-0.15) while solubility of Sn in solid Bi-2212 and in BSCCO melt was limited to a few mol %. The $Sr_1 - xCa_xSnO_3$ particles were found to be partially included in Bi-2212 large grains, partially agglomerated in-between. The composites had T_c of 80-90K and exhibited increased intragrain pinning in comparison with the undoped Bi-2212 samples. Transport J_c of 1000 A/cm^2 were measured for the samples containing up to 1.6 mol $Sr_1 - xCa_xSnO_3$ per 1 mol Bi-2212. In addition, substantial increase in mechanical strength was observed for the composites with the high second phase content.

The work was supported by Russian Ministry of Science (project "Composite"), Russian Foundation for Basic Research (project 97-03-33249a), and BMBF-VDI (Germany, project 13N6761).

4–4

Electrical, mechanical and thermal characterisation of LFZ Bi-2212 textured thin rods.

E. Natividad[1], *J.C. Díez*[1], *L.A. Angurel*[1], *M. Castro*[1], *R. Burriel*[1], *R. Navarro*[1], *J.Y. Pastor*[2], *P. Poza*[2], *J. Llorca*[2], *J. Calero*[3], *L. García-Tabarés*[3] and *P. Abramian*[4] [1]Instituto de Ciencia de Materiales de Aragón (C.S.I.C.-Universidad de Zaragoza), María de Luna, 3, 50015 Zaragoza (Spain). [2]Departamento de Ciencia de Materiales, E.T.S. Ingenieros de Caminos, U.P.M., Ciudad Universitaria, 28040 Madrid (Spain). [3]CEDEX AlfonsoXII, 3, 28014 Madrid (Spain). [4]CIEMAT Av Complutense 22, 28040 Madrid (Spain).

The design of hybrid current leads is strongly related to the physical properties of the superconducting material. Bi-2212 thin rods, textured with a Laser Floating Zone (LFZ) technique, have been used to construct a 600 A current lead. In this communication, a full characterisation of these rods (1.7 mm of diameter and a length of 10 cm), including electrical, mechanical and thermal properties, is presented. Electrical measurements include the temperature dependence of the normal resistivity and the evolution of the I-V characteristics with temperature in the range 65-77 K and with magnetic field at 77 K. An analysis of the homogeneity of the samples along the length is also presented. The me-

chanical properties at room temperature were determined through longitudinal and transverse tension tests in order to determine the anisotropy in the mechanical response of the rods. Furthermore, the temperature dependence of the thermal conductivity has been measured from 4.2 K to room temperature by a steady state longitudinal flow method.

4–6

Scale-up and production of ~1000A current elements from MgO fibre textured Bi-2212.

K.A. Kursumovic[1], *B.A. Glowacki*[1], *J.E. Evetts*[1], *M.A. Henson*[2], *M.P. Hills*[2] and *R.M. Henson*[2]. [1]IRC in Superconductivity and Department of Materials Science and Metallurgy, University of Cambridge, Cambridge CB2 3QZ, UK. [2]Advanced Ceramics Limited, Castle Works, Stafford ST16 2ET, UK.

Composite Reaction Texturing (CRT) of Bi-2212 is a partial melting process that depends on multi-seeding with aligned high aspect ratio MgO fibres. The MgO fibres (10wt%) and Bi-2212 precursor powder are dispersed in an organic binder and aligned by the doctor blade tape casting method. About 5wt% Ag-powder is added to the original Bi-2212 precursor (MERCK), in order to avoid contact dissolution during melt processing. Sample batches are limited in size only by furnace hot zone dimensions. This process yields material that exhibits a critical current density of $10^5 A/cm^2$ at 10K and 12T, and is self-field limited to about $1.5\text{-}4x10^3 Acm^{-2}$ at 77K. It is shown, in scaling-up the process, that uniformity and quality of all the precursors, especially MgO fibres, plays an important role in achieving optimal superconducting properties. However, it is clearly demonstrated that this method can readily produce robust elements of ~1000A critical current. The in-situ contacts show low resistivity ($<10^{-6}\Omega$cm) and support current transients up to 10 times the critical current. The peak in J_C, for optimised oxygen post-anneal, does not coincide with the maximum in T_C, optimum J_C values are shifted towards the overdoped regime. This is believed to be due to the occurrence of the so-called normal state gap. This work was supported under an EPSRC LINK project.

4–7

An Analysis for Finding a Suitable Design Condition to Improve J_C of a Bi-System by SRPM Method.

H. Nakane[1], *S. Haseyama*[2], *S. Yamazaki*[1], *H. Miyairi*[1] and *S. Yoshizawa*[3]. [1]Kogakuin Univ., Shinjuku-ku, Tokyo 163-8677, Japan. [2]Dowa Mining Co. Ltd., Hachioji-shi, Tokyo 192-0001, Japan. [3]Meisei Univ., Hino-Shi, Tokyo 191-8506, Japan.

Since an appropriate method for pinning a Bi-based sintered bulk has not yet been found out, attempt to increase the density and improve the orientation of the crystallization has been made by controlling the sintering time and repeating the CIP (cold isostatic pressing) process to increase J_C so far. The SRPM method has been developed to measure the values related to the surface impedance of samples within the frequency band of kHz from MHz. In the SRPM method, the difference in the impedance of a solenoid coil with and without a rod-shaped sample is measured. The Bi 2223-system samples made under various conditions were measured by the SRPM method. It was confirmed that the temperature dependence of the difference in the coil impedance generated showed a remarkable change by controlling the sintering time and repeating CIP. For the samples made by different sintering time without CIP, the difference among 2212, 2223 and the other phases could clearly be distinguished. The relation between the values of J_C and the temperature dependence of the difference in the impedance is analyzed and the results are reported.

4–8

HTSC bulk materials - shielding elements and their properties.

H. Altenburg[1], *J. Plewa*[2], *W. Jasczcuk*[1] and *N. Munser*[1]. [1]Fachhochschule Münster - University of Applied Sciences Stegerwaldstraße 39 48565 Steinfurt Germany. [2]SIMa - Steinfurter Initiative für Materialforschung e.V. Uhlandstraße 17 48565 Steinfurt Germany.

The subject of this presentation is the preparation of powder materials of YBCO, BSCCO and NBCO and the characterization of their properties, the production, forming and texturing of HTSC bulk materials and also the evaluation of the magnetic and electrical properties of shielding elements. Liquid-phase sintered, not textured HTSC hollow-cylinders and rings (diameter of 2-10 cm and lenghts of 10-50 cm) were processed. With a Hall probe, fully shielding of dc fields was measured up to to 2 mT for YBCO and up to about 8 mT for BSCCO. Additional measurements were made on BSCCO and Cryoperm tubes with a HTSC-SQUID magnetometer and with an improved inductive method on NBCO and BSCCO rings. With SQUID's we could compare screening properties of tubes made from different materials. The shielding effect of a triple Cryoperm cylinder is less than the BSCCO single cylinder. The value of the magnetic shielded field for two superimposed cylinders of HTSC was smaller than the sum of their single values.

4–9

Holes Control Superconductivity and Critical Current Densitiy in $Bi_2Sr_2(Ca_{1-x}Y_x)Cu_2O_{8+\delta}$.

R. S. Liu[1], *I. J. Hsu*[1], *J. M. Chen*[2] and *L. Y. Jang*[2]. [1]Department of Chemistry, National Taiwan University, Taipei, Taiwan, R.O.C. [2]Synchrotron Radiation Research Center, Hsinchu, Taiwan, R.O.C.

We have prepared a series of the $Bi_2Sr_2(Ca_{1-x}Y_x)Cu_2O_{8+\delta}$ system which has a maximal superconducting transition temperature of around 92 K at x = 0.2. Across the homogeneity range $x = 0.5 \sim 1.0$, the materials also undergo a Metal-Insulator Transition. Here we demonstrate the variation of the hole concentration within the CuO_2 planes and the local structure across the $Bi_2Sr_2(Ca_{1-x}Y_x)Cu_2O_{8+\delta}$ series samples by XANES (X-ray absorption near edge structure) and EXAFS (Extended X-ray absorption fine structure), respectively. The hole concentration within the CuO_2 planes in $Bi_2Sr_2(Ca_{1-x}Y_x)Cu_2O_{8+\delta}$ can be tuned by the chemical substitution between Ca^{2+} and Y^{3+} as observed by XANES. The disordering effect induced by the chemical substitution in $Bi_2Sr_2(Ca_{1-x}Y_x)Cu_2O_{8+\delta}$ may play a crucial role to reach the optimum (highest) T_c. Moreover, we found that there existed a strong correlation between hole concentration and critical current density in $Bi_2Sr_2(Ca_{1-x}Y_x)Cu_2O_{8+\delta}$ which may give useful informa-

tion for the future application.

4–10

Large area deposition of high quality YBCO films by pulsed injection CVD.

A. Teiserkis[1], *A. Abrutis*[1], *V. Kubilius*[1], *Z. Saltyte*[1], *J.P. Senateur*[2] and *F. Weiss*[2]. [1] Vilnius University, Dept. of General and Inorganic Chemistry, LT-2006 Vilnius, Lithuania. [2]LMPG-ENSPG, CNRS UMR 5628, BP 46, 38402 St Martin D'Heres, France.

YBCO growth process was optimized in a built new pulsed injection CVD reactor assigned for large area deposition. Microdoses of an organic solution cotaining a mixture of Y, Ba, Cu 2,2,6,6-tetramethyl-3,5-heptandionates were injected in an evaporator by means of a special computer controled injector. The resulting vapor vas transported by a mixed Ar-O_2 flow into the growth chamber. Homogeneity of the critical temperature was verified by deposition on nine small substrates distributed on large area (~70 mm in diameter) of 3 inches substrate holder. All films (~0.2 μm) had very sharp superconducting transition (ΔT_{full}=0.1-0.2 K) at 91-92 K. One YBCO film (~0.2 μm) was deposited on 3 inches $LaAlO_3$ substrate and the distribution of critical current density (Jc) was established by AC susceptibility measurements (resolution 5 mm). Film had Tc=92.1 K, ΔTc=0.15 K. High Jc values of 4-6 MA/cm^2 were obtained over the wide area of 65-70 mm in diameter.

4–12

The Influence of Elevated Magnetic Fields on the Texture Formation of Melt-Processed Bi-2212.

E. Cecchetti, *P.J. Ferreira* and *J.B.V. Sande*. Massachusetts Institute of Technology (MIT) Department of Materials Science and Engineering Cambridge, MA, 02139, USA.

Melt-processing of BSCCO high-TC superconductors under elevated magnetic fields is an effective technique for producing superconductors with enhanced critical current. This result is a consequence of the high degree of crystallographic texture achieved in the polycrystalline superconductor processed under a high magnetic field. Possible mechanisms for the orientation of Bi-2212 plate-like crystals under the influence of a magnetic field have been analyzed, in particular, the orientation of superconductor embryos during nucleation and the orientation of Bi-2212 grains during grain growth. In order to understand the relevance of each of these mechanisms, we have studied the effect of an applied magnetic field during different stages of the partial-melt process. Experimental results confirm that most of the alignment is achieved in the early stages of crystal growth. This result may have important consequences on the large-scale implementation of this process.

4–13

Numerical stability analysis for a solenoidal HTS coil.

J. Lehtonen, *R. Mikkonen* and *J. Paasi*. Laboratory of Electromagnetics, Tampere University of Technology P.O.Box 692, 33101 Tampere, Finland.

Knowledge of stability is essential when designing superconducting applications. Stability considerations for low temperature superconductors (LTS) are well established but high temperature superconductors (HTS) have a few intrinsic features very different to those of LTS. Examples of those features are the slanted electric field - current density E(J)-characteristics, the wide margin between the operating and the critical temperature, and the anisotropic magnetic field dependence of the critical current density. Basic principles of a numerical model for stability considerations in HTS magnets are reviewed. The model is based on Maxwell's equations and heat conduction equation. The anisotropic magnetic field dependence of the E(J)-characteristic of HTS material is taken into the consideration. The equations are solved by using the Finite Element Method. Using the model the operating conditions which result in stable operation for solenoidal HTS coil are studied. The effects of anisotropy are discussed. The results show that the maximum allowable power dissipation is a more suitable design criterion for HTS magnets than the critical current.

4–14

Copper Oxides Superconductors Containing Phosphate Group.

J. C. Gonzalez[1], *A. Bustamante*[1], *D. Landinez*[2] and *J. Albino*[2]. [1]Laboratorio de Superconductividad, Facultad de Ciencias Fisicas, Universidad Nacional Mayor de San Marcos, Apartado Postal 14-0149, Lima 14 - Peru. [2]Departamento de Fisica, Universidad Federal de Pernambuco, 50670-901 Recife PE, Brazil.

After the discovery of high T_c superconductivity in multinary cuprates, a large number of different superconductors have been synthesized by varing the chemical composition and structural features of the insulating layers which connect the superconducting CuO_2 layers. Although experimental studies initially focused on aliovalent cationic substitutions in these layers, it was subsequently discovered that oxyanions groups: $(CO_3)^{2-}$, $(NO_3)^{1-}$, $(BO_3)^{3-}$, $(SO_4)^{2-}$, $(PO_4)^{3-}$, can also be located on some cationic sites to provide an additional means of the controlling the electronic properties of the superconducting regions. Here we present the composite $[Y_{1-x}Ca_x]SrBaCu_{2.80}(PO_4)_{0.20}O_y$ ($0.10 \leq x \leq 0.40$) prepared at normal pressure and temperature conditions. X-ray diffraction pattern show that the samples containing Ca crytallize into 123 tetragonal structure without any impurity phase peak. The ac susceptibility measurements using a SQUID show that the materials are superconductors with the variation of the Ca concentration (for x=0.10 T_c=46K and x=0.40 T_c=75K). This demonstrates the importance of doping of Ca^{2+} into the site Y^{3+} in the generation of the holes in the CuO_2 layers. In the normal region the measurements of the χ_{ac} show a typical Curie-Weiss behavior.

4–15

Improving thermal and electrical conductivity of cylindrical superconducting YBCO magnetron targets.

I. Van Driessche[1], *F. Persyn*[1], *R. Mouton*[1], *G. De Mey*[2] and *S. Hoste*[1]. [1]University Gent, Department Inorganic and Physical Chemistry, Gent, 9000, Belgium. [2]University Gent, Department of Electronics and Information Systems, Gent,9000, Belgium.

This study forms part of the Brite Euram industrial project ≪ MUST ≫ dealing with the development of a cost effective multi-functional flexible HTSC tape, exhibiting a critical current density in the film > 10^6 A/cm^2 at 77K using sputter deposition of 0.5 - 1 micron thick YBCO films on metallic and polymer substrates. To allow a high power throughput the electrical and thermal conductivity at room temperature and elevated temperatures of the YBCO targets needs to be improved by the addition of metals that are not detrimental to the superconductivity in YBCO films. This study describes a rapid and accurate technique for the determination of the bulk thermal conductivity of superconducting oxides using an infra-red camera measuring heat transfer through the samples. The relation between conductivity and composition, density and synthesis method is described. Values of K = 6 Wm^{-1}K^{-1} are obtained for undoped YBCO samples. The addition of Ag has a positive effect on thermal and electrical conductivity (e.g. a factor 4 for 15 wt% Ag addition) but also influences density of the materials therefore complicating the expected relationship between conductivity and Ag content. Percolation effects and improvement of the Ag distribution in the materials are studied.

This work has been supported under the Brite-Euram project "Multi-functional flexible high temperature superconducting tape (MUST)", contract BRPR-CT97-0331.

4–16

Development of cylindrical superconducting magnetron targets by flame spraying and atmospheric plasma spraying.

I. Van Driessche[1], *R. Mouton*[1], *F. Persyn*[1], *E. Georgiopoulos*[2], *A. Tsetsekou*[2] and *S. Hoste*[1]. [1]University Gent, Department Inorganic and Physical Chemistry, Gent, 9000, Belgium. [2]Ceramics and refractories technological development company, CERECO S. A., Chalkida, Evia, 34100, Greece.

This study forms part of the Brite Euram industrial project ≪ MUST ≫ dealing with the development of a cost effective flexible HTSC tape, exhibiting a critical current density in the film > 106 A/cm2 at 77K using sputter deposition of 0.5 - 1 micron thick YBCO films on metallic and polymer substrates. To achieve this cost effective process it is imperative to reach the highest deposition rate possible from specially designed magnetron sources. This study describes the development of such high power YBCO targets by both atmospheric plasma and flame spraying. The YBCO was doped with Ag to increase the electrical and thermal conductivity and mechanical stability of the targets. Spray drying was used for the preparation of large quantities dedicated precursors. Suitably prepared stainless steel substrates were employed which were cooled below 60°C using flowing water, liquid nitrogen or air cooling. This avoids thermal stresses between coating and substrate providing a good bond for layers up to 5 mm thick and 30 cm long on cylindrical substrates of 13 cm diameter. The coatings were characterised by XRD, SEM, scratching and mechanical impact tests. A decomposition of the YBCO phase occurs during spraying in both cases. However, after post-spraying heat treatment the superconducting phase can be reformed and pure YBCO-123 coatings can be produced. An electrical resistivity at room temperature of 0.05 mOhm cm, a thermal conductivity of 21 W/m K and a Tc of 90K were obtained. This work has been supported under the Brite-Euram project "Multi-functional flexible high temperature superconducting tape (MUST)", contract BRPR-CT97-0331.

4–17

Low Pressure Plasma Spraying of Superconducting Powders.

E. Georgiopoulos[1] and *A. Tsetsekou*[2]. [1]CERECO S.A, P.O Box 146, Chalkida, Greece. [2]CERECO S.A, P.O Box 146, Chalkida, Greece.

Superconducting Y-Ba-Cu-O coatings were deposited on stainless steel substrates by the low-pressure plasma spraying technique with the aim to produce high power magnetron targets for thin film deposition on flexible tapes by sputtering. This work is part of the Brite-Euram industrial project "MUST: Multifunctional Flexible High Temperature Superconducting Tape". Various coatings were produced using as starting material a homemade powder produced by spray drying from nitrate solutions of Y, Ba and Cu. The plasma spraying parameters (pressure, plasma and carrier gas, powder feed rate, spraying distance, plasma power) were optimised in order to produce good quality coatings. X-ray diffraction analysis, SEM studies combined by EDS microanalysis and scratching test experiments were carried out in order to characterise the adhesion of the coatings to the substrate, the coatings morphology, thickness and crystalline structure as well as the powder phase transformations during spraying. It was shown that the low pressure employed during spraying influences to a great degree the results obtained in terms of coatings density and phase composition. As pressure decreases, less decomposition of the YBCO phase during spraying is observed and denser coatings are produced. Thus, by this way, the step of the post heat treatment that is usually necessary for the restoration of the superconducting <123> phase after the production of thermal sprayed coatings can be avoided.

4–18

Quantitative Phase Analysis of HTSC-Multifilamentary-Tapes by X-ray Diffraction using the Rietveld Method.

A. Risch, *P.O.G. Gaeberlein*, *J. Neubauer* and *M. Goebbels*. Department of Mineralogy, Friedrich-Alexander University Erlangen-Nuernberg, Schloßgarten 5a, 91054 Erlangen, Germany.

Phase content of HTSC- multifilamentary-tapes is playing an important role for their current carrying capacity.Generally the phase content is calculated by the ratio of the strong (00l) or (115) X-ray diffraction intensities for the 2212- and 2223-phases. This does not consider additional phases and variation of the chemical compositions of the phases i.e. solid solution. Hence the resulting phase assemblage is attached with uncertainties in content. A new type of standardless quantification of the phase content of HTSC-multifilamentary-tapes is based on the Rietveld refinement, a structurally dependent full pattern fitting. The Rietveld refinement makes use of both the digitized X-ray diffraction powder pattern and calculated X-ray diffraction pattern. The calculated pattern is based on the crystallo-

graphic data of all possible phases of the particular HTSC tape and global parameters. These data are combined in the control file. In this study the phase assemblage of fully processed HTSC-multifilamentary-tapes were quantified by X-ray diffraction using the Rietveld method including the phases 2201, 2212, 2223, 3321, several plumbates, cuprates and silver.

4–19

AC Susceptibility measurements and simulation of magnetic percolation effect in Bi2223 composites with MgO.

E. Bruneel[1], *A.J. Ramirez-Cuesta*[2], *R. Mouton*[1], *F. Persyn*[1] and *S. Hoste*[1]. [1]Department of Inorganic and Physical Chemistry, Solid State and Superconducting Materials Division, University of Gent, 9000 Gent, Belgium. [2] Department of Chemistry, University of Reading Whiteknights, PO Box 224 Reading RG6 AD, United Kingdom.

The superconducting properties of a series of BPSCCO-MgO composites with variable volume fractions were studied. Percolation effect is observed in resistivity as well as in susceptibility measurements and the effect of variation in temperature is investigated. A model is proposed to analyse the relationship between AC-susceptibility and composition in superconducting composites. The model is based on a random distribution of superconducting and non-superconducting phases and on the occurrence of shielding when a non-superconducting area is encapsulated by superconducting material. A two dimensional simulation is is in good agreement with our experimental data.

4–20

Quantitative Rietveld Phase Analysis of BPSCCO-2223 Precursor Powders using XRD.

P.O.G. Gaeberlein, *A. Risch*, *J. Neubauer* and *M. Goebbels*. Department of Mineralogy, Friedrich Alexander University, Schlossgarten 5a, 91054 Erlangen, Germany.

The production of BPSCCO-2223 tapes by the powder in tube method requires high quality precursor powders. Qualitative and quantitative phase composition of the precursor powders influence current carrying capacity of the BPSCCO-2223 tapes. Different processing conditions during precursor formation lead to different phase compositions and phase contents. A high level quality control has to guarantee a stable phase content. Rietveld refinement offers new possibilities for accurate quantitative phase analysis by X-ray powder diffraction. The Rietveld method allows standardless phase quantification of powder patterns within a few minutes. Data sets - supported by a new Windows software package - were developed for precursor powders of different origin. It will be shown that XRD combined with Rietveld refinement is an efficient, fast and user friendly tool for quality control of BPSCCO-2223 precursor powders.

4–21

Preparation of Bi-2223/Ag multilayered sintered bulk.

S. Yoshizawa[1], *S. Nemoto*[1], *I. Tezuka*[1] and *S. Haseyama*[2]. [1]Meisei University, Advanced Materials R & D center, Hino, Tokyo, 191-850, Japan. [2]Dowa Mining Co., Ltd., Tobuki, Hachioji, Tokyo, 192-0001 Japan.

The Jc obtained is 2,000 A/cm^2 at 77 K and 0T for Bi-2223 sintered bulk that was produced by repeating and intermediate pressing in a conventional sintering. Superconducting wire made by a powder-in-tube method using the Bi-2223 phase approaches the high Jc which is required for applications. It is expected that the Jc of the sintered bulk could be increased possibly by introducing Ag into the superconductor. Bi-2223/Ag multilayered sintered bulk was designed and prepared by the sintering method. Calcined powder and Ag foils 50 μ m in thickness were stacked and molded with metal dies using a coaxial pressing equipment. The molded bulk was sintered at 840°C in atmosphere. Then, the sintered bulk was pressed intermediately by CIPing and sintered again at 840°C. By repeating the process several times, a sintered pellet of 10 mm in diameter and 1 mm in thickness was obtained where superconductor layers were laminated with several Ag foils. As increasing the number of Ag foil, Jc increased to be 2,000 A/cm^2 in the sample without CIPing. Bi-2223 phase was easily grown improving the grain boundary and the crystal orientation on the Ag surface, which was confirmed by the results of XRD patterns and SEM images.

4–22

Effect of CaF2 additions on the formation of the (Bi,Pb)2Sr2Ca2Cu3Oy phase.

J.-C. Grivel[1,2]. [1]Nordic Superconductor Technologies A/S, Priorparken 685, DK-2605 Broendby, Denmark. [2]Materials Department, Risoe National Laboratory, DK-4000 Roskilde, Denmark.

In an attempt to improve both grain connectivity and flux pinning, the influence of the addition of CaF2 as a sintering aid on the formation and properties of the (Bi,Pb)2Sr2Ca2Cu3Oy phase has been studied. Various amounts of this additive were mixed into calcined precursor powders. The mixtures were heat-treated both in form of pellets and as the ceramic core of Ag-sheathed tapes. By means of differential thermal analysis and x-ray diffraction, the effect of this additive on the sintering temperature and phase formation kinetics was studied. The differences induced in the microstructure of the ceramic were investigated by scanning electron microscopy. ac-susceptibility as well as transport measurements were conducted in order to study the influence of CaF2 on the superconducting properties of the (Bi,Pb)2Sr2Ca2Cu3Oy compound.

Session Motors, bearings and levitation

4–23

Parasitic Resonances in Contactless Bearings.

A.A. Kordyuk, *E.A. Laptev* and *V.V. Nemoshkalenko*. Institute of Metal Physics, Kyiv 252680, Ukraine.

The parasitic resonances in contactless bearings were studied with physical computer simulation. A thin structure of the resonances was investigated for different models of damping and elasticity. The energy loss law for HTS bearings was derived from comparison with the experimental data on the high-speed magnetic rotor. A question how to decrease the parasitic resonances amplitude in real systems was also examined.

4–24
Characterization of melt-textured YBCO for Superconducting Magnetic Bearings.
U. Sutter, M. Adam, R. Wagner, R. Koch, M. Kläser and *M. Sander*. Forschungszentrum Karlsruhe GmbH, INFP, P. O. Box 3640, D-76021 Karlsruhe.

Superconducting Magnetic Bearings (SMBs) utilizing the interaction between a permanent magnet (PM) and HTS material, are completely passive devices: They allow stable levitation of e.g. fast rotating machinery without any active control, which should provide additional safety margins compared with active magnetic bearings. To make use of another attractive feature, the very small bearing losses, it is necessary to employ sufficiently homogeneous HTS materials of high quality i.e. of high critical currents and good pinning properties. Using our in-house developed test-bench, force measurements under FC and ZFC conditions were carried out, and remanent flux profiles were recorded after various magnetizing processes. Quite generally, it turned out that pulsed magnetization experiments, reveal more details about inhomogenities than FC or ZFC force measurements or flux mappings utilizing permanent magnets in a quasi-DC mode. In addition, the properties of a model SMB were characterized by static and dynamic measurements in a temperature range from 50K to 80K. Forced oscillations of a PM-ring levitated above a HTS ring were recorded and analyzed with respect to radial stiffness and damping.

4–25
Numerical analysis of a rotating superconducting magnetic bearing.
E. Portabella, R. Palka, H. May and *W.R. Canders*. Institut für Elektrische Maschinen, Antreibe und Bahnen. Technische Universität Braunschweig. Braunschweig, 38106, Germany.

A numerical calculation method, combining the critical state model and the trapped flux model, has been developed to study the interaction between permanent magnet (PM) and high-temperature superconductor (HTSC). The method has been applied to the analysis of an axial magnetic HTSC bearing. A permanent magnet arrangement with flux concentrating iron poles and optimised pole pitches has been used. The current distribution inside the HTSC sample and the levitation force between the bulk superconductors, placed in the stator, and the permanent magnet rings, fixed in the vertical shaft, have been computed during the loading process for the upper and lower bearings. Radial and axial forces and stiffness associated to small amplitude displacements have been evaluated by means of the trapped flux model. The design of the magnet arrangement, that is the number magnetic poles and the dimensions of magnets and soft iron poles, has been optimised to obtain a high performance of the bearing for a given operational gap. The effect of different cooling processes on the forces and stability of the system has also been explored.

4–26
Stability and stiffness of superconducting bearings.
R.J. Storey, T.A. Coombs, A.M. Campbell and *R.A. Weller*. IRC in Superconductivity, University of Cambridge, Cambridge CB3 0HE, UK.

Investigation is being made at Cambridge into the stability of superconducting bearings under static and / or oscillating imposed loadings in both the axial and radial directions. In order to devise general rules to define a safe operating region for a superconducting bearing the conditions required for bearing failure are being investigated. Resonant behaviour is stimulated using various excitation amplitudes in order to study different modes of behaviour, including possible bearing collapse, depending on the size of disturbance force applied to the bearing. A cellular model of the interaction between magnet and superconductor, developed in Cambridge, is being used to simulate vibrations in a superconducting bearing. The results from this are compared with the measured data, with the eventual aim of producing simulation software to aid design of safe superconducting bearing systems.

4–27
Application of High Performance Bulk Sm-Ba-Cu-O to Superconducting Magnetic Bearings.
T. Otani, M. Tomita and *M. Murakami*. ISTEC, Superconductivity Research Laboratory, 1-16-25 Shibaura, Minato-ku, Tokyo 105-0023, Japan.

Superconducting magnetic bearings (SMB) for the flywheel energy storage system (FESS) require high load capacity and large stiffness along with low rotational loss. In order to satisfy these demands, large single-grain LRE-Ba-Cu-O (RE: Nd, Sm, Eu, Gd) bulk superconductors with high critical current densities have been employed as stators of the SMB. LRE-Ba-Cu-O exhibit a secondary peak effect in that the critical current density (J_c) increases with increasing the external magnetic field. Since the magnetic field generated by the permanent magnet is below the peak value, magnetic relaxation in LRE-Ba-Cu-O is very small. In addition, large Jc values can be maintained even when the applied field is increased. Therefore, the high performance is expected by using the LRE-Ba-Cu-O/permanent magnet combination. In the present study, we used bulk Sm-Ba-Cu-O superconductors with fan-shape to make a ring 204 mm in outer diameter. We will also report the results of the field test with such a bearing. This work was supported by the New Energy and Industrial Technology Development Organization (NEDO).

4–28
Numerical Simulation of Reluctance Motors Containing Bulk High Temperature Superconducting Materials in the Rotor.
G.J. Barnes, M.D. McCulloch and *D. Dew-Hughes*. Dept. Engineering Science, University of Oxford, Parks Road, Oxford OX1 3PJ, U.K.

This paper describes the development of a numerical technique based on the finite element method to solve for the hysteretic critical state current distribution in high temperature superconductors (HTS). The finite element method is used to solve for the field both in the superconductor and its surroundings and an adapted method of moments algorithm is used to obtain the superconducting current distribution. The advantages of this technique are that it can readily handle non-uniform fields, arbitrary geometries and domains containing materials of differing permeabilities and

current sources. These properties make this technique suitable for modelling electrical machines which use bulk high temperature superconducting material. The machine chosen here is a reluctance motor where HTS materials are attached to an iron rotor to enhance the machine's performance. The results presented show that the HTS materials increase the power output by factors of 2-4 by improving the effective saliency of the rotor and also providing an additional hysteresis torque. This hysteresis torque is desirable for the run up properties and also the stability of the machine. Different designs of rotor are investigated and their simulated performance compared with experimental measurements when available.

4–29

6-DOF superconducting magnetic bearing with high accuracy of the rotor positioning.

A.V. Filatov, *O.L. Poluschenko* and *N.A. Nigelskiy*. Moscow N.E. Bauman State Technical University, Moscow, 107005, Russia.

A 6-degree-of-freedom passive magnetic bearing utilizing high-temperature superconducting rings made of single-domain melt-textured YBaCuO ceramic is presented. The bearing is featured by high stiffnesses and load capacities in both axial and radial directions, low force-displacement hysteresis (less than 4%), and low drag rotation torque. With the bearing outer diameter of 113mm and thickness of 32mm, the bearing load capacities in both axial and radial directions were estimated to be more than 53N with rotor displacements not exceeding 0.5mm. Therefore, the suspension stiffness can be evaluated to be approximately the same in axial and radial directions and to be in excess of 100 N/mm. The angular suspension stiffnesses about axes perpendicular to the rotation axis were estimated to be more than 4Nm/degree. High values of stiffness and load capacity make this bearing especially promising for applications requiring high accuracy of the rotor positioning such as momentum exchange wheels, centrifuges, etc.

4–31

Construction and Experiments of a Superconducting Cylindrical Linear Induction Motor with AC Superconducting Primary Windings.

M. Tomita, *T. Kikuma*, *M. Tsuda* and *A.I. Ishiyama*. Dept. of EECE, Waseda University, Shinjuku-ku, Tokyo 169-8555, Japan.

For realizing of AC superconducting applications , we are constructing a model Superconducting Cylindrical Linear Induction Motor (SCLIM) to clarify the behavior(AC loss , stability and so on) of AC superconducting windings in a realistic operational environment of electrical rotating machines. Until now the studies of an AC superconductor's development in regard to the reduction of AC loss and the improvement of current capacity have been advanced. From now on, the characteristic evaluation of AC superconducting windings in a realistic operational environment of electrical machines should be investigated. In the previous paper we presented the design and construction of SCLIM model system (i.e. AC superconducting primary windings , FRP cryostat and VVVF power supply with quench detection and protection circuit) and the results of fundamental driving experiments. In this paper, we focus on the optimization of current distribution in primary windings to enhance the torque characteristics, and a new quench detection and protection system for AC superconducting machines.

4–32

Superconducting Magnetic Bearing based on the Magnetic Gradient Levitation Concept.

H. Ohsaki, *N. Nozawa* and *Y. Fukasawa*. The University of Tokyo, Bunkyo-ku, Tokyo, 113-8656, Japan.

We have studied a novel superconducting magnetic bearing based on the magnetic gradient levitation concept, which uses bulk superconductors as a field shaping material. This bearing system needs only a steel component on the rotor side. The bulk superconductors or circular coils generate main magnetic field and stable levitation force on the steel component in the rotor without active control. The system is expected to have low rotational drag. Fundamental levitation characteristics have been demonstrated successfully with the small experimental model. In the paper, the structures of the superconducting bearings based on the magnetic gradient levitation concept are presented, and then the flux density profiles and electromagnetic force characteristics are investigated based on the experimental and numerical analysis results. The influence of the initially applied field during field cooling on electromagnetic characteristics is discussed in relation to the critical current density of the superconductor. The rotor dynamics and the magnetic drag during high-speed rotation are also examined. For the future application the possibility of a large bearing system of this concept is discussed.

4–33

The principles of construction and computer simulation of superconducting graviinertial sensors.

G.E. Shunin, *S.A. Kostryukov* and *V.V. Peshkov*. Voronezh State Technical University, Voronezh, RU, 394026, Russia.

The report contains a brief review of elaborations in cryogenic accelerometers, gravimeters and gravitational gradiometers, whose operation principle is based on the phenomenon of superconductivity. In theory, such devices have an own noise level $\sim 10^{-12} m \cdot s^{-2} \cdot Hz^{-1/2}$ and zero drift $\sim 10^{-11} m \cdot s^{-2}$ per day. However, the practical achievement of these values is connected with optimization of their construction and overcoming of some technological difficulties of their manufacture. The reviewing of construction principles of superconducting graviinertial sensors occupies the main part of the report. The physical processes in sensor elements influencing on a sensitivity threshold, zero drift and work reliability are analyzed. The mathematical models describing the dynamics of proof mass of sensor located on vibrating foundation are adduced. The results of elaboration of computer simulation system for the physical processes in a sensor are reported. The development is based on the finite element method. With the developed system the computer simulations of superconducting screens, proof mass suspensions and other elements of sensor were carried out, the main parameters and characteristics of these devices were calculated.

4–34

Finite Element Simulation of Autostable Superconducting Magnet Rails.

G.C. da Costa[1], *A.S. Pereira*[2], *L. Landau*[1] and *R. Nicolsky*[2]. [1] LAMCE - Laboratório de Métodos Computacionais em Engenharia, PEC/COPPE/UFRJ Cx.P. 68552, Rio de Janeiro 21949-900, Brazil; e-mail: gian@lamce.ufrj.br. [2]LASUP - Laboratório de Aplicações de Supercondutores, IF/UFRJ Cx.P. 68528, Rio de Janeiro 21945-970, Brazil; e-mail: agnaldo@if.ufrj.br.

The application of the finite element method (FEM) in the simulation of the electromechanical machines with superconducting components has been seriously limited by the lack of suitable programs for working with the diamagnetic response, a characteristic feature of the superconducting materials, mainly for the type II superconductors. In this work we have applied a methodology able for calculating the magnetic levitation forces generated by repulsion between a permanent magnet rail and the high-Tc superconducting levitator by means of an ordinary FEM program. The rails are designed in two distinct geometries: flat and roof-shaped. The calculation of levitation forces was made possible by introducing the B × H curve of the YBaCuO levitator in the material database of the program. As these curves are not available in the usual handbooks, we have constructed them using the Bean critical state model adjusted for the rail symmetry. The introduction of this magnetization curve allows treating the superconductor as an ordinary magnetic material, in the frame of a commercial FEM program, avoiding the need for specific softwares. We also present a model for the transversal mechanical stability based on the vortex collective pinning.

4–35

Hybrid superconducting/electromagnetic bearing for induction machines.

R. de Andrade, Jr.[1], *A.S. Pereira*[2], *D.F.B. David*[3,4], *J.A. Santisteban*[5], *A. Ripper*[4], *R.M. Stephan*[1,6] and *R. Nicolsky*[2]. [1]LASUP, DEE/EE/UFRJ, Cx.P. 68515, Rio de Janeiro 21945-970, Brazil. [2]LASUP, IF/UFRJ, Cx.P. 68528, Rio de Janeiro 21945-970, Brazil. [3]TEM/UFF, Niteroi 24210-240, Brazil. [4]LASUP, PEM/COPPE/UFRJ, Rio de Janeiro 21945-970, Brazil. [5]DEE/UFF, Niteroi 24210-240, Brazil. [6]LASUP, PEE/COPPE/UFRJ, Rio de Janeiro 21945-970, Brazil.

A hybrid magnetic bearing with superconducting passive axial levitation and active radial electromagnetic positioning for induction machines has been designed and tested. This bearing/motor prototype has been designed on the basis of a previous one reported by Salazar-Stephan as 4-pole 2-phase induction machine using windings of a standard motor which have, simultaneously, torsional and radial positioning functions. The active radial bearing uses four eddy-current sensors for measuring the shaft-position and a PID control system for correcting it. The superconducting bearing has been designed with two commercial NdFeB permanent magnets, disc- and ring-shaped, fixed on the bottom of the shaft of the rotor, in a concentric anti-parallel configuration. The superconductors are seeded-melt-textured YBCO blocks in different spatial arrangements. The levitation forces at 77 K, have been measured for field cooling at different distances. The resulting air gap, the distance between the permanent magnets and the superconductors, as well as the elastic and damping constants show a strong dependence on the cooling position and the particular display of the superconductors. The different configuration have been modelled and simulated by finite element method. The experimental results have shown a reasonable agreement with simulations within the limits of the models.

4–36

Thickness effects in the levitation of superconducting cylinders and disks.

C. Navau and *A. Sanchez*. Departament de Fisica, Universitat Autonoma de Barcelona, 08193 Bellaterra, Barcelona, Spain.

Many devices are based on the levitation of superconductors or permanent magnets which arises from their magnetic interaction. The levitation forces are dependent on many factors, including the characteristic critical current density of the superconducting material and the permanent magnet strenght, but also from other extrinsic factors such as the device spatial configuration or the geometry and shape of the components. In this work we concentrate in systems with cylindrical symmetry and analyze the effect that the dimensions of the superconductor and the permanent magnet have in the levitation forces. A method based on energy minimization in the superconductor allows us to calculate the force as a function of its thickness. The limiting cases of infinite cylinders and thin disks are discussed as well.

Session Wires, tapes and coated conductors

4–37

Preparation of Bi 2223 Multifilamentary Tapes by Two-Step Heat Treatment Process.

S.K.Xia[1], *A.Polasek*[1], *M.B.Lisboa*[1], *E.T.Serra*[1] and *F.Rizzo*[2]. [1]CEPEL-Electric Power Research Center, Rio de Janeiro, RJ, 21944-970 Rio de Janeiro, RJ, Brazil. [2]Pontifícia Universidade Católica - PUC-Rio, Rua Marques de Sao Vicente, 225 22453-900 Rio de Janeiro, RJ, Brazil.

Owing to the simplification for tape processing, the two-step method, which includes a high temperature sintering and a lower temperature annealing during the heat treatment cycle, has exhibited great advantage for large-scale fabrication of Bi 2223/Ag tapes. The main advantage of such method is the reduction of the number of thermomechanical cycles when compared to the traditional process. Results on monofilamentary tapes prepared by two-step method bave been reported in the literature. In this work, 19-filament tapes habe been prepared by two heat treatment cycles with only one intermediate tape deformation, and with the two-step method applied on the second heat treatment cycle. The effect of several processing parameters on the critical current density (Jc) of the mutifilamentary tapes was studied. These parameters included the intermediate deformation load, the overall tap thickness, and the sintering and annealing temperatures. For the optimized deformation and tape thickness conditions critical current densities greater than 25kA/cm^2 are reproductible.

4–38

A new type of superconductor/ferromagnet heterostructures for high-current applications.

Yu.A.Genenko[1,2], *A.Usoskin*[1], *A.Snezhko*[2,3] and *H.C.Freyhardt*[1,4]. [1]Zentrum für Funktionswerkstoffe gGmbH, 37073 Göttingen, Germany. [2]Donetsk Physical and Technical Institute NAS Ukraine, 340114 Donetsk, Ukraine. [3]Charles University, 180 00 Prague 8, Czech Republik. [4]Institut für Materialphysik, Universität Göttingen, 37073 Göttingen, Germany.

Transport current distribution over superconductor/ferromagnet heterostructures of various design is studied theoretically and experimentally. Substantial enhancement or strong suppression of the maximum nondissipative current is predicted for different configurations which results from the enhanced or suppressed effect of the edge barrier in a superconducting strip. Analyical solutions for the case of strong ferromagnets as well as numerical studies at arbitrary magnetic permeabilities show that the effect depends strongly on the geometry of a structure and much less on the magnetic permeability of magnets. Preliminary results of experimental studies of YBaCuO/Fe and YBaCuO/Ferrites structures exhibit the critical current enhancement by 15% and suppression by 50% in different geometries in qualitative agreement with the theory.

4–39

Influence of irradiation on the superconducting properties of uranium-doped $Bi_2Sr_2Ca_2Cu_3O_x$-tapes.

S. Tönies[1], *C. Klein*[1], *H.W. Weber*[1], *B. Zeimetz*[2], *Y.C. Guo*[2], *S.X. Dou*[2], *R. Sawh*[3], *Y. Ren*[3] and *R. Weinstein*[3]. [1]Atomic Institute of the Austrian Universities, Vienna, A-1100,Vienna, Austria. [2]Institute of Superconducting and Electronic Materials, University of Wollongong, Wollongong NSW 2522, Australia. [3]Institute for Beam Particle Dynamics, University of Houston, Houston, TX 77204-5506, USA

BiSCCO-2223-tapes containing small amounts of UO_4 powder were prepared by the powder in tube method. Irradiation by thermal neutrons causes fission of the uranium. The resulting defects significantly improve flux pinning and shift the irreversibility line. The superconducting properties of the samples were characterised by transport measurements in fields up to 6T. The rotation of the sample holder in the horizontal field of a Helmholtz-coil allows us also to measure the angular dependence of J_c. At higher fields we find enhancements of J_c due to irradiation in the uranium-doped samples by a factor of 10 at 3T for HIIab and a factor of 20 at 0.7T for HIIc at 77K. The J_c anisotropy is reduced by irradiation by an order of magnitude for the uranium doped samples (from 12 to 1.6). Furthermore, inter- and intragranular critical current densities of these samples were determined from the remanent moments. We report on results for samples with different amounts of uranium and compare them with those on undoped samples.

4–40

Assembled conductors of Bi2223/Ag-tapes for AC-applications.

J. Rieger, *M.P. Oomen*, *P. Kummeth*, *W. Herkert*, *R. Nanke* and *M. Leghissa*. Siemens AG, Corporate Technology, P.O.Box 3220, D-91050 Erlangen, Germany.

For power energy applications like transformers a high transport current in a single HTS-conductor is desirable to ease the fabrication. We cabled single insulated multifilament Bi2223/Ag-tapes to form assembled conductors. We applied different preparation routes depending on the insulation material. Mechanical tests were performed to find limits for bending the conductor along its edge and high voltage tests to qualify the electrical insulation. The critical current of the multifilament tapes is not degraded by the insulating and cabling process. We studied the influence of the mutual self field contributions on the critical current. We performed AC-loss measurements in an external AC-field. Cabled conductors with a perfect insulation have an AC-loss level as high as the sum of the losses of the single tapes. Electrical contacts between elementary tapes cause, similar to the filaments in a multifilament tape, extra losses caused by coupling currents.

This work was supported by the German Ministry for Education, Science, Research and Technology, BMBF, under grant no. 13N6481A.

4–41

Design of HTS pancake coil by the optimization of tape width.

S.S. Oh, *H.B. Jin*, *H.S. Ha*, *D.W. Ha*, *D. Y. Jeong* and *K.S. Ryu*. Applied Superconductivity Lab., Korea Electrotechnology Research Institute, Changwon 641-120, Korea.

The high temperature superconducting pancake coil fabricated by React & Wind method is usually consisting of several double pancake elements with the same tape's width. The critical current of tape conductor in the each double pancake element is dependent on the strength and the direction of magnetic field generated from the coil itself. The critical current becomes maximum at center part of the coil and minimum at the uppermost and lowermost parts where the radial magnetic field is maximum. In this paper, we have suggested a new design method with different tape's width to improve the efficiency of magnetic field strength in a pancake type HTS coil considering the magnetic field distribution with respect to the coordinates of each double pancake element. From the optimization of tape's width, the center magnetic field was confirmed to be increased compared to the conventional method using the tape with same width.

4–42

Quench characteristics of Ag sheathed Bi-2223 superconducting tapes with different Ag/SC ratio.

S.S. Oh[1], *H.M. Jang*[1], *H.S. Ha*[1], *D.W. Ha*[1], *K.S. Ryu*[1] and *S.H. Kim*[2]. [1]Applied Superconductivity Lab., Korea Electrotechnology Research Institute, Changwon 641-120, Korea. [2]Gyeongsang National University, Chinju 660-701, Korea.

The influence of Ag/SC ratio on the quench characteristics and stability of Ag sheathed Bi-2223 tapes was investigated.

The Ag sheathed Bi-2223 tapes with various Ag/SC ratios were prepared using PIT method. Minimum quench energy and normal zone propagation(NZP) velocity of the tape were measured changing the temperature, operating current and magnetic field. Those experimental results were analyzed and compared with the results calculated by solving nonlinear heat conduction equations. The temporal variation of temperature and voltage were also measured and discussed. It was made clear that the NZP velocity becomes faster when the Ag/SC ratio is increased. The dependence of Ag/SC ratio on MQE was much influenced by the operating current.

4–43
Thermal and Electrical Properties of Bi-2223 tape conductors.
A.K. Shikov[1], *N.I. Kozlenkova*[1], *I.I. Akimov*[1], *P.A. Kuznetsov*[1], *D.N. Rakov*[1], *F.V. Popov*[1], *I.V. Bogdanov*[2], *S.S. Kozub*[2], *A.A. Olunin*[2] and *P.A. Sherbakov*[2]. [1]SSC RF Bochvar's All – Russia Seientific Research Institute of Inorganic Materials, Moscow, Rogova St., 123060, Russia. [2]SSC RF Institute for High Energy Physics, Protvino, Moscow region, Russia.

Applying HTSC tape conductors in current leads require alloying silver sheath with other elements. This approach allows to reduce thermal conductivity in the temperature range between 4.2K and 77K. On the other hand alloying of sheath should not lead to degradation of critical temperature and current. In frame of this work thermal and electrical properties Bi-2223 tape conductors sheathed with silver and silver alloy (Ag+1at.%Au, Ag+10at.%Au) were investigated. This paper presents the full characterization of BiPb2223 conductors: critical current and parameter "n" dependencies on temperature and magnetic field up to 12T; the temperature transition profiles; the data on electrical and thermal conductivity, heat capacity and thermal expansion coefficient in the range of temperature from 300K to 50K as well as results of the sheath thermal expansion coefficient measurement. The data on the degradation of critical current on bending deformation are presented also. The investigation carried out have shown that properties of conductors under study allow the current leads with heat leak much lower than that for conventional copper current leads to be manufactured.

4–44
Optimization of deformation processing for Bi-2223 composite superconductors.
A.D. Nikulin, *A.K. Shikov*, *A.E. Vorobieva*, *I.I. Akimov*, *F.V. Popov*, *A.V. Rekudanov*, *D.B. Gusakov*, *M.I. Medvedev* and *O.I. Lomov*. SSC RF Bochvar's All – Russia Seientific Research Institute of Inorganic Materials,Moscow, Rogova St. 5a, 123060, Russia.

The model approach is proposed to calculate the optimal design as well as optimal deformation regimes for Bi-2223 composite superconductors. The effects of different parameters such as area reduction ratio on each step, roller diameter and lubrication material were investigated on the conductor sizes evolution during processing, structure and superconducting properties as well for different designs of tapes and wires. The set of perspective HTSC-wires design was presented which were made by the OPIT technique and HTSC mono- and multilayer plates having large surface area among them. The influence of initial precursor properties on geometrical and critical characteristics for HTSC-conductors have been analyzed. Some model electrotechnical articles made on base of different HTSC-conductors are presented.

4–45
Cooling studies of BSCCO/Ag Tapes in 8% Oxygen.
L. G. Andersen[1], *Y.L. Liu*[1], *J.-C. Grivel*[1,2], *H.F. Poulsen*[1] and *W.G. Wang*[2]. [1]Materials Research Department, Risø National Laboratory, DK-4000 Roskilde, Denmark. [2]Nordic Superconductor Technologies, Priorparken 878, DK-2605 Brøndby, Denmark.

We have earlier shown that during cooling of BSCCO/Ag tapes in air two processes taking place: a) a conversion of $(Ca,Sr)_2CuO_3$ and a liquid phase to 2212 + 2223 and at lower temperatures to 2201, b) a decomposition of 2223 to 3221 or $(Ca,Sr)_2PbO_4$. Both can be detrimental to the critical current density J_c. In this work multi-filamentary BSCCO/Ag tapes already annealed are investigated during cooling in an oxygen partial pressure of 8%. Different two-step temperature profiles are used for the final heat treatment. The temperature of the second step and the two cooling rates are systematically varied. The tapes are characterised by means of transport measurements (J_c) and by scanning electron microscopy (SEM). The phase assemblage, after the cooling procedure, is investigated by means of high-energy synchrotron x-ray diffraction. This method is also used to study phase transformation *in-situ* during cooling for a selected temperature profile. The synchrotron technique provides information of the concentration and stoichiometry changes. Furthermore a phase diagram, depicting of temperature versus oxygen partial pressures, is established using the same tapes. Precipitation and decomposition mechanisms are discussed. Finally we compare the 8% O_2 data with results of air-cooling and the phase diagram. Support is provided by the Danish Energy Agency and by the companies ELSAM and ELKRAFT. The synchrotron experiments took place within the framework provided by Dansync and the Engineering Science Center for Structural Characterization and Modeling of Materials.

4–46
Current carrying capacity and the anisotropy of Bi-2212/Ag ROSATwire.
M. Okada[1], *K. Tanaka*[1], *K. Ohata*[2], *J. Sato*[2], *H. Kitaguchi*[3], *H. Kumakura*[3], *K. Togano*[3], *T. Kiyoshi*[3] and *H. Wada*[3]. [1]Hitachi Research Laboratory, Hitachi, Ltd., Hitachi, Ibaraki 319-1292, Japan. [2]Advanced Research Center, Hitachi Cable, Ltd., Tsuchiura, Ibaraki 300-0026, Japan. [3]National Research Institute for Metals, Tsukuba, Ibaraki 305-0047, Japan.

Bi-2212/Ag round-shaped wires with tape-shaped multifilaments have been successfully developed. The wires includes 126-960 tape-shaped filaments with triple rotation symmetry, having a good crystal alignment in each filament. We named the new wire ROSATwire, (ROtation-Symmetric Arranged Tape-in-tube wire). We found that the present wire fabrication process markedly improves not only productivity and lowers cost, but also enhances the transport Jc of the Bi-21212/Ag wire. The Ic and Jc reached >340A and

1000A/mm2 at 28T and 4K

4–47

Improving the Mechanical Properties of Multifilament Ag/Bi-2223 Tape.

M.H.Apperley, *R. Zhao*, *F. Darmann*, *G.D. McCaughey* and *T.P. Beales*. Australian Superconductors Pty. Ltd., Eveleigh, NSW, 1430, Australia.

The powder-in-tube technique is a viable process for the fabrication of multifilament Ag clad Bi-2223 tape and continuous lengths up to 1 km are readily available. A consequence of using pure Ag as the cladding metal, however, is that the tape is mechanically very weak and the filaments within easily damaged by handling during the production process or the fabrication of devices. Two methods for improving the mechanical properties of Bi-2223 tape have been investigated. The first of these involved replacing the outer Ag sheath of conventional PIT tape with a Ag-Mg alloy which strengthened the tape by an oxide dispersion mechanism. The second method involved the stacking of multifilament tapes between pure Ag or alloy backing tapes followed by the processing in such a way that the final dimensions of the composite were similar to conventional PIT tape. The tolerance of tape Ic at 77 K to tensile, bending and torsion strains was assessed and compared to pure Ag clad tape. It was found that the modified PIT tapes could tolerate higher levels of mechanical strain before Ic degraded with bend strains over 1% measured on some samples before Ic decreased to below 95% of Ico.

4–48

Estimation of the upper limit of the critical currents of Bi(2223)Ag tapes with various orientation of filaments.

J. Pitel, *P. Kovac* and *I. Husek*. Institute of Electrical Engineering Slovak Academy of Sciences Dubravska 9 842 39 Bratislava Slovakia.

Anisotropy of the critical current versus magnetic field at 77 K can be considered a serious disadvantage of the flat rolled Bi(2223)Ag tapes, resulting in natural limitation of the operating current of the magnets. It has been believed that this problem can be overcome by producing the multifilamentary tapes using the two-axial rolling technique. It is being shown that the anisotropy of such a new type of tapes with the filaments oriented in parallel as well as perpendicular direction to the tape surface decreases considerably. Unfortunately, a simultaneous decrease in the current carrying capacity is observed as well. Simple mathematical model has been built, enabling to estimate the values of the critical current of the tapes with various orientation of the filaments as a function of both the magnitude and the direction of an external magnetic field. The data obtained for short samples were used to predict the critical currents of the cylindrical iron free magnets in order that to show the changes in the position of the weak spots in the winding, when designed of different types of tapes.

4–49

The effective resistance between superconducting filaments in tapes.

S. Takács[1], *K. Funaki*[2] and *M. Iwakuma*[2]. [1]Instiute of Electrical Engineering, Slovak Academy of Sciences, 842 39 Bratislava, Slovakia. [2]Research Institute of Superconductivity, Graduate School of Information Science and Electrical Engineering, Kyushu University, 6-10-1 Hakozaki, Higashiku, Fukuoka 812-8581, Japan.

We consider two effects which can strongly influence the effective resistance between crossing filaments in twisted tapes. Tapes with BSCCO filaments in silver matrix in perpendicular magnetic fields are considered as model structure (strands on flat cables behave similarly). At first, the silver matrix between the filaments increases the effective conductance compared with the direct current paths (proportional to the touching area of filaments). The increase factor is about two and can be easily suppressed by other effects, like the contact resistance between the superconductor and the matrix. However, due to the strong anisotropy of critical parameters for high temperature superconductors, this effect can compensate the usually weaker critical current density perpendicular to the tape, causing the current to flow not only directly between the filaments. The second effect is the existence of induced voltage between any points of crossing filaments. This increases the effective conductance by a factor quadratically proportional to the total filament number. Therefore, for obtaining low AC coupling losses, structures with smaller filament number should be preferred. This result is analogous to the round structures (A.M. Campbell), leading to AC losses proportional to the square of the layer number in the field direction.

4–50

Mechanical Properties and Fracture of Ag-BSCCO Tapes.

N.McN. Alford[1], *O.O. Oduleye*[2] and *S.J. Penn*[3]. [1]South Bank University, London, SE1 0AA UK. [2]Clarendon Laboratory, Oxford, OX1 3PU, UK. [3]South Bank University, London, SE1 0AA UK.

Experiments have been carried out to determine the elastic modulus in bending, Eb, the model (opening) fracture toughness, K1c and the critical flaw size of 1 mm extruded (Bi,Pb)SrCaCuO rods. This provides a good model for the core in Ag-BSCCO conductors. These properties are crucial in developing a clearer idea of the behaviour of BSCCO superconductors in service and are a pre-requisite for modelling using for example finite element techniques. The experiments show the effect of pore volume on these mechanical properties. It is found that the critical defect length is BSCCO is surprisingly large and this has important implications on the processing of the materials and to the limits of application. Finite element analysis reveals that that the BSCCO core is subject to considerable tensile forces even on cooling the Ag-BSCCO composite.

4–51

Detection of Pores and Cracks in Bi-2223/Ag Multifilamentary Tapes.

A. Kasztler[1], *M. Polak*[2] and *H. Kirchmayr*[1]. [1] Institute for Experimental Physics, University of Technology Vienna, Austria Austria. [2]Institute of Electrical Engineering, Slovak Academy of Sciences, Bratislava, Slovak Republic.

Using potential taps distanced by 1 mm we measured local V-I curves and estimated the local Ic-values of a 55 filament Bi-2223 tape. The cross-section of the tape in the subsection with lowest Ic showed pores and cracks in many filaments. No similar defects were observed outside this weak section. Cracks were only found in filaments where pores were present, which indicates that cracks result from mechanical stress in the vicinity of pores. Near these defects some linear sections of the V-I curves were observed.
This work has been partly conducted within the association EURATOM-OEAW (Austrian Academy of Science) (Task No. GB6-MAG-M16/02) and within the project 2/4052/97 supported by the Slovak Grant Agency VEGA.

4–52

Influence of Ge addition on phase formation and electromagnetic properties in internal tin processed Nb_3Sn wires.

D.W. Ha[1], *S.S. Oh*[1], *H.S. Ha*[1], *N.J. Lee*[1], *K.S. Ryu*[1] and *H.K. Baek*[2]. [1]Applied Superconductivity Lab., Korea Electrotechnology Research Institute, Changwon 641-120, Korea. [2]Department of Metallurgical Engineering, Yonsei University, Seoul 120-749, Korea.

In previous study, Ge addition to the Cu matrix in the internal tin processed wire was confirmed to suppress the growth of Nb_3Sn layer and to improve the high field Jc property. Compared to the Nb_3Sn wire made by Cu-Sn-Ge/Nb bronze process, the influence of Ge addition on the microstructure was not so clear in the Cu-Ge/Nb/Sn internal tin process. In order to investigate correlation between the Ge addition and the microstructure change related to the Nb_3Sn formation in detail during the reaction heat-treatment, we prepared 4 kinds of internal tin processed wires with pure Cu and Cu-Ge alloys containing 0.4 wt% , 0.8wt% and 1.2 wt% Ge. We analyzed diffusion behavior of Ge element in the matrix and Nb core. Variation of electromagnetic properties of AC loss, Tc and Jc in magnetic fields due to the amount of Ge addition was also investigated.

4–53

The temperature dependence of the critical currents in commercial Nb_3Sn superconductors with respect to applied field and strain.

A. Godeke, *H.J.G. Krooshoop*, *B. ten Haken* and *H.H.J. ten Kate*. University of Twente, Faculty of Applied Physics, P.O. Box 217, 7500 AE Enschede, The Netherlands.

In order to extend the available conductor data necessary for the stability codes of large magnet systems, two conductor types are analyzed over a wide range of temperature, applied background field and axial strain. The conductors are two bronze-processed wires produced by different manufacturers. The critical current is measured at temperatures from 4.2 K to 20 K, in background fields from 1 T to 16 T and at axial strain values ranging from 0.8 % to + 0.5 %. The acquired data are evaluated with an earlier introduced improved relation for the critical current density as a function of field, temperature and strain for A15 materials. The emphasis is on the temperature dependence that is described in the existing literature by various empirical models.

4–54

The effect of strain on the critical current density of Nb_3Sn wires.

D. P. Hampshire, *N. Cheggour* and *S. A. Keys*. Superconductivity Group, Dept of Physics, Durham University, South Road, Durham DH1 3LE England.

The effect of strain on the critical current density (Jc) of superconductors in high magnetic fields is important for applications and for a better understanding of the mechanisms that determine Jc. We present systematic measurements of Jc as a function of field, temperature and strain (in tension and compression) for Nb_3Sn wire. The change in the functional form of Jc caused by hot isostatic pressing at 2000 atmospheres has been measured and is considered within the framework of the fietz-Webb pinning scaling law. We discuss a minimum data set from which the magnetic field, temperature and strain dependence of Jc, required for the design of high field systems, can be determined for a given strand of wire.

4–55

Direct study of transport characteristics in YBCO coated-conductors.

S.B. Kim[1], *Y. Takahashi*[1], *K. Matsumoto*[1], *T. Takagi*[2], *T. Machi*[2], *N. Koshizuka*[2], *A.I. Ishiyama*[3] and *I. Hirabayashi*[1]. [1]Superconductivity Research Laboratory ISTEC, Nagoya, 456-8587, Japan. [2]Superconductivity Research Laboratory ISTEC, Tokyo, 135-0062, Japan. [3]Department of EEC Engineering Waseda University, Tokyo, 169-8555, Japan.

We have been developing a YBCO coated-conductor for high current applications. The challenge now is to scale-up the fabrication techniques to investigate the long length conductors with high critical current density. In order to develop the YBCO conductor with high critical current density, understanding what is presently limiting the critical current density would be helpful and the information will be feedback to fabrication processing. In the prersent work, how much the critical current density is restricted by grain boundaries, cracks, second phases, porosity and highly misaligned regions has been studying directly with magneto-optic imaging technique (MOI) and scanning electron microscopy (SEM), etc. The samples used in this work were YBCO coated-conductors prepared by pulsed laser deposition (PLD) on single crystalline MgO and biaxially oriented Ni substrates. This work was supported by the New Energy and Industrial Technology Development Organization (NEDO).

4–56

Fabrication of biaxially textured substrates and buffer layer architectures for Tl-1223 thick films.

T.A. Gladstone, *J.C. Moore*, *A.J. Wilkinson* and *C.R.M. Grovenor*. Department of Materials, University of Oxford, Oxford, UK.

Power applications of HTS materials operating at or near 77K in moderate magnetic fields require a choice of superconducting phase with a high irreversibility line, such as Tl-1223 and YBCO, and production of long lengths of biaxially textured superconducting tape. There has been a significant amount of interest in achieving this texture by the epitaxial deposition of superconductors onto rolling-assisted biaxially-textured substrates (RABiTS). We have investigated texture formation under different thermomechanical process conditions in Ag and several Ni-based materials including pure Ni and Ni-Cr alloys. XRD and EBSD measurements have been used to compare the degree and stability of the texture obtained. Lanthanum nickelate has been identified as a possible buffer layer material and we have fabricated coatings on both single crystal substrates and cube textured Ni tape by RF magnetron sputtering. We have examined the compatibility of LaNiO3 with Tl-1223 films fabricated by spray pyrolysis and sputtering, and initial indications suggest that adverse reactions occur. We are investigating other compounds to include in LaNiO3 based buffer layer architectures to achieve a biaxially textured substrate suitable for the deposition of Tl-1223 films.

4–57

Variations of superconducting properties with F content in F-dopped Tl-1223/Ag tapes.

D. Y. Jeong[1], *H. K. Kim*[1], *H. Y. Lee*[1], *H. S. Ha*[1], *S. S. Oh*[1], *J. H. Lee*[2], *B. J. Kim*[2] and *Y. C. Kim*[2]. [1]Korea Electrotechnology Research Institute, Changwon 641-120, Korea. [2]Pusan National University, Pusan 609-735, Korea.

Previously the present authors reported the clear occurrence of grain-texturing and high J_c's over 25,000 A/cm^2 at 77 K and 0 T in $Tl_0.8Bi_0.2Pb_0.2Sr_1.8Ba_0.2Ca_2.2Cu_3O_x$/Ag tapes. However, there existed significant weak-links in the tapes, indicating that the grain-connectivity is still far from the desired one and need to be enhanced by a certain manner. Recently, Hamdan et al. and Bellingeri et al. reported significant increases in T_c and width of magnetization hysteresis loop resulting from the partial substitution of fluorine for oxygen in Tl-1223 materials. In the present study, therefore, the effects of partial substitution of fluorine on superconducting properties were studied in $Tl_0.8Bi_0.2Pb_0.2Sr_1.8Ba_0.2Ca_2.2Cu_3O_xF_y$ ($0 \pounds \frac{1}{4} y \pounds \frac{1}{4} 2$) tapes. The tapes were prepared using the powder-in-tube method incorporating an in-situ reaction method. In the present study, T_c, phase evolution, the changes of morphology and J_c's during thermo-mechanical treatments, the field dependence of transport and magnetization Jc's, and intergranular coupling characteristic in the tapes with different F contents will be presented.

4–58

Comparative study of microstructures in Tl-1223/Ag tapes with different chemical compositions and J_c's.

D. Y. Jeong[1], *H. K. Kim*[1], *H. Y. Lee*[1], *H. S. Ha*[1], *S. S. Oh*[1], *S. Horiuchi*[2], *Y. Matsui*[2], *J. H. Lee*[3], *B. J. Kim*[3] and *Y. C. Kim*[3]. [1]Korea Electrotechnology Research Institute, Changwon 641-120, Korea. [2]National Institute for Reseach in Inorganic Materials, Tsukuba, Ibaraki 305-0044, Japan. [3]Pusan National University, Pusan 609-735, Korea.

The microstructures of a $Tl_0.8Bi_0.2Pb_0.2Sr_1.6Ba_0.4Ca_2Cu_3O(9+\delta)$/Ag tape with J_c of 18,000 A/cm^2 at 77 K and 0 T and two $Tl_0.8Bi_0.2Pb_0.2Sr_1.8Ba_0.2Ca_2.2Cu_3O(O9+??)$/Ag tapes with J_c's of 17,000 and 25,000 A/cm^2 prepared using the powder-in-tube method and an in-situ reaction method, were investigated using scanning electron microscopy and high-resolution transmission electron microscopy, and compared each other. In the tape preparation history, an intermediate rolling process was not added during final heat-treatment for the first and the second tapes, but for the third. The microstructural analysis revealed clear differences in grain-texturing, crystallographic defects and impurity phases, depending on the chemical composition of the tape. While the grain-texturing in the first tape appeared to be poor, that in the second tape appeared to be more or less prominent. The grain-texturing was much enhanced by the intermediate rolling. In crystallographic defects, while stacking faults were prevalent in the former composition, dislocations and voids were frequently observed in the latter. Also impurity phases were appeared to be more abundant in the latter than in the former.

4–59

Texturation of YBCO films deposited by an electrophoretic technique.

E. Meunier[1], *F. Weiss*[2], *C. Chabaud-Villard*[3], *J.W. Park*[4] and *F. Hardinghaus*[5]. [1]CRETA - BP 166 - 38042 Grenoble CEDEX 09 - France. [2]LMGP - Domaine Universitaire BP 46 - 38402 ST Martin d'Heres CEDEX - France. [3]CRTBT - BP 166 - 38042 Grenoble CEDEX 09 - France. [4]Solvay Barium Strontium GmBH, Hans-Bockler Allee 20, 53557-Bad Honningen, Germany. [5]Solvay Barium Strontium GmBH, Am Guterbacker Hof, 53557-Bad Honningen, Germany.

Electrophoresis has been investigated as a deposition technique for both thick and thin films of YBCO on silver substrates. We report results on electrophoretic deposition (EPD) at room temperature using acetone as suspending medium. Intense magnetic fields are used for texturation of the deposits (8-12T). Thick films (30-60μm) are investigated for their current carrying ability, they must be prepared under high magnetic fields (8-10T) to obtain good uniaxial texture. Typically, a 60μm-thick YBCO deposit displayed an XRD peak intensity ratio (005)/(103) of 1.22, which corresponds to a transport Jc value of 2000 A/cm^2 at 77K. The use of additives such as Y211 or PtO_2 proved to be very important regarding film behaviour during thermal treatment. Thin films are rather similar to "veils" since the substrate occupation rate ranges from 50 to 70%. This kind of EPD film is very promising for multiseeding purposes. We have achieved the deposition of YBCO particles on a silver sub-

strate with a 50% occupation rate and an XRD (005)/(103) ratio of 4.2. Conventional melt processing techniques could then be used to texture a thicker layer deposited on top of such "veils".

4–60

Processing of YBCO Thick Films on Ag Substrates in Low $p(O_2)$ Environments.

T.C.Shields[1], *J.S.Abell*[1], *T.W.Button*[2], *W.Haessler*[3], *J.Eickemeyer*[3] and *L.Schultz*[3]. [1]School of Metallurgy and Materials, University of Birmingham, Birmingham, B15 2TT, UK. [2]IRC in Materials for High Performance Applications, University of Birmingham, Birmingham, B15 2TT, UK. [3]IFW Dresden Institute of Solid State and Materials Research, D-01171 Dresden, Germany.

Ag substrates with different textures have been fabricated by varying their rolling and recrystallisation procedures. YBCO thick films have been prepared on these substrates by the screen printing method. The screen printed films were initially heated in a low $p(O_2)$ environment and then the gas switched to $p(O_2)$=5% at a peak temperature of 955°C, in order to drive the crystallisation of the 123 phase. The microstructures and superconducting properties of the thick films are dependent on the degree of texture in the Ag substrates. The initial $p(O_2)$ content also has an influence on the properties of the films. A $p(O_2)$ of less than 1% is required to produce melt textured films that are c-axis textured. Different microstructures have also been produced by control of the dwell times at peak temperature and the subsequent cooling rates. The influence of the microstructures on the critical current densities at 77K will also be discussed.

4–61

Texture development of YBCO thick films by directional solidification on metallic substrates.

M. Najib[1], *S. Piñol*[1], *T. Puig*[1], *J.M. Chimenos*[2], *E. Varesi*[1] and *X. Obradors*[1]. [1]Institut de Ciencia de Materials de Barcelona. Consejo Superior de Investigaciones Cientificas. Campus de la UAB. Bellaterra. Barcelona. 08193 Spain. [2]Departament d'Enginyeria Química i Metal·lúrgia, Facultat de Química, Universitat de Barcelona, Diagonal 647, E-08028, Barcelona, Spain.

We have investigated the influence of different metallic substrates on the texture of the superconducting YBCO thick films, prepared by screen printing and solidified directionally at different speeds after melting, in a furnace with Chalmers configuration. The metallic substrates were prepared by RABiTS procedure (Rolling Assisted Biaxially Textured Substrates) in order to prepare long HTS superconducting tapes. The metallic substrates studied in this work are: silver (110), Ni (100) <001> and polycristalline Ag-Pd alloys (5-12.5% at Pd). In addition, epitaxial cube textured NiO (100) layers growth on textured Ni (100) metallic foils, have also been obtained. Surface morfology and texture of the substrates and superconducting thick films were characterised by means of SEM, X-ray diffraction, rocking curves and pole figures. Superconducting properties were measured by SQUID magnetometry and transport critical currents.

4–62

Epitaxial growth of Re-123 (Re: Gd, Nd) superconducting phases on pure Ag single crystals.

M. Schindl[1], *E. Koller*[1], *J.-Y. Genoud*[1], *E. Walker*[1], *G. Triscone*[1], *H. Suo*[1,2], *Ø. Fischer*[1] and *R. Flükiger*[1]. [1]DPMC, University of Geneva, 24 quai E.-Ansermet, 1211 Geneva 4, Switzerland. [2]Beijing Polytechnic University, 100022 Beijing, China.

Sputtering techniques were used to study the epitaxial growth of $GdBa_2Cu_3O_{7-\delta}$ (Gd123) and $NdBa_2Cu_3O_{7-\delta}$ (Nd123) on pure oriented Ag single crystals. In the Gd123 case, the commensurability between the superconducting cell and the three (100), (110) and (111) Ag planes was studied in details. No preferential orientation was found on the Gd123 phase sputtered on the (111) Ag orientation. Two biaxial orientations, 45° apart were obtained on the (100) face whereas a univoque orientation was found on the (110) oriented crystals. X-ray f-scan gave FWHMs of respectively 12° and 30° . If the results are in principle similar for the two rare earth compounds, a very promising improved film quality was obtained when Nd was used. FWHM as sharp as 3° are found on the Nd123 films grown on (110) Ag. In the Ag (100) case, the intensity ratio between the two biaxial orientations is changed by a factor of 10 with Nd as to compare to Gd where both orientations showed similar intensities. Those results also showed the good chemical and crystallographical compatibility of pure silver with the superconductor, no buffer layer is required. Ag is therefore a very good alternative for substrate for thin film preparation. It is also one of the most promising substrate for coated conductors if textured tapes of sufficient quality can be produced.

4–63

Preparation of (100) and (110) textured Ag tapes for superconducting biaxially aligned coated tapes.

H. Suo[1,2], *J.-Y. Genoud*[1], *E. Walker*[1], *G. Triscone*[1], *M. Schindl*[1], *E. Koller*[1], *Ø. Fischer*[1] and *R. Flükiger*[1]. [1]DPMC, University of Geneva, 24 quai E.-Ansermet, 1211 Geneva 4, Switzerland. [2]Beijing Polytechnic University, 100022 Beijing, China.

The texturing mechanisms in pure Ag were studied in details. The deformation and recrystallization parameters were optimised in order to obtain the two (100)<001> cube texture and (110) texture that are known to be of high interest for in-plane aligned superconducting coated tapes preparation. A pure cube texture is obtained when a fine grains Ag ingot is pre-heated at 100°C before cold rolling and annealed in a primary vacuum at 700°C for 30 min. The FWHMs of the three X-ray pole figures are with no more than 10° the smallest ever reported for cube textured Ag. Oriented Distribution Function (ODF) was used to carefully control and understand the texture transformations from the deformation texture to the final recrystallization texture. The (110)<uvw> texture was obtained after a high level of standard cold rolling deformation followed by an annealing at 800°C in a primary vacuum. The ODF data showed that if the (110) orientation is of high quality, several <uvw> directions are found along the same Ag tape. In a small length scale, those (110) tapes are suitable for Re-123 (Re=Nd) epitaxial growth: $NdBa_2Cu_3O_{7-\delta}$ sputtering on

those (110) tapes gave a unique biaxial orientation with a FWHM as small as 6° in the X-ray pole figures. This proves that those Ag tapes are suitable for biaxially aligned coated tapes preparation.

4–64

Pulsed laser deposition of oxide layers onto metallic substrates for coated conductor applications.

A.P. Bramley[1], *N.A. Rutter*[1], *G. Gibson*[1], *B.A. Glowacki*[1], *E. Maher*[2], *Z.H. Barber*[1] and *J. E. Evetts*[1]. [1]Department of Materials Science and IRC in Superconductivity, University of Cambridge, Pembroke Street, Cambridge, CB2 3QZ. [2]Oxford Instruments plc, Eynsham, Witney, Oxon, OX8 1TL.

The development of a viable HTS coated conductor technology requires the deposition of biaxially aligned oxide layers onto flexible metallic substrates. Using pulsed laser deposition we have deposited CeO_2/YSZ heterostructures onto biaxially textured Ni and Ni-alloy substrates to act as a buffer layers for the subsequent deposition of $YBa_2Cu_3O_x$ films. The texture in the layers has been characterised using X-ray Diffraction and Electron BackScatter Diffraction. Both techniques show that the buffer layers have excellent biaxial alignment with XRD ω and ϕ scans having FWHM values of 3.5° and 6° respectively, and EBSD misorientation maps showing percolation for a grain boundary misorientation angle of 6°. The growth of the layers has also been studied using Atomic Force Microscopy and Transmission Electron Microscopy. $YBa_2Cu_3O_x$ films have been deposited onto the buffered metallic substrates using pulsed laser deposition. We will describe the influence of various processing parameters on the texture of the heterostructures produced and will discuss some of the issues involved in the deposition of oxide films onto textured Ni-based alloy substrates.
This research was carried out in the frameworks of the Brite Euram programmes CONTEXT (Contract No. BRPR-CT97-0607) and MUST (BRPR-CT97-0331).

4–65

Development of a deposition system for continuous production of YBCO coated conductor.

J. Denul[1], *G. De Winter*[2], *R. De Gryse*[1] and *H. te Lintelo*[3]. [1]Centre for Vacuum and Materials Sciences, Gent, B-9000, Belgium. [2]University of Gent, Gent, B-9000, Belgium. [3]Innovative Sputtering Technology, Zulte, B-9870, Belgium.

A modular vacuum system has been built which can be used for different deposition processes at the same time in order to prepare several metres of YBCO coated conductor in-situ. In the first module annealing under reducing atmosphere is performed in order to texture the Ni-alloy substrate foil. The second module is used for sputter deposition of a YSZ buffer layer. YBCO can be deposited on this buffered foil in the third module. In this system several metres of Ni-alloy foil have been successfully annealed in a continuous mode. Pole figures revealed that this annealing procedure resulted in cube texture with FWHM(phi) less than 9°. A (002) oriented YSZ buffer layer was successfully deposited in line on the annealed foil, resulting in a cube textured layer with FWHM(phi) less than 15°. While annealing the Ni-alloy tape and depositing the buffer layer, the substrate foil was passing through the system at a speed of 2 cm/min. In this process no dramatic oxidation of the substrate was observed. This research was supported by the Brite-EuRam project MUST (Multi-functional flexible high temperature superconducting tape) (contract BRPR-CT97-0331).

Session Josephson Junctions

4–66

Efficient Multi-Josephson Junction Oscillator using a Cavity.

G.Filatrella[1], *N.F. Pedersen*[2] and *K. Wiesenfeld*[3]. [1]INFM Unit Salerno and Science Faculty, University of Sannio,. [2]Department of Electric Power Engineering Building 325, Technical University of Denmark DK-2800 Lyngby, Denmark [3]School of Physics, Georgia Institute of Technology, Atlanta.

A theory is presented for a highly efficient microwave oscillator consisting of a large number of underdamped Josephson junctions in a high-Q cavity. The junctions – with a spread in the parameters – interact with each other only through the cavity. Numerical calculations show the following behavior: As the junctions are switched to the voltage state one at a time, at a threshold number of junctions the system enters a coherent state. At this coherent state all the active junctions oscillate in phase at the resonant frequency of the cavity. This sudden phase transition of nonlinear oscillators is somewhat similar to that found in a gas laser. The conversion efficiency from DC power to Ac (microwave) power is very high, typically $10 - 20\%$. The model explains recent experimental results by Barbara et al. on a multi Josephson junction microwave oscillator very well.

4–67

Induced ferroelectric state and the intrinsic Josephson effect in cuprate superconductors.

S. Shafranjuk. RIEC, Tohoku University, 2-1-1 Katahira, Aoba-ku, Sendai 983.

The Josephson plasma mode (JPM) in cuprate superconductors is strongly affected by the external tunneling injection and/or by the ac field applied. The screening properties of the cuprate superconductors in respect to c axis polarized fields are described by the dielectric function $\epsilon(\omega)$ and are determined by the interlayer electric currents having presumably a tunneling origin. In the model of the c axis tunneling transport, we calculate the dielectric function $\epsilon(\omega)$ and find the shift $\delta\Omega_0$ of the transverse JPM Ω_0 due tothe non-equilibrium deviation of the electron distribution function. For the cases of the tunneling injection and the microwave, we obtain the conditions when the resonance vanishes. It causes the arising of a non-equilibrium instability in respect to the transition into a ferroelectric state characterized by a genuine bias voltage along the c axis of a cuprate superconductor sample that can be observed experimentally.

4–68

Quantum fluctuations of current in superconducting tunnel junctions.

G.I.Urushadze and *Z.Z.Toklikashvili*. Tbilisi State University, Tbilisi, 380028, Georgia.

The question of tunneling of electrons in SIS junctions taking into account the effect of the narrowing of the junction was investigated. It is known that this effect creates en impeding fluctuating potential across the barrier which together with the potential from the external source forms the total current (TC). The general expression for the TC was found and the cases of various temperatures, voltages and other parameters have been considered. For example, in the strong fluctuating case $e/2C \gg kT/e$ (where e is the electron charge, C is the junction capacitance, k is the Boltznann's constant and T is the absolute temperature) an interesting deviation of the conductivity from ordinary long junctionns conductivity law accur at voltages near to $V \sim e/2C$ where TC has logarithmically singularity. This and the other cases show that in strong fluctuation case a "Coloumb gap" appears which is add to the energetic gap of one of the superconducting electrodes. The result obtained apart from independent neaning will be apply for derivation of the Fokker-Planck equation for the Josephson contact.

4–69

Analysis of a hot-spot response of a long Josephson junction in the flux-flow regime.

M. V. Fistul and *A. V. Ustinov*. Erlangen-Nürnberg Universität, Erlangen, D-91058, Germany.

Low temperature scanning microscopy (LTSM) allows to study static and dynamic properties of large Josephson junctions. LTSM techniques use a focused laser or electron beam for local heating of a sample. A hot-spot induced variation of the voltage drop on the sample is recorded versus the hot spot coordinates. We theoretically investigate a LTSM response of a long Josephson junction in the flux-flow regime. The LTSM response appears here due to the presence of a spatially inhomogeneous interaction between Josephson current wave and linear electromagnetic waves propagating in the junction. We show analytically and verify numerically that the shape of the LTSM response crucially depends on the ratio L/ℓ, where L is the Josephson junction length and ℓ is the dissipative decay length for linear electromagnetic waves in the junction. In the limit $L/\ell \gg 1$ the LTSM response displays small oscillations and two pronounced maxima nearby the junction boundaries. In the opposite limit, $L/\ell \ll 1$, the maxima disappear and the linear dependence of LTSM response on the coordinate along the junction is obtained. A good agreement between our theory and earlier LTSM experiments on long Josephson junctions is found.

4–70

The possibility of sound wave amplification in Josephson junctions (JJ).

G.I.Urushadze. Tbilisi State University, Tbilisi, 380028, Georgia.

A longitudinal sound passing through the junction perpendicular to the barrier plane creates a voltage oscillation in the junction. This voltage performs work upon the normal and superconducting electrons tunneling through the barrier. As a result intensive energy exchange between acoustic oscillations and electrons arises in the junction.We will focus our attention on the case when the energy from the JJ transits to the acoustic vibrations and therefore the sound wave of the definite frequency passing through the JJ is amplified.We survey the regime of amplification of the sound when:(i)the JJ is in bias current situation,(ii)the frequercy of the sound is resonant to the JJ oscillation, and (iii) the sound frequency is resonant to the Anderson plasma oscillations in the junction.The regime of amplification in these cases are essentially determined by sound, current and junction parameters and we compare these cases for the best choosing such parameters that make JJ to work under the conditionof maximum amplification of the sound.The high temperature superconducting JJ BSCCO and PBCCO are discuss from the viewpoint of their application as sound wave amplification objects.

4–71

Supercurrent enhancement by coherent tunneling in double-barrier Nb/Al-AlO_x-Al-AlO_x-Nb devices.

I. P. Nevirkovets[1] and *J. B. Ketterson*[2]. [1]Northwestern University, Department of Physics and Astronomy, Evanston, Illinois 60208 Permanent address: Institute for Metal Physics, National Academy of Sciences of the Ukraine, 36 Vernadsky Blvd., UA-252680 Kyïv-142, Ukraine. [2]Northwestern University, Department of Physics and Astronomy, Evanston, Illinois 60208.

Recently, the SINIS junctions have demonstrated their potential for various applications. For some of them, it is important to have maximum IcRN product and non-hysteretic behavior. However, at present, neither theoretical no experimental works can provide a reliable recipe for optimization of the above parameters. We propose that Andreev bound states can be used as a physical mechanism to increase superconducting critical current in the SINIS system. We have carried out the experiments on Nb/Al-AlO_x-Al-AlO_x-Nb double-barrier junctions with "dirty" middle Al layer. At low temperatures, the devices displayed the critical current larger than that possible for a system considered as a simple, series-connection, of the two (Nb/Al-AlO_x-Al and Al-AlO_x-Nb) junctions. Rather, the AlO_x-Al-AlO_x trilayer acts as a single barrier, and it turns out that this fairly thick (of order 10 nm) structure can, under some conditions, maintain almost as large a supercurrent as a single AlO_x barrier in Nb/Al-AlO_x-Nb junctions.

4–72

The influence nonharmonisity of current-phase relation on $I-V$ curve of Josephson junction.

I.N. Askerzade. Institute of Physics, Azerbaijan Academy of Sciences, H. Cavid ave. 33, 370143, Baku, Azerbaijan.

After the discovery of HT superconductivity a varity types of Josephson junctions have been suggested and experimentally tested. From the point of veiew of practical and scientific interest the following junction types are most important: step edge SNS junctions with noble metal interlayer, ramp type structures and grain boundary junctions. Analysis of experimental data shows that current-phase ralation in these junctions has a modified form, which is connected with $d_{x^2-y^2}$ symmetry of order parameter.
The goal of the present contribution is the study influence nonharmonocity of current-phase relation on characteristic JJ. We calculate I-V curve in the framework modified RSJ-model with nonharmonic character current-phase relation and discuss qualitatively the influence of this factor.

The microtheoretical approach of Josephson effect in d-wave superconductor junctions by Tanaka et al and Barash et al. An analytical formula shows that the d.c. Josephson current is very sensitive to the varying grain boundary angle. As shown by Likharev and Kupriyanov, anharmonicity in current -phase relation is equivalent to the introducing of self- inductance of JJ. Using experimental data for the HT SC JJ we can say that the inductance l is equal to 0.2. For this value of the inductance we can choose special form for the supercurrent. Accoding to the experimental data the McCumber parameter of capacity for the JJ is equal $\beta = \frac{2\pi I_c {R_N}^2 C}{\Phi_0} \cong 1$, where C is the capacity of JJ, R_N is the resistivity of JJ. The dynamics of the JJ in this case is described by the equation with quadratic resistance , which can be solved in quadratures in the case nonsmall capacity. Finally using analytical solution we derived next formula for the *IV* curve. We have calculated I (V) curve of JJ for the different values parameter for the case $l = 0$ and $l = 0.2$. It is shown that at $l = 0.2$ the lower switching current is increased. Finally , decreasing of the hysteresis is connected with the inductance of anharmonicity of JJ. Thus, this pecularities of dynamics of HTSC JJ has been taken into account in considering schems on the base such junctions.

4–73

Fabrication and Dynamical Analysis of Etching Process on $SrTiO_3$ Step Substrates for Step-edge YBCO Josephson Junctions.

QianSheng Yang, *GengHua Chen*, *Jin Wang*, *Shiping Zhao* and *FengZhi Xu*.

A way to determine some important etching parameters in step fabrication for high Tc step-edge Josephson junctions is given based on a dynamical analysis of etching process. The optimum thickness of etch mask is defined with negligible recession of mask edge during etching. The equilibrium angle of the steps etched on $SrTiO_3$(STO) substrate with Nb mask has been calculated to be about 76^O. With carefully controlled mask thickness, its sidewall sharpness and the straightness of its edge, some high quality steps on STO substrates with step height from 200nm to 300nm and step angle about 70^O were made. Some Josephson junctions and DC SQUIDs with high reproducibility and less parameter scatter are also practised on the step substrates.

4–74

Transition properties of $YBa_2Cu_3O_7$ step-edge junctions with various step orientations.

S.G. Lee[1], *Y. Hwang*[2] and *J.T. Kim*[3]. [1]Korea University, Jochiwon, Chungnam, 339-800, Republic of Korea. [2]Korea University, Seoul, 136-701, Republic of Korea. [3]Korea Research Institute of Standards and Science, Taejon 305-600, Republic of Korea.

We have fabricated $YBa_2Cu_3O_7$ step-edge junctions with different step orientations and studied their transition properties. Steps with different orientations were prepared on a $SrTiO_3$ (100) substrate by argon ion milling with photoresist mask, and Josephson junctions were made by pulsed laser deposition and ion mill patterning. 12 junctions were made on a single substrate with the step orientation angle ranging from 0^o to 165^o with respect to one of the major axes of substrate at a 15^o interval. We investigated current-voltage characteristics, the critical current, and the transition temperature as a function of the angle. The transition temperature did not show a temperature-dependence. However, the critical current showed a modulation with a maximum near 0^o or 90^o and minimum near 45^o and 135^o. We believe that the critical current variation with the step orientation is at least partially associated with the symmetry of high Tc superconductor.

4–76

Characteristics of step-edge $YBa_2Cu_3O_y$ junctions on various step-angle substrates.

S.Y. Yang[1], *C.H. Chen*[1], *J.T. Jeng*[1], *H.E. Horng*[1] and *H.C. Yang*[2]. [1]Department of Physics, National Taiwan Normal University, Taipei 117, Taiwan. [2]Department of Physics, National Taiwan University, Taipei 106, Taiwan.

The Josephson coupling was investigated by measuring the characteristics of YBCO Josephson junctions on step-edge substrates with various step angles. The step angle used in this work was varied over a range up to 70^o to obtain a series of grain-boundary orientations for YBCO Josephson junctions. It was found that the critical current density J_c of the junction decreased with raising the step angle. And also, the I_cR_n's of the junctions on various step angles were observed to fall onto a single scaling line $I_cR_n \propto (J_c)^p$ with $p \sim 0.5$. This implies that the physical mechanism of the Josephson coupling is similar for all various grain-boundary orientations, but differs in coupling strength. The influences of the step angle on the characterizations, such as the flux-voltage transfer function and the flux noise, of step-edge YBCO SQUIDs are also reported.

4–77

On the Combination of $YBa_2Cu_3O_{7-\delta}$ (YBCO) and Niobium Technology: Material and Electrical Interface Characterization.

H.J.H. Smilde, *D.H.A. Blank*, *G.J. Gerritsma* and *H. Rogalla*. University of Twente, Low Temperature Division, P.O.Box 217, 7500 AE Enschede, The Netherlands.

In a larger context of taking advantage of both materials in high frequency and digital applications, first results are presented about the combination of the $YBa_2Cu_3O_{7-\delta}$ (YBCO) material and niobium. YBCO is an anisotropic high temperature supeconductor, and its charge carriers are assumed to be hole-like. While, on the other hand, niobium is a low temperature superconductor, characterized by its s-type superconductivity and having electron-like charge carriers. The interface between both types of materials is characterized chemically as well as electrically. Although a gap structure is clearly visible, a natural, amorphous but uncontrollable interface layer, which is due to the reactivity of niobium with the oxide from the YBCO, avoids a supercurrent to be observed. Several metallic barrier materials are tried in order to prevent this chemical reaction at the interface, while aiming the electrical contact to be good. Although silver has been chosen often as a chemical barrier, some mechanism at the interface between YBCO and silver prevents a good contact, possibly due to a non-superconducting top-layer. Better results have been obtained using other metallic materials. The first results show a beautiful RSJ-like Josephson character. A few different contact configurations

will be presented, each showing different results.

4–78

Anomalous resistance peaks in highly transmissive ScS contacts with microwave irradiation.

K. Hamasaki[1], *A. Saito*[1] and *Z. Wang*[2]. [1]Department of Electrical Engineering, Nagaoka University of Technology, Nagaoka, Niigata 940-2188, Japan. [2]KARC, Communication Research Laboratory, M.P.T. 588-2, Iwaoka-chou, Nishi-ku, Kobe, 651-2401, Japan.

We report on oscillatory dV/dI peaks in the microwave response of highly transmissive superconductor-constrictions-superconductor (ScS) contacts. The constriction was fabricated by applying a pulse electric field (<2 V/nm) to the insulating Nb/Insulator(3-10 nm)/NbN sandwiches. By this method, we can continuously vary the Andreev reflection probability in the constriction from zero to unity in liquid helium. Most features of the first derivative dV/dI for ScS contacts with long constrictions were well explained by single-Andreev reflection model. Microwave induced steps (Shapiro steps) due to the AC Josephson effect were observed in lower voltage region, but in higher voltage region we observed new microwave induced steps only for highly transmissive contacts. The voltage spacing and height of these new dV/dI peaks increased with increasing bias voltage. The voltage spacing, however, was constant in the frequency range 2-20 GHz. The observed oscillatory peaks up to 2.5 mV differ from the features of well-known microwave-assisted tunneling or LC resonance peak structures. We suggest that the mechanism of these new microwave-induced dV/dI peaks may be related to modulation of Andreev reflection currents by microwave irradiation.

4–80

Effects of He^+ irradiation on electromagnetic properties of $YBa_2Cu_3O_{7-\delta}$ grain boundary Josephson junctions.

M. A. Navacerrada, *M. L. Lucia* and *F. Sanchez-Quesada*. Departamento de Fisica Aplicada III, Facultad de Ciencias Fisicas, Universdidad Complutense, 28040 Madrid, Spain.

We report a study of electromagnetic and transport properties of long and small $YBa_2Cu_3O_{7-\delta}$ Josephson junctions made on bicrystalline substrates and irradiated with He^+ at 80keV. After irradiation no changes have been observed in the shape of the magnetic field dependence of the critical current, $I_c(B)$. A decrease of the critical temperature always occurs as a consequence of degradation of the electrodes by irradiation. However the outstanding result is that more than 60% of the irradiated junctions show an increase of the critical current: for instance, a small junction irradiated at 5×10^{13} cm^{-2} presents an increase of 10% at 15K. In the framework of the filamentary model, we present a comparative analysis on the dose effects in junctions of the same width but with different shape of the $I_c(B)$ curve, so with different distribution of superconductive filaments in the grain boundary. The results suggest that the increase of the critical current can be connected to the effects of irradiation preferentially on the highly disordered resistive refions of the barrier.

This work bas been supported by CICYT grant MAT97-0675

4–81

Zero-crossing Steps in Over-damped Josephson Junctions.

A.Takada[1], *A.Chiba*[1] and *T.Noguchi*[2]. [1]Hakodate National College of Technology,Hakodate,042-8501,Japan. [2]Nobeyama Radio Observatory,Nobeyama,Nagano,384-1305,Japan.

The Shapiro steps crossing the zero-current axis in a current-voltage characteristic, so called zero-crossing steps, for the over-damped Josephson junction irradiated with an rf-signal is numerically simulated based on the resistively shunted junction model. As an rf-signal, either a pulse train signal or a biharmonic signal is adopted. The amplitude of the Shapiro step and zero-crossing step are simultaneously examined as a function of rf-amplitude. For example, under the condition of Ω=0.44, β=0.01 and 25% in duty cycle of the pulse train, the part of 25% in the first order step having the amplitude of approximately I_C crosses the zero-current axis, where Ω, βandI_C are reduced frequency, hysteresis parameter and the maximum Josephson current, respectively. Furthermore, the small duty cycle for fixed Ω seems preferable to avoid the undesirable phenomena due to the attenuation of rf-power in the junction array. It is estimated that the rise-time of the pulse shorter than 50ps is needed to establish the pulse train with 10% in duty cycle under the assumption of I_C R =5μV and Ω=0.44. We consider that the obtained results can be applied to the conventional dc-voltage standards without the crisis of chaos.

4–82

Preparation and characterization of a-axis oriented $NdBa_2Cu_3O_{7-\delta}$ / doped $PrBa_2Cu_3O_{7-\delta}$ / $NdBa_2Cu_3O_{7-\delta}$ trilayers.

M. Sato, *G.A. Alvarez*, *F. Wang*, *T. Utagawa*, *K. Tanabe* and *T. Morishita*. International Superconductivity Technology Center, Koto-Ku, Tokyo, 135-0062, Japan.

a-Axis oriented $NdBa_2Cu_3O_{7-\delta}$ (a-NBCO) / doped $PrBa_2Cu_3O_{7-\delta}$ (doped a-PBCO) / $NdBa_2Cu_3O_{7-\delta}$ (a-NBCO) trilayers were prepared on (100) $SrTiO_3$ substrates. The trilayers were sputtered using a DC-95MHz hybrid plasma. $PrBa_2Cu_{2.8}Co_{0.2}O_{7-\delta}$, $PrBa_2Cu_{2.6}Co_{0.4}O_{7-\delta}$, $PrBa_2Cu_{2.0}Ta_{1.0}O_{7-\delta}$ were employed as a doped a-PBCO. The I-V characteristics of the trilayers dependent on the doped PBCO materials were analyzed. The junction with a 50 nm thick $PrBa_2Cu_{2.8}Co_{0.2}O_{7-\delta}$ barrier showed a resistively shunted junction (RSJ)-like behavior whose critical current value was 0.52 mA and normal resistance was 10 mΩ at 4.2 K. The clear Shapiro steps for 7-20 GHz microwave irradiation and the Fraunhofer pattern for applied magnetic fields up to 1 mT were observed at 4.2 K. The trilayers have good crystallinity, the minimum channeling yield of 3.7 %, and smooth surface, a mean roughness of 2.32 nm over 5 $\mu m \times 5\mu m$ area, as revealed by Rutherford backscattering spectrometry and atomic force microscopy, respectively. This work was supported by New Energy and Industrial Technology Development Organization (NEDO).

4–83

Electrical characteristics of all-NbCN Josephson junctions with TiN films as barriers.

H.Yamamori, *S.Kohjiro*, *H.Sasaki* and *A.Shoji*. Electrotechnical Laboratory, 1-1-4, Umezono, Tsukuba, 305-8568, Japan.

Electrical characteristics of NbCN/TiN/NbCN Josephson junctions have been investigated as functions of TiN-film resistivity ρ and thickness d. First, TiN films were prepared on Si wafers by reactive-magnetron sputtering in mixtures of Ar and N_2 and their resistivities were measured by a four-terminal method. Then, junctions were fabricated using TiN films with different resistivities and thicknesses. A junction fabricated using a TiN film with a relatively low resistivity ($\rho = 90$ $\mu\Omega$ cm) showed a small product of critical current and normal-state resistivity I_cR_n (0.8 μV), while a junction fabricated using a TiN-film with a high resistivity ($\rho = 500$ $\mu\Omega$) a moderately large I_cR_n value (20 μV). We also measured change of I_cR_n for junctions as a function of TiN-film thickness. I_cR_n approached 10 μV when d increased up to 65 nm. The largest I_cR_n (100 μV) was obtained for a junction with the highest J_c (58 kA/cm^2).

4–84

Effects of Post Ion-milling, Pre-annealing, and Post-annealing on the Characteristics of High-T_c Ramp-edge Junctions.

G.Y. Sung[1], *C.H. Choi*[1], *K.Y. Kang*[1], *M.C. Lee*[2] and *S.G. Lee*[3]. [1]Electronics and Telecommunications Research Institute, Taejon, 305-350, Rep. of Korea. [2]Dept. of Physics, Korea University, Seoul, 136-701, Rep. of Korea. [3]Dept. of Physics, Korea University, Jochiwon, Chungnam, 339-800, Rep. of Korea.

We fabricated high-Tc superconducting $YBa_2Cu_3O_{7-\delta}$(YBCO)/$YBa_2Cu_{0.79}Co_{0.21}O_{7-\delta}$(C0-doped YBCO) /YBCO ramp-edge Josephson junctions on (001) $SrTiO_3$ single crystal substrates and studied the effects of post ion- milling and pre-annealing of the ramp-edge prior to the top layer and post annealing process. The ion beam voltage, the ion beam incident angle, and the photoregist mask angle to yield smooth slopes with an angle of about 30°C were optimized. The morphology of the edge was improved by the post ion milling, as were the edge-surface-induced epitaxial growth and the small interface resistance between the top YBCO layer and the Co-doped YBCO barrier. Annealing prior to barrier deposition recovered the ramp-edge surface and increased the T_c of the edge. Annealing helped epitaxial growth of the top YBCO layer on the ramp edge. Post-annealing at a temperature above the deposition temperature and cooling at 500 Torr O_2 induced the epitaxial rearrangement of Co-doped YBCO at a high oxygen vapor pressure. The current-voltage characteristics of the junctions showed RSJ-like behavior.

4–85

Dynamics of Josephson vortices in intrinsic Josephson junctions in $Bi_2Sr_2CaCu_2O_y$ single crystal mesas.

A. Irie[1,2] and *G. Oya*[1,2,3]. [1]Department of Electrical and Electronic Engineering, Utsunomiya University 7-1-2, Yoto, Utsunomiya 321-8585, Japan. [2]Crest (Core Reserch for Evolutional Science and Technology) of Japan Science and Technology Corporation (JST). [3]Department of Energy and Environmental Science, Utsunomiya University 7-1-2, Yoto, Utsunomiya 321-8585, Japan.

Josephson vortex dynamics in stacks of intrinsic Josephson junctions (IJJs) in $Bi_2Sr_2CaCu_2O_y$ single crystal mesas has been investigated experimentally and numerically for the purpose of high-frequency device applications of IJJs. In a magnetic field ($B \leq 0.18$ T) parallel to the copper oxide layers of the junctions, flux-flow branches (FFBs) were observed in addition to multiple resistive branches on the current-voltage characteristics of the mesas with area of $(160,320)\times 40\mu m^2$ and 20-100 IJJs at 4.2 K. Then, vortex flow occurred only in 10-20 % of IJJs in each mesas. From the field dependence of the maximum voltage of FFB the vortex velocities were estimated to be in the range of $(1-4)\times 10^6$m/s, which is close to the highest characteristic velocity for electromagnetic waves in IJJs. Simulations based on the coupled sine-Gordon equations also showed that the vortex motion with the highest velocity mode was stable rather than that with the lowest velocity mode, when not all junctions but some in a stack are concerned in vortex flow, and indicated that the FFBs observed experimentally were caused by synchronous motions of vortices in different junctions in mesas.

4–86

On the phase difference in Josephson equations.

D.-X. Chen[1], *J. J. Moreno*[1], *A. Hernando*[1] and *A. Sanchez*[2]. [1]Instituto Magnetismo Aplicado, RENFE-UCM, P.O.Box 155, 28230 Las Rozas, Madrid, Spain. [2]Grup d'Electromagnetisme, Departament de Fisica, UAB, 08193 Bellaterra, Barcelona, Spain.

Two different expressions for the gauge-invariant phase difference θ_{12} in the Josephson equations, $\theta_{12} = \theta_{12}^{(1)} = \gamma_2 - \gamma_1 - \frac{2e}{\hbar}\int_1^2 \mathbf{A}\cdot d\mathbf{l}$ and $\theta_{12} = \theta_{12}^{(2)} = \gamma_1 - \gamma_2 - \frac{2e}{\hbar}\int_1^2 \mathbf{A}\cdot d\mathbf{l}$, have been used in the literature. We show from analyzing Feynman's treatment on Josephson effects and the current density in continuous superconductors that the correct one is $\theta_{12}^{(2)}$.

4–87

Cross-section TEM characterization on measured microbridges of artificial grain boundary Josephson Junctions.

K. Verbist[1], *G. Van Tendeloo*[1], *F. Tafuri*[2], *F. Miletto Granozio*[2] and *H. Bender*[3]. [1]EMAT, University of Antwerp (RUCA), Antwerp, Belgium. [2] INFM-Dipt. Scienze Fisiche, University of Napels "Fed. II", Napels, Italy. [3]IMEC, Leuven,Belgium.

It is challenging to analyse by cross-section transmission electron microsocpy (XTEM) the barrier region of a junction area with measured transport properties due to the need for

submicron localisation during specimen preparation and the required high yield when dealing with unique samples. We report on a method combining precision mechanical polishing and focussed ion beam (FIB) thinning to obtain,with high yield, XTEM samples with large transparent areas at the barrier. This method allows to elucidate the possible microstructural origin of variations in Josephson junction (JJ) properties. The principle is demonstrated on biepitaxial JJ comprising [100] 45^o tilt and twist AGB in YBCO grown on (110) $SrTiO_3$ with MgO seed layer. The transport properties indicate clear Josephson coupling. The obtained microstructure is compared to results obtained on conventional XTEM samples. Different interface configurations are observed consisting of low index planes of either of the electrodes. Facetting of the interface, as observed in plan view, will also be discussed. K. Verbist is a postdoctoral fellow of the FWO Flanders.

4–88

Fabrication and Properties of Sr_2AlTaO_6/YBCO Interface-treated Junctions.

G.Y. Sung, C.H. Choi, S.K. Han, J.D. Suh and *K.Y. Kang.* Electronics and Telecommunications Research Institute, Taejon, 305-350, Rep. of Korea.

We fabricated ramp-edge Josephson junctions with barriers formed by interface treatments instead of epitaxially grown barrier layers. Low-dielectric Sr_2AlTaO_6(SAT) layer was used as an ion-milling mask as well as an insulating layer for the ramp-edge junctions. An ion-milled $YBa_2Cu_3O_{7-x}$ (YBCO)-edge surface was not exposed to solvent through all fabrication procedure. The barriers were produced by structural modification at the bottom YBCO edge using plasma treatment prior to deposition of the top YBCO electrode. We investigated the effects of pre-annealing and post-annealing on the characteristics of the interface-treated Josephson junctions. The spreads in the critical current (I_c) as well as the junction parameters such as T_c, I_c, R_n were measured and discussed in relation to the interface states.

4–89

Characteristics of ramp-type $YBa_2Cu_3O_{7-\delta}$ / $SrRuO_3$ / $YBa_2Cu_3O_{7-\delta}$ junctions prepared with interfaces grown in situ.

L. M. Wang[1], *H. H. Sung*[1] and *J. H. Chen*[2]. [1]Department of Electronic Engineering, Da-Yeh University, Changhua 515, Taiwan, R. O. C. [2]Department of Physics, National Taiwan University, Taipei 106, Taiwan, R. O. C.

$YBa_2Cu_3O_{7-\delta}$(YBCO) and $SrRuO_3$(SRO) films have been grown to fabricate YBCO/SRO/YBCO ramp-type junctions. Jousephson junctions with SRO barriers have been fabricated ex situ in a ramp-type geometry, and in a sandwich geometry with both interfaces grown in situ using the shadow mask technique. The atomic force microscopy (AFM) images, I-V curves, microwave induced Shapiro steps, and flux noise spectrums have been used to characterize the junctions. The junctions show a resistively shunted-junction-like current voltage characteristics with $I_cR_N \sim 100\ \mu V$ and the vortex noise $S_{\Phi,1kHz}{}^{1/2} \sim 10^{1/2}$-5 $\Phi_o/Hz^{1/2}$ at 77 K. Results indicate the junction properties are improved with junctions grown in situ.

4–90

Fiske Resonance in YBCO/PBCO/YBCO Ramp-type Josephson Junctions.

H. H. Sung[1], *L. M. Wang*[1] and *C. H. Chen*[2]. [1]Department of Electrical Engineering, Da-Yeh University, Changhua, 51542, Taiwan. [2]Department of Physics, National Taiwan University, Taipei, 10660, Taiwan.

We have studied the current-voltage characteristics of ramp-type YBCO/PBCO/YBCO Josephson junctions under the application of magnetic fields. The magnetic-field-induced current singularities due to Fiske resonances were observed. We determined the effective shunting capacitances from the voltages of the resonances. The McCumber constant estimated from the capacitances is in agreement with the current-voltage curves. Finally, the magnetic field dependence of the height of these singularities is analyzed, and the results are discussed in the model of nonuniform junction current density.

4–91

Superconducting structures on tilted $NdGaO_3$ substrates.

P.V. Komissinski[1,2], *G.A. Ovsyannikov*[2], *Z.G. Ivanov*[1], *I.M. Kotelyanskii*[2] and *T. Claeson*[1]. [1]Chalmers University of Technology and Gothenburg University, Gothenburg, S412-96, Sweden. [2]Institute of Radio Engineering and Electronics RAS, Moscow,103907, Russia.

$YBa_2Cu_3O_x$ superconducting thin films with critical temperatures of Tc's >89K were grown on (120) $NdGaO_3$ substrates at 790°C and 0.8mbar oxygen pressure by laser ablation technique. Three layer structures of $Nb/Au/YBa_2Cu_3O_x$ and $YBa_2Cu_3O_x/PrBa_2Cu_{2.6}Ga_{0.4}O_x$ $/YBa_2Cu_3O_x$ were obtained on the basis of these films. X–ray $\Omega - 2\theta$ scan showed, that the c-axis of $YBa_2Cu_3O_x$ thin films were 18.4° tilted from the normal to the substrate, providing a current flow along the direction, which is a superposition of c-axis and a-b-plane crystallographic orientations of $YBa_2Cu_3O_x$ thin films. Contact areas, 8x8μm2, were defined in three layer structures, using a standard photolithography and ion milling methods. Current-voltage characteristics and the dependencies of the differential resistance on the bias voltage were investigated at different magnetic fields and temperatures in terms of presence of a Josephson coupling and zero bias anomaly.
This work has been supported by Russian Foundation of Fundamental research, INTAS program of EU, ESPRIT project HTS-RSFQ-23429, and Swedish Material Consortium on Superconductivity.

Session Passive Devices

4–93

TBCCO based HTS Channel Combiners for Digital Cellular Communications.

A.P. Jenkins[1], *D.M.C. Hyland*[2], *D. Dew-Hughes*[1], *D.J. Edwards*[1] and *C.R.M. Grovenor*[2]. [1]Department of Engineering Science, University of Oxford. [2]Department of Materials, University of Oxford.

Linearity and spectral re-growth are issues that are becoming of increasing importance in cellular base station trans-

mitter subsystems. If HTS technology is to have an impact on this application area then devices operated under realistic signals need to be demonstrated. To this end this paper reports on the testing of disk resonator structures fabricated from TBCCO based 2212 thin films. The Rs of such films has been measured at 5.5GHz using a sapphire dielectric resonator and shown to be less than 0.5 milli-ohms scaled to 10GHz and at 80K. Devices designed for operation in the PCS and DCS1800 cellular bands have been tested using multiple GMSK signals at power levels as high as 5W. Measures such as error vector magnitude and spectral re-growth will be reported that show the effects of non linearity on the performance of such digital modulation schemes. In addition, a two channel combiner will be demonstrated that operates in a cryocooler at 70K as well as the co-existence of 3rd Generation UMTS like signals alongside GSM using HTS filters.

4–94

Thermal breakdown of HTS devices based on S/N transition.

E. Loskot, *M. Sitnikova* and *V. Kondratiev*. St.-Petersburg Electrotechnical University, St.-Petersburg, 197376, Russia.

A special problem of application of microwave high temperature superconducting (HTS) devices based on transition from the superconducting state (S-state) to the state of the normal electrical resistivity (N-state), such as microwave switches, power limiters and phase shifters is thermal spontaneous switching. Theoretical analysis of thermal destruction of the S-state in HTS microwave switching element is presented. Switching element performed as a transmission line section based on HTS film on a dielectric substrate is controlled by dc current. We obtained the closed form equation for the minimum current of the normal phase expanding and equation for the velocity of the S/N boundary movement. The results of modeling thermal processes in such structure allow to select a regime of the film control without spontaneous switching. One can define the nature of switching process (thermal or non-thermal) and predict the behavior of HTS film on the substrate with given parameters. In addition to the theoretical description, the validity of the model was verified experimentally. The work was supported by the Science Council on Physics of Condensed Matter (Project 98063) in Russia.

4–95

HTS switchable diplexer.

V. Kondratiev, *A. Svishchev* and *I. Vendik*. St.-Petersburg Electrotechnical University, St.-Petersburg, 197376, Russia.

Multiplexer is an important component of microwave receivers and transmitters. A high quality multiplexer can be designed using thin film microwave circuits based on high temperature superconducting (HTS) technology. It is known a switched two channel filter bank incorporating HTS filters : the channel switching was provided by PIN diodes. Instead of the semiconductor diodes we propose to use a HTS switch controlled by dc current. The surface resistance of a superconducting film changes drastically under a transport current. This effect was successfully used for a design of S-N microwave switches and digital phase shifters. We present the results of a simulation, design and experimental investigations of a switched HTS diplexer consisting two 5-pole band-pass filters with 0.9% bandwidth centered at 8.4GHz and 9.06GHz. The filters with Chebyshev characteristic are designed as end-coupled half wavelength resonators. The in-band insertion loss is less than 1 dB, the return loss is about 15dB. The isolation between the channels is 21 dB. The S-N switch is designed as a narrow (w = 10 μm) strip 1.5 mm long connected in series with a radial chock. The S-N switch is connected in shunt with the first resonator of the filter in each channel. The switchable diplexer is manufactured on 200 nm thick YBCO film on $LaAlO_3$ substrate of 0.5 mm thickness . The control current is 40 mA. The results of experimental investigation at T = 77 K are in a good agreement with simulated characteristics. The work was supported by the Science Council on Physics of Condensed Matter (Project 98063) in Russia.

4–96

Optical Modulator with Superconducting Resonant Electrodes for Subcarrier Optical Transmission.

K. Yoshida[1], *H. Morita*[1], *H. Kanaya*[1], *Y. Kanda*[2], *T. Uchida*[3], *H. Shimakage*[3] and *Z. Wang*[3]. [1] Graduate School of Information Science and Electrical Engineering, Kyushu University, Fukuoka 812-8581, Japan. [2] Fuculty of Engineering, Fukuoka Institute of Technology, Fukuoka 811-0295, Japan. [3] KARC Communications Research Laboratory, Kobe 651-2401, Japan.

A new design of LiNbO3 optical modulator with superconducting resonant electrodes has been proposed for use in subcarrier optical transmission of microwave signals. By incorporating a superconducting broadband impedance matching circuit , it is shown that gain-bandwidth product of the proposed device can be much larger than the existing devices using a stub for impedance matching. Experiments using high Tc superconducting electrodes to demonste the proposed performance have been made.

4–97

$YBa_2Cu_3O_{7-\delta}$ thin films grown by RF sputtering on buffered $LiNbO_3$ substrates.

L. Fàbrega[1], *R. Rubí*[1], *F. Sandiumenge*[1], *J. Fontcuberta*[1], *C. Collado*[2] and *J.M. O'Callaghan*[2]. [1]Institut de Ciència de Materials de Barcelona (C.S.I.C.), Campus de la U.A.B., 08193 Bellaterra (SPAIN). [2]Dpt. Teoria del Senyal i Comunicacions, Campus Nord UPC, Jordi Girona 1-3, 08034 Barcelona (SPAIN).

The growth of high temperature superconductors (HTS) on technologically interesting substrates has been a challenge since their discovery; it would allow the incorporation of these materials in currently commercial electronic devices, improving their performances without involving drastic changes in the actual industry and users' habits. In this contribution we report on the microstructural and superconducting properties (critical current, RF losses) of $YBa_2Cu_3O_{7-\delta}$ thin films grown by RF magnetron sputtering on $LiNbO_3$ with a YSZ buffer layer. LiNbO3 is an electrooptic crystal widely used in surface acoustic wave devices and electrooptic modulators; the substitution of HTS for conventional Au electrodes in these devices would allow an

improvement of their performances (speed,working power, ...). We show that the use of the YSZ buffer layer allows the obtaining of superconducting $YBa_2Cu_3O_{7-\delta}$ thin films with high critical currents and RF performances suitable for fabrication of electrodes for electrooptical applications.

4–98

Tl-2212-Films for Microwave Devices.

H.Schneidewind[1], *M.Zeisberger*[1], *H.Bruchlos*[1], *M.Manzel*[1] and *T.Kaiser*[2]. [1]Institut für Physikalische Hochtechnologie, Jena, Thuringia, D-07743, Germany. [2]Bergische Universität Gesamthochschule Wuppertal, Wuppertal, Nordrhein-Westfalen, D-42097, Germany.

High-temperature superconductor (HTS) microwave devices in satellite communication systems require working temperatures as high as possible to enhance the efficiency of the applied cooling systems. In order to fulfil the requirements of the satellite payload Tl-HTS-phases with critical temperatures higher than 100 K are very useful. Two inches $Tl_2Ba_2Ca_1Cu_2O_x$ (2212)-films on $LaAlO_3$- and also on CeO_2 buffered sapphire-substrates were prepared using the two-step method. Tl-free precursor films were prepared by reactive off axis sputtering followed by a special annealing process in a Tl_2O-loaded atmosphere. The best Tl-2212-films prepared on $LaAlO_3$ and buffered sapphire show very low surface resistances: R_s(19 GHz, 77K) = 490 $\mu\Omega$ and R_s(5.6 GHz, 77K) = 100 $\mu\Omega$, respectively. We used the double sided Tl-2212-films on $LaAlO_3$ to fabricate narrow-band n-pole filters with a center frequency of 4 GHz. The performance of two-pole filters based on λ -dual-mode ring resonators exhibited low insertion loss at 77 K (< -0.2 dB) and more than -23 dB in return loss over the bandwidth of 17.5 MHz. The influence of the thin film technology on the filter performance will be discussed. Work supported by the German BMBF under Grant No. FKZ: 13 N 7386.

4–99

High temperature superconducting microwave filtrs for space applications.

J.P.Shivhare, *D.Balasubrnayam*, *O.P.Kaushik*, *A.D.Dadve* and *Dr.H.O.Gautam*. Space Applications Centre ,India Space Research Organisation,Govt of India.

As per the experts views the progress in the field of HTS technology is quite right on its way. The future is bright.It is expected that by the end of year 2020 A.D.the HTS technology will be multi- billion dollar technology like semiconductor and fiber optics technology.In our centre we have designed and develoved one HTS broad band filter at 4035 MHz, two narrow band filters at 3885+/- 18 MHZ and 3925+/- MHZand a 3 dB hybrid in frequncy range 3700-4200 MHZ. We hahe already tested the broad band filter at 77 K(-196 deg.C).The achieved results are very close to the predicted results.The narrow band filters are to be tested by the end of April"99. The 3 dB hybrid also to be tested soon.These HTS devices will be used for our own communication payload to be kept on our own Satellite to be launched by our own geosynchronous launch vehicle from our own country(India).By knwing the performance of these HTS devices we want to develop the filters equivalent to the exiting metal cavity filters which bulkier in weight and larger in volume.By using the HTS tech the reduction in weight and volume will be 80-90 percent compare to the metal cavity filters.So for our future communication payloads we may use dozens of filters and dozens of hybrid to increase te number of communication channels. Thus the HTS technology will be very useful technology in next mellinium.

4–100

Spectral-domain Modelling of Superconducting Microstrip Structures.

Z. D. Genchev[1], *A. P. Jenkins*[2] and *D. Dew-Hughes*[2]. [1]Institute of Electronics, Bulg. Ac. Sci.,1784 Sofia,Bulgaria. [2]Department of Engineering Science, Parks Road, Oxford OX1 3PJ, UK.

We present an analysis of thin parallel plate microstrip superconducting structures in which the effects of the superconducting material, of finite complex conductivity and finite thickness, are taken into account through the concept of sheet impedance coupled with spectral-domain immittance approach. The full-wave analysis performed by Pond and co-workers [1;IEEE Trans. Microwave Theory Tech. 37,181 (1989)]for transmission line consisting of two very thin superconducting layers ($h<<\lambda$) double sided on $LaAlO_3$ substrate was generalized to multilayer case. In our layered media we have for the scalar permittivity in the whole space:$\epsilon= \epsilon_1$,x>L/2+D;$\epsilon=\epsilon_2$, L/2,x,L/2+D;$\epsilon=\epsilon_3$,-L/2<x<L/2; $\epsilon=\epsilon$-4,-L/2-d<x<-L/2,$\epsilon= \epsilon$-5,x<-L/2-d).At each boundary x=const. four different resistive boundary conditions have been applied. Analytical formulas for the real and imaginary parts of propagation constant have been derived.

4–101

Large-area and Double-sided PLD YBCO:Ag Thin Films for Microwave Applications.

M.A. Lorenz[1], *H. Hochmuth*[1], *D. Natusch*[1], *K. Kreher*[1], *T. Kaiser*[2], *M. A. Hein*[2], *R. Schwab*[3] and *R. Heidinger*[3]. [1]Universität Leipzig, Fakultät für Physik und Geowissenschaften, D-04103 Leipzig, Germany. [2]Bergische Universität Wuppertal, Fachbereich Physik, D-42097 Wuppertal, Germany. [3]Forschungszentrum Karlsruhe, Institut für Materialforschung I, D-76021 Karlsruhe, Germany.

A large-area pulsed laser deposition (PLD) process for high-quality YBCO thin films on both sides of R-plane sapphire substrates with ceria buffer layer is used routinely to develop planar microwave stripline filters for satellite and mobile communication systems. A relatively simple PLD arrangement with fixed laser plume and rotating substrate, and an offset of the laser plume to the center of the substrate is employed to deposit lateraly homogeneous 3-inch diameter Ag-doped YBCO thin films. The YBCO:Ag films of about 250 nm thickness show homogeneous critical current densities (j_c) of 4 MA/cm^2 at 77 K and laterally homogeneous maps of microwave surface resistance (R_s) of about 40 mΩ at 145 GHz and 77 K measured by an open resonator technique. The R_s at 8.5 GHz and 77 K determined in the center position of the YBCO:Ag films with a sapphire resonator technique remains constant at about 380 $\mu\Omega$ up to a microwave surface magnetic field of about 10 mT. With the experience of more than 600 double-sided 3-inch diameter YBCO thin films a high degree of homogeneity and reproducibility of j_c and R_s is reached. Currently our large-

area PLD technique is extended to the very large substrate diameter of 8-inch which is an important step to a more effective series deposition of 3-inch diameter YBCO films by means of PLD. The PLD-YBCO:Ag films are suitable for the envisaged microwave applications in future communication systems by Robert BOSCH GmbH Stuttgart.
Supported by the German BMBF under Grant No. 13 N 6829, and within BMBF-Leitprojekt "Supraleiter und neuartige Keramiken für die Kommunikationstechnik der Zukunft" of Robert BOSCH GmbH, and by the SMWK Dresden.

4–102
Voltage Tunable $YBa_2Cu_3O_7$ -$BaTiO_3$ - Microwave Ring Resonator Processing and Characterization.
A.I. Lacambra, *J.C. Blanco*, *G. Dimarco*, *D.D. Dixon*, *F.A. Leon*, *M. Rossman*, *Yu.A. Vlasov* and *G.L. Larkins,Jr.*. Florida International University (CEAS 3850) 10555 W. Flagler Street Miami, Florida 33174, USA.

We have integrated a tunable coplanar capacitor with a $YBa_2Cu_3O_7$ ring resonator on $LaAlO_3$ substrate allowing the control of the odd resonant frequency with the application of an external bias. $BaTiO_3$, a well-known ferroelectric material, has been selected as dielectric material. The electrodes are made by creating an interdigitated gap on the $YBa_2Cu_3O_7$ ring. Then dielectric $BaTiO_3$ thin film has been deposited on top of $YBa_2Cu_3O_7$ electrodes on a $LaAlO_3$ substrate. Both the $BaTiO_3$ and the $YBa_2Cu_3O_7$ thin film were grown by pulsed laser deposition technique. The growth conditions for the $YBa_2Cu_3O_7$ thin film were 750°C in 500 mTorr of O_2. The $BaTiO_3$ thin film was deposited at a temperature in the region of 600 - 650°C and 100 mTorr of O_2. $YBa_2Cu_3O_7$ films revealed zero-resistance temperature $T_{(R=0)}$ in the region of 86-88 K with a T_c of ~89 K. We are currently collecting additional experimental data, but so far some voltage driven tunability has been demonstrated. Thin film properties and growth conditions, microwave characterization and measurements will be presented along with detailed results.
This work has been supported by the United States Air Force's Office of Scientific Research under grant number F49620-95-1-0519 and by the Office of Naval Research under grant number N00014-99-190315.

4–103
Characteristics of Electrically Tunable Phase Shifter Using YBCO/Ferroelectric Thin Films.
S. K. Han, *S. J. Lee*, *S. D. Jung* and *K. Y. Kang*. Telecomm. Basic Research Lab., ETRI, Taejon 305-350, South Korea.

We prepared a coplanar-type electrically tunable phase-shifter using a superconductor and a ferroelectric oxide multi-layer structure. $YBa_2Cu_3O_{7-\delta}/(Ba_{1-x}Sr_x)TiO_3$ /MgO thin films were fabricated by pulsed laser deposition method. The phase shifter of the coplanar waveguided transmission line structure with the width of 5 μm and the gap of 5 μm was designed to be operated in the range of 8-12 GHz. A phase shift of above 40° was obtained with an insertion loss of below 10 dB at 10 GHz, V_{dc} = 30 V, and 40 K. We observed the microwave optimized responsivity of the device as functions of DC bias-voltage and temperature. From the results, the devices will be effectively used in the field of monolithic integrated microwave circuits because the phase shifter is able to be modulated under the effect of an externally applied electric field and a light weight.

4–104
Modeling and Fabrication of a Microelectromechanical Switch for H-Tc Superconductive Applications.
I.O. Hilerio[1], *J.R. Reid*[2], *J.S. Derov*[2], *T.M. Babij*[1] and *G. Larkins*[1]. [1]Florida International Univeristy, Miami, FL, 33199, USA. [2]Air Force Research Laboratory / SNHA, Hanscom AFB, MA, 01731, USA.

RF Microelectromechanical (MEM) capacitive switches have been fabricated using surface micromachining technique. This work has led to ongoing development of a micromechanical switch for microwave high Tc superconductive (HTS) application. This work covers the design, modeling, and fabrication of such switches. By combining numerical calculations with finite element analysis different dimensions and topologies were obtained. The switch with overall dimensions of 0.6mm wide by 1.5mm long is triggered by the application of voltage differential between the membrane and the waveguide. When the potential is high enough, the air bridge collapses, coming into contact with the dielectric, resulting in the shunt to ground of the signal. Simulations performed show the switch to possesses low insertion loss (< 1dB @ 20 GHz), and high isolation (> 15dB @ 20 GHz). RF characterization is currently underway and is compared to simulations in order to validate the design process. An intensive surface micromachining design process was implemented. A lanthanum aluminate substrate coated with a thin YBCO layer is used. The YBCO is etched in H−2PO−4, forming the CPW. A dielectric is deposited to avoid metal-to-metal contact between plates. Finally, the gold membrane is then deposited, followed by its wet-etch release process. Currently, all steps have been performed but the material selection is being optimized. This work promises to provide small, cheap, and reliable switches for HTS applications. This work covers the design, modeling, and fabrication of MEMS switches compatible with superconductive applications.

4–105
Fabrication of YBCO films and its application to microwave devices.
S. Ohshima, *M. Mukaida*, *M. Kusunoki*, *T. Tomiyama*, *Y. Takano*, *K. Chiba* and *T. Kinpara*. Yamagata University, Yonezawa, Yamagata, 992-8510, Japan.

We have investigated the formation process of HTS films, (YBCO) for superconducting filters and antennas. The YBCO films were prepared by the plasma-coupled magnetron sputtering and Laser ablation methods. We need YBCO thin films with perfect oriented grains which c axis is normal to the substrate. It was found that the grain orientation could be controlled using the buffer layer. The buffer layers of MgO and sapphire substrates are $BaSnO_x$ and CeO_2, respectively. The T_c and surface resistance of each films were quite good. Superconducting band pass filters are expected to be small insertion loss, sharp skirt property, low pass band ripple and high attenuation at out band. We need many resonators in the filter to realize such prop-

erties, however, the size of filter is restricted, because it is very difficult to fabricated large size HTS films.The elliptic function filter is superior to the Chebyshev function filter to reduce the size. We have examined cross-coupled filter which is an elliptic function filter. It was found that the filter properties of the cross-coupled filter was superior to that of the normal hair pin filter.

4–107

Planar electrooptical phase modulators: An intermediate step towards superconducting Mach-Zehnder integrated modulators.

E. Rozan, *C. Collado*, *J. Prat* and *J.M. O'Callaghan*. Campus Nord UPC, D3 Barcelona 08034 Spain.

Even though the use of high temperature superconductors (HTS) deposited onto Lithium Niobate (LNO) substrates might lead to a substantial improvement in the performance of integrated, travelling-wave Mach-Zehnder modulators, no published reports are easily found on successful attempts to build and test such devices. Part of the problem lies in the fact that, while deposition processes are still under development, there are several difficult requirements that have to be simultaneously met: 1) good quality HTS material over large areas; 2) high power, large bandwidth signal source to test the device; 3) custom-made optical waveguide (OWG) layout in the LNO; 4) tight alignment between the OWG and the HTS electrodes. While these constrains may be achievable with a mature technology, having to comply with all of them while the technology is being developed complicates the fabrication and testing of prototypes, and slows down technology development. To circumvent this, the use of HTS resonant modulators is proposed for both amplitude and phase modulation. Coplanar (CPW) and slot-line topologies are studied, and their fabrication and testing requirements are analyzed. The performance of these devices is analyzed as a function of the quality factor of the resonant electrodes, and the critical current of the HTS material.

4–108

Experimental determination of nonlinear parameters in HTSC transmission line using a multiport harmonic balance algorithm.

J. Mateu[1], *C. Collado*[1], *L.M. Rodriguez*[2] and *J.M. O'Callaghan*[1]. [1]Universitat Politecnica de Catalunya (UPC) Campus Nord UPC-D3 Barcelona 08034, Spain. [2]Centro de Investigacion Cientifica y de Educacion Superior de Ensenada (CICESE) Km 107 Carretera Tijuana-Ensenada Ensenada, B.C. Mexico 22860.

The multiport harmonic balance (MHB) algorithm is a highly efficient numerical method to calculate the intermodulation and harmonic spurious generated by distributed nonlinear effects, which occur along a superconducting transmission line. By specifying the current dependence of the inductance and resistance per unit length of the line (L(I); R(I)), the MHB algorithm is able to find the current distribution in the transmission lines for the fundamental frequency, and all the spurious frequencies. For example, MHB can determine the intermodulation performance of a superconducting coupled-line filter, provided that L(I) and R(I) of its lines are known. This work explores the possibility of using MHB calculations to determine L(I) and R(I) from experimental measurements of single line resonators. Depending of the intrinsic properties of the material and the geometry of the transmission line, there will be two main situations to be considered: one where L(I), R(I) have a quadratic dependence with I (and sometimes one of them is considered to behave linearly); and a second situation where higher order terms can not be neglected in L(I), R(I). It will be shown that the experimental procedures to be used to determine L(I), R(I) depend on which of these two situations describes the superconducting lines being considered.

4–109

Computer simulation of the non-linear response of superconducting devices using the Multiport Harmonic Balance algorithm.

C. Collado, *J. Mateu* and *J.M. O'Callaghan*. Universitat Politecnica de Catalunya (UPC) Campus Nord UPC-D3 Barcelona 08034 Spain.

This work describes the application of the multiport harmonic balance (MHB) algorithm to the calculation of the non-linear response of superconducting devices and circuits. The algorithm does not restrict the order of the nonlinearities and is very well suited for calculating harmonic spurious and intermodulation products in superconducting filters and resonators. These calculations are difficult to perform in time domain since they simultaneously require high frequency resolution (for the excitation signals and the in-band intermodulation products) over a broad frequency band (to cover one or several harmonics of the excitation signals), and this requires simulating a long time interval with a small time step, resulting in a high computational burden. The MHB algorithm (an evolution of the harmonic balance used to analyze circuits with lumped elements) overcomes this by analyzing the linear parts of a circuit in frequency domain, and the non-linear ones in time domain. An extension of the classical HB was necessary to take into account the distributed nature of the nonlinearities in superconducting lines and resonators. Both one-dimensional and two-dimensional extensions have been developed to simulate superconducting transmission lines (1D) and planar patches or quasi-lumped structures (2D). Excellent agreement has been found with theoretical predictions performed on simple resonators.

4–110

Modelling the Nonlinear Microwave Surface Impedance of a Superconducting Weak Link.

A. V. Velichko[1,2] and *A. Porch*[1]. [1]School of Electronic and Electrical Engineering, University of Birmingham, Birmingham B15 2TT, UK. [2]Institute of Radiophysics and Electronics, NAS of Ukraine, Kharkov 310085, Ukraine.

A phenomenological model is presented which describes the effect of both dc and rf magnetic fields, H, on the microwave surface impedance, $Z_s = R_s + jX_s$, of a superconducting weak link modelled as a Josephson Tunnel Junction. The nonlinear response of the junction is considered for two geometries; a weak link between two grains, shunted by another third grain, and a non-shunted weak link. In both cases, R_s and X_s were found to be non-monotonic functions of H. Under certain conditions, the values of Z_S in the applied field can fall below the corresponding zero-field values. The model findings are discussed in the light of the unusual

features in $Z_s(H)$ of high-quality HTS thin films, recently observed by several research groups.

4–111

Weakly Coupled Grain Model for High Tc Superconducting Thin Films Taking Account of Anisotropic Complex Conductivities.

K. Yoshida[1], *H. Takeyoshi*[1], *H. Morita*[1], *H. Kanaya*[1], *T. Uchida*[2], *H. Shimakage*[2] and *Z. Wang*[2]. [1] Graduate School of Information Science and Electrical Engineering, Kyushu University, Fukuoka 812-8581, Japan. [2]KARK Communications Research Laboratory, Kobe, 651-2401, Japan.

Weakly coupled grain model for high Tc superconducting thin films has been extended to the general case of finite film thickness. Analitical expressions for the transmission line parameters for high Tc superconducting thin films have been obtained, which take account of the effects of anisotropic complex conductivities resulted from weaklinks. We generally discussed the effects of anisotropy in terms of three basic parameters, i.e., grain size, strength of coupling and film thickness. Comparisons between theory and experiment are also discussed.

ORAL SESSION 5A: Coated Conductors I

Tuesday Afternoon, September 14th, 17:30-19:00

17:30 *5A–1

Low-cost YBCO coated conductor technology.

A.P. Malozemoff[1], *S. Annavarapu*[1], *L. Fritzemeier*[1], *Q. Li*[1], *V. Prunier*[1], *M. Rupich*[1], *C. Thieme*[1], *W. Zhang*[1], *A. Goyal*[2], *M. Paranthaman*[2] and *D.F. Lee*[1] [1]American Superconductor Corporation 2 Technology Dr., Westborough MA 01581 USA. [2]Oak Ridge National Laboratory, Oak Ridge TN 37831 USA.

To insure a cost-effective YBCO coated conductor technology superior to the well-developed BSCCO-OPIT HTS wire technology, it will be important to avoid costly high vacuum deposition techniques. To this end, American Superconductor has explored the trifluoroacetate solution-based precursor technique originally developed by the group of Cima et al. at MIT. Films with performance levels greater than 1 MA/cm^2 have been achieved on oxide single crystal substrates, including film thicknesses over 1 micron. Additional challenges with this technique applied to textured metal substrates are being addressed. It is also desirable from a cost perspective to prepare buffer layers with the solution-based precursor technique. Encouraging results have been obtained on single crystal substrates, but further work is required to extend these results to textured metal substrates.

18:00 5A–2

In-plane Aligned YBCO Thick Films on Ag and $LaAlO_3$ Substrates by Ultrasonic Mist Pyrolysis.

J.J. Wells[1], *A.L. Crossley*[1], *M.J. Vallet-Regi*[2] and *J.L. MacManus-Driscoll*[1]. [1]Department of Materials, Imperial College of Science Technology and Medicine, Prince Consort Road, London SW7 2BP, England. [2]Dep. De Quimica Inorganica, Facultad de Farmacia, Universidad Complutense, 28040 Madrid, Spain.

An ultrasonic mist pyrolysis system has been used to deposit thick films of $YBa_2Cu_3O_{7-x}$ on (100) $LaAlO_3$ and (110) Ag single crystal, and {110}⟩110⟨ polycrystalline Ag substrates. Nitrate precursors with an Y:Ba:Cu ratio of 1:2:0.6 have been used with a deposition temperature of 900°C. Growth rates as high as 1mm per minute have resulted in epitaxial growth of biaxially aligned 5mm thick $YBa_2Cu_3O_{7-x}$ films. The film microstructure is very dense and grain connectivity is good. The degree of structural disorder within the YBCO films has been studied as a function of nitrate concentration, growth rate, and post-annealing. The superconducting properties of the films have been measured and will be reported.

18:15 5A–3

Sol-gel technique applied to buffer deposition on textured flexible substrates for YBCO coated conductor.

S.Lesca[1], *P.Caracino*[2], *P.Scardi*[3] and *R.Scotti*[4]. [1]INFM, UdR di Milano, Università Statale - Dipartimento di Scienza dei Materiali, Via Cozzi, 53, 20126 Milan, Italy. [2]PIRELLI CAVI & SISTEMI SpA, viale Sarca 222, 20126, Milan, Italy. [3]Università di Trento, Dipartimento di Ingegneria dei Materiali, 38050 Mesiano TN Italy. [4]Universita' Statale di Milano -Dipartimento di Scienza dei Material, Via Cozzi, 53, 20126 Milan, Italy.

The present study is focused on the deposition via sol-gel technique of CeO_2 buffer layers on Ni textured substrates for the realisation of YBCO coated conductors. Among high-T_c superconductors, YBCO is one of the most promising materials for the preparation of high J_c thick films for power transmission applications, whereas CeO_2 is an excellent buffer layer. Due to its chemical compatibility and low thermal expansion, ceria is suitable to make interconnections between metal and superconducting phase. Between the deposition techniques, the sol-gel process is a viable route to deposit oxide layers on long-length tapes by applying a solution of precursors to the substrate by spinning or dipping methods. Among the advantages of the sol-gel technique it should also be considered the low deposition temperature and the high homogeneity achievable. CeO_2 buffers were deposited starting from different precursors, such as nitrate-based salts and colloidal cerium oxide. To optimise the deposition process, the viscosity of the solution was measured. Buffer deposition was carried out on textured Ni substrates, both as obtained after recrystallisation and after a thin epitaxial NiO layer was grown by thermal oxidation. Surface morphology and texture of the buffer layers were characterised by means of SEM and X-ray diffraction, respectively.

18:30 5A–4

Superconducting Thick Films of $YBa_2Cu_3O_{7-\delta}$ with Y_2O_3 Additions on Ag Substrates.

W. Hässler[1], *P. Schätzle*[1], *L. Schultz*[1], *T.C. Shields*[2], *T.W. Button*[2] and *J.S. Abell*[2]. [1]Institut of Solid State and Materials Research Dresden, PF 270016, D-01171 Dresden, Germany. [2]School of Metallurgy and Materials, The University of Birmingham, Edgbaston Birmingham, B152TT, UK.

Thick film technology is an attractive commercial alternative to vacuum based PVD techniques such as IBAD and RABiTS, providing bi-axially textured layers can be produced. Thick films of $YBa_2Cu_3O_{7-\delta}$ (YBCO) have been prepared on Ag substrates by screen printing and a modified melt processing method. This involves heating the films in low $p(O_2)$ and switching to higher $p(O_2)$ at peak temperature to initiate the crystallisation mechanism of YBCO. Two different processes have been investigated: i) films prepared from stoichiometric YBCO and ii) with an addition of Y_2O_3 oxide. An addition of Y_2O_3 oxide reduces the peak temperature and enhances the liquid phase based on a modified phase diagram. Thermodynamic considerations on the modified phase diagram regarding the processing parameters $p(O_2)$ and peak temperature have been undertaken. The influence

of these parameters, together with dwell time and cooling, on the microstructure and superconducting properties of the films has been studied. An addition of Y_2O_3 results in films consisting of larger grains with a prefered c-axis texture. The influence of textured Ag substrates on the microstructure of the films will also be discussed.

18:45 5A–5
Development of Cube Textured Nickel-Alloys as Substrate for Superconducting Tapes.
N. Reger, *B. de Boer*, *B. Holzapfel*, *J. Eickemeyer*, *R. Opitz* and *L. Schultz*. Institute of Solid State and Materials Research Dresden, Institute of Metallic Materials PO-Box 270016, D-01171 Dresden, Germany.

Rolling Assisted Biaxially Textured Substrates (RABiTS) is a promising route for the deposition of buffered high temperature superconducting films on long tapes for application in magnetic fields at 77K. Ni is well suited as a substrate material due to the formation of a sharp cube texture and its resistance to oxidation. However, disadvantages are its ferromagnetism that leads to magnetization losses and its low tensile strength. In this work several binary and ternary Ni-alloys were examined according to their suitability for RABiTS-processing. First criterion for the choice of alloying elements was lowering the Curie temperature below 77K while keeping the cube texture. Texture was controlled by EBSP-mappings and orientation distribution functions calculated from x-ray data. As a result, the three alloying elements Cr, Cu, and V remained. Tensile strengths were estimated by hardness measurements. The potential of solution hardening and precipitation hardening is discussed. Finally, the surface oxidation behaviour of these alloyed tapes was examined by XPS and AES and their mechanical and thermal processing were optimized to improve the cube texture.
This work is supported by the Federal Ministry of Education, Science, Research and Technology, Germany (BMBF, 13N7265)

ORAL SESSION 5B: Flux Pinning I

Tuesday Afternoon, September 14th, 17:30-19:00

17:30 *5B–1
New Method to Induce Periodic Pinning in 3D Vortex Structures: High and Low Temperature Superconductors
F. de la Cruz. Centro atómico de Bariloche, 8400 S.C. de Bariloche, Rio Negro, Argentina

We have developed a new technique to generate periodic vortex pinning in extended regions of superconducting samples. The technique is based in the Bitter decoration method, used to visualize vortex structures. Nanoparticles of Fe are deposited on the inhomogenous magnetic field induced by the vortex structure at the surface of the sample. The idea is to use the iron dots that mimic the vortex structure as pinning centers for subsequent decorations. The resulting pinning structure is shown to be an effective weak two dimensional periodic system. In this way we have been able to investigate elastic static and dynamic vortex structures, in low and high temperature superconductors, in the presence of periodic pinning.

18:00 5B–2
Flux pinning in thick $YBa_2Cu_3O_7$ films by the BaF_2 process.
L.-J. Wu, *V. F. Solovyov*, *H. J. Wiesmann* and *M. Suenaga*. Brookhaven National Laboratory, Upton, New York, 11793 USA.

The nature of flux pinning was investigated for thick (3 - 5 $\propto m$) films of $YBa_2Cu_3O_7$ on $SrTiO_3$ by the BaF_2 process. Critical currents were measured as a function of applied dc magnetic fields and of the angle between the film plane normal and the c-axis. A small but sharp peak in critical current was observed when the applied field is parallel to the c-axis. This suggested the twin boundaries in these films acting as the main pinning sites. However, transmission electron microscopy, TEM, studies of the films revealed that the boundary spacing (30 nm) for these films were essentially unchanged for all of these filsm. TEM also revealed the presence of highly dense Y_2O_3 precipitates. The sizes of the precipitates varied by a factor of five, $\sim$ 20 to $\sim$ 100 nm. Furthermore, in 5 $\propto m$ thick films, the films consisted of very fine grains (500 nm) where the grain boundaries were primarily low angle boundaries. Possible interactions of these pinning sites in attainment of high critical current densities ($\sim$ 2 x 10^9 A/m^2 at 1 T applied field which is parallel to the c-axis.) in these films will be discussed.
This work was performed under the auspices of the U. S. Department of Energy, Division of Materials Sciences, under Contract # DE-AC02-98CH10886.

18:15 5B–3
Irreversibility line in $HgBa_2CuO_{4+\delta}$ single crystal.
D. Stamopoulos[1], *M. Pissas*[1], *D. Niarchos*[1] and *M. Charalambous*[2]. [1]Institute of Materials Science National Center for Scientific Research "Demokritos" 153-10, Aghia Paraskevi, Athens GREECE. [2]Centre de Recherches sur les Tres Basses Temperatures, CNRS, BP166X,38042 Grenoble FRANCE.

Among the high temperature cuprate superconductors the $HgBa_2CuO_{4+\delta}$ (Hg-1201) compound is a very promising candidate for microwave applications due to its high T_c. It is well known that the irreversibility line (IL) is affected by three different mechanisms: bulk pinning, surface and geometrical barriers. We will present the effect of surface barriers on the location of IL for the Hg-1201 compound. A comparison between the activation energies U_B, U_S of the two competitive mechanisms of bulk and surface pinning is presented via relaxation measurements at low fields and high temperatures.

18:30 5B–4

Geometry, vortex pinning, and surface-barrier effects in platelet and "prism" shaped BSCCO single crystals.

T.B. Doyle[1], *R. Labusch*[2] and *R.A. Doyle*[3]. [1]School of Pure and Applied Physics, University of Natal, Durban, 4001, South Africa. [2]Institut fuer Angewandte Physik, Technischen Universitat Clausthal, Clausthal-Zellerfeld 3992, Germany. [3]c/0 Interdisciplinary Research Centre in Superconductivity, University of Cambridge, Cambridge CB3 OHE, UK.

The results of numerical calculations for the isothermal, spatial field profiles and global magnetisation $M(H_a)$ behaviour, in transverse applied field H_a, of high-T_c superconducting single crystal BSCCO specimens, for both disc (platelet) and cone ("prism") specimen geometry, are presented and contrasted. The treatment is based on a rigorous theoretical analysis which includes proposed, explicit, equilibrium constitutive B(H*loc*) behaviours for the solid and liquid vortex phases, their respective explicit $J_c(B)$ dependence's, and a model for the surface-barrier. This allows, inter alia, for the effects of vortex pinning, vortex melting and the arrowhead phenomenon to be included in the treatment. The predicted $M(H_a)$ behaviour is compared with isothermal experimental M-H_a data for both specimen geometries and the relative contributions of specimen geometry, surface-barrier and pinning effects are established within the validity of the surface-barrier and pinning models used in each case.

18:45 5B–5

Interlayer metallization and plastic deformation: two ways to improve flux pinning in Hg-based superconductors?.

L. Fàbrega[1], *A. Sin*[1], *A. Calleja*[1], *S. Piñol*[1], *J. Fontcuberta*[1], *D. Eyidi*[2] and *J. Rabier*[2]. [1]Institut de Ciència de Materials de Barcelona (C.S.I.C.), Campus de la U.A.B., 08193 Bellaterra (SPAIN). [2]Laboratoire de Métallurgie Physique, UMR 6630 CNRS, Université de Poitiers, SP2MI, BP 179, 86960 Futuroscope Cedex (FRANCE).

There have been recently intense efforts pursuing the enhancement of flux pinning in Hg-based high temperature superconductors (HTS). In spite of their high critical temperature (134K for $HgBa_2Ca_2Cu_3O_8$), these materials display very low critical currents and irreversibility lines, which prevent their development for applications at liquid nitrogen temperatures. The weak flux pinning in Hg-based HTS has been ascribed to two reasons: the high anisotropy of these materials, and the low effectivity of their defects as pinning centers. Therefore, two approaches have been undertaken in order to rise Jc: i) reducing the superconductor anisotropy, via the metallization of the interlayers, which is pursued by partially substituting Hg by other cations (Tl, Bi, Cr, In, Re, ...); and ii) introducing new defects which might be able to pin flux more effectively, by irradiation or plastic deformation. In this contribution we report our recent work in both these approaches. We focuss on the Re-substituted samples. Based on magnetization and μSR experiments, we discuss the role of Re, oxygen and alkalin-earth cations on the rise of magnetic irreversibility and anisotropy change, which are not as clear as earlier claimed. Finally, plastic deformation experiments on bulk Hg-1223 reveal the sensibility of these materials to mechanical stress, and point to an enhancement of bulk pinning, caused by the deformation-induced high density of dislocations.

ORAL SESSION 5C: SQUIDS and SQUIDS Applications

Tuesday Afternoon, September 14th, 17:30-19:00

17:30 *5C–1

High-T_c SQUIDs: Gradiometers and Microscopes.

J. Clarke. Department of Physics, University of California, Berkeley, CA 94720-7300 and Materials Sciences Division, Lawrence Berkeley National Laboratory, Berkeley, CA 94720.

A high-transition-temperature, first-order gradiometer is described in which a planar asymmetric flux transformer on one substrate is bonded to a SQUID magnetometer on a second substrate; the baseline is 48 mm. The signals from two such gradiometers are subtracted to form a second-derivative gradiometer; in addition, the signals from three orthogonal magnetometers are subtracted to reduce the response to uniform magnetic fields. The overall balance of the system is 20 ppm, and is sufficient to obtain magnetocardiograms in an unshielded environment. In the microscope, a SQUID, cooled to 77 K, is mounted just below a silicon nitride window; the separation of the SQUID from samples at room temperature and pressure is as low as 15 micrometers. The microscope is used to study the dynamics of magnetotactic bacteria, which contain a chain of magnetite particles. This technique can be extended to the magnetic tagging of other biological samples This work was performed in collaboration with M. Adamkiewicz, J. Borgmann, B.B. Buchanan, Y.R. Chemla, H.L. Grossman, R.H. Koch, K.A. Kouznetsov and R. McDermott and supported by the U.S. Department of Energy under contract number DE-AC03-76SF00098.

18:00 5C–2

HTS SQUID current comparator for ion beam measurements.

L. Hao[1], *J.C. Gallop*[1], *J.C. Macfarlane*[2] and *C. Carr*[2]. [1]Centre for Basic and Thermal Metrology, National Physical Laboratory, Teddington, TW11 0LW, UK. [2]Dept. of Physics and Applied Physics, Strathclyde University, Glasgow G4 0NG, UK.

Direct current comparators are unique superconductivity-based devices which allow extremely accurate direct current ratios to be established. Up to the present they have been used only with low temperature superconductors and SQUIDs. We have begun investigations into HTS current comparator designs, with a readout SQUID also made from HTS. The longer term aim of this work is to produce a system capable of high accuracy non-invasive measurement of an ion beam current (in the range 1uA to 1mA). Here we report preliminary measurements on the current ratio accuracy achievable with a simple HTS current comparator and our experimental results are compared with theory.

18:15 5C–3

An HTS SQUID Magnetometer Using Coplanar Resonator with Vector Reference for Operation in Unshielded Environment.

Y. Zhang[1], *G. Panaitov*[1], *N. Wolters*[1], *L.H. Zhang*[2], *R. Otto*[1], *J. Schubert*[1], *W. Zander*[1], *M. Bick*[1], *H.-J. Krause*[1] and *H. Bousack*[1]. [1]Institut für Schicht- und Ionentechnik (ISI), Forschungszentrum Juelich (FZJ), D 52425 Juelich, Germany. [2]Institute of Physics Chinese Academy of Sciences, Beijing 100080, China.

Using a HTS rf SQUIDs vector reference, we built an HTS SQUID-magnetometer for operation in unshielded environment. The reference consists of three magnetometer SQUIDs oriented in x, y and z directions. The sensing SQUID magnetometer is z-oriented and positioned at (baseline) distance of 7.5 cm from the z-reference. The balance (common mode rejection) was electronically adjusted by the subtraction of the reference SQUIDs output signals. The two z-oriented SQUIDs are coupled to coplanar resonators via 8x8 mm2 flux-focusing washers. For the x- and y-oriented SQUIDs with 3.5 mm diameter washer, we have used the conventional tank circuits. The dynamic range of each SQUID-magnetometer is more than 600 nT. The magnetic field resolution of the system in unshielded environment was found to be 120 fT/sqrt(Hz) at frequencies above 10 Hz. To demonstrate the performance of the system, magnetocardiographic (MCG) measurements were successfully performed. The system can be used also for non-destructive evaluation, for example the detection of very small-size ferrous particles in a nonmagnetic matrix.

18:30 5C–4

A Second Order Electronic Gradiometer for Nondestructive Evaluation.

C. Carr, *E.J. Romans*, *A.J. Millar*, *A. Eulenburg*, *C.M. Pegrum* and *G.B. Donaldson*. Physics and Applied Physics, University of Strathclyde 107 Rottenrow Glasgow G4 0NG United Kingdom.

For operation in an unshielded environment, first order HTS single layer gradiometers can significantly reduce the effect of unwanted magnetic fields. Here, we incorporate two such devices fabricated from YBCO thin films on 10mmx10mm STO bicrystal substrates to form a second order electronic gradiometer using room-temperature differencing. We report on the spatial response of the system, comparing it with modelled results and discuss the noise performance in both shielded and unshielded environments. finally, we present eddy current NDE results with aluminium and steel samples.

18:45 5C–5

HTS RF SQUID Gradiometer With Long Baseline For the Inspection of Aircraft Wheels.

M. Maus, *H.-J. Krause*, *Y. Zhang*, *H. Bousack*, *M. Vaupel*, *R. Kutzner* and *R. Wördenweber*. Institute of Thin Film and Ion Technology, Research Centre Juelich, 52425 Juelich, Germany.

A drawback of our automated aircraft wheel inspection system using a HTS SQUID sensor is the small baseline of our planar double hole rf gradiometers. The cracks to be

detected are typically located 10mm beneath the wheel surface. A detailed calculation of the optimum value for the baseline, with optimization of the signal-to-noise ratio and environment parameters, is presented. The enlargement of the baseline to the optimum value of 10-15mm leads to a higher white flux-noise because of the raised SQUID inductance. This causes a suppression of the amplitude of the SQUID signal, so that the SQUID cannot be operated in flux-locked-loop-mode any more. Two technological approaches to achieve the required baseline are presented: The parasitic slit inductance is reduced either by covering the slit with a superconducting ground plane or by reduction of the slit width using the direct electron beam writing lithography. For a gradiometer with 5mm baseline prepared using the former technique, a reduction of the white flux noise from $144\mu\phi_o\sqrt{Hz}$ to $73\mu\phi_o\sqrt{Hz}$ was observed when covering the slit. The corresponding increase of the gradient-to-flux coefficient from $15nT/(\phi_o$ cm) to $33nT/(\phi_o$ cm) confirms the reduction of the effective pickup area. Work is in progress to further increase the baseline.

This work was supported by German BMBF under Grant No. 13N6682.

ORAL SESSION 5D: Mixers and Detectors

Tuesday Afternoon, September 14th, 17:30-19:00

17:30 *5D–1

The role of the geometry in superconducting tunnel junctions detectors.

R. Cristiano. Istituto di Cibernetica del CNR Arco Felice, Napoli, I-80072 Italy.

Recently, experimental results on superconducting tunnel junctions as high energy resolution radiation detectors demonstrated performances close to intrinsic limits. On one side this opens new perspectives for applications, on the other side makes urgent to solve problems related to the efficiency and simplification of the working conditions. The role of the junction geometry enters various issues in the solution of such problems. An example is the need of optimal junction geometry to obtain the suppression of Josephson critical current at lowest magnetic field and this requirement becomes relevant when arrays of junctions are used to improve the collecting efficiency. In this work, various aspects related to the superconducting tunnel junction detector configuration will be discussed, reporting on an overview of recent experiments made on Nb-based junctions with various geometry. In particular, results referring to the annular geometry, which have an interest beyond the particular application, will be presented and discussed.

18:00 5D–2

Superconducting YBCO nanobridges for submillimeter-wave detectors.

A. Gaugue[1], *C. Ulysse*[1], *A. Sentz*[2], *C. Gunther*[3], *D. Robbes*[3], *J. Gierak*[4], *C. Vieu*[4], *G. Beaudin*[5], *M. Fourrier*[2] and *A. Kreisler*[1]. [1]LGEP - UMR8507 CNRS, Universités Paris 6 & Paris 11; Supélec plateau de moulon; GIF sur YVETTE 91192 France. [2]LDIM, EA 253 MENRT, Tour 12, Université Paris 6; 4 place de jussieu; PARIS 75252 France. [3]GREYC, URA 1526 CNRS, ISMRa et Université de Caen; 6 Bd du Marechal Juin; CAEN 14050 France. [4]L2M, UPR 20 CNRS; 196 Av. Henri Ravera; BAGNEUX 92225 France. [5]DEMIRM Observatoire de Paris; 61 Av de l'Observatoire; Paris 75014 Paris.

New heterodyne detectors, using high temperature superconducting materials, are presently emerging for many applications at submillimeter wavelengths. Due to their low local oscillator power requirements and reasonably high operating temperature (liquid N2), they provide good performance vs. implementation compromise, offering an attractive choice as compared with Schottky or SIS junction mixers. These hot electron bolometers (HEB) use the possibility that electrons - under the effect of incident photons - can reach thermal equilibrium at a temperature different from the crystal lattice. To be effective, this phenomenon however requires very small superconducting microbridges, so interest in HTS HEBs has prompted the development of YBaCuO microstructures of nanometer scale. In this paper, we describe a processing method to obtain YBCO nanobridges that includes two main steps. Using standard photolithography, micrometer-size bridges are predefined first; the length and width of the bridge are then reduced by focused ion beam milling. As a preliminary result, bridges of 300 nm

width and 1 μm length have been obtained. Besides, the nanobridge is embedded in a log-periodic antenna structure which size is adapted to the submillimeter-wave range. Detection experiments performed with the 119 μm radiation from a water vapour discharge laser will be given.

18:15 5D–3

Methods of submillimeter wave Josephson spectroscopy.

M. Tarasov[1,3], *E. Stepantsov*[1,2], *A. Shul'man*[3], *E. Kosarev*[4], *O. Polyansky*[3], *D. Golubev*[1,5], *M. Darula*[6], *O. Harnack*[6], *A. Vystavkin*[3] and *Z.G. Ivanov*[1]. [1]Chalmers University of Technology and University of Gothenburg, S-41296, Sweden. [2]Institute of Crystallography of the RAS, Moscow, RU-117333, Russia. [3]Institute of Radio Engineering and Electronics of the RAS, Moscow, RU-103907, Russia. [4]P.L.Kapitza Institute for Physical Problems of the RAS, Mo cow, RU-117973, Russi. [5]P.N.Lebedev Physical Institute of the RAS, Moscow, RU-117810, Russia. [6]Institut fur Schicht und Ionentechnik, Research Center Juelich GmbH, Juelich, D-52425Germany.

A HTS Josephson spectrometer has been designed, fabricated and experimentally studied. The spectrometer circuit consists of a YBCO bicrystal Josephson junction integrated with a double-slot or log-periodic antenna, connected in parallel with a gold low-inductance shunt. The YBCO films were deposited by laser ablation on sapphire and MgO bicrystal substrates with misorientation angle of 24 degrees. The selective detector response and RF response at intermediate frequency IF=1.4 GHz were measured in the signal frequency range 60-1250 GHz and the linewidth of Josephson oscillations (LJO) was determined by using three different methods. (1) The Hilbert spectroscopy approach was used in processing the selective detector response. (2) In the case IF<LJO the detector and RF responses have a similar shape that allows to extract the spectrum and LJO from the RF response and even process by Hilbert spectroscopy approach. (3) The RF response at IF>LJO corresponds to the frequency down-conversion in a self-pumped Josephson mixer mode. For processing of RF response in this case we suggest a novel method that allows extracting the signal spectrum by means of simple operations: shifting, summing and subtracting. The advantages of RF response method are in its simplicity, higher sensitivity, better frequency resolution due to low-inductive shunting.

18:30 5D–4

Single photon imaging spectrometers using superconducting tunnel junctions.

L. Frunzio, *K. Segall*, *C. Wilson*, *L. Li*, *M. C. Gaidis* and *D. E. Prober*. Department of Applied Physics, Yale University, New Haven, CT 06520-8284, USA.

We are developing superconducting, single photon, imaging detectors for x-ray, visible and UV photons. The detectors use a Tantalum absorber and Aluminum-Aluminum Oxide-Aluminum tunnel junctions for readout. Photons absorbed in the Tantalum create excess quasiparticles which are trapped in the Aluminum tunnel junctions and cause an increase in their subgap current. The integrated charge is proportional to the photon energy. Two tunnel junctions are connected laterally to a single absorber and the resulting charge division allows one dimensional imaging. We have measured an energy resolution of $26eVFWHMfor6keV$ x-rays over an $18\mu m \times 100\mu m$ absorber area and a simultaneous position resolution of $0.5\mu m$ over the same range. The energy resolution is within a factor four of the theoretical limit and is limited by fluctuations in the electronic readout. We have also fabricated smaller junction devices designed to detect optical photons which display very good junction quality ($R_{dyn}/R_{nn} > 10^5$). The noise characteristics of these junctions appears good enough to see visible photons, although at the time of this writing we have not yet tested their photon response. We will discuss the detector design, spatial and spectral resolution and potential applications.

18:45 5D–5

Cryogenic microcalorimeters for high resolution energy dispersive x-ray spectroscopy.

J. Höhne[1], *M. Altmann*[2], *G. Angloher*[2], *M. Bühler*[1], *F. v. Feilitzsch*[2], *P. Hettl*[2], *T. Hertrich*[1], *J. Jochum*[2], *S. Pfnür*[2] and *J. Schnagl*[2]. [1]CSP Cryogenic Spectrometers GmbH, Bahnhofstr. 18a, D-85737 Ismaning, Germany. [2]Technische Universität München, Physik Department E15, D-85747 Garching, Germany.

The use of superconducting detector technology allows energy dispersive X-ray spectrometry with energy resolution and energy threshold far beyond the level of semiconductor detectors. Especially for the detection of light elements in material analysis applications cryogenic detectors combine the excellent energy resolution of wavelength dispersive spectroscopy (WDS) with the energy dispersive analysis of EDS. We are developing microcalorimeters based on superconducting tunnel junctions (STJs) and superconducting transition edge sensors (TESs) with energy resolutions as good as 12 eV (FWHM) for 6 keV X-rays. For microanalysis applications a cryostat system was developed allowing the use of our microcalorimeters on a SEM or a synchrotron beam line. First results will be discussed.

POSTER SESSION 6

Tuesday Evening, September 14th, 19:00-21:00

Session Bulk materials and materials aspects

6–1

Inhomogeneous Magnetic Properties of Melt-Textured YBCO.

T. Habisreuther, *D. Litzkendorf*, *M. Zeisberger* and *W. Gawalek*. IPHT, Jena, 07702, Germany.

Vibrating sample magnetometric measurements performed with small samples of melt textured $YBa_2Cu_3O_{7-\delta}$ show critical current densities up to 50000 Acm^{-2} at 77K and in zero field. The highest remanent inductions measured with bulk samples of 3cm diameter are approximately 1 T at 77 K which corresponds to a much lower critical current density. This discrepancy shows that the inhomogeneity is an important property of this material. In this contribution we present a statistical investigation of the inhomogeneity in the magnetic properties of $YBa_2Cu_3O_{7-\delta}$-bulk material by vibrating sample magnetometry and ac-susceptometry. The relation of the inhomogeneity and the crystal imperfections, e. g. micro cracks and sub-grain boundaries, is analyzed. The work was supported by the German BMBF under Grant No. FKZ: 13 N 6854.

6–2

Multi seeded YBCO - bars for cryogenic applications.

G. Krabbes, *P. Schaetzle*, *G. Stoever*, *N. Mattern*, *D. Stephan*, *D. Schlaefer* and *G. Fuchs*. Institute of Solid Sate and Material Research Dresden, P.O. Box 270016, D-01171 Dresden,.

Large bars of the $YBa_2Cu_3O_{7-\delta}$ (YBCO) HTSC material are prepared by a multi seeded melt crystallization process (MSMCP). Starting from up to four biaxial oriented Sm-123 seeds placed on the top of rectangular shaped YBCO bars (up to 100 x 40 x 15 mm^3) oriented single grains are grown. They joined together by partially coherent grain boundaries with an improved current transport capability and high levitation forces with overall values of 70 - 80N. The bars were used as rotor elements in an reluctance motor resulting in an output power of 12 kW. Results of investigations on the real structure and crystallization process of the YBCO - bars prepared by MSCP are presented. The real structure of the single grains was investigated as a function of the position on the YBCO - bar using a microdiffractometer system. X-ray diffraction with 200 mm beam size were used to analyze position resolved the local microstructure and the local grain orientation by rocking curve measurements. Normal X-ray pole figures were additionally measured to characterize the integral texture at interesting positions and the orientation distributions in mm regions. Results of optical microscopy and measurements of magnetic properties are compared with the X-ray diffraction results.

6–3

The effect of the addition of gold on secondary phase formation in RE-Ba-Cu-O (RE = Nd, Y, La).

P.J. Smith, *N. Hari Babu*, *D.A. Cardwell* and *Y.H. Shi*. I.R.C. in Superconductivity, University of Cambridge, Madingley Road, Cambridge, CB3 0HE, England.

The formation, size and distribution of non-superconducting secondary phases in the RE-Ba-Cu-O (RE = Nd, Y, La) matrix is considered essential for obtaining a high critical current density in these materials. The addition of small amounts of platinum and cerium oxide results in a reduction of the size and a finer dispersion of secondary phase particles throughout the bulk material. The influence of gold on the formation of secondary phases in REBCO is investigated in the present study. Small amounts of this dopant (0.1 wt %) have been added homogeneously to the REBCO matrix via a solution based technique which involves dissolving a soluble gold salt in an acidified solution of the base cations. The presence of gold is found to have a remarkable effect on the decompositon temperature of the reacted powder and consequently on the range of seeds that may be suitable for subsequent melt processing.

6–4

Fabrication of 100mm-diameter Y-Ba-Cu-O bulk QMG Superconductors with Larger Levitation Forces.

T. Fujimoto, *M. Morita*, *N. Masahashi* and *T. Kaneko*. Advanced Technology Research Laboratories, Nippon Steel Corporation.

Y-Ba-Cu-O type Quench and Melt Growth (QMG) bulk superconductors have become one of the most promising materials for practical applications, e.g., high-field magnets or flywheel energy storage systems. Controlling the crystallinity of the QMG superconductors is a key for enhancing the superconducting properties. We have investigated the relative misorientation angles of the adjacent subgrains, and the results obtained suggest that the growth conditions strongly influence the relative misorientation angle. On the basis of the results, we are able to fabricate 100 mm diameter Y-Ba-Cu-O bulk QMG superconductor disks with improved levitation forces, and a record-high value of 171 kgf has been achieved. Such high quality QMG superconductors provide a significant technological break-through for realising large-scale flywheel energy storage systems in which larger-diameter flywheels with massive weight rotating at higher speeds are required to store a plentiful amount of energy. Furthermore, we have also performed Electron Back Scattering Diffraction (EBSD) analyses which enable us to determine the misorientation angles of finer scale structures such as crystallites with much higher accuracy. We will show the EBSD data and discuss the crystallinity of the QMG superconductors.

6–5

Magnetooptic Imaging System for Studies of Magnetic Flux and Current Flow in Superconductors.

A. Polyanskii[1], *L. Dorosinskii*[2] and *H. Bocuk*[2]. [1]Applied Superconductivity Center, University of Wisconsin-Madison, WI 53706, USA. [2]National Metrology Institute,P.K.21, 41470 Gebze-Kocaeli, Turkey.

We present a magnetooptic imaging system which allows one to study the spatial distribution of magnetic field in superconductors. The field distribution is visualized using indicator garnet films with in-plane anisotropy. The film is placed on top of a superconducting sample, and magnetic field penetrating the sample results in the Faraday rotation

of the polarization of the light passing through the film. The pattern of filed distribution is observed in a polarizing optical microscope. Due to the high spatial resolution of the method (1 μm) one can see the effect of various defects on the penetration and pinning of magnetic flux and on the flow of transport current in superconductors. Therefore, the method proves to be very useful not only for characterizing the quality of superconducting samples but also for understanding the mechanisms limiting the pinning strength and the current- carrying capacity. We present results of studies of the flux penetration and pinning and of the transport current flow in YBCO bulk materials and BSCCO tapes.

6–6

Top seeding growth and microstructure of large grain Nd123/422 superconductors.

M.Gombos[1], *A.E.Carrillo*[1], *V.Gomis*[1], *X.Obradors*[1], *S.Pace*[2] and *A.Vecchione*[2]. [1]Institut de Ciència de Materials de Barcelona (CSIC). Campus UAB, 08193 Bellaterra (SPAIN). [2]Istituto Nazionale di Fisica della Materia, unità di Salerno e Dipartamento di Fisica, Università di Salerno, Via S.Allende, Baronissi (Salerno), Italia.

Single domain top seeded melt textured superconducting pellets of Nd123/Nd422 composites have been prepared using Nd210 additions in the precursors.The temperature window has been determined allowing to achieve grain nucleation at MgO seeds in air avoiding additional nucleations.The single grain Nd123/422 composites are found to display some porosity and new microstructural features. It has been found that microscopic cracks may be developped both parallel and perpendicular to ab-plane with a well defined in-plane orientations ({100}, {010}). Nd422 precipitates have been found to distribute homogeneously and its mean size progresively decreases as the initial Nd210 content increases. The influence of high temperature annealing in Ar atmosphere on Tc has been investigated.

6–7

Magnetic field dependences of rf absorption in HTS ceramics as a way to grains quality evaluation.

G.V. Golubnichaya, A.Ya. Kirichenko, I.G. Maximchuk and *N.T. Cherpak*. Usikov Institute of Radiophysics and Electronics of National Academy of Sciences, Kharkov, 310085, Ukraine.

Peculiarities of the electromagnetic power absorption at extreme points of magnetic field dependences in high-T_c ceramics are investigated. The absorption power was measured by the inductive technique at a frequency of 2.5 MHz at liquid nitrogen temperature. The hysteresis loop of the absorption of rf energy and the losses in the sample with a trapped magnetic flux in zero magnetic field have been recorded. A linear dependence of absorption on the magnetizing field at the points of minima on the curves is established. The values of losses at the minimum of the curve recorded in a decreasing magnetic field are approximately twice as large as rf losses at the minimum of the absorption curve recorded on a sample with a trapped magnetic flux during magnetization reversal. A good agreement to the Bean's model as well as linear dependences of the absorption lead to the conclusion that losses at the minima of magnetic fiels dependences is mainly due to absorption directly in grains. In spite of the generally accepted opinion that rf losses in magnetic fields are mainly associated with losses in the intergranular medium, the absorption takes place predominantly in grains for certain values of magnetic fields on magnetic fiels curves. The magnitude of losses at these points can be used to estimate the quality of grains.

6–8

Persistent current in melt-processed YBCO-rings.

N.A. Nijelskiy[1], *O.L. Poluschenko*[1], *A.V. Kalinov*[2], *I.F. Voloshin*[2] and *S.V. Shavkin*[3]. [1]Moscow N.E.Bauman State Technical University, 5 2nd Baumanskaya str, Moscow 107005, Russia. [2]All-Russian Electrical Engineering Institute, 12 Krasnokazarmennaya str, 111250 Moscow, Russia. [3]RRC "Kurchatov institute", Kurchatov sq, 123182 Moscow, Russia.

The persistent currents in YBCO-rings and their grain structure were studied. The rings with outer diameter 15 mm, inner diameter 7 mm and thickness 2.5 mm were produced from disks prepared by the top-seeding melt-texturing method with Sm-123 seeds. The X-ray pole figures analysis indicates the microstructure to consist of several block crystals up to 5 mm in size, with **ab**-plane being parallel to the ring surface. A supercurrent capability of the rings was studied by the scanning Hall probe technique as well as by the measurements of the magnetic flux penetration into the ring at the external magnetic field up to 2 T. The Hall magnetometry was used to visualize the magnetic induction distribution on the sample surface in FC and ZFC regimes. The magnetic field mapping gives the possibility to find the persistent circular current in the sample and to localize the 'weak' grain boundaries. These maps are compared with the data of the X-ray analysis of the grain structure. The magnetic flux measurements were used to estimate the magnetic field dependence of the critical current density. The best ring shows a single domain structure and gives $J_c \approx 15$ kA/cm^2 in the self-field and $J_c \approx 9$ kA/cm^2 at $H = 1$ T. is considered now as the most promising way to improve supercurrents in large scale bulk HTS materials. This classical method allows to control and minimize effectively a misorientation of grains in a polycrystalline ingot. Recently (A.S. Parikh, B. Meyer, K. Salama, Supercond. Sci. Technol. 7 (1994) 455) developed a processing Liquid Phase Removal Method (LPRM) to eliminate secondary phases and reduce microcracks at the grain boundaries in YBCO superconductors. The late method gives a possibility to improve a supercurrent capability of large angle grain boundaries. The critical currents through grain boundaries are measured usually by pulsed DC methods giving not so reliable information as a conventional DC four-probe method. To avoid some current input problems we have prepared O-rings from TSMT YBCO disks and studied the supercurrents in them by contactless magnetic methods.

6–9

Preparation of Melt-Textured YBCO with optimized shape for Cryomagnetic Applications.

D. Litzkendorf, T. Habisreuther, M. Zeisberger and *W. Gawalek*. Institut fuer Physikalische Hochtechnologie e. V., Helmholtzweg 4, PF 100239, D-07702 Jena, Germany.

Alternative to a batch process of cylindrical YBCO blocks

we report some results on a batch process preparing quadratic shaped YBCO plates with well developed melt texture technology. Up to 16 quadratic YBCO plates with a edge length of 40 mm and a height of 18 mm can reproducible prepared in one box furnace run. For a standard composition of $Y_{1.5}Ba_2Cu_3O_{7-X}$ + 1 % CeO_2 a commercial prereacted $YBa_2Cu_3O_{7-X}$ powder with an excess of Y_2O_3 was used. Small MgO single crystal seeds were put on top of the samples. The quality of the plates is checked by integral levitation force measurements and field mapping. We reached zero field cooled levitation forces at 77 K higher than 60 N and we found a homogeneous distribution of the levitation force in one run. At 77K a remanent induction of 600 mT was frozen in a single domain sample. Batch processed material with quadratic shape is used for a number of magnetic applications, e. g. for electromotors and magnetic bearings. For these applications constructions of joined YBCO structures with more complex geometries are necessary. To build these YBCO structures rectangular plates can be used superior to cylindrical blocks, because the plates enable to make a simple construction and less costs of assembling. The additional expenditure by cutting and machining of cylindrical blocks and the loss of useable YBCO material caused by cutting can be much more reduced by using a minor number of quadratic shaped YBCO plates. A bonding technique was used to assemble the tiles. By the change from cylindrical to quadratical material the bonding face of the YBCO plates decreases about 60%. This results also in better cryomagnetic quality of our function elements.

6–10

An Approach to Homogeneity in YBCO Melt Texturing.

F.N. Werfel[1], *U. Flögel - Delor*[1], *L. Woodell*[2], *S. Remke*[2] and *M. Gerards*[2]. [1]Adelwitz Technologiezentrum GmbH, D-04886 Adelwitz, Germany. [2]MERCK KGaA,Darmstadt, Germany.

Polycrystalline melt textured YBCO rods and plates are a promising concept for the modular up-scaling of current transport components if the weak - link behaviour of grain boundaries can be reduced. A Ceramo-Crystal-Growth Bridgman-like directional solidification with an applied temperature gradient was performed on $Y_{1+x}Ba_2Cu_3O_{7-\delta}$ in order to minimise cracks, mechanical stress and grain boundary decoupling effects. Both the growing rates and a predetermined temperature gradient are important process parameters. Using small grain band - width precursor powders with Y rich stoichiometry the grain boundary spacings were decreased with increasing growing rate. Two types of precursor powder were compared, an Y rich 123 formulation and a 123-211 mixture to control the liquid phase influence on the weak - link behaviour of the grain boundaries. "In - situ drying" by compacted Y_2O_3 bars supporting the samples during the texturing process improves the transport current characteristics. With increased growing rate the mesoscopic structure of the samples were changed to smaller grains and hence from cellular with a high tendency to form hot - spots and cracks at the grain boundaries, to more homogeneous. This resulted in improved transport current carrying properties within the multigrain YBCO bulk parts. We report current - voltage measurements on YBCO plates and rods. Melt growth rods can carry currents in excess of 5 $kAcm^{-2}$.

6–11

Processing of superconducting Y-123 cylindrical bars.

A. Calleja[1], *M. Segarra*[1], *I. García*[2], *J.M. Chimenos*[1], *M.A. Fernández*[2], *F. Espiell*[2], *E. Mendoza*[3], *T. Puig*[3], *S. Piñol*[3] and *X. Obradors*[3]. [1]DIOPMA, Llacuna 162-166, Barcelona, E-08018, Spain. [2]Departament d'Enginyeria Química i Metal.lúrgia, Facultat de Quimica, Martí i Franques 1, E-08028, Barcelona, Spain. [3]Institut de Ciència de Materials de Barcelona-C.S.I.C., Campus de la UAB, Bellaterra, Barcelona, E-08193, Spain.

Y-123 monodomain bars are finding succesful application as superconducting elements useful for current transportation in fault current limiters and current leads. They are able to carry high current densities of 10,000-20,000 A/cm^2 at liquid nitrogen (T=77 K) and self field. Precursor powders were also prepared corresponding to a Y-123/Y-211 mixture. From an economic point of view, cost reduction of the materials is sought from the actual values both of the precursors and materials processing. The fabrication method consists of a patented melt solidification process by the Bridgman technique in which the cold-pressed green bars are hung vertically. Then, a motor-driven mechanism pulls the bar out of the furnace. The solidification occurs as the whole lenght of the bar crosses the peritectic temperature at a thermal gradient of 20°C/cm. After the run, monocrystalline bars display the following typical dimensions: L=80 mm and ⌀=6 mm, with an overall critical current I_c=1500 A. In this work, we show the industrial obtention of cylindrical-shaped Y-123 bars with good transportation properties. The superconducting elements can be used as current leads and in fault current limiters.

6–12

Homogeneity of Top-Seeded Single-Grained (RE)BCO Superconductors.

I.-G. Chen[1], *S.-H. Hsu*[1], *S.-Y. Chen*[1] and *M.K. Wu*[2]. [1]Dept. of Materials Sci. & Eng., National Cheng Kung Univ., #1 Ta-Hsueh Rd., 70101, Tainan, Taiwan, R.O.C. [2]Materials Science Center, National Tsing Hua Univ., Hsinchu, 30043, TAIWAN, R.O.C.

Recent studies indicated that single grained samples of other (RE)BCO system, where RE=Sm, Nd, etc. can also be produced with even better Jc(H,T) properties. However, the homogeneity of the Jc(H,T) of different (RE)BCO systems with different processing parameters have not been fully studied, which have a strong influence on the overall superconducting performance of the sample. In this study, we have conducted a systematic study on the single grained sample with different (RE)BCO systems. Two methods have been used to characterize the single grained samples. One is to measure the contour of trapped magnetic field distribution to reveal the relative the persistent current pattern and weak-links. And the other method is to use SQUID to measure the Jc(H,T) on small samples cut from various location on a single grained sample. For YBCO sample with Sm seed, the sample 3-6 mm below the seed shows a largest single peak with a highest trapped field and Jc(H,T). For samples far away from the seed, very complicate patterns were

observed which reveals the development of inhomogeneities and weak links.

6–13

Improvement of the mechanical properties of bulk-superconductors by impregnation of epoxy resins.

M. Tomita and *M. Murakami*. Superconductivity Research Laboratory,1-16-25 Shibaura, Minato-ku, Tokyo 105-0023, Japan.

Large single-grain bulk RE-Ba-Cu-O (RE: rare earth elements) superconductors can trap large fields exceeding several teslas and thus can function as very strong quasi-permanent magnets, however, the maximum trapped field is essentially limited by the mechanical strength of bulk-superconductors. The stress produced by refrigeration sometimes causes cracking. A large electromagnetic force will also act on the superconductors, when they trap large magnetic fields, which occasionally leads to the fatal failure. We have recently found that epoxy resin can penetrate into the bulk superconductors under proper conditions. Microstuctural observation revealed that macrocracks as well as microcracks or porosities can be impregnated with epoxy resin, which greatly improves the mechanical properties of bulk RE-Ba-Cu-O and thus results in the improvement of field trapping capability. This work was supported by New Energy and Industrial Technology Development Organization (NEDO).

6–14

Fabrication of Large Single-Domained Y-Ba-Cu-O Superconductor by Multiseeding in Top-Seeded Melt Growth.

Y.A. Jee, *G.W. Hong* and *C.J. Kim*. Functional Materials Lab, Korea Atomic Energy Research Institute, PO Box 105, Yusong, Taejon 305-600, South Korea.

Fabrication of large single-domained YBCO superconductors has been investigated so far with various points of view, and the single domain can be grown up to 10-15cm diameter at the present level. With general top-seeded melt growth (TSMG) process, however, hundreds of hours is required only for undercooling heat treatment, and parasitic nucleation during the process is difficult to restrain. Moreover, as the demand for larger samples with specific shape increases recently, it is getting difficult to satisfy the requirement with conventional TSMG. Accordingly, more interests are being given to the new trial such as multiseeding or bonding to obtain large samples easily. However, sudden degradation of superconducting properties is generally observed across grain boundaries in samples prepared by multiseeding. In this study, we tried to understand the reason for intergranular property degradation and suggested various kind of multiseeding technique in attempt to reduce the problem.

6–15

Different limitations of trapped fields in melt-textured YBCO.

G.Fuchs[1], *C.Wenger*[2], *A.Gladun*[2], *S.Gruss*[1], *P.Schaetzle*[1], *G.Krabbes*[1], *J.Fink*[1], *K.-H.Müller*[1] and *L.Schultz*[1]. [1]Institute of Solid State and Materials Research Dresden, D-01171 Dresden, Germany. [2]Technical University Dresden, D-01062 Dresden, Germany.

Bulk melt-textured YBCO material with single-domain grains up to 35 mm in diameter has been prepared by a modified melt-texture process. The trapped field of the samples was found to be limited by the pinning properties at high temperatures, by the mechanical strength of the material at medium temperatures around 50 K and by magnetic instabilities at low temperatures. The maximum trapped field measured in the 1 mm gap between single-grain disks increases from 1 T at 75 K up to 9.6 K at 46 K. Very high trapped fields up to 9 T at 43 K were observed also at the top surface of a YBCO cylinder 26 mm in diameter. In order to reinforce the samples against tensile stresses they were surrounded by tubes from stainless steel which were additionally filled by epoxy. Improved pinning properties have been achieved by modified precursors in the melt crystallization process. These materials showing the peak effect in the field dependence of the critical current density were found to be favourable for obtaining high trapped fields. The occurrence of flux jumps at low temperatures ($\leq$ 20 K)in bulk samples was investigated by thermal and magnetic measurements. The dependence of the flux jump field on the heat transfer coefficient, the sweep rate of the applied magnetic field and the temperature of the sample was studied. The measured instabilities in the critical state are discussed in the frame of existing criteria.

6–16

Trapped fields up to 9 T in bulk $YBa_2Cu_3O_{7-\delta}$ material.

S. Gruss, *G. Fuchs*, *P. Schaetzle*, *G. Krabbes*, *J. Fink*, *K.-H. Müller* and *L. Schultz*. Institute of Solid State and Materials Research Dresden, P.O. Box 27 00 16, 01171 Dresden, Germany.

A modified melt texture process using Sm-123 seed crystals was used to produce bulk $YBa_2Cu_3O_{7-\delta}$ material with domain sizes up to 34 mm in diameter. The samples were characterized by field mapping and levitation force measurements at 77 K. The trapped magnetic field was measured in the 1 mm gap between two disks (mini-magnet) and at the surface of single disks. Maximum values of 9.6 T at 46 K for the mini-magnet and 9.0 T at 43 K for the single disks were reached. We observe a pronounced peak in the field dependence of the critical current density in samples manufactured with a modified precursor powder. The activation energy for flux creep was investigated by relaxation measurements. The improved pinning properties of samples showing the peak effect were found to be caused by an enhancement of the density of pinning sites, whereas the pinning energy of the pinning defects remains unchanged. For applications of bulk YBCO material in superconducting magnetic bearings an effective method for the magnetizing procedure of the superconductor is required. Results of magnetizing YBCO samples at 77 K by applying pulsed magnetic fields with different rising times will be presented.

6–17

YBaCuO monoliths of complex shapes processed by welding and optimized by infiltration.

H. Walter[1], *M.P. Delamare*[2], *B. Bringmann*[2], *A. Leenders*[1,2] and *H.C. Freyhardt*[1,2]. [1]Zentrum für Funktionwerkstoffe Göttingen gGmbH, Windausweg 2, 37073 Göttingen, Germany Zentrum für Funktionwerkstoffe Göttingen gGmbH, Windausweg 2, 37073 Göttingen, Germany. [2]Institut für Materialphysik, Universität Göttingen, Hospitalstrasse 3-7, 37073 Göttingen, Germany.

Melt textured YBCO samples were cut parallel to their c direction and joined under a pressure of 0.5 MPa with $YbBa_2Cu_3O_x$ or $ErBa_2Cu_3O_x$ powder as welding agent. This welding technique enables the preparation of larger monoliths and also of monoliths with complex shapes for technical applications, e.g. in superconducting bearings of HTS hysteresis motors or energy storage systems. However, this technique must be further investigated not only to reach large volume tiles but also to obtain both high and homogeneous distributed trapped fields and good mechanical properties. Indeed, a successful joining of two monodomains, leading to a low-angle grain boundary, guarantees both a good connectivity and high intergrain critical currents. The remanent induction of these samples can be further improved by applying an infiltration technique with $YbBa_2Cu_3O_x$ as infiltration agent. After infiltration, the trapped field of an YBCO sample can be increased by 100-300 mT from a level of about 1000 mT (quadratic samples (38 x 38 x 12) mm^3).

6–18

$BaZrO_3$ and $YBa_2ZrO_{5.5}$ additions in melt textured $YBa_2Cu_3O_{7-\delta}$: influence on the microstructure and physical properties.

A. E. Carrillo, *T. Puig*, *V. Gomis*, *S. Piñol*, *J. Plain*, *F. Sandiumenge* and *X. Obradors*. Institut de Ciència de Materials de Barcelona, Campus UAB, 08193 Bellaterra, Barcelona, Spain.

We report the effects of non-reactive new additions, namely $BaZrO_3$ and $YBa_2ZrO_{5.5}$, in the top seeding melt-texturing growth TSMTG of Y123+30%wt211 composites. Their microstructure and physical properties have been systematically analysed in the compositional range between, 1%wt and 10%wt of $BaZrO_3$ or $YBa_2ZrO_{5.5}$. The initial average particle size has been carefully controlled. Energy Dispersive Spectroscopy (EDS) and polarized optical microscopy reveal a strongly pushing mechanism which surprisingly leads to twinned single domains free of Y211 precipitates and few $BaZrO_3$ particles. Critical superconducting temperatures of 91K have been obtained with transition width of $\delta T_c \cong 0.7K$. The absence of 211 inclusions was further confirmed by magnetisation measurements of the paramagnetic signal. Whereas critical current densities at 5K of 10^6 A/cm^2 demonstrate the high quality of the single domain, a strong decrease of $J_c^{ab}$is observed when the pinning by 211 precipitates should become efficient (i.e. at high temperature and high field). A comparison with Y123+30%wt211 TSMTG and YBCO single crystal is performed. We confirm this method as a potential way to obtain good quality Y123 MTG single domains free of 211 precipitates. This has enabled us to study vortex pinning effects in MTG Y123 without the contribution of the 211 phase.

Financial support from the EU-TMR Network Supercurrents, EBR 4061 PL 97-0281, is acknowledged.

6–19

Top seeding growth and superconducting properties of bulk YBCO - Ag composites.

E. Mendoza[1], *M. Carrera*[2], *E. Varesi*[1], *A.E. Carrillo*[1], *T. Puig*[1], *J. Amorós*[3], *X. Granados*[1] and *X. Obradors*[1]. [1] Institut de Ciencia de Materials de Barcelona Consejo Superior de Investigaciones Cientificas Campus de la UAB Bellaterra 08193 Barcelona Spain. [2]DMACS. Universitat de Lleida Jaume II, 69 Lleida 25001 Spain. [3]Departament de Matematica Aplicada Universitat Politecnica de Catalunya Diagonal 647 08028 Barcelona Spain.

Melt textured $YBa_2Cu_3O_7$ / Y_2BaCuO_5 composites have been prepared by top seeding growth with an addition up to 20% wt of submicrometric silver precipitates, in order to study their mechanical and superconducting properties. A thorough analysis of the different compositions by thermogravimetric analisys has indicated a decrease of the peritectic temperature of 30 ^{o} C which has required a full optimization of the solidification process. Polarized optical microscopy, SEM and EDX analisys show good quality growth monoliths with an homogeneous distribution of silver particles in the range of 5 to 50 μm. Inductive critical currents measurements of small pieces confirmed an increase of J_c^{ab} by a 100% reaching values of $2 \cdot 10^6$ A/cm^2 at 5K and 10^5 A/cm^2 at 77K. These results are contrasted with global measurements of levitation force and trapped magnetic field. For the latter Hall probe scanning measuring system in the remanent state has been used and the current distribution in the sample has been determined by solving the inverse problem from magnetic flux maps.

Session Wires tapes and coated conductors

6–20

Magnetic field of bent BSCCO tapes carrying magnetisation currents.

J. Kvitkovic and *M. Polak*. Institute of Electrical Engineering, Slovak Academy of Sciences, Bratislava, 842 39, Slovak Republic.

One of most interesting application of BSCCO tapes are HTS magnets. R&W method has several advantages. The disadvantage of the method is that during winding procedure the critical parameters of the tapes are affected by bending. Double bending was used in our experiments. Hall magnetometry was used for tape parameter inspection. We investigated transversal and longitudinal profiles of all three components of magnetic field above bent BSCCO tapes carrying magnetisation currents. Magnetic field was measured by special AXIS-3 Hall probe and moved by computer controlled positioning system. Reduction of the amplitude of magnetic field with decreasing bending diameter was compared with the reduction of the transport critical current versus bending diameter. Homogeneity of the reduction of transport Ic was studied using several potential taps.

6–21

Some aspects of Bi(2223)/Ag tapes with resistive barriers.

P. Kovac[1], *I. Husek*[1], *F. Gömöry*[1], *L. Cesnak*[1], *T. Melisek*[1] and *W. Pachla*[6]. [1]Institute of Electrical Engineering of Slovak Academy of Science, Bratislava, 842 39, Slovakia. [2] High Pressure Research Center of Polish Academy of Science, Warszawa, 01 142, Poland.

In the last time, a new conductor configurations with a quite novel composite matrix having a ceramic resistive barriers inside the Ag matrix have been developed. The aim is to reduce the coupling losses by enhancing the resistivity of the matrix material between the filaments. The preparation of these multi-component composites is not trivial, and it brings also new effects which influence the properties of Bi-2223 filaments. A several characteristics of Bi-2223/Ag/barrier/Ag single-core and multicore tapes with various barrier material (BaZrO2, SrCO3, ZrO2 and Al2O3) have been studied. AC susceptibility measurements, V-I curves (in a range of 10-9-10-3 V/cm) and the effects of twisting were measured. It was found that the shape of I-V curves, transfer lengths as well as current densities are strongly influenced by barrier material, its thickness, porosity and continuity as well. The resistive barrier influences also the oxygen diffusion and consequently it determines the quality of Bi-2223 core.

6–22

Quality measurement of Bi(2223)/Ag tapes by Hall probe array.

P. Kovac, *V. Cambel* and *J. Pitel*. Institute of Electrical Engineering of Slovak Academy of Sciences, Bratislava, 842 39, Slovakia.

A gliding four probe method and contactless field monitoring measurements have been used for homogeneity studies of Bi(2223)/Ag tapes. The gliding potential contacts moved along the tape surface and a sensitive system based on an integrated Hall probe array containing 16 or 19 in-line probes supported by PC-compatible electronics with software allowed to make a comparison of contact and contactless measurements at any elements of Bi(2223)/Ag sample. The nature of BSCCO compound and application of powder-in-tube technique lead usually to not uniform quality across and/or along the ceramic fibbers and finally to variations in critical currents and its irregular distribution in Bi(2223)/Ag tape. The results of four probe and Hall probe measurement show very good correlation and possibility to use sensitive Hall probe array for monitoring the final quality of Bi(2223)/Ag tapes. The self field calculation and monitored field have also been compared with the aim to show the effect of irregular current flow in the filaments.

6–23

Transport current and texture of Bi-2223 grains in multicore Ag sheathed tapes.

P. Kovac[1], *T. Melisek*[1], *A. Kasztler*[2], *W. Pachla*[3], *J. Pitel*[1], *R. Diduszko*[4] and *H. Kirchmayr*[5]. [1]Institute of Electrical Engineering of Slovak Academy of Sciences, Bratislava, 842 39, Slovakia. [2]Institute of Experimental Physics of Technical University, Wien, A-1030, Austria. [3]High Pressure Research Center of Polish Academy of Sciences, Warszawa, 01 142, Poland. [4]Institute of Vacuum Technology, Warszawa, 00 241, Poland. [5]Institute of Experimental Physics of Technical University, Wien, A-1030, Austria.

Angular, field and temperature dependences of the critical current were measured in multifilamentary Bi(2223)/Ag tape. Due to the not ideal alignment of the Bi-2223 grains in Ag sheathed tapes there is always a component of the external magnetic field which is parallel to the c-axes even if it is oriented parallel to the tape plane. Thus the magnetic field multiplied by sinus of the average misalignment angle gives the field component parallel to the c-axes. This method was used to determine the so called magnetic angle of Bi-2223 grains from critical currents measurement at parallel and perpendicular field orientation. Magnetic angle at various temperatures were estimated and it was shown that is not simply equal to the structurally measured misalignment angle. SEM and RTG analysis were used for structural characterisation especially near the filament surface. They have shown a gradient of the texture and phase content from filament surface to its centre. Consequently, the flow of current at various fields and temperatures is not uniform and the relation of local structure to transport current is not simple.

6–24

Stoichiometric variations in Bi-2212 thick film conductors: electrical and microstructural characterisation.

B.R. Balmer[1], *G.W. Grime*[1], *C.J. Salter*[1], *R. Riddle*[2] and *C.R.M. Grovenor*[1]. [1]Dept. of Materials Science, University of Oxford, Oxford OX1 3PH, U.K. [2]Merck Research and Development UK, University of Southampton, Highfield SO17 1BJ.

There have been many reports of phase diagram studies on Bi 2212 powder, some varying the stoichiometry, and some introducing small amounts of substituting elements. However, there has been little work on the effect such changes would have on the transport properties of melt processed thick films on silver. For example, it is still not clear how the distribution of impurity phases may be affected by such changes. We have carried out a systematic study of the effects of powder composition on the microstructure, volume fraction and composition of insulating impurity phases, and J_c values. The composition of the melt processed 2212 has also been analysed by EPMA and scanning proton microscopy in order to ascertain any effect of source powder stoichiometry. J_c values have been optimised for 77K, with 4.2K testing being carried out on the best from each composition, and systematic variations have been observed for very small changes in stoichiometry.

6–25

Vortex pinning and anisotropy in Ag/Bi(Pb)SrCaCuO-2223 tapes by means of surface columnar defects.

R.Gerbaldo[1], *G.Ghigo*[1], *L.Gozzelino*[1], *E.Mezzetti*[1], *B.Minetti*[1], *L.Martini*[2] and *G.Cuttone*[3]. [1]I.N.F.M. UdR Torino Politecnico; I.N.F.N. Sez. di Torino; Dipartimento di Fisica, Politecnico di Torino, Torino, Italy. [2]ENEL-SRI, Segrate (Milano), Italy. [3]I.N.F.N. Laboratorio Nazionale del Sud, Catania.

Surface columnar defects, SCDs, are produced in high quality Ag/BSCCO tapes by irradiating them with 0.25 GeV gold ions only on a top layer up to about 10% of the full volume. The ion beam is orthogonal to the tape plane. Such defects shift the irreversibility lines (ILs) towards high temperatures and magnetic fields, enhance the critical current densities and strongly decrease the dependence of ILs on frequency. In this paper we concentrate on the shutdown of the IL anisotropy (low current regime) as well as on the decrease of the critical current density anisotropy (high current regime) in high quality Ag/BSCCO tapes. IL anisotropy is also studied as a function of the angle between the applied magnetic field and the ion tracks. Two are the results to be emphasized, because they are particular of the SCD topology: 1) the enhancement of the superconducting properties when the magnetic field is applied parallel to the ion tracks does not compromise the superconducting properties with the field perpendicular to the ion tracks, unchanged. This aspect leads to the shut down of the anysortopy between B^* ($B^*<B_\phi$) and $2B_\phi$ (with B_ϕ we mean the field which would be ideally required to fill each track with a flux quantum). 2) A dose dependent zone of the ILs exists (toward highest temperature and lowest magnetic field), where SCDs do not affect the intrinsic properties of the material. On the contrary a Bose glass-like phase starting just at the mentioned dose dependent (T_{onset}, B_{onset}) point phase is induced by the defects. A correlation between the two features is discussed on the basis of recent models.

6–26

Filament by filament mapping of BISCCO2212-2223 conversion in multifilamentary tapes.

J. Tundidor, *R. Dudley*, *E. Young*, *Y. Yang* and *C. Beduz*. Institute of Cryogenics, University of Southampton, Southampton SO17 1BJ, UK.

The conversion from BSCCO-2212 to BSCCO-2223 in multifilamentary tapes has been analysed in each filament separately by XRD and mapped across the entire cross sectional area. A special window was used to narrow the x-ray beam to the width of each filament. The tapes have been made using the standard PIT method and sheathed in Ag-Ni(0.25)Mg(0.25) alloy using two intermediate sintering/rolling processes and the analysis was done in tapes with different final sintering times. We observed general inhomogeneous conversion among filaments since the speed of conversion is higher for the central filaments. Even in an optimised critical current we can see that conversion could vary by more than 50% for different filaments. In contrast, the inhomogeneity is less pronounced in pure silver sheath tapes. The cause of the differences in phase conversion between silver and alloy sheath tapes could be that the mean density of the core and its spread in silver sheathed tapes are less than those of alloy ones. The differences in conversion rate could be related to inhomogeneous density during mechanical processing.

6–27

Normal-zone Propagation Properties in BSCCO Silver Sheathed Tapes.

S. Shimizu[1], *A.I. Ishiyama*[1] and *S.B. Kim*[2]. [1]Dept. of EECE, Waseda Univ., Shinjuku-ku, Tokyo 169-8555, Japan. [2]SRL, ISTEC, Atsuta-ku, Nagoya 456-8287, Japan.

The normal-zone propagation properties are very important for issue of high-temperature superconducting (HTS) coil design. Therefore in this paper, we present the results of experiments and computer simulations to make clear the normal-zone propagation properties in Bi-2223/Ag superconducting multifilament tape. We developed a computer code based on the two-dimensional finite element method (2-D FEM). Computed voltage and temperature traces during a quench agree well with the experimentally recorded voltage and temperature traces. Good agreement validates the computer code, making a useful tool in developing protection strategies for HTS coils. We simulate the quench process in a single pan cake coil wound with Bi-2223/Ag superconducting multifilament tape with background magnetic filed up to 10 T at 20 K using the developed computer code. The normal-zone propagation properties and stability in HTS coils are discussed and compare with those in low-temperature superconducting (LTS) coils. Especially we focus on the estimation of the amount of Joule heating in a current-sharing region.

6–28

A Systematic Comparison of the Phase Development in Powders from the PBSCCO 2223 System, considered in PIT Processing, prepared by Solid State Processing, Co-Precipitation, Citrate Gel and Spray Pyrolysis.

Y.W. Hsueh[1], *R.S. Liu*[1], *L. Woodall*[2] and *M. Gerards*[2]. [1]Department of Chemistry, National Taiwan University, Taipei, Taiwan, R.O.C. [2]Merck KGaA Darmstadt, D-64271 Darmstadt, Germany.

We have synthesized precursor phase mixtures from the Bi-2223 [$(Bi,Pb)_2Sr_2Ca_2Cu_3O_{10+\delta}$] system using solid-state reaction, co-precipitation, citrate gel and spray pyrolysis. The analytical techniques, TGA/DTA, IR, XRD and SEM/EDS, were used to study the phase formation in these powders. The phases present change as both the calcination temperature and holding time increase. First we obtained the Superconducting Bi-2201 [$(Bi,Pb)_2Sr_2Cu_1O_{6+\delta}$] with secondary phases and then the Bi-2212 [$(Bi,Pb)_2Sr_2CaCu_2O_{8+\delta}$] with minority phases, including Ca_2PbO_4, 3321 and CuO. Preliminary Quantitative Rietveld refinement data will also be presented. The importance of the secondary phases in the conversion of Bi-2212 to Bi-2223, and their suitability to PIT processing, will be discussed.

6–29

Quantitative Phase Analysis of PBSCCO 2223 Phase Mixtures used in PIT Processing.

S. Raeth[1], *W.W. Schmahl*[1], *L. Woodall*[2] and *M. Gerards*[2]. [1]Institut für Mineralogie, Ruhr Universität, D-44780 Bochum, germany. [2]Merck KGaA Darmstadt, D-64271 Darmstadt, Germany.

A PIT precursor powder was calcined under air and in flowing nitrogen at different temperatures. Quantitative phase analysis and determination of the lattice constants of the 2212-phase were carried out by Rietveld refinement of the X-ray powder diffractograms. This analysis is potentially very useful as a form of quality control when processing bulk, multi-kilogram quantities of these phase mixtures. Calcining under nitrogen at 760°C produces a precursor powder containing primarily 2212 phase, Ca_2CuO_3, Ca_2PbO_4, 14:24 phase ($Sr_{14-x}Ca_xCu_{24}O_{41}$) and CuO. This phase composition changes at higher temperatures with the amounts of 14:24-phase and calcium plumbate decreasing and finally disappearing at 770°C. At this point the Pb-content in the 2212-phase reaches a maximum. At temperatures above 770°C the 2212-phase decomposes again and the first melt occurs at 780°C. The phase composition as seen in air is very different consisting of Pb-free 2212, Ca_2PbO_4, 3321, 14:24 and the 1:1 phase ($Ca_{1-x-y}Sr_xCuO_{2-\delta}$ around 800 °C. The proportions of the secondary phases changes above 800°C with a noticeable decrease in the amount of Pb-containing secondary phases.

6–30

Prospects of Utilization of HTSC Having High Critical Currents due to Nuclear Fission Fragment Tracks.

I.N.Goncharov. Joint Institute for Nuclear Research, Dubna, 141980, Russia.

One of the most effective methods of increasing a critical current is due to the production of nuclear fission fragment tracks almost uniformly distributed inside HTSC. These fissions can be caused either by high energy particle irradiation for Hg,Tl,Pb,Bi, which belong intrinsically to HTCS, or by neutron/gamma irradiation for doped U nuclei. The problems of optimum radiation fluences, radioactivity and cost are analyzed in this paper. The prospect of utilization of such modified HTCS materials for various superconducting systems are also considered.

6–31

Influence of the precursor powder properties on phase formation and critical current density of (Bi,Pb)-2223-tapes.

F. Schwaigerer, *B. Sailer*, *A. Trautner*, *W. Wischert*, *H. J. Meyer* and *S. Kemmler-Sack*. Universität Tübingen, Institut für Anorganische Chemie, Auf der Morgenstelle 18, D-72076 Tübingen, Deutschland.

Ag-clad (Bi,Pb)-2223 tapes made by the PIT-process are most suitable for application with high-Tc-superconductors. Much effort has been made to produce these high-Tc-wires with excellent current carrying capabilities in good reproducibility. In the present study the effect of the phase assemblage of the precursor powders has been examined: (1) One important feature of all cuprate superconductors is the oxygen stoichiometry. Controlling the oxygen content means controlling the concentration of defect electrons influencing directly the superconducting properties. But during the thermo-mechanical treatment the oxygen diffusion is rapidly hampered by the growth of extended 2212- or 2223-plates. So attempts optimizing the oxygen content of the (Bi,Pb)-2223-ceramic by varying the oxygen content of the precursor-powder were made and its effect on phase-formation and critical current density were studied. (2) The development of 2223 is strongly influenced by the formation of a liquid phase. But no general agreement about its composition has been achieved. The effect of adding Ca_2PbO_4, $CaBi_2O_4$ and Ag to the standard precursor on phase formation and the development of critical current density is examined. We show how these dopants are involved in the reaction acting as a flux. This work was supported by the Bundesministerium für Bildung, Wissenschaft und Technologie (FKZ 13N6481 A/6) and the Siemens AG

6–32

Lattice constant differentiation and texture distribution within the monocore (Bi,Pb)-2223/Ag tapes.

W. Pachla[1], *R. Diduszko*[2], *P. Kovac*[3] and *I. Husek*[3]. [1]High Pressure Research Center, Polish Academy of Sciences, ul. Sokolowska 29, 01-142 Warszawa, Poland. [2]Institute of Vacuum Technology, ul. D[3]uga 44/50, 00-241 Warszawa, Poland. [3]nstitute of Electrical Engineering, Slovak Academy of Sciences, Dubravska cesta 9, 842-39 Bratislava, Slovak Republ.

XRD spectra of the ceramic monocores made by the powder-in-tube (PIT) method at different depths have been made. The texture distribution throughout the thickness of the ceramic cores has been quantified and discussed with respect to optimal process parameters leading to maximal texturization. To differentiate tapes in texturization degree and phase content the sequence of thermomechanical steps involving two-axial and eccentric rolling was applied. Results obtained have confirmed different susceptibility to texturization between the two main phases ('high' for 2223 and 'weak' for 2212) and have visualized differences between ceramic at Ag-interface vs. core center. Evidence of 2223-phase c-axis constant decrease within the ceramic core has been demonstrated. The texture distribution followed the general trend to that at the Ag/ceramic interface: better texturizaton at the interface led to deeper grain alignment beneath the surface and higher texturization degree in the region closer to core axis. Detailed study of the relationships between the mechanical deformation and texture distribution across the cores have been performed. Thermomechanical treatment has produced a stronger texture in 2223-phase which has penetrated deeper into the ceramic core than in 2212-phase. This effect is additionally enforced by the higher volume content of the first.

6–33

An XRD Rietveld Analysis of the Phase Assemblage in PBSSCO PIT Precursor Powders.

W.W. Schmahl[1], *S. Raeth*[1], *B. Seipel*[1], *L. Woodall*[2], *M. Bartels*[2] and *M. Gerards*[2]. [1]Ruhr Universität - Bochum and Tübingen Universität, Germany. [2]Merck KGaA Darmstadt, D-64271 Darmstadt, Germany.

The metastable phase assemblage in the PBSCCO precursor powders for 2223-PIT HTSC tapes investigated here consist mainly of Pb-free 2212 and the 'minor' phases $(Ca_{1-x}\ Sr_x)_2\ PbO_4$, "3321" :$(Pb_{3-x}Bi_x)(Sr_{3-y}\ Ca_y)(Ca_{2-z}\ Sr_z)Cu_{1-u}O_{9+\delta}$, "1-1" : $(Ca_{1-x}\ Sr_x)_{0.8}$ Cu $O_{2-\delta}$, "14-24": $(Sr_{14-x}\ Ca_x)Cu_{24}O_{41+\delta}$. Despite strongly overlapping diffraction peaks we positively identified these phases by careful synthesis of the correct member of the solid solution series. The CuO and $Ca_{2-x}Sr_xCuO_3$ phases are not present. For the Rietveld analysis we used commensurate approximations to all structures. The incommensurate satellite peaks of the 2212 phase, however, are comparable in intensity to the peaks of the minor phases; the satellite peaks were included by a Le Bail fit based on the incommensurate wave vector q = 0.209 a* - c*. We automatized the Rietveld refinement strategy for routine determination of the relative abundance of these phases.

6–34

Preparation of Bi(2223) tape conductors with resistive matrix components and new composite structures.

W.Goldacker, *R.Nast*, *H.Eckelmann* and *J.Krelaus*. Forschungszentrum Karlsruhe-Institut für Technische Physik, Eggenstein-Leopoldshafen, Baden-Württemberg, 76344, Germany.

The application of Bi(2223) Tapes in AC operated components of energy technique, like transformers, motors, coils (SMES) and cables requires an improved conductor performance with respect to all the aspects: filament twist, low AC losses, mechanical reinforcement and high transport currents. New tape concepts as resistive barrier matrix and the ring bundled barrier conductor with stranded filament structure have changed boundary conditions for the preparation of the conductor and the heat treatment to react the Bi(2223) phase compared to standard Bi(2223) tapes. We present the different preparation techniques for resistive barrier tapes and for novel ring bundled barrier tapes with stranded filaments and we present our investigations of the consequences for the thermomechanical treatment of the final conductors to form the Bi(2223) phase and to obtain an optimised transport current density. Special interest was invested in the oxygen exchange conditions between the superconducting filaments and the annealing atmosphere for the different sheath configurations including a dispersion hardened AgMg component, investigated by means of TG measurements. The results will be correlated and discussed with the achieved superconducting performance and the AC loss properties of the conductors. work partially performed under EC-contract BRPR-CT95-0030

6–35

Thermal Quenches in Monolayer Bi-2223 Coil.

F. Chovanec[1], *P. Usak*[1], *L. Jansak*[1], *A. Kasztler*[2], *H. Kirchmayr*[2] and *M. Polak*[1]. [1]Institute of Electrical Engineering, Slovak Academy of Sciences,Bratislava,Sk 84239, Slovakia. [2]Institut fur Experimentalphysik, Technische Universitat Wien, Austria.

E - J characteristics and thermal quenches of a single layer He gas cooled Bi-2223 coil were examined over the temperature range of 4.2K to 77K in various external magnetic fields. The quenches were induced by DC as well as AC current. The conventional concept for the critical current density charakterised by 1 μV/cm criterion is compared with that of a maximum admissible dissipation due to the heat/quench propagation. It is shown that the stability consideration of the high temperature superconducting coil is very different from that of low temperature one. Due to variation of local critical current along the tape the dissipation has also a local character. The approach to designing of high temperature superconducting windings and magnets is discussed.

6–36

Bi,Pb(2212) grain growth and relationship between the initial and final texture in Ag-sheathed Bi,Pb(2223) tapes.

J.-C. Grivel[1,2], *Y.L. Liu*[1], *H.P. Poulsen*[1], *L.G. Andersen*[1], *T. Frello*[1], *N.H. Andersen*[1] and *W.G. Wang*[2]. [1]Risø National Laboratory, DK-4000 Roskilde, Denmark. [2]Nordic Superconductor Technologies, Priorparken 685, DK-2605 Bröndby, Denmark.

In Ag-sheathed Bi,Pb(2223) tapes, it has previously been shown that the texture of the Bi,Pb(2212) phase present in the precursor powders significantly improved during the first heating step. We present studies of the Bi,Pb(2212) phase texture development during this stage. After the initial tape deformation, the Bi,Pb(2212) grains are either isolated or gathered in compact groups. During heating (T > 700C) grain boundaries in the compact groups vanish rapidly and these have a greater tendency to grow as one big grain as compared to the small single grains. As a result of the preferential growth process the volume fraction of the aligned 2212 is increased, leading to texture sharpening. The mechanisms of the preferential growth process are discussed. In view of studying the influence of the initial Bi,Pb(2212) texture on the final tape, a short pre-annealing treatment was performed in order to obtain various initial Bi,Pb(2212) average textures. These tapes were then heat treated several times in order to convert the precursor powders into Bi,Pb(2223). The initial Bi,Pb(2212) and final Bi,Pb(2223) textures have been investigated by means of synchrotron diffraction and scanning electron microscopy. The relationship between the initial and final texture and its influence on the critical current of the Ag-sheathed tapes are discussed.

6–37

YBCO Coated Tapes Fabricated by Magnetron Deposition.

K.H. Müller, *N. Savvides*, *S. Gnanarajan*, *A. Katsaros*, *A. Thorley*, *J. Herrmann* and *R. Clissold*. CSIRO Telecom. and Industrial Physics, Lindfield, NSW 2070, Australia.

YBCO coated superconducting tapes represent the second generation of high-J_c conductors which are expected to extend the application of HTS to high magnetic fields. We have used magnetron deposition techniques to fabricate YBCO tapes. The biaxially aligned YSZ and CeO_2 buffer layers, 300 nm thick, were deposited at room temperature onto Hastelloy substrates by magnetron IBAD. The technique combines a magnetron to sputter a YSZ target or a Ce metal target to provide the condensing species with a Kaufman-type ion beam source to provide concurrent bom-

bardment by Ar^+ ions at 55° from the normal to the substrate. The epitaxial $YBa_2Cu_3O_7$ thin films, 150 - 300 nm thick, were deposited at 750°C by magnetron sputtering using a stoichiometric $YBa_2Cu_3O_7$ target sputtered in an argon/oxygen plasma. X-ray θ - 2θ diffraction, rocking curves (ω scans), ϕ scans and pole figures are used to determine the crystalline quality and biaxial alignment of the films. The buffer layers have (111) poles in the direction of the ion beam and a minimum full-width at half-maximum (FWHM) $\Delta\phi = 13°$. For the best YBCO tapes the (103) pole gives $\Delta\phi = 10°$ and $\Delta\omega = 2°$, and the critical current density $J_c = (0.9\text{–}1.5)\times10^6$ A cm^{-2} at 77 K.

6–38

Characterisation of substrates and buffer layers for next-generation HTS coated conductor tapes.

C. Prouteau[1], *J. S. Abell*[1], *T. W. Button*[1], *E. Maher*[2], *K. Marken*[3] and *B.A. Glowacki*[4]. [1]School of Metallurgy, University of Birmingham, Edgbaston, Birmingham B15 2TT. [2]Oxford Instruments plc, Old Station Way, Eynsham, Witney, Oxford, OX8 1TL. [3]Oxford Superconducting Technology, 600 Milik Street, PO Box 429, Carteret, New Jersey, 07008 0429, USA. [4]Dept. of Materials Science and Metallur y, University of Cambridge, Pembroke Street, Cambridge CB3 OH.

Grain boundaries are ubiquitous within $YBa_2Cu_3O_{7-\delta}$ films grown on buffered metallic substrates. Since the critical current density of superconductors is reduced by grain boundaries, metallic tapes and buffer layers with a high degree of texture need to be developed. The use of Electron Back Scattering Diffraction in the SEM is a powerful technique to evaluate the quality of such tapes. Crystal orientation maps obtained by EBSD can be processed into misorientation grain maps to show grain size and grain boundary distribution. EBSD also allows evaluation of the homogeneity of the substrate and can track the improvement of the texture at each stage of the growth. A much better statistical view is obtained by acquiring large area orientation maps and distributed discrete maps using automated stage scanning to cover larger samples. The combination of EBSD and other characterisation techniques such as AFM or TEM to assess the different layers as well as correlation of these results with critical current density measurement will lead to a better understanding of the growth process and superconducting behaviour of these tapes. Texture and surface characterisation of substrates and layers will be presented and the influence of substrate quality and growth parameters will be discussed.

6–39

YBCO - deposition on metal tape substrates.

J. Egly[1], *R. Nemetschek*[1], *W. Prusseit*[1], *B. Holzapfel*[2] and *W. Goldacker*[3]. [1]THEVA Thin Film Technology GmbH, 85386 Eching, Germany. [2]IFW Dresden, 00171 Dresden, Germany. [3]FZ Karlsruhe, 76021 Karlsruhe, Germany.

Ni and Ni-alloy substrates fabricated at the IFW Dresden and FZ Karlsruhe were used for the deposition of YBCO - tape conductors. In plane texture of the metallic substrates was achieved by mechanical rolling (RABiTS technique) and re-crystallisation at temperatures > 850°C resulting in well aligned grains of typical 100 μm size. The substrates were characterised by X-ray pole figures, exhibiting a FWHM in plane texture of 6°, and by electron backscattering patterns (EBSP). Short length tape samples were heated up to the deposition temperature of 670°C in reducing Ar/H_2 - gas ambient to avoid oxidation of the Ni substrate surface. Subsequently, CeO_2 - based buffer layers were deposited by vacuum evaporation. YBCO films were grown by thermal coevaporation and intermittent oxidation in a rotating disk substrate holder - a technique known as Garching process. We obtained transition temperatures up to 87 K and critical current densities at 77K of up to 0.2 MA/cm^2 on unpolished and 0.4 MA/cm^2 on polished substrates. Currently, this evaporation technique is modified for continuous operation employing AAS rate control, automatic refilling of the boat sources, and a reel to reel tape winding mechanism capable of YBCO - deposition on 10 mm wide, long length tape with a speed of 4 m μm/hour.

6–40

LPE Growth of REBCO Thick Films.

X. Qi, *J.J. Wells* and *J.L. MacManus-Driscoll*. Dept of Materials, Imperial College, London SW7 2BP.

Liquid phase epitaxy (LPE)is a fast and scalable method to produce thick films for high-Jc applications. A LPE growth system has been built to grow thick REBCO films under controlled pO_2 pressure. Films of different RE ions and their mixtures, such as Yb_xEr_{1-x} have been grown on $LaAlO_3$ substrates. XRD and SEM showed good quality of the films, which were (001)-oriented and typically 10-15 μm thick after growth in the high-temperature solution for about 10 mins. With a suitable composition and combination of different RE ions, the growth temperature could be lower than 930 °C, at which silver substrates could be used for the film growth without other additives in the high- temperature solution. Details of LPE growth and structural and electrical characterisation of grown films will be reported.

6–41

Study of the recrystallisation of nickel and Ni-based alloy substrates for YBCO coated conductors.

B. Lehndorff[1], *M. Hortig*[1], *B. Mönter*[1], *H. Piel*[1], *J. Pouryamout*[1], *N. Pupeter*[1] and *E. Bischoff*[2]. [1]Cryoelectra GmbH, Wettinerstr. 6h, D-42287 Wuppertal, Germany. [2]MPI für Metallforschung, Seestr. 92, D-70174 Stuttgart, Germany.

Nickel and nickel based alloys like Cu-Ni, Ni-Cr and Ni-Mo are good candidates for substrates of YBCO coated conductors. Upon strong mechanical deformation and annealing in vacuum a cube texture is built in these materials. Consequently they may serve as biaxially textured substrates for epitaxial growth of YBCO on appropriate buffer layers. On these multilayer systems YBCO is known to carry high critical currents /1/. Recrystallisation experiments on Nickel and various Ni-based alloys are presented. Good cube texture was achieved for example in a Ni-Cu composite tape. The texture was analyzed using EBSD (electron backscatter diffraction). Measurements of surface roughness are also presented.

/1/ A. Goyal et al; Epitaxial superconductors on rolling-assisted biaxially-textured substrates (RABiTS): A route to-

wards high critical current density wire. Appl. Supercond. **4, (1998) 402**

6–42

Biaxially textured Ni and CuNi alloy substrate tapes for HTS coated conductor applications.

A.Tuissi[1], *R.Corti*[1], *A.P.Bramley*[2], *M.E.Vickers*[2] and *J.E.Evetts*[2]. [1]Istituto per la Tecnologia dei Materiali e dei Processi Energetici del Consiglio Nazionale delle Ricerche - CNR TEMPE, C.so P.Sposi 29, 23900 Lecco, Italy. [2]University of Cambridge, Department of Materials Science and Metallurgy, Pembroke Street, Cambridge,CB2 3QZ, U.K.

Since the demonstration of the RABiTS (Rolling Assisted Biaxially Textured Substrate) procedure as a viable approach for the production of long HTS superconducting tapes, several studies have been directed towards the development of suitable metallic substrates. In this work, $Cu_{90}Ni_{10}$, $Cu_{70}Ni_{30}$ (at.%) non-magnetic tapes and Ni tapes have been prepared as substrates for high critical current density YBCO film deposition. CuNi alloys were prepared using a plasma arc furnace and the biaxially textured tapes were formed by recrystallization after heavy cold rolling. The microstructure of the CuNi tapes has been investigated by Θ-2Θ X-ray diffraction as a function of recrystallization temperature and the texture has been studied using pole figure X-ray analysis. The mechanical properties and the roughness of the tapes produced have also been characterised by stress-strain measurements and Atomic Force Microscopy respectively. The cube recrystallization conditions for CuNi alloys have been defined and a degree of biaxial grain alignment comparable to that in Ni tapes has been achieved using $Cu_{70}Ni_{30}$. The mechanical properties of Ni and $Cu_{90}Ni_{10}$ are quite similar while the $Cu_{70}Ni_{30}$ alloy has higher mechanical strength. $Cu_{70}Ni_{30}$ can therefore be used as a viable non-magnetic, low cost, biaxially textured metallic substrate for YBCO film deposition.

6–43

Texture Development in Pd and Ag Layers on Ni-based Substrates for Coated Conductor Applications.

N.A. Rutter[1,2], *M.E. Vickers*[1], *Z.H. Barber*[1,2], *A.P. Bramley*[1], *B.A. Glowacki*[1,2], *J.E. Evetts*[1,2] and *E. Maher*[3]. [1]Department of Materials Science and Metallurgy, University of Cambridge, Pembroke Street, Cambridge, CB2 3QZ, U.K. [2]IRC in Superconductivity, Madingley Road, Cambridge CB3 0HE, U.K. [3]Oxford Instruments plc, Old Station Way, Eynsham, Witney, OX8 1TL, U.K.

Silver buffer layers, with the cube texture, {100}⟨001⟩, have been deposited onto nickel based substrates, using palladium as an intermediate layer. The substrates used were textured Ni-alloy tapes, suitable for large scale conductor development and also thin film Ni, grown on (100) MgO single crystals as a control. The overall texture of the substrates and films has been characterised by X-ray pole figures and rocking curves and the surface texture analysed by Electron BackScatter Diffraction (EBSD). Depending on the deposition temperature used, alternative in-plane orientations were observed in the Ag layer, consistent with a near coincidence site lattice model. In those films deposited on the almost perfectly aligned Ni (on MgO), the crystallographic alignment of each layer was found to be less perfect than the underlying one. However, in the films deposited on the Ni-alloy tapes, an improvement in alignment was evident in each successive layer. By improving the texture in this way, a Ag buffer layer with in-plane and out-of-plane FWHM values of around 4° has been produced. Experiments have been carried out to investigate the interdiffusion of the layers in order to predict the conditions which may be used for superconductor deposition.

6–44

Formation of native cube textured oxide on a flexible Ni-alloy tape substrate for coated conductor applications.

N.A. Rutter[1,2], *B.A. Glowacki*[1,2], *J.E. Evetts*[1,2], *H. te Lintelo*[3], *R. De Gryse*[4] and *J. Denul*[4]. [1]Department of Materials Science and Metallurgy, University of Cambridge, Pembroke Street, Cambridge, CB2 3QZ, U.K. [2]IRC in Superconductivity, Madingley Road, Cambridge CB3 0HE, U.K. [3]Innovative Sputtering Technology, Karreweg 18, B-9870 Zulte, Belgium. [4]Centrum voor Vacuum en Materiaalwetenschappen (CVM), Krijgslaan 281 / S1, B-9000 Gent, Belgium.

The oxidation behaviour of a Ni based alloy with a strong cubic (100)<001> texture has been investigated in an attempt to develop buffer layers suitable for deposition of well aligned superconductors. It is known that pure Ni may be oxidised to produce a cube textured oxide in a process known as surface oxidation epitaxy, but the addition of an alloying element with a different oxygen affinity complicates the process. Though a cube textured oxide was not produced initially under any of the oxidation conditions used, an additional stage, involving oxide removal and re-oxidation leads to the formation of an oxide with an excellent cube texture, having in-plane and out-of-plane X-Ray FWHMs of around 8 °. We will report attempts to deposit further buffer layers and superconducting layers on the native cube textured oxide.

6–45

Recrystallization Kinetics of Biaxially Textured Ni Substrates for YBCO Coated Conductors.

R. Nast[1], *W. Goldacker*[1], *B. Obst*[1] and *G. Linker*[2]. [1]Forschungszentrum Karlsruhe, Institut für Technische Physik, Karlsruhe, D-76021, Germany. [2]Forschungszentrum Karlsruhe, Institut für Nukleare Festkörperphysik, Karlsruhe, D-76021, Germany.

Cubic recrystallized Ni substrates are used to produce YBCO coated conductors with intermediate epitactical coating with buffer layers (CeO_2 and YSZ). The quality of the cubic structure, grain alignment and content of wrongly aligned grains determines considerably the texture quality and thus the attainable transport current in the superconducting YBCO layer. Small tape thickness are desired for high technical current densities. In order to ensure a spatial delimitation of the texture errors (untextured grains) small grain sizes, as small as possible, are targeted. Nickel tapes of 20 - 100 μm thickness were examined systematically with regard to the influence of the Nickel purity and the annealing temperature on the recrystallization texture

quality. Special attention was given to the phase formation of the cubic structure. With a new annealing technique and device in combination with x-ray structure analysis a time resolved detection of the cubic phase formation was possible which allows a characterization of the recystallization kinetics. During the first seconds of the annealing process the grain nucleation initiates and depending on temperature most of the recrystallization process has occurred during the first minutes. Our investigations extend the possibilities for improved heat treatment procedures for a further optimized microstructure of the substrate tapes.

6–46

Raman and X-ray Characterisation of Structural Disorder in YBCO Thick Films Grown at High Rates for IBAD Conductors.

G. Gibson[1], *S. R. Foltyn*[2], *N. Malde*[3], *L.F. Cohen*[3], *P.N. Arendt*[2], *E.J. Peterson*[2], *D.E. Peterson*[2] and *J.L. MacManus-Driscoll*[3]. [1]Dept. of Materials Science and Metallurgy, Cambridge University, Pembroke St., Cambridge, CB2 3QZ. [2]Superconductivity Technology Center, Los Alamos National Laboratory, Los Alamos, New Mexico 87545, U.S.A. [3]Centre for High Temperature Superconductivity, Imperial College of Science Technology and Medicine, Prince Consort Road, London SW7 2AZ, U.K.

In order to achieve scaleability in processing of IBAD conductors for commercial applications, rapid YBCO film growth rates (>100Å /s) are required. The same is also true for other growth routes for YBCO conductor thick films (e.g. via LPE or CVD). However, rapid growth leads to crystalline disorder in the film, with the formation of planar and point defects (including cation disorder). We have grown films by PLD on SrTiO-3- substrates at rates from 2Å /s to 240Å /s, and have measured the cation disorder in the films by Raman spectroscopy and x-ray diffraction. We will report on the correlation between growth rate, intensity of the Raman (580) to (340) ratio, 'c' lattice parameter, intensity of the (005) to (006) ratio, non-uniform strain, Jc, and the influence of post-annealing on disorder and resultant microstructure.

6–47

Heteroepitaxial growth of oxide buffer layers by pulsed laser deposition on biaxially oriented Ni and Ni-alloy tapes.

B. Holzapfel[1], *L. Fernandez*[1], *M. Arranz*[2], *N. Reger*[1], *B. de Boer*[1], *J. Eickemeyer*[1] and *L. Schultz*[1]. [1]IFW Dresden, Institute of Metallic Materials, D-01171 Dresden, Germany. [2]Departamento de Fisica Aplicada, Facultad de Ciencias Quimicas, UCLM, 13071 Ciudad Real, Spain.

The use of Rolling Assisted Biaxially Textured Substrates (RABiTS) is a very promising route for producing Y123 coated conductors. The heteroepitaxial growth of the oxide buffer layers is a critical point in this approach and there are serious problems connected to the formation of NiO on the metal surface prior to the buffer layer deposition, to diffusion of Ni at the elevated deposition temperatures, and to cracking of the buffer layers. Here we report on pulsed laser deposition (PLD) of YSZ, $SrTiO_3$ and Y_2O_3 buffer layers on recrystallised Ni and nonmagnetic NiCr tapes with an in-plane orientation width (FWHM) of less than 10°. The heteroepitaxial growth of the oxide films and their microstructure was investigated using standard ex-situ techniques (x-ray diffraction, SEM, AFM). Also model experiments using single crystalline Ni and Ni-alloy films prepared by e-beam evaporation were performed to look at the heteroepitaxial growth conditions and the Ni-diffusion in these multilayer structures.

6–48

Effects of impurities on texturing of Ni tapes and the properties of YBCO films.

S.H. Oh, *J.E. Yoo*, *K.C. Chung*, *H.S. Kim*, *B.S. Lee*, *K.H. Lee*, *J.S. Lee*, *H.K. Lee* and *D. Youm*. KAIST, 373-1, Kusong-dong, Yusong-gu, Taejon, 305-701 Korea.

Texturing of rolled and annealed Ni tapes with the impurities, Fe, Mn, Co, Cr was investigated. The concentration range of the impurities was 0 to 1%. The results of XRD measurements shows the textures strongly depended on the impurities and their concentrations. The Ni tape with 0.2% of Fe gave the best quality of texture. However the tape with 0.1% Mn showed a large stiffness for the elastic property although its texture was not the best. Using the buffer layer, $CeO_2/YSZ/CeO_2$, the YBCO film was deposited on the tapes. According to the texture qualities of Ni tapes with various impurities, the T_c and J_c were in wide ranges. The best one showed $5x10^5 A/cm^2$ at 77K.

6–49

High J_c YBCO Thick Films on Biaxially Textured Ni-V Substrate with CeO_2/NiO Intermediate Layers.

V. Boffa[1], *T. Petrisor*[1,2], *F. Fabbri*[1,3], *C. Annino*[1], *D. Bettinelli*[1,3], *G. Celentano*[1], *L. Ciontea*[1,2], *U. Gambardella*[1,4], *G. Grimaldi*[1] and *A. Mancini*[1]. [1]ENEA-Centro Ricerche Frascati. [2]Technical University of Cluj, 3400 Cluj-Napoca, Romania. [3]Under PIRELLI-ENEA contract. [4]INFN-LNF, 00044 Frascati, Rome, Italy.

Biaxially aligned $YBa_2Cu_3O_{7-\delta}$ thick films were successfully deposited by pulsed laser ablation on biaxially textured Ni-V metallic substrate, using NiO as a first buffer layer. With respect to Ni, the main advantages of using a Ni-V substrate consist in lower ac losses, higher strength after recrystallization and easier formation of (100)[001] NiO textured layer on its surface. The epitaxially YBCO thick film grown on CeO_2/NiO buffer layer structyre has the T_c onset of 90.9K and zero resistance at 86K. The critical current density, J_c, of the YBCO film epitaxially grown on this configuration is higher than 10^5 A/cm^2 at 77K and in zero magnetic field. The Φ-scans and ω-scans of YBCO thick film have a FWHM of 11° and 8°, respectively. The preliminary results are encouraging for the futher scaling up of the process to YBCO long tape fabrication.

6–50

Deposition of Buffer and YBCO-Layers on Textured Metal Tapes Using RF and DC Sputtering Techniques.

S. Kreiskott[1], *M. Getta*[1,2], *B. Lehndorff*[1,2], *B. Mönter*[1,2], *G. Müller*[2], *B. Skriba*[1], *R. Wagner*[1,2] and *E. Bischoff*[3]. [1]Cryoelectra GmbH, Wettinerstr. 6H, D-42287 Wuppertal. [2]Bergische Universität Wuppertal, Gaußstr. 20, D-42097 Wuppertal. [3]MPI f. Metallforschung, Seestr. 92, D-70174 Stuttgart.

Techniques are reported for sputter deposition of biaxially oriented buffer layers and epitaxial YBCO films on textured metal tapes produced from Ni, NiCr, NiMo and NiCu alloys and Ni-Cu composite tapes. These tapes can be applied as long flexible substrates for the heteroepitaxial growth of biaxially aligned YBCO films with high critical current density J_C. RF sputtering was used to deposit biaxially oriented CeO_2, YSZ and MgO layers on the metallic substrates. The oxide layers serve both as a chemical and a structural buffer. The buffer layers were characterized by scanning electron microscopy, electron backscatter diffraction, Rutherford backscattering and optical microscopy investigations. Subsequent YBCO films were deposited by high-pressure DC sputtering. The YBCO films were investigated by inductive measurements ($J_C - T_C - Tester$) and electron and optical microscopy. Preliminary results of microscopy investigations of CeO_2-YSZ-CeO_2 buffer layers show smooth surfaces on a μm-scale. A strong influence of substrate temperature on the behaviour of film growth was found.

6–51

Non magnetic $Ni_{100-x}V_x$ Biaxially Textured Substrates for YBCO Tape Fabrication.

T. Petrisor[1,5], *V. Boffa*[1], *S. Ceresara*[2], *C. Annino*[1], *D. Bettinelli*[1,6], *F. Fabbri*[1,6], *U. Gambardella*[1,7], *G. Celentano*[1], *P. Scardi*[3] and *P. Caracino*[4]. [1]ENEA-Centro Ricerche Frascati. [2]CNR-TEMPE, C.so Promessi Sposi, 29, 22053 Lecco, Italy. [3]Università di Trento, Dipartimento di Ingegneria dei Materiali, 38050 Mesiano, Trento, Italy. [4]PIRELLI CAVI&SISTEMI, viale Sarca 222, 20126 Milan, Italy. [5]Technical University of Cluj, 3400 Cluj-Napoca, Romania. [6]Under PI ELLI-ENEA contract. [7]INFN-LNF, 00044 Frascati, Rome, Italy.

One of the most promising techniques for high J_c YBCO tape fabrication is the deposition of superconducting thick film on a biaxially oriented metallic substrate. Until now, Ni has been the most used substrate. The ferromagnetic behaviour and the low strength after recrystallization represent the main drawbacks of the Ni substrates. This paper presents the magnetic, mechanical and structural properties of a new non magnetic metallic substrate based on $Ni_{100-x}V_x$ solid solution. The role of vanadium is to decrease the Curie temperature of Ni and as a consequence to reduce the ac losses in the substrate. At the same time Ni-V alloy preserves the crystalline properties of Ni. The (100)[001] texture was induced by cold-rolling processing followed by a recrystallization thermal treatment. For the whole range of concentration (0<x<12) the sample exibits a sharp well developed cube texture with FWHM of Φ-scans and ω-scans of 11.3° and 5.5° respectively. The Curie temperature linearly decreases with vanadium concentration reaching the zero value for about 11.5 at %. The stress-strain diagram at room temperature shows that the $Ni_{89}V_{11}$ substrate Yield Strength is improved with respect to Ni one. At 77K this improvement is about one order of magnitude.

6–52

Influence of external strains on YBCO films deposited on thin buffered technical substrates.

F. García-Moreno[1,2], *A. Usoskin*[1], *H.C. Freyhardt*[1,2], *J. Wiesmann*[2], *J. Dzick*[2] and *J. Hoffmann*[2]. [1]Zentrum fuer Funktionswerkstoffe Goettingen gGmbH, Windausweg 2, D-37073 Goettingen, Germany. [2]Institut fuer Materialphysik, Universitaet Goettingen, Windausweg 2, D-37073 Goettingen, Germany.

The strain behaviour at 77 K and 0 T of YBCO films with high critical densities J_c of 2 MA/cm2 on Ni, 1.2 MA/cm^2 on YSZ and stainless steel was investigated. The substrates - Ni, YSZ and stainless steel tapes - were previously polished and covered with a biaxially textured YSZ IBAD layer. A study of J_c of 600-800 nm-thick YBCO films under compressive and tensile strains, caused by substrate bending, has been performed at 77 K by employing different bending tecniques, using e.g. 4-point measuraments, in situ variation of the bending radius, etc. The critical current densities of the films were measured by dc as well as by ac inductive methods. The ranges of the J_c reversibility of under alternating strains was found. Within this range J_c is almost constant for a tensile strain, but shows pecularities under compression. Characteristic defects of the films induced by high tensile and compressive loads were analyzed by SEM. Changes of the film resistivity in the normal state in the course of bending were determined and used to interprete the electron-transport mechanisms.

This work is supported by the German BMBF and kabelmetal elctro GmbH (Project Nr. 13 N 6924/6)

6–53

YBCO Tape Coating by Thermal Reactive Co-Evaporation.

U.Schmatz, *Ch.Hoffmann*, *R.Metzger*, *M.Bauer*, *P.Berberich* and *H.Kinder*. Physikdepartment E10, Technische Universität München, 85747 Garching, Germany.

Coated tape conductors of YBCO require a deposition process allowing to obtain a high volume growth rate in order to produce long lengths of tape in a reasonable amount of time. Thermal reactive co-evaporation of the metals Y, Ba, and Cu has proven to be a very reliable and economical method to grow high quality YBCO films on large area substrates up to 20x20 cm^2. To use this area fully for the fast coating of a tape of 1 cm width we have developed a coating system where 15 loops of the travelling tape are coated simultaneously at 700°C. For high critical current densities, in-plane alignment of the YBCO film is necessary. Inclined substrate deposition (ISD) is a technique that allows to deposit in-plane oriented buffer layers suitable for YBCO growth. As high growth rates can be achieved with this technique, this process is compatible with the YBCO coating process. Results of YBCO films grown on ISD buffer layers of MgO deposited by simple e-gun evaporation on metallic substrates will be presented.

6–53P1

Evidence for the Influence of the Grain Structure of Textured Nickel Substrates on the YBCO Layer in Coated Conductors.

D.M. Feldmann, *J.L. Reeves*, *A. Polyanskii*, *S.E. Babcock* and *D.C. Larbalestier*. Applied Superconductivity Center University of Wisconsin - Madison 1500 Engineering Drive Madison, WI 53706 USA.

Evidence has been collected which strongly suggests that the grain structure of textured nickel substrates is directly influencing the connectivity of the YBCO layer in high J_c Coated Conductors (CC). Magneto-Optical Imaging (MOI) of CC samples from multiple sources shows similar electromagnetic granularity in the YBCO layer, on a scale which is the same as that of the underlying nickel grains. Combined BEKP, MOI, light microscopy and SEM show that induced currents flow in intra-granular regions and across low angle grain boundaries, selectively avoiding high angle grain boundaries and deep trench boundaries.

Session Cables, transformers and generators

6–54

Discussion of the current leads for AC magnet.

K. Kaiho[1], *H. Yamaguchi*[1], *K. Arai*[1], *T. Saitoh*[2], *S. Sadakata*[2], *H. Fuji*[2] and *M. Yamaguchi*[3]. [1]Electrotechnical Laboratory, Tsukuba, Ibaraki, 305-8568, Japan. [2]Fujikura Co.Ltd., Koto-ku, Tokyo, 135-0042. Japan. [3]Niigata Univ., Niigata-shi, Niigata, 950-2102, Japan.

Current leads of the superconducting magnet are usually the dominant source of extraneous heat leaking into the cryostats. Considerable attention has therefore been given to the current lead design. The development of fine filaments superconducting wires with high resistive matrix or high Tc superconductor permitted sufficiently reduce AC losses to have possibility to operate at power frequency. But up to now, there is no theoretical discussion on the current leads for AC operation magnet. In AC ope ration, current transfer uniformity from the normal metal conductor to the superconductor and the skin effect in the normal metal conductor have to be taken into consideration. In order to realize the uniform current transfer from the normal metal conductor to the superconductor, the shape of SN joint configuration is considered to be cylindrical. To eliminate the concentration of current to the narrow boundary area due to the skin effects, the cross-section of the normal metal around the SN boundary area is designed to be conical shape. A theoretical optimization is performed for the length and the cross-section of the normal metal conductor around SN boundary. As a results of study, some aspects in practical design are also discussed.

6–55

The magnetic field distribution in a transmission superconducting cables.

V.E. Sytnikov, *G.G. Svalov*, *P.I. Dolgosheev* and *N.V.Polyakova*. JSC"VNIIKP", Moscow, 111024, Russia.

The magnetic field distribution in a transmission superconducting cables. V.E. Sytnikov, G.G. Svalov, P.I. Dolgosheev, N.V. Polyakova. JSC "VNIIKP",shosse Entuziastov Moscow, 111024, Russia. The results of the theoretical and experimental study of the three-dimensional magnetic field distribution in a multilayer tape cable core are offered. One- and four-layer cable conductors from the tape superconductors are analyzed. The solutions are the engineering formulas for a calculation of the component of the three-dimensional magnetic field distribution in the vicinities of superconducting tapes. Study shows the effect of the relative gap between superconducting tapes on the inhomogeneity level of the magnetic field. The influence of the tape number in a layer on the magnetic field distribution with the removing from a superconductor surface has been analyzed. The results and equations of this study are the base for the analysis of the cable constructive parameters influence on the electromagnetic additional losses and critical current.

6–56

The study of additional losses in multilayer transmission cable.

G.G. Svalov, *V.E. Sytnikov*, *P.I. Dolgosheev* and *N.V. Polyakova*. JSC"VNIIKP", Moscow, 111024, Russia.

The study of additional losses in multilayer transmission cable G.G. Svalov, V.E. Sytnikov, P.I. Dolgosheev, N.V Polyakova. JSC "VNIIKP", Shosse Entuziastov,5 Moscow, 111024, Russia. The questions connected with the influence of cable design and of the transport current distribution between the layers on the energy losses are described. Theoretically it was investigated the influence of relative gap between tapes, the twisting angles of a tape in layers, the electrical and critical characteristics of a material on the losses in superconducting (hysteresis losses) and normal conducting (eddy current losses) cable elements. The results are reported. The factor of the losses increasing to the account of a gap between tapes has been offered. The increasing of these losses can reach several ten of percents in the superconductor and several hundred percents in the normal conducting constructive and stabilizing cable elements. The possibility of the minimization the energy losses by the selecting of the cable design parameters is discussed.

6–57

Transport AC losses in a coaxial cylindrical cable.

F. Gömöry. Institute of Electrical Engineering, Slovak Academy of Sciences, Dubravska 9, 84239 Bratislava, Slovak Republic.

To estimate the AC losses in superconducting cables for electric power transport, the monoblock model is often used. In this model, the cable is replaced by a solid tube with the radius and thickness corresponding to those of the real cable, and only the axial flow of current is considered. In the present work this approach is applied to the coaxial arrangement. In this case, the return conductor is a superconducting tube placed coaxially with the go conductor. Because the magnetic field is confined to the space between the tubes, it penetrates the return conductor from inside. Then, the straightforward application of the monoblock model derived for the field penetration from outside would be incorrect for loss calculation in the return conductor. Due to rotational symmetry of the problem, an analytical solution for total AC losses can be easily found. In the limit of thin-walled tubes

it approches the result obtained by applying the monoblock model also for the return conductor.

6–58

Influence of spread in tape properties on DC critical current of a superconducting cable.

F. Gömöry and *L. Frolek*. Institute of Electrical Engineering, Slovak Academy of Sciences, Dubravska 9, 84239 Bratislava, Slovak Republic.

DC critical current is one of the main characteristics of a superconducting cable. Its experimental determination should not represent any ambiguity, if all the tapes used in the cable were identical. However, real cables consist of tapes with properties given by production statistics. Then, one can expect the determination of critical current will depend on which tape the voltage taps have been soldered. In our paper a theoretical simulation of such an experiment is given. As a first step, the current-voltage characteristic of a multifilamentary BiSCCO-2223/Ag tape was replaced by a two-member polynomial. Then, the set of nonlinear equations for an array of parallel tapes was resolved in numerical way, taking into account the existence of contact resistances on current terminations. We consider the tapes are insulated along the cable, thus the redistribution of current in the cable happens in the terminal zone only. Important conclusion from our calculations is that the spread in cable critical current determined with voltage taps placed on different tapes increases with the resistance of the tape contact on the current termination.

6–59

A 10-20 kVA Single Phase High Temperature Superconducting Demonstrator Transformer.

M.K. Al-Mosawi[1], *C. Beduz*[1], *M. Webb*[1] and *A. Power*[2]. [1]Institute of Cryogenics, University of Southampton, Southampton SO17 1BJ, UK. [2]The National Grid Company plc, UK.

We report on the design, construction and characterisation of a 50Hz single phase High Temperature Superconducting (HTS) transformer which is designed to deliver 10kVA at 77.4K and 20kVA at 65K. The transformer is made of two windings positioned at the middle limb of a three limb iron core. The secondary winding is made of nine double pancake superconducting coils, using silver sheathed BPSCCO-2223 multifilamentary tapes with nominal critical current of 20A (at 77.4K and self field). The primary winding is made of copper to perform a direct comparison between HTS and conventional windings. Utilising a superinsulated non-metallic doughnut shaped dewar with low background heat intake, the AC losses in the superconducting winding have been measured by calorimetric method. Two powdered iron flux diverters (relative permeability of approximately 6) have been used inside the dewar at both ends of the superconducting winding in order to reduce the radial component of leakage flux density in the HTS tapes. This work was supported by The National Grid Company plc, UK. The Superconducting tape was supplied by Intermagnetics General Corporation , IGC.

6–60

A model for the current distribution and ac losses in superconducting multi-layer power cables.

M. Däumling. NKT Research Center, DK-2605 Brøndby, Denmark.

A superconducting cable consisting of a several layers is described theoretically. Discretised equations are given that can be used to describe the current distribution in the cable as a function of cable current. Solutions are worked out for the case of an ideal Bean type II superconductor, taking into account layer current saturation at the critical current Ic. The ac loss is shown to exhibit two different regimes. In a low current regime the current in each layer is below its respective Ic value, resulting in hysteresis loss in the presence of simultaneous currents and fields. In this regime all layer currents and the local magnetic fields are in phase with the externally applied current. As the critical current in a layer is reached current redistribution occurs and an additional loss mechanism appears that stems from the distortion of the local current and magnetic field values. Calculated ac loss values are compared to three cables from the literature, and good agreement is found.

6–61

Electrically and Thermally Insulated Connection for Liquid Nitrogen Transfer.

C.N. Rasmussen and *J.T. Holboell*. Technical University of Denmark Department of Electric Power Engineering Lyngby DK-2800 Denmark.

A prototype of a LN_2-cooled superconducting cable is currently under construction. The peripheral cooling circuit is kept at ground potential while the cable conductor is on high voltage. This requires a LN_2 feed-through that is electrically and thermally insulated. Foams are thermally insulating but generally not recommended for use in high electrical fields. However, recently Expancel has proved to withstand large electrical fields ($E_{Breakdown}$ = 6 kV/mm) at room temperature. In this work the electrical and thermal properties are investigated on full-size constructions at temperatures between 77 K and 300 K. The model constitutes 2 coaxial glass fibre reinforced polymer (GFRP) tubes with Expancel foam in-between. The goal is to construct a LN2 feed-through for a system voltage of 36 kV. Limitations of the approach are discussed and suggestions on how to connect superconducting components at high voltage will be given.

6–62

Bending test of a 3 meter long, 2 kArms HTS cable conductor.

C.N. Rasmussen[1], *S. Hutchinson*[1], *M. Däumling*[1], *D.W.A. Willén*[1], *Martin Andersen*[2], *K. Høj Jensen*[3], *C. Træholt*[3] and *O. Tønnesen*[3]. [1]NKT Research Center, Priorparken 878, DK-2605 Brøndby, Denmark. [2]NKT Cables, Priorparken 510, DK-2605 Brøndby, Denmark. [3]Technical University of Denmark, Department of Electric Power Engineering, Bldg. 325, DK-2800 Lyngby, Denmark.

The mechanical flexibility of a high temperature superconducting (HTS) cable needs to be comparable to a conventional cable so that it can be spooled on to a cable drum, transported, and installed using conventional cable techniques. The HTS tapes are known to be sensitive to mechan-

ical stresses and strain. In order to reduce the mechanical stress on the tapes when the HTS cable is bent the tapes are spirally wound on a carrier (former), which also forms the cooling duct for a circulating coolant. This contribution present a test series where a 3 meter long cable conductor has been subjected to bending with progressively smaller radius of curvature. After each bending the I_C of the conductor was measured and compared with that of the virgin cable conductor. The result shows that it is necessary either to take precaution to reduce the stress and strains on the tapes, or design the cable with the degradation of I_C in mind.

6–63

Theoretical and experimental investigation of the effect of the gap between tapes on the critical current in a cable-like environment.

A. Bentien, *M. Däumling* and *D. W. A. Willén*. NKT Research Center, Priorparken 878, 2605 Brondby, Denmark.

Measurements have been performed on high-temperature superconducting (HTS) Bi-2223/Ag-alloy tapes in a magnetic field environment that resembles that of a single-layer superconducting cable. The HTS tapes in a single-layer cable model were connected in series using individual return leads that form a co-axial shield. The electrical properties were then measured for various configurations of these tapes. In particular, the value of the critical current was determined as a function of the gaps between the tapes. In self-field at 77 K, the tapes displayed a critical current of 22-24 A. In the cable-like environment, this value could increase by approximately 2-5 %. The magnetic field environment was also modeled using a commercial FEM software. The field-dependent current distribution within each tape was then modeled numerically using a critical-state approach. These calculations resulted in a theoretical estimate of the critical current of each tape that corresponded well with the measured results.

6–64

BSCCO/Ag Resonator Coil with an Air - Gap Iron Yoke.

O. A. Shevchenko[1], *A. Godeke*[1], *J. J. Rabbers*[1], *H. J. G. Krooshoop*[1], *G.C. Damstra*[2], *C. J. G. Spoorenberg*[3], *B. ten Haken*[1] and *H. H. J. ten Kate*[1]. [1]Faculty of Applied Physics, University of Twente, Enschede, The Netherlands. [2]University of Eindhoven, Eindhoven, The Netherlands. [3]Smit Transformatoren, B.V.,Postbus 9107,6500 HJ, Nijmegen, The Netherlands.

A potential application of high temperature superconductors and BSCCO/Ag tape in particular is in high quality AC coils operating at liquid nitrogen temperature. The paper presents results of a coil development that combines a high quality factor with a high specific inductive power. An air-gap iron yoke that provides much higher self-inductance surrounds a coil made of BSCCO/Ag tape. Optimal sizing of the air gap keeps the additional ac loss in the yoke at acceptable level. Depending on the application, the yoke can operate at room temperature or placed in liquid nitrogen. In addition, the stray field of the coil is greatly reduced. This is an important advantage, as a high quality factor requires low operating magnetic field. The latter requirement leads to relatively large dimensions of the coil and subsequently of the area where a high stray field is present. Both static and ac voltage-current curves of a 10-kVA superconducting model coil are measured. They are compared with those calculated from short sample results extracted for the same tape. The competitiveness of the superconducting coil is increased this way, as the price of high-T_c tapes is remarkably higher than of both iron and copper.

Work supported by the Netherlands Technology Foundation STW, Utrecht, The Netherlands

6–64P1

Theoretical geometric considerations about design of coreless superconducting transformers.

A. Alvarez, *P. Suarez* and *D. Caceres*. Universidad de Extremadura Escuela de Ingenierías Industriales Avda. de Elvas s/n. Apdo de correo, 382 06071 Badajoz (Spain).

When the core of a transformer is taken out, because of the very high magnetic field possible with superconducting currents, the lines of the field get out from the common path that concatenates the electrical circuits. Therefore, the transformer would work with a very low coupling factor k, not interesting in usual applications. Nevertheless, there are two geometric shapes that can make the electrical circuits share most of the field lines; these are: the annular and the toroidal geometries.

The first of one was studied by Fontana [Rev. Sci Instrum. 66 (3), March 1995], getting a coupling factor $k = 0.91$ with a 115 mm mean radius ring. The toroidal geometry is the other way to share all the field, because this vanishes out of the torus. So, if we place both electrical circuits (wire or tape) over the torus surface, the coupling factor must get close to $k = 1$. At present, we are studying this geometry and this paper shows the theoretical conclusions of it.

Furthermore, we can think of an intermediate geometry made with a torus but winding the wire or tape in a direction other than that with minimum radius. The current has a component along the torus direction that behaves just like the currents in the Fontana's transformer.

Session Materials related to electronic applications

6–65

Even and Odd Hall Effects in YBCO Thin Films.

V.Shapiro, *A.Verdyan*, *I.Lapsker* and *J.Asoulay*. Center for Technological Education Holon affiliated with Tel-Aviv University.

Hall resistivity measurements as a function of temperature in vicinity of T_c were carried out on thin film YBCO superconductors. On the same films we have observed the anomalous odd Hall effect and even Hall effect that was insensitive to the direction of magnetic field along c-axis of the film. The even Hall effect is discussed on the basis of directional motion of vortices along certain net of channels. Direction of the channels is defined by condition of perpendicularity to pinning forse. The magnitude of the even Hall voltage depends on quantity and distribution of pinning centers. As well presence as the random character of even Hall effect are connected with pinning distribution in the film.

6–66
High pressure behavior of ferroelectric-superconducting composites $Pb_2(ScTa)O_6$-$YBa_2Cu_3O_{7-\delta}$.
J. Marfaing[1], *C. Caranoni*[1], *M. Krupski*[2], *J. Stankowski*[2], *S. Przybyl*[2], *B. Andrzejewski*[2], *A. Kaczmarek*[2] and *B. Hilczer*[2]. [1]Lab. MATOP-CNRS, Case 151, F-13397 Marseille Cedex 20. [2]Inst. of Molecular Physics, Pol; Aca. Sci., Pl-60179 Poznan.

In high-T_c cuprate superconductors, high-pressure influences the superconducting hole-like carrier concentration resulting in a shift of T_c under pressure. Moreover, the variations of T_c with the hole concentration n in the CuO_2 planes are approximated by inverted parabola, similarly to the dependence of T_c under high pressure. For $YBa_2Cu_3O_{7-\delta}$ (YBCO), both T_c and its pressure dependence, dT_c / dp , strongly vary with the oxygen content δ. Recent results concerning ferroelectric-superconductor composites $Pb_2(ScTa)O_6$(PST)-YBCO reveal the change of the T_c with the PST variable fraction in weight x. We investigate the effect of hydrostatic pressure ($p < 0.6$ GPa) on T_c in PST-YBCO composites using the method of magnetically modulated microwave absorption . The T_c dependence on x (0, O.25, 0.5 and 0. 75) is approximated by an inverted parabola function whereas the influence of pressure on T_c is represented by the equa tion dT_c / dp = 0.061(2) - 1.72(6) x. The result can be explained assuming that PST influences the superconducting carrier concentration similar to chemical substitution in YBCO. It is suggested that Sc^{+3} ions diffuse from PST to Y or Cu sites in the YBCO lattice during the sintering.

6–67
Peculiarities of Noise Behavior of YBCO Films Showing Strong Pinning.
I.A Khrebtov[1], *A.D. Tkachenko*[1], *A.V. Bobyl*[2], *F.C. Klaassen*[3], *J.M. Huijbregtse*[3] and *B. Dam*[3]. [1]S.I. Vavilov State Optical Institute, St. Petersburg, 199034, Russia. [2]St. Petersburg State Technical University, 195251, Russia. [3]Vrije Univers., De Boelelaan 1081, 1081HV Amsterdam, Netherlands.

At present devices of HTS electronics such as detectors and SQUIDs are being developed. HTS films with high critical currents and low noise are necessary for the achievement of high performance of those devices. The results of noise research on YBaCuO fillms are reported. The films were deposited by means of laser ablation on STO substrates. XRD and AFM techniques were used for structural characterization of the films. The current dencity j_s(B,T) (up to 10^12 A/m^2 at T=4.2 K and B=0 T) was measured using torque magnetometry. The temperature, resistance and current dependences of excess 1/f noise were investigated in the frequency region of 1 Hz-1 kHz and temperature interval of 80-300 K. The peculiarity of the excess noise behavior is the comparatively large noise in the normal phase and the absence of noise at $T \ll T_c$ at j_s near the critical current density. The mosaic block model of strongly mismatched epitaxial films was used for the interpretaition of the obtained X-ray data.
The Monte-Carlo annealing model of the spatial oxygen distributions in the Cu plane allowed us to investigate the action of the block sizes on the energy spectra of the thermally activated oxygen jumps between sublattice positions of this plane and explain the behavior of flicker noise in YBaCuO films observed in the experiment. The absence of excess noise at the tail of the superconducting transition is due to strong pinning effects.

6–68
Surface resistance of YBCO thin films at THz-frequencies.
I.Wilke[1], *C.Rieck*[1], *C.Jaekel*[2] and *H.Kurz*[2]. [1]Universität Hamburg, Jungiusstrasse 11, D-20355 Hamburg, Germany. [2]Institut für Halbleitertechnik II, RWTH Aachen, Sommerfeldstrasse 24, D-52056 Aachen, Germany.

Hitherto, the surface resistance of high temperature superconductors (HTS) at THz-frequencies has been rather unexplored. However, due to advances in HTS thin film deposition, improvement and availability of compact closed-cycle coolers and the invention of new HTS THz-electronic devices, interest in THz-frequency properties of HTS thin films is strongly increasing. We present a study of the surface resistance of YBCO thin films at frequencies $87GHz < f < 2THz$ and temperatures $50K < T < 120K$ by time-domain Terahertz-transmission spectroscopy (TDTTS). We have investigated c-axis oriented YBCO thin films deposited on MgO substrates by laser ablation and thermal evaporation for various thickness between $80nm < d < 120nm$. We measure a surface resistance R_S=0.66Ω at T=77K and f=1THz. At T=53K and f=1THz the surface resistance is reduced to R_S=0.21Ω. Over the entire range of temperatures and frequencies investigated the measured surface resistance agrees very well with calculations by nested Fermi-liquid (NFL) theory. In our work the measurement of the surface resistance of HTS thin films by TDTTS is extended to higher frequencies and thicker films than previously by numerical solution of the complex transmission coefficient. Moreover, we sucessfully apply nested NFL-theory ,which incorporates the model of d-wave superconductivity, to the explanation of the temperature and frequency dependence of the surface resistance of YBCO in the THz-range. With our experimental and theoretical study of YBCO thin films we provide valuable reference data for HTS THz-electronic device simulation and performance prediction.

6–69
Development of Tl-2212 Films for Device Applications.
D.M.C. Hyland[1], *O.S. Chana*[2], *A.P. Jenkins*[1], *P.A. Leigh*[1], *P.A. Warburton*[2], *C.R.M. Grovenor*[3] and *D. Dew-Hughes*[1]. [1]Department of Engineering Science, University of Oxford, Parks Road, Oxford, OX1 3PJ, UK. [2]Department of Electronic Engineering, King's College London, Strand, London, WC2R 2LS, UK. [3]Department of Materials, University of Oxford, Parks Road, Oxford, OX1 3PH, UK.

HTS thin films of $Tl_2Ba_2CaCu_2O_8$ on $LaAlO_3$ substrates have been fabricated for a variety of device applications using a standard two stage process. An amorphous precursor film is R.f. sputtered from a ceramic Ba-Ca-Cu-O target, then subsequently annealed ex-situ in a sealed crucible with a suitable thallium source. Typical films have a

J_c of $10^5 Acm^{-2}$ and T_c of 105-108K. A successful micron scale lithography process for amorphous precursor films has been developed to fabricate microbridges on vicinally cut $LaAlO_3$ substrates which are then annealed post-patterning to form the 2212 phase. The resulting microbridge definition and superconducting transport properties have been investigated with a view to exploiting intrinsic Josephson effects. Large scale 2 inch diameter 2212 films on $LaAlO_3$ have also been fabricated, both single and double sided, for microwave power applications. Surface resistance measurements on these films have been correlated against microstructure and physical characteristics to establish a rapid quality control strategy. Conventional patterning post-annealing has been used to fabricate these (comparatively) macroscopic devices and their performance will be described.

6–70

Plasma sprayed superconducting YBCO and Dy-substituted YBCO coatings.

R. Enikov, *T. Koutzarova*, *D. Oliver* and *I. Nedkov*. Institute of Electronics, Bulg. Acad. Sci., Sofia, 1784, Bulgaria.

Microcrystalline YBCO and Dy substituted YBCO coatings were deposited using the plasma spraying technique on a home made d.c. plasmatron with air as plasma-forming gas. This technological approach opens the possibility for covering large surfaces while the process does not depend strongly on the substrate crystalline-chemical composition. The plasmatron's parameters were: Electrical powder-30kW; Plasma jet temperature-6000K; Nozzle-substrate-distance-0.12m. A coating with 200μm thickness and 1cm^2 area was prepared for 0.5s. To optimize the spraying process, we performed spectroscopic measurements and determined the plasma temperature and the temperature of the particles in the jet at different distances from the nozzle. This enabled us to avoid the overheating of the particles and to preserve their crystalline-chemical structure. Coatings with general chemical formulas: $YBa_2Cu_3O_{7-y}$ and $Y_{1-x}Dy_xBa_2Cu_3O_{7-y}$ where x=0.4, 0.6 and 1.0 were investigated. The substrates were of Al_2O_3, SiO_2 and Cu. The work discusses the technological particularities of this new technique for HTS coatings deposition. The results pointed at the particular importance of the chemical composition of the initial powder and of the post-deposition annealing of the films. One of the aims of the investigation was to obtain and study thick coatings of Dy substituted YBCO. The Raman spectroscopy showed that the DyBCO coatings are affected weakly by the partial oxygen pressure in the plasmatron chamber. The XRD and SEM spectroscopy were used for microstructure investigations and the correlation between the morphology and R(T) and microwave R_s properties of the coatings were analyzed. All this allowed us to establis the technological conditions for formation of substituted YBCO coatings. The work discuss some aspects for electronic applications of the coatings.

6–71

Microwave Properties of Screen-Printd Bi2223 Thick Films on Ba(Sn,Mg,Ta)O_3 Dielectric Ceramics.

Y. Kintaka[1], *T. Tatekawa*[1], *N. Matsui*[1], *H. Tamura*[1], *Y. Ishikawa*[1] and *A. Oota*[2]. [1] Murata MFG Co.Ltd.,Nagaokakyo,Kyoto,617-8555,Japan. [2] Toyohashi University of Technology,Toyohashi,Aichi,441-8580,Japan.

Screen-printed Bi2223 thick films were fabricated on both sides of Ba(Sn,Mg,Ta)O_3 dielectric ceramics disk (3mm thick and 35mm in diameter) of relative dielectric constant ϵr=24. The temperature dependence and incident power dependence of the unloaded quality factor on TM_{010} mode were measured at 2.1GHz. The typical value of unloaded quality factor measured at 10dBm was 30000 at 70K and 90000 at 20K, which correspond to surface resistance of 0.8m-ohm and 0.3m-ohm,respectively.By addressing this,1.8GHz TM dual-mode resonators are designed and constructed using 25mm-cubes of Ba(Sn,Mg,Ta)O_3 with Bi2223 thick films as superconductor electrodes.Results for the resonators under TM_{010} mode operation will be present.

Session SQUIDs, and SQUIDs applications

6–72

Direct measurement of vortex motion in Nb variable-thickness-bridges.

S. Hirano[1], *S. Kuriki*[1], *M. Matsuda*[2], *T. Morooka*[3] and *S. Nakayama*[3]. [1]Research Institute for Electronic Sciences, Hokkaido University, Sapporo, 060-0812, Japan. [2]Muroran Institute of Technology, Muroran, 050-8585, Japan. [3]Seiko Instruments Inc., Matsudo, Chiba, 270-2222, Japan.

We have measured flux noise characteristic of variable-thickness-bridges (VTBs) made on Nb thin films by the direct flux detection method. The magnetic flux fluctuation was directly detected using a concentric thin-film planar gradiometer coupled to a dc SQUID in the monopole approximation scheme. The VTB with length l = 200 nm and width 47 μ m fabricated using focused-ion-beam (FIB) on an epitaxial Nb film showed random telegraph noise (RTN) of the flux in a time trace above the critical current, which was determined from the onset of the flux noise increase. The power spectrum of the flux noises showed Lorentzian-like form corresponding to the RTN. For the fabricated VTB (l = 5.5 μ m, w = 450 μ m) on a polycrystalline Nb film, long time period observation showed the flux noise in a sequence of multiple steps. The occurrence of the sequences of different steps varied with time at fixed current bias. The distribution of the step size S was roughly approximated by the power law,$S^{-\alpha}$ with $\alpha = 2$. This power-law distribution suggests a self-organized criticality, that is associated with the occurrence of "avalanche" of trapped vortices under fixed driving force.

6–73

Thermal Noise in Digital DC SQUID.

G.H. Chen, *H. Du* and *Q.S. Yang*. Institute of Physics,Chinese Academy of Sciences,Beijing 100080,China.

The intrinsic noise expression of digital DC SQUID (under

low damping limite) can be obtained by means of mechanical analogy and numerical method.It shows that the noise has temperature dependence of $T^{4/3}$,and that it is inversely proportional to the pulse frequency ω_b of the bias current.

6–75

The simulation and design of HTS RSQUID noise thermometers.

L. Hao[1], *J.C. Gallop*[1], *J.C. Macfarlane*[2], *D.A. Peden*[2] and *C.M. Pegrum*[2]. [1]Centre for Basic and Thermal Metrology, National Physical Laboratory, Teddington, TW11 0LW, UK. [2]Dept. of Physics and Applied Physics, Strathclyde University, Glasgow G4 0NG, UK.

Josephson noise thermometry has provided a method of primary thermometry in the temperature region below 1K for a number of years. An HTS Josephson noise thermometer extending the temperature range of application of such primary thermometers to as high as 50K has been proposed. The HTS Josephson junction with critical current shunted by a metallic resistor (R-SQUID) is magnetically coupled to a HTS dc SQUID pre-amplifier. Measurement of the linewidth of Josephson radiation due to thermal noise in the shunt resistor provides the absolute temperature. In practice a large value of RSQUID loop inductance L is needed to ensure efficient coupling to the readout SQUID. We present calculations which indicate that, for practical design parameters, the amplitude of the circulating RSQUID current measured by the readout SQUID is seriously reduced , and its power spectral density is modified in a manner that makes it impossible to relate the linewidth accurately to temperature. We are now extending our work to use the directly-coupled two-junction RSQUID, as has been successfully used at LHe temperature. Simulations show that this device avoids the effects due to high loop inductance, and in this case the Josephson linewidth should be determined only by the thermal noise in the shunt resistor. This device was designed on the basis of numerical simulations, and these, together with ongoing experimental measurements will be reported in this paper.

6–76

Integrated resistors in $YBa_2Cu_3O_{7-\delta}$ thin films suitable for superconducting quantum interference devices with resistively shunted inductance.

F. Kahlmann[1], *W.E. Booij*[1], *M.G. Blamire*[1], *P.F. McBrien*[1], *N.H. Peng*[2], *C. Jeynes*[2] and *E.J. Tarte*[1]. [1]IRC in Superconductivity, University of Cambridge, Madingley Road, Cambridge CB3 0HE, United Kingdom. [2]urrey Centre for Research into Ion Beam Applications, School of Electronic Engineering, Information Technology and Mathematics, University of Surrey, Guildford GU2 5XH, United Kingdom.

Previously, we have demonstrated that the performance of high-T_c dc SQUIDs can be significantly improved by resistively shunting their inductance. During the course of this former work the integrated resistors were fabricated by focussed electron beam irradiation. In this study we set out to evaluate the feasibility of ion implantation and conventional photolithography in order to reduce the complexity of the resistor fabrication process. Firstly, it was found that the resistivity of 200 nm thick YBCO films irradiated with 100 keV H_2^+ ions in a dose range from $1.2x10^{16}$ ions/cm^2 to $1.9x10^{16}$ ions/cm^2 was nearly independent of temperature around 77 K. The absolute values of the resistivity ranged from 800 $\mu\Omega$cm up to 2000 $\mu\Omega$cm. Secondly we have shown that using a 2.2 μm thick AZ photoresist mask and varying the slit width from several microns down to 1 μm it is possible to obtain resistor values in a range from 30 Ω to 5 Ω, respectively. The results obtained are also discussed in terms of (a) the influence of the implantation induced defects upon the transport properties of the irradiated YBCO films, (b) the influence of the proximity effect upon the resistance values and (c) the suitability of the fabricated resistors for integration in resistively shunted dc SQUIDs.

6–77

Effect of the thermally activated phase slippage on characterizations of step-edge YBCO SQUIDs.

H.E. Horng[1], *S.Y. Yang*[1], *C.H. Chen*[1], *J.T. Jeng*[1] and *H.C. Yang*[2]. [1]Department of Physics, National Taiwan Normal University, Taipei 117, Taiwan. [2]Department of Physics, National Taiwan University, Taipei 106, Taiwan.

In this report, we investigate the effect of the thermally activated phase slippage (TAPS) on the characterizations of a step-edge YBCO SQUID. It was observed that the V-I curves at temperatures from 10 K to 77 K show nonzero dynamic resistances with the bias current close to zero. This fact is attributed to the TAPS in the SQUID and reveals that TAPS is present over a considerable temperature rage. Owing to the nonzero dynamic resistance of the SQUID, the voltage of the SQUID was found to be modulated by external magnetic fields under zero bias current. And also, the bias current corresponding to the maximum V_{pp} in the V-Φ curve was observed to be smaller than that predicted from the RSJ model. This deviation suggests that the TAPS reduces definitely the effective critical current of Josephson junctions. All the details will be discussed.

6–78

$YBa_2Cu_3O_{7-\delta}$ dc SQUID array magnetometers and multichannel flip-chip current sensors.

J. Ramos, *R. IJsselsteijn*, *R. Stolz*, *V. Zakosarenko*, *V. Schultze*, *A. Chwala*, *H.-G. Meyer* and *H. E. Hoenig*. Institute for Physical High Technology, Dept. of Cryoelectronics, P. O. Box 100239, D-07702 Jena, Germany.

We have prepared arrays of single layer washer-type dc superconducting quantum interference devices (SQUIDs) on bicrystal substrates. The array can be used as a multichannel magnetometer or current sensor if inductively coupled to an array of input coils. Arrays with nine or eleven SQUIDs have been prepared on one chip. The washer side of the SQUID equals 500 μm and 400 μm respectively. Each SQUID in the array is equiped with a modulation loop, enabling a separate operation of them. The field sensitivity of the SQUIDs is 85 nT/Φ_0 in the 11-devices and 105 nT/Φ_0 in the 9-devices arrays. The crosstalk between neighbouring SQUIDs has been found to be 5 %. The equivalent flux noise of 80 % of the SQUIDs on a chip is typically $\leq 20\mu\Phi_0 Hz^{-1/2}$ down to 1 Hz with bias reversal. A field resolution $\leq$ 2 pT Hz$^{-1/2}$ has been measured for these devices. By using multiturn input coils and mounting them in a flip-chip configuration, multichannel current sensors can

be realised. The small-signal current sensitivity equals 0.9 - 1.1 $\mu A\Phi_0$ depending on the alignment accuracy of the flip-chip sample. The resolution of the current sensors is $\leq$ 20 pA $Hz^{-1/2}$.

6–79

Smart DROS Sensor with Digital Readout.

M. Podt, *D. Keizer*, *J. Flokstra* and *H. Rogalla*. Low Temperature Division, Department of Applied Physics, University of Twente, P.O. Box 217, 7500 AE Enschede, The Netherlands.

Previously, we have demonstrated a Double Relaxation Oscillation SQUID (DROS) with the complete flux locked loop on a single chip, i.e. the smart DROS. The integrator is realized as a superconducting storage loop, interrupted by two write gates to add or extract flux quanta. In the prototype version of the smart DROS, a conventional dc SQUID was used for the readout, which limited the system performance. The pulsed output of the smart DROS is particularly suitable for digital readout. In this readout scheme, no readout SQUID is used but the output pulses of the DROS are counted by a differential counter at room temperature. A 100 MHz DROS has demonstrated the operation principle. In order to increase the slew rate and the linear flux range, we are developing advanced smart DROSs. With a DROS operation at a relaxation oscillation frequency of 1 GHz and a well-chosen quantization unit, the slew rate can be as high as 10^8 Φ_0/s. By applying the signal flux and the feedback flux to the same superconducting input loop coupled to the DROS, the current in this loop is constantly nulled. This makes the dynamic range virtually infinite.

6–80

Low-noise S-band DC SQUID Amplifier.

G.V. Prokopenko[1], *S.V. Shitov*[1], *D.V. Balashov*[1], *V.P. Koshelets*[1] and *J. Mygind*[2]. [1]Institute of Radio Engineering and Electronics RAS, Moscow, Russia. [2]Department of Physics, Technical University of Denmark, Lyngby, Denmark.

The RF amplifier based on a dc SQUID (SQA) is a good choice for an IF amplifier integrated with a SIS mixer and a flux-flow oscillator (FFO) in a fully superconducting submm receiver. SQA has a number of advantages over traditional semiconductor low noise amplifiers, due to its ultra-low power consumption and natural compatibility with both SIS mixer and FFO. Following the concept of a completely integrated superconducting receiver, the study on SQA is a logical step towards an imaging array receiver with dense packaging. A 6 mm · 6 mm chip comprising two identical SQAs has been designed, fabricated and tested as a one-stage and a two-stage RF amplifier in the frequency range of 4 GHz. The SQA consists of a double washer type dc SQUID with two 1 mm^2 of area Nb-AlO_x-Nb junctions each shunted by a Ti film resistor. The integrated input circuit comprises a planar coil inductively coupled to the washer of the SQUID and two tuning capacitors. To avoid saturation, the test noise signal was applied to SQA through a tuneable 40 MHz band-pass YIG-filter. The following characteristics have been measured for a two-stage SQA at 3.7 GHz at the small-signal mode: gain (15±1) dB, noise temperature (6.5±1) K, 3 dB bandwidth about 250 MHz. The RF mismatch between the input/output of SQA was measured experimentally. Taking into account the reflection data , one can estimate two-stage SQA gain (17.5±1) dB, noise temperature (4±1) K. To reduce the input/output reflections, a new RF launcher system with improved design of transition to coplanar line of the SQA chip is under development and test. To increase the dynamic range of SQA, two possible approaches are discussed: 1) a fully integrated (internal) RF feed-back circuit; 2) an external RF feed-back circuit using an adjustable coolable attenuator and phase shifter.

The work was supported in parts by the Russian SSP "Superconductivity", the INTAS project 97-1712, the Danish Research Academy, and the Danish Natural Science Foundation.

6–81

Noises study of high-T_c $YBa_2Cu_3O_y$ SQUIDs magnetometers under microwave irradiation.

H.C. Yang[1], *M.P.H. Chang*[1], *J.H. Chen*[1], *H.W. Yu*[1], *H.E. Horng*[2], *J.T. Jeng*[2] and *S.Y. Yang*[2]. [1]Department of Physics, National Taiwan University, Taipei 106, Taiwan. [2]Department of Physics, National Taiwan Normal Unversiy, Taipei 117, Taiwan.

The noise spectral density, $S_\Phi(f)$, of high-T_c $YBa_2Cu_3O_y$ SQUIDs magnetometers at varied microwave powers was measured to investigate the effects of the microwave irradiation on the noise characteristics. The normal state resistance and the critical current of magnetometers were ~2.8 Ω and ~35.2 μA respectively at 77 K. The flux noise at 77 K was 9 ~ 36 $\mu\Phi_o/Hz^{1/2}$ at 1 kHz which corresponds to a field noise of 70 ~ 240 $fT/Hz^{1/2}$. The microwave changes the I_c and the dynamic resistance of SQUIDs. It also varies the peak-to-peak value ΔV_{pp} of the V-Φ curves and increases the noise. The increased noises are attributed to the decreased transfer function of the V-Φ curves. The results are discussed.

6–82

HTS-DC-SQUID Flux-Locked-Loop based on a cooled integrated electronics.

J. Kunert[1], *V. Zakosarenko*[1], *V. Schultze*[1], *R. Gross*[2], *F. Nitsche*[2] and *H.-G. Meyer*[1]. [1]Institut fuer Physikalische Hochtechnologie, Abteilung Kryoelektronik, PF 100 239, D - 07702 Jena, Germany. [2]MAZeT GmbH, In den Weiden 7, D - 99099 Erfurt, Germany.

HTS-DC-SQUIDs with direct read out Flux-Locked-Loop (FLL) electronics can currently be realized with high cut-off frequency and good noise behaviour. Bandwidths up to 15 MHz and electronics input noise of 500 pV/sqrt(Hz) are reached. However, remarkable further bandwidth increase is limited by some factors. One of them is the distance between the electronics located at room temperature and the SQUID in liquid nitrogen. A second one is the input noise of the electronics. Our idea was to realize the electronics as an integrated circuit near the SQUID. This extremely short distance should prevent delay times and furthermore decrease the thermal noise in the electronics. To reach this aim all of the components of the integrated circuit are specially designed for a working temperature of 77 Kelvin. The integrated circuit consists of differential amplifiers, operational amplifiers, and CMOS switches. This read out electronics

has an ultra low input noise of 260 pV/sqrt(Hz) and a gain-bandwidth-product of 10 GHz. Our measurements proved the electronics noise to be negligible compared to the SQUID noise. This is due to the low electronics noise but also to the high voltage-to-flux transfer coefficient of our SQUIDs. So, finally a compact and fast SQUID system could be realized based on these components.

6–83

Radio Frequency Amplifier Based on a Niobium dc SQUID with Microstrip Input Coupling.

M.Mueck[1,2], *M.-O. Andre*[1], *J.Clarke*[1], *J.Gail*[2], *C.Heiden*[2] and *C.Hagmann*[3]. [1]Department of Physics University of California at Berkeley Berkeley, CA 94720, U.S.A. [2]Institut fuer Angewandte Physik Justus-Liebig-Universitaet Giessen 35392 Giessen, Germany. [3]MS 414, Lawrence Livermore National Laboratory Livermore, CA 94550, U.S.A.

We have developed a high frequency amplifier using a dc SQUID in a new configuration in which the input coil of the SQUID is used as a microstrip resonator. The input signal is coupled between one end of the coil and the SQUID loop, which acts as a groundplane for the microstrip resonator; the other end of the coil is open. In this configuration, such an amplifier exhibited a gain of more than 20 dB in the frequency range of 100 MHz to 1 GHz. The -3 dB bandwidth of the amplifier was typically 10 % to 20 % of the resonant frequency of the microstrip resonator formed by the input coil. By connecting a GaAs varactor to the open end of the input coil, the frequency of maximum gain of the amplifier could be tuned over a wide frequency range. With a bath temperature of 4.2 K and a room temperature post-amplifier, the system noise temperature ranged from 0.5 K $\pm$ 0.3K at 80 MHz to 1.6 $\pm$ 1.2 K at 1 GHz. An even lower noise temperature, about 100 mK at a frequency of 90 MHz, and about 120 mK at a frequency of 440 MHz, was obtained at a bath temperature of about 0.4 K with a cooled post-amplifier. This work is supported by the National Science Foundation under grant number FD96-00014.

6–84

HTS dc SQUID behavior under the influence of external fields.

V. Schultze, *A. Chwala*, *R. IJsselsteijn*, *J. Ramos*, *R. Stolz*, *V. Zakosarenko* and *H.-G. Meyer*. Institute for Physical High Technology Jena Dept. of Cryoelectronics P.O.Box 100239 D-07702 Jena Germany.

Different dc SQUIDs made of high temperature superconductors (HTS) are investigated concerning their behavior under the influence of external fields. These fields include static magnetic fields superimposed to the SQUIDs and the earth magnetic field including environmental field noise. The SQUIDs differ in their layout what includes single layer and multilayer configurations. The influence of lateral patterning into small structures which should hinder the penetration of flux into the superconducting areas is investigated. Furthermore, the influence of the patterning technology on the durability of the SQUID structures against external fields is examined.

6–85

Alternative structures in washer-type high-T_c dc SQUIDs.

A.B. Jansman[1], *P.G. Jeurink*[1], *A.I. Gómez-Corona*[2], *M. Izquierdo*[2], *J. Flokstra*[1] and *H. Rogalla*[1]. [1]Low Temperature Division Department of Applied Physics University of Twente P.O. Box 217 Enschede 7500 AE Netherlands. [2]On leave from Low Temperature Division Department of Applied Physics University of Twente P.O. Box 217 Enschede 7500 AE Netherlands.

The excess low-frequency noise of field cooled high-T_c dc SQUIDs was shown to be suppressed by the implementation of slots or holes in the SQUID washer. The effective area of such SQUIDs is maximal for the half-slotted case. The remaining outermost strip of a half-slotted SQUID is expected to be too wide to avoid flux penetration in background fields in the order of 100 μT. In this paper, we present half slotted-SQUIDs with the outermost strip provided with structures ranging from small holes to various slot configurations. These SQUIDs are supposed to take profit of the maximum effective area of the half-slotted case while keeping the line width small. A flux quantization model applied to these SQUIDs is most successful for concentric structures. The actual $YBa_2Cu_3O_{7-\delta}$ SQUIDs, fabricated on a $SrTiO_3$ bicrystal substrate, show effective areas, which are close to those of the completely slotted SQUIDs, somewhat lower than expected. Nor the half-slotted nor the new structures showed excess low frequency noise when cooled in a fields up to 60 μT.

6–86

Superconductive and traditional electromagnetic probes in eddy current nondestructive testing of conductive materials.

M. Valentino[1,2], *A. Ruosi*[1], *G. Pepe*[1] and *G. Peluso*[1]. [1] Istituto Nazionale per la Fisica della Materia (INFM), Unita' di Napoli Università di Napoli "Federico II", Piazzale Tecchio 80, 80125 Napoli, Italy. [2] Dipartimento di Ingegneria dei Materiali per la Produzione Università di Napoli "Federico II", Piazzale Tecchio 80, 80125 Napoli, Italy.

Currently different kinds of electromagnetic probes are used for eddy-current nondestructive analysis such as induction coils and flux-gates. Each one has advantages and drawbacks and hence it is difficult to state which of them is the most effective for a particular application. In this context, a comparative study of perfomance of traditional device like induction coil and flux-gate and the innovative HTc-SQUID-based magnetometer is presented here. Single-layer and multi-layers aluminium-alloy structures with artificial defects commonly encountered in the aircraft industry, i.e. holes, slots and cracks, have been examined. In particular, the higher sensitivity of SQUID magnetometer allows higher performances in the inspection of weakly conducting or multi-layered structures, where traditional electromagnetic probes fail. The experimental data have been validated through numerical simulations obtained by a rigorous 3D vector volume integral formulation of the wavefield for a damaged metallic planar isotropic layer. Preliminary results obtained by SQUID based measurements for composite materials with impact damaging will be shown.

6–87

HTS dc-SQUID with a gradiometric multilayer flux transformer.

M.I.Faley[1], *U.Poppe*[1], *K.Urban*[1], *D.N.Paulson*[2], *T.N.Starr*[2] and *R.L.Fagaly*[2]. [1]Institut fuer Festkoerperforschung, FZ-Juelich GmbH D-52425 Juelich, Germany. [2]Tristan Technologies inc., San Diego, CA 92121 USA.

To demonstrate the application of sensitive HTS dc-SQUID sensors in a magnetically unshielded environment, we use a gradiometric configuration of the pick-up coil and a multiturn multi-layer flux transformer in a flip-chip configuration with a dc-SQUID using quasiplanar Josephson junctions. The gradiometer has a base length of about 1 cm, sensitivity of about 1.6 nT/phi0, and white noise better than 50 fT/cm.sqrt(Hz). At 1 Hz, the noise increases to about 150 fT/cm.sqrt(Hz). Even better values are expected with the use of gradiometric flux antennas with multi-turn multilayer flux transformers on larger wafers. The laboratory environmental noise is significantly larger then the intrinsic noise of the gradiometer, but can practically be eliminated with the help of a reference gradiometer. These gradiometers can be moved and/or rotated in Earth's field during operation. Possible applications for biomagnetism or NDE will be discussed.

6–88

Field-Cooled Noise Characteristics in the SQUID Magnetometers with Holes.

J.T.Jeng[1], *Y.C. Liu*[1], *S.Y. Yang*[1], *J.R. Chiou*[2], *H.E. Horng*[1], *J.H. Chen*[2] and *H.C. Yang*[2]. [1]Department of Physics, National Taiwan Normal University, Taipei 117, Taiwan. [2]Department of Physics, National Taiwan University, Taipei 106, Taiwan.

High-T_c SQUIDs with various arrays of holes in washers were fabricated to investigate the influence of the magnetic flux on the noise $S_\phi{}^{1/2}$ in the field-cooled situation. In this work, the arrays of holes in the SQUID washers were arranged to be hexagonal or rectangular structure with a fixed distance between the edges of two neighboring holes. It was found that the low frequency flux noise $S_\phi{}^{1/2}$ of the SQUIDs with the hexagonal array of holes remained unchanged when the cooling field was lower than a threshold value H_{th}, at which $S_\phi{}^{1/2}$ increased obviously. When the field applied for cooling process was further raised, the $S_\phi{}^{1/2}$ was observed to oscillate periodically with the field. The SQUIDs with the rectangular array of holes also exhibited the similar behavior of $S_\phi{}^{1/2}$ -H curve, but showed different H_{th} and period. The variation in H_{th} for these two types of SQUIDs is resulted from the various hole densities in the washers. Thus, the Hth can be further increased by properly designed hole structures to achieve a better performance of the SQUIDs under higher magnetic fields.

Session Mixers/Detectors

6–89

Realisation of a flux-flow dc-transformer using high temperature superconductors.

S.Berger, *K.Bouzehouane*, *D.Crete* and *J.P.Contour*. Unite Mixte de Pysique CNRS / Thomson, Domaine de Corbeville, 91404 Orsay Cedex, France.

We report on the first realisation using high temperature superconducting films of the device proposed in 1965 by Giaever: the dc-dc transformer, which involves flux-flow vortex motion in two superimposed thin films, separated by an insulating layer. The device was fabricated using the ramp based multilayer technology from an $YBa_2Cu_3O_7$ based SIS structure grown by pulsed laser deposition. Transport measurements exhibiting the coupling and decoupling phenomena between the two vortex arrays are obtained. We study the possibility of widening the working range of this device, which can be applied to RF detection. This work constitutes an important result in the effort to use high temperature superconductors for electronics.

6–91

Far-Infrared Hilbert-Transform Spectrometer based on Stirling Linear Cooler.

O.Y. Volkov[1], *V.V. Pavlovskii*[1], *Y.Y. Divin*[2] and *U. Poppe*[2]. [1]Institute of Radioengineering & Electronics of RAS, Moscow 103907, Russian Federation. [2]Institut fuer Festkoerperforschung, Forschungszentrum Juelich GmbH, 52425 Juelich, Germany.

The design and the characteristics of first Hilbert-transform spectrometer operating with Stirling cryocooler is reported. The principle of operation of Hilbert-transform spectrometer is based on the ac Josephson effect. High-quality epitaxial YBaCuO thin-film Josephson junctions have been fabricated on untwinned (110) NdGaO3 bicrystal substrates to satisfy the operational requirements of Hilbert-transform technique. The operation temperature of the spectrometer of 50 K is reached with the help of Stirling cryocooler. The characterization of the spectrometer has been made in the range of frequencies 60 GHz – 4.25 THz, using a far-infrared optically-pumped laser, a backward-wave oscillator and a harmonic multiplier as sources of monochromatic radiation. The effective coupling of radiation to Josephson junction has been achieved with a help of Si hyperhemispherical substrate lens. The operation of the spectrometer has been demonstrated in the over-a-decade frequency range 0.16 – 3.1 THz with the resolution of 4 GHz at the large part of the range. The comparison of Hilbert-transform spectrometers with conventional spectroscopic devices will be presented.

6–92

Development and Characterization of NbN Phonon Cooled Hot Electron Bolometer Mixers at 810 GHz.

C. Rösch, *F. Mattiocco* and *K.F. Schuster*. Institut de Radio Astronomie (IRAM) 300, rue de la piscine Domaine Universitaire de Grenoble 38406 St. Martin d'Heres France.

We report about the progress in developing phonon cooled hot electron bolometers (HEB) based on thin film NbN microbridges. Since first devices with single dipol antennas had shown good performance in simple mixer tests we investigated a double dipol structure with two different integration schemes of the HEB mixer elements. To determine the frequency dependent response of the detector Fourier Transform Spectroscopy (FTS) measurements were performed using the bolometer element in the direct detection mode. Furthermore noise temperatures were obtained for local oscillator (LO) frequencies in the range of 795 GHz to 813 GHz and intermediate frequencies (IF) from 1.0 GHz to 1.7 GHz.

Impedance measurements to determine the IF bandwidth proposed by Karasik in 1997 were performed in a dipstick. Data was recorded for different operating points and its evaluation clearly shows a change in roll-off frequency with bias voltage. Results for the IF bandwidth are compared with results obtained by superposing the signals of two LOs and show reasonably good accordance.

6–93
Current Tunable IF-Phase Using High-Tc Superconducting 100GHz Mixer.
K. Suzuki, *K. Kashiwagi* and *Y. Enomoto*. Superconductivity Research Laboratory, ISTEC 1-16-25, Shibaura, Minato-ku, Tokyo, 105-0023, Japan.

A current controlled phase shifter has its future application in steerable microwave and millimeter wave antenna systems. It provides tunable shifted phase, easy access and fast response. Here we report on millimeter wave mixer performances of high-Tc superconductor (HTS) Y-Ba-Cu-O (YBCO) Josephson junctions on MgO substrates with a log-periodic antenna. The 6 junctions with 1.5-micron space apart from each other make it possible to build current controlled phase shifter devices that are suitable for millimeter wave integrated circuits. We describe the experimental characterization for the phase shifter in which the HTS juncton bias current has been adjusted to give a large change in intermediate frequency (IF) output with 100 GHz harmonic mixer modes. The magnitude of IF phase change have several steps more than 200 degrees. It means that they are not depending on plus or minus sign of the junctionÕs bias current. The IF phase shift as functions of bias currents and the power of local frequencies (LO) were examined from 100.0 GHz to 100.5GHz at 50K in a practical small size millimeter wave cryostat. The LO was an X band frequency for harmonic mixing modes which were suitable to practical application to phase array systems.

6–94
Relaxation Times and Noise in Sub-Micron Long HTS Hot-Electron Mixers.
O. Harnack[1,2], *B. S. Karasik*[1], *W. R. McGrath*[1], *A. W. Kleinsasser*[1] and *J. B. Barner*[1]. [1]Center for Space Microelectronics Technology, Jet Propulsion Laboratory, California Institute of Technology, 4800 Oak Grove Drive, MS 168-314, Pasadena, CA 91109, USA. [2]Institute of Thin Film and Ion Technology, Research Center Juelich, 52425 Juelich, Germany.

The hot-electron bolometer (HEB) mixer made from a high-T_c superconductor (HTS) was introduced recently as an alternative to a Schottky mixer at THz frequencies. The mixer performance depends on the total thermal conductance for heat removal from the phonon sub-system due to either length-dependent phonon diffusion or phonon escape to the substrate. We present a systematic study of the length and temperature dependencies of the thermal relaxation times, as inferred from the -3dB intermediate frequency (IF) bandwidth, and of the noise properties of HTS HEB mixers on MgO and CeO_2/sapphire substrates. For 50nm to 400nm long devices on MgO, the bandwidth was 100MHz at 65K and about 2GHz at temperatures close to T_c, while 50nm and 80nm long mixers on CeO_2/sapphire showed bandwidths of about 1.9GHz and 2.4GHz at similar temperatures. Noise measurements at 65K and around 2.7GHz gave SSB mixer noise temperatures of 8000K and 9700K at IFs of 120MHz and 1GHz, respectively. The impact of low-frequency effects on the measured device performance and the importance of the device geometry for optimizing the total thermal conductance will be discussed. This research was funded by NASA. Funding for O.H. was provided by the German Academic Exchange Service (DAAD).

6–95
Heterodyne type response in SIS direct detector.
A. Karpov[1], *J. Blondel*[1], *P.N. Dmitriev*[2] and *V.P. Koshelets*[2]. [1]Institut de Radioastronomie Millimétrique, St. Martin d'Hères, France. [2]Institute of Radio Electronics and Engineering, Moscow, Russia.

We present the first observation of single photon mixing in an SIS detector, providing a heterodyne type response in a direct detection experiment. A broad band (40%) SIS direct detector is studied under the effect of the black body radiation. A 1.5 GHz intermediate frequency low noise amplifier is connected to the detector. No local oscillator power is applied in this experiment. At the same time a typical periodical heterodyne response appeared in the intermediate frequency power versus bias voltage dependence. Tien - Gordon like steps are observed in the current voltage characteristic (CVC) of the SIS junction. The Y factor of about 2 is measured in a standard experiment with liquid nitrogen cooled and ambient temperature loads. The heterodyne response may be explained as single photon mixing within the detector band. The effectiveness of single photon mixing is due to the quantum nature of the interaction. The mode of operation presented here may serve to build a sensitive detector for the millimeter and sub millimeter bands using a SIS junction.

6–96
Metal - High Tc Superconductor Point Contact Resonce to Millimeter Wave Radiation.
A. Laurinavicius, *K. Repsas*, *R. A. Vaskevicius* and *A. Deksnys*. Semiconductor Physics Institute, Vilnius, A. Gostauto 11, 2600 Vilnius, Lithuania.

In this paper, we present the experimental results of normal metal -high Tc superconductor point contact response to millimeter wave radiation. The experiment was carried out at 25-35 GHz frequences in the incident power range 0,1-40 mW. The superconducting Bi-Sr-Ca-Cu-O layers with a thickness about 30 micrometers were used for the investigation. Samples were prepared on cleaved MgO(100) faces by the melt processing technology, i.e. by melting and recrystalyzing coatings of the superconducting powder. The response measurement results show that the detected signal has a weak dependence on temperature even in the region of transition from the normal state to the superconductive one. The response was also observed at room temperature. So, we conclude that the response is not related to the superconducting phenomenon. Thus, we assume that the response could be associated with the degradated metal-high Tc superconductor interface. The increase of the response signal when temperature is decreased and the large point contact resistance show that the nature of the interface layer

shoud be semiconductive. The point contact voltage-power characteristics are presented at liquid nitrogen and room temperatures, respectively, and compared with analogous of semiconductor detectors based on hot electron phenomenon. The obtained results could be usefull for design hibrid cryo-electronic components that integrate both superconducting and non-superconducting elements.

6–97

Performance of Inhomogeneous Distributed Junction Arrays.

M.Takeda[1] and *T.Noguchi*[2]. [1]The Graduated University for Advanced Studies, Nobeyama, Minamisaku, Nagano, 384-1305 Japan. [2]Nobeyama Radio Observatory, Nobeyama, Minamisaku, Nagano, 384-1305 Japan.

The distributed junction arrays made up of a number of junctions connected in parallel with an identical tuning inductance separating every two junctions has been proposed [C.Shi. and T.Noguchi. IEIC Trans. Electron., **E81-C**, NO.10 October 1998]. This type of junction arrays has demonstrated excellent mixer performance such as low J_c, large bandwidth and low noise. However, mixer performance of the distributed junction arrays deteriorate at some frequency bands determined by both tuning inductances and junction capacitances, so that they never show flat frequency dependence as far as the junction critical current density or the number of junctions is not increased. In order to overcome this problem, we propose inhomogeneous distributed junction array, which have different lengths of tuning inductance or junction sizes. In the simulation of mixer performance, we compared the mixer performance of inhomogeneous types of junction arrays with that of homogeneous one, providing same conditions on the critical current density, number of junctions and width of strip line. We found that an inhomogeneous type of distributed junction arrays show excellent mixer performance and that its deterioration of noise temperature at some furequency bands are considerably suppressed compared with the homogeneous junction arrays, if the tuning inductances and junction capacitances are optimized well. The details in this paper will be reported at the Conference.

6–98

Ka-Band High-T_c Superconductor and III-V Semiconductor Hybrid Balanced Mixer.

S. K. Han, *J. D. Suh*, *G. Y. Sung* and *K. Y. Kang*. Telecomm. Basic Research Lab., ETRI, Taejon 305-350, South Korea.

We demonstrated a balanced mixer of the combination of High-T_c superconductor (HTS) and III-V Schottky GaAs beam lead diodes operating at cryogenic temperature. The HTS hybrid mixer was designed with a center frequency of 28 GHz and a bandwidth of 2 GHz, and consists of a rat-race coupler circuit with beam-lead diodes attached to its balanced ports. The HTS hybrid mixer with 2 GHz RF bandwidths exhibits a conversion loss of 10 dB. A LO-to-RF isolation was greater than 20 dB in the range of operating frequencies. Since the HTS/III-V hybrid devices have lower noise and conversion loss, this technique provide us with new capabilities that can be effectively utilized in the field of multi-point distribution service (MDS) systems.

6–99

HTSC-Bolometer for IR-Spectrometer -Processing and Operation-.

K.-S. Roever[1], *T. Heidenblut*[1], *B. Schwierzi*[1], *T. Eick*[2], *W. Michalke*[2] and *E. Steinbeiss*[2]. [1]Institut fuer Halbleitertechnologie UNI-Hannover, Appelstrasse 11A, Hannover, Niedersachsen, 30167, Germany. [2]Institut fuer Physikalische Hochtechnologie e.V., Helmholtzweg 4, Jena, Thueringen, 07743, Germany.

$GdBa_2Cu_3O_{7-x}$-(GBCO) superconducting bolometers with T_c around 90K and very high detectivity D* were fabricated and characterized. A specially developed Silicon-On-Nitride (SON) substrate was used to create c-Si/Si_xN_y-membranes with very low thermal conductivity G. A crystalline YSZ/CeO_2 double-buffer layer was deposited onto the remaining thin silicon top-layer to enable the epitaxial growth of the superconducting thin film. Noise measurements of the fabricated bolometers showed a low 1/f noise level as well as very small phonon noise. As a result a remarkable high D* of 2×10^{10} cm $Hz^{1/2}/W$ at a wavelength of 10μm was achieved. Furthermore a new operational mode for bolometers was developed, the so called resistance-bias. Compared to current- and voltage-bias, simulations and measurements showed great advantage in response time. With this mode electrical time constants τ_{el} below 1ms were achieved. This makes even bolometers with very high D*, which are usually slow, usable for measurements in the frequency range up to 200Hz

6–100

A superconducting integrated receiver with phase-lock loop.

S.V. Shitov[1], *V.P. Koshelets*[1], *L.V. Filippenko*[1], *P.N. Dmitriev*[1], *A.M. Baryshev*[2], *V.L. Vaks*[3], *W. Luinge*[2], *J.-R. Gao*[2,4] and *N.D. Whyborn*[2]. [1]Institute of Radio Engineering and Electronics (IREE), Moscow 103907, Russia. [2]Space Research Organization of the Netherlands (SRON), Groningen 9700 AV, the Netherlands. [3]Institute for Physics of Microstructure (IPM), Nizhny Novgorod 603600, Russia. [4]Department of Applied Physics and Materials Science Center, University of Groningen, the Netherlands.

An integrated superconducting heterodyne receiver for radio astronomy containing a phase-locked flux-flow oscillator has been designed and is being studied at about 350 GHz. The circuit of the chip receiver contains a quasioptical low-noise SIS mixer, FFO as a local oscillator, a harmonic SIS mixer and a SIS multiplier as an optional source for the harmonic mixer. The FFO has to be phase-locked to the 35th harmonic of a 10 GHz synthesized source using custom-design room temperature electronics with the PLL loop bandwidth of about 10 MHz and IF = 400 MHz. The RF scheme and layout of the chip will be presented along with numerical simulation of its performance; comparison to the experimental data will be reported as well.

The work was supported in parts by the Russian SSP "Superconductivity", the INTAS project 97-1712, Science Foundation and the Netherlandse Organisatie voor Wetenshappelijk Onderzoek (NWO).

6–101

Numerical Simulation based on a Five-Port Model of the Parallel SIS Junction Array Mixer.

M.-H. Chung and *M. Salez*. DEMIRM, Observatoire de Paris, 61 avenue de l'Observatoire, 75014 Paris, France.

The bandwidth of SIS quasiparticle mixer is limited due to several reasons. One of the constraints of large bandwidth is related to the inductive circuits for tuning out the geometrical capacitance of SIS junctions. Recently the parallel SIS junction array mixer was proposed to have larger bandwidth of SIS quasiparticle mixers and there were encouraging experimental results. Since the analysis of the parallel SIS junction array mixer is a non-linear problem, it needs a general approach to analyze the performance of mixer. The large signal analysis is performed in the frequency domain by using the voltage update method to determine the local oscillator voltage waveforms across multiple SIS junctions and we calculate the harmonic performance of the parallel SIS junction array mixer using five-port model and Tucker's quantum theory of mixing. A comparison between the results of three-port approximation and five-port model is reported.

6–102

The Characterization of Radiation Beam Pattern and Fabrication of Superconducting Hot Electron Bolometer Mixer.

C.C. Chin[1], *P.Z.Y. Pan*[2], *C.C. Chi*[2], *S.F. Horng*[3], *Y.S. Yang*[1], *S.S. Shen*[1] and *R. Hu*[1]. [1] Institute of Astronomy and Astrophysics, Academia Sinica, Nankang, Taipei, Taiwan. [2] Center for Material Science and Department of Physics, Tsing Hwa University, Hsin Chu, Taiwan. [3] Department of Electrical Engineering, Tsing Hwa University, Hsin Chu, Taiwan.

Because of the low T_c and high diffusion constant of aluminum, Al hot electron bolometer (HEB) mixer are expected to have lower noise temperature and wider band width. We have setup a research program on Al HEB. Firstly, we will fabricate 200 GHz Al HEB and then will try higher frequency. An Al HEB mixer is composed of the Al HEB chip and the corrugated feed horn. The design of the horn follows that of Raymond Blundell *etal* .[1]. Those horns are manufactured under tight tolerance. Any defects or dimensions derivation from the design may seriously affect the radiation pattern.We have set up a 200 GHz near field measurement system to characterize the radiation pattern of the corrugated feed horn. The measured contours of the field pattern were highly circular. The short and long term phase fluctuations of the system were respectively 0.2° and 2°. The system has successfully characterized the quality of the horn. The fabrication process of the Al HEB chip has been setup. Recently, we can achieve sub μm Al microbridge by e-beam photolithography. As a test of the process, we have first successfully applied the process on Nb HEB. We are now working on using the process on Al HEB chip. We will report the design of our near field measurement system and the fabrication process. [1] Ray Blundell *etal*. A Wideband Fixed-Tuned SIS Receiver for 200 GHz Operation, IEEE Transaction on Microwave Theory and Techniques Vol. 43, #4, 1995, p.933.

6–103

Surface Resistance of NbN and NbC_x N_{1-x} Films in the Frequency Range of 0.5-1.5THz.

S. Kohjiro and *A. Shoji*. Electrotechnical Laboratory, Tsukuba, Ibaraki, 305-8568, Japan.

Superconducting receivers composed of Josephson local oscillators and quasiparticle tunneling (SIS) or hot electron bolometer (HEB) mixers are candidates for global monitoring and astronomical observation. Recent progress on SIS and HEB mixers motivates the investigation on such low-noise receivers operating above 0.7THz, i.e., the gap frequency of Nb. For such applications, an electrode material with low surface resistance R_s above 0.7THz is required. In this paper, we report R_s of NbN and NbC_x N_{1-x} films in the frequency range of 0.5-1.5THz. In our measurement, we used Fiske resonant modes in NbN(or NbC_x N_{1-x})/MgO/NbN(or NbC_x N_{1-x}) Josephson tunnel junctions whose electrodes were deposited on (100) MgO substrates heated up to 300°C. We have found R_s of NbC_x N_{1-x} is about 1/2 of NbN's, which would be attributed to the frequency dependence of their magnetic penetration depth. Typical R_s value of NbC_x N_{1-x} is 50mΩ at 1THz, less than 1/2 of highly conductive copper's.

6–105

Fabrication and Testing of Microcalorimeter for X-ray spectroscopy.

M. Ukibe, *F. Hirayama*, *M. Koyanagi*, *M. Ohkubo* and *N. Kobayashi*. Electrotechnical Laboratory, 1-1-4, Umezono, Tsukuba-shi, Ibaraki, 305-8568, Japan.

We are developing X-ray microcalorimeters using superconducting transition edge sensors(TES), which can be operated at relatively high temperatures in a 3He cryostat, and DC-SQUID current amplifiers to realize a X-ray spectroscopy with a high energy resolution and a high counting rate. For this purpose we have selected (Ti/Au) bilayers as TES. Our X-ray microcalorimeters were constructed from a (Ti:60 nm/Au: 20 nm) bilayers as TES, a Au film (200 nm) as absorber, and Nb electrodes (100 nm) on a silicon nitride membrane of 500 - 1000 nm. All films were deposited by rf- or dc-sputtering. The electrodes and SiN were patterned by RIE, TES by chemical etching, and the absorber by liftoff method. The Tc and the DTc of TES were about 0.5 K and 3 mK, respectively. Our DC-SQUID amplifier has the single stage consisting of the series SQUIDs of 200 to 1000. The typical voltage gain of series 200 SQUIDs was about 200 V/A. The microcalorimeter and series SQUIDs were placed on the same low temperature bed. The detection trial of the X-ray will be reported in detail.

6–106

A Compact High-resolution X-ray Detector System using STJ and SQUID Amplifier.

T. Ikeda[1], *H. Kato*[1], *K. Kawai*[1], *H. Miyasaka*[1], *T. Oku*[1], *W. Ootani*[1], *C. Otani*[1], *H. Sato*[1], *Y. Takizawa*[1], *H. M. Shimizu*[1], *H. Watanabe*[1], *H. Nakagawa*[2], *H. Akoh*[2], *M. Aoyagi*[2] and *T. Taino*[3]. [1] The Institute of Physical and Chemical Research (RIKEN), 2-1 Hirosawa, Wako, Saitama 351-0198, Japan. [2] Electrotechnical Laboratory (ETL), 1-1-4 Umezono, Tsukuba, Ibaraki 305-8568, Japan. [3] Department of Nuclear Engineering, Kyushu University, Hakozaki, Fukuoka 812-8581, Japan.

A compact system for high-resolution X-ray detection using STJ and SQUID amplifier has been developed. It requires no specially shielded room. In order to detect X-ray, an STJ of Nb/Al/AlOx/Al/Nb fabricated in RIKEN is employed at 0.3 K. And SQUID amplifier, which is commercially available, is located at 4K stage. Generally, there are some difficulties in using both STJ and SQUID amplifier correctly, e.g., the temperature and magnetic sensitivity differences between them. Moreover, the methods of the transfer of the current from STJ to SQUID amplifier and biasing them should be well studied. Our system has already worked as an X-ray detector with a fine tuning of the peripheral circuit. The performance of the compact system consisting of STJ, SQUID amplifier and their peripheral circuit will be reported in terms of energy resolution, a limit of bandwidth, pulse shapes, comparison with the results of simulation and so on. This system was designed to be inside a compact low-temperature stage. Also the configuration of STJ and SQUID amplifier inside a volume smaller than 10x10x10 cm^3 will be shown. Especially, the SQUID amplifier well works in the field for STJ of about 100 Gauss. The specially designed magnetic shield at low temperature will be reported.

6–107

Sensitivity of a NbN phonon-cooled hot-electron mixer in the frequency range from 0.7 THz to 5.2 THz.

A.D. Semenov[1], *J. Schubert*[2], *G.N. Gol'tsman*[1], *H.-W. Huebers*[2], *G. Schwaab*[3], *E.M. Gershenzon*[1] and *B.M. Voronov*[1]. [1]Physical Department, State Pedagogical University of Moscow, M.Pirogovskaya 29, 119435 Moscow, Russia. [2]DLR Institute of Space Sensor Technology, D-12489 Berlin, Germany. [3]Physical Chemistry II, Ruhr-University Bochum, D-44801 Bochum, Germany.

The sensitivity is a parameter important for the application of a mixer in any practical heterodyne receiver since it determines the integration time required for resolving a particular temperature contrast. So far mainly the noise temperature of various hot-electron mixers has been studied. Here we report first sensitivity measurements of a NbN phonon-cooled hot-electron bolometric mixer. The device represents a 0.2-micrometer long and 1.7-micrometer wide bridge from 3-nm thick film embedded into a planar complementary log-spiral antenna. Measurements were performed at frequencies ranging from 0.7 THz to 5.2 THz. When corrected for optical coupling losses, the DSB noise temperature increases linearly with frequency starting from 700K at 0.7 THz and approaching twenty times the quantum limit of a DSB receiver in the whole frequency range. In the interval of bias voltages corresponding to the lowest noise temperature we found the sensitivity close to the theoretical limit. Although, at small voltages the sensitivity degraded due to enhanced root mean square noise at the device output. From our results we estimate an upper frequency limit of 7 THz for the present design of the mixer and antenna.

6–108

Fabrication of Diffusion-cooled Nb Hot-Electron-Bolometer Mixer for Terahertz Applications.

M. Frommberger, *P. Sabon*, *M. Schicke*, *K.H. Gundlach* and *K.F. Schuster*. IRAM, 300 Rue de la Piscine, 38406 St. Martin d'Heres, France.

Diffusion-cooled Nb hot-electron bolometer (HEB) are one of the most promising candidates for heterodyne frequency mixing in the terahertz regime. We present general investigations on the properties of thin (2nm- 200nm) Nb films used for such devices. Particulary critical temperature, resistance ratio R_{300K}/R_{10K}, sheet resistance and their dependence on film thickness. Ellipsometry and anodisation were applied to controll as well the Nb layer as resist thicknesses. Furthermore the IRAM HEB fabrication process is shown where the subμm lateral structures of the bolometer are defined out of a 12nm thick Nb layer in two step E-beam lithography. Limiting factors of the process are discussed and first promising results are presented.

6–109

Anodic oxidation for NbN film thickness measurements.

M. Schicke[1], *K. H. Gundlach*[1] and *K. Mizuno*[2]. [1]Institut de Radioastronomie Millimétrique, 300 rue de la piscine, Saint Martin d'Hères, 38406, France. [2]Central Research Laboratories, Matsushita Electric Industrial Co. Ltd., 3-4 Hikaridai, Seika-Cho, Soraku-Gun, Kyoto, 619-02, Japan.

It is well known that the thickness of some metallic layers (e.g. Nb, Al, Ta, Ti) can be evaluated by anodic oxidation. Under appropiate conditions they anodize at a constant rate (Nb: 0.9 nm/V) up to thicknesses above 100 nm. The thickness is determined from the voltage span in the anodization profile. Previous anodization experiments with NbN films were generally done for thicknesses > 20 nm. These films do not anodize at a constant rate and the anodization profile is not reproducible. During the development of Hot Electron Bolometer (HEB) mixers with thin (3 to 10 nm) NbN microbridges we have re-examined the anodization of thin NbN films and found a reproducible constant anodization rate of approximately 1.3 nm/V for 2 to 13 nm thick films. This can be of interest for various applications including the investigation of superimposed layers or the passivation of the edges of NbN tunnel junctions. As for NbN HEB mixers the film thickness is an important parameter for the speed, the impedance, and the transition temperature. Its simple evaluation by anodic oxidation before the actual definition of the microbridge can be very useful. We also discuss a model describing the anodization-behaviour of NbN films.

6–110

Conductivity and Kinetic-Inductance Response of the YBaCuO Bicrystal Josephson Junctions Array.

A.P. Lipatov[1], *D.V. Meledin*[1], *A.S. Kalabukhov*[2], *A.N. Zherikhin*[3], *G.N. Goltsman*[1] and *O.V. Snigirev*[2]. [1]Moscow State Pedagogical University, Moscow,119435 Russia. [2]Moscow State University, Moscow, 119899, Russia. [3]Scientific Research Center for Technological Lasers, Toitzk, Moscow region,142092 Russia.

We studied a conductivity and a kinetic-inductance response of an one-dimensional YBaCuO Josephson junctions array (JJA) and a thin-film junctions array (JA) fabricated on 36.8° $NdGaO_3$ bicrystal substrates. Both the JJA and JA were patterned as a meander line with 3-5 μm width in 55 nm thick YBCO film. Critical temperature, Tc, and critical current density, jc , were equal to 88 K, 5×10^6 A/cm^2 and 70 K, 5×10^3 A/cm^2 for the JA and JJA correspond-

ingly. The conductivity of JJA in temperature range 4.2 - 88 K has demonstrated the deviations from the RSJ model due to localized states formed at bicrystal boundary. The kinetic-inductance responses of JJA and JA were measured under 780 nm laser radiation modulated at frequencies 1 - 500 MHz. Measured responses had temperature dependency with a maximum at 53-58 K. A kinetic-inductance response was found at temperatures below the maximum, and mixed kinetic-resistive bolometric response was found at higher temperatures.

6–111

A Superconducting Tunnel Junction with Superconducting Microstrip Coil for X-ray Detector.

T.Taino[1,2], *H.Nakagawa*[1], *M.Aoyagi*[1], *H.Akoh*[1], *K.Maehata*[2], *K.Ishibashi*[2], *H.Satoh*[3], *T.Ikeda*[3], *T.Oku*[3], *C.Otani*[3], *W.Otani*[3], *H.Kato*[3], *K.Kawai*[3], *H.Miyasaka*[3], *H.M.Shimizu*[3], *H.Takizawa*[3] and *H.Watanabe*[3]. [1]Electrotechnical Laboratory (ETL), Tsukuba, Ibaraki, 305-8568, Japan. [2]Kyushu University, Fukuoka, Fukuoka, 812-8581, Japan. [3]The Institute of Physical and Chemical Research (RIKEN), Wako, Saitama, 351-0198, Japan.

We have proposed and demonstrated a superconducting tunnel junction (STJ) with superconducting microstrip coil for X-ray detector. The superconducting microstrip coil has advantages of an external magnetic field free and a high reproducibility operation for X-ray detector. Since the superconducting microstrip coil is integrated on the STJ, directional fluctuations between magnetic field and STJ doesn't have to consider. Using the superconducting microstrip coil with superconducting ground plane, magnetic field can be closed around the STJ. This feature allows that STJ for X-ray detector with suppression of Josephson current and digital processing circuit of signal from X-ray detector with use of Josephson current can be integrated on the same chip. The STJ with superconducting microstrip coil was fabricated by Nb/Al/AlO_x/Nb junction technology with $2\mu m$ design rule. Magnetic field dependence of the STJ using the superconducting microstrip coil was investigated. Details of design and fabrication and experimental results will be presented.

6–112

Mm and submm wave mixing and selective detection by YBCO bicrystal Josephson junctions on sapphire.

K. Y. Constantinian[1], *G. A. Ovsyannikov*[1], *A. D. Mashtakov*[1], *N. G. Pogosyan*[2], *A. A. Hakhoumian*[2], *J. Mygind*[3] and *N. F. Pedersen*[3]. [1]Institute of Radio Engineering and Electronics RAS, 103907, Moscow, Russia. [2]Institute of Radiophysics and Electronics Armenian National Academy of Sciences, 378410, Ashtarak-2, Armenia. [3]Department of Physics, Technical University of Denmark, DK-2400, Lyngby, Denmark.

We present the results of mm wave (40 – 140 GHz) and submm wave (270 –550 GHz) frequency down conversion and selective detection in Josephson junctions, prepared by 100 nm thick and 4 mm wide YBCO thin film deposition on bicrystal sapphire substrates. Authonomous I-V characteristics exhibit some minor deviations from RSJ model. Shapiro step amplitudes also fitted to RSJ model within spread less than 5%. At the same time the linewidths of Josephson oscillation, obtained from selective detector response function, measured at 505 GHz and ambient temperature 17-20 K, were 3.5 - 4 times wider, than predictions of RSJ model. Down converted frequency mixing products were measured by cryocooled 1.5 GHz amplifier. The heterodyne mixing, using the 3-rd harmonic pumping at 149 GHz has demonstrated strong down converted signal 450 GHz. Reducing the frequency of heterodyne oscillator down to 65 GHz, the mixing has been observed also for harmonics of signal source at frequencies of order of 500 GHz . Linear dependence of output IF signal vs power of applied submm signal indicated the absence of stray response, which may take place due to nonperfect matching and signal refractions. An other indicator was the only one sign for down converted output signal in modulator-demodulator regime.
The work was partially supported by the Russian Program "Actual Problems of Condensed Matter Physics", subdivision "Superconductivity", Fund for Basic Research, NATO and INTAS Research Programs.

6–113

Investigation of quasiparticles diffusion to the edge process in superconducting tunnel junction detectors.

E. Esposito[1,3], *R.Cristiano*[1], *L.Frunzio*[1], *M.Lisitski*[1], *C.Nappi*[1], *G.Ammendola*[2], *L.Parlato*[2,3], *G.Pepe*[2], *H.Kraus*[4] and *P.Valko*[4]. [1]Istituto di Cibernetica del C.N.R., Arco Felice, Napoli, I-80072, Italy. [2]INFM-Dipartimento di Scienze Fisiche dell'Università di Napoli Federico II, Napoli, Italy. [3]Osservatorio Astronomico di Capodimonte, Napoli, I-80131 Ital. [4]Dept. of Physics, Particle and Nuclear Physics, University of Oxford, Oxford OX1 3RH, UK.

Superconducting tunnel junctions (STJs) are promising devices for high energy resolution radiation detection. The progress recently achieved in this field opens the possibility of new applications like advanced instrumentation for material analysis. Several low-Tc superconductors have been considered for STJ-detectors. Among them, Niobium has the highest Tc and is therefore less demanding in terms of operational temperature. Nb-based STJs, however, do not achieve the theoretical limit of the energy resolution. The diffusion to the edge process of the quasiparticles, with the accompanying losses of quasiparticles themselves, in the bulk and at the edge of the junction, can be considered one of the mechanisms which reduces the energy resolution. Moreover, the efficiency of the charge collecting mechanism in such devices can be improved when both the electrodes contribute to the tunnelling so that charge amplification processes caused by multiple tunnelling of quasiparticles take place. We present a model for the detector response which takes into account both the multiple tunnelling and the diffusion of the quasiparticles. We compare our theoretical predictions with measurements data from X-ray irradiation of Nb/Al2O3/Nb junctions where the diffusion to the edge process is relevant and we show that our model is able to reproduce all the major features of the experimental results.

6–114

Development of Superconducting Tunnel Junctions with Al Trapping Layers for X-ray Detectors.

H. Sato[1], *K. Kawai*[1], *H. Miyasaka*[1], *T. Oku*[1], *W. Ootani*[1], *C. Otani*[1], *H.M. Shimizu*[1], *H. Watanabe*[1], *H. Nakagawa*[2], *T. Taino*[3], *T. Ikeda*[1], *H. Kato*[1] and *M. Aoyagi*[2]. [1]The Institute of Physical and Chemical Research (RIKEN), 2-1 Hirosawa, Wako, Saitama 351-0198, Japan. [2]Electrotechnical Laboratory (ETL), 1-1-4 Umezono, Tsukuba, Ibaraki 305-8568, Japan. [3]Department of Nuclear Engineering, Kyushu University, Hakozaki, Fukuoka 812-8581, Japan.

Superconducting tunnel junctions (STJs) have a potential for being X-ray detectors with good energy resolution because of their small band gap energy. In order to realize high energy resolution, large number of quasiparticles should be produced and led to the read out electronics circuit when an X-ray is absorbed in a STJ. For this purpose, fabrication of STJs with Al layers on either side of a tunnel barrier (Nb/Al/AlOx/Al/Nb) has been started. In such STJs, quasiparticles created in the Nb layer are diffused and trapped in the Al layers. This trapping effect is known to enhance the signal gain which leads to an improvement of the signal-to-noise ratio. At present, by irradiating X-rays with an energy of 5.9 keV from a ^{55}Fe radioisotope source, 10 to 20 times greater signals than that of our Nb-based STJs have been observed. The detail of our fabrication processes, the quality of the STJs and the results of the X-ray measurements will be discussed.

6–116

Performance of NbN hot electron bolometric mixers at terahertz frequencies.

P. Yagoubov[1], *M. Kroug*[1], *H. Merkel*[1], *E. Kollberg*[1], *J. Schubert*[2] and *H.-W. Hubers*[2]. [1]Department of Microelectronics, Chalmers University of Technology, S-412 96 Gothenburg, Sweden. [2]DLR Institute of Space Sensor Technology, D-12489 Berlin, Germany.

The aim of this research is to design and fabricate sensitive wideband heterodyne receivers for operation in the terahertz frequency range. They are needed in particular for atmospheric observation and radio astronomical applications. The devices are superconducting Hot Electron Bolometric (HEB) mixers. The bolometer element is made out of ultrathin, 3-4 nm, NbN superconducting film deposited on a high resistivity Si substrate. The length of the bolometer microbridge is 0.1-0.2 um, the width is 1-2 um. It is integrated with a planar spiral antenna on the same substrate and placed on the backside of a Si elliptical lens. The choice of superconducting material is determined by the potential to achieve a wide intermediate frequency bandwidth together with a very low, almost quantum limited at terahertz frequencies, noise. The gain bandwidth of 3-4 GHz and noise bandwidth of 5-8 GHz have been already measured for NbN based HEB mixers. In this paper we present results of heterodyne mixing at frequencies between 0.7 and 3.1 THz. The best results of the total DSB receiver noise temperature are: 800 K at 0.7 THz, 1100 K at 1.6 THz, 2000 K at 2.5 THz and 4700 at 3.1 THz.

6–117

Particle Detection with Geometrically-Metastable Type-I Superconductors.

M.R. Gomes[1], *T.A. Girard*[1], *C. Oliveira*[2] and *V. Jeudy*[3]. [1]Centro de Fisica Nuclear, Universidade de Lisboa, Lisboa 1649-003 Portugal. [2]Departamento da Fisica, Instituto Tecnologico e Nuclear, Sacavem 2685, Portugal. [3]Groupe de Phsysique des Solides (CNRS UMR 75-88), Universites de Paris 7/6, Paris 75251, France.

Recent results in the electron irradiation of geometrically-metastable tin lamina by Jeudy et. al. suggest the use of rhenium in detector development as a result of its intrinsically higher stopping power. We report a similar response study with lamina of 25 and 50 micron thick rhenium at 330 mK under electron and X-ray irradiation, using a fast-pulse induction system which records the irreversible flux transfer associated with the particle interactions. Experiments yield fully-resolved energy spectra, with a linear response and high efficiency. The results additionally provide information on the thermal evolution of the geometrical energy barrier, and associated flux instabilities.

6–118

$(YBCO/STO)_n$ mutilayers : a way to avoid substrate micromachining of microbolometers ?.

N.Cheenne[1,2], *D.Robbes*[1], *J.P.Maneval*[3], *S.Flament*[1], *B.Mercey*[2], *J.F.Hamet*[2] and *L.Mechin*[1]. [1]GREYC-Instru - UPRES-A 6072, CAEN, 14050, France. [2]CRISMAT - UMR 6508, CAEN, 14050, France. [3]Ecole Normale Superieure, PARIS, 75231, France.

We have refined thermal conductance measurements for two distinct types YBCO / STO buffer / MGO structures : YBCO single layer and YBCO decoupled by a superposition of ultra-thin (7 nm + 8 nm) YBCO/STO bilayers. Excitation of the films was performed using either a modulated laser beam at 780 nm that heats a reference sample and a multilayered $600\times40\mu m^2$ strips and smaller microbridges , as well as samples with a shorter period of the decoupling layer. In the single-layer and the multilayered samples respectively, we got thermal conductances per unit area of 1000 W/K/cm^2 and 60 to 100 W/K/cm^2. The latter values lead to thermal conductance of small microbridges, say $1\times3\mu m^2$, falling in the muW/K range that is suitable for antenna-coupled microbolometers at the pW/$sqrtHz$ level, close from the best achieved performances using substrate micromachining. Finally we propose a novel method, using the transient response to critical current steps, for measuring the phonon escape times at 77K.

6–119

A Self-Consistent Hot Spot Mixer Model for NbN Phonon-Cooled Hot Electron Bolometer.

H. F. Merkel, *P. Khosropanah*, *P. Yagoubov*, *M. Kroug* and *E. Kollberg*. Department of Microwave Electronics, Chalmers University of Technology, S 412 96 Göteborg, Sweden.

Based on a one-dimensional power balance for electrons and phonons, the bolometer bridge resistance as a function of bias and RF heating is determined where the dependence of the electron thermal conductivity and of the electron-phonon interaction with electron temperature is taken into

account. An analytic approximation for the electron temperature profile is given where the electron phonon interaction has not been linearized. A hot spot is formed where the electron temperature exceeds the critical temperature. Under such hot spot conditions a small signal model is derived in a specific operating point where the conversion gain and the thermal fluctuation noise are calculated. Results for the IV characteristic, gain and noise figures are in close coincidence with experimental data for several different HEB mixers obtained at 1THz and 2.5THz. Optimum operating points for 200nm long and 1um wide 3.5um thick devices are predicted around 0.8mV where about a third of the device length is normal conducting. There is a tradeoff between conversion gain being maximum when the hot spot is smallest and fluctuation noise being smallest when the electron temperature slope around the critical temperature is largest. Indeed optimum operating points for such HEB mixers are found at 0.8mV

6–120

Investigation of the far-infrared absorption processes in high temperature superconductors for construction fast infrared radiation detectors.

E. A. Kafadaryan. Institute for Physical Research National Academy of Scienses, Ashtarak-2,378410,Armenia.

The resonant absorption processes between 200-600cm-1 arised from electron excitations located on the Fermi surface of high Tc superconductors are used to induce nonequilibrium electron heating with potential to build fast and sensitive radiation detectors operated at wavelength longer than 50 micron at wide temperature region.

6–121

Disordered suspensions of metastable superconducting microgranules.

A. Peñaranda, *C.E. Auguet* and *L. Ramírez-Piscina*. Departamento de Física Aplicada, E.U.P.B., Universidad Politècnica de Catalunya, c/ Dr. Marañón, 44, 08028 Barcelona.

Some proposed detectors of neutrinos and dark matter are based on the phase transitions induced by radiation in a disordered suspension of superheated superconducting microgranules. The metastable state is achieved by an external magnetic field. We perform simulations of the successive transitions when the external magnetic field is slowly increased from zero. We study systems with different fractions of volume occupied by the microgranules (filling factor ρ), from 0.001 up to 0.20. In the calculus of the surface magnetic field of each microgranule we consider the multipolar magnetic contributions of the remainder superconductor granules by an iterative method which allows us to control the results accuracy. We compare systems with different initial ρ that after successive transitions evolve to the same final value. We find that the successive transitions induce a strong ordering mechanism on the systems. They behave in such a way that both the spatial inhomogeneities and the surface magnetic field distributions tend to homogenize. We also compare simulations with previous analytical perturbative results. Theory provides the correct qualitative behaviour of transitions and surface magnetic field, but the range of validity appears to be limited to extremely diluted samples

PLENARY SESSION 7

Wednesday Morning, September 15th, 8:30-10:00

8:30 7–1

Advances in large scale applications of superconductors

P. Komarek. Forschungszentrum Karlsruhe GmbH Institute for Technical Physics D76021 Karlsruhe, P.O. Box 3640.

Advances can be reported in principle from most areas where superconductivity use is under investigation or already established. Most of the existing applications rely still on LTS use. This concerns research applications as well as industrial applications. One must mention the magnet systems for large accelerators as LHC and the systems for magnetic fusion devices (LHD, W7-X and the ITER model coils). Further, high field NMR spectroscopy systems are approaching the 1000 MHz class (23,5 T in the magnet bore), a challenge to the most advanced LTS as well as to HTS. In the MRI business trends for HTS use have successfully been demonstrated, however economy will still depend on HTS wire cost reductions. This problem is also decisive for other HTS applications already technically feasible, as cryogenfree magnets, small SMES and magnetic separation. Well in use with advantages for new constructed magnets are already HTS current leads for medium currents, for very large currents their development is well proceeding too. The large potential for HTS in electric power equipment is the basis for intensive development programmes for transmission cables, fault current limiters, transformers and motors. Here can be refered to another plenary talk in this conference.

9:15 7–2

Materials for Superconducting Electronics.

H. Rogalla. University of Twente, Low Temperature Division, 7500AE Enschede, the Netherlands.

With the advancement of superconducting electronics, materials properties and their tailoring to applications become more and more important. Whereas, e.g., for a long time single barrier Niobium Josephson junctions were fully adequate to the requirements of certain applications or, e.g., single-layer techniques for high-$T_(c)$ devices, new applications and concepts require double barrier Josephson junctions or multiple high-$T_(c)$ layers applying compositional control in its thickness on an atomic or molecular level. This also holds for devices, which will make use of special symmetries of wave functions in certain superconducting materials. Here also high lateral control will be very important. Furthermore, the application in complex analog or digital circuits require a high degree of reproducibility of the device characteristics and thus of the materials properties. In this talk a few typical applications from classical and high-$T_(c)$ electronics and the interdependence between the material properties, preparation methods and resulting device characteristics will be discussed. A focus will lie on the recent achievements in the control of layer deposition by pulsed laser methods with in-situ RHEED-analysis. In addition, the local control of material parameters for the tailoring of weak coupling between superconductors as needed for the preparation of Josephson junctions will be discussed.

ORAL SESSION 8A+9A: Wires and Tapes- BSCCO I

Wednesday Morning, September 15th, 10:30-12:45

10:30 *8A–1

Thermal Equilibrium and Texturing in Ag/Bi,Pb(2223) and Ag/RE(123) Tapes.

R. Flükiger, *E. Giannini*, *F. Marti*, *R. Passerini*, *M. Schindl*, *H. L. Suo*, *E. Koller* and *J.-Y. Genoud*. Département de Physique de la Matière Condensée Université de Genève 24, quai Ernest Ansermet CH-1211 Genève 4, Switzerland.

In Ag/Bi,Pb(2223) tapes, thermal equilibrium is influenced by the reaction history and by the cooling conditions. A recent high temperature neutron diffraction study confirmed the formation of the Bi,Pb(2223) phase by nucleation and growth. During the cooling process, the phase Bi,Pb(2223) was found to remain stable, i.e. the phase limits are almost temperature independent. At the same time, however, a newly formed Bi(2212) phase was observed, as a result of the decomposition of the Bi(2201) and 14/24 phases. We have recently found that the Pb content inside Bi,Pb(2223) filaments shows a decrease with reaction time, correlated to an enhancement of Tc from 107.8 to 109.2 K after 200h in air at 838°C. The question is discussed, whether the decrease of Pb content is correlated to the reasons about the various unsuccessful attempts to recover the Bi,Pb(2223) phase after treating above the decomposition temperature: the solution of this problem, involving a better knowledge about the formation conditions, may lead to an improvement of jc. An EBSD study showed no correlation between the orientations of the Ag sheath and of the Bi,Pb(2223) in the ab plane. In Ag/R.E.(123) systems, however, there is commensurability between the Ag surface and the superconducting cell. A single orientation was found in R.E.(123) layers, sputtered on Ag single crystals and textured Ag ribbons, but only for the (110) orientation. The best results were obtained for Nd(123), where FWHM values of 3° were observed. The specific problems to be solved on the way towards high jc R.E.(123) layers on Ag ribbons are discussed with regard to the thermal equilibrium of the composite.

11:00 *8A–2

Long Length PIT Conductors Realized by Rectangular deformation Route.

P. F. Herrmann[1], *G. Duperray*[1], *D. Legat*[1], *A. Leriche*[1], *C-E. Bruzek*[2], *Y. Parasie*[3] and *J. Bock*[4]. [1]Alcatel, F-91461 Marcoussis, France. [2]Alcatel, F-59460 Jeumont, France. [3]Alcatel, 75411 Paris, France. [4]Aventis Research & Technologies, D-50351 Hürth, Germany.

Alcatel pursues the development of multifilamentary Bi-2212 and Bi-2223 tape-conductors by the rectangular deformation route. The Bi-2212 conductor represents today the optimum cost versus performance solution for magnet applications in the intermediate temperature range 20-30 K. This interest for the Bi-2212 conductor is related: 1. to higher current density in the intermediate temperature range and 2. to the higher stability range at the formation temperature of the superconducting phase in the silver matrix which results in a simple single step heat treatment. Both of these facts result

in a cost-effective solution for magnets. For the assessment of the conductors test coils have been realized both by the W&R and by the R&W technique. For the time being km length are available for the W&R process and 400 m lengths of fully reacted conductors with good tolerance to bending are available for R&W process. The Bi-2223 conductor remains of course the best solution for 77 K applications where the conductor which is realized by the rectangular route shows a strongly reduced field dependency compared to conventional PIT conductors.

11:30 8A–3
Performance at 10-50K of Bi-2212/Ag multilayer tapes fabricated by using PAIR process.
H. Kitaguchi[1], *K. Itoh*[1], *T. Takeuchi*[1], *H. Kumakura*[1], *H. Miao*[1,2], *K. Togano*[1,2], *T. Hasegawa*[3] and *T. Koizumi*[3]. [1]National Research Institute for Metals. [2]CREST, Japan Science and Technology Corporation. [3]Showa Electric Wire & Cable Co. Ltd.

We developed PAIR (Pre-Annealing and Intermediate Rolling) process, which is a fabrication procedure for Bi-2212/Ag composite tapes, in order to improve their superconducting properties. High transport critical current density (J_c-oxide) > 500kA/cm^2 at 4.2K, 10T can be obtained for Bi-2212/Ag tapes fabricated by using PAIR and melt-solidification process. In this paper, we report high temperature properties of PAIR processed Bi-2212/Ag multilayer tapes in order to show their potential for practical applications operated at cryocooling temperatures. Magnetic field dependence and angular dependence of J_c are investigated at temperatures ranging 10-50K by using He gas cooling and liquid Ne. Transport resistivity is also measured in the temperature range of 15-90K, in magnetic fields ranging 0-10T in order to determine irreversible fields. High temperature performance of the tapes is attractive to consider future applications. For example, a straight short sample carries (J_c-oxide) = 150kA/cm^2 (I_c = 264A, engineering-J_c = 300A/mm^2) and 50kA/cm^2 (92A, 100A/mm^2) at 27.1K (in liquid Ne), in magnetic fields (parallel to the tape surface) of 2T and 10T, respectively. Engineering-J_c of 100A/mm^2 is obtained even in the perpendicular field of 0.5T at 27.1K.

11:45 9A–1
Advanced rolling techniques for Bi(2223)/Ag wires and tapes.
P. Kovac[1], *I. Husek*[1] and *L. Kopera*[1]. [1]Institute of Electrical Engineering of Slovak Academy of Sciences, Bratislava, 842 39, Slovakia.

Most of the multifilamentary Bi(2223)/Ag composites are usually produced by drawing and flat rolling which results in a limited fill factor of BSCCO/Ag composite, a regions of various density and generation of transversal cracks. Therefore, the advanced deforming techniques as two-axial (TAR) and eccentric rolling (ER) were aslso used recently for Bi(2223)/Ag composites. TAR allows to increase the fill factor of BSCCO/Ag and to improve the filament density and homogeneity as well. Consequently, engineering current density is increased and filaments show improved resistance to mechanical stress. The homogeneous deformation of BSCCO/Ag/barrier/Ag by TAR is also possible. The next advantage of TAR is the texturization of Bi-2223 grains in two perpendicular directions which allows to reduce the anisotropy of critical current. A new rolling technique, eccentric rolling allows to perform tape pressing in long continuous lengths at speeds comparable to the rolling operation. The apparently higher transport critical current densities were measured for various sinle-, 19- and 61-filament tapes deformed by ER in comparison to flat rolling. The magneto-optical imaging shows that ER samples had a significantly reduced number of transversal cracks which is a vital aspect for increasing the critical current density in rolled tapes.

12:00 9A–2
High critical current and defect free km long Bi-2223 alloyed multifilament tapes.
W.G. Wang, *M.D. Bentzon*, *J. Goul*, *A. Barkani*, *M.B. Jensen*, *P. Skov-Hansen*, *Z. Han* and *P. Vase*. Nordic Superconductor Technologies A/S, Priorparken 685, DK-2605 Broendy, Denmark.

Highly homogenous, defect free, high strength, and high critical current (I_c) Bi-2223 tapes are produced in km lengths. For many applications of the high temperature superconducting wires and tapes, such as cables, magnets, transformers, and current limiters, it is extremely important to make the long Bi-2223 tape with high quality and in particular free of defects. The number of defects and the sensitivity of I_c degradation was measured by a continous Hall probe set up. This set up has much higher spatial resolution and efficiency than normal four probe transport current measurement. The homogeneity and the defect level of the tapes are related to the amount of cracks and bubbles. By improvement of the processing technique, km long Bi-2223 tapes with I_c higher than 50 A, J_e higher than 8 kA/cm^2, I_c standard deviation of less than 4 %, and with no bubbles have been produced and measured at 77 K in self-field by Nordic Superconductor Technologies.

12:15 9A–3
Bi-2223 tape processing.
B. Fischer[1], *T. Arndt*[1], *J. Gierl*[1], *H. Krauth*[1], *M. Munz*[1], *A. Szulczyk*[1], *M. Leghissa*[2] and *H.-W. Neumüller*[2]. [1]Vacuumschmelze GmbH, 63450 Hanau, Germany. [2]Siemens AG, 91050 Erlangen, Germany.

For large scale applications in power engineering like transmission cables, transformers and motors different Bi-2223 tapes in long length are required. With respect to this applications we produce 55-filament tapes with a high strengthed matrix of lengths up to 600 m carrying currents up to 75 A (overall current density up to 8,5 kA/cm^2). In short samples critical current densities over 40 kA/cm^2 were measured. An overview of the fabrication process and the optimasation of different process parameters of the multifilamentary tapes are given. Besides the mechanical and microstructural properties of different Ag, Ag-alloy and coated tapes we present the current carrying capability in differnt magnetic fields and at different temperatures as well as the AC loss characteristics of these tapes. This work is supported by the german BMBF, grant-no: 13N6481A/6

12:30 9A–4

Novel, internally stranded "Ring Bundled Barrier" Bi-2223 tapes for low AC loss applications.

J. Krelaus, *R. Nast*, *H. Eckelmann* and *W. Goldacker*. Forschungszentrum Karlsruhe - ITP, P.O.Box 3640, D-76344 Karlsruhe, Germany.

For application of Bi-2223 tapes in transformers, energy storage devices or motors, novel ring bundled barrier (RBB) tapes open up the field of up-scaled transport currents at low AC losses: An internal-stranding technique increases the cross section simultaneously observing the thermodynamic limitations of standard tape preparation. A resistive barrier guarantees optimal AC characteristics even in perpendicular alternating magnetic fields. The conductor is prepared by bundling multifilamentary strands in an outer tube around a resistive core ($SrCO_3$). This precursor is swaged, twisted and rolled to a tape which is thermomechanically reacted to obtain the final conductor. It resembles the well-known Rutherford cable where single strands are wound around a resistive profile thus effectively reducing losses in perpendicular fields. The filaments are situated near the surface of the composite, so phase formation is not drastically changed with respect to standard tapes having smaller cross sections. Superconducting properties of prototype RBB conductors are investigated. Dependencies of critical currents on DC fields ($I_c(B)$, $I_c(\vartheta)$) and temperatures ($I_c(T)$) are presented. In addition, the impact of mechanical stresses on I_c is studied. Main parameters of interest are different resistive core/matrix materials and twist pitches – AC characteristics are presented in a separate contribution at this conference.

ORAL SESSION 8B+9B: Motors, Bearings and Levitation

Wednesday Morning, September 15th, 10:30-12:45

10:30 *8B–1

Electric Machines With the Bulk HTS Rotor Elements. Recent Results and Future Development.

L.K. Kovalev[1], *K.V. Ilushin*[1], *S.M.A. Koneev*[1], *V.T. Penkin*[1], *V.N. Poltavets*[1], *W. Gawalek*[2], *T. Habisreuther*[2], *B. Oswald*[3] and *T. Strasser*[3]. [1]Moscow State Aviation Institute (Technical University). [2]Institut fur Physikalische Hochtechnologie (IPHT), Jena, Ger. [3]Oswald Elektromotoren GmbH, Miltenberg, Germany.

New types of HTS electric machines are considered. The first type is hysteresis motors and generators with cylindrical and disk rotors containing bulk HTS elements. It was shown theoretically and experimentally that at the temperature level of liquid nitrogen the specific mass-dimension parameters of the hysteresis HTS machines are 2-5 times better then the similar one for the conventional hysteresis electrical machines. The second type is reluctance motors with the compound HTS-Ferromagnetic rotors. The compound HTS-Ferromagnetic rotors consisting of the joined alternating bulk HTS and ferromagnetic plates provide a new active material for the electromechanical purposes. Such rotors have anisotropic properties (ferromagnetic in one direction (x) and diamagnetic in perpendicular one (y)). It allows to improve the power characteristics of HTS motors. The simulation and experimental data show that the cryogenic HTS reluctance motors operating in liquid nitrogen have mass-dimensional and power parameters 3-5 times better in comparison with the traditional reluctance and asynchronous motors. It is important to mention that the reluctance HTS motors have rather high values of power factor (cosfi=0.7-0.8) at the output power rating 5-15kW and more. The third type is the ≪trapped-field≫ motors with the rotors containing the compound HTS-Ferromagnetic core surrounding by the HTS cylindrical shell. The HTS shell is used for the ≪field-trapping≫ and the anisotropic core determines the direction of the magnetic momentum. The theoretical investigations demonstrated that such motors posses 4-6 times better output characteristics. A series of hysteresis HTS motors with output power rating 1kW (50Hz)-4kW (400Hz, synchronous rotating velocity =24000rpm) and a series of reluctance HTS motors with output power 2-15kW (50Hz) was constructed and successfully tested. The future HTS motors with bulk YBCO elements operating in the medium of liquid nitrogen and high output power $\sim$ 125 kW (and more) and higher power factor ($cos\phi > 0.75$) are discussed. The future applications of the novel types of HTS electrical machines with bulk HTS elements are discussed.

11:00 8B–2

High - Speed Rotor Systems with HTS Bearings.

F. N. Werfel, *R. Rothfeld*, *D. Wippich* and *U. Flögel - Delor*. Adelwitz Technologiezentrum GmbH, Adelwitz, D-04886, Germany.

Engineering prototype high - speed wheel assemblies with passive HTS bearings (smb) were designed and fabricated to suspend a centrifugal rotor and an optical mirror com-

ponent and rotate up to 180 000 rpm at 77 K. In air the speed of a 4 cm rotor is limited to about 90 000 rpm due to air friction. Measurements of bearing stiffness and damping, drag torque, and wheel performance are presented. Among several advantages of smb, this concept does not limit the rotation speed at the level of the bearings. With v = 570 m/s circumference velocity the rotors are designed to accept high stresses to maximise the profit of the high rotation speed for centrifuges and scanning devices. The combination of YBCO bore - bulks and permanent magnet rotors in radial configuration are investigated to gather basic and practical data on the smb technology. The polycrystalline melt textured YBCO rings with a radial - like texture provides both high stiffness, rapid damping of the critical rotor vibrations and very low rotational energy losses. With respect to the high - speed rotation alternating magnetic fields due to non- ideal rotors cause energy loss and eddy currents in the YBCO rings. The double - bearing wheel construction increases the maximum imbalance stability of a centrifugal system relative to commercial one by a factor of five. It is concluded that the superconducting magnetic bearings with integrated cooling devices are capable of providing reliable, long -life operation in centrifugal systems and other high-speed applications.

11:15 8B–3
Stability of magnetic HTSC bearings under axial vibrations.
E. Portabella, *R. Palka*, *H. May* and *W.R. Canders*. Institut für Elektrische Maschinen, Antreibe und Bahnen. Technische Universität Braunschweig. Braunschweig, 38106, Germany.

Melt-processed superconductors provide the possibility to build rotational bearings with low friction and high stability. In such systems vibrations induce a cycling loading which can lead to levitation drift and anomalous dynamics. A new experimental set up has been designed to study the dynamic behaviour of the permanent magnet-superconductor interaction. The system consists of a force measuring system coupled to a cryocontainer, where the high temperature superconductor is fixed, and a permanent magnet arrangement linked to an electrodynamic shaker. The phase shift between the excitation (vibrational motion of the magnets) and the response of the system (magnetic force on the superconductor) has been measured for different frequencies and amplitudes. The central issues of stability, stiffness and damping associated with axial vibrations are discussed. The influence of the levitation gap as well as of the cooling process have also been studied.

11:30 8B–4
Superconducting Motors with HTS Bulk Material for Medium Power Range.
B. Oswald[1], *T. Strasser*[1], *M. Krone*[1], *M Soell*[2], *J. Oswald*[1] and *K.J. Best*[1]. [1]OSWALD Elektromotoren GmbH, D-63897 Miltenberg, Germany. [2]Fachhochschule Landshut, Germany.

On the basis of experimental results of superconducting motors with increased power up to 10 kW a conceptual design is presented for motors with incorporated YBCO bulk material. This is anticipated for the use up to a power range of 100 kW. With this respect we emphasise on the optimisation of the main motor parameters efficiency, power factor and motor dimensions. The major advantage of this type of motors is having both a high power density and a high efficiency.

11:45 9B–1
Levitated Liquid Hydrogen Cryotank For Automotive Applications.
J. Bock[1], *M. Baecker*[1], *G. Brommer*[1], *L. Cowey*[1], *M. Kesten*[2], *H. Fieseler*[2], *W. R. Canders*[3], *H. May*[3], *H. C. Freyhardt*[4] and *A. Leenders*[4]. [1]Aventis Research & Technologies, D-50351 Huerth, Germany. [2]Messer, D-47805 Krefeld, Germany. [3]University of Braunschweig IMAB, D-38023 Braunschweig, Germany. [4] 4ZFW gGmbH, D-37073 Goettingen, Germany.

A functional model of a levitated cryotank for storing liquid hydrogen was presented by the consortium in 1998. For the first time the principle of inherent stable levitation with high temperature superconductors and permanent magnets was applied to the interior container of a cryotank. Comparative measurements with a conventional liquid hydrogen tank showed an improvement of the insulation by more than 100%. Now the first real prototype, suitable for automotive applications, with improved design and capacity is under development and will be tested in close cooperation with a German car manufacturer. The new design consists of a cylindrical interior tank suspended on a fixed central tube. This permits a compact tank, suitable for direct incorporation into automobiles. The design requires HTS parts shaped as a hollow cylinder and the characterization of their levitation properties. A new measuring device allows the measurement of levitation and guiding forces of large HTS cylinders up to vanishingly small gaps between superconductor and permanent magnet. First measurements of the radial stiffness of cylindrical HTS bearings at 20 K show that both MCP (Melt-Cast-Process) Bi-2212 and Melt-Growth Y-123 bulk material show sufficient forces to levitate the interior tank with 140 l of liquid hydrogen.

12:00 9B–2
Superconducting Thrust Bearings.
T.A. Coombs and *A.M. Campbell*. IRC in Superconductivity, Cambridge University, Madingley Road, Cambridge CB4 0HE United Kingdom.

A great deal of research effort has been devoted to the development of superconducting thrust bearings. These are seen as replacements for conventional rolling element type bearings and direct competitors to other non-contact type bearings such as Electromagnetic Bearings. We have constructed an experimental rig which is designed to test superconducting bearing systems for energy storage flywheels. The rig is built in two main sections, a demountable "top hat" cylindrical section, and this is supported on an aluminium base plate. The resulting experimental chamber has a volume of 0.4 m3. Evacuation is performed by a rotary pump and a turbomolecular pump. Cooling is provided by a CTI 350CP cryocooler. Control and datalogging is by computer program written under Visual Basic 5.0. The flywheel rig is complemented by a vibration analysis rig which is used to test the effect of vibrations by providing biaxial stimulation in a

range of known waveforms to individual YBCO pucks. The flywheel under test was supplied by British Nuclear Fuels, weighs 40kg and is representative of the Pirouette flywheel system. The experimental rig incorporates a loading mechanism, for inducing and measuring out of balance forces, together with optical measurement systems, for measuring rotation speeds and displacements.

12:15 9B–3

Development and Test of a 300Wh/10kW Flywheel Energy Storage System.

R. Koch[1], *R. Wagner*[1], *U. Sutter*[1], *M. Sander*[1] and *H. J. Gutt*[2]. [1]Forschungszentrum Karlsruhe GmbH, INFP, P. O. Box 3640, D-76021 Karlsruhe. [2]Universität Stuttgart, IEMA, Pfaffenwaldring 47, D-70569 Stuttgart .

The overall performance of high speed flywheel systems, which appear increasingly attractive not only for short term but also for long term stationary energy storage, depends on several critical components. One of them is the bearing. Superconducting Magnetic Bearings (SMBs) can stabilize a flywheel rotor without any active control, and at the same time, they provide a remarkable reduction of bearing losses. Based on our experience with SMB technology, we developed an integrated high speed flywheel system (300Wh/10kW), which is especially designed for long-term stationary energy storage. The dynamic behavior of the system was tested and evaluated with respect to axial and radial stiffness, damping and critical speeds. Rotational loss characteristics were measured, and the energy efficiency of our system has been estimated by analyzing different components of the flywheel system for a whole charge/standby/discharge cycle.

12:30 9B–4

1 kW Bearingless Superconducting Motor with Axial Field Exitation.

J. Pallarés[1,2], *X. Granados*[1], *R. Bosch*[2] and *X. Obradors*[1]. [1]Institut de Ciència de Materials de Barcelona, Bellaterra, Barcelona, 08193, Spain. [2]Escola Tècnica Superior d'Enginyers Industrials de Barcelona (UPC), Barcelona, 08028, Spain.

A superconducting motor has been constructed by using conventional iron-copper armature and a disk shaped superconductor rotor The armature consists of two plane iron cores with 24 slots which are wounded with standard copper in a 8 poles-3 phases configuration. The flux is thus distributed axially between the poles of both cores. The rotor has been made by a glass fiber reinforced epoxy disk with 8 superconducting cylindrical pieces homogeneously distributed according to the situation of the poles in the armature. The rotor is placed in the gap between both armatures. The mabnetic field in the gap is responsible of both, driving and levitating forces. The performance of the motor has been measured by means of the torque, load angle, position and applied magnetic field. The centering and levitating forces have also been measured.

ORAL SESSION 8C+9C: Josephson Junctions I

Wednesday Morning, September 15th, 10:30-12:45

10:30 *8C–1

Intrinsic josepson junctions and grain boundary π-junctions in high temperature superconductors

A. Yurgens, V. Krasnov, Z. Ivanov, T. Claeson. Physics and Engineering Physics, Chalmers, SE-41296 Göteborg, Sweden.

Pre-contacted, small mesas can be etched into a single crystal or an epitaxial film of a high temperature superconductor while the sample is cooled and transport measurements are performed during the etching process. The latter can be stopped at appropriate times, allowing detailed studies. Tunneling between superconducting planes occurs in the c-axis direction, resulting in so called intrinsic Josephson junctions. These can be applied, for example, to study current transport in the c-axis direction under magnetic fields and under rf irradiation.
The properties and possible applications of intrinsic junctions as well as of the well studied grain boundary junctions will be discussed. The d-wave character of the oxide superconductors results in so called pi-junctions that may be used to study the feasibility of quantum computing.

11:00 *8C–2

C-axis Microbridge Junctions for HTS Single Flux Quantum Circuits.

R.G.Humphreys, P.J.Hirst, J.S.Satchell, I.L.Atkin and *M.J.Wooliscroft.* DERA, Malvern, Worcestershire WR14 3PS, UK.

It is widely recognised that reproducible junction critical currents are necessary to implement single flux quantum logic. It has recently been shown that the minimisation of stray inductances is just as important: a technology with low strays can tolerate a larger spread in critical currents than one with large strays. The c-axis microbridge (CAM) technology has an inherently low inductance (0.8pH per square) due to its groundplaned geometry. For a target critical current of 0.5mA at 40 to 60K the CAM junctions must be about 0.5 microns in diameter. Junctions of this type have been fabricated using an electron beam lithography process and show promising reproducibility ((Ic<15%) and high IcRn (>1mV) products at the target operating temperatures.The CAM fabrication technology has been carefully reassessed and a number of simplifications have been made which contribute to reducing stray inductances. The junction properties obtained from this simplified process will be presented.

11:30 8C–3

Mechanisms controlling the electric field effect in High-T_c Josephson Junctions.

C.W. Schneider, A. Schmehl, B. Goetz, H. Bielefeldt, R.R. Schulz, H. Hilgenkamp and *J. Mannhart.* Experimentalphysik VI, Center for Electronic Correlations and Magnetism,Institute of Physics, Augsburg University, 86135 Augsburg, Germany.

Extensive work over the last years showed, that the elec-

tric transport properties in high-T_c grain boundary junctions are being controlled by the dislocation structure of the boundary, the predominant d-wave symmetry of the order parameter for most high-T_c materials and the possibility of band-bending at the boundary interface, thereby forming a depletion layer. Considering all these aspects, the experimental results of three-terminal Josephson junctions based on the electric field effect are analyzed. For these devices, perpendicular electric fields are applied to control the transport properties of the grain boundary. We identified a new mechanism controlling the critical current density of the Josephson junction, acting in addition to the well-known modification of the charge carrier density using an applied electric field. The effect is based on the modification of the electrical screening length of the junction due to a change of the permittivity of the gate dielectric, affecting the width of depletion layer and therefore the critical current density of the Josephson junction.

11:45 9C–1
Current-Phase Relation in High-T_c YBCO Josephson Junctions.
E.Il'ichev, *V. Zakosarenko*, *R.P.J. Ijsselsteijn*, *H.E. Hoenig*, *V. Schultze* and *H.-G. Meyer*. Institute for Physical High Technology, Dept. of Cryoelectronics, P.O. Box 100239, D-07702 Jena, Germany.

The current-phase relation (CPR) of YBCO step-edge, ramp-type as well as several configurations of bicrystal grain boundary Josephson junctions (JJ) has been investigated experimentally. The CPR was obtained from the measurement of the impedance of the phase-biased junction. In the presence of large thermal fluctuations the apparent CPRs for all types of junctions were found to be nonsinusoidal. When thermal noise is negligible the only remarkable deviation from a sinusoidal dependence has been found for the CPR of 45 degree grain boundary JJs. Moreover, for asymmetrical 45 degree grain boundary JJs a large π-periodic component of the CPR has been experimentally observed. These results are consistent with *d*-wave pairing symmetry. Possible explainations are discussed.
Financial support by the DFG (Ho 461/1-1) and INTAS (No. 11459) is gratefully acknowledged.

12:00 9C–2
Meandering of resistive states in two-dimensional arrays of underdamped Josephson tunnel junctions.
D.Abraimov[1], *P.Caputo*[1], *G.Yu.Logvenov*[2], *M.V.Fistul*[1], *A.V.Ustinov*[1] and *G.Filatrella*[3]. [1]Physikalisches Institut III, Universitaet Erlangen-Nuernberg Erwin-Rommel-Str. 1, D-91058 Erlangen, Germany. [2]OXXEL oxide electronics technology Fahrenheitstrasse 9 D-28359 Bremen Germany. [3]INFM Unit and Physics Department University of Salerno, I-84081 Baronissi, Italy.

A well know feature of two-dimensional arrays of underdamped Josephson junctions is the switching of rows of junctions transverse to the bias current. The hysteresis of the *I-V* curve allows to determine the number of rows which are at the gap voltage state while the other rows remain in the superconducting state. We report on the experimental observation of resistive states in two-dimensional arrays of different geometries by means of the low temperature laser scanning microscopy (LTLSM). The novel feature found in our studies is that resistive states can meander from row to row giving raise to the contemporary presence of superconducting and resistive junctions in the individual rows. Numerical simulation have shown that such percolative paths can occur in absence of both positional disorder and thermal noise. We therefore conclude that it is an intrinsic feature of the system to give rise to the meandering of the resistive lines.

12:15 9C–3
A high sensitivity directly coupled Josephson-Fraunhofer-Meissner magnetometer.
E.Sassier, *Y.Montfort*, *C.Gunther* and *D.Robbes*. GREYC, UPRES-A 6072, ISMRA Universite de Caen, Caen, 14050, FRANCE.

A high sensitivity Josephson-Fraunhofer-Meissner magnetometer (JFM) has been derived from the well-known directly coupled dc SQUID design. The pick-up loop (washer) is closed by a strip line at the edge of which is patterned a Josephson Junction instead of a dc SQUID. The whole sensor is 0.85×0.85 cm^2 large. It exhibits a tranfer coefficient of 550 V/T or 1100 A/T as it is respectively current or voltage biased. The measured white noise is 600 fT/$\sqrt{Hz}$ and the 1/f noise corner is around 400 Hz. In agreement with several other team's voltage noise measurements, the white noise level is about 5 times higher than it is predicted by the standard RSJ theory. We have investigated some effects of thermal fluctuations of the superconducting electrodes in the vicinity of the edges of GBJ, as done earlier by Voss & Clarke. Experimental works are also in progress on possible 1/f noise reduction using networks of micro-strip lines to define the pick-up structure.

12:30 9C–4
Spatially inhomogeneous temperature effects in Josephson tunnel junctions.
D. Abraimov[1], *M. V. Fistul*[1], *P. Caputo*[1], *A. V. Ustinov*[1] and *G. Yu. Logvenov*[2]. [1]Physikalisches Institut III, Erlangen-Nürnberg Universität, Erwin-Rommel-Str.1, D-91058 Germany. [2]OXXEL GmbH, Technologiepark Universität, Fahrenheitstraße 9, D-28359, Bremen, Germany.

Low Temperature Laser Scanning Microscopy (LTLSM) is a spatially resolved method for electrical characterization of superconducting filaments, thin films and Josephson circuits. In this report we present an experimental observation of a spatially inhomogeneous LTSM response of small homogeneous tunnel junctions of a dc SQUID interferometer. We shown that, in the absence of external magnetic field, interplay between a non-linear current-voltage characteristic of a single Josephson junction and inhomogeneous temperature distribution in superconducting electrodes leads to the appearance of various inhomogeneous LTLSM patterns in the form of "rings" around small Josephson junctions of dc SQUID. Simple theory of this inhomogeneous thermoelectric effect allows us to describe the dependence of the ring parameters on the bias current, amplitude and dc offset of the laser beam modulation. In the presence of magnetic field, we have found that the response of the dc SQUID drastically changes. We argue that this change is the evidence of the thermomagnetic effect caused by the presence of a tem-

perature gradient across a tunnel Josephson junction in a quantum interference device.

ORAL SESSION 8D: Oscillators and Volt Standards

Wednesday Morning, September 15th, 10:30-11:45

10:30 *8D–1

Josephson Arrays for DC and AC Voltage Metrology.

J. Niemeyer. Physikalisch-Technische Bundesanstalt Bundesallee 100 D-38116.

The development of versatile voltmeters on the basis of quantum effects requires the preparation of large and perfect series arrays of overdamped Josephson junctions. Up to now damping of Josephson junctions has often been achieved by external shunting of SIS (superconductor/insulator/superconductor) junctions. In this case the critical current and the normal state resistance of the junction can be determined independently of each other, but the technology of fabrication is complex and space consuming.
In the case of SNS (superconductor/normal metal/superconductor) junctions, strong damping is reached by internal shunting. The very low normal state resistance of this junction type leads to a low critical voltage - and thus to restrictions in high-frequency operation - unless the junction area is very small. To overcome this disadvantage, the N-layer can be replaced by a semiconductor barrier or the S/N interfaces can be disturbed in the extreme case by introducing an insulating barrier at both interfaces resulting in double barrier SINIS junctions. Arrays of up to more than 8000 SINIS junctions and up to more than 30000 SNS junctions were successfully operated at the 1V DC level. In the case of SINIS arrays, it has been shown that coherent oscillations of the complete array can be phase-locked to the external oscillator. As only a few junctions at the input of the array must be phase-locked, much lesser microwave power is needed to generate reference voltages from the complete array than this is the case for conventional SIS arrays.
Besides their application in large arrays for voltage metrology and oscillators, the described junction types may also become very useful for the preparation of highly integrated single-flux quantum digital circuits.
The work is supported by the European Communities (Project No. SMT4-CT98-2239) and by the BMBF (Projects 13N6835 and 13N7259).
Work financied partially by E.U. under contract B.E. 97-4829 (BYFAULT).

11:00 8D–2

Externally Phase Locked Sub-MM Flux Flow Oscillator for Integrated Receiver.

V.P. Koshelets[1], *A.M. Baryshev*[1,2], *J. Mygind*[3], *V.L. Vaks*[4], *S.V. Shitov*[1], *L.V. Filippenko*[1], *P.N. Dmitriev*[1], *W. Luinge*[2] and *N. Whyborn*[2]. [1]Institute of Radio Engineering and Electronics, Mokhovaya 11, 103907, Moscow, Russia. [2]SRON-Groningen, P.O.Box 800, 9747 AV Groningen, the Netherlands. [3]Department of Physics, Technical University of Denmark, B309, DK-2800 Lyngby, Denmark. [4]Institute for Physics of Microstructure, GSP-105, 603600 Nizhny Novgorod, Russia.

Flux flow oscillators (FFO) has proven to be a reliable wideband and easy tunable local oscillator suitable for integra-

tion with a SIS-mixer in a single-chip sub-mm wave receiver. A noise temperature (DSB) of about 100 K has been achieved for an integrated receiver with the FFO operating near 500 GHz. For spectral radio-astronomy applications besides the noise temperature the instant linewidth of the local oscillator and its long-time stability are required. The dependence of the microwave linewidth of Nb-AlOx-Nb FFOs of a new design on the junctions parameters has been measured in the frequency range 250 - 600 GHz. The linewidth were measured both for autonomous FFO and FFO locked to an external synthesizer via a wideband feedback loop. Experimental data are compared with theoretical estimates to evaluate the influence of the possible mechanisms responsible for the broadening of the FFO linewidth. The feasibility of FFO phase locking to an external reference oscillator is demonstrated experimentally. A FFO linewidth as low as 1 Hz has been measured in the frequency range 270 - 440 GHz. This linewidth is far below the fundamental level given by shot and thermal noise of the free-running tunnel junction.
The work was supported in parts by the Russian SSP "Superconductivity", the INTAS project 97-1712, the Danish Research Academy, the Danish Natural Science Foundation and the Netherlandse Organisatie voor Wetenshappelijk Onderzoek (NWO).

11:15 8D–3

Microwave Circuts with High-T_c Josephson Junctions for Programmable Voltage Standard and Voltage Calibrator.

A.M. Klushin[1,2], *C. Weber*[1], *Kh.A. Ainitdinov*[2], *S.I. Borovitskii*[2], *V.D. Gelikonova*[2], *A.V. Komkov*[2] and *R. Semerad*[3]. [1]Institut fuer Schicht- und Ionentechnik, Forschungszentrum Juelich GmbH, Juelich, 52425, Germany. [2]Institute of Electronic Measurements "KVARZ", Nizhny Novgorod, 603009, Russia. [3]Technical University of Munich, Physic Dept. E10, Garching, 85748, Germany.

We discuss two important metrology applications of Josephson junctions: digital-to-analog conversion (DAC) and voltage calibration. In both cases we are using high-temperature superconducting (HTS) shunted $YBa_2Cu_3O_{7-\delta}$ junctions on bicrystal Y-ZrO_2 substrates operating at 78 K. Two types of microwave circuits for drive frequencies of 30 GHz to 40 GHz and of 70 GHz to 90 GHz were designed and fabricated. Thus far, we successfully tested the circuit operating at 30 to 40 GHz, and are now in the process of evaluating the higher-frequency version. The performance of both circuits will be presented at the Conference. Three experiments with the first version of Josephson voltage calibrator (JVC) have been carried out. First, we compared the steps produced by the niobium reference junction at 4.2 K and the HTS junctions and found no difference with a relative accuracy of $\sim 10^{-6}$. Second, we investigated the form of constant voltage steps and found no measurable step slope. Third, we tested the JVC with the best commercially available counterpart (Zener's voltage standard Fluke 734 B) and did not see any deviations from reference voltage. These results demonstrated that the bicrystal junctions are promising for metrological applications. Work supported by German BMBF under Project 13/N6946/4.

11:30 8D–4

MM wave Josephson radiation in High-Tc bicrystal junction arrays.

K. Y. Constantinian[1], *A. D. Mashtakov*[1], *G. A. Ovsyannikov*[1], *V.K. Kornev*[2], *N.A. Shcherbakov*[2], *M. Darula*[3], *J. Mygind*[4] and *N. F. Pedersen*[4]. [1]Institute of Radio Engineering and Electronics RAS, 103907, Moscow, Russia. [2]Moscow State University, Moscow, Russia. [3]Research Centre Juelish, Juelish, Germany. [4] Department of Physics, Technical University of Denmark, DK-2400, Lyngby, Denmark.

High-Tc Josephson junction arrays with coupling circuits of short-circuited superconducting (5 mm wide and 0.1 mm thick) coupled microstrip lines, provided dc bias in parallel, were fabricated on bicrystal sapphire substrates for experimental investigation of the phase-locking phenomenon. Josephson self radiation, emitted by the array was measured by an external 90 GHz receiver for different applied dc magnetic fields. The minimum linewidths of self radiation for array found is of the same value as the linewidth expected for a single junction with the same normal state resistance and critical current. The array was also studied by numerical simulation. The coupled microstripe lines were modeled as a circuit with lumped LC-parameters. The coupling superconducting circuits provide Josephson-junction interaction as at dc current, so at high frequencies corresponding to the standing wave excitations. The strong interaction between Josephson junctions and standing waves of currents within coupling circuits provides both an additional reduction in the oscillation linewidth and the phase-locked oscillation state in phase regardless to applied dc magnetic field. According our calculations, the required strong interaction exists at small damping less than 0.001. The conditions for the maximum amplitude of the output oscillating voltage have been analyzed and optimized topology of the multijunction system has been suggested.
The work was supported in part by Russian Foundation for Basic Research, Russian State Program "Modern Problems of Solid State Physics", "Superconductivity" division, INTAS programs of EU and NATO Collaborative Research Program.

ORAL SESSION 9D: Bulk Materials and Materials Aspects II

Wednesday Morning, September 15th, 11:45-12:45

11:45 9D–1

A Model for Texture Development in BSCCO High-Tc Superconductors.

E. Cecchetti, *P.J. Ferreira* and *J.B.V. Sande*. Massachusetts Institute of Technology (MIT) Department of Materials Science and Engineering Cambridge, MA, 02139, USA.

Textured BSCCO high-Tc superconductors are studied and the various mechanisms for alignment of BSCCO grains addressed. To date, surface energy effects leading to texture development in BSCCO superconductors have been considered only with respect to the free surface of melt-processed Bi-2212 thick films. However, these previous considerations have not included the surface interactions between BSCCO crystals and other solid surfaces present in the BSCCO system. The present work attempts to analyze systematically the implications of a variety of mechanisms through a simple formalism based on surface thermodynamic properties. A careful examination of the different stages involved during the partial melt process gives an explanation for the various observed phenomena. During the early stages of solidification, when the peritectic liquid is abundant, BSCCO crystals are rather mobile, facilitating their contact and interaction. As a result, if a crystal has its wide planar c-surface in contact with a foreign surface (silver substrate, secondary phase, or another BSCCO crystal), it can minimize its surface energy and likely adhere to that surface. This mechanism, applied to a system with planar constrains like a 2212/Ag film, will result in a textured sample, depending on the thickness of the superconducting layer. In a bulk sample, however, BSCCO crystals many only minimize their surface energy by adhering to other BSCCO crystals or second-phase particles, which consequently will form clusters of locally aligned crystals, with no long-range texture. In a similar fashion, we may also address the role of silver in promoting texture development in BSCCO superconductors

12:00 9D–2

Synthesis and densification of Hg- and Hg(Re)-1223 superconductors.

A. Tampieri[1], *G. Celotti*[1], *D. Martínez*[2], *S. Piñol*[2], *A. Calleja*[3], *T. Puig*[2], *A. Sin*[2] and *X. Obradors*[2]. [1]IRTEC-CNR, via Granarolo,64-48018 Faenza, ITALY. [2]ICMAB-CSIC, campus de la UAB-E08193 Bellaterra, SPAIN. [3]DIOPMA. Llacuna 162-166 Barcelona, E-08018, Spain.

The preparation of discrete amounts of Hg-based superconductors, as single 1223 phase, remained a serious challenge until now, essentially due to the difficulty of reaction between HgO vapour and solid state precursors mixture; moreover the thermal lability of such a phase, made practically impossible to obtain it as dense bulk material.The synthesis and simultaneous densification of Hg-Ba-Ca-Cu-O and Hg(Re)-Ba-Ca-Cu-O with nominal composition 1223, was performed directly through "reactive sintering" by hot isostatic pressing (HIP) at 830°C, 0.15 GPa for 5 hours starting from simple oxides canned in silver tubes. At the same time, experiments of densification of 1223 pure phase, prepared by the sealed quartz vessel technique were performed by HIP. The microestructure, phase purity and density of these samples have been compared with that achieved at low presures using $CaHgO_2$ as external mercury source. Magnetic characterization and critical current measurements were carried out and correlated to final density, 1223 phase volume fraction and microstructural features of obtained samples.

12:15 9D–3

Effect of Fluorine substitution in HTCS: new structures in Bi-based superconductor.

E. Bellingeri[1], *G. Grasso*[1,2], *R. Gladyshevskii*[1,3], *E. Giannini*[1], *F. Marti*[1], *M. Dhallé*[1] and *R. Flükiger*. [1]DPMC, Université de Genève 24, Quai Ernest Ansermet CH-1211 Genève 4, Switzerland. [2]Present address: INFM Unità di Genova, Via Dodecaneso 33, Genova, Italy. [3]Present address: Department of Inorganic Chemistry, L'viv State University, Ukraine.

New superconducting structures were produced in the Bi system, by a low temperature (200-400 °C) fluorination process. The fluorine substitutes completely the oxygen sites in the Bi layers and additional F atoms are inserted. One of the new F-containing phases (Bi(2223)F) differs from the pristine phase by more than 1.7 Angstrom in the c axis parameter while also the arrangements of cation and anions are changed especially in the Bi and partially in the Sr layer. This new phase shows superconducting behaviour at temperatures under 70 K. Just as in the Bi-based superconductors, there is evidence that the fluorine substitutes almost completely for oxygen in the heavy metal layer of Tl(1223). However, no significant differences in the crystal structure have been observed in the Tl-based samples with F inclusions. The critical temperature (116 K) remains unchanged but a significant increase of the irreversibility field at low temperature was found. The different behaviour of Tl- and Bi-based superconductors is probably due to the fact that the Tl atoms can lower their valency state resulting in a substitution of one F for each O atom, while Bi is already in the minimum valency state and is obliged to accommodate two F for each O atom.

12:30 9D–4

Magneto-optic characterisation of artificial grain boundaries in melt textured YBCO.

G.J. French[1], *S.A.L. Foulds*[1], *J.S. Abell*[1], *W.Lo*[2], *A. Bradley*[2], *R.A. Doyle*[2] and *D.A. Cardwell*[2]. [1]School of Metallurgy and Materials, University of Birmingham , Birmingham B15 2TT. [2]IRC in superconductivity, University of Cambridge, Cambridge CB3)he.

The resistance to magnetic flux penetration of artificially engineered grain boundaries in large grained melt textured YBCO has been studied by magneto-optical imaging. The characteristics of the joins have been observed in swept field, remnant state and swept temperature regimes. The magnetic behaviour of the joins varies, but in some cases they showed no difference in behaviour to the adjacent grains, indicating that the artificially engineered boundaries were of the highest quality. An inversion procedure to generate two-dimensional current distributions from the magneto-optic data has confirmed that there is no deviation in the current

flow and distribution across the artificial boundary.

POSTER SESSION 10

Wednesday Afternoon, September 15th, 15:30-17:30

Session Bulk materials and materials aspects

10–1

Scaling of the critical current density vs specific contact resistance in ceramic $Y_1Ba_2Cu_3O_{7-\delta}$ superconductors.

S.R. Currás, *J.A. Veira*, *J. Maza* and *F. Vidal*. Laboratorio de Bajas Temperaturas y Superconductividad, Universidad de Santiago de Compostela Santiago de Compostela, E-15706, Spain.

We will report measurements of the critical current density at zero applied magnetic field, J_c, of ceramic $Y_1Ba_2Cu_3O_{7-\delta}$ samples with different average grain size, a, and normal state resistivity. From the normal state resistivity versus temperature curve the average intergrain resistivity, ρ_{wl}, is extracted by using the empirical equation: $\rho(T) = \alpha^{-1}[\rho_{ab}(T) + \rho_{wl}]$, where α is a granularity parameter and ρ_{ab} is the average intragrain resistivity. Our results show that at a given temperature J_c depends only on the specific contact resistance of the average grain boundary junction, $\rho_\Box$, defined as the product $\rho_{wl}a$, so that the product $J_c\rho_\Box$ is sample independent. This finding that $\rho_\Box$ is a key factor in J_c, but not a, is in contrast with most previous results and could point to the revision of the applicability of the continuous Josephson medium approach to ceramic superconductors.

10–2

Current-Voltage characteristics in granular superconductors at very low magnetic field.

M.T. González, *S.R. Currás*, *J. Maza* and *F. Vidal*. Laboratorio de Bajas Temperaturas y Superconductividad, Universidad de Santiago de Compostela Santiago de Compostela, E-15706, Spain.

We study the current-voltage characteristics (VI) in granular $Y_1Ba_2Cu_3O_{7-\delta}$ at very low magnetic fields in the range 2-20 Oe, with the voltage spanning three orders of magnitude. Measurements were taken by applying a variable magnetic field compensating the increasing self-field along a VI curve, so as to keep the total average magnetic field constant. A dissimilar behavior of the voltage to a change of sign of the total magnetic field is observed. This asymmetry is interpreted in terms of the intergrain junctions' behavior. In this respect, the data would lend direct empirical evidence that in granular Y-based superconductors junctions are "large" in nature, i.e., the largest effective dimension is greater than the Josephson penetration length.

10–3

Determination of inter- and intragrain critical current densities of YBCO ceramics in high fields by Hall magnetometry.

H.Varmhram[1], *M.Reissner*[1], *W.Steiner*[1] and *H.Hauser*[2]. [1]Institut für Angewandte und Technische Physik, Technische Universität Wien, A-1040, Austria. [2]Institut für Werkstoffe der Elektrotechnik, Technische Univresität Wien, A-1040, Austria.

A Hall magnetometer was built up to determine both the inter- and the intragrain critical current densities in ceramic superconductors at high fields. To obtain the required high sensitivity and resolution a differential method was adapted, where the difference of the signal of two Hall sensors - one measuring only the external field, the other both the external and the local field - was used. Both currents were separated by comparison of the results obtained from measurements on ceramics (inter- and intragrain currents) and on powders (only intragrain currents). To calculate critical current densities from the measured local field at the position of the Hall sensor, a model was developed which takes into account the special geometry of the samples. Whereas the intergrain currents are flowing around the whole sample, for the powder sample the signal from each individual grain has to be considered. From the thus determined inter- and intragrain current densities the Hall signal for the ceramics could be calculated. A comparison with the measured signals gives deviations of less than 10%,thus confirming the validity of the chosen model.

10–4

Non-contact Measurements of Resistivity of HTS materials.

W. Nawrocki[1], *J. Pajakowski*[1], *P. Seidel*[2] and *K-U. Barholz*[2]. [1] Poznan University of Technology Institute of Electronics and Telecom. ul. Piotrowo 3A, PL-60965 Poznan Poland. [2] Friedrich Schiller University Institute of Solide State Physics Helmholtzweg 5, D-07743 Jena Germany.

We have developed an instrument for measurement of resistivity r of HTS samples using the non-contact method. The sample to be tested is put in a magnetic circuit of an electrical coil which electrical quality factor Q is measured. The quality factor depends on the eddy-current induced in the sample. In turn, the eddy-current is the function of resistivity. This method has several advantages. First, there is no physical contact with the tested sample (thin film samples are very sensitive to contact). Second, the sample is easy to prepare of the material for testing. Third, there is the possibility of measuring of spatial distribution of resistivity. The data of the sensor used for the measurements of resistivity: core material – Ferroxide U31; number of turns of copper winding – 70; frequency of maximum sensitivity – 1.5 MHz; maximum quality factor – 200. Resistivity of YBCO material of the thin sample from Jena University is about 0.02 W cm at the room temperature. The results of the measurement of some YBCO samples in the function of the temperature using the described method and the four-point method are presented. The non-contact method is suitable for testing of HTS material before it is used for fabrication of Josephson junctions (or SQUID sensors).

10–5

The Upper Critical Field and Irreversibility Field of the Chevrel Phase Superconductor Tin-Molybdenum-Sulphide Doped with Europium.

N. R. Leigh, *I. J. Daniel* and *D. P. Hampshire*. Superconductivity Group, University of Durham, Department of Physics, South Road, Durham, DH1 3LE. U.K.

Chevrel Phase superconductors with upper critical field values of up to 60 T, are candidate materials for the next generation of high field magnets. We have investigated the effect of doping tin-molybdenum-sulphide with the magnetic ion europium, to improve the critical parameters and the flux pinning in this material. Samples were prepared at 1450 °C to ensure the europium was uniformly distributed throughout the material and then sintered using a Hot Isostatic Press operating at a pressure of 2000 atmospheres. Calorimetric, resistive and susceptibility measurements have been completed in magnetic fields up to 15 T as a function of temperature. Magnetization measurements up to 15 T have been performed at 4.2 K and sample purity has been verified by x-ray analysis. The temperature dependance of the upper critical field of these samples are presented . Upper critical field values for the undoped sample of 39 T and over 50 T for the doped samples have been determined. We investigate the effect of doping on the critical current density and the irreversibility field. The change in critical parameters with doping is discussed in terms of a change in the fundamental properties of the material rather than the quality of the grain boundaries.

10–6

Modelling of Current Transfer in Current Contacts to Superconducting Devices.

R. P. Baranowski[1,2], *K. A. Kursumovic*[1,2] and *J. E. Evetts*[1,2]. [1]IRC in Superconductivity, Madingley Road, Cambridge, CB3 OHE, UK. [2]Department of Materials Science, University of Cambridge, Cambridge CB2 2QZ, UK.

Solutions of a 2D finite element model of the anisotropic current flow in a contact to a superconductor with a non-linear current-voltage characteristic are presented. Experimental studies of current transfer by in-situ current contacts to composite reaction textured (CRT) Bi-2212 reveal that at applied currents in excess of the critical current, the behaviour of the total power dissipation across the contact is non-ohmic. The power dissipation at the metal-superconductor contacts was estimated by monitoring the voltage drop during continuous current ramp in self and applied fields. The voltage distribution along the contact and power loss have been found to agree well qualitatively with experimental results; which suggests that the bulk resistivity of a superconducting device is not negligible and leads to non-ohmic current transfer behaviour in current contacts at high applied currents. The work was supported under the European Union TMR Network SUPERCURRENT, an EPSRC LINK project and an Oxford Instruments CASE Award.

10–7

Preparation and characterization of electrical contacts to bulk high-temperature superconductors.

J.G. Noudem, *M. Tarka* and *G.J. Schmitz*. ACCESS e.V., Intzestr. 5, D-52072 Aachen, Germany.

Much effort has been devoted to the development of manufacturing processes of bulk high temperature superconducting components with high critical current densities in the last decade. Besides these components themselves, their interfaces with other -especially normal conducting- materials are essential for the design of practical systems for application like e.g. current leads or fault current limiters. Espe-

cially ohmic losses at contacts between superconductor and snormal conductor in the cryogenic environment have to be minimized. Following a short summary of present knowledge in the field, perspectives and first results of investigations aiming towards a robust and reliable preparation of low resistance contacts to both REBaCuO and BISCCO bulk superconductors will be presented focussing especially on: · Low temperature soldering processes · Improved wetting between solder and superconductor · Determination of apparent and effective contact area · Maximization of contact area

10–8

Spin dynamics effects on the resistivity and the magnetoresistance of the $La_{1.85}Sr_{0.15}(Cu_{1-x},Li_x)O_4$ system with $0.0 < x < 0.15$.

S. García[1], *J. E. Musa*[2] and *E. M. Baggio-Saitovitch*[2]. [1]Centro Brasileiro de Pesquisas Físicas (CBPF-DME). rua Dr. Xavier Sigaud 150, Urca, Rio de Janeiro 22290-180, RJ, Brazil. Permanent address: Laboratorio de Superconductividad, Facultad de Física-IMRE, Universidad de La Habana, San Lázaro y L, 10400, Ciudad de La Habana, Cuba. [2]Centro Brasileiro de Pesquisas Físicas (CBPF-DME). rua Dr. Xavier Sigaud 150, Urca, Rio de Janeiro 22290-180, RJ, Brazil.

The interplay between the hole-doping, the spin fluctuations and the unusual normal-state properties in the layered cuprates is relevant for the physics of the high temperature superconductors. Looking for a better understanding of the role of the magnetic interactions on the conduction mechanism, a systematic study of the normal-state resistivity ρ(x,T) of the title system was performed down to 4.2 K. Initially, the ρ(x,T) values decreased with the increase in x, while T_c remains unchanged. An upward deviation from the high-temperature linearity was also observed on cooling. As x increases further, T_c is gradually suppressed without broadening. For the highest Li content, both the metallic behavior and superconductivity were completely suppressed, while a steep divergence at low temperatures emerges. A logarithmic contribution was found to properly describe the ρ(x,T) behavior, with the corresponding coefficient following a quadratic dependence on x. Scattering of the carriers by the spin fluctuations at the Cu-O_2 conduction planes is proposed to be the source of the Kondo-like behavior. Negative magnetoresistance measurements up to 8T, with an increasing intensity with x, confirm the role of the spin degrees in the resistivity behavior.

10–9

Moessbauer characterization of the prospective Pr1.9Ba1.1Cu3O7+y substrate material.

A.V.Kravchenko, *I.S.Bezverkhy*, *E.A.Goodilin* and *Yu.D.Tretyakov*. Moscow State University, Chemistry Faculty, Inorganic Chemistry Divison, Lenin Hills, 119899, Moscow, Russia.

In the present work Pr1+xBa2-xCu3O7+y substrate materials (Pr123ss) were studied to control a mismatch with deposited superconducting films by the x parameter adjustment. The homogeneity field of Pr123ss was investigated, and a new solution with x=0.9 (a=3.848, b=3.900, c=11.581A) was prepared by freeze-drying followed by sintering at 950C in air for 60h. The solution stayed permanently orthorhombic and possessed a small oxygen nonstoichiometry. To probe local oxygen arrangement, the sample was doped with Fe-57 (Pr1.9Ba1.1Cu2.85Fe0.15O7+y) at a temperature (1000C) above the thermal stability of the pure phase (955C). Its Moessbauer spectrum can be fitted by a superposition of two doublets (IS1=0.04; IS2=0.23 mm/c; QS1=0.50, QS2 =1.49 mm/s). The spectral contribution of the second doublet rises up from 53 to 65% after full oxygenation at 350C in oxygen. It can be assumed that iron atoms are localized in pyramids formed by the CuO2 plane and apical oxygens; another part of Fe-57 becomes five-coordinated after oxygenation. Therefore extra oxygen atoms exist in the basal plane at fixed positions prohibited in the x=0 case. The Pr1.9Ba1.1Cu3O7+y phase is isostructural with Nd1.9Ba1.1Cu3O7+y, and can be applied as a new substrate material. This work is supported by RFBR (grant 98-03-32575à).

10–10

Routine method for determination of stoichiometric ratios of elements in high temperature superconductors.

D. Geilenberg[1], *J.A.C. Broekaert*[2] and *M. Gerards*[3]. [1]University of Dortmund Department of Chemistry-Analytical Chemistry D-44227 Dortmund Germany. [2]University of Leipzig Institute for Analytical Chemistry D-04103 Leipzig Germany. [3]Merck KGaA, Darmstadt Werk Gernsheim D-64579 Gernsheim Germany.

High precision and fast routine method for the determination of metallic elements was developed by using simultaneous ICP-optical emission spectroscopy. High precision was achieved through careful and standardized sample preparation and through a statistical approach of data collection. In respect of spectral interferences the appropriate selection of emission lines and matrix adjustment of calibration standard solutions are essential for accurate results. New standard operation procedure for e.g. BSCCO powders gives relative standard deviation better than ± 2 % for each elemental stoichiometric factor. A proposal for the format of exchange of analytical data among HTSC community is presented.

10–11

Local Studies of high-Tc Superconductors using a Cryogenic Microwave Near-Field Microscopy.

A.F. Lann[1], *M. Abu-Tair*[1], *M. Golosovsky*[1], *D. Davidov*[1], *A. Frenkel*[2], *S. Djordjevic*[3], *N. Bontemps*[3] and *L.F. Cohen*[4]. [1]Racah Institute of Physics, Hebrew University of Jerusalem, Jerusalem 91904,Israel. [2]M.S.I. Engineering Software Ltd., Tel-Aviv, Israel. [3]Ecole Normale Superieure,rue Lhomond 24, Paris, France. [4]Imperial College, London, UK.

We report a vacuum cryogenic ($80K < T < 350K$) near-field microwave scanning microscope based on a 90 GHz transmitting/receiving slit antenna with a capacitive control of the probe-sample separation. The probe allows local measurement of surface impedance at varying temperature with the spatial resolution of 20-50μm. The mm-wave probe is integrated with the eddy-current (mutual inductance) probe which allows global measurement of resistance of conduct-

ing and superconducting samples. (1) We compare local sheet resistance of YBCO thin films measured by our local mm-wave probe to the oxygen content measured by Raman microscopy and find an excellent agreement. (2) We use our integrated probe for local study of superconducting transition in high-T_c superconducting thin films. In some films we find difference in T_c as detected globally through mutual inductance and locally through microwave reflectivity, and attribute the difference to film inhomogeneity and percolation behavior. Our present probe has sensitivity of less than 1 Ohm which is enough to detect variations in surface reactance but not enough to measure surface resistance. We report a new scanning probe which is based on a dielectric resonator and operates at 30 GHz. It has enhanced sensitivity and is intended to map surface resistance with a micron spatial resolution.

10–12

Local magnetic-field-modulated microwave reflection - a new tool contactless technique for detection of superconductivity.

M. Abu-Tair[1], *A.F. Lann*[1], *M.Golosovsky*[1], *D.Davidov*[1], *A.Goldgirsh*[2] and *V.Beilin*[2]. [1]Hebrew University of Jerusalem, Racah Institute of Physics. [2]Hebrew University of Jerusalem, Applied Physics Department.

We report a new contactless material characterization tool - a magnetic-field-modulated microwave reflectivity (FMMR) measured locally using a near-field microwave scanning probe with a 20-50μm spatial resolution. The technique allows (i) to detect and to localize minute quantities of superconductor in a nonsuperconducting matrix, (ii) to distinguish between several superconducting transitions occurring in a small spot. The technique is based on a microwave scanning probe integrated with an ac-excitation coil. Ac magnetic field modulates the surface impedance of the sample which is measured through the local microwave reflectivity. We report measurements on YBCO thin films and a 110 K BSCCO pellet and show that our technique is an excellent characterization tool for material homogeneity, for example, in BSCCO we detect minute traces of 85K phase and surface degradation. We report dependence of local FMMR on temperature and on dc-magnetic field and show that they are very different from field and temperature dependences of the linear and nonlinear ac-susceptibility (measured simultaneously on the same samples). We show that FMMR probes surface properties while the ac-susceptibility probes bulk properties.

10–13

Surface resistance $R_S(T,f)$ of YBCO and its quantification below $0.8T_C$ by weak links.

A. Dierlamm, *E. Keskin*, *R. Schwab* and *J. Halbritter*. Forschungszentrum Karlsruhe, Institut für Materialforschung I P.O.Box 3640, D-76021 Karlsruhe, Germany.

Superconductors in an rf-field are plagued by rf-residual losses $R_{res}(T,f)$, being in YBCO more than two orders of magnitude larger than for bulk Nb. The higher $R_{res}(T,f)$ - values of YBCO can be explained by the very much reduced critical Josephson currents j_{CJ} and the enhanced leakage currents (normal conducting) grain boundary resistance $R_{bl}(R_{bn})$ of weak links. In YBCO, j_{CJ}, R_{bl} (R_{bn}) and $j_{CJ}R_{bn} = \hbar/2e\tau_J$ are at least degraded by factors of 5 compared to intrinsic, perfect contacts without any localised states. The finite rf-residual losses $R_{res}(T,f) \propto f^{\alpha}/j_{CJ}(T)^{3/2}a_J R_{bl}$ by weak links in distances a_J are quantified by the finite normal conducting leakage currents $R_{bl}(T < 0.8T_C) \approx$ const, where the T-dependence is dominated by $j_{CJ}(T) \approx j_{CJ}(0)(1-T/T_C)^m$ ($m \approx 1$) and the frequency dependence $\alpha \leq 2$ by the distribution of Josephson frequencies $1/\tau_J$. Quantitative agreement with experimental $R_S(T < 0.8T_C, f)$ is found by measured values of $a_J(\approx 0.2 - 20\mu m)$, of $j_{CJ}((\approx 1 - 10^7$ A/cm$^2)$ and of $R_{bn} \approx R_{bl}(10^{-7}-10^{-9}\Omega$ cm$^2)$ obtained by percolation analysis of $\rho(T)$ with $j_{cJ}R_{bl}^2 \approx 10^{-12}$ AΩ^2cm^2, where the latter value agrees with other YBCO - junctions. Hence for sintered and epitaxially grown YBCO $R_S(T < 0.8T_C, f)$ can be described quantitatively by weak links with one $j_{cJ}R_{bl}^2$-value and measured values for a_J, R_{bn} and j_{cJ}.

Session Flux pinning and ac losses

10–14

Electrical transport properties of high temperature superconductors at intense current densities.

W. Goeb[1], *W. Lang*[1], *R. Roessler*[2], *J.D. Pedarnig*[2] and *D. Baeuerle*[2]. [1]Institut fuer Materialphysik der Universitaet Wien, Kopernikusgasse 15, A-1060 Vienna, Austria [2]Angewandte Physik, Johannes-Kepler-Universitaet Linz, A-4040 Linz, Austria.

Understanding the nature of the electrical transport properties and the vortex state in high temperature superconductors is crucial for developing high-current-carrying applications of these materials. We report on measurements of the resistivity and the mixed-state Hall effect in thin films of high-temperature superconductors in magnetic fields from $B = 60$ mT to $B = 1$ T and current densities j up to $3MA/cm^2$. To reduce the problem of sample heating, we have employed a pulsed current technique and developed a new heating correction procedure. In optimally doped samples, we observed a double sign reversal of the Hall resistivity in the mixed state, resulting in two peaks which both depend on B and j. The position of the sign changes only varies with B, but is found to be independent of j. The Hall conductivity turns positive again in the superconducting regime and dramatically increases towards lower temperatures in high current densities where vortex pinning is reduced. In underdoped samples, however, both sign changes disappear and the Hall conductivity remains positive and monotonically increases with decreasing temperatures. The results are discussed with respect to recent theories.

10–15

Non-Destructive Critical Currents Determination in Large Grain HTS Bulks.

A.A. Kordyuk[1], *V.V. Nemoshkalenko*[1], *R.V. Viznichenko*[1], *W. Gawalek*[2] and *T. Habisreuther*[2]. [1]Institute of Metal Physics, Kyiv 252680, Ukraine. [2]Institut für Physikalische Hochtechnologie, Jena D-07743, Germany.

A set of non-destructive contactless experimental techniques that based on permanent magnet-superconductor interac-

tion has been developed to study the macroscopic magnetic properties of HTS bulks. The resonance oscillations technique gives an opportunity to recover the critical current density profiles in thin undersurface layer and to study the influence of the surface treatment and degradation on a.c. losses in this materials. We have also developed a simple approach to determine the critical current density in melt-textured HTS bulks from the levitation force measurements. From the local measurements, using the permanent magnet much less than HTS sample, we obtain the critical current density in ab-plain as a function of the magnetic field parallel to this plane. The first and second hysteretic loops calculated from these Jc(B) dependencies without any fitting parameters completely coincide with experimental data. An optimization criterion of the levitation force measuring technique to minimize the influence of random parameters like sample shape or surface condition on Jc determination was considered.

10–16

Experimental and theoretical study of heating of bulk HTSC samples due to AC losses.

V. Sokolovsky, *V. Meerovich* and *M. Gladstein*. Ben-Gurion University, Beer-Sheva, 84105, Israel.

It is shown that a very low thermal conductivity of HTSC materials results in nonuniform temperature distribution inside a bulk HTSC sample placed in AC magnetic field. The characteristic properties of this distribution and the influence of this phenomenon on the values of the AC losses and critical current are discussed. The theoretical treatment is based on the critical state model supplemented by the heat equation. The evaluations show that, at the magnetic field of the complete penetration, the maximum overheating temperature inside a HTSC sample increases directly proportional to the fourth power of the sample thickness and the square of the critical current density. To confirm the theoretical conclusions, we measured the temperature distribution in the wall of a BSCCO hollow cylinder in AC magnetic field. Although the cylinder possesses the relatively low critical current density of 550 A/cm2 (determined by 1 mkV/cm criterion), the overheating of interior parts of the cylinder relative to the outside coolant was up to 2.5 K at the magnetic field amplitude of about 0.04 T. The overheating temperature is increased linearly with frequency and as the third power of the applied magnetic field. In bulk samples with higher critical current density, the overheating of interior parts can result in the pronounced discrepancy between the critical current values measured under AC and DC conditions.

10–17

The extended critical state model for a nonuniform Type II superconductor.

A.Y. Galkin[1], *B.A. Ivanov*[2] and *V. Kambersky*[3]. [1] Institute for Metal Physics, Vernadsky 36, 252142 Kiev, Ukraine. [2] Institute of Magnetism, Vernadsky 36b, 252142 Kiev, Ukraine. [3] Institute of Physics, Na Slovance 2, 18040, Prague8, the Czech Republic.

Here we propose a simple model (on the base of the critical state model) of a two-component layered slab, with critical current density varying periodically along the current direction. In the simplest case of a superconductor divided into periodical layers with the different critical current density values the magnetic hysteresis curve might be calculated analytically. The shape of hysteresis curve essentially differs from the standard dependence predicted by the Bean model for a homogeneous superconductor. In particular, in the case of the virgin curve the standard quadratic dependence becomes more complicated, polynomial, with coefficients strongly dependent on the sample geometry and ratio of the critical current density in weak and strong region. The geometry of critical current flow in the several examples considered show interesting non-trivial features like current closed loops in the layered model and discontinuities in current directions in all cases. While the explicit results, for either constant or field-dependent critical current values, may be insufficient for quantitative comparison with experiments in granular materials, with three-dimensional grain distributions, they may be perhaps useful for drawing qualitative conclusions on the distribution of material parameters.

10–18

Real Time Dynamics of Flux Expulsion from Type-I Superconducting Strips.

G. Jung[1,5], *V. Jeudy*[2], *D. Limagne*[2], *G. Waysand*[2], *T.A. Girard*[3], *M.J. Gomes*[3] and *B.Y. Shapiro*[4]. [1] Department of Physics, Ben Gurion University of the Negev, P.O.Box 653, 84105 Beer Sheva, Israel. [2] Groupe de Physique des Solides Universite Paris VII, 75251 Paris Cedex 05, France. [3] Centro de Fisica Nuclear Universidade de Lisboa, 1649-003 Lisboa, Portugal. [4] Department of Physics, Bar-Ilan University, Ramat-Gan, 52900, Israel. [5]Instytut Fizyki PAN, 02668 Warszawa, Poland.

Dynamics of expulsion of magnetic flux from type-I superconducting tin strips induced by decrease of a perpendicular magnetic field following field increase-induced flux penetration, is investigated in real time by detecting voltage pulses associated with flux variation. The presence of the geometrical surface barrier introduces irreversibility to the system and results in three different flux expulsions regimes. The magnetic field ranges of the distinct expulsion regimes correspond in general to the different regimes of the initial flux penetration. Magnetic history of the sample strongly influences the dynamics of the flux expulsion leading to only two expulsion regimes following the incomplete flux penetration.

10–19

Effets of columnar defects on flux lines pinning in $Bi_2Sr_2Ca_{1-x}Y_xCu_2O_8$ single crystals.

L.Ammor[1], *R.De Sousa*[1], *J.C. Soret*[1], *V. Ta Phuoc*[1], *G. Villard*[2], *A. Ruyter*[1], *A. Wahl*[2] and *E. Olive*[1]. [1]Laboratoire LEMA Université F.Rabelais UFR Sciences 37200 Tours France. [2]Laboratoire CRISMAT,ISMRA 6 Bd Marechal juin 14050 Caen France.

The introduction of columnar defects into high-Tc superconductors by high-energy heavy ion irradiation has shown to be a promising method to improve the performance in technical application of type-II superconductors in external magnetic fields. The main features of the after-irradiation in these compounds are the enhancement of the critical current density Jc and the upward shift of the irreversibility

line. In this study, we report on the vortex phase diagram in $Bi_2Sr_2Ca_{1-x}Y_xCu_2O_8$ single crystals irradiated with the ion beam parallel to the c-axis with doses corresponding to matching field B_ϕ=0.75 and 1.5T, using transport measurements. We have examined the behavior of the isothermal current-voltage characteristics for magnetic fields parallel to columnar defects. The magnetic field dependence of the Bose-glass transition temperature in various regimes has been extracted from the analysis of scaling proprieties of I-V curves predicted by the Bose-glass(BG)theory. Our experimental phase diagram, reveals various vortex pinning regimes that strongly depend on a filling fraction f=(B/B_ϕ). The obtained results show evidence that columnar defects control the dynamics of the vortex system (defect-vortex interactions, strong pinning) only between two characteristics temperatures $T_0 \approx 0.72T_c$ (f≈0.8) and $T_1 \approx 0.83T_c$(f≈0.1). Moreover, beyond this interval, the vortex system is increasingly dominated by the vortex-vortex interactions (weak pinning) and / or thermal fluctuations and the irreversibility line appears to recover the first-order melting line T_m for the unirradiated single crystals. We obtained good quantitative agreement between our experimental results and the predictions of the BG theory for correlated disorder.

10–21

Pinning of grain-boundary vortices by neighboring Abrikosov vortices in the nearby grains.

D.H. Kim[1], *M.B. Field*[2], *D.J. Miller*[2], *K.E. Gray*[2], *Y.H. Kim*[3] and *T.S. Hahn*[3]. [1]Yeungnam University, Kyungsan, 712-749, S. Korea. [2]Argonne National Laboratory, Argonne, IL 60439, USA. [3]Korea Institute of Science of Technology, Seoul, 136-791, S.Korea.

The critical current densities J_c of the YBCO grain boundaries of 90-degree [100] symmetric tilt showed a hysteretic behavior depending on how the external magnetic fields were applied. At 77K for fields less than $\sim$ 1 T, the field-cooled J_c of grain boundaries was larger than the zero-field-cooled J_c. This result is consistent with the model in which the grain-boundary vortices can be pinned by neighboring Abrikosov vortices in the nearby grains.

10–22

Twin planes pinning in the ab-planes of large YBCO monodomain samples.

A. Sulpice[1], *S. Sanfilippo*[2], *D. Bourgault*[2], *O. Laborde*[1], *X. Chaud*[3] and *R. Tournier*[2]. [1]Centre de Recherches sur les Tres Basses Temperatures, CNRS, Grenoble, BP 166, 38042 Grenoble CEDEX 9 France. [2]Laboratoire de Cristallographie, CNRS, Grenoble, BP 166, 38042 Grenoble CEDEX 9 France. [3]Centre de Recherches et d'Etudes Techniques Avancees, CNRS, Grenoble, BP 166, 38042 Grenoble CEDEX 9 France.

Twin planes effect on the pinning is studied in large monodomain YBCO textured samples with the size along the c-axis greater than the others. This unique configuration allows to investigate the influence of the twin planes (TP) on pinning properties in the ab-plane with a current directed along the c-axis. B is applied in the ab-plane and makes a variable angle F with one TP direction. The magnetic field angular dependencies of the transport and magnetic c-axis critical current density, of the irreversibility line $I.L_{ab}$ and of the c-axis resistivity show clearly strong improvements of the pinning properties at high temperatures (T > 40 K) when B is close to the TP directions. The irreversible properties in the ab plane are enhanced due to the reduced sensitivity of the pinning potential along the plane to thermal depinning. An experimental phase diagram is proposed with a possible existence of a Bose glass phase in the ab-plane induced by the two directions of the TP. Surprisingly these effects still exist for field intensity higher than 8 T when the vortices outnumber the TP, up to 20 T in the resistivity measurements.

10–23

Direct evidence for a transition from elastic to plastic regimes in the vortex phase diagram of $YBa_2Cu_3O_{7-\delta}$.

S. Kokkaliaris[1], *A. A. Zhukov*[1,2], *P. A. J. de Groot*[1], *R. Gagnon*[3], *L. Taillefer*[3] and *T. Wolf*[4]. [1]Department of Physics and Astronomy, University of Southampton, Southampton, SO17 1BJ, UK. [2]Physics Department, Moscow State University, Moscow 117234, Russia. [3]Department of Physics, McGill University, Montreal, Quebec, H3A 2T8, Canada. [4]Forschungszentrum Karlsruhe, Institut für Technische Physik, Postfach 3640,D-76021 Karlsruhe, Germany.

We have performed partial magnetization loops in order to study history effects in high quality $YBa_2Cu_3O_{7-\delta}$ single crystals with various types and densities of pinning sites. Results obtained on detwinned single crystals with very low densities of point defects have disclosed the transition from a dislocation-free Bragg glass to a disordered vortex phase. The transition line has been mapped in the field - temperature phase diagram and found to be in proximity to the onset of the second magnetization peak. This boundary is found to shift to lower fields with decreasing oxygen stoichiometry in a broad region near optimal doping ($6.908 \leq 7\text{-}\delta \leq 6.999$) in agreement with theoretical predictions. Above the transition, metastable topological disorder invades the vortex system leading to a pronounced dependence of the critical current density on the thermomagnetic history of the superconductor. The latter, however, diminish at high fields but only for the lowest oxygen concentrations under investigation. The influence of extended defects like twin boundaries and columns is also discussed.

10–24

Study of Collective Flux Creep in Directionally Solidified YBCO.

R. A. Ribeiro[1], *O. F. de Lima*[1], *X. Obradors*[2], *B. Martínez*[2] and *T. Puig*[2]. [1]Instituto de Fisica "Gleb Wataghin", UNICAMP, Brasil. [2]Institut de Ciencia de Materials de Barcelona, CSIC, Spain.

The fast relaxation of the irreversible magnetization is one of the important features of high temperature superconductors. Among the most significant parameters extracted from such data is the activation energy for flux creep. We present a magnetic flux creep study, in a directionally solidified Y123 (82% Y123 + 17% Y211 + 1% CeO_2) sample, using Maley's procedure and collective-pinning theory. Here we use the expression $U = kT(ln|dM/dT| - C)$, where $C = ln[HX\nu_0/(2\pi d)]$, X is the hopping distance, ν_0 the

attempt frequency for flux hopping, and d the thickness of the sample. In collective pinning theory, an inverse power law $U = U_c(J_c/J)^{\mu}$ is proposed for current densities not too close to the critical current density. U_c is the activation energy for $J = J_c$. Our results for different fields allow the determination of the exponent μ for the different regimes of tridimensional vortex creep.

10–25

Anisotropic pinning defects in melt textured $YBa_2Cu_3O_7$ / Y_2BaCuO_5 composites by cold isostatic pressing.

J.Figueras[1], *T.Puig*[1], *F.Sandiumenge*[1], *X.Obradors*[1] and *J.Rabier*[2]. [1]Institut de Ciència de Materials de Barcelona (ICMAB-CSIC), Bellaterra, Barcelona, 08193, Catalunya, Spain. [2]Laboratoire de Métallurgie Physique, UMR 6630 CNRS, Université de Poitiers, 86960 Futuroscope Cedex, France.

Cold isostatic pressing (CIP) effects on vortex pinning in the liquid state of Y123/211 melt-textured composites have been analysed by angular magnetoresistance measurements and the corresponding magnetic phase diagram has been drawn. These magnetization measurements have enabled the separation of isotropic from anisotropic pinning effects. Samples prepared by top seeding growth and oxygenated at 1bar and 450°C for 120 hours were subsequently submitted to a CIP treatment, i.e. 2 kbar of Ar at 300°C for 4 hours. TEM analysis revealed that the CIP process induces the growth of nanometric stacking faults parallel to the 110 twin boundary directions. Consequently, a strong increase of the partial dislocation length associated to the stacking faults was observed. Angular magnetoresistance measurements show that partial dislocations behave as linearly correlated defects for H //{110} with the Lorentz force lying within the ab plane. Additionally they lead to an upward shift of the irreversibility line. Instead, pinning by partial dislocations is not especially important in the liquid vortex state when these act as point defects (H//c), contrary to that observed in the solid vortex state by inductive measurements, which showed an increase of $J_c{}^{ab}$ by 100 % at 77 K.

Financial support from the EU-TMR network Supercurrents, EBR 4061PL97-0281, is acknowledged.

10–26

Microwave surface resistance measurements in YBCO/Au bilayer films and observation of proximity effect.

V. M. Pan[1], *V. F. Tarasov*[1], *M.A. Lorenz*[2], *A. Y. Ivaniuta*[3] and *G. A. Melkov*[3]. [1]Institute for Metal Physics, Kiev 252142, Ukraine. [2] Institute of Experimental Physics II, University of Leipzig,Leipzig D-04103, Germany. [3] Department of Cryo- Taras Shevchenko University of Ukraine at Kiev, Kiev 252030, Ukraine.

Measurements of surface resistance, R_S, for bilayer normal metal/HTSC film systems with varied (2.5−300 nm) normal metal layer thickness, d_n, are carried out at 67 and 32 GHz in temperature range 100−60 K. A model calculation is performed to determine $R_S(d_{Au})$ -function at 77 K for Au/YBCO bilayers. The calculated $R_S(d_{Au})$ increases versus low Au thicknesses and, passing maximum, comes to bulk Au surface resistance. The measured $R_S(d_{Au})$ turns out to differ crucially from predictions supposedly due to YBCO/Au-interface proximity effect. This assumption allows to understand two observed features: 1) $R_S(d_{Au})$-maximum shifts to much lower (comparatively with calculated) d_{Au}; 2) Enlargement of $R_S(d_{Au})$-maximum height. In the vicinity of Au/YBCO interface a proximity results in an enhancement of conductivity of adjacent Au layer with large enough correlation length ξ_{Au} (in contrast to YBCO where proximity effect propagation is limited by one unit cell). As a result effective conductivity σ_1 of Au-layer at the interface increases sharply while the thickness of proximity layer with enhanced conductivity is much lower than skin depth, what leads to the observed shift of the $R_S(d_{Au})$-maximum. Furthermore, due to the σ_1-enhancement the normal layer losses elevates, resulting in the remarkable raise of R_S maximum height.

10–27

Grain Boundary Magnetic Flux Pinning in High-T_C Superonductors.

A. Tuohimaa[1], *J. Paasi*[1] and *T. Di Matteo*[2]. [1]Tampere University of Technology, Tampere, FIN-33720, Finland. [2]University of Salerno, Baroniss i,(Salerno), I-84081, Italy.

Critical current densities in grain boundaries with meandering grain boundary path have been found to be significantly higher than in grain boundaries with almost a straight grain boundary path. By taking into account that in most high-T_C materials the $d_{x^2-y^2}$-wave symmetry of the superconducting order parameter seems to dominate, we present a model which enables us to explain the difference in the critical currents. The model consists of narrow (0)- and (π)-types of Josephson junctions in an inductive one-dimensional array. The pinning capacity and the critical current density of the array are studied numerically as a function of the percentage of π-junctions present in the array. We discuss the results in the viewpoint of granular bulk materials and grain boundary junctions. The results suggest that the grain boundary flux pinning can have an important role in the magnetic flux pinning and in determining the critical current density of high-T_C superconductors in low magnetic fields.

10–28

Effect of Inhomogeneous Distribution of Flux Pinning Strength on Critical Current Characteristics in Bi-2212 Tapes Prepared by PAIR Process.

M. Kiuchi[1], *A. Yamasaki*[2], *T. Kiss*[1], *T. Matsushita*[1,2], *M. Takeo*[1] and *H. Kumakura*[3]. [1]Graduate School of Information Science and Electrical Engineering, Kyushu University, 6-10-1 Hakozaki, Higashi-ku Fukuoka 812-8581, Japan. [2]Department of Computer Science and Electronics, Kyushu Institute of Technology, 680-4 Kawazu, Iizuka 820-8502, Japan. [3]National Research Institute for Metals, 1-2-1 Sengen, Tsukuba 305-0047, Japan.

It is known that the vortex glass-liquid transition line and the critical indices predicted by the vortex glass-liquid transition theory are not intrinsic properties of the material but determined by the flux pinning strength and its inhomogeneous distribution. Especially, the critical indices are correlated with the distribution of flux pinning strength. Hence,

it is necessary to understand the effect of distribution on the critical current characteristics. It was recently reported that the critical current density of Bi-2212 tape was much improved by introduction of the PAIR (Pre-Annealing and Intermediate Rolling) process. This improvement is speculated to originate from a better alignment of Bi-2212 grains by the PAIR process. This suggests that the distribution of flux pinning strength becomes sharp after this process. In this study, current-voltage curves in the PAIR processed Bi-2212 tape are measured under a magnetic field along the *c*-axis. Experimental results of the transition line and the critical indices are compared with the theoretical results of the theoretical analysis using the flux creep-flow model. The change in the distribution of flux pinning strength due to the PAIR process is discussed.

10–29

Magnetically investigated E-J characteristics of Bi-2212/Ag tape conductors.

H. Kumakura, *H. Kitaguchi*, *T. Mochiku* and *K. Togano*. National Research Institute for Metals Tsukuba, Ibaraki 305-0047 Japan.

Investigation of electric field(E) vs. current density(J) characteristics is important not only for the understanding of the flux dynamics but also for the practical applications. We compared E-J characteristics of several Bi-2212/Ag tapes. Tapes were prepared under the oxygen partial pressure of 0.25atm and 1atm. 180MeV Cu^{11+} irradiated tapes were also prepared. For comparison, Bi-2212 single crystal was investigated. Magnetization(M) was measured with a vibrating sample magnetometer. E was calculated from the sweep rate of the magnetic field and J was estimated from M. At 5K, logE-logJ curves of all samples showed linear behavior. The slope of the curve(n-value) of ~45 was obtained in low fields for the tapes(0.25atm). This n-value decreased to ~19 at 4T. The tape(1atm) showed larger n-values than the tape (0.25atm). This enhancement should be attributed to the improved pinning characteristics introduced by an over doping of carrier. Cu^{11+} irradiation significantly enhanced n-values at low fields. However, these large n-values decreased rapidly with increasing field. At 25K, n-values of 15-11 were obtained at low fields for the tapes. These n-values decreased more rapidly with increasing field than those at 5K. However, the irradiation much decreased the field dependence of n-values. At 40K, logE-logJ curves were not liner anymore except for the irradiated tapes.

10–30

Dynamic flux patterns of multifilamentary Ag/Bi2Sr2Ca2Cu3010-d tapes at 8K-77K temperatures.

B.A.Glowacki[1,2], *K. Van der Beek*[3] and *M.Konczykowski*[3]. [1] Department of Materials Science and Metallurgy University of Cambridge, Pembroke Street, Cambridge CB2 3QZ, U. K. [2]IRC in Superconductivity, University of Cambridge, Madingley Road, Cambridge CB3 OHE,U.K. [3]Laboratoire des Solides Irradies, Ecole Politechnique, 91128 Plalaiseau, France.

Current percolation in composite conductors such as Ag/Bi2Sr2Ca2Cu3010-d is determined by the different kinds of grain boundaries and interfilamentary intergrowth and by the conductance of the Ag matrix. We present and discuss magneto-optical measurements made at low frequency (0.2Hz) and power frequency (50Hz) versus temperature on two type of the multifilamentary tapes with magnetic field applied perpendicular to the tape plane. One type was a 19 filamentary tape with well separated filaments and the second was 37 filamentary tape with distorted and bridged filaments. The quantitative analysis of the magnetic field distribution on the surface of the conductors was conducted by numerical analysis of the colour intensity of magneto-optical images using Image Analysis Software. The results prove that interfilamentary bridging effects significantly the flux penetration profile and also critical state model. Since current through the interfilamentary bridges is very high this alter also the development of critical state of superconductor filaments. The temperature dependencies of the flux trapped in the volume of the superconducting region of the tape agrees with the irreversibility line vs temperature dependence. A video recorded research data of the magnetic field penetration into volume of such conductors vs frequency and temperature will be demonstrated during presentation at the conference.

10–31

Surface nanostructuring and optimization of the vortex confinement in melt textured YBCO.

L.Gozzelino[1], *R.Gerbaldo*[1], *G.Ghigo*[1], *E.Mezzetti*[1], *B.Minetti*[1], *P.Schätzle*[2], *G.Krabbes*[2], *E.Carlino*[3] and *A.Rovelli*[4]. [1]I.N.F.M. UdR Torino Politecnico; I.N.F.N. Sez. di Torino; Dipartimento di Fisica, Politecnico di Torino, Torino, Italy. [2]Institute of Solid State and Materials Research Dresden(IFW), Dresden, Germany. [3]C.N.R.S.M - PA.S.T.I.S., Brindisi, Italy. [4]I.N.F.N. Laboratorio Nazionale del Sud, Catania. [5].

In the present paper the magnetic properties of high quality melt textured $YBa_2Cu_3O_{7-\delta}$ irradiated with 2 GeV Au-ions are studied. The irradiation affects a surface layer of 50 μm (about 10% of the whole sample thickness), while linearly correlated columnar defects are estimated to be present up to about 46 μm. The paper is focused on the magnetic property analysis of the material before and after irradiation, as determined by the competition and/or correlation between surface columnar defects and intrinsic defects. In the intermediate/high temperature region (T > 45 K), the surface columnar defects are very effective as it results from critical current density, pinning force (F_p), creep rate and irreversibility line measurements. In particular the detailed study of the F_p vs. B curves at 75 K by means of a modified Dew-Hughes model shows that, before and after irradiation, several kinds of defects are effective in different ranges of field. After irradiation, the columnar defects deeply modify the full scenario near an accommodation field lower than the dose equivalent field. The detailed analysis shows that at least at higher temperatures, the strong pinning of the vortices in the surface layers induces easier confinement of the vortices trapped by volume and planar defects in deeper layers.

10–32

Influence of the grain size on I-V curves and critical current density in granular superconductors in the self-field approximation.

A. Kilic[1], *K. Kilic*[1] and *S. Senoussi*[2]. [1]Abant Izzet Baysal University Department of Physics, Bolu/Turkey. [2] Laboratoire de Physique des Solides (associé au C.N.R.S, URA, 0002) Université Paris Sud, 91405 Orsay Cedex, France.

In the self-field approximation, the influence of the grain radius on the current-voltage characteristics and associated critical current density J_c have been investigated in terms of the Lorentz Force driven flux flow motion of the vortices. In the calculations, the direct summation theory of Campbell et al. has been modified and could be adopted to the granular systems by considering the fact that a weak link can be considered as type-II superconductor. It has been shown that I-V characteristics and associated critical current density depend on the mean grain size of the samples implying that J_c is enhanced as the size of the grains is decreased. The case of the critical current density being greater for smaller grains which is consistent with both transport and low-field magnetization measurements is discussed by the weak links between the superconducting grains and also with the percolation model.

10–33

The ab-plane and c-axis studies of vortex pinning in $Y_{0.4}Ho_{0.6}Ba_2Cu_3O_{7-\delta}$ high-T_C superconductor crystal.

Y.S. Chen[1], *W.K. Chu*[1], *C.C. Lam*[1], *X. Jin*[2], *L.J. Shen*[1], *J.Q. Li*[1] and *J. Feng*[1]. [1]Department of Physic and Materials Science, City University of Hong Kong, Kowloon, Hong Kong. [2]National Laboratory of Solid State Microstructures and Department of Physics, Nanjing University, Nanjing 210008, P.R. China.

AC susceptibility measurement were performed in the $Y_{0.4}Ho_{0.6}Ba_2Cu_3O_{7-\delta}$ single crystal over a range of magnetic which is parallel to the c-axis of crystal and related to the frequency. Two dissipation peaks in the imaginary part (χ'') is observed. We suggested that the low temperature peak (T_{P1}) is the flux line travelling along the copper oxide layer, and the higher temperature peak (T_{P2}) is the flux line passing through the copper oxide layer. By using the AC susceptibility measurements, temperature, current density, and magnetic field dependences of the effective pinning potential U_{eff} have been determined. The difference in effective pinning potential between the ab-plane and c-axis can be shown.

10–34

Chemical Introduction of flux pinning centres in Bi-2212 and YBCO.

A.V. Berenov[1], *A.L. Crossley*[1], *A.D. Caplin*[2] and *J.L. MacManus-Driscoll*[1]. [1]Department of Materials, Imperial College, London, SW7 2BP. [2]Department of Physics, Imperial College, London, SW7 2BP.

In Bi-Sr-Ca-Cu-O superconductors at temperatures above 40K, intra-grain flux motion is thought to be the dominant dissipation mechanism. In YBCO, intergrain weak links dominate the dissipation and is overcome by processing the material to yield low angle grain boundaries. In this study, knowledge of the complex phase equilibria in the Bi-Sr-Ca-Cu-O system has been exploited to quantitatively introduce high concentrations of lead into bulk and tape materials. Magnetisation measurements and microstructural characterisation have been undertaken in order to assess the effects on high lead concentrations on pinning within the grains. Nano-precipitates of (Bi,Pb)-2212 were found to be incorporated in a matrix of (Bi,Pb)-2212 platelets, leading to a marginal increase in J_c above 40K. In the YBCO system, studies of preferential grain boundary doping of the various cation sites have been undertaken to determine whether a change in the local charge at the boundary improves the grain boundary coupling.

10–35

The role of the LRE-rich phase in the formation of the peak effect in LRE-123 superconductors.

M. R. Koblischka[1], *M. Muralidhar*[1], *T. Higuchi*[1], *K.Waki*[1], *N. Chikumoto*[1], *M. Murakami*[1] and *T. Wolf*[2]. [1]SRL/ISTEC, Div.3, 1-16-25 Shibaura, Minato-ku, Tokyo 105, Japan. [2]Institut fuer Technische Physik, Forschungszentrum Karlsruhe, D-76023 Karlsruhe, Germany.

Superconducting transitions were measured in field-cooled cooling (FCC) and field-cooled warming (FCW) modes in external magnetic fields ranging between 1 mT and 7 T on various LRE-based superconductors of the 123 type, e.g. NdBCO single crystals and melt-processed samples, and on melt-textured ternary compounds of the type $(Nd_{0.33}Eu_{0.33}Gd_{0.33})$-123 (NEG) with varying additions of 211 particles. All LRE-based superconductors investigated exhibit a two step transition when being cooled/warmed in fields larger than 4 T with the exception of single crystals showing a transition temperature T_c of about 96 K. In this case, the Nd/Ba solid solution is practically suppressed. Therefore, we ascribe this effect to the presence of the LRE-rich phase providing a spatial scatter of T_c throughout the sample. Due to the proximity effect, the presence of the LRE-rich phase with a smaller T_c is masked when measuring the samples in a typically small field ($\sim$1 mT). We show that the presence of the two step transitions is directly linked to the occurrence of the peak effect in the magnetization loops.

10–36

Current-Voltage Characteristics and Flux Creep in Melt-Textured YBCO Strips.

H. Yamasaki and *Y. Mawatari*. Electrotechnical Laboratory, Tsukuba, 1-1-4 Umezono, Ibaraki, 305-8568, Japan.

Current-voltage (E-J) characteristics of superconductors shows how dissipation occurs due to current, and thus it is an important parameter for power applications. We investigated the E-J characteristics in melt-textured YBCO strips by measuring the field-sweep rate dependence of magnetization. We corrected the current density distribution in the specimen by a new method. For a wide temperature and field range (60-80 K, 0.2-5.0 T) the E-J curves showed power-law behavior, and the power index n generally became smaller at higher fields and higher temperatures. The E-J characteristics in the lower E windows were also derived from the relaxation of magnetization, flux creep. Combining both measurements, we found that the E-J characteristics show

almost power-law behavior but that there is a slight downward curvature in the logE vs logJ plots. This downward curvature is expected from the vortex-glass theory, which shows that the dissipation approaches zero when the current is substantially reduced. It is then expected that the flux creep is greatly reduced if the current is much reduced from the critical state. We demonstrate a drastic decrease of flux creep by decreasing temperature slightly in a fixed magnetic field.

10–37

Characterisation of the magnetization hysteresis in RE-123 superconductors by exponentially decaying functions.

M. Jirsa[1], *M. R. Koblischka*[2], *T. Higuchi*[2] and *M. Murakami*[2]. [1]Institute of Physics, ASCR, Na Slovance 2, CZ-182 21 Praha 8, Czech Republic. [2]SRL/ISTEC, Div. 3, 1-16-25 Shibaura, Minato-ku, Tokyo 105, Japan.

The characteristic (fishtail) shape of the magnetization hysteresis loops (MHLs) in RE-123 bulk materials has been successfully described by means of the exponentially decaying function $j_n = b^m \exp[(1-bn)m/n]$ where j_n and b are the current density and the applied field normalized to the coordinates of the fishtail maximum. The use of this phenomenological formula, which can also be expressed in terms of the pinning force density, is discussed with emphasis on the elucidation of the physical background of these expressions. We show that the parameter n determines the position of the fishtail peak with respect to the irreversibility field and also relates to the width of the normalized magnetization curve. The definition of n implies that the presence or absence of MHL scaling with temperature is bound to the properties of the pinning barrier distribution in the sample. None of the classical models is able to provide a similarly good fit of the experimental data on high T_c materials because the strong flux creep cannot be ommited. The only pinning mechanism proposed for conventional superconductors, which might at least qualitatively account for the fishtail data in high-T_c materials, is $\triangle\kappa$ pinning.

10–38

Distribution of vortex lattice melting obtained from electrical resistivity.

M. Pekala[1] and *M. Ausloos*[2]. [1]Department of Chemistry, University of Warsaw, Al. Zwirki i Wigury 101, PL-02-089 Warsaw, Poland. [2]SUPRAS, Institut de Physique, Universite de Liege, Liege, B-4000 Sart Tilman, Belgium.

xperimental stucies of the electric and heat currents in the normal, superconducting and mixed states of high critical temperature superconductors (HTSC) supply a valuable characterization, complementary to the data obtained from other techniques. A magnetic field superimposed on the superconducting sample with an orientation perpendicular to the electric or temperature gradient, generates the magneto - transport phenomena, like excess electrical resistivity, excess thermoelectric power, Nernst effect. Different behaviors for the various effects allow to distinguish various dissipation mechanisms, like quasi particle scattering, vortex motion dissipation and superconductivity fluctuations. The location of the mixed state in a phase diagram of HTSC as well as the behavior of vortices play a key role in the understanding of superconductivity and for technological applications. In addition to strictly magnetometric and calorimetric methods most often used for characterisation of HTSC, also the magneto - transport studies offer sensitive probes in the mixed state of superconductors. Precise electrical resistivity measurements performed over broad temperature and magnetic field ranges are analysed in order to unveil the vortex lattice melting processes in the Bi- based HTSC. A relatively simple model assuming a Gaussian distribution of local melting temperatures has allowed us to reconstruct the resistivity versus temperature curves up to about a half of the normal state resistivity. Parameters characterizing the melting transition have been calculated. The mean melting temperature has been found to diminish with the increasing magnetic field. This is accompanied by a broadening of the melting transition width. The temperature derivative of the second critical magnetic field dBc2/dT and the intervortex viscosity increase roughly proportionally to the external magnetic field. The melting line located in the phase diagram remarkably above the percolation line of electrical resistivity indicates that the melting line has the distinguished nature as compared to the percolation and irreversibility lines lines determined from electric and magnetic measurements, respectively. For the polycrystalline materials only the average values are available, whereas for single crystals, textured and oriented thin film superconductors, the observed transport anisotropy and correlates with their layered structure. The experimental transport studies not only enable to test theoretical superconductivity models but also allow to control and tailor HTSC properties by the production and treatment processes. The further investigation lines are defined

10–39

Anisotropic current transport property and its scaling in a YBCO film under the magnetic fields up to 27T.

T. Kiss[1], *M. Inoue*[1], *M. Kiuchi*[1], *M. Takeo*[1], *T. Matsushita*[1,2], *S. Awaji*[3] and *K. Watanabe*[3]. [1]Dept. of Electrical and Electronic Systems Engineering, Kyushu University, Fukuoka 812-8581, Japan. [2]Kyushu Institute of Technology, Iizuka 820-8502, Japan. [3]Institute for Material Research, Tohoku University, Sendai 980-8577, Japan.

In the previous paper, we proposed a method to extract a statistic critical current distribution from a measured transport E-J characteristic. In this study, based on that method, we studied the influence of the magnetic field angle to the transport properties in a c-axis oriented YBCO film. By measuring the transport E-J characteristic, as well as its magnetic field angle dependencies systematically, over wide range of temperature and magnetic fields up to 27T, we studied the stochastic distribution of pinning strength and its scaling. When the field is applied parallel to the ab-plane, the transition fields are enhanced three to four times larger than that of the case when the field is parallel to the c-direction, however, the angle dependencies are scaled for the reduced fields. The other important result is that the statistic characteristics of the pinning and its scaling are almost independent of the field direction. Namely, the volume pinning force densities are scaled for any field angle if we eliminate the influence of the pin distribution. As a result,

we can describe and predict the nonlinear current-voltage characteristics as a function of temperature, magnetic field and its direction.
Research supported in part by the NSF and the State of Florida under cooperative grant DMR 9527035.

10–40
Neutron irradiation and annealing effects in single crystalline Y-123.
F. M. Sauerzopf[1], *M. Zehetmayer*[1], *H. W. Weber*[1] and *M.A. Kirk*[2]. [1]Atomic Institute of the Austrian Universities, Vienna, A-1020, Austria. [2]Argonne National Laboratory, Argonne, IL 60439, USA.

In view of the increase in T_c observed upon annealing irradiated Y-123 crystals, which is accompanied by a rather small decrease of J_c, optimization experiments for the critical current densities by sequential irradiation and annealing steps were made. We find that an optimization is hardly possible, since the optimal density of strongly pinning cascade defetcs is reached in a very small "window" of the neutron fluence. In the same window, important contributions of smaller defects to flux pinning are observed, which are partly removed by the annealing treatment.At the same time, this plays an essential role for the enhancement of T_c.

10–41
Magnetic relaxation measurements in a thin disk of $YBa_2Cu_3O_{7-\delta}$ superconductor.
E. Moraitakis, *M. Pissas*, *G. Kallias* and *D. Niarchos*. Institute of Materials Science, NCSR "Demokritos", 15310 Ag. Paraskevi, Athens,Greece.

The relaxation of the magnetic moment of a thin disk of $YBa_2Cu_3O_{7-\delta}$ superconductor in a perpendicular magnetic field shows a logarithmic dependence on time for the examined temperature range T : $10 - 60$ K. Data are analyzed within the analytical model, which was described by A. Gurevich and E. H. Brandt [Phys. Rev. Lett. **73**, 178 (1994)], assuming a steep $E(j)$ relation. The estimated j_c values show a rather power law dependence on the applied field of the form $j_c(H) \propto H^{-b}$ with $b \simeq 0.50$, and a rather exponential dependence on temperature $j_c(T) = j_c(0)\exp(-T/T_0)$ with $T_0 \simeq 25$ K. The estimated pinning potential U_0 shows a maximum at a temperature where the start of the strong increase of the normalized relaxation rate $S = d\ln m/d\ln t$ happens, which shifts to lower temperatures for higher fields. The E vs j characteristics obtained for the disk geometry from the relaxation data at the circumference of the disk, show a very steep $E(j)$ relation described by a power law $E(j) = E_c(j/j_c)^n$, while a change of this behavior is observed for $T = 60$ K.

10–44
He Irradiation and oxygen disorder in epitaxial $YBa_2Cu_3O_{7-\delta}$ thin films.
D. Arias[1], *Z. Sefrioui*[1], *M. Varela*[2], *C. Leon*[1], *G. D. Loos*[1] and *J. Santamaria*[1]. [1]Departamento de Física Aplicada III, Universidad Complutense de Madrid, 28040-Madrid, Spain. [2]Departamento de Física, Universidad Carlos III de Madrid, Leganés 28911- Madrid, Spain.

Ion damage on high Tc superconductors has been a subject of great interest in recent years. Although high energy irradiation with heavy ions is known to cause amorphous tracks, which act as pinning centers, the effect of light ions (He) at lower energies (10-1000 kV) is still not well characterized. In this contribution we report on the effect of He bombardement (40-160 kV) on high quality epitaxial $YBa_2Cu_3O_{7-\delta}$films at doses between 1E14-1E15 cm-2. The samples for this study were high quality epitaxial $YBa_2Cu_3O_{7-\delta}$ films grown on (100) $SrTiO_3$ using a high pressure (3.6 mbar pure oxygen) sputtering system. Substrate temperature was 800 °C, and oxygen content was adjusted in situ following a stability line of the pressure-temperature phase diagram during sample cool down. The overall effect of irradiation is a reduction of the critical temperature and an increase of the resistivity. This effect is discussed in terms of oxygen displacements from the Cu-O chains into interstitial positions, which increase scattering in planes and act as pairbreakers. A comparison between irradiated and oxygen depleted samples with some thermally induced disorder in the oxygen sublattice, is presented. It leads to the conclusion that there is a tight relationship between the effect of ion irradiation and oxygen disorder. Irradiation of deoxygenated samples at small doses, cause basically oxygen disorder in the chains, an effect which completely recovers with room temperature annealing. Higher doses result in displacements into interstitial positions as mentioned above.
Acknowledgements: Financial support from CICYT grant nr. MAT94-0604 is acknowledged.

10–45
The influence of the propagation of the critical state in the Ag-(Bi,Pb)2Sr2Ca2Cu3Ox sequentially pressed tape conductor on V-I characteristic.
B.A.Glowacki[1,2]. [1]IRC in Superconductivity, University of Cambridge, Madingley Road, Cambridge CB3 OHE,U.K. [2]Department of Materials Science and Metallurgy University of Cambridge, Pembroke Street, Cambridge CB2 3QZ, U. K.

The analysis of the critical state propagation induced by macro-modulations and micro-cracks in the high current silver clad (Bi,Pb)2Sr2Ca2Cu3Ox tapes manufactured by cold continuous sequential pressing is presented using direct current measurements. It has been explained how the change of the current direction relative to the micro-cracks direction may cause appearance of the maximum on the I-V characteristic.

10–46
Surface resistance measurements on HTS films with a high- power niobium-shielded sapphire resonator.
T. Kaiser[1], *M. A. Hein*[2] and *G. Müller*[2]. [1]Cryoelectra GmbH, Wettinerstr. 6H, D-42287 Wuppertal, Germany. [2]Bergische Universität Wuppertal, Fachbereich Physik, Gaußstr. 20, D-42097 Wuppertal, Germany.

We have constructed a niobium shielded sapphire resonator for surface resistance measurements on HTS films up to 3" in diameter. The niobium cavity offers very low background losses ($R_S = 80\mu\Omega$ at 4.2 K and 19 GHz) yielding a measurement limit of about $20\mu\Omega$. The thermally isolated HTS sample can be separately heated while the niobium cavity and the sapphire rod stay at 4.2 K. This technique has been

used for sensitive measurements of the temperature and field dependent surface resistance $R_S(T, B_S)$ between 4.2 K and T_c up to field levels $B_S \approx 50$ mT on films provided by different laboratories. At 4.2 K, $YBa_2Cu_3O_{7-\delta}$ films on sapphire show a 20% R_S-increase at an average field level of 10.7 mT while the corresponding field amplitude for films on $LaAlO_3$ is only 6.6 mT. This difference can be explained by the higher thermal conductivity of sapphire. At higher temperatures, however, films on sapphire often suffer from lower T_c values and exhibit an average R_S value of 2.7 mΩ (at 19 GHz and 77 K), which is about two times larger than for films on $LaAlO_3$. This results in comparable onset fields for nonlinear behavior at 77 K, i.e. a 20% R_S-increase is observed at an average field of 5 mT for films on $LaAlO_3$ and sapphire.

10–47

Low frequencies method to estimate the Labusch parameter and the depinning current in thin YBCO films.

M.Pannetier[1], *P.Bernstein*[1,2], *Ph.Lecoeur*[1,2], *T.D.Doan*[2] and *J.F.Hamet*[2]. [1]LUSAC-EIC (EA-2607) Site Universitaire de Cherbourg F50130 Octeville France. [2]CRISMAT-ISMRA (UMR-CNRS 6508) F14050 Caen France.

In a previous paper, we have described the motion of vortices in a YBaCuO superconducting microbridge with the help of a diffusion model. From the experimental current-voltage characteristics at low frequency, we can determine some physical quantities, such as the pinning energy and the pinning range, and estimate the vortex mobility. In this work, we show how other interesting quantities can be determined or estimated from measurements with the help of the model and of a simple harmonic oscillator description of the pinning potential well. In particular, we estimate the Labusch parameter, which is a significant parameter for the interaction of vortices with pinning sites in a short-range elasticity context. The obtained values are of the same order of magnitude than those given by microwave frequencies measurements from other authors. We also determine the depinning current, and show that the results are consistent with the values measured in the flux flow regime for the same samples.

10–48

Crossover from 3D to pure 2D vortex-glass transition in deoxygenated $YBa_2Cu_3O_{7-\delta}$ thin films.

Z. Sefrioui[1], *D. Arias*[1], *M. Varela*[2], *M. A. Lopez de la Torre*[3], *C. Leon*[1], *G. D. Loos*[1] and *J. Santamaria*[1]. [1]Departamento de Física Aplicada III, Universidad Complutense de Madrid, 28040- Madrid, Spain. [2]Departamento de Física, Universidad Carlos III de Madrid, Leganés 28911-Madrid, Spain. [3]Departamento de Física Aplicada, Universidad de Castilla-La Mancha, 13071 Ciudad Real, Spain.

Current-voltage (I-V) characteristics were used to investigate the response of the vortex glass (VG) phase transition in a oxygen depleted $YBa_2Cu_3O_{7-\delta}$ films, in magnetic fields up to 8T. The samples for this study were high quality epitaxial $YBa_2Cu_3O_{7-\delta}$ films grown on (100) $SrTiO_3$ using a high pressure (3.6 mbar pure oxygen) sputtering system. Substrate temperature was 800 C, and oxygen content was adjusted in situ following a stability line of the pressure-temperature phase diagram during sample cool down. We show that varying the oxygen content, the scaling analysis reveals a crossover from 3D to a pure 2D VG transition with Tg = 0. While, at small oxygen deficiencies (7-δ=6.75), the resistivity vs current curves scale according to the 3D VG model, at intermediate oxygen content (7-δ=6.48), the VG phase transition behaves completely analogous to the highly anisotropic $Bi_2Sr_2CaCu_2O_8$ (BSCCO) samples, showing a quasi 2D VG transition. However, for a very deoxygenated samples (7-δ=6.4), the result is consistent with a pure 2D vortex-glass model similar to the observed in highly anisotropic $Tl_2Ba_2CaCu_2O_8$ thin films. In summary, we conclude that the anisotropy of high quality oxygen depleted samples is comparable to that of the highly anisotropic superconductors.

Acknowledgements: Financial support from CICYT grant nr. MAT94-0604 is acknowledged.

10–48P1

Comparative study of Ca-doped and undoped $YBa_2Cu_3O_{7-\delta}$ thin film bicrystals lying in the low angle to high angle crossover regime.

G.A. Daniels[1], *A. Gurevich* and *D.C. Larbalestier*. University of Wisconsin - Applied Superconductivity Center 1500 Engineering Drive, Madison, WI 53706 USA.

Recently the Augsburg group has reported dramatic changes in the properties of $YBa_2Cu_3O_{7-x}$ thin film 24° [001] tilt bicrystals when Ca is partially substituted into the lattice. J^o(0T, 4K) is greatly enhanced and the grain boundary resistivity markedly decreased, consistent with the fact that Ca additions permit the hole content of the grain boundary and its conductivity to be enhanced. We here report studies of a range of thin film bicrystals (3-24° [001] tilt), paying attention to the change in character of the intergrain properties as a function of misorientation, doping state and electric field. Early results show a distinct reduction of grain boundary resistance with overdoping 5 and 7° [001] tilt boundaries, but no significant enhancement of the J^o(H) characteristics. Detailed temperature and magnetic field dependence of the properties will be presented.

Session Josephson Junctions

10–49

Josephson effects and anisotropy in Tl-2212 thin films.

O.S. Chana[1], *D.M.C. Hyland*[2], *R.J. Kinsey*[3], *W.E. Booij*[3], *M.G. Blamire*[3], *C.R.M. Grovenor*[4], *D. Dew-Hughes*[2] and *P.A. Warburton*[1]. [1]Department of Electronic Engineering, King's College London, Strand, London, WC2R 2LS, UK. [2]Department of Engineering Science, University of Oxford, Parks Road, Oxford, OX1 3PJ, UK. [3]Department of Materials Science, University of Cambridge, Pembroke Street, Cambridge, CB2 3QZ, UK. [4]Department of Materials, University of Oxford, Park Road, Oxford, OX1 3PH, UK.

$Tl_2Ba_2CaCu_2O_8$ (Tl-2212) films have been grown on vicinal $LaAlO_3$ substrates with up to 20° misalignment. Microbridges are patterned into the epitaxial film. The T_c of the microbridge is between 105 and 108K. The microbridges are patterned aligned with the (0 1 0) and ($\cos\theta$ 0 $\sin\theta$)

directions, where θ is the vicinal angle. In the former direction, current transport is parallel to the copper oxide planes whilst in the latter there is a non-zero component of current in the c-direction. The ratio of the resistivity in the two directions is 120 at 300K at 250 at 110K. This strongly suggests that there is an inherent difference in the mechanism responsible for the flow of current within these two directions. Josephson like current-voltage (I-V) characteristics have been measured for microbridges in the ($\cos\theta$ 0 $\sin\theta$) direction. These exhibit hysteresis. This is suggestive of intrinsic Josephson effects. The ratio of Jc in the two directions is 5 at 77K. I-V measurements in the (0 1 0) direction show vortex flow characteristics. The temperature and magnetic field dependence of the microbridges has also been investigated.

10–50

Structure modification and superconducting properties of La- and Nd-substituted Bi-2201 crystals.

K.K. Uk[1], *T.E. Os'kina*[2], *Yu.D. Tretyakov*[2], *V.F. Kozlovskii*[2], *A. Krapf*[3], *M.A. Lorenz*[4] and *Ya.G. Ponomarev*[5]. [1] M.V. Lomonosov Moscow State University, Faculty of Physics, 119 899 Moscow, Russia. [2] M.V. Lomonosov Moscow State University, Faculty of Chemistry, 119 899 Moscow, Russia. [3] Humboldt-Universität zu Berlin, Institut für Physik, Invalidenstr. 110, D-10 115 Berlin, Germany. [4] Bergische Universität Wuppertal, Fachbereich Physik, Gaußstr. 20, D-42 097 Wuppertal, Germany. [5] M.V. Lomonosov Moscow State University, Faculty of Physics, 119 899 Moscow, Russia.

The effect of doping on the crystal structure and superconducting properties of $Bi_2Sr_{2-x}R_xCuO_6$ (R=La, Nd) system (Bi-2201) has been investigated. The crystals were grown from copper-oxide-rich melt and characterized by XRD, resistance measurements, point-contact and tunneling spectroscopy. The X-ray diffraction pattern of the Bi-2201 phase showed the pseudo-tetragonal symmetry with $a = 0.538 - 0.539$ nm for all tested powders and crystals. At the same time the c-axis lattice parameter demonstrated the strong dependence on La doping decreasing from $c = 0.2483(1)$ for $x = 0.01$ to $c = 0.2455(4)$ for $x = 0.2$. By comparing the c-parameters of initial powders and grown crystals on each doping level it has been deduced that the enrichment factor for the crystals was close to 2. The gap parameter Δ was measured in the underdoped, optimally doped and overdoped single crystals of Bi-2201 in a wide range of temperatures 4.2 K$\leq T \leq T_c$ by point-contact and tunneling spectroscopy. For Bi-2201 the ratio $2\Delta/kT_c = 12-13$ was found to be practically constant in the whole range of doping. This is in conflict with the available experimental data for Bi-2212.

10–51

Dependence of the gap parameter on the number of CuO_2 layers in a unit cell of the optimally doped BSCCOO, TBCCO and HBCCO.

Ya.G. Ponomarev[1], *N.Z. Timergaleev*[1], *K.K. Uk*[1], *M.A. Lorenz*[2], *C. Janowitz*[3], *A. Krapf*[3] and *R. Manzke*[3]. [1] M.V. Lomonosov Moscow State University, Faculty of Physics, 119 899 Moscow, Russia. [2] Bergische Universität Wuppertal, Fachbereich Physik, Gaußstr. 20, D-42 097 Wuppertal, Germany. [3] Humboldt-Universität zu Berlin, Institut für Physik, Invalidenstr. 110, D-10 115 Berlin, Germany.

We measure the gap parameter Δ in optimally doped single crystals of $Bi_2Sr_2Ca_{n-1}Cu_nO_{2n+4}$ ($n = 1$: Bi-2201, $n = 2$: Bi-2212 and $n = 3$: Bi-2223) in a wide range of temperatures 4.2 K $\leq T \leq T_c$ by point–contact spectroscopy. In the current-voltage characteristics (CVCs) of S–c–S contacts (point-contact regime), a clear defined subharmonic gap structure (SGS) caused by multiple Andreev reflections has been observed. The dips composing the SGS in the dI/dV-characteristics had a symmetric shape which points to the absence of a strong anisotropy of the gap parameter. It has been found that $\Delta(4.2\ \mathrm{K})$ within experimental errors is proportional to the number n of CuO_2 layers in the optimally doped samples of Bi-2201, Bi-2212 and Bi-2223. The critical temperature T_c^{max} *vs.* n does not obey this simple relation. We have also measured the gap parameter Δ for optimally doped polycrystalline samples of Hg-1212 ($n = 2$), Hg-1223 ($n = 3$) and for single crystals of Tl-2223 ($n = 3$) at $T = 4.2$ K. Combining these results with the data obtained by other authors for Hg-1201, Tl-2212 and Tl-2201, we have found a linear relation between Δ and n for these compounds. For a given number of CuO_2 layers n the value of Δ increases slightly in a row BSSCO → TBCCO → HBCCO.

10–52

Three-dimensional Josephson junction networks: general properties and possible applications.

R. De Luca. INFM - Dept. of Physics - University of Salerno - Baronissi (SA) 84081 ITALY.

The study of the electrodynamic properties of one-dimensional or two-dimensional Josephson junction arrays has brought about a large variety of applications. Only very recently detailed analyses of three-dimensional Josephson junction networks have been carried out. In particular, a current-biased inductive cubic network of Josephson junctions has been proposed as a model system of a vectorial magnetic field sensor. In the present work a general approach to the study of the electrodynamic properties of inductive cubic networks with different types of bias current configurations is presented. Potential applications of these model systems are briefly discussed.

10–53

Current transport mechanism in YBCO bicrystal junction on sapphire.

G. A. Ovsyannikov, A. D. Mashtakov, I.V. Borisenko and *K. Y. Constantinian*. Institute of Radio Engineering and Electronics RAS, 103907, Moscow, Russia.

YBCO junctions were made on sapphire bicrystal substrates in which the directions <1120> for both parts of the sub-

strate have the angle 12° with the plane of boundary. YBCO film with thickness 100 nm was deposited by dc sputtering on the plane 1102 of bicrystal substrate after deposition of CeO2 buffer layer. The junctions were tested at dc and mm waves. The junction with width 5 mcm have high resistance 10-20 Ohm and IcRN= 1-2 mcV for width of junction 4-5 mcm and tolerance of RnS around 30% on chip. DC, microwave and magnetic characteristics of the junctions have been investigated experimentally. The microwave dynamics of the junction with superconducting current-phase relation fits with sin j relation better than 5%, that clear indicates on tunnel conductivity between two YBCO electrodes. It was found that critical current density depends as square root on the interface transparency in accordance with prediction of superconducting current transport via Andreev-bound surface states. The work was partially support by Russia Foundation of Fundamental research and INTAS program of EU and NATO Scientific program.

10–54

Observation of subharmonic gap structures in NbN/AlN/NbN tunnel junctions.

Z. Wang[1], *A. Saito*[2] and *K. Hamasaki*[2]. [1]Kansai Advanced Research Center, Communications Research Laboratory 588-2 Iwaoka, Iwaoka-cho Nishi-ku, Kobe, 651-2401 Japan. [2]Nagaoka University of Technology 1603-1 Kamitomioka-cho, Nagaoka, 940-2188 Japan.

NbN tunnel junctions are promising for applications of high-frequency and high-speed Josephson devices. In order to obtain high performances for the devices, however, the junctions must have large IcRN products and small RNCJ constants. This requires that the junctions have a high current density, because the RNCJ constants scale with the 1/Jc. We have recently made an advantage in development of high current density and high quality NbN/AlN/NbN tunnel junctions for submillimeter wave SIS mixers. The junctions showed excellent tunneling characteristics with a current density up to 100 kA/cm2 and sensitive heterodyne mixing properties in submillimeter wave regions. These junctions exhibited significant subgap current, which is interesting to analysis noise properties of SIS mixers. In this paper, we report on the investigations of subgap current for our NbN/AlN/NbN tunnel junctions. Subharmonic gap structures were observed in the I-V characteristics at voltage 2D/ne, where D is the superconducting energy gap and n is an integer. We show that multiple-Andreev reflection is responsible for the subgap current in NbN/AlN/NbN tunnel junctions, and try to relate the subgap current with noise properties of the junctions.

10–55

Effect of trapped Abrikosov vortices on the critical current of YBCO step-edge junctions.

K.H. Müller, *E.E. Mitchell*, *C. Andrikidis* and *C.P. Foley*. CSIRO, Telecommunications and Industrial Physics, Sydney 2070, Australia.

We have measured the Josephson critical current I_c of YBCO thin-film step-edge junctions at 77 K and 4.2 K as a function of an applied perpendicular magnetic field H_a and the junction width w. Above a certain field, depending on the width w, Abrikosov vortices form in the film near the junction causing the appearance of sudden jumps in the data of I_c versus H_a. We have developed a theoretical model to calculate the Josephson critical current $I_c(H_a)$ for a junction in planar geometry in a perpendicular field H_a taking the presence of Abrikosov vortices fully into account. Comparing our experimental data with our calculations, we are able to predict the likely positions of newly formed vortices as well as vortex rearrangements. In addition, our model correctly predicts the experimentally observed dependence of $I_c(H_a)$ on the junction width w. In large magnetic fields (several tesla) $I_c(H_a)$ shows strong hysteretic behaviour. Our theoretical model quantitatively explains this hysteretic behaviour as being caused by the partial cancellation of vortex and Meissner currents close to the junction.

10–56

A high-T_c multilayer ramp-edge junction process for digital circuit applications.

I.H. Song[1], *E.H. Lee*[1], *S.Y. Yoon*[1] and *G. Park*[2]. [1]Samsung Advanced Institute of Technology, P.O.Box 111, Suwon 440-600, Korea. [2]Sogang University, C.P.O.Box 1142, Seoul 100-611, Korea.

Reliable $YBa_2Cu_3O_{7-\delta}$ (YBCO) ramp-edge junctions with a Ga-doped YBCO barrier have been fabricated by pulsed laser deposition. In order to produce high-T_c digital circuits, it is necessary to develop a circuit process which integrates reliable and reproducible junctions into epitaxial multilayers. In-situ rf plasma cleaning process enabled to control the interface resistance of ramp-edge junctions and enhance the epitaxial growth. These junctions exhibited clear resistively-shunted-junction-like current-voltage characteristics with high values of I_cR_n products at 65 K. We have examined interface resistance of the junctions in an edge junction geometry. Critical current uniformity is required to keep device performance reliable. We have measured spreads in the junction's critical currents as low as 10% (1-σ). The temperature dependence of the critical currents and normal resistance for junctions are qualitatively consistent with the behavior predicted by the conventional proximity effect. The normal coherence length of the Ga-doped YBCO barrier estimated from the fittings indicates that the junctions are in the dirty limit regime. DC SQUIDs fabricated with these junctions exhibited excellent voltage modulations in response to applied fields at 65 K.

10–57

Fabrication of YBCO step-edge Josephson junctions.

M.J. Chen[1], *H.W. Yu*[1], *J.R. Chiou*[1], *J.H. Chen*[1], *H.C. Yang*[1], *H.E. Horng*[2], *S.Y. Yang*[2], *J.T. Jeng*[2], *C.H. Chen*[2] and *Y.C. Liu*[2]. [1]Department of Physics, National Taiwan University, Taipei 106, Taiwan. [2]Department of Physics, National Taiwan Normal Unversiy, Taipei 117, Taiwan.

We report a systematic study of the fabrication process of YBCO step-edge Josephson junctions on MgO substrates. The optimum microlithography process pre-determines the straight step profile while the non-optimum process gives a curvy one. To achieve a smooth inclined plane in step-edge profile without trench or redeposit protrusion, the argon ion-

beam incident angle is aligned to incident at 65 degree with respect to the normal direction of the substrate and parallel to the edge of the photoresist mask. The current-voltage (I-V) curves of the straight step-edge junctions are RSJ-like while curvy ones show flux-flow behavior. For uniform RSJ-like junctions with the same step angle, the I-V characteristics depend on the ratio of the film thickness to the step height (t/h). These junctions exhibit larger IcRn product with smaller t/h value. Further clarifications of the junctions are obtained by fitting the data to I-V and I_c-B curves. The results are discussed.

10–58

Influence of the passive region on zero field steps for window junctions.

A. Benabdallah[1], *J. G. Caputo*[2] and *N. Flytzanis*[3]. [1]Laboratoire de Matématiques Institut National de Sciences Appliquées and Unité C.N.R.S. 6085, B. P. 8, 76131 Mont-Saint-Aignan Cedex France. [2]Laboratoire de Physique Mathématique et Théorique Université de Montpellier II and Unité C.N.R.S. 5095 34095 Montpellier cedex 05 France. [3]Physics Dept. University of Crete POB 2208 710 03 Heraklion Greece.

Modern Josephson junctions due to their process of fabrication are surrounded by a passive (linear) region where the thickness of the oxide layer prevents the passage of the supercurrent. This protects the oxide layer from degradations due to the environment and provides an electromagnetic cavity to enhance the power of the device. We present a numerical and analytic study of the influence of the passive region on fluxon dynamics where we examine the effect of the extension of the passive region and its electromagnetic characteristics, its surface inductance L_I and capacitance C_I. When the velocity in the passive region v_s is equal to the Swihart velocity (1) a one dimensional model describes well the operation of the device. When v_s is different from 1, the fluxon adapts its velocity to v_s. In both cases we give simple formulas for the position of the limiting voltage of the zero field steps. Large values of L_I and C_I lead to different types of solutions which are analysed.

10–59

Laminar phase flow for an exponentially tapered Josephson oscillator.

A. Benabdallah[1], *J. G. Caputo*[2] and *A. C. Scott*[3]. [1]Laboratoire de Matématiques Institut National de Sciences Appliquées and Unité C.N.R.S. 6085, B. P. 8, 76131 Mont-Saint-Aignan Cedex France. [2]Laboratoire de Physique Mathématique et Théorique Université de Montpellier II and Unité C.N.R.S. 5095 34095 Montpellier cedex 05 France. [3]Department of Mathematics, University of Arizona, Tucson, AZ, 85721, U.S.A. Department of Mathematical Modeling, Technical University of Denmark, Lyngby, Dk.

Exponential tapering has previously been proposed as a means to improve the performance of a Josephson flux flow oscillator by extending the parameter range over which flux quanta move smoothly (laminar flow) toward the load. Extensive numerical results are presented here that support this claim and demonstrate that exponential tapering increases power output while improving the spectral purity of the output voltage waveform. Since exponential tapering is not expected to increase the difficulty of fabricating a flux flow oscillator, we suggest that this feature should be incorporated in future designs.

10–60

Characterisation of ramp-edge Josephson junctions and junction arrays with Ga-doped $PrBa_2Ga_xCu_{3-x}O_7$ and $SrTiO_3$-barrier.

H. Burkhardt, *A. Rauther* and *M. Schilling*. Institut fuer Angewandte Physik und Zentrum fuer Mikrostrukturforschung der Universitaet Hamburg, Jungiusstrasse 11, 20355 Hamburg, Germany.

Ramp-edge Josephson junctions from high-temperature superconductors are needed for several applications like digital circuits, magnetometers and voltage standards because of their circuit design flexibility. Beyond this they provide the potential to investigate the conduction mechanism of Cooper pairs and quasi-particles through the barrier material. In this work ramp-edge junctions with a sandwich structure of $YBa_2Cu_3O_7$/barrier/$YBa_2Cu_3O_7$ are investigated. As barrier materials we use the semiconductor $PrBa_2Ga_xCu_{3-x}O_7$ with different doping concentrations x=0-0.4 of Gallium and the insulator $SrTiO_3$ with different barrier thickness. We investigate the RSJ-behaviour, especially the excess current in the I(V)-curves, their derivative, and the temperature- and field-dependent conductivity. We find hopping conductivity with a radius of the localised states of about 6nm at 50K. In further experiments we apply magnetic and rf-fields. To verify our results, we pay special attention to the spread of the characteristic parameters like critical current density j_c and specific normal state resistance ρ_n by investigating small Josephson junction serial arrays. This work is supported by the Deutsche Forschungsgemeinschaft in the Sonderforschungsbereich SFB 508 „Quantum materials - lateral and hybrid structures".

10–61

Flux flow properties of $Bi_2Sr_2Ca_1Cu_2O_{8+y}$ Intrinsic Josephson junctions fabricated by Si ion implantation.

K. Nakajima[1,3], *S. Sudo*[1], *T. Tachiki*[1] and *T. Yamashita*[2,3]. [1]Research Institute of Electrical Communication, Tohoku University, Sendai, Japan. [2]New Industry Creation Hatchery Center, Tohoku University, Sendai, Japan. [3]CREST, Japan Science & Technology Cooporation, Japan.

Flux flow properties have been studied for the $Bi_2Sr_2Ca_1Cu_2O_{8+y}$ intrinsic Josephson junctions fabricated by Si ion implantation. For the Si-implanted intrinsic Joosephson junctions, the junction length corresponding to the height of conventional mesa type junctions is defined by penetration length of implanted Si ions in BSCCO. It has been reported that the Si-implanted junctions show branching I-V curves typical of intrinsic Josephson effect and the number of branches is consistent with Si penetration depth. We claim the advantage of the Si ion implantation process to fabricate the intrinsic junctions that embedded in the BSCCO single crystal since the implantation doesn't change the crystal structure while the superconductivity is suppressed. In this paper, we present flux flow properties. Flux flow peaks due to vortices lock-in into ab-planes are clearly observed in an-

gler dependencies of voltage across the junctions measured under various external magnetic fields. Obvious vortices lock-in and flux flow velocities estimated from the flux flow voltage peaks reveal that the Si-implated BSCCO intrinsic junctions are comparable to conventional mesa junctions.

10–62

SNS Ramp Type Josephson Junctions for Highly Integrated Superconducting Circuit Applications.

R. Pöpel, *D. Hagedorn*, *F.-Im. Buchholz* and *J. Niemeyer*. Physikalisch-Technische Bundesanstalt, Bundesallee 100, D-38116 Braunschweig, Germany.

At PTB, a new fabrication process has been developed to produce small SNS Josephson junctions for application in highly integrated superconducting circuits. The technological process based on a combination of standard non-contact photolithography using an optical wafer stepper and etching techniques has been optimized to produce Nb/PdAu/Nb junctions in a Ramp Type Junction (RTJ) configuration. Test circuits of single RTJs and RTJ arrays containing up to 10,000 junctions with contact areas of A = 0.25 μ m × 1.3 μm have been fabricated and experimentally and theoretically investigated. With a thickness of the PdAu normal metal layer of d = 40 nm, values of junction parameters of about $j_C = 200\ kA/cm^2$ and of about $I_C \cdot R_N = 21\mu V$ have been achieved for the critical current density and for the product of critical current and normal state resistance. The junctions exhibit excellent hysteresis-free current-voltage characteristics with small parameter spread. The measurement results are in good agreement with theory. Even under inhomogenuous microwave coupling conditions, stable Josephson voltage steps have been observed in arrays containing up to 1,000 junctions. The fabrication process fulfils the requirements for an implementation of sub-micron Josephson junctions in highly integrated circuits in the fields of programmable Josephson voltage standards and Rapid Single Flux Quantum applications.

The work is partly supported by the European Communities (proj. no. SMT4-CT98-2239) and by the Deutsche Forschungsgemeinschaft (DFG), Germany (proj. no. NI 253/3-1).

10–63

Effect of pressure on the c-axis critical current of Bi-2212 intrinsic Josephson junctions.

A. Yurgens, *D. Winkler* and *T. Claeson*. Department of Microelectronics and Nanoscience, Chalmers University of Technology, S-41296, Gothenburg, Sweden.

We have experimentally found that the c-axis critical current of $Bi_2Sr_2CaCu_2O_{8+\delta}$ (Bi-2212) intrinsic Josephson junctions drastically increases with pressure $P < 1$ GPa (up to 120 % GPa^{-1}). This observation may provide a basis for further improvements in processing of long-length Bi2212 and Bi2223 tapes for high-current applications.

10–64

Vortex dynamics and Cherenkov radiation of linear waves in long narrow Josephson junction connected with wide stripline.

A.V. Chiguinev[1] and *V.V. Kurin*[2]. [1]IPM RAS, Nizhny Novgorod, 603600, Russia. [2]IPM RAS, Nizhny Novgorod, 603600, Russia.

We consider a long Josephson junction connected built in a wide stripline. A sine-Gordon equation with nonlocal integro-differential operator describing the dynamics of such a system is obtained. We get analytical expressions for a uniformly moving soliton in cases of small and large width of an idle region. The Cherenkov radiation of a moving vortex is predicted both by numerical simulation and by the analysis of dispersion characteristics of linear waves. A general theoretical scheme of studying the Cherenkov radiation of a moving vortex in equations of the sine-Gordon type with nonlocality is present

10–65

Josephson Current along the c-axis of the Mesa-structured $Bi_2Sr_2CaCu_2O_{8+\delta}$.

K. Hirata and *T. Mochiku*. [1]National Research Institute for Metals, 1-2-1 Sengen, Tsukuba,Ibaraki, 305-0047, JAPAN. [2]1-2-1 Sengen, Tsukuba,Ibaraki, 305-0047, JAPAN.

Intrinsic Josephson effect has been recognized as one of the significant features in the anisotropic high T_c superconductors. In order to study the Josephson current in the intrinsic junction, the mesa-structure has been fabricated on the $Bi_2Sr_2CaCu_2O_{8+\delta}$ single crystal, and the current-voltage characteristics have been studied in a magnetic field perpendicular and parallel to the c-axis. In the magnetic fields, it is found that I-V characteristics reflect strongly the vortex states and the arrangements of the vortices in the material.

10–66

Effects induced by microwaves on S-I-N-I-S junctions.

G. Carapella, *G. Costabile* and *R. Latempa*. Dipartimento di Fisica and Unita' INFM, Baronissi 84081, Italy.

We fabricated and tested double barrier devices consisting of Nb-AlOx-Al-AlOx-Nb films, in which the AlOx barriers are thin ($\approx$ 2 nm) and the Al film is thinner than the coherence length in Nb (thinner than $\approx$ 30 nm). The devices exhibit Josephson critical current and their I-V characteristic is highly hysteretic and shows in zero magnetic field evenly spaced resonances which become very unstable when an external magnetic field is turned on. When the devices are irradiated with microwaves, Shapiro steps are observed. At low rf power, the resonances are more stable than the zero voltage current. Increasing the rf power, they appear as current branches symmetrical aside a Shapiro step. Increasing further the rf power, they are turned into resistive steps alternated to the Shapiro steps. If the microwave is chosen to have twice the frequency related to the resonance voltage spacing by the Josephson relation, Shapiro steps of half integer order appear in the I-V characteristic.

10–67
Submicron $YBa_2Cu_3O_{7-\delta}$ Step-Edge Josephson Junctions For A Scanning SQUID Microscope Sensor.
P.Larsson[1], *A.Tzalenchuk*[1,2], *Z.G.Ivanov*[1] and *T.Claeson*[1]. [1]Department of Physics, Chalmers University of Technology and University of Göteborg, S-412 96 Göteborg, Sweden. [2]Institute of crystallography RAS, 117333 Moscow, Russia.

We report on design, fabrication and properties of SQUID sensors for a scanning SQUID microscope. The sensors are based on submicron step-edge Josephson junctions (SEJJ) with RSJ type current-voltage characteristics and good reproducibility. The SQUID modulation voltage was of the order of 40 μV. En-route to achieving these results we have studied various aspects of technology-dependent properties of Josephson junctions formed on the edge of the step etched in the substrate. Although wide ($\geq$ 2 μm) step edge junctions have a high characteristic voltage and the possibility of arbitrary positioning on the chip, their application is hindered by the lack of reproducibility. We have fabricated submicron SEJJ in $YBa_2Cu_3O_{7-\delta}$ thin films on a $LaAlO_3$ substrates by e-beam lithography and ion-beam etching through an amorphous carbon mask. There properties were studied in magnetic fields up to 5 T. Three types of behaviour were clearly distinguished: (i) junctions with low critical current, high normal resistance and RSJ characteristics, (ii) junctions with high critical and excess currents, and low resistance, and (iii) tunnel junctions with zero Josephson current. Techniques to reproducibly create submicron SEJJ will be summarised. This work has been supported in part by TFR, STINT, Materials consortium on Superconductivity and RFBR.

10–68
Calculation of flux focusing efficiency of grain-boundary Josephson junctions electrodes.
C.Cordier, *S.Flament*, *C.Dubuc* and *E.Sassier*. GREYC - ISMRA , 6 Bd Marechal Juin F-14050 CAEN Cedex, France.

The Josephson Fraunhofer Magnetometer (JFM), firstly described during the previous EUCAS of 1995, is a superconducting magnetometer including a single Josephson junction whose critical current dependence on the applied magnetic field is precisely measured. It has promising applications in absolute magnetometry insofar as its resolution is only one order lower than the resolution of a SQUID with the same geometry of flux focuser. As an example, Lee et al have obtained a 35fT/rtsq(Hz) resolution for a directly coupled SQUID having a 1cmX1cm washer while we have recently measured a 600fT/rtsq(Hz) resolution for a JFM with similar geometry having a 0,85cmX0,85cm washer. The present work deals with further improvement in the JFM resolution. Whereas the flux focusing effect produced by large washer has been widely studied, there are very few papers dealing with the optimization of the geometry in the neighbourhood of the junctions. We have used the finite element method so as to describe the superconducting Meissner state. This method has turned out to be well suited to the description of the focusing effect obtained with proper design of the strip joining the grain-boundary junction to the flux focuser. We present the calculated results and compare them with experimental data.

10–69
Highly localised light ion irradiation of $YBa_2Cu_3O_{7-\delta}$ using metal masks.
W.E. Booij[1], *N.H. Peng*[2], *F. Kahlmann*[1], *R. Webb*[2], *E.J. Tarte*[1], *D.F. Moore*[1], *C. Jeynes*[2] and *M.G. Blamire*[1]. [1]IRC in Superconductivity, University of Cambridge, Cambridge, CB3 0HE, United Kingdom. [2]Surrey Centre for Research into Ion Beam Applications, School of Electronic Engineering, Information Technology and Mathematics, University of Surrey, Guildford, GU2 5XH, United Kingdom.

Irradiation of $YBa_2Cu_3O_{7-\delta}$ with H_2^+ ions with an energy in the range of 10-50 keV can be used to fully suppress superconductivity. Simulations suggest that such an irradiation process in combination with a high-aspect ratio metal mask can be used to create highly localised damage regions in thin YBCO films (50-200 nm). We describe results obtained on verification of this using the following experimental method. When the metal mask is electrically isolated from the YBCO layer it can be accurately patterned down to 30 nm with a Ga^+ Focused Ion Beam in combination with in-situ resistance monitoring. The sample is than transferred to a broad ion beam implanter in which the sample can be cooled down to any temperature between 20 K and room temperature while its electrical characteristics are monitored during irradiation with light ions (H_2^+).

10–70
Two-dimensional arrays of tunnel junctions: transport properties and phase transitions.
I. Wooldridge[1], *B. Camarota*[2] and *P. Delsing*[1]. [1]Chalmers University of Technology and Göteborg University, 412 96 Göteborg, Sweden. [2]CNRS-CRTBT, BP166, 38042 GRENOBLE CEDEX 9, France.

We describe the transport properties of two-dimensional arrays of $Al/Al_2O_3/Al$ tunnel junctions, such as the current voltage characteristics and the Hall resistance. The dependence of these properties on temperature and external magnetic field is discussed. The arrays have been fabricated using electron-beam lithography and angle shadow evaporation. Two different substrates with very different values of electrical permittivity, silicon oxide and strontium titanate, were chosen. By altering the oxidation conditions during the fabrication we are able to control the ratio between the charging energy and the Josephson coupling energy and hence the dynamics of the arrays. The various phenomena exhibited by these arrays, such as magnetic field tuned superconductor-insulator transitions, are discussed

10–71
Statistical analysis of the size dependence of *c*-axis critical currents in Bi2212 mesas.
V.M. Krasnov[1,2]. [1]Department of Microelectronics and Nanoscience, Chalmers University of Technology, S-41296 Göteborg, Sweden. [2]Institute of Solid State Physics, 142432 Chernogolovka, Russia.

We present systematic analysis of the *c*-axis critical current in small area Bi2212 mesas as a function of the size of the

mesa. Measurements were made for mesas with large variety in area, fabricated simultaneously on top of Bi2212 single crystals. Strong suppression of critical current density with decreasing mesa area is observed. Possible mechanisms of the suppression are discussed.

10–72

Influence of the passive region on zero field steps for window junctions.

A. Benabdallah[1], J. G. Caputo[2] and N. Flytzanis[3]. [1]Laboratoire de Matématiques Institut National de Sciences Appliquées and Unité C.N.R.S. 6085 B. P. 8, 76131 Mont-Saint-Aignan cedex, France. Place Emile Blondel, B.P. 08 76131, Mont Saint Aignan France. [2]Laboratoire de Physique Mathématique et Théorique, Université de Montpellier II and Unité C.N.R.S. 5095 34095 Montpellier cedex 05, France. [3]Department of Physics University of Crete POB 2208 710 03 Heraklion, Greece.

Modern Josephson junctions due to their process of fabrication are surrounded by a passive (linear) region where the thickness of the oxide layer prevents the passage of the supercurrent. This protects the oxide layer from degradations due to the environment and provides an electromagnetic cavity to enhance the power of the device. We present a numerical and analytic study of the influence of the passive region on fluxon dynamics where we examine the effect of the extension of the passive region and its electromagnetic characteristics, its surface inductance L_I and capacitance C_I. When the velocity in the passive region v_s is equal to the Swihart velocity (1) a one dimensional model describes well the operation of the device. When v_s is different from 1, the fluxon adapts its velocity to v_s. In both cases we give simple formulas for the position of the limiting voltage of the zero field steps. Large values of L_I and C_I lead to different types of solutions which are analysed.

10–73

Laminar phase flow for an exponentially tapered Josephson oscillator.

A. Benabdallah[1], J. G. Caputo[2] and A. C. Scott[3]. [1]Laboratoire de Matématiques Institut National de Sciences Appliquées and Unité C.N.R.S. 6085 B. P. 8, 76131 Mont-Saint-Aignan cedex, France. Place Emile Blondel, B.P. 08 76131, Mont Saint Aignan France. [2]Laboratoire de Physique Mathématique et Théorique, Université de Montpellier II and Unité C.N.R.S. 5095 34095 Montpellier cedex 05, France. [3]Department of Mathematics, University of Arizona, Tucson, AZ, 85721, U.S.A. Department of Mathematical Modeling, Technical University of Denmark, Lyngby, Dk.

Exponential tapering has previously been proposed as a means to improve the performance of a Josephson flux flow oscillator by extending the parameter range over which flux quanta move smoothly (laminar flow) toward the load. Extensive numerical results are presented here that support this claim and demonstrate that exponential tapering increases power output while improving the spectral purity of the output voltage waveform. Since exponential tapering is not expected to increase the difficulty of fabricating a flux flow oscillator, we suggest that this feature should be incorporated in future designs.

Session Passive Devices

10–75

Frequency dispersion of tunability and losses in ferrite/superconducting structures.

A. Kuzhakhmetov[1], A. Jenkins[1], D.M.C. Hyland[1], M. Koledintseva[2] and D. Dew-Hughes[1]. [1] Department of Engineering Science, University of Oxford Department of Engineering Science, University of Oxford, Parks Road, Oxford OX1 3PJ, UK. [2]Department of Radio Engineering, Moscow Power Engineering Institute, Moscow 111250, Russia.

The results of experimental research of tunable microwave structures based on HTS resonators combined with ferrite plane elements of various geometry are presented. Tunability by means of external magnetic field and microwave losses in these structures are studied. Split ring resonators are made of superconducting TlBaCaCuO films (0.3 micron thick) deposited on LaAlO3 substrates. TlBaCaCuO films have the following average parameters: Tc=103-105K and Rs=0.5 mOhm (at 10 GHz, 77K). The resonator unloaded Q-factor is 4500 at the fundamental mode 2.4 GHz (at 77K). The Q-factor of resonators is not affected by the magnetic field up to 2000 Oe. In the structures under investigation the resonator is placed on the ferrite planes or thin films (5 and 10 micron thick) on GGG substrates. Saturation magnetisation of the employed ferrites is 4*pi*Ms = 300-1760 G at room temperature. External magnetic field is applied parallel to the ferrite and LaAlO3 planes along the wave propagation direction. Tunability and losses are observed at fundamental and minor modes in the range 2-15 GHz. At 2.4 GHz maximum tunability of about 10% and an insertion loss -20 dB with Q=500 obtained. At 11.4 GHz the maximum Q-factor is 3500 (ferrite with 4*pi*Ms =300 G), the best reported recently, and the achived tunability is 1.2%.

10–76

Comparative study of YBaCuO thin film microwave surface resistance measurement methods.

A. Dégardin[1], A. Gensbittel[1], P. Crozat[2], M.S. Boutboul[3], M. Achani[4], Y. Roelens[4], S. Sautrot[3], J-C. Carru[4], M. Fourrier[3] and A. Kreisler[1]. [1]LGEP - UMR 8507 CNRS - Universités Paris 6 & Paris 11 - Supélec, Plateau de Moulon, 91190 Gif-sur-Yvette, France. [2]IEF - UMR 8622 CNRS - Université Paris 11 - Bâtiment 220, 91405 Orsay, France. [3]DIM - Université Paris 6 - Tour 12, 4 Place Jussieu, 7 005 Paris, France. [4]IEMN - UMR 8520 - Université Lille 1 - Avenue Poincaré, BP 69 - 59652 Villeneuve d'Ascq, France.

The knowledge of the surface resistance R_s of high critical temperature superconductors plays a major role in the development of passive microwave devices. In order to study devices made from YBaCuO thin films deposited by rf magnetron sputtering on MgO single crystals, we have undertaken several measurements in the 50 MHz to 35 GHz frequency range involving two aspects. The first one is related to R_s determination from conical cavity resonator measurements on unpatterned films. The second aspect has concerned microwave measurements on such structures as coplanar waveguides and resonators as well as microstrip resonators, patterned in YBaCuO films using conventional

lithographic process followed by ion beam etching. Experimental results confirm a frequency independent phase velocity for superconducting transmission lines. Concerning resonator characterizations, the magnetic penetration depth as well as the kinetic inductance have been evaluated from the temperature dependence of the resonance frequency. Quality factor measurements of resonators, for which non linear effects have been observed as a function of incident microwave power, have allowed to determine R_s values which are discussed using various theoretical models found in the literature. Finally, the comparison between the surface resistance of unpatterned and patterned films will be considered.

10–77
Ion milled YBaCuO films for microwave applications.
R. Monaco[1], *U. Gambardella*[2], *C. Beneduce*[3], *F. Bobba*[3], *M. Boffa*[3], *A.M. Cucolo*[3] and *M.C. Cucolo*[3]. [1]Istituto di Cibernetica del C.N.R., Arco Felice (Na), Italy. [2]Centro Ricerche ENEA, Frascati, Italy. [3]Dipartimento di Fisica, Universita' di Salerno, Baronissi (Sa), Italy.

The low microwave surface resistance of superconducting thin film allows for the fabrication of high-Q microstrip resonators, and thus of low loss, highly selective filters. However, the high current densities that arises due to the small size and to the thin film nature of these structures together with nonlinear loss mechanisms are responsible for large losses even at incident power levels as small as 1mW. Further, since the rf current in a microstrip line is peaked at the film edges, losses can be dramatically high if the film profile is not step-like. We have measured the microwave losses and imaged the film edge profile of YBaCuO thin film resonators patterned with both liquid etch and argon ion milling. The high quality c-axis oriented films were deposited on $LaAlO_3$ substrates by an in situ dc sputtering process in high oxygen pressure. These shoved $T_c(\rho = 0) > 91$ K and $\Delta T_c < 0.5$ K. By SEM imaging we found that the resonators etched with the ion milling had a sharper edge profile and, from Q-factor measurements, a surface resistance as low as 1mΩ at 1.2 GHz and 77K.

10–78
Development of superconductive microwave filters for UMTS mobile communications.
B.Marcilhac, *Y.Lemaitre*, *D.Mansart* and *J.C. Mage*. U.M.R.137 Thomson-CSF LCR / CNRS, Orsay,France.

Future mobile communication specifications (UMTS) require microwave filters with narrow band-pass, typically 5 MHz at 1950 MHz (0.25%), and sharp edges (40dB at 400kHz). These targets are attainable with superconductive technology but the development of such filters with more than ten poles requires a controlled and reproducible process. We optimised our procedure for designing HTS filters that do not require tuning after fabrication. The goal was to estimate how far accuracy and precision of the bandwidth and centre frequency of the filter are influenced by variations in the dielectric constant and thickness of the substrate and also by the patterning and processing of the circuit elements. Lanthanum aluminate was used as substrate, the complete geometry was modelled by EM software and results on a 12-pole 1950 MHz band-pass filter will be presented.

This work was partially supported by the French government in RNRT contract "SUPRACOM"

10–79
Calculation of RF spurious in planar superconducting structures.
J. Parrón, *C. Collado*, *J. Mateu*, *E. Úbeda*, *J. M. O'Callaghan* and *J. M. Rius*. Universitat Politécnica de Catalunya Campus Nord UPC, D3 Barcelona 08034 Spain.

A general algorithm has been developed to calculate intermodulation and harmonic spurious generated by planar superconducting structures such as a single resonator or a filter consisting of several coupled resonators. The algorithm combines a numerical tool used in electromagnetic calculations (Method of Moments optimized at UPC and LEMA-EPFL for analysis of single and multi-layer planar structures) with Harmonic Balance routines which are normally used for calculating the nonlinear response in electronic circuits with lumped components. With these techniques, the nonlinear response of planar structures can be calculated without restrictions in their shape. Thus, resonators of any shape can be analyzed, as well as planar filters consisting of several -and not necessarily identical- resonators. The only inputs to the algorithm developed are: the frequencies of the fundamental and spurious signals, a geometrical description of the structure, the parameters of the dielectric (permittiviy and loss tangent), and parameters to characterize the dependence of the superconductor's surface impedance with current density. With these, the program calculates the current distribution at the fundamental frequency, and at the frequency of each spurious. Examples will include the calculus of the fundamental, third harmonic, and third-order intermodulation products of a microstrip resonator coupled with capacitive gaps.

10–80
Full wave analysis of YBCO Coplanar transmission lines on Lithium Niobate Substrates.
E. Rozan[1], *J.M. O'Callaghan*[1], *J. Byun*[2] and *F.J. Harackiewicz*[2]. [1]Universitat Politècnica de Catalunya Campus Nord, Modulo D3 Jordi Girona 1-3 08034 Barcelona Spain. [2]Southern Illinois University Dpt of Electrical Engineering 62901 Carbondale, Il USA.

Full-wave Method of Moments (MoM) and Finite Difference Time Division (FDTD) Method are presented in this paper. The methods have been used to characterize coplanar transmission lines (CPW) made with high T_c superconductors, YBCO films in this case. The configuration studied evolves a multi-layer system composed by Lithium Niobate (LNO), YBCO and a buffer layer Yttria-Stabilized Zirconia (YSZ), structure with important specific features: the high permittivity of both YSZ and LNO, the presence of a strong LNO anisotropy, and the proper particular behavior of HTS film. The original MoM formulation was only taking in account isotropic substrates. Additional conditions were introduced in the formal Green functions system to simulate the effect of the LNO cut and the complex surface impedance of the superconductor. A FDTD formulation algorithm has also been used in the analysis. As MoM, the original algorithm was modified for this peculiar structure. The comparison of both methods will be used to check the

validity of the modifications introduced in the original analysis. Special attention will be paid in describing the influence of the LNO cut used. The determination of line parameters (characteristic impedance, effective propagation index, and attenuation) will serve to predict the performance of a Mach-Zehnder electro-optical modulator.

10–81

Simulation of Global Heating Effects on Non-linear Resonance Curves at Microwave Frequencies.

A. Cowie[1], *S. Thiess*[1], *N. Lindop*[2], *J.C. Gallop*[3] and *L.F. Cohen*[1]. [1]Blackett Laboratory, Imperial College Prince Consort Rd, London SW7 2BZ. [2]Dept. of Biological Sciences, University of Warwick, CV4 2AL. [3]National Physical Laboratory, Queens Rd, Teddington, Middlesex.

In experiment a thin film parallel plate HTS resonator was observed to produce skewed resonance curves at high microwave power and a pronounced shift of resonance frequency. In order to explore whether the skewed shape and frequency shift observed originated from thermal effects a model was set up to simulate global heating of the films. In the present work simulated results are compared with experiment under different conditions. The simulation produces similar skewed curve shapes at similar input powers to experiment with a calculated global temperature rise of 2.7K. However, in order to produce a resonance frequency shift of a magnitude comparible to experiment the global heating would have to be of the order of 15K. As this rise in temperature is unphysical in the cryogenic environment in which the experiments were performed, namely flowing helium gas (i.e. a continuous flow cryostat was used), this suggests that mechanisms other than global heating are responsible for the experimental observation.

10–82

Forward coupled superconducting filters for DCS1800 mobile phone base stations.

M. Salluzzo[1], *A. Andreone*[1], *M. Iavarone*[1], *F. Palomba*[1], *G. Pica*[1], *R. Vaglio*[1], *G. Panariello*[2], *R. Monaco*[3], *A. Guidarelli Mattioli*[4] and *E. Petrillo*[5]. [1]INFM Unita' di Napoli and Universita' di Napoli "Federico II", Napoli, Italy. [2]Dip. di Ingegneria Elettronica, Universita' di Napoli "Federico II", Napoli, Italy. [3]INFM Unita' di Salerno and Universita' di Salerno, Salerno, Italy. [4]Omnitel Pronto Italia, Ivrea, Italy. [5]Ansaldo C.R.I.S., Napoli, Italy.

HTS bandpass planar filters for use in cellular base stations have been fabricated. Different filters have been designed to operate as superconducting or hybrid superconducting/semiconducting front-end receivers for DCS1800 mobile phone system. A special cryocooler has been developed to house a superconducting filter and a very low noise cryogenic amplifier. A d.c. sputtering system has been used to grow in pure oxygen high pressure all in situ gold coated YBCO double side films on 2" diameter $LaAlO_3$ substrates. The layout of interdigital planar filters having a Tchebicev response has been produced and optimized using an advanced Computer Aided Design software. The microwave response of various L-band Niobium and YBCO filters has been compared with the electromagnetic simulation. The power handling capability of each device has been studied at various temperatures. This is accomplished measuring both the overall frequency response of the filters vs the circulating microwave power, and two tones third order intermodulation products. YBCO planar filters spanning the frequency range 1710 MHz to 1785 MHz and capable to handle several watts of input power with a linear response have been successfully obtained.

10–83

Varactor switchable/tunable HTS-notch filter for the mobile communication system.

B.A.Aminov[1], *H.Chaloupka*[1], *S.Kolesov*[1], *H.Piel*[1], *J.Bohult*[2], *H.Medelius*[2] and *A.Rogachev*[3]. [1]Cryoelectra GmbH, Wettinerstr. 6h, D-42287 Wuppertal, Germany. [2]Ericsson Radio Access AB, Gullfossgatan 6, S-16493 Stockholm, Sweden. [3]Bergische Universitat, Fachbereich Elektrotechnik, D-42097, Wuppertal, Germany.

HTS technology provides a mean to realise switchable and tunable filters for the receiver front-end of mobile communication base stations, which is highly demanded for the evolution towards a reconfigurable system. Such adaptive RF-prefiltering permits a frequency selective control of the amplification within the access bandwidth, which lower demands for high linearity in the low noise-amplifier and mixer as well as demands for a high dynamic range and sampling rate of the analogue/digital converters. We present design and test of the first varactor-controlled HTS band-reject ("notch") filter with midband frequency of 2GHz. The filter bank consists of two filters with the stopband of about 1MHz at 3dB level and 20dB midband attenuation. The narrow filter band and high attenuation levels are provided by a HTS lumped-element resonator with double symmetry having unloaded quality factor $Qo \leq 50000$ at $T \sim 60K$. The controlling element GaAs-based varactor is weakly-coupled to the resonator without strong effecting of the Q-factor ($Qo \geq 20000$) of resonator in the switched state (voltage on varactor $V<0$) and producing high dissipation and the frequency shift ($\Delta f<10MHz$) in the unswitched state ($V=0$). This work was supported in part by German BMBF under the contract 13N7387.

10–84

Superconductor Band-Pass Analog-to-Digital Converter.

V.K. Semenov[1] and *E.B. Wikborg*[2]. [1]Department of Physics, SUNY, Stony Brook, NY 11794, USA. [2]Ericsson Components AB, Kista-Stockholm, SE 164 81, Sweden.

The majority of Analog-to-Digital Converters (ADCs) simultaneously measure AC and DC signal components. The sensitivity of ADCs to a DC signal limits their application for radar and communication systems dealing with narrowband signals. In radio communication systems, an early analog-to-digital conversion, at either the intermediate or radio-frequency stage, will result in a more robust system and provide opportunities for dealing with multiple standards. This report describes our first attempt at analyzing a band-pass ADC, based on rapid single flux quantum (RSFQ) technology. A theoretical analysis and numerical simulation of Delta and Delta-Sigma band-pass ADCs combined with an RSFQ mixer and digital filters is presented.

10–85

Performance of passive microwave devices made from thin films of $YBa_2Cu_3O_{7-\delta}$ superconductor.

E. Moraitakis, *M. Pissas* and *D. Niarchos*. Institute of Materials Science, NCSR "Demokritos", 15310 Ag. Paraskevi,Athens,Greece.

High quality thin films of $YBa_2Cu_3O_{7-\%\delta}$ superconductor were deposited on $LaAlO_3(100)$ substrates with sizes up to 1 in x 1 in, with a simple sputtering technique. Two passive microwave devices were designed and fabricated from these films: a two-pole filter and a disk resonator with centre frequency of 13 GHz. A *YBCO* filter exhibits at 77 K an insertion loss of more than 5 dB lower than an equivalent Au filter at the same temperature. Furthermore the nonlinearity of the resonators is discussed and analyzed in terms of a critical state model.

10–86

Third-order local nonlinear microwave response of $YBa_2Cu_3O_7$ thin films.

R.K.Belov, *V.V.Kurin*, *Yu.N.Nozdrin* and *E.E.Pestov*. Institute for Physics of Microstructures(RAS),Nizhny Novgorod,603600,Russia.

HTS thin film continue to be of interest for passive device application at microwave frequencies ,but nonlinear effects may limit the performance. We report a set of experimental data on local third-harmonic generation at microwave frequencies(ω :0.5 GHz) in $YBa_2Cu_3O_7$ from 77° K to T_c. For the local investigation of the nonlinear response it was elaborated the probe with inductive coupling. The probe consists of 50 μm conductor connecting the inner and outer conductor of the coaxial cable. It is plotted the map of nonlinear microwave response HTS film $YBa_2Cu_3O_7$ below T_c with resolution of about 50 μm in one coordinate. The third-harmonic power is measured as function of temperature,inpute power ,and dc magnetic field at some places of the film. The temperature dependence demonstrates a peak of nonlinearity below T_c.The behavior of the third-harmonic power versus the input power can be described the power-low with exponent n≈1.5-2.5. Also it is shown relation between dc pinning density J_c^p and nonlinear microwave response.

10–87

Study of the tunability of superconducting passive microwave components by laser light.

M. S. Boutboul[1], *S. Sautrot*[1], *A. Dégardin*[2], *H. Kokabi*[1], *A. Kreisler*[2], *M. Pyée*[1] and *M. Fourrier*[1]. [1]LDIM - University Pierre and Marie Curie 4, place Jussieu - 75252 Paris - France. [2]LGEP - Supelec plateau Moulon - 91190 Gif sur Yvette - France.

Passive microwave components made of superconducting microstrip have shown not only their superiority compared to their metal competitors but also their interest for wireless telecommunication. One of the major challenges in the future is the tunabilty of those circuits. We have studied on an original method which would make possible to carry out tunable components. It consists in illuminating a superconducting microstrip resonator to modify its kinetic inductance and thus its resonance frequency. We have observed the evolution of the first harmonic of an YBaCuO microstrip resonator with respect to various parameters: illumination spot width, laser power, wavelength and microwave power. We have used a laser diode (λ= 1.3 μm) and an Argon laser (λ = 514 nm). The illumination is guided by an optical fiber arriving at a few tens of micrometers of the film which is plunged in a liquid nitrogen bath. A displacement of 6 MHz from the center frequency (5.1 GHz) has been found in a reproducible way using the argon laser with a power of 200 mW. In addition, it comes out from this study that the local heating of the superconductor by laser light seems to mask all other phenomenon acting on kinetic inductance.

10–88

Surface Wave High Temperature Superconducting Resonators.

G.A. Melkov[1], *Y.V. Egorov*[1], *A.N. Ivanyuta*[1], *V.Y. Malysh*[1] and *A.M. Klushin*[2,3]. [1]Kiev Taras Shevchenko University, Kiev, 252017, Ukraine. [2]Institut fuer Schicht - und Ionentechnik, Forschungszentrum Juelich GmbH, Juelich, 52425, Germany. [3]Institute of Electronic Measurements "KVARZ", Nizhny Novgorod, 603009, Russia.

Microwave electronics and measuring techniques use microstrip and parallel-plate resonators. They must contain two superconducting films to have a high quality Q. Besides the manufacturing of such resonators for the short-wave part of the millimeter waveband is accompanied by both the difficulties of design and increase of losses in the input microstrip and coaxial circuits. We have elaborated several microwave resonators using a single metal or HTS surface (the existence of other surfaces only decreases Q). All resonators operate on the surface waves, running along the metal. Those can be surface waves running along a solitary metal surface with a finite conductivity (Zennek waves) or surface waves along the metal (even an ideal one) covered with dielectric. Theoretical analysis of the resonant frequencies has been carried out by decomposition method. The resonator, containing two dielectrics and placed in the waveguide has been considered. The dependence of the first mode resonant frequency and quality of such a resonator on its length and temperature was measured. The coincidence of the results in the experiment and theory was demonstrated with the accuracy better than 5%. Possible new applications of surface wave resonators in cryoelectronic will be discussed.

10–89

Microwave power handling capabilities and intermodulation distortion in sputtered YBCO films on sapphire and $LaAlO_3$.

P. Lahl, *J. Einfeld* and *R. Wördenweber*. Institut fuer Schicht- und Ionentechnik (ISI), Forschungszentrum Juelich, 52425 Juelich, Germany.

The use of YBCO films for microwave devices enables the fabrication of high quality devices with small sizes, which automatically results in large hf power densities. Therefore, for hf applications it is essential to examine the power handling capabilities and generation of intermodulation distortions (IMD), which is ascribed to a nonlinear surface resistance in these films. In this work microwave properties (surface resistance R_S, power handling capabilities R_S and IMD versus hf power) of epitaxial YBCO films on CeO_2 buffered sapphire substrates and $LaAlO_3$ substrates were examined using dielectric resonator techniques and coplanar waveguide and resonator experiments in ambient dc magnetic fields. The influence of various defects in the films upon R_S, power handling and IMD was investigated. Low R_S values (1,4mW at 77K and 110μW and 4,2K) and large power handling capabilities ($B_{HF,max}$=17,5mT at 77K and >54 mT at 4.2K) have been obtained for YBCO thin films on both substrates. However, a small nonlinearity was observed in the surface resistance as function of hf-power. Despite this nonlinearity, no enhanced IMD products could be measured. Moreover, the third order intercept of the $2f_1$-f_2 IMD product coincides with the steep increase in R_S.

Session Materials related to electronic applications

10–90

Undestructive Microwave Characterization of Large-Area Single Crystal Dielectric Substrates and Ferroelectric Thin Films.

N.T.Cherpak[1], *Yu.G.Makeev*[1], *A.P.Motornenko*[1], *I.N.Chukanova*[2] and *E.V.Izhyk*[1]. [1] Usikov Institute of Radiophysics and Electronics, National Academy of Sciences, Kharkov, 310085, Ukraine. [2] Institute of Single Crystales , National Academy of Sciences, Kharkov, 310001, Ukraine.

Design of planar HTS-based microwave devices requires an accurate knowledge of dielectric properties of the substrates. In addition integration of both HTS and ferroelectric (FE) films technologies gives perspective for a number of highly functional microwave devices. However the problem of the quality and the loss tangent still remains the main obstacle to exploitation of large-area single crystal dielectric substrates and FE thin films intended for the following fabrication of microwave devices. Two techniques have been worked out and used. One is based on 8mm waveband quasioptic dielectric resonator perturbed by a radial slot. It allows the microwave measurement of the substrate anisotropy axis orientation. Another techniques uses a resonator on base of branching evanescent circled and radial waveguides.The measurements of dielectric permittivity of Al_2O_3, $LaAlO_3$ and $NdGaO_3$ substrates and also FE films $Pb(Zn_0.5Ti_0.5)O_3$ on $LaAlO_3$ substrate have been carried out in 2cm waveband. Averaged absolute meanings of permittivity were measured with accuracy of about 1%, relative ones are evaluated with accuracy of about 0.1%. Under certain conditions the both techniques have a potential for the loss tangent determination.

10–91

Ferroelectric polarisation charging in $YBa_2Cu_3O_{7-\delta}/SrTiO_3/Pb(Zr_{0.54}Ti_{0.46})O_3/Au$ heterostructures.

R. Aidam, *D. Fuchs* and *R. Schneider*. Forschungszentrum Karlsruhe, Institut für Nukleare Festkorperphysik, P.O.B. 3640, D-76021 Karlsruhe, Germany.

Ferroelectric superconductor field effect transistors (FSuFETs) consisting of $YBa_2Cu_3O_{7-x}$ (YBCO) base layers and $Pb(Zr_{0.54}Ti_{0.46})O_3$ (PZT) gate insulators were fabricated. The PZT films were epitaxially grown on top of (001) oriented YBCO layers with high remanent polarizations of up to 61 $\mu C/cm^2$. In order to prevent contamination of the YBCO layers we inserted 10 nm thick (100) oriented $SrTiO_3$ buffer layers between YBCO and PZT. Ferroelectric polarization charging effects were observed in YBCO films thinner than 20 nm. The modulations of the resistivity, the critical temperature and the critical current clearly reflected the ferroelectric hysteresis of the PZT layer. The changes amounted to 10 %, 1 K and 16 %, respectively. By reversing the polarization state we measured a nonvolatile change of the YBCO properties. The modulations and their polarity dependencies were consistent with a charging effect and the p type conduction in YBCO.

10–92

Mosaic structure of epitaxial films (001) $YBa_2Cu_3O_{7-\delta}$ (10.2)Al_2O_3 and microwave properties of microstrip resonators.

O.D. Poustylnik. SRC "Phonon" Kiev KPI-3240 Ukraine.

The monophase films $YBa_2Cu_3O_{7-\delta}$ (δ=0.15) with c-orientation on substrates Al_2O_3 obtained by a method of a laser deposition, as well as microwave regector microstrip resonators on their basis, were investigated. The increase of mosaic blocks disorientation leads to the increase of their surface resistance (at the frequency of 135 GHz) and to the increase of value R_s^p for the linear microstrip resonators at the frequency 34 GHz.It is estabiliched that the surface resistens of films R_s and surface resistence of films in microwave resonators R_s^p is a lineare function of mosaic structure degree M. Mosaic structure degree M was determind as the relation of radial disorientation of $YBa_2Cu_3O_{7-\delta}$ films to radial disorientation of Al_2O_3 substate. With increase of thickness of epitaxial $YBa_2Cu_3O_{7-\delta}$ films, grown by the pulse laser deposition method on sapphire substrates, the increase of disorientation of the mosaic structure, caused by appearance of heterogeneous structures, was observed. It significantly increases the films surface resistance, and makes worse the performancies of integrated microwave devices on their basis. Thus, optimum thickness of $YBa_2Cu_3O_{7-\delta}$ films, suitable for microwave applications, have to lie within 350-400 nm.

10–93

Plasma Optical Emission Studies during HTSC Thin Film Deposition Process Optimisation.

V.N. Tsaneva[1,3], *C. Christou*[1], *J.H. Durrell*[1,2], *G. Gibson*[1,2], *F. Kahlmann*[2], *E.J. Tarte*[2], *Z.H. Barber*[1,2], *M.G. Blamire*[1,2] and *J.E. Evetts*[1,2]. [1]Cambridge University, Dept. of Materials Sci., Cambridge CB2 3QZ, UK. [2]IRC in Superconductivity, Cambridge University, Cambridge CB3 0HE, UK. [3]Institute of Electronics, Bulg. Acad. Sci., Sofia 1784, Bulgaria.

The HTSC thin film deposition process has been empirically modelled by Response Surface Methodology (RSM) in a system for high-pressure on-axis sputtering equipped with a radiative-type heater. The input parameters were pressure of the sputtering gas mixture and heater temperature, while specific application-aimed responses were optimised, such as film electrical parameters (measured by contact and contactless methods), film structure, orientation and morphology (characterised by AFM and X-ray diffraction). The glow discharge luminosity was monitored during the optimisation. The plasma optical emission spectra were correlated with the properties of the films, deposited under various conditions, allowing the plasma parameters for optimal and non-optimal deposition conditions to be evaluated.

This research was supported in part by the UK EPSRC and Bulgarian NFNI

10–94

New Prospects for Using Layered Superconductors in Electronics.

A.Lykov. P.N.Lebedev Physical Institute of RAS, 117924, Moscow, Russia.

In this work, an idea of creation of the electromagnetic pulses generator was developed using layered superconductors. In a magnetic field slightly tilted to the layers, a system of kinks on vortex lines can arise in such superconductors. The rotation of the sample leads to the existence of the kink structure even in parallel magnetic field if the intrinsic pinning centers in the superconducting layers are strong enough. Avalanche transition of the vortex lattice into ground state without the kink structure leads to the generation of the electromagnetic pulse. This idea can also be used for the amplification and detection of electromagnetic pulses. The operational principle of these devices is based on the avalanche disappearance of kinks, which can be initiated by a weak electromagnetic pulse. For detection a transport current through the specimen must be used. The bias current defines set points on the current-voltage curves of the specimen with the flux vortex lattice in the excited state. The transition of the vortices into an equilibrium state stimulated by a start pulse leads to an increase in the critical current of the sample and a decrease in the voltage across the sample, which can be detected. In this work the possibility of realization of this idea is analyzed, and an equation for time dependence of trapped magnetic field in layered superconductors is obtained which gives the conditions for the avalanche disappearance of the kinks.

10–95

Dynamic electrical response of YBaCuO thin films as a function of substrate crystallinity for electronic applications.

A. De Luca, *A. Dégardin*, *É. Caristan*, *G. Klimek*, *A. Gaugue*, *J. Baixeras* and *A. Kreisler*. LGEP - UMR 8507 CNRS - Universités Paris 6 & Paris 11 - Supélec, Plateau du Moulon, Gif-sur-Yvette, 91190, France.

Obtention of high critical current densities on superconducting films is necessary for development of such applications as power and / or agile microwave devices. For this purpose we have studied the behaviour of superconducting YBaCuO thin film properties as a function of temperature and applied static magnetic field. The films were sputtered on MgO and $SrTiO_3$ single crystals as well as polycrystalline YSZ substrates. In order to avoid heating effects during four probe transport measurements, I-V characteristics have been obtained using a pulsed current technique. The voltage appearing between the voltage contacts was measured by a programmable digital oscilloscope after being amplified by a variable gain low noise voltage amplifier. Inductive effects observed on the voltage response could be attributed to superconducting material, thus allowing to determine the maximum energy stored inside the film. Moreover, a theoretical model to describe the resistive transition, based on a statistical treatment of the motion of vortices in an arbitrary pinning potential, has been used to determine the parameters governing the critical current density. Finally, experimental results both on unpatterned YBaCuO films and on microbridges etched on these films will be discussed in relation with film microstructure, substrate crystallinity and smoothness.

10–96

Protective layers for the encapsulation of YBCO - thin film devices.

W. Prusseit. THEVA Thin Film Technology GmbH, 85386 Eching, Germany.

Long term stability of electronic devices based on YBCO - thin films becomes a major issue for field and outer space applications. Humidity, aggressive ambient, and thermal cycling usually degrade the superconducting properties of YBCO - films and hence the long term device performance. Possible preventive measures are either protective layers on top of the YBCO - films or hermetically sealed encapsulations. The latter, however, is expensive and often complicated to realise since e.g. microwave filters require access for mechanical tuning. Obviously, appropriate protective layers applied after fabrication and bonding of thin film devices would be highly favourable. However, the demands on such layers are numerous and very tough. Residual moisture diffusion, thermal expansion and material compatibility rule out most of the standard compounds developed for the protection of semiconductor devices. We have studied a variety of candidates for such protective layers, amongst them inorganic, organic and silicon-based compounds. Their feasibility for cryogenic microwave applications, compatibility with HTS material, step coverage, and long term stability will be discussed in detail.

10–97

Fabrication of Low Microwave Surface Resistance $YBa_2Cu_3O_y$ Films on MgO Substrate by Self-template Method.

M. Kusunoki, *Y. Takano*, *M. Mukaida* and *S. Ohshima*. Yamagata University, Yonezawa, Yamagata, 992-8510, Japan.

In-plane aligned c-axis $YBa_2Cu_3O_y$ (YBCO) which has low microwave surface resistance (R_s) was fabricated on MgO substrate by self-template method. Pulsed laser deposition was used to prepare the YBCO films. The ratios of 0° and 45° orientations I(0°)/I(45°) had been measured by XRD ϕ-scans. The amount of 45° grain boundaries strongly depended on the substrate temperature. From these results, four kinds of YBCO templates with different I(0°)/I(45°) ratios were prepared. Thickness of the template layer was 60 nm. The upper main YBCO layers were deposited using the same condition where critical temperatures of more than 88 K were obtained. The R_s's at 22 GHz were measured by the sapphire dielectric resonator method in a cryocooler. The R_s's systematically changed corresponding to the amount of 45° grain boundaries. Perfect 0° in-plane aligned YBCO film showed R_s of 0.60 mΩ at 20 K and 3.26 mΩ at 77 K. The R_s's scaled to 10 GHz were 0.12 mΩ at 20 K and 0.67 mΩ at 77 K, respectively. The R_s value of this film is comparable to that of in-plane aligned YBCO on a $BaSnO_3$ buffer layer.

10–98

Atomic force microscopy with conducting tips: an original and efficient way to probe superconducting film surface.

O. Schneegans, *A. Dégardin*, *É. Caristan*, *P. Chrétien*, *F. Houzé*, *A. De Luca*, *L. Boyer* and *A. Kreisler*. LGEP - UMR 8507 CNRS - Universités Paris 6 & Paris 11 - Supélec, Plateau du Moulon, Gif-sur-Yvette, 91190, France.

High quality superconducting thin films are of significant interest for such applications as microwave devices or radiation detectors. To test this quality, YBaCuO thin film surfaces have been studied with an original laboratory-made device associated with a commercial atomic force microscope. Using a doped silicon probe coated with doped diamond, topographical and local electrical contact resistance surface images can be obtained simultaneously within a given area of the sample. YBaCuO films of various thicknesses (in the 50 to 200 nm range) sputtered on MgO and $SrTiO_3$ single crystals have been observed and results are discussed in relation with superconducting film properties. The electrical connection areas between grains are visible on the electrical images, that can be correlated to the good electrical transport properties of the thickest films. Moreover, island-shaped grains exhibiting terraces of one unit cell height can be observed, on close inspection of films grown on MgO substrates. For YBaCuO elaborated on $SrTiO_3$ substrates, the observed grain structure clearly exhibits a spiral shape. Finally, electrical images will be discussed in relation with other near-field techniques like transmission electron microscopy or scanning microwave microscopy, in order to improve the understanding of YBaCuO growth processes.

10–99

Columnar defects as a tool to investigate vortex confinement mechanisms in YBCO films.

G.Ghigo[1], *C.Camerlingo*[2], *G.Cuttone*[3], *R.Gerbaldo*[1], *L.Gozzelino*[1], *E.Mezzetti*[1], *B.Minetti*[1] and *A.Rovelli*[3]. [1]I.N.F.M. UdR Torino Politecnico; I.N.F.N. Sez. di Torino; Dipartimento di Fisica, Politecnico di Torino, Torino, Italy. [2]Istituto di Cibernetica del C.N.R., Arco Felice (NA), Italy. [3]I.N.F.N. Laboratorio Nazionale del Sud, Catania, Italy.

In the paper we show that the irradiation of films with a controlled dose of columnar defects is a powerful tool to understand the vortex confinement properties. Two sets of YBCO films were prepared by magnetron sputtering, the first one composed by oxygen deficient films, the second one by fully oxigenated films. The two sets were irradiated by 0.25 GeV Au ions, at two different dose equivalent fields (0.3 T and 1.5 T). The critical current densities vs. applied field were measured at several temperatures. The position of the irreversibility line (IL) and its possible shift due to the irradiation was analyzed. The main experimental achievements are: 1) the underdoped films exhibit critical temperatures lowered by the irradiation, while in optimally doped films T_c results unchanged, thus excluding the presences of weak links; 2) near the IL the film behaves mostly as a "continuum bulk medium" and the columnar defects enhance the IL through a Bose-glass like mechanism; 3) in the high current regime, the effects of intergrain defects appear; the defects do not enhance the critical current densities, but widen the log(J_c)-log(B) plateau by shifting the maximum field of the plateau (accomodation field) towards the dose equivalent field; 4) above the accommodation field the critical current density decreases, but after irradiation a number of fluxons equal to half the applied field is accommodated without further dissipation. We successfully fitted our J_c (B) data with a model based on an hidden network of high-current carrying channels along grain boundary interfaces modulated by defects. The network is composed by a parallel array of short Josephson junctions with statistically distributed lengths and field-dependent magnetic thickness.

Session SQUIDs, and SQUIDs applications

10–100

Optimization of Inductance for the Directly-coupled SQUID Gradiometer.

J.T. Jeng[1], *Y.C. Liu*[1], *S. Y. Yang*[1], *H.E. Horng*[1], *J.H. Chen*[2] and *H.C. Yang*[2]. [1]Department of Physics, National Taiwan Normal University, Taipei 117, Taiwan. [2]Department of Physics, National Taiwan University, Taipei 106, Taiwan.

To minimize the field noise $S_B^{1/2}$, the directly-coupled gradiometers with the various self-inductance L_s of the SQUIDs were investigated. The inductance Ls measured by directly current injection method were quite comparable to those calculated from the voltage amplitude in the V- ϕ modulation at the corresponding temperature. In the meanwhile, the effective area A_{eff} of the gradiometer was also determined by the V- ϕ modulation period. It was found that the effective area of the gradiometer was in proportional to L_s of the SQUID. However, the flux noise density $S_\phi^{1/2}$ increased

more rapidly as L_s of the SQUID became larger. In addition, we have also observed a strong enhancement of the flux noise density $S_\phi{}^{1/2}$ by temperature. Since the field noise $S_B{}^{1/2}$ or the field gradient resolution with a fixed baseline is the ratio of the flux noise density $S_\phi{}^{1/2}$ and the effective area A_{eff}, therefore the optimal L_s at the corresponding temperatures will be investigated in this report.

10–101
Detection of Internal Defects using HTS-SQUID for Non-destructive Evaluation.
Y.H Hatsukade[1,2], *N.K. Kasai*[2], *F.K. Kojima*[3], *H.T. Takashima*[2] and *A.I. Ishiyama*[1]. [1]Waseda Univ.,3-4-1 Ohkubo,Shinjuku-ku,Tokyo,169-8555,Japan. [2]Electrotechnical Laboratory,1-1-4 Umezono,Tsukuba-shi,Ibaraki,305-8568,Japan. [3]Kobe Univ.,1-1 Rokkodai-cho,Nada-ku,Kobe,657-8501,Japan.

SQUID has an extremely high magnetic sensitivity and its sensitivity is independent in frequency. Due to the potential of SQUID, several studies about detection of deep lying flaws in metals using SQUID have been reported. We have studies the method to know the shape of the flaws, especially the method to know the shape of internal flaws by changing the frequency of the current injected into specimen. We have fabricated a HTS-SQUID gradiometer and developed a SQUID-NDE system with the HTS-SQUID gradiometer in a magnetically shielded room. We prepared a Copper sample plate, which has a stair-stepped through hole. We measured the magnetic field induced by the flowing current through the sample plate by changing the frequency of the injected current using our SQUID-NDE system. The distribution of the induced magnetic field changed depending on the frequency. We tried to estimate the shape of the flaw using the measurement data by a computational method based on the finite element method.

10–102
Development of an HTS Cryogenic Current Comparator.
M. D. Early[1] and *M. A. van Dam*[1,2]. [1] Meaurement Standards Laboratory, Industrial Research Limited, P O Box 31-310, Lower Hutt,6009, New Zealand. [2]Present Address: School of Engineering, University of Canturbury, Private Bag 4800, Christchurch, New Zealand.

Low temperature cryogenic current comparators (CCC's) can be used to establish current ratios to better than 10^{-10}. This performance is achieved by harnessing the flux sensitivity of a SQUID and the magnetic shielding properties of a superconductor. The practical difficulties of helium systems have restricted the use of low temperature CCC's, but an HTS CCC could be expected to be extremely advantageous in a wide range of applications. However the complex three-dimensional geometry and the difficult mechanical properties of HTS materials have so far thwarted the construction of a similarly accurate HTS version of the device. A general problem with proposed HTS CCC designs is that the windings are not completely encircled by the shielding. We have designed a toroidal geometry to minimize this effect. By calculating the current distribution on the shielding we have numerically evaluated this additional source of error and expect that an accuracy significantly better than 10^{-7} should be achievable. We are currently working on a low temperature prototype to test our model and will be reporting on the performance of this device. We also hope to present progress on the development of an HTS version of the prototype at the conference.

10–103
Development of HTS Resistive SQUIDs for Noise Thermometry.
D.A. Peden[1], *J.C. Macfarlane*[1], *L. Hao*[2], *R.P. Reed*[2] and *J.C. Gallop*[2]. [1]Department of Physics and Applied Physics, University of Strathclyde, Glasgow G4 0NG, UK. [2]Centre for Basic and Thermal Metrology, National Physical Laboratory, Teddington, TW11 0LW, UK.

The use of a High-T_c resistive SQUID (R-SQUID) for Noise Thermometry is currently under investigation. This technique has the potential to provide realisation of the absolute temperature scale in the range 4 K — 50 K. An R-SQUID consists of a noble metal resistor connected as a shunt across a YBCO grain boundary junction, where the shunt resistance R_S is significantly smaller than the junction normal state resistance R_n. Resistors based on a YBCO/Au bilayer intersected by a meandering gap have been fabricated. A second ex-situ Au layer forms the resistive path, and $R_S \leq 1$ mΩ has been measured at 77 K. Resistors have been used in both single junction and double junction devices. Single junction R-SQUIDs have been interrogated using an inductively coupled HTS dc SQUID. Double junction R-SQUIDs with a directly coupled readout are also under investigation. Experimental results in the temperature range of 30 K to 77 K are presented for both types of devices, together with one dimensional current flow simulations. Simulations have indicated the significance of the loop inductance as it affects the circulating current at the Josephson frequency.

10–104
Application of SQUID based position detectors for testing the Weak Equivalence Principle at the Drop Tower Bremen.
W. Vodel, *S. Nietzsche*, *H. Koch*, *J.v. Zameck Glyscinski* and *R. Neubert*. Friedrich Schiller University Jena, Institute of Solid State Physics, Helmholtzweg 5, 07743 Jena, Germany.

Due to their high sensitivity and universality SQUIDs can be applied even in position detectors providing an extreme high position resolution at the order of $10^{-14}\frac{m}{\sqrt{Hz}}$. Using this sensor technique gravitational experiments can be performed such as the test of the Weak Equivalence Principle on earth using drop tower facilities or at the orbit like the Satellite Test of the Equivalence Principle (STEP) of NASA/ESA. This contribution describes an experimental set-up which is presently tested at the Drop Tower Bremen, Germany, providing a free-fall height of 109 m which corresponds to a measurement time of 4.7 sec. In principle, this apparatus consists of two free falling test bodies, a 2-channel LTS DC SQUID based position detector, magnetic bearing, a caging mechanism, and a liquid helium cooling. All systems are qualified for operation at the drop tower and have to resist, especially, against the high-deceleration phase of 50 g at the end of each drop. Finally some recent results are

discussed.

10–105
High Temperature SQUID Magnetometers for Nondestructive Evaluation.
J.T. Jeng[1], *J.H. Chen*[2], *H.C. Yang*[1] and *H.E. Horng*[2].
[1]National Taiwan Normal University Department of Physics 88 Section 4, Ting-Chou Road Taipei,117-18 Taiwan. [2]National Taiwan University Department of Physics One Section 4, Roosevelt Road Taipei,106-17 Taiwan.

We have designed a SQUID system using high-T_c magnetometers for nondestructive evaluation in unshielded environments. In this system, the cryostat was made of nonmagnetic fiberglass in order to minimize the noise induced by metallic materials near the SQUID. Furthermore , the cold-to-hot distance at the bottom of the liquid nitrogen dewar was reduced to less than 5 mm to improve the spatial resolution of the system. When the system was operated in unshielded environment, the obtained SQUID signal was subtracted by the environment disturbances detected by a reference magnetometer. In this way, the field resolution of the system was optimized. The system was applied to inspect some artificial flaws. The current distribution in these flaws was simulated by superposition current dipoles. It was found that the spatial resolution of the system was approximately the same as the distance from the sensor to the flaw, and is consistent with that estimated from the proposed model.

10–106
Effect of asymmetric junction configurations on the voltage to magnetic flux transfer function in resistively shunted dc SQUIDs.
G. Testa[1,2], *E. Sarnelli*[1], *S. Pagano*[1] and *M. Russo*[1].
[1]Istituto di Cibernetica - CNR, Arco Felice, I-80072, Italy. [2]Istituto Nazionale di Fisica della Materia, Unita di Napoli, Italy.

The effect of asymmetric configuration of the Josephson junctions on the voltage-to-magnetic flux transfer function $h = \partial V/\partial \Phi$ in resistively shunted dc SQUIDs has been analyzed. Simulations have been carried out for SQUIDs with damping resistance and different values of the screening parameter $\beta = LI_c/\Phi_0$, where L and I_c are the inductance and the critical current of the device, and Φ_0 is the magnetic flux quantum respectively. An increase of the h parameter with respect to the case of symmetric shunted dc SQUIDs is achieved for any values of β and is larger in the case of large β. This is related to the appearance of structures on the current-voltage characteristics. Such new configurations may become advantageous for the fabrication of single layer high-T_c superconducting (HTS) magnetometers. In fact, with larger values of L, better matching between pick-up coil and SQUID inductance may be achieved; as a result the responsitivity of HTS magnetometers increases. On the other hand, considering thermal noise contributions, $\beta = 1$ represents the optimum value for operating both symmetric shunted SQUIDs and asymmetric unshunted SQUIDs. The noise characteristics of asymmetric shunted SQUIDs is actually under investigation.

10–107
Radiofrequency dc SQUID Amplifier with Microstrip Inpit Coil: Simulations and Experiment.
M.A. Tarasov[1], *A.S. Kalabukhov*[2], *S.I. Krasnosvobodtsev*[3], *O.V. Snigirev*[2], *Z.G. Ivanov*[4] and *A. Kovalenko*[1].
[1]Insitute of Radioelectronics and Engeneering, Moscow,103907 Russia. [2]Moscow State University, Moscow, 119899, Russia. [3]Lebedev Institute of Physics, Russian Academy of Sciencies, Moscow,117924, Russia. [4]Department of Physics, Chalmers University of Technology and University of Geteborg, Geteborg, Sweden.

We designed layouts and fabricated samples both of the YBCO and Nb dc SQUID radio-frequency amplifiers to attain effective matching of microwave signal to the SQUID loop. The input signal was applied to the microstrip line fabricated above the SQUID washer. A model taking into account coupling of a slit below the microstrip to the SQUID loop indiuctance was developed. High-Tc dc SQUID amplifiers were made on 32° YSZ bicrystal substrates. The SQUIDs revealed high values of IcRn product in the range 100-150 μV. The integrated input spiral microstrip line was made from gold on 100 nm thick ZrO_2 isolation layer. The isolation layer was deposited by pused laser ablation. No degradation of the high-Tc dc SQUID parameters was observed after deposition process. Both experimental data and simulations results will be presented in the conference report.

10–108
Noise Characteristics of a Two Stage dc SQUID-based Amplifier.
D.E. Kirichenko[1], *A.B. Pavolotskij*[2], *I.G. Prokhorova*[1], *O.V. Snigirev*[1], *R. Mezzena*[3], *S. Vitale*[3], *Y.V. Maslennikov*[4] and *V.Y. Slobodtchikov*[4]. [1]Department of Physics, Moscow State University, 119899 Moscow, Russia. [2]Nuclear Physics Institute, Moscow State University, 119899 Moscow, Russia. [3]Department of Physics, University of Trento, 38050 Trento, Italy. [4]Cryoton Co. Ltd., 142092 Troitsk, Moscow Region, Russia.

An integrated version of a two stage dc SQUID-based amplifier with double transformer coupling scheme has been designed and tested at temperature 4.2 K earlier. The noise characteristics of this amplifier measured in the temperature range 1.2-4.2 K are presented in this report. The effective input inductance of the amplifier was close to 2.9 μH, the loop inductance of the first stage SQUID was of about 11 pH, and an effective coupling k^2 was close to 0.24. The white noise level of the amplifier was found close to 0.3 $\mu\Phi_0/Hz^{0.5}$ at 4.2 K for the undamped version of the first stage SQUID, and 0.6 $\mu\Phi_0/Hz^{0.5}$ at 4.2 K for the first stage SQUID with an additional distributed damping system. The energy resolution of both versions of the amplifier linearly scales down with temperature with zero residual value at 0 K.

10–109

A scanning SQUID microscopy of the HTS thin-film specimens at 77 K.

S.A. Gudoshnikov[1], *M.I. Koshelev*[2], *A.S. Kalabukhov*[2], *O.V. Snigirev*[2], *L.V. Matveets*[1], *M. Muck*[3], *J. Dechert*[3] and *C. Heiden*[3]. [1]Institute of Terrestrial Magnetism, Ionosphere and Radio Wave Propagation, Russian Academy of Sciences, (IZMIRAN), Troitsk, Moscow region 142092, Russia. [2]Moscow State University, Moscow, 119899, Russia. [3]Institut fur Angewandte Physik Justus Liebig Universitat Giessen, 35392 Giessen, Germany.

A scanning HTS dc SQUID microscope with a spatial resolution of about 30 μm and a magnetic field sensitivity close to 100 $pT/Hz^{1/2}$ was used to image a magnetic flux distribution $B_z(x,y)$ in the YBCO specimens at 77 K in a perpendicular geometry in a low magnetising field ranging from 0.1 to 70 A/m. The magnetic field images of thin-film SQUIDs and different square-shaped samples were measured for the cases of applying an external field to zero field-cooled (ZFC) and field-cooled (FC) superconducting samples. Images corresponded to individual vortices and vortex clusters trapped in a superconducting film have been obtained for ZFC samples. Magnetic flux penetration in HTS samples was observed for FC samples.

10–110

Low-field NMR and MRI of room temperature samples detected with a high-T_c SQUID.

K. Schlenga[1], *R.E. de Souza*[2], *A. Wong-Foy*[2], *R. McDermott*[1], *A. Pines*[2] and *J. Clarke*[1]. [1]Department of Physics, UC Berkeley and LBNL, Berkeley, CA 94720 USA. [2]Department of Chemistry, UC Berkeley and LBNL, Berkeley, CA 94720 USA.

We have constructed a high-T_c SQUID spectrometer to detect pulsed nuclear magnetic resonance (NMR) signals from samples at room temperature in magnetic fields up to 3 mT. The multiloop SQUID magnetometer is operated in vacuum at 77 K, and is separated from the sample, which is less than 1 mm away, by a sapphire window. We present NMR spectra of protons and fluorine nuclei in thermal equilibrium, as well as spectra of hyperpolarized, isotopically-enriched ^{129}Xe. In a magnetic field comparable to that of the Earth, we can resolve the proton spin echo produced by 1 ml of mineral oil at 2.5 kHz after 2000 averages. When the field is increased to 2 mT we can detect the proton spin echo at 86 kHz in a single shot. In addition to the spectroscopic data we present images obtained from proton signals in mineral oil filled phantoms. With 0.4 ml of mineral oil in a field of 2 mT we are able to obtain two-dimensional magnetic resonance images (MRI) with a spatial resolution of about 0.6 mm. In our experiments with hyperpolarized xenon at 15 kHz we obtain a signal-to-noise ratio of 100 in a single shot.

10–111

A 40-channel double relaxation oscillation SQUID system for biomagnetic multichannel applications.

Y. H. Lee, H. C. Kwon, J. M. Kim, Y. K. Park and *J.-C. Park.* Korea Research Institute of Standards and Science, P.O. Box 102, Yusong, Taejon, 305-600, Republic of Korea

We developed a 40-channel planar gradiometer system based on double relaxation oscillation SQUIDs (DROSs). For a multichannel system, we simplified the DROS design by using a single reference junction instead of the reference SQUID. The SQUIDs were fabricated from hysteretic Nb/Al-oxide/Nb junctions using a simple 4-level process. Due to the large flux-to-voltage transfers of DROSs, the flux-locked loop electronics could be made simple. The pickup coil is an integrated planar gradiometer type with a baseline of 4 cm. The SQUID insert was designed to have low thermal load, and the SQUID gradiometers were distributed in a rectangular array to measure tangential components of biomagnetic fields. The typical field gradient noise of the SQUIDs is 1.2 $fT/cmHz^{0.5}$ at 100 Hz, measured inside a magnetically shielded room. The 40-channel DROS planar gradiometer system was operated successfully to measure neuromagnetic fields.

ORAL SESSION 11A: Coated Conductors II

Wednesday Afternoon, September 15th, 17:30-19:00

17:30 *11A–1

Prospects of YBCO coated conductors for applications

H.C. Freyhardt[1,2], *F. García-Moreno*[2,1], *J. Hoffmann*[1], *J. Dzick*[1], *S. Sievers*[1], *A. Usoskin*[2] and *C. Jooss*[1]. [1]Institut fuer Materialphysik,Universitaet Goettingen,D-37073 Goettingen. [2]Zentrum fuer Funktionswerkstoffe gGmbH,D-37073 Goettingen.

With physical vapour deposition methods, like pulsed laser deposition, thermal coevaporation and sputtering, efficient processing techniques have been developed fo the YBCO coating of tapes, sheets and tubes. Essebtial for applications in the selection of suitable substrates, ceramic (in particular YSZ) or metallic (Ni, Ni-based alloys,recently also strainless steel), polycrystalline or well textured, which determines the methods to be used for the deposition if the intermediate functional buffer layers (heteroepitaxial growth, IBAD,ISD). In this contribution recent progress in preparation of larger-area, high-current-density (> 1MA/cm^2, 0T, 77K) coated conductors will be critically evaluated with respect to specific applications.

18:00 11A–2

Microstructure in $YBa_2Cu_3O_{7-\delta}$ Coated Conductors and Their Buffer Layers.

S.E. Babcock[1], *Chau-Yun Yang*[1], *Yuehong Wu*[1], *D.M. Feldman*[1], *A. Polyanskii*[1], *A. Ichinose*[1], *D.C. Larbalestier*[1], *A. Goyal*[2] and *S.R. Foltyn*[3]. [1]University of Wisconsin, Madison Wisconsin, USA. [2]Oak Ridge National Laboratory, Oak Ridge Tennessee, USA. [3]Los Alamos National Laboratory, Los Alamos New Mexico, USA.

This presentation will describe results of our on-going studies of the microstructure features of the buffer and $YBa_2Cu_3O_{7-\delta}$ layers of a variety of $YBa_2Cu_3O_{7-\delta}$ coated conductors and their relationships to the electromagnetic granularity as signaled by magneto optic imaging and the J_c value of the films. X-ray diffraction, scanning electron microscopy imaging and microanalysis, and transmission electron microscopy are used in coordination to study the subgrain size and crystallography, the dislocation density and arrangement, the local and long range degree of crystallographic alignment of the oxide layers. This characterization is done in conjunction with magneto-optic imaging studies of the same films with the goal of discovering relationships among the electromagnetic performance and the microstructure. Studies of films produced by the RABiTS technique (materials provided by Goyal, Paranthaman, Norton, Beach, Kroger, Feenstra and List of Oak Ridge National Laboratory) and by the IBAD (materials provided by Arendt and Foltyn of Los Alamos National Laboratory) reveal a hierarchy of defects that contribute to the J_c performance of the film, ranging from micron + -scale defects like porosity, cracking and second phase to fine scale grain-to-grain misalignments. Rather homogeneous $YBa_2Cu_3O_{7-\delta}$ films are observed on inhomogenous buffer layers and vice versa. This presentation will compare and summarize our most recent microstructural characterizations and understanding of their implications. This work is supported NSF-MRSEC on Nanostructured Materials at the University of Wisconsin & the US Department of Energy through Oak Ridge National Laboratory.

18:15 11A–3

Multi-functional flexible high temperature superconducting tape (MUST).

J. Denul[1], *I. Van Driessche*[2], *H.T. Lintelo*[3], *R. De Gryse*[1], *A. Testsekou*[4], *E. Georgiopoulos*[4], *S. Hoste*[2], *B.A. Glowacki*[5], *R. Garre*[6] and *E. Maher*[7]. [1]Centre for Vacuum and Materials Sciences, Gent, B-9000, Belgium. [2]University of Gent, Gent, B-9000, Belgium. [3]Innovative Sputtering Technology, Zulte, B-9870, Belgium. [4]Cereco, Chalkida, 34100, Greece. [5]University of Cambridge, Cambridge, CB2 3QZ, United Kingdom. [6]Europa Metalli, Fornace di Barga, 55052, Italy. [7]Oxford Instruments, Eynsham, Witney, OX8 1TL, United Kingdom. [8]Cryogenic, London, W3 7QE, United Kingdom. [9]KTH, Stockholm, S-10044, Sweden. [10]GAIKER, Zamudio, 48170, Spain.

Ten partners (comprising six industrial partners) from six European countries are cooperating in the Brite-EuRam project MUST. This consortium has a clear industrial objective : the development of a cost effective multi-functional flexible HTS tape exhibiting a high critical current, using high power sputter deposition of 0.5 - 1 micron thick YBCO films on metallic and polymer substrates. The commercial possibilities of this end product will be demonstrated by using the flexible superconducting tape for the fabrication of simple components which will allow assessment of coated conductor in HTS high field insert coils for LTS magnets, new NMR and MRI applications and fault current limiters. By combining the unique talents of the partners involved, the following innovations crucial to the new technology will be established : textured metal foils, large scale magnetron sputter deposition of YBCO on metal substrates at high temperatures, small scale sputter deposition of YBCO on polymer substrates at low temperatures, development of industrial sized cylindrical YBCO targets and low cost target reconstruction, and demonstration of components for high performance magnet applications and fault current limiters. This research was supported by the Brite-EuRam project MUST (Multi-functional flexible high temperature superconducting tape) (contract BRPR-CT97-0331).

18:30 11A–4

Laser deposition of biaxially aligned MgO buffer layers.

R. Huehne[1], *B. Holzapfel*[2], *C.-G. Oertel*[1], *L. Schultz*[2] and *W. Skrotzki*[1]. [1]Institut fuer Kristallographie und Festkoerperphysik, Technische Universitaet Dresden, 01062 Dresden, Germany. [2]Institut fuer Metallische Werkstoffe, Institut fuer Festkoerper- und Werkstofforschung, PF 270016, 01171 Dresden, Germany.

The growth of biaxially oriented buffer layers by Ion Beam Assisted Deposition (IBAD) on polycrystalline metal substrates is one promising route to achieve biaxially textured YBCO films for the preparation of long tapes with high critical currents in magnetic fields. Therefore MgO thin films were prepared by ion-beam assisted pulsed laser deposition

on non-textured substrates, using a low divergence rf plasma source as an assisting source. The texture has been investigated using X-ray pole figures. Without using the ion beam the films show strong fibre textures. The orientation changes from (220) at room temperature over (200) to (111) at 650°C. Using an ion beam, biaxially textured films have been grown with in-plane orientations of about 20° FWHM. We report on the influence of deposition parameters such as substrate temperature, film thickness and ion beam energy on the quality of the in-plane texture. Furthermore MgO thin films with a FWHM of about 30° were fabricated with pulsed laser deposition on inclined substrates. The microstructure has been investigated by SEM and AFM.

18:45 11A–5

Fabrication and Characterization of Textured YBCO Superconductor Thick Films on Oxide/Cu Sheets.

M. Jin[1], *E. Kim*[1], *T.H. Sung*[2], *S.C. Han*[2] and *K. No*[1]. [1] Electronic and Optical Materials Laboratory, Dep. of Mat. Sci.& Eng., Korea Advanced Institute of Science and Technology 373-1, KuSung-dong, YuSung-gu, TaeJon, Korea 305-701,. [2]Materials and Corrosion Research Laboratory, Korea Electric Power Research Institute 103-16 Munji-dong, Yusong-gu, Taejon, Korea 305-380.

A new fabrication technique of textured YBCO superconductor thick films on Oxide/Cu sheets was invented for high power applications. Pure Cu sheets of the thickness of 50§ were fabricated using hot and cold rolling. The Cu sheets were heat treated to induce the biaxial texturing. Various oxide thin films: MgO and/or ZrO2, were coated on the textured Cu sheets to prevent possible reaction between Cu sheets and YBCO superconductors, to reduce possible cracking due to thermal expansion mismatch and to hold the lattice mismatch for biaxial texturing. Textured superconductor thick films were fabricated on the textured Oxide/Cu sheets using screen printing and melt texturing to fabricate textured YBCO/Oxide/Cu sheets for high power applications. The texturing and the superconducting properties of YBCO/Oxide/Cu sheets were studied.

ORAL SESSION 11B: Cables, Transformers ans Generators

Wednesday Afternoon, September 15th, 17:30-19:00

17:30 *11B–1

Development and test of a 100 kVA superconducting transformer operated at 77 K.

P. Kummeth[1], *R. Schlosser*[2], *P. Massek*[1], *H. Schmidt*[2], *C. Albrecht*[1], *D. Breitfelder*[2] and *H.-W. Neumüller*[1]. [1]Siemens AG, Corporate Technology, Erlangen, D-91052, Germany. [2]Siemens AG, Power Transmission and Distribution, Nuremberg, D-90027, Germany.

High temperature superconducting transformers are very promising candidates for application in electrical power engineering. Their main advantages are reduced size, weight and better efficiency compared to existing conventional transformers. This is due to the high critical current densities and low losses of Bi2223 tape conductors. Additionally the use of HTS transformers reduces potential fire and environmental hazards since the nonflammable liquid nitrogen is used as coolant. We have designed, constructed and tested a 100 kVA high temperature superconducting power transformer as a functional model. The nominal primary and secondary currents (voltages) are 18 A (5.6 kV) and 92 A (1.1 kV), respectively. Iron core and HTS coils are cooled by liquid nitrogen at a temperature of 77 K in a G-FRP cryostat. Untwisted multifilamentary silver sheathed Bi2223 tape conductors with 55 filaments were used for coil manufacturing. The primary winding consists of a stack of 30 pancake coils connected in series while each of the two secondary windings is a solenoid coil with five tapes wound in parallel. The primary and secondary windings are arranged concentrically and the secondary windings are connected in series. No-load tests, short-circuit tests and load tests proved repeatedly that the transformer has the rated capacity. HTS winding losses of 21 W and iron losses of 403 W were measured. - Work on a 1 MVA demonstrator transformer is underway.

18:00 *11B–2

Test of a 10 meter long, 2 kArms high-temperature superconducting cable conductor model based on Bi-2223/Ag-alloy tapes.

S.K. Olsen[1], *C. Træholt*[1], *C.N. Rasmussen*[1], *K. H. Jensen*[1], *O. Tønnesen*[1], *M. Däumling*[2], *C. N. Rasmussen*[2] and *D. W. A. Willén*[2]. [1]Department of Electric Power Engineering, Technical University of Denmark, Building 325, DK-2800 Lyngby, Denmark. [2]NKT-Research Center, Priorparken 878, DK-2605 Brøndby, Denmark.

The AC-loss of a superconducting cable conductor carrying an AC current is small. Therefore the ratio between the inductive and the resistive voltages over the conductor is high. This results in phase angles between the current and the voltage over the cable close to 90 degrees which has the effect that the loss can not be derived directly using most commercial lock-in amplifiers due to their limited absolute accuracy. However, by using two lock-in amplifiers and an appropriate correction scheme, the high relative accuracy of such lock-in amplifiers can be exploited. In this paper we present the results from AC-loss measurements on a low loss 10 meter long high temperature superconducting cable con-

ductor using such a correction scheme. Measurements were carried out with and without a compensation circuit that could reduce the inductive voltage. The 1 μV/cm critical current of the conductor was 3240 A at 77 K. At an rms current of 2 kA (50 Hz) the AC-loss was derived to be 0.6 $\pm$ 0.15 W/m. This is, to the best of our knowledge, the lowest value of AC-loss of a high temperature superconducting cable conductor reported so far at these high currents.

18:30 11B–3

Short-Circuit Test of a Bi-2223 Model Winding for a High-Voltage-Type HTS Transformer.

K. Funaki[1], *M. Iwakuma*[1], *K. Kajikawa*[1], *T. Bohno*[2], *S. Nose*[2], *M. Konno*[3], *J. Kuwayama*[3], *H. Maruyama*[4], *T. Ogata*[4] and *K. Tsutsumi*[5]. [1]Kyushu University, 6-10-1 Hakozaki, Higashi-Ku, Fukuoka 812-8581, Japan. [2]Fuji Electric Corporate Research & Development, Ltd., Ichihara, Chiba 290-8511, Japan. [3]Fuji Electric Co., Ltd., Shinagawa, Tokyo 141-0032, Japan. [4]Kyushu Transformer Co. Ltd., Fukuma-Cho, Munakata 811-32, Japan. [5]Kyushu Electric Power Co., 2-1-47 Shiobaru, Minami-Ku, Fukuoka 815-8520, Japan.

Transformer windings have a large over current for an accidental short-circuit in practical power grids. In case of high T_c superconducting (HTS) transformers, the current density may be designed about ten times higher than that in conventional oil ones. This means that the mechanical and thermal stress is much more severe for the HTS windings compared with the conventional ones in the accidental short-circuit. For the development of practical HTS transformers, we esti-mated electromagnetic force of the windings in the accidental case and considered the winding structure for the mechanical and thermal stress. In order to confirm the design concept, we constructed a small-sized model coil of Bi-2223 Ag/Mn tapes with the same winding structure and performed a short-circuit test of the model coil. For the over current more than ten times higher than the rated level, we had no degradation in current-voltage characteristics of the HTS tapes. We will design and construct a 22/6.9 kV HTS transformer on the basis of the test results.
This work is supported by the New Energy and Industrial Technology Development Organization, Japan.

18:45 11B–4

Manufacture and Testing of a HTS Prototype Cable for Power Transmission.

G. Pasztor[1], *A. Anghel*[1], *B. Jakob*[1], *A.M. Fuchs*[1], *D. Trajkovic*[1], *R. Wesche*[1], *G. Vécsey*[1] and *R. Schindler*[2]. [1]Centre de Recherches en Physique des Plasmas, Technologie de la Fusion Ecole Polytechnique Fédérale de Lausanne, CH-5232 Villigen PSI, Switzerland CH-5232 Villigen. [2]Brugg Kabel AG, CH-5201 Brugg, Switzerland.

A 5 m long, single-phase HTS prototype cable for power transmission has been designed, manufactured and tested. Investment cost optimization studies and the requirement to reduce cable losses to acceptable levels, have led to optimum operating temperatures in the range of 50 to 60 K, suggesting that neon gas cooling may be an attractive approach for power cables based on HTS. The cable consists of two oppositely wound helical layers on a 53-mm-diameter former with glass fibre tape separating the layers. Bi-2223 commercial tapes with high strength silver alloy matrix were employed. Evacuated superinsulant was used as thermal insulation. A test set-up devoted to evaluation of HTS cable performances under dc and ac conditions has been designed and built. Cooling is provided by a neon refrigeration system. The dc voltage-current characteristics, measured separately for each layer, indicate that the cable manufacturing doesn't significantly affect the critical current of the cable. The current distribution is measured under both dc and ac currents. The self-field ac losses at 50 Hz are determined using the double lock-in amplifier technique and compared with theoretical predictions. This work describes the cable and the test set-up and presents test results on the prototype cable. This work was partly supported by the Swiss Federal Office of Energy and the PSEL.

ORAL SESSION 11C: Passive Devices II

Wednesday Afternoon, September 15th, 17:30-19:00

17:30 11C–1

Investigations on the unloaded quality factor of planar resonators with respect to substrate materials and packaging.

A. Baumfalk, *M. Reppel*, *H. Chaloupka* and *S. Kolesov*. University of Wuppertal FB13, Wuppertal, 42119, Germany.

The unloaded quality factor Q_0 of various planar HTS resonators has been investigated, involving different resonator types, HTS materials, substrate materials, and packaging. It has been shown that for different temperatures Q_0 derives from different loss contributions (surface resistance R_s of the HTS film, dielectric losses of the substrate and losses due to housing contributions). Taking this fact into account, the loss mechanisms in disk- and in microstrip resonators have been classified in order to achieve higher Q-factors for temperatures of technical interest (55 K - 80 K). For disk resonator structures (4 GHz), a Q_0 of 140,000 at 75 K (298,000 at 60 K) has been measured on low-loss $LaAlO_3$ substrates, which is an improvement of a factor of 2 (respectively 3) compared to standard $LaAlO_3$ substrates. For double-symmetric microstrip resonators at 1.8 GHz a Q_0 of 40,000 at 77 K and of 65,000 at 60 K has been achieved for 0.5 mm standard $LaAlO_3$ substrates. These results suggest that the known loss contributions of substrate material and packaging can considerably be reduced so that the obtained unloaded quality factor is mainly due to the surface resistance of the HTS thin films.

17:45 11C–2

Progress towards superconducting optoelectronic modulators.

J.M. O'Callaghan[1], *J. Fontcuberta*[2], *L. Torner*[1], *R. Pous*[1] and *A. Cardama*[1]. [1]Universitat Politecnica de Catalunya (UPC) Campus Nord UPC-D3 Barcelona 08034 Spain. [2]ICMAB-CSIC, Campus UAB Bellaterra 08193 Spain.

This work describes the technological steps being taken to develop high-speed superconducting optoelectronic Mach-Zehnder integrated modulators to be used in fiber-optic communication systems. The most relevant figure of merit in these devices is the ratio between the bandwidth of the device and the power of the RF modulating source, which can be improved by lowering the RF losses in the metal electrodes of the modulator. Therefore, the use superconductive electrodes might lead to devices operating at higher modulation speed with weaker electrical signals. Efforts have been made to prove: 1) That the performance of standard electrooptical modulators improves when they are cooled down to liquid nitrogen temperatures; 2) That superconducting YBCO with low RF losses can be grown on electrooptic (lithium niobate) substrates; 3) That other factors affecting the performance of these modulators (i.e., the mismatch in propagation velocities between the optical and electrical signal) do not mask the performance improvements due to the use of superconducting electrodes. The tasks performed under these three concepts will be described.

18:00 11C–3

Applications of coupled dielectric resonators using HTS coated SrTiO3 pucks: tuneable resonators and novel thermometry.

J.C. Gallop and *L. Hao*. National Physical Laboratory, Teddington, TW11 0LW, UK.

The combination of very low dielectric loss single crystal materials with a high temperature superconductor shielding enclosure has led to the achievement of high Q resonators operated in the temperature range 40K-80K which show great promise for frequency standard applications. We have already reported how high frequency stability with minimum temperature control may be achieved be means of composite dielectric pucks. Another requirement is that it should possess a specified frequency. With an artefact standard such as a resonator this requires accurate manufacture of dimensions and control of material parameters but some further tuning is required to bring the final frequency within tolerance. Here we report investigation of electronic tuning of a sapphire dielectric puck resonator by using a HTS coated STO tuning element situated in the evanescent field region outside the sapphire puck. In the opposite limit corresponding to weak coupling between the sapphire resonator and the STO element we have shown how the strong temperature dependence of the STO permittivity allows very small temperature changes (<1 micron Kelvin) to be readily detected. We present results on the potential sensitivity and reproducibility of such a thermometer which seems capable of providing nanokelvin resolution at temperatures in the range 40-80 K, where such high sensitivity is unknown using other methods. This microwave driven thermometer has the further advantage that no direct connections to the sensing element are necessary.

18:15 11C–4

Bandpass filter on a parallel array of coupled coplanar waveguides.

A. Deleniv[1], *V. Kondratiev*[1], *P.K. Petrov*[2] and *I. Vendik*[1]. [1] St.-Petersburg Electrotechnical University, St.-Petersburg, 197376, Russia. [2] Chalmers University of Technology, Goteborg, S-412 96, Sweden.

A novel bandpass filter using a parallel array of coplanar waveguides (CPW) is developed. The CPW properties do not depend strongly on the substrate thickness, and a wide range of impedance is achievable on rather thick substrates with reasonably small dimensions of the CPW cross-section. This allows to miniaturize microwave planar filters based on the CPW structure. The simulation procedure based on quasi-TEM analysis is briefly discussed. A coplanar waveguide three-pole Chebyshev bandpass filter with 14 % equal-ripple bandwidth at 1.775 GHz was simulated and designed. The filter was manufactured using high-temperature superconducting film (YBCO) on $LaAlO_3$ substrate. The experimental investigation revealed 0.6 dB insertion loss at T = 78 K. A good agreement between measured and simulated data was observed. The 5-pole bandpass filter is designed. The experimental investigation is in a progress. The work was supported by the Science Council on Physics of Condensed Matter (Project 98063) in Russia, and by the Royal Swedish Academy of Sciences.

18:30 11C–5

High - temperature superconducting microwave circuits with ferrimagnetic or ferroelectric tuning.

D. Schemion, *M. Winter*, *R. Ott* and *N. Klein*. Forschungszentrum Jülich GmbH Institut of Solid State Research 52425 Jülich Germany.

One of the most promising applications of high-temperature superconductors (HTS) are passive microwave devices. In general, these devices are based on microstrip or coplanar transmission lines and/or lumped element capacitors and inductors, which are fabricated by photolithography from HTS thin films deposited on low loss dielectric substrates like e.g. sapphire. Such circuits are e.g. bandpass filters, which are much smaller in size and weight than the conventionally employed waveguide or dielectric filters. Therefore are considered to be very useful for base stations in mobile communication and satellite technology. For many applications electrical tunability is an important issue. Two very promising approaches are tuning with low-loss ferrites or ferroelectric materials. In case of ferroelectric we have produced $SrTiO_3$-layer on sapphire substrates with a CeO_2-buffer layer. The layers have been optimised for low microwave losses employing characterisation by quasioptical submillimeterwave-spectroscopy. Since HTS films cannot be deposited easily on ferrite substrates, flip-chip geometries can be employed for magnetic tuning. For the determination of both dielectric and magnetic microwave losses of different ferrites at cryogenic temperatures we have designed a special resonator. Our first device tested is a HTS/ferrite bandreject filter based on an HTS hairpin resonator.

18:45 11C–6

Progress in superconducting preselect filters for mobile communications base stations.

J.S. Hong[1], *M.J. Lancaster*[1], *D. Jedamzik*[2], *R.B. Greed*[2] and *J.C. Mage*[3]. [1]SEEE, Univ. of Birmingham, Edgbaston, Birmingham B15 2TT, UK. [2]Marconi Res.Cen.,Great Baddow,Chelmsford Essex,CM2 8HN, UK. [3]Thomson-CSF/CNRS,UMR137,Domaine de Corbeville F-91404,France.

The technology and system challenges of next generation mobile communications have stimulated the research and development of high temperature superconducting (HTS) bandpass filters. In this paper, we summarise the recent progress of novel HTS preselect bandpass filters that have been developed for an European research project called Superconducting Systems for Communications (SUCOMS). The objective of the project is to construct a HTS based transceiver for mast mounted DCS1800 base stations. The HTS preselect receive filters have been designed to have a quasi-elliptic function response in order to provide low insertion loss and very steep roll-off at the filter band edges. The filters cover a 15 MHz sub-band of a receive band which ranges from 1710 to 1785 MHz. The filters have been fabricated using double-sided YBCO thin films on MgO or LAO substrates with a size of 22.5x39 mm. The filters have been tested in both liquid nitrogen and vacuum coolers. Very good performance has been measured. The filters have been integrated with low noise amplifiers (LNA) into a r.f. module for encapsulation. The measurements have been performed with the encapsulated r.f. module.

ORAL SESSION 11D: Flux Pinning II

Wednesday Afternoon, September 15th, 17:30-19:00

17:30 *11D–1

Flux pinning in textured high temperature superconductors by artificial defects.

H.W. Weber. Atominstitut der Österreichischen Universitäten, A-1020 Wien, Austria.

Recent results on the flux pinning action of artificial pinning centers introduced into melt textured bulk 123 superconductors and into PIT Bi-2223 tapes will be reviewed. Special emphasis will be placed on two kinds of radiation-induced defects, namely spherical collision cascades (produced by fast neutrons) and extended columnar defects (produced by fission products as a consequence of thermal neutron induced fission of uranium additions to the superconductors). In the melt textured bulks, we find significant enhancements of the critical current densities and the trapped fields at 77 K, but almost no change of the irreversibility lines. The flux pinning effect is comparable for both kinds of defects, which can be understood on the basis of a simple model for the defect configuration in the 123 system. In BiSCCO, the extended defects turn out to be highly efficient flux pinning centers, especially at high temperatures. For fields applied perpendicular to the tape surface, the critical current densities are enhanced by approximately two orders of magnitude. As a consequence, their angular dependence becomes very weak. Moreover, the irreversibility fields are doubled at 77 K. These observations and the characteristic differences between the pinning forces exerted by these extended defects and by the smaller spherical defects will be discussed in terms of the magnetic microstructure prevailing in BiSCCO.

18:00 11D–2

Pinning force diagram of the ternary superconductor (Nd,Eu,Gd)-123 with secondary phase additions.

M. R. Koblischka, *M. Muralidhar* and *M. Murakami*. SRL/ISTEC, Div.3, 1-16-25 Shibaura, Minato-ku, Tokyo 105, Japan.

$(Nd_{0.33}Eu_{0.33}Gd_{0.33})Ba2Cu3Oy$ ("NEG") samples are prepared containing extremely fine insulating 211 particles, which are uniformly dispersed in the supercon-ducting matrix. Even though $(Nd,Eu,Gd)_2BaCuO_5$ powders about 3 μm in diameter were added to the precursor, we have found that Gd_2BaCuO_5 (Gd-211) inclusions about 0.1 μm in diameter were finely distrib-uted in the NEG matrix. As a function of the concentration of the 211 particles, the shape of the $J_c(B)$ curves at $T = 77$ K can be changed from a very pronounced fishtail behaviour to a plateau-like behaviour, yielding a nearly constant current density up to 2.5 T. This suggests that the peak effect is an unique property of the superconducting matrix (i.e. oxygen vacancy clusters), whereas the 211 particles provide effective pinning in the entire temperature range acting quasi as a "background" pinning mechanism for the peak effect. Based on these observations we construct a pinning force diagram for the NEG system.

18:15 11D–3

Vortex pinning dynamics anisotropy for perfect YBCO films with $J_c(77K) > 3\,MA/cm^2$ studied by direct transport measurements of $J_c(H,T,\theta)$.

V.M. Pan[1], *V.A. Komashko*[1], *A.L. Kasatkin*[1], *V. L. Svetchnikov*[1], *A. G. Popov*[1], *A. V. Pronin*[1], *A. Yu. Galkin*[1], *C.L. Snead*[2], *M. Suenaga*[2] and *H.W. Zandbergen*[3]. [1]Institute for Metal Physics, Kiev 252142, Ukraine. [2]Brookhaven National Laboratory, Upton, NY 11973, USA. [3] National Centre for HREM, TU Delft, Rotterdamseweg,34, AL Delft 2628, The Netherlands.

$J_c(H,T,\theta)$ is studied in highly biaxially oriented YBCO thin films with $J_c(77K) > 3\,MAmp/cm^2$ produced by DC magnetron sputtering as well as pulse laser deposition. Three sorts of the $J_c(\theta)$ angular dependencies are observed: (1) with the single $J_c(\theta)$-maximum at $H \parallel C$-axis; (2) with the single $J_c(\theta)$-maximum at $H \parallel ab$-plane; (3) with two $J_c(\theta)$ -maxima at $H \parallel C$ and $H \parallel ab$, their relative heights changing in a wide range due to structure variation. Comparison of the HRTEM data and J_c field/angular dependencies for YBCO films deposited onto different substrates exhibits how the dislocation distribution can affect the field/angular critical current behavior. HRTEM of YBCO films deposited onto buffered sapphire substrates reveals very high density ($> 10^{11}\,lines/cm^2$) of edge dislocations having their lines perpendicular and/or parallel to the substrate surface depending on a film growth mode which is predetermined by a state of sapphire/cerium-oxide/YBCO interfaces. High J_c in epitaxial YBCO films and its remarkably varied field/angular dependencies are in accordance with observed densities, distribution and line directions of edge dislocations. The 2D VLL correlated disorder induced by linear defects is shown to be responsible for the critical current density as a function of the applied magnetic field, mosaicity domain size and misorientation angle.

18:30 11D–4

Surface columnar defects as a tool to tune the static and dynamic superconducting properties of HTS bulks without any damage.

E.Mezzetti, *R.Gerbaldo*, *G.Ghigo*, *L.Gozzelino* and *B.Minetti*. I.N.F.M. UdR Torino Politecnico; I.N.F.N. Sez. di Torino; Dipartimento di Fisica, Politecnico di Torino, Torino, Italy.

his paper presents the outstanding characteristics of the confinement of vortices into superconducting materials by means of columnar defect implantation (bulk materials). In particular, the quite peculiar advantages of the implantation of columnar defects for about 10% of the whole thickness are emphasized by means of a wide spectrum of dc and ac experimental data concerning Ag/BSCCO-2223 tapes (see abstract ID-349) and melt textured YBCO materials (see abstract ID-347), irradiated with 0.25 GeV and 2.0 GeV Au ions, respectively. Surface columnar defects do not damage the T_c, the J_c and the irreversibility lines when the magnetic field is applied perpendicular to the c-axis (i.e. to the ion tracks). They enhance the critical current densities and the irreversibility lines in a quite controllable range of magnetic fields, when the magnetic field is applied parallel to the c-axis (for BSCCO-2223 tapes the position of the c-axis is only known within an error of 10%). They shut down the anisotropy between a point phase (T_{onset}, B_{onset}) up to about $2B_\phi$, also when the applied field is tilted with respect to the c-axis direction. They strongly dump the dependence of the ac losses on the frequency of the applied field. Two models are also proposed in the framework of a guide for technological applications. The two models concern the irreversibility lines (E.Mezzetti et al., Phys. Rev. B 59, 3890) and the pinning force, respectively. Both models fit the data quite well and allow to have a picture of vortices confined in a surface layer by columnar defects, and keeping some ordering also in deeper layers trough a favorable arrangemet of intrinsic defects. Finally, the confinement proper ies of surface defects on 3D systems are compared with the confinement properties of crossing defects on 2D systems (YBCO films) (see abstract **10-99**) by pointing out either analogies or differences

18:45 11D–5

Flux pinning forces in irradiated a-axis oriented $EuBa_2Cu_3O_7$ films.

J. I. Martin[1], *E. M. Gonzalez*[1], *W. K. Kwok*[2] and *J. L. Vicent*[1]. [1]Dpto. Fisica Materiales, Universidad Complutense, 28040 Madrid (SPAIN). [2]Materials Science Division, Argonne National Laboratory, IL. 60439 (USA).

a-axis oriented $EuBa_2Cu_3O_7$ films have been fabricated by dc magnetron sputtering technique on (100)$SrTiO_3$ substrates. In these films the CuO_2 planes are perpendicular to the substrates and they show a peculiar microstructure with 90° microdomains. These films were irradiated using heavy ions 1.4 GeV ^{238}U and 2.5 GeV ^{131}Xe and the matching fields were 1 T and 0.5 T. Three different types of columnar defects were fabricated, perpendicular to the substrates (paralell to the CuO_2 planes), 30° off the direction perpendicular to the substrate and +45°, -45° (splayed defects) off the perpendicular to the substrate direction. The angular critical current dependence has been measured, close to T_c, using a 90 kOe magnet and a computer controlled rotatable sample holder. The angular dependence of the pinning forces and the enhancement of the critical current are governed by the competition between the intrinsic anisotropy of the 123 cuprates and the different types of defects, that could be natural (90° microdomains) or artificial (columnar) defects. The critical currents and pinning forces show a weaker dependence on these artificially induced extended correlated defects than in the case of irradiated single crystals.

POSTER SESSION 12

Wednesday Evening, September 15th, 19:00-21:00

Session Bulk materials and materials aspects

12–1

Melt processing and flux pinning behaviors of (Nd, Sm)-Ba-Cu-O superconductors.

A.M. Hu, *G. Krabbes*, *P. Schätzle* and *W. Bieger*. Insitute of solid state and materials researchs Dresden, P.O. Box: 270016, D-01171 Dresden, Germany.

High quality binary(Nd, Sm)-Ba-Cu-O monoliths were successfully grown in air via a chemically controlled melt processing technique. Melt-processed Nd123 crystals were used as the seeds to initialize the crystallization and the influence of (Nd,Sm)2BaO4, Ag and Pt additives was investigated. Tc's value up to 96K with a sharp transition can be achieved using the presently modified melt processing. The critical current density at 77K reaches 3.8  104 A/cm2 in 2T and a magnetic field of 250mT is trapped in a cylinder with a diameter of 15 mm. The scaling behaviors of critical current densities and volume pinning forces also were investigated using a series of high quality melt-processed (Nd, Sm)-Ba-Cu-O crystals with varying postannealing in Ar and O2. Enhanced superconducting performance can be attributed to the dramatic suppression of the chemical substitution between rare earth element and Ba in the superconducting matrix and the striking refinement of non-superconducting second phase particles.
This work is supported by the Alexander von Humboldt Stiftung, the German Minister of Research and Education, and the Fonds der Chemischen Industrie.

12–2

Decomposition of the supersaturated $Nd_{1+x}Ba_{2-x}Cu_3O_z$ solid solution as a way to superconductors with strong vortex pinning.

E.A.Goodilin, *A.P.Soloshenko*, *V.V.Lennikov*, *A.V.Knot'ko* and *Yu.D.Tretyakov*. Moscow State University, Chemistry Faculty, Inorganic Chemistry Divison, Lenin Hills, 119899, Moscow, Russia.

A new generation of materials with strong pinning centers related to nanoscale Nd3+/Ba2+ fluctuations was born by the superconductor NdBa2Cu3Oz (Nd123). In the present study fundamental features of the Nd1+xBa2-xCu3Oz homogeneity field are discussed for a wide range of temperatures (600-1100°) and the substitution ratio x (0<x<1). A particular attention is paied for Time-Temperature-Transformation (TTT) diagrams of solid state decomposition of the supersaturated solution with x~0 to find conditions of forming a spectra of nanocomposites with desired properties. To produce reactive, highly homogeneous and carbon-free submicron precursors, the spray-drying technique is applied followed by vacuum decomposition. It is found that less-substituted solid solutions (Tc=94K) exist in air at 980-1030C while x=0.05-0.1 are reached below and above this range. As a result, growth of Nd123ss whiskers is observed upon partial melting at 1060-1080°; the solid state decomposition into a solution with x>0 and BaCuO2 may occure with suppression of Tc down to 45-50K under regular oxygenation (600°, O2). Finally, the shape and the internal fine structure of the Nd123ss solution field are established, and a ≪chemical pressure≫ model is suggested to explain compositionally induced structural phase transitions. This work is supported by RFBR (grant 98-03-32575à).

12–3

Thermodynamics of the $RE_1Ba_2Cu_3O_{7-x}$ (REBCO) Phases.

J.A.G. Nelstrop and *J.L. MacManus-Driscoll*. Departement of Materials, Royal School of Mines, Prince Consort Road, London SW7 2BP, England.

Lower melting onset temperatures are required if the REBCO phases are to be processed for conductor applications via liquid assisted routes, e.g.by LPE or conventional (peritectic) melt processing. In order to determine the minimum melting onset temperatures, we have studied the thermodynamics of different REBCO phases (including RE mixtures), with and without fluorine additions by a coulometric titration method. The thermodynamic information has been obtained in the temperature range 850°C - 1020°C, and oxygen partial pressure range 1.0×10^{-6} - 2.0×10^{-1} atm. We have found that the minimum peritectic temperature, T_p, can be lowered to 860°C± 10°C under reducing conditions. In addition, T_p at a given pO_2 decreases with decreasing RE ion size, with a lowering of T_p as much as 100°C for RE ions smaller than Y. T_p is further lowered by the presence of fluorine. Additional information about the kinetics of formation of the different REBCO phases have also been obtained, and it has been found that, at a given temperature, the rates of grain growth decrease with decreasing RE ion size.

12–4

Effects of Nd partial substitution on the Y123/Y211 composites.

R. Cabré[1], *Jna. Gavaldà*[2], *R. Solé*[2], *J. Massons*[2], *M. Aguiló*[2] and *F. Díaz*[2]. [1]Dept. d'Enginyeria Electrònica, Elèctrica i Automàtica, Univ. Rovira i Virgili, 43005 Tarragona, Spain. [2]Lab. de Física Aplicada i Cristal.lografia, Univ. Rovira i Virgili, 43005 Tarragona, Spain.

In this study, cylindrical samples of Y123/Y211 composites with different neodymium oxide additions were textured using the Partial Melting Zone method in order to investigate how these additions affected the morphology, the structure and the superconducting properties of the samples when different concentrations of Nd^{3+} ions are partially substituted in the structure of the composites . The melting and crystallization temperatures for all the samples were first determined and compared with those of the samples without Nd additions. It was found that neodymium increases the melting temperature but maintains the crystallization temperature. The morphology of the samples was analysed by optical microscopy. Image processing techniques were applied to the micrographs to measure the size and distribution of Y211 particles. They showed that if initial neodymium concentration is low (≈2%), the size of the precipitates is small, its distribution homogeneous and the single domain generated is large. However, if neodymium concentration increases (up to ≈5%), the final distribution of precipitates is more inhomogeneous and an aggregate of small domains appear. The microstructure of the samples was also analysed by TEM. This study showed that neodymium intro-

duces more defects into the Y123 structure. Electron Probe Microanalysis applied to the samples reveals that the Nd^{3+} ions only substitute the Y^{3+} ions, in the Y123 and the Y211. X-ray diffraction and texture analysis show that,of all the cell parameters, only the c parameter is appreciably modified when neodymium is incorporated into the unit cell. Finally, the samples are electrically and magnetically characterized.

12–5

Peculiarities of high pressure-high temperature processing of MeBCO (Me=Y, Nd).

T. Prikhna[1], *W. Gawalek*[2], *V. Moshchil*[1], *V. Melnikov*[3], *F. Sandiumenge*[4], *P. Nagorny*[1], *T. Habisreuther*[2], *P. Shaetzle*[5], *Ch. Wende*[2] and *S. Dub*[1]. [1]Institute for Superhard Materials, Kiev, 254074, Ukraine. [2]Institut fuer Physikalische Hochtechnologie, Jena, D-07743,. [3]Institute of Geochemistry, Mineralogy and Ore-Formation, Kie. [4]Instituto de Cincia de Materiales de Barcelona, Bellaterra,. [5]Institut fuer Festkrper- und Werkstofforschung, Dresden, D-0.

Among the known high temperature bulk superconductors melt-textured Me123 (Me=Y, Nd) - based (MT-MeBCO) possess the highest level of cryomagnetic properties, which makes these materials the most promising for application in the devices working on the principals of levitation. We investigated the peculiarities of the MT-MeBCO structure, superconductive and mechanical properties variation depending on parameters of high pressure-high temperature (HP-HT) treatment. The HP-HT effect influence on single-phased Me123 (Me=Y, Nd) and HP-HT sintering features of Y123 powder will be presented as well. It has been found that high pressures (2-5 GPa) allow us to maintain the orthorhombic superconductive Me123 structure when heated up to high temperatures (1073-1673 K). Besides, it is possible to densify the material and improve its mechanical and superconductive properties. The four-order increase in dislocation density may be one of the reasons of critical current density increase.

12–6

Directional solidification in air of NdBaCuO bulk superconductor.

A. Vecchione[1,2], *P. Tedesco*[1], *M. Gombos*[1,2], *M. Polichetti*[1,2] and *S. Pace*[1,2]. [1]Dipartimento di Fisica Università di Salerno Via Salvador Allende, Baronissi (SA), I-84081 Italia. [2] Istituto Nazionale per la Fisica della Materia Unità di Salerno Via Salvador Allende, Baronissi (SA), I-84081 Italia.

NdBaCuO bulk samples have been fabricated by directional solidification using both top-seeding and horizontal Bridgman techniques. In order to avoid the lowering of the transition temperature due to substitution of Nd in Ba sites in the superconducting phase, the samples were prepared by admixtures of $NdBa_2Cu_3O_{7-\delta}$ and a Nd-poor insulating brown phase ($Nd_{4-2z}Ba_{2+2z}Cu_{2-z}O_y$ with $z = 0.2$). Single-domain samples of about 1 centimetre have been obtained, and their compositional homogeneity has been checked by energy dispersive spectroscopy. Transition temperatures of about 90 K have been measured in samples grown in air and successively annealed at low temperature in a pure oxygen atmosphere. Measurements both of the temperature dependence of magnetisation and of the magnetisation hysteresis loops up to 10 T show the presence of a residual phase characterised by a low critical temperature.

12–7

Microstructure development in thick YBCO films grown by liquid phase epitaxy.

K.A. Kursumovic[1,2], *Y.S. Cheng*[1,2], *A.P. Bramley*[1], *B.A. Glowacki*[1,2] and *J.E. Evetts*[1,2]. [1]Department of Materials Science and Metallurgy, University of Cambridge, Pembroke Street, Cambridge CB2 3QZ, UK. [2]IRC in Superconductivity, Cavendish Laboratory, Madingley Road, University of Cambridge, Cambridge CB3 0HE, UK.

There is increasing interest in Liquid Phase Epitaxy as a high rate processing route for the production of thick film YBCO and ReBCO for high current applications. The technique involves the undercooling of a flux (e.g. $Ba_3Cu_5O_8$) supersaturated with rare earth in the presence of a suitable substrate. The substrate is rotated in order to establish forced convection of the melt. The film growth in an initial transient regime is based on diffusion growth from the flux rich in yttrium. Classical $t^{1/2}$ growth kinetics is found in this regime. In the subsequent steady state regime the growth rate becomes almost linear in time depending on the delivery of fresh supersaturated liquid through the establishment of forced convection. We report here a microstructural study on samples varying in thickness from 1μm to 350μm. For optimum conditions the samples had nearly perfect c-axis orientation. The initial growth was initiated by multinucleation in a Stranski-Krastanov like mechanism. However, films thicker than ~2.5μm showed a dislocation stress-relief mechanism and growth became dislocation mediated. The larger sub-grains increase in size as films get thicker showing growth-death competition. This research was carried out in the framework of the Brite Euram programme CONTEXT (Contract No. BRPR-CT97-0607).

12–8

Statistical Thermodynamics of Point Defects, Dopant Segration, and Carrier Densities Near Dislocations, Grain Boundaries, and Other Interfaces in $YBa_2Cu_3O_x$.

D. O. Welch. Department of Applied Science, Brookhaven National Laboratory, Upton, New York 11973-5000 USA.

Critical current densities across grain boundaries and twin boundaries, as well as flux pinning by twin boundaries, stacking faults, dislocations, and precipitates in $YBa_2Cu_3O_x$ are sensitively influenced by the nearby state of oxygen content and order, segregation of dopants and point defects, and elastic strain state. These factors influence the density of charge carriers, electronic band bending, and the strength of superconducting pairing in the vicinity of lattice defects and these, in turn, control the superconducting properties. In this paper, I will describe various statistical thermodynamic models which can be used to describe these effects. Such models are useful for correlating and understanding the relation of experimental data on superconducting properties and the results of studies of defect structure by analytic and imaging methods of electron microscopy. This research was performed under the auspices of the U.S. Department of Energy, Division of Materials Sci-

ences, Office of Basic Energy Sciences under Contract No. DE-AC02-98CH10886.

12–9

Rf field dependencies of the surface impedance of YBCO: A new analysis of the ratio $r = dX_s/dR_s$.

K. Numssen[1], *E. Gaganidze*[2] and *J. Halbritter*[2]. [1]TU Muenchen, James-Frank Str. 1, D-85747 Garching, Germany. [2]Forschungszentrum Karlsruhe, IMF 1, Postfach 3640, D-76021 Karlsruhe, Germany.

The application of HT_c-superconducting wafers in rf devices requires a profound knowledge of [the mechanisms which govern] the rf field dependent surface impedance $Z_s = R_s + iX_s$. It has been found that the mechanisms yielding a nonlinear behaviour $Z_s(H)$ can best be classified on the basis of the ratio $r = dX_s/dR_s$. In contrast to $R_s(H)$ and $X_s(H)$, the determination of this quantity is independent of any geometric factor of the measurement set-up. With increasing rf field, however, a certain difficulty occurs: frequency domain measurements (sweep method), which are usually applied to derive δX_s from the shift of the resonance frequency, fail at high rf power levels because of heating, while time domain measurements (decay method) yield $R_s(H)$ but no information on the frequency shift. We present a pulse measurement technique which allows to directly determine the ratio r and to identify thermal effects by analysing the nonlinear response. Furthermore, a closer examination of the excess transmission at the beginning of the pulse response gives hints on the dynamics of the underlying nonlinear mechanisms. From the observed r-values, $r = 1..10$, and material dependencies we conclude, that Josephson fluxons in weak links play the most important role.

12–10

Gold-Doped YBCO Superconducting Samples.

A. Marino, *M. Sanchez*, *D. Riano* and *H. Sanchez*. Department of Physics, Universidad Nacional de Colombia, Bogota, Colombia.

Superconducting $YBa_2Cu_{3(1-x)}Au_{3x}O_{7-\delta}$ bulk samples with nominal Au content $0 \leq x \leq 0.1$ have beeen prepared by the solid state reaction method. The Au doping affected both the superconducting properties and the structure of the YBCO system. An enhancement of the critical current density for low Au-doping levels ($x \leq 0.01$) was observed and assigned to pinning effects.

12–11

Enrichment of NdBCO Superconducting Powders by Electromagnetic Separation.

E.Broide[1], *G.E.Shter*[2] and *G.S.Grader*[2]. [1]Separator Ltd.,Kiryat Weizmann Science Park,Ness-Ziona,70400,Israel. [2]Chemichal Engineering Dept.,Technion,Haifa,32000,Israel.

The aim of this work is to demonstrate the possibility to enrich the NdBCO superconducting powders by electromagnetic separation to fractions that are significantly different in their physical, chemical and superconducting properties. The method of Electromagnetic Separation (EMS)is based on the interaction of HTSC particles and an alternating magnetic field at their transition temperature and extracting of the fractions characterized by higher critical currents. The method and device used in work was developed by "Separator, Ltd.".The NdBCO material was prepared by oxalate coprecipitation and then partially degraded powders were treated by EMS. The different conditions of separation were studied to find the optimal parameters. As a result of separation, the powders were divided to "concentrate" and "tail" fractions.Phase composition, morphology and electromagnetic properties such as inductance, impedance, resonant frequencies were investigated for each of fractions. A significant difference of the properties for these fractions was shown. The "concentrate" amounted to an average of 60-70%wt. and characterized by better superconducting properties while the "tail" properties were essentially lower as require for preparation of superconductors. The "concentrate" is actually an enriched superconducting powder with optimal quality and the "tail" is a recycle fraction needed an additional thermo-chemical treatment.Thus, the EMS may be used as an effective and simple method for enrichment and improvement of NdBCO superconducting powders.In addition, the possibility to use of EMS for rapid evaluation of powders quality and immediately correction of processing parameters will be discussed.

12–12

Superconducting Properties of Textured $YBa_2Cu_3O_{7-\delta}/Y_2BaCuO_5$ Grown with Addition of Nanoparticles.

Z.H. He[1,2], *O.B. Surzhenko*[1], *T. Habisreuther*[1] and *W. Gawalek*[1]. [1]Institut für Physikalische Hochtechnologie e.V., Postfach 100239, D-07702, Jena, Germany. [2]Department of Physics, Zhongshan University, Guangzhou, 510275, P.R. China.

It has been well known that the critical current density (J_c) of the high T_c bulk superconductor can be increased if the nonsuperconducting flux-pinning centers are reduced in size. To introduce nanometer size particles to the high T_c superconductors, nanopowders of SnO_2, $BaTiO_3$ were prepared and added to the blend of $YBa_2Cu_3O_{7-\delta}/Y_2O_3$, in a supersonic-vibrating alcohol, for texture growth. With the help of vibrating sample magnetometer (VSM), superconducting properties were measured and analyzed. For slightly SnO_2-doped samples, J_c(H,T) was found comparable with that of the best of the undoped samples. The fishtail effect in J_c(H) was found for most of the sample at 77K. The collective flux-pinning model, however, did not seem to be effective to explain the experimental data. For the $BaTiO_3$ doped samples, the superconducting temperature (T_c) dropped with $BaTiO_3$ content. In this case, the data agreed with the collective flux-pinning model. Relationship between the superconducting properties, the pinning mechanisms and the nanopowder doping will be discussed. This work was supported by the German BMBF project (contract number 13N6854), the Alexander von Humboldt Foundation, and the National Nature Science Foundation of China.

12–13

Exploring the ternary superconductors of the type (Nd,Eu,Gd)-123.

M. Muralidhar, *M. R. Koblischka* and *M. Murakami*. SRL/ISTEC, Div.3, Tokyo 105, Japan.

Recent experiments have demonstrated the superior performance of $(Nd_{0.33}Eu_{0.33}Gd_{0.33})Ba_2Cu_3O_y$ bulk superconductors as compared to YBCO or NdBCO. Similar to NdBCO, the transition temperature, T_c, is of the order of 95 K and the magnetization loops exhibit a very pronounced secondary peak effect at fields of about 2.5 T. Addition of NEG-211 particles to the starting composition leads to the formation of submicron-sized Gd-211 particles embedded in the superconducting matrix which are very effective pinning sites. Originally starting from an even ratio of the light rare earth elements (LRE) in the matrix and in the 211 particles, we now explore the effect of variations of this initial LRE mixing ratio.

12–14

High transport critical current of Y123 zone melted samples processed in a microwave cavity.

S. Marinel[1], *D. Bourgault*[2], *O. Belmont*[3], *A. Sotelo*[1], *G. Desgardin*[1] and *B. Raveau*[1]. [1]CRISMAT laboratory-CNRS UMR 6508, 6 Bd. Du Marechal Juin, 14050 Caen cedex. France. [2]Laboratoire de Cristallographie-CRETA, 25 Avenue des Martyrs, 38042 Grenoble Cedex 9, France. [3] Centre de Recherches sur les Très Basses Températures Centre National de La Recherche Scientifique 25 Avenue des Martyrs, 38042 Grenoble Cedex 9, France.

The unidirectional solidification method is currently used to prepare well textured $YBa_2Cu_3O_{7-\delta}$ (Y123) bars for applications such as current leads. We describe here a new technique based on microwave heating to prepare single-domain textured bars between 10-15 centimeters in length. This new technique is very interesting to apply a high thermal gradient (higher than 200^0C/cm) which is very difficult to obtain in a conventional furnace and beneficial to improve the texture quality of Y123, even when we use a relatively high solidification speed (higher than 2 mm/h). The microwave method consists of using a TE102 single mode cavity working at 2.45 GHz and equipped with a conductor susceptor which consists of a tube which is positioned in the middle of the microwave applicator perpendicularly to the electrical field. Thus, the susceptor is placed in the maximum of the magnetic field and consequently is heated by an induction mechanism. The thermal profile thus obtained has demonstrated to be beneficial for preparing Y123 single-domain bars by the floating zone method. The microstructure of bars are investigated and correlated with transport properties measured along several centimeters of the bar by the four point method using pulse current. J_c higher than 20000A/cm^2 were obtained with a high reproducibility even if the (ab) plane orientation is far from the bar axe. We have also investigated the possibility of improving the (ab) plane orientation using appropriate seeds.

Session Flux pinning and ac losses

12–15

Surface effect on the M-H diagram of the current-carrying superconductor in a parallel field.

Yu.A.Genenko[1,2] and *H.C.Freyhardt*[1,3]. [1]Zentrum für Funktionswerkstoffe gGmbH, 37073 Göttingen, Germany. [2]Donetsk Physical and Technical Institute NAS Ukraine, 340114 Donetsk, Ukraine. [3]Institute für Materialphysik, Universität Göttingen, 37073 Germany.

Magnetic flux entry in and exit from the flux-filled pin-free type-II superconductor cylinder carrying a transport current and subjected to a parallel magnetic field are studied in the frame of a modified Meissner state model. The Bean-Livingston barrier and the repulsion from the internal magnetic flux determine the condition for the right-handed spiral flux line entry: $H^2 + H_I^2 = H_c^2 + B^2$ where H, H_I and H_c are the external magnetic field, transport current self-field and thermodynamical critical field, respectively, and B is an average magnetic induction in the sample. The above relation as well as the analysis of a left-handed vortex exit from the sample allows us to estimate a hysteresis of the magnetisation of the current-carrying superconductor which results from the surface barrier effect alone.

12–16

AC transport losses in self fields for superconducting parallel-conductors cables.

A. Oota[1], *R. Inada*[1] and *T. Fukunaga*[2]. [1]Toyohashi University of Technology, Tempaku-cho, Toyohashi, Aichi 441-8 580, Japan. [2]Gifu National College of Technology, Shinsei-cho, Motosu-gun, Gifu 501-0495, Japan. .

A method is proposed to calculate the shape of field-free core, the current distribution and the AC transport losses in self fields as a parameter of current amplitude for superconducting parallel-conductors cables. Numerical calculations were made on the models of cables composed of a single-layer or a multi-layer configuration of superconducting tape strands with rectangular cross section on a cylindrical former. It is found from calculations that the tapes on a former show significant edge effect under current transmission so that the losses in the cables mainly generate near the tape edges. Narrowing the tape gap in a single-layer configuration suppresses the edge effect and lowers the loss values. A decrease in a distance between adjacent tapes in a multi-layer configuration also lowers the loss generation. Taken together, an improvement for design and construction of power cables should provide the possibility to suppress the loss values significantly and approach a demand for a practical use.

12–17

AC Losses in BiPbSrCaCuO/Ag 19-filaments tape in form of a helix measured by different potential taps.

M.Majoros[1,2], *B.A.Glowacki*[1,3], *A.M.Campbell*[1], *Z. Han*[4] and *P. Vase*[4]. [1]IRC in Superconductivity,University of Cambridge,Cambridge,CB3 OHE,U.K. [2]Institute of Electrical Engineering,SAS,Bratislava,842 39,Slovak Republic. [3]Department of Materials Science and Metallurgy,University of Cambridge,Cambridge,CB2 3QZ,U.K. [4]Nordic Superconductor Technology,Brondby,DK-2605,Denmark.

Transport ac losses in BiPbSrCaCuO-2223/Ag multifilamentary tape in form of a helix with a 3 mm gap between the turns were measured at power frequencies. Different positions of potential taps on outer and inner surface of the tape were used. Potential wires were led along the tape axis as well as along the axis of the helix. At currents lower than the critical current it was found that there was a strong dependence of the apparent ac losses on potential tap position, and on the configuration of the potential wires. A comparison of the results with short sample measurements is made. Suitably wound contact-less pick-up coils to detect magnetic flux of different magnetic field components were also used. They allowed us to measure the "magnetisation" part of the apparent losses, even when the sample was in the resistive state. The results of the losses at the gap in the tape are compared with the existing theoretical model.

12–18

Influence of matrix resistivity on transport ac losses and current-voltage characteristics of BiPbSrCaCuO-2223/Ag multifilamentary tapes.

M.Majoros[1,2], *B.A.Glowacki*[1,3], *A.M.Campbell*[1], *Z. Han*[4] and *P. Vase*[4]. [1]IRC in Superconductivity,University of Cambridge,Cambridge,CB3 OHE,U.K. [2]Institute of Electrical Engineering,SAS,Bratislava,842 39,Slovak Republic. [3]Department of Materials Science and Metallurgy,University of Cambridge,Cambridge,CB2 3QZ,U.K. [4]Nordic Superconductor Technology,Brondby,DK-2605,Denmark.

Transport ac losses and dc current-voltage characteristics of BiPbSrCaCuO-2223/Ag multifilamentary tapes with different matrix resistivities were measured. Powder-in-tube samples with 19 filaments were prepared with pure Ag, Ag-Mg alloy and Ag-Au (11 at %) alloy sheaths. AC losses were measured in the frequency range 40 Hz - 120 Hz. It was found that increasing the matrix resistivity increases the steepness of the dc current-voltage characteristic. The same effect was also observed for the ac loss dependencies at currents higher than the critical current. In this region the ac losses of the sample with Ag-Au matrix are much higher than the others. At currents lower than the critical current the ac losses of the samples with Ag-Mg and Ag-Au matrices are comparable, and slightly lower than those of the sample with pure Ag matrix. The losses of all samples are purely hysteretic.

12–19

Influence of defects on transport ac losses and current-voltage characteristics of BiPbSrCaCuO-2223/Ag multifilamentary tapes.

M.Majoros[1,2], *B.A.Glowacki*[1,3], *A.M.Campbell*[1], *Z. Han*[4] and *P. Vase*[4]. [1]IRC in Superconductivity,University of Cambridge,Cambridge,CB3 OHE,U.K. [2]Institute of Electrical Engineering,SAS,Bratislava,842 39,Slovak Republic. [3]Department of Materials Science and Metallurgy,University of Cambridge,Cambridge,CB2 3QZ,U.K. [4]Nordic Superconductor Technology,Brondby,DK-2605,Denmark.

Transport ac losses and dc current-voltage characteristics on different parts of a BiPbSrCaCuO-2223/Ag 19-filaments tape with an Ag matrix were measured. The influence of a localized defect on local and overall dc current-voltage characteristics, and ac losses, was studied. AC losses were measured in the frequency range 40 Hz - 120 Hz using a lock-in technique. It was found that the presence of a defect influences substantially the ac loss dependence and the form of the dc current-voltage characteristics. The problem of ac loss normalization and critical current definition is discussed and comparison of the normalized ac losses with different theoretical models is made.

12–20

Time constants and coupling losses in superconducting cables and in magnetic systems.

S. Takács. Institute of Electrical Engineering, Slovak Academy of Sciences, 842 39 Bratislava, Slovakia.

The possible sources of causing differences in AC losses and time constants in measuring arrangements and their expected values in real magnetic systems are summarized. These include the induced currents in the end portions, the field variations in time and space, the mixed contributions from substructures and normal parts, the longitudinal field effects, etc. These effects are supposed to be important at evaluating the expected losses, time constants and discharging processes in superconducting cables. In the last years, the size effects and the spatially changing fields were calculated and measured extensively, but in the low frequency limit only. However, some other effects are at least equally important, like the uncertainties in determining the effective resistances (or conductances) and effective volumes for the current loops, or the inductive coupling of current loops on the cable (mainly at higher frequencies). These effects can also cause considerable deviations in finite cable measurements, compared with the situation in different magnetic systems. The role of these differences, which can be decisive for the design of large superconducting magnets with required stability and quench behaviour, is emphasized. In addition, some special features for high temperature superconducting structures are discussed.

12–21

Voltage and Losses in Hard Superconductors Carrying Alternating Transport Current.

A.N.Ulyanov. Donetsk Physico-Technical Institute Ukrainian Academy of Sciences, 340114 Donetsk-114, Ulyanov.

Due to the high critical current density, high-temperature superconductors can be used for power applications, such as for transport of a dc and an ac current, as in wire for superconducting magnets, as current leads from liquid nitrogen temperature to liquid helium. Nevertheless for a lot of experimental and theoretical works devoted to the tranport properties of superconductors, some aspects of this topic are not studied well. Here, in terms of critical and resistive state model, the voltage, voltage wave form, and losses in superconductors carrying the alternating and direct current are calculated for an arbitrary relation between the values of transport and critical current. Obtained results agree well with the experimental ones. It is shown that the origin of the voltage rectification observed earlier is the shifting of the working point of the current-voltage characteristic of the superconductor carrying both dc and ac component of

transport current. The peculiarities of the voltage across the superconductors with high value of the ac transport current are predicted.

12–22

Numerical modeling of the Critical State and calculation of AC losses and current profiles in multifilamentary Bi-2223 tapes.

Y. Yang, *E. Martínez* and *C. Beduz*. Institute of Cryogenics, University of Southampton, Southampton, United Kingdom.

Existing numerical modeling of multifilamentary tapes based on the finite element method has been proved to be successful to estimate their AC losses. Nevertheless, those models present the drawback of requiring high performance computers. Beside those, the method proposed by E.H. Brandt, is able to calculate the current profile in monofilamentary tapes with power-law I-V characteristics, and then to estimate their electric and magnetic behaviour. This method, which is based on solving the integral equation of motion for the electric field, has some advantages with respect to the former ones, as they can run in PCs and require just short calculation times, giving reasonable results even using a small number of grids. In this paper we present the modeling of multifilamentary tapes using a refined Brandt's method that allows grids of large aspect ratio, which reduce the number of grids necessary for the calculation. The AC losses have been calculated for different frequencies and for parallel and perpendicular fields. The contributions of the superconductor and the metal matrix to the losses have been analysed. The comparison between the calculated AC losses and the experiments is presented.

12–23

Temperature Dependence of AC Losses in High-Temperature Superconductors.

N. Magnusson[1], *N. Schönborg*[1] and *S. Hörnfeldt*[2]. [1]Royal Institute of Technology, Electric Power Engineering, SE-100 44 Stockholm, Sweden. [2]ABB Corporate Research, SE-721 78 Västerås, Sweden.

When a high-temperature superconductor is to be used in electro-technical applications, it will have an optimal operating temperature. To determine this temperature it is essential to study the temperature dependence of the AC losses. In this work we have measured the AC losses of a Bi-2223 multi-filamentary tape at different temperatures. The sample was exposed to combinations of externally applied AC magnetic fields and AC transport currents. The losses were measured calorimetrically, at four temperatures between 38 K and 80 K, with a measuring system which provides the possibility to vary the temperature, the magnetic field, the transport current and the frequency independently. The losses are discussed in terms of an existing semi-empirical model based on the critical state model.

12–24

Transport ac losses and current-voltage characteristics of BiPbSrCaCuO-2223/Ag multifilamentary tapes with Ag and AgMg sheaths.

M.Majoros[1,2], *B.A.Glowacki*[1,3], *A.M.Campbell*[1], *M.Leghissa*[4], *B.Fischer*[5] and *T.Arndt*[5]. [1]IRC in Superconductivity,University of Cambridge,Cambridge,CB3 OHE,U.K. [2]Institute of Electrical Engineering,Slovak Academy of Sciences,Bratislava,842 39,Slovak Republic. [3]Department of Materials Science and Metallurgy,University of Cambridge,Cambridge,CB2 3QZ,U.K. [4]Siemens AG, ZT EN 4,Erlangen,D-91050,Germany. [5]Vacuumschmelze GmbH,HT-SE,Hanau,D-63450,Germany.

Transport ac losses and dc current-voltage characteristics of BiPbSrCaCuO-2223/Ag multifilamentary tapes with Ag and AgMg sheaths were measured. The samples were made by powder-in-tube technique and had 55 filaments. All samples were non-twisted and with respect to the filament arrangements they had the same architecture. AC losses were measured in the frequency range 40 Hz - 120 Hz. Some frequency dependence of the losses in the sample with the Ag sheath was observed at currents I/Ic <0.1. AC losses in the sample with the AgMg sheath were purely hysteretic. At I/Ic <0.2 the ac losses of the sample with the AgMg sheath were higher than those of the sample with the pure Ag sheath. Experimental results were compared with existing theoretical models. The possible influence of the intergrowths on dc current-voltage characteristics and ac loss behaviour was studied.

12–25

Superconductor modelling : an useful tool for ac losses.

E. Vinot[1], *P. Tixador*[1], *G. Meunier*[2] and *G. Donnier-Valentin*[1]. [1]CNRS-CRTBT/LEG, Grenoble, 38042, France. [2]LEG - CNRS/INPG-UJF, Saint Martin d'Heres, 38402, France.

A.c. losses play an important part in many superconducting applications to design the refrigerator system and to calculate the device efficiency. A.c. losses are calculated in general by analytical methods. These are based on the critical state model (J =± Jc or 0). But only simple geometries may be considered for analytical calculations. Otherwise high Tc materials do not show a sharp quench around Jc and so the critical state model can not be strictly used from a theoretical point of view. Only a numerical model may take into account practical geometries and the real E(J) curve (E : electrical field ; J : current density). A model of superconducting area based on the E(J) curve with a power law has been implemented into an existing finite element code (Flux3D). At present only 2D or axisymmetrical problems may be considered. Several numerical problems have been solved using an electromagnetic formulation with a suitable state variable. It has been possible for example to study geometrical effects and the stiffness of the quench ("n" value). The finite geometry is very important part in some cases. Some numerical calculations have been compared to experimental measurements and classical formula.

12–26

Magnetization and transport loss of Bi-2223 tapes in alternating magnetic field.

M.P. Oomen[1], *J. Rieger*[1], *M. Leghissa*[1], *J.J. Rabbers*[2] and *B. ten Haken*[2]. [1]Siemens AG, Corporate Technology, PO Box 3220, 91050 Erlangen, Germany. [2]Low Temperature Division, Faculty of Applied Physics, University of Twente, PO Box 217, 7500 AE Enschede, The Netherlands.

The magnetization loss in Bi-2223 superconducting tapes plays an important role in applications like power transformers. This type of AC loss can be significantly decreased only when the filaments in the tapes are electrically decoupled by twisting the filaments and increasing the matrix resistivity. We measured the magnetic AC loss at power frequencies with a pickup method at 77K. In moderate fields parallel to the tape plane, the filaments can be decoupled and the AC loss is decreased by filament twist, even if the matrix is pure silver. In tapes with high-resistance ceramic barriers between the filaments, decoupling is observed also in low-amplitude 50 Hz fields oriented perpendicular to the tape plane. The increase in matrix resistivity caused by such barriers is quantified by measuring the frequency-dependence of the magnetization loss. When the tape carries a DC or AC transport current close to its critical current, the transport loss becomes important as well. This transport loss with DC current in AC field is described by a dynamic resistance which depends on the field amplitude. The dynamic resistance in a superconducting slab with field-dependent critical current is calculated and compared to measurement results.

12–27

Scanning Hall Probe Imaging of Multifilamenary HTS Conductors: Implications for AC Losses.

G.K. Perkins, *J.E. Everett* and *A.D. Caplin*. Centre for High Temperature Super-conductivity, Blackett Lab., Imperial College London SW7 2BZ, UK.

The AC electrical characteristics of multifilamentary Ag-sheathed BSCCO tapes are crucial to the development of power applications incorporating these materials. One of the major concerns about present conductors is the hysteretic AC loss associated with current flow along superconducting intergrowths between individual filaments. Using a scanning hall probe technique we have studied the properties these intergrowths by imaging the sample magnetic remnance with spatial resolution approaching 10 microns. At this resolution we are able to resolve individual filements close to the sample surface, allowing the study of large scale defects and areas where intergrowths appear to be present.

12–28

Self-field losses and I-V curves of Bi-2223 tape without silver sheath.

M. Polak and *L. Jansak*. Institute of Electrical Engineering, Slovak Academy of Sciences Bratislava, 842 39 Slovakia.

I-V curves and self-field losses of a monocore $(BiPb)_2Sr_2Ca_2Cu_3O_x$ tape without silver sheath have been measured. The silver sheath was chemically removed from 1 cm long section of the sample to eliminate effects of Ag sheath (current sharing, eddy current losses). I-V curves of the bare tape carrying sinusoidal ac current $i = I_0 \sin\omega t$ with frequencies 23Hz, 83Hz and 203Hz were measured and compared with those measured under DC conditions (f≅5mHz). Three components contribute to the measured voltage: the resistive voltage, V_r, associated with movements of fluxoids, the self-field voltage, V_{sf}, generated by the flux changes due to the AC transport current, and the voltage V_i induced in the loop formed by potential wires and the tape. As predicted by the theory, the I-V curves measured with current increasing from - I_0 to + I_0 differ from those measured with current decreasing from +I_0 to -I_0, so that the I-V curves for the whole cycle show hysteresis. Transport current losses, P(W/m), were measured in the frequency range from 5 Hz to 203 Hz. Below the critical currrent (14A at 1μV and DC conditions) they are proportional $(I_0/I_c)^n$, where n was found $n = 3.6 \pm 0.1$. The n-factor was practically independent on the frequency in the range 5 Hz to 203 Hz. The energy loss per unit length per cycle, Q (J/m/cycle), for AC currents with $I_0 < I_c$ and 5 Hz < f < 203 Hz is frequency independent. With increasing amplitude I_0 the loss per cycle, Q, decreases with frequency f.

12–29

Weak AC Magnetic Field Influence on Nonlinear Flux Diffusion in the Mixed State of Superconductors.

A.L. Kasatkin, *V. V. Vysotskii* and *V. M. Pan*. Superconductivity Dept., Institute of Metal Physics, 36 Vernadsky str., Kiev 252142, Ukraine.

Several experiments have demonstrated the strong effect of weak AC magnetic field component on both the resistivity and the magnetization decay rate in the mixed state of type II superconductors. In the present work these effects are considered for the slab geometry on the basis of nonlinear flux diffusion equation, accounting for the existence of shielding or transport current inside the superconductor and also periodical boundary conditions due to the AC field influence. We have obtained the results for the AC field-induced 'dynamical' DC resistivity as well as for the increase of magnetization decay, which correspond to increasing of the flux creep rate caused by the AC field in nonlinear flux diffusion case, and are characterized by power-like dependencies on the AC field amplitude and frequency.

12–30

What causes the steep increase of the critical current density below 20 K in Bi-based superconductors?.

M. R. Koblischka and *M. Murakami*. SRL/ISTEC, Div.3, 1-16-25 Shibaura, Minato-ku, Tokyo 105, Japan.

In all Bi-based superconductors (Bi-2212, Bi-2223) the critical current density is found to increase steeply when decreasing the temperature below 20 K. The origin of this increase provides an important issue to understand the pinning mechanism in these strongly layered superconductors. Recent magneto-optic (MO) observations on monofilamentary Bi-2223 tapes have shown that the granularity increases when lowering the temperature below 20 K, which clearly points to an increase of the intragranular pinning. Measuring superconducting transitions in field-cooled cooling (FCC) and Ewarming (FCW) modes in external magnetic fields between

1 mT and 7 T on various Bi-based superconductors (Bi-2212 single crystal, Bi-2212 partial melt-textured compound, Bi-2223 mono- and multifilamentary tapes) shows that there is a second step in the transitions, appearing in fields > 2 T at temperatures between 20 and 40 K, depending on field and sample type. Possible reasons for this second step are discussed

12–31

Alternative approach to the hysteresis of transport current in Bi-based tapes.

P. Nalevka[1], *M. Jirsa*[1], *M. R. Koblischka*[2] and *D. Dew-Hughes*[3]. [1]Institute of Physics AV CR, Na Slovance 2, 182 21 Praha 8, Czech Republic. [2]SRL/ISTEC, Div. 3 1-16-25 Shibaura, Minato-ku Tokyo 105 [3]Department of Engineering Science, University of Oxford, Oxford OX1 3PJ, UK.

Tapes of Bi-2212 and Bi-2223 prepared by different technologies were studied in a wide range of temperatures and external magnetic fields. As a major source of information, we use critical current densities associated with the total magnetic moment induced in the sample by a linearly varying applied magnetic field. To distinguish between intragranular and intergranular (transport) superconducting currents, the samples were bent to a small diameter, and measured both before and after the bending. After subtracting the contribution due to intragranular currents obtained from the latter measurement, the behaviour of intra- and intergranular currents could be investigated separately. As a result, a hysteresis of the transport current density was observed. Character and appearance of this effect in Bi-2212 tapes is very similar to that usually found in Bi-2223 tapes but not so pronounced. To describe this effect more exactly, we propose an alternative phenomenological description. This model allows us to compare different samples and to draw conclusions on a possible origin of such a behaviour. We conclude that the observed data cannot be explained by stray fields from intragranular currents.

12–32

Transport AC losses in (Bi,Pb)SrCaCuO-2223/Ag (6+1) multifilamentary tapes with different architecture.

M.Majoros[1,2], *B.A.Glowacki*[1,3], *A.M.Campbell*[1], *M.Apperley*[4] and *F.Darmann*[4]. [1] IRC in Superconductivity, University of Cambridge, Madingley Road, Cambridge CB3 OHE,U.K. [2]Institute of Electrical Engineering, SAS, Bratislava, Slovak Republic. [3]Department of Materials Science and Metallurgy University of Cambridge, Pembroke Street, Cambridge CB2 3QZ, U. K. [4]Metal Manufactures Ltd., Australian Technology Park, Eveligh, 1430, Australia.

Transport ac losses in multifilamentary (Bi,Pb)SrCaCuO-2223/Ag tapes with different filament arrangements have been measured. The samples were untwisted and had 7 filaments, which were arranged in columns, in slanted columns or evenly distributed across the tape cross-section. The aspect ratio of the samples as well as their filamentary regions was the same. The ac losses were measured in the frequency range 40 Hz – 120 Hz. Two different methods to determine the critical current were used: from dc current-voltage characteristics and from the saturation value of ac losses. The experimental results were compared with theoretical models. The normalized ac losses approximately follow the theoretical dependence for a tape with rectangular cross-section of similar aspect-ratio. It was found that the sample with filaments stacked in columns had slightly lower normalized losses at low currents in comparison with other filament arrangements. It was also observed that tapes containing bridged filaments, but having similar critical currents, had variable normalized ac loss.

12–33

Introduction of Flux-Pinning Defects in Bi-2212 Superconducting Tapes.

T. Haugan, *W. Wong-Ng*, *L. P. Cook*, *H. J. Brown* and *L. Schwartzendruber*. National Institute of Standards and Technology Gaithersburg, MD 20899 U.S.A.

The lack of intrinsic flux-pinning centers in $Bi_2Sr_2CaCu_2O_{8+x}$ (Bi-2212) high temperature superconductors (HTS) limits their usefulness for applications >20K. This paper will study the effect of adding defects to practical Bi-2212 conductors to enhance flux-pinning, and raise the effective operating temperature of these conductors. Possible defects to be studied include intrinsic secondary phase defects $(Sr,Ca)_{14}Cu_{24}O_{41+y}$ (14:24) or $Bi_3(Sr1\text{-}xCax)_7O_y$ (3430) and artificial defects including ZrO_2, MgO, and Al_2O_3. Reactions of defects with the melt, their influence on phase assemblages, and possible methods of compensating for reaction effects will be examined. The effect of flux-pinning defect size and density on critical current density (J_c) will be evaluated, and compared to the theoretical model, $J_c \sim V_f/d$, where V_f is the volume fraction of pinning defect, and d is the defect size. Preliminary results show improvement of flux-pinning with introduction of $V_f < 4\%$ of Al_2O_3 and 14:24 defects.

12–34

Transport Properties of $Bi_2Sr_2CuO_{6+\delta}/CaCuO_2$ Multilayers Obtained by Molecular Beam Epitaxy.

S.L. Prischepa[1], *M. Salvato*[2], *C. Attanasio*[2], *G. Carbone*[2] and *L. Maritato*[2]. [1] State University of Informatics and RadioElectronics, State University of Informatics and RadioElectronics, Minsk, 220600, Belarus. [2]INFM and Dipartimento di Fisica Università di Salerno, Baronissi, Salerno,84081,Italy.

Transport properties of $(Bi_2Sr_2CuO_{6+\delta})_m/(CaCuO_2)_n$ multilayers, obtained by Molecular Beam Epitaxy (MBE) with the same number of $Bi_2Sr_2CuO_{6+\delta}$ unit cells (n=1) and different numbers (m) of $CaCuO_2$ layers, have been studied. Resistivity vs. temperature and current voltage characteristics, measured at different values of the external magnetic field and bias current, show a strong structure dependence of the superconducting properties. The superconducting anisotropy parameters have been estimated from the experimental results. The irreversibility line has been extracted from the R vs. T measurements for different samples and an explanation of its nature has been proposed.

12–35

Influence of collective interaction of turns on transverse-field losses in superconducting multifilamentary wires.

K. Kajikawa, *A. Takenaka*, *M. Iwakuma* and *K. Funaki*. Kyushu University, Fukuoka, 812-8581, Japan.

It is very important to understand an accurate AC loss property of superconducting wire because it is one of the key parameters to design superconducting devices or apparatuses for AC use. In this paper, we quantitatively evaluated the AC losses of some sample coils with different distances between turns of a NbTi multifilamentary wire. The AC losses of the sample coils exposed to a transverse magnetic field were measured by a pickup-coil method. The obtained transverse-field losses scarcely depend on frequency, and are hysteretic. The AC losses of the sample coils have a good agreement with each other in the higher range of amplitude of external magnetic field. On the other hand, the AC losses in the smaller range are influenced by the distance between turns of the sample coils. Taking into account an effective demagnetization factor defined by the geometrical parameters of the sample coils, the AC losses are plotted on a master curve for the magnetic field on the surface of the sample wire.

12–36
AC Losses in Bi-2223 Multifilamentary Tapes.
F. Sumiyoshi[1], *K. Fukushige*[1], *M. Nakagami*[1] and *H. Hayashi*[2]. [1]Kagoshima University, Kagoshima, 890-0065, Japan. [2]Kyushu Electric Power Co. Inc., Fukuoka, 812-0053, Japan.

Short and straight samples of Bi-2223 multifilamentary tapes are measured in liquid nitrogen in case of simultaneous sweep of ac transport currents and external transverse ac magnetic-fields. A new system is developed for this measurement, in which Poynting vectors around the sample are measured by using a movable set of a potential lead pair and a miniature pick-up coil for each flat face of tapes. This is considerably useful for various external condition of transport currents and transverse magnetic fields applying to short samples as long as longitudinal change in the magnetic field can be neglected. In order to compare and discuss the result of the short sample, moreover, ac loss measurements of coils which are wound by this tape into double pancake shape are also carried out by using another new system.

12–37
AC losses in filamentary YBCO/hastelloy superconducting tapes.
K.H. Müller, *N. Savvides* and *J. Herrmann*. CSIRO, Telecommunications and Industrial Physics, Sydney 2070, Australia.

The AC hysteresis loss of a long YBCO thin-film superconducting strip in a perpendicular AC magnetic field can be reduced by subdividing the film into narrow parallel strips (filaments). The hysteresis loss depends on the film critical current density J_c, the film thickness d, the filament width $2a$ and the lateral spacing L between filaments as well as on the AC magnetic field amplitude H_m. In addition, if the film is deposited onto a YSZ/hastelloy substrate to form a flexible tape, eddy current loss occurs in the hastelloy metal. The eddy current loss depends on the resistivity ρ of the hastelloy, the width $2w$ and thickness d_m of the hastelloy substrate as well as on the frequency f and amplitude H_m. We have calculated the hysteresis and eddy current losses as a function of J_c, d, a, L, ρ, w, d_m, f, and H_m to find optimal design parameters for a YBCO/hastelloy tape. As the AC loss is related to the loss component χ'' of the AC susceptibility, we have measured χ'' at different frequencies f and amplitudes H_m for several filamentary designs of YBCO/hastelloy tapes and compared our experimental results with our model calculations.

12–38
Magnetic AC Loss Measurements using Hall Sensor Magnetometry.
M.P. Staines[1], *S. Rupp*[1], *A.D. Caplin*[2] and *S. Fleshler*[3]. [1]Industrial Research Ltd, Lower Hutt, New Zealand. [2]Imperial College, London SW7 2BZ, UK. [3]American Superconductor Corporation, Westborough, MA 01581, USA.

Hall sensor magnetometers have found use in the measurement of magnetic AC loss in superconductor tapes largely because of their simplicity and good low frequency response compared to pick-up coil methods. However calibration to give the total moment of the sample, and hence the loss, is difficult because the field measured at the sensor depends on the details of the current distribution in the tape. We show that the induced currents for fields normal to the face of the tape can be decomposed into circulating currents flowing: (i) at the edges of the tape, or (ii) penetrating to its centre, as in the critical state model. By making measurements at an appropriate distance from the tape, close enough that Hall sensors still have adequate sensitivity, but far enough away for higher order moments of the current to be negligible, these idealised current distributions lead to reliable estimates of the magnetic moment. We present a simple interpretation of the loss curve as a function of frequency for multifilament tapes which makes it straightforward to identify the relevant current distribution regimes.

Session Fault current limiters and related materials

12–39
Current Limiting Properties of YBCO-Films on Sapphire Substrates.
A. Heinrich[1], *R. Semerad*[1], *H. Kinder*[1], *H. Mosebach*[2] and *M. Lindmayer*[2]. [1]Technical University of Munich, Physics Department E10, 85748 Garching, Germany. [2]Technical University of Braunschweig, Institut für Hochspannungstechnik, D-38023 Braunschweig, Germany.

We have studied the switching of YBCO thin film resistive fault current limiting devices. Films of 300 nm thickness were deposited on 2 inch and 4 inch sapphire substrates by thermal co-evaporation. Bridges 10 mm wide and 22 mm long (2 inch) or 42 mm long (4 inch) were structured by standard photolithography. Contacts were made by in-situ gold overlayers and soft solder. The gold film was removed from the switching area so that the YBCO film was not shunted. The films were tested by 30 μs DC pulses and 50 Hz AC pulses for 50 ms. We find evidence that at the AC tests heat propagates over several cm under these conditions in sapphire so that hot spots can be avoided even without shunt layer with the prospect of higher switching power. The highest destruction free switching power - the rms critical current times rms voltage after switching - was 57 kVA. The highest switching power density achieved was 2.5 kVA/cm^2.

12–40
Shaping and Assembling of HTS Bulk Materials for High-Current Applications.
J. Reichert, R. Ochs, M. Kläser and *M. Sander*. Forschungszentrum Karlsruhe GmbH, INFP, P. O. Box 3640, D-76021 Karlsruhe.

Shaping and assembling techniques are prereqisites for the fabrication of High-Temperature Superconductor-(HTS)-based components like current leads or current limiters. First of all, this includes pressing of HTS powders to near end-shapes, melt-texturing processes to obtain high-quality HTS parts as well as cutting and polishing steps. More complex and larger structures, however, make additional steps necessary: In this respect we used a joining technique, which employs YbBaCuO as a superconducting solder for our YBaCuO parts. The critical currents obtained for such superconducting joints are comparable to those of our melt-textured YBaCuO. Finally, high transport-current applications require high-quality metal contacts to reduce contact heating. By using commercially available Ag pastes and solders, specific contact resistances of below 1 $\mu\Omega cm^2$ can be obtained routinely. Details of electrical and microstructural characterizations will be presented.

12–41
Ceramic Substrates for Bi-2212 Partial Melt Processing.
S. Köbel, D. Schneider, R. Nussbaumer and *L.J. Gauckler*. Swiss Federal Institute of Technology, CH-8092 Zürich, Switzerland.

Melt processing of polycrystaline thick films of high-temperature superconductors requires substrate materials that are inert against the oxide melt and closely match thermal expansion of the film. Different oxide ceramic materials (Al_2O_3, CeO_2, MgO, $BaZrO_3$) are evaluated in respect of reaction behavior, diffusion of cations (to/from the superconductor) and especially resulting electric properties of Bi-2212 films. As compared to thick films processed on silver substrates, only MgO does have a favourable combination of the evaluated properties. Thick Films processed on MgO do have the same high critical current densities as those processed on silver. The thick films processed here are due to their high current capacities and their nonconductive substrate promising candidates for applications in devices like resistive type current limiters.

12–42
Critical Current Densities in Bi-2212+Ag / MgO Thick Films.
S. Köbel, D. Schneider, L. Fall, P. Sütterlin and *L.J. Gauckler*. Swiss Federal Institute of Technology, CH-8092 Zürich, Switzerland.

Thick films of Bi-2212 with silver additions (0-6 wt.-%) were produced by tape-casting and subsequent partial melting. The aim of this study was to investigate the influence of silver additons on processing parameters and critical current densities (77K, selffield) of Bi-2212 thick films processed on polycrystalline MgO substrates. Silver additons are known to decrease the peritectic melting temperature of Bi-2212. It was found, that critical current densities of melt processed films depend strongly on Ag content and that maximum densification temperature had to be within a narrow processing window slightly above the solidus temperature of the particular composition. Current carrying capacities of up to 50 A/cm^2 were reached in untexured thick films. Those films are thus highly suitable for applications in power engineering.

12–43
Non-Uniformities In Multifilament Superconductors - Influence On Quench Currents Under Fast Current Change.
V.S. Vysotsky[1,2], *Y.A. Ilyin*[1,2], *K. Funaki*[1], *M. Takeo*[1], *K. Shimohata*[3], *S. Nakamura*[3], *T. Kaito*[4], *K. Hasegawa*[4] and *A.L. Rakhmanov*[5]. [1]Kyushu University, Fukuoka, 812-8581, Japan. [2]Visiting scientists from Kurchatov Institute, Moscow, Russia. [3]AT R& D Center, Mitsubishi Electric Co, Japan. [4]TRC, Kansai Electric Power Company, Japan. [5]SCAPE, Russian Academy of Science, Moscow, Russia.

The magnitude of quench currents under fast current change is a very important parameter for designing of resistive type Fault Current Limiters. We studied quench currents under fast current rise in several samples of multifilament superconducting wires with highly resistive matrix. The samples have different wire diameters, different length and different cooling conditions. All samples were provided by several potential taps to find out the quench spots along the length. We observed sufficient scattering of quench currents along the samples. Quench current in each part of the sample depends on current rise rate and may differs as much as 1.5 times. At relatively slow current rise, only one normal spot is the source of normal zone that propagates along a sample. At average ramp rate, several normal spots may appear in different points independently. At very fast current rise rate, entire sample quenches simultaneously. Variation of quench currents along a wire may have a serious impact on Fault Current Limiter behavior. We analyzed the reason of quench current scattering and suggested that variation of cooling conditions along the sample is a major reason. Anyway, critical current variations and mechanical looseness may contribute also.

12–44
Non-Uniformities In Multifilament Superconductors - Influence On Quench Development Under Fast Current Change.
V.S. Vysotsky[1,2], *Y.A. Ilyin*[1,2], *K. Funaki*[1], *M. Takeo*[1], *K. Shimohata*[3], *S. Nakamura*[3], *T. Kaito*[4], *K. Hasegawa*[4] and *A.L. Rakhmanov*[5]. [1]Kyushu University, Fukuoka, 812-8581, Japan. [2]Visiting scientists from Kurchatov Institute, Moscow, Russia. [3]AT R& D Center, Mitsubishi Electric Co, Japan. [4]TRC, Kansai Electric Power Company, Japan. [5]SCAPE, Russian Academy of Science, Moscow, Russia.

Normal zone propagation velocity (NZPV) under fast current rise is a major parameter for resistive type Fault Current Limiters design. Normal zone propagation contributes to the total resistance rise during current ramp that determines limiting properties of FCL. We studied quench currents and NZPV under fast current change in several samples of multifilament superconducting wires with highly resistive matrix. All samples demonstrated sufficient scattering of

quench currents along samples. That fact leads to corruption of meaning of NZPV, especially if it is measured by total voltage rise. Different parts of a sample quench at different times. NZPV in these parts depends on both current and current rise rate values. Rather erratic combination of quench events in different parts of the sample contributes to total resistance increase. When current rise rate reaches certain value, almost all sample parts quench simultaneously. In that case, it is impossible to say anything reasonable about "normal zone propagation" also. We observed such simultaneous quench in our experiments. In the paper we present experimental data about quench development under fast current rise in different samples with non-uniformities along their length. We also analyze the impact of wires non-uniformity on quench development and limiting properties of FCL

12–45

Quench behaviour of high temperature superconducting bulk material in resistive fault current limiters.

M. Noe[1], *K.-P. Juengst*[1], *F. N. Werfel*[2], *M. Baecker*[3], *J. Bock*[3] and *S. Elschner*[4]. [1] Forschungszentrum Karlsruhe, Institut fuer Technische Physik, Eggenstein-Leopoldshafen, 76344, Germany. [2] Adelwitz Technologiezentrum GmbH, Adelwitz, 04886, Germany. [3] Aventis Research & Technologies, Hürth, 50351, Germany. [4] Fachhochschule Mannheim, Mannheim, 68157, Germany.

Both the resistive and the inductive superconducting fault current limiter (SFCL) are higly attractive. So far, BSCCO bulk material for the inductive SFCL as well as YBCO thin films for the resistive one have been favoured. For resistive SFCL, the use of superconducting bulk material may provide a cheaper alternative. For this reason, first experiments with melt textured YBCO and melt cast (MCP) BSCCO bulk materials have been carried out in order to prove the suitability of these materials to limit fault currents effectively. Test results with differently shaped YBCO and BSCCO and with a BSCCO bifilar coil are presented. This bifilar coil enables a superconductor length of 1,8 m without any intermediate contact. The experiments to measure the quench propagation show a strong influence of material inhomogenities and contact resistances on the quench behaviour. Furthermore, a simple method to adjust the temperature of rod shaped superconductors has been applied. The measurements show that the investigated materials are candidates for the use in resistive SFCL's.

12–46

Computer Modelling of Superconducting Fault Current Limiters.

R.A.Weller, *A.M.Campbell*, *T.A.Coombs* and *R.J.Storey*. IRC in Superconductivity, Madingley Road, Cambridge CB3 0HE, UK.

Two computer models have been developed to aid in the design of superconducting fault current limiters (SCFCLs). The first is an overall FCL model which models the interaction between a FCL and the line / load characteristics, giving as output the resultant current waveform and superconductor temperature. The second is a 'cellular' model which addresses the problem of material inhomogeneity. The cellular model allows us to predict the effect of variations in Jc, thickness, and resistivity over the surface of a film, and thermal properties such as heat capacity and substrate conductivity can be explored. It is hoped that this model will provide us with details of 'acceptable limits' of manufacture, allowing materials processing to be directed towards optimising the superconductor for a given application. In order to confirm computer predictions we have developed an automated testing rig, which subjects FCLs to typical fault conditions. This allows physical processes to be recorded and ensures good correlation between predicted and measured results.

12–47

Characteristics of Bulk Superconducting Cylinder for Magnetic Shielding Type Superconducting Fault Current Limiter.

S.N. Noguchi, *A.I. Ishiyama* and *H.U. Ueda*. Dept. of EECE, Waseda University, 3-4-1 Ohkubo, Shinjuku-ku, Tokyo 169-8555, Japan.

The superconducting fault current limiter (SCFCL) is expected to be a new application of bulk High-Temperature superconductors (HTS) in power systems. To develop a magnetic shielding type superconducting fault current limiter, we have carried out some fundamental experiments concerning the magnetic shielding characteristics of bulk HTS cylinders, and have analyzed its magnetic characteristics using the Finite Element Method (FEM). Test sample is Bi-2223 cylinder with OD 52mm, ID 47m and 70mm height. The AC magnetic field is applied to the sample by the coaxial copper winding coil excited by AC sinusoidal- and triangular-waveform currents in the frequency range of 0.1Hz to 100Hz. We have also developed a FEM computer program for evaluation of the magnetic field including the bulk HTS considering E-J characteristic. However, the dynamic characteristics of the bulk HTS cylinder in real operation of SCFCL is affected on the evolution temperature distribution in the bulk HTS. In this paper, the analytical results on the thermal and electromagnetic behaviors of the bulk HTS cylinder of SCFCL in the current operation are shown.

12–48

Utility Survey of Requirements for a HTS Fault Current Limiter.

J.N. Nielsen[1], *P. Joergensen*[1], *J.J. Oestergaard*[1] and *O. Toennesen*[2]. [1]DEFU Research Institute of Danish Electric Utilities, P.O. Box 259, 2800 Lyngby, Denmark. [2]Department of Electric Power Engineering, Technical University of Denmark, 2800 Lyngby, Denmark.

Utility Survey of Requirements for a HTS Fault Current Limiter J. N. Nielsen, P. Joergensen, J.J. Oestergaard, O. Toennesen Department of Electric Power Engineering, Technical University of Denmark DK-2800 Lyngby, Denmark DEFU, Research Institute of Danish Electric Utilities P.O. Box 259, 2800 Lyngby Denmark The application of Superconducting Fault Current Limiters (SFCL) in the electric utility industry will clearly be dependent on to what extension the needs and requirements from the utilities can be met by the ongoing development of SFCL technology. Up to now, a number of studies have been carried out concerning different design concepts of fault current limiters and their

potential applications in different locations of the power system networks. Although a full-scale and cost-effective SFCL has not been presented yet, there is no doubt that SFCL will be a strongly alternative to the existing protection systems in the coming highly deregulated electric power sector. This paper considers a questionnaire survey of which needs and expectations the Danish electric utilities have to this new state-of-the-art technology. Based on the results of that investigation design and operating specifications required for a SFCL, addressed for transmission, medium and distribution voltages are stated. It also gives a review of how the short-circuit capacity can be reduced in a distribution substation by use of a SFCL. The advantages and limitation performance of the SFCL are compared with the existing protection system.

12–49

Resistive current limiter with Bulk Bi:2223.

J.G. Noudem[1,2], *J. M. Barbut*[2], *O. Belmont*[2], *D. Bourgault*[1], *J. Sanchez*[2], *P. Tixador*[3] and *R. Tournier*[1]. [1]CRETA, CNRS, B.P. 166, 38042 Grenoble cedex 09, France. [2]SCHNEIDER ELECTRIC S.A, A3, rue Volta,38050 Grenoble cedex 09, France. [3]CRTBT/LEG, CNRS, B.P. 166, 38042 Grenoble cedex 09, France.

Two forms of the samples have been elaborated and investigated at 77 K using pulsed currents with a duration of 20 ms. The rod formed by isostatic pressure and classical sintering. 60 rods have been assembled in serie. This assembling has been tested up to 1100 V at 1080 A instead of a theoretical value of 5000 A. In order hand the pellet textured by hot forging have been made. Short bar and meander sample connected have been prepared and tested. The critical current density up to 3500 A/cm2 at 77 K has been measured. In the normal state, electrical fields of 1600 V/m have been obtained without any degradation of the materials. Here we Study the recorery of the superconducting state and analyse the transition of the samples.

12–50

Key Design Issues of YBCO Current Leads: Low Resistance Contacts.

U.F. Delor, *R. Rothfeld*, *D. Wippich* and *F.N. Werfel.* Adelwitz Technologiezentrum GmbH, Adelwitz, D-04886, Germany.

Low heat transfer at high currents is the key issue of HTS current leads. Practical application of the excellent high transport critical currents of up to 10 kA/cm^2 of multi -grain bulk YBCO is severely limited, due to insufficient large contact resistances and a degradation behaviour of the joints after several cooling cycles. Joule heating locally at the small contacts cause inhomogeneous current transport properties and a catastrophic quench dynamics in the kA range. Tests has been performed on fabricated melt textured functionally gradient YBCO rods with a longitudinal a - b crystal orientation and different contact shapes. We have compared in - situ contact processing and YBCO ex - situ surface preparation techniques of Ag, Au , Cu metals giving values $<1\mu$W / cm^2 at current densities of 5 kA/cm^2 and 77 K. We report the preparation of low resistance metallic contacts on bulk YBCO at an economical level. Current - voltage measurements of the contacts in different directions exhibit a superconducting to normal state transport characteristic of the interface correlating with the local orientation of the YBCO crystals. Electrical leads can be directly clamped or soldered to the > 10 μm thick and mechanically stable metallic interfaces on YBCO.

12–51

Quench transition in high current bulk YBCO elements for Fault Current Limiters.

E. Mendoza[1], *X. Granados*[1], *T. Puig*[1], *E. Varesi*[1], *L. García-Tabarés*[2] and *X. Obradors*[1]. [1]Institut de Ciència de Materials de Barcelona, CSIC, Campus UAB, 08193 Bellaterra, Spain. [2]Centro de Estudios de Técnicas Aplicadas, CEDEX, Alfonso XII, 6, 28040 Madrid, Spain.

Melt textured $Yba_2Cu_3O_7/Y_2BaCuO_5$ composites have been grown in a bar shape by means of Bridgman growth, which leads to single domains having the ab planes oriented at $\simeq 30^o$ from the long axis. The use of these elements as variable impedances in a hybrid-type Superconducting Fault Current Limiter has been analysed. First of all, a non-destructive technique for the long bars has been developed based on the measurement of levitation forces in a system having a localised magnetic gradient. The system is based on the measurement of local hysteresis loops.
The quench transition of bar elements having a total length of $\simeq$ 30-40 mm has been investigated using ac currents up to $\simeq$ 3.500 A in a transformer system where the superconducting elements are protected from excessive energy dissipation. It has been found that the quench transition in high critical current elements with a diameter of 6 mm are invariably initiated at the electrical contacts, even with contact resistances as low as $0.5\mu\Omega$cm^2. An strategy to overcome this problem and be able to induce an homogeneous quench transition through all the sample will be discussed in conjunction with the study of the electrothermal behaviour of these superconducting elements during the quench transition will be discussed.
Work partially financed by the EU through BE97-4829 (BY-FAULT project).

12–52

Large - Area YBCO-Sputter Deposition for Fault Current Limiters.

W. Klein[1], *U. Pyritz*[2], *R. Wördenweber*[1], *B. Holländer*[1], *R. Kutzner*[1], *H. Schiewe*[2], *J. Einfeld*[1], *S. Bunte*[1] and *U. Krüger*[2]. [1]Forschungszentrum Jülich, ISI, D-52425 Jülich, Germany. [2]Siemens AG, ZT MF5, Siemensdamm 50, D-13629 Berlin, Germany.

The development of a reliable and reproducible process for the deposition of large-area (up to 20x50 cm2) HTS films requires serious modifications of existing conventional planar sputter devices, in order to adopt a suitable stable high-pressure and high-temperature process. Especially, high-pressure magnetron cathodes and substrate heater have to be developed. Due to the requirements of a project on fault current limiters and using our experience of the successful YBCO deposition dc sputter devices for 2" substrates we constructed and developed a sputter device for deposition of up to 20x50 cm2 substrates. The automised sputter device is equipped with three 70cm long planar magnetron cathods driven by unipolar pulse dc-power supply at vari-

able frequencies between 50 and 250 kHz. Substrate heater and cathode are successfully tested. Optimal pulse frequencies for YBCO targets proved to range about 135 kHz. First YBCO depositions are executed. The films are characterised via x-ray, RBS, resistive and inductive measurements. The technological problems with emphasis on the stabilisation of the plasma and homogeneity of the substrate temperature as well as depositions results will be presented and discussed in the context of given requirements.

12–53
Thermal characterization of an inductive fault current limiter*.
L.G. Sanz, *M.R. Osorio*, *S.R. Currás*, *J.A. Veira*, *J. Maza* and *F. Vidal*. Laboratorio de Bajas Temperaturas y Superconductividad, Universidad de Santiago de Compostela Santiago de Compostela, E-15706, Spain.

We will report experimental results about the electromagnetic and thermal responses of a superconducting inductive fault current limiter. The device is based on the magnetic coupling between a coil, fed with low frequency A.C. current, and a superconducting ring through a metallic core. Dimensions of the samples are from 1 cm height, 1 cm internal diameter and 0.2 cm thickness. These are textured rings with critical current densities from 300 A/cm^2, which can be measured by using the device itself. The response of the system will be characterized at different refrigeration conditions and for various core materials. Other thermal dissipation aspects will also be studied. *This work has been supported by a grant from UNIÓN-FENOSA, Spain.

12–54
Current limitation by YBCO single domains.
P. Tixador[1], *J.M. Duval*[1], *D. Bourgault*[2], *R. Tournier*[2] and *D. Isfort*[2]. [1]CNRS-CRTBT/LEG, Grenoble, 38042, France. [2]CNRS-Laboratoire de Cristallographie, Grenoble, 38042, France.

The natural quench of a superconductor from the superconducting state to a resistive state by overstepping a threshold current brings a new function : the limitation of fault currents under high voltages. Not possible by conventional techniques, this is very attractive and of real need. The YBaCuO single domains show high performances in term of critical current density and resistive state electrical field but they are very sensitive to hot spots. The samples are very often destroyed after a limitation in liquid nitrogen. By adapting the material properties and above all the operating temperature it is possible to avoid destructive hot spots. This paper will present theoretical requirements based on a self protected concept and some experiments using several YBCO samples tested in liquid argon. A sample is self protected when the dissipated energy may be absorbed without damage by its enthalpy. From this concept a maximum critical current density may be deduced and an order of magnitude is 100 MA/m^2. This value may be achieved by an operation at temperatures higher than 77 K. The reduction of the temperature margin with the normal state is another favourable point. Samples with "low" J_c have effectively shown reproducible quenches without damage.

12–55
Rectifier Type Fault Current Limiter by Use of Micro SMES.
T.Ise, *T.Oka*, *N.H.Nguyen* and *S.Kumagai*. Department of Electrical Engineering, Graduate School of Engineering, Osaka University, 2-1, Yamada-oka, Suita, Osaka, 565-0871, JAPAN.

This paper proposes a rectifier-type fault current limiter using Micro SMES (Superconducting Magnetic Energy Storage). The proposed system is composed of a small superconducting coil, a three phase diode rectifier connected in series with the power line through a coupling transformer and an ac/dc converter connected in parallel with the power line. The superconducting coil is automatically inserted to the line through the diode rectifier and can limit the increase of the line current when a fault is occurred. Features of the system are as follows. 1) Fault current can be limited immediately and automatically without detecting the fault. 2) The system returns to a normal operation automatically after clearing the fault. 3) The ac/dc converter do not have to be operated at a usual condition, which is operated at the initial charging of the superconducting coil and at compensating the voltage drop of the bus caused by the fault in the utility grid network. The system is suitable for an interface device between a utility grid network and dispersed type generators such as a co-generation system and an IPP (Independent Power Producers). Design of the system, computer simulation and experimental results will be presented in the paper.

12–56
The Effect of Jc and Magnetic Shielding Capacity on the Performance of Superconducting Screening Fault Current Limiter.
I.-G. Chen and *J.-M. Lin*. Dept. of Materials Sci. & Eng., National Cheng Kung Univ., 1 Ta-Hsueh Rd., Tainan, Taiwan, R.O.C.

The single-grained YBCO high Tc superconductors (HTS) offer applications in the field of Superconducting Screening Fault Current Limiters (SSFCL) in electric power networks. The current limiting mechanism is related to the magnetic shielding effect of superconductor. Current limitation can be accomplished by means of the non-linear impedance of a transformer with a primary winding carrying the power circuit current and a short-circuited secondary winding consisting of a hollow cylinder or rings of single grained YBCO material. The latter remains superconductive at normal load level, which act as a magnetic flux shielding device to provide low impedance. If a defined current level is exceeded a certain level, which generates a sufficient high magnetic flux penetrating into the superconducting ring, the secondary winding turns resistive, providing a high impedance which limits the prospective fault current. Ring-shaped single grained YBCO materials with different thickness, height, and Jc(H) have been produced by Top-Seeding Melt-Textured method. The relationship between the superconducting properties and the current limiting performance will be reported.

12–57

Current Induced Transition into a Highly Dissipative State: Implication for the Fault Current Limiter.

L. Antognazza[1], *M. Decroux*[1], *N. Musolino*[1], *J.-M. Triscone*[1], *W. Paul*[2], *M. Chen*[2] and *Ø. Fischer*[1]. [1]Department of Condensed Matter Physics, University of Geneva, 24 Ernest Ansermet, 1211 Genève 4, Switzerland. [2]ABB Corporate Research, 5405 Baden, Switzerland.

In this presentation we report on the I-V characteristics at high current densities measured on $YBa_2Cu_3O_7$ thin films grown on 2" sapphire substrates. These experiments were carried out with short, constant, current pulses, ranging from a few microsecondes to a milliseconde, applied to superconducting strip lines with lengths ranging from 0.2 to 4 cm. Several pairs of voltage leads attached to the 4 cm line allow to map the time and position dependence of the I-V characteristics. When the current exceeds 2-3 times the conventional critical current, an abrupt transition into a highly dissipative state occurs. Detailed investigations on the thermal behavior of the superconducting line during the current pulse show that its temperature is still below T_c when the highly dissipative state appears. This indicates that this transition is indeed induced by the current as previously reported by Doettinger et al and Xiao et al. Direct measurements of the temperature of the superconducting line during the current pulse support this idea. The implications of these results for thin films based fault current limiters will be discussed.

12–58

A Small Scale Test Model for an AC-Fault Current Limiter.

B.A.Aminov[1] and *H.Piel*[1,2]. [1]Cryoelectra GmbH, Wettinerstr. 6H, 42287 Wuppertal, Germany. [2]Bergische Universitaet, Gaussstr. 20, 42096 Wuppertal, Germany.

We report on a small scale model of a resistive ac-fault current limiter for testing various ideas of conductor architectures based on YBCO-coated substrates suitable for this application. Attention is focussed on a planar YBCO conductor incorporating a new method of thermal stabilization. The trapped $1 \div 10\,\mu m$ thick normalconducting patches silver or gold were deposited on the YBCO film instead of ordinary used continuos thin (less than 100nm) stabilizing layer. This method permits essentially increase the FCL-resistance in the triggered (switched) state, utilizing high resistivity of HTS- material, and to increase the heat "mass" of conductor. As a result the required conductor length can be drastically decreased compare to the thin film stabilization method, and a current limiter for essentially higher power levels can be constructed. The described method was successfully tested on the small scale 24V/10A YBCO film FCL-model. The obtained experience will be applied for the constructing of a resistive FCL based on YBCO-coated metallic biaxially textured substrates. This work was supported in part by German BMBF under the contract N137265.

12–59

Properties of the quench release in current-carrying thin film HTS.

B. Heismann. B. Heismann, Siemens AG Erlangen, ZT EN 4, Paul-Gossen-Str. 100, 91050 Erlangen, Germany.

For the implementation of YBaCuO thin films in the construction of a resistive fault current limiter, the homogeneity of the phase transition between the superconducting and the normal state is deceisive. A direct optical observation method based on high-speed imaging of the local energy dissipation is used to gain information on the spatial release and propagation of a quench. Digital image anaylsis of an image series yields two-dimensional time- and space resolved maps of the superconductor state. Combined with magnetic hall array measurements the results allow to investigate the fundamental properties of superconducting loss mechanisms. Their correlation to intrinsic material properties like defects and the $j_(c)$ distribution or extrinsic aspects like the geometry of a current- carrying strip is discussed.

12–60

Current Limiting Characteristics of Inductive Fault Current Limiter Using YBCO Bulk Superconducting Ring.

D. Ito, *S. Harada* and *O. Miura*. Tokyo Metropolitan University, Hachioji, Tokyo, 192-0397, Japan.

High TC superconductors will be applied to fault current limiters. An inductive fault current limiter model using a single domain YBCO bulk ring has been built and tested. In the fault current limiting behaviors, voltage spikes were observed in higher voltage tests. Limiting behavior of the limiter accompanied with voltage spikes is different from the performance of inductive limiters with Bi bulk rings. The origin of the voltage spikes could be explained by resistance variation resulting from the transition from a flux flow state to a normal state.

12–61

Preparation of switching elements for a resistive type HTS fault current limiter.

R. Nies[1], *W. Schmidt*[1], *B. Seebacher*[2], *B. Utz*[1] and *H.-W. Neumüller*[1]. [1]Siemens AG, Corporate Technology, 91052 Erlangen, Germany. [2]Siemens AG, Corporate Technology, 81730 Munich, Germany.

High quality superconducting thin films on large-area insulating substrates are required to build a resistive type fault current limiter. As a substrate material we used partially stabilized zirconia ceramics (PSZ) with a size of $10 \times 10\,cm^2$, polished to a residual roughness r_A of less than 5 nm. Onto these substrates we deposited a 1 μm biaxially aligned buffer layer of yttria stabilized zirconia (YSZ) using an ion-beam assisted deposition (IBAD) system. A thin yttria diffusion barrier is followed by a 700 nm thick superconducting YBCO layer deposited by thermal coevaporation (TCE). An in-situ gold layer serves as an electrical shunt-resistance and allows to make low-ohmic electrical contacts to the superconductor. The texture of the deposited films is characterized by ϕ-scans measured with a four-circle x-ray diffractometer. The FWHM of the YSZ (111) ϕ-scans is better than 15° and the FWHM of the YBCO (103) ϕ-scans is better than 10°. The superconducting properties of the YBCO are characterized by measurements of the critical current density at 77 K using an inductive scanning system. All over the substrate j_c exceeds 10^6 A/cm^2 with a homogeneity better than ±20%. The work is co-funded by the German BMBF under contract number 13N6482.

12–62

Study of MCP BSCCO 2212 bulk material with respect to application in resistive current limiters.

S. Elschner[1], *J. Bock*[2], *G. Brommer*[2] and *L. Cowey*[2]. [1]FH Mannheim, University of Applied Sciences, D-68163 Mannheim, Germany. [2]Aventis Research & Technologies, D-50351 Huerth, Germany.

Melt-cast processed (MCP-) BSCCO 2212 is a promising candidate for the use in resistive or inductive current limiters. The soft transition from superconducting to resistive state permits stable toleration of large over-currents. In additional it can be simple manufactured and machined in long lengths with varying geometries. For effective fault current limitation, the ratio between the fault current and normal current should be minimised. This requires the HTS to be operated close to its critical current level. Design of a limiter requires knowledge of both the current threshold up to which it can be run safely and the behaviour of the material at elevated temperatures in order to simulate the conditions in a fault limiting case. This threshold has been determined for different sample geometries and both AC- and DC-currents. It strongly depends on the mechanism of heat removal. This results is qualitatively explained by a theoretical estimation based on the U(I)- characteristics and on a simple model for the heat transfer.

12–63

Transport Critical Current Measurements in a Pressurised Liquid Nitrogen Vessel.

B. Zeimetz[1], *B. A. Glowacki*[1], *Y. S. Cheng*[1], *K.A. Kursumovic*[1], *E. Mendoza*[2], *X. Obradors*[2], *S. X. Dou*[3], *J. E. Evetts*[1] and *T. Puig*[2]. [1]Department of Materials Science, Cambridge University, Cambridge CB2 3QZ, UK. [2]ICMAB-CSIC, Campus de la Universitat Autonoma de Barcelona, 08193 Bellaterra, Spain. [3]ISEM, University of Wollongong, NSW 2522, Australia.

A high-pressure liquid nitrogen vessel was used to carry out measurements of DC critical currents in high temperature superconductors (HTS). Temperature control between 77 K and the critical temperature was achieved by variation of the nitrogen pressure, allowing liquid nitrogen cooling and thus high-power DC measurements at elevated temperatures. At present, DC currents up to 880 A can be passed through the sample. Current-voltage characteristics and transport critical currents as function of magnetic field and temperature were measured for a range of HTS materials, including Bi2223 powder-in-tube tapes, Bi2212 composite-reaction-textured bars and Y123 films and bulk material. Possible dissipation mechanisms in these HTS are discussed.

Session Wires tapes and coated conductors

12–64

Weak Link Path Model and E - J Characterisitcs in Ag/Bi2223 Tapes.

K. Osamura[1], *K. Ogawa*[1], *T. Thamizhavel*[1] and *A. Sakai*[2]. [1]Department of Materials Science and Engineering, Kyoto University, Sakyo-ku, Kyoto 606-8501, Japan. [2]Mesoscopic Materials Research Center, Kyoto University, Sakyo-ku, Kyoto 606-8501, Japan.

In order to elucidate the influence of weak link to the E-J characterisitcs in silver sheathed Bi2223 tapes, the second differential of E-J curve has been analysed using the Weibull distribution function. The four parameters of the function are examined to investigate the microstructural nature of the samples, that were prepared under different experimental conditions. Further the computer simulation has been carried out based on a new weak link path model considering correlated-network of weak links among SC/non SC grains. The present model is flexible for changing the distribution of strength of weak links for local electric and magnetic fields and their spatial distribution. The calculated results can well explain the Weibull distribution of local current densities determined by experiments.

12–65

Effect of intermediate treatment on the structure of monocore Bi-2223/Ag tapes made by two-axial and eccentric rolling.

W. Pachla[1], *R. Diduszko*[2], *P. Kovac*[3] and *I. Husek*[3]. [1]High Pressure Research Center, Polish Academy of Sciences, ul. Sokolowska 29, 01-142 Warszawa, Poland. [2]Institute of Vacuum Technology, ul. Długa 44/50, 00-241 Warszawa, Poland. [3]Institute of Electrical Engineering, Slovak Academy of Sciences, Dubravska cesta 9, 842-39 Bratislava, Slovak Republic.

Monocore (Bi,Pb)-2223 tapes have been made by sequence of thermomechanical steps involving two-axial and eccentric rolling and anneling between 20h and 120h. Commercially available BPSCCO precursor of nominal composition 2223 has been used to manufacture tapes of critical currents reaching 8,000Acm^{-2}. Special attention has been made to evaluate phase purity and content at the Ag-interface. Texture degrees, phase content and purity were measured by X-ray diffraction (XRD) and core morphology and composition by scanning electron microscope (SEM) equipped with energy dispersive X-ray analysis (EDS). Results obtained have confirmed the predominant role of thin layer at the Ag-interface in creation of texturization and phase content as the prevelage path for supercurrents within the HT$_c$ ceramic cores. Evidence of c-axis constant decrease, 2223-phase content and purity increase, higher texturization degree and smaller volume of secondary phases have been found and demonstrated for this interfacial layer. Observed properties are discussed and related to process parameters applied for each individual tape and its influence on the critical current density J$_c$ in final tapes is analyzed. Mode of cooling (high vs. slow) are incorporated into the analysis.

12–66

Relating the Magnetic Field Response to the Transport Properties of BSCCO/Ag Superconducting Tapes.

W.F.A. Klein Zeggelink[1], *J.J. Rabbers*[1], *B. ten Haken*[1], *H.H.J. ten Kate*[1], *M.D. Bentzon*[2] and *P. Vase*[2]. [1]Faculty of Applied Physics, University of Twente, P.O. Box 217, 7500 AE Enschede, The Netherlands. [2]Nordic Superconductor Technologies, Priorparken 878, 2605 Brøndby, Denmark.

A contact-less magnetic measurement is used to characterise long lengths of superconducting tape. A perpendicular AC magnetic field is applied to a tape in an industrial inline

testbed for superconductors. The magnetic response is determined by the critical current density of the superconducting material inside the tape and the exact geometry of the conductor. The critical current measured over a certain length of conductor is determined in principle by the same set of properties. A comparison is made at 77 K, between the magnetic response, as measured in the testbed, and the critical current, measured with a 4-probe technique at regular intervals of 10 mm. The relation between the critical current and the magnetic response is investigated experimentally in various tapes with different transport properties. The experimental results are compared with model-calculations on a two-dimensional tape with a rectangular cross-section and an arbitrary magnetic field dependent voltage-current relation. It is concluded that the magnetic technique can be used to accurately locate various kinds of defects in the tape.

12–67

The Investigation of the Formation of Bi-2223 in Bi-2223/ Ag-Tapes by in situ XRD.

T. Fahr, *K. Fischer*, *W. Pitschke* and *H.-P. Trinks*. IFW Dresden, Dresden, D-01069, Germany.

The formation of the Bi-2223 phase is investigated by in situ X-ray diffraction at Bi-2223/Ag tapes with the upper silver sheath peeled off from the tape. The changes in the phase assemblage have been detected in the early stage of the reaction starting from a precursor containing Bi-2212, Ca2PbO4 and alkali earth cuprates. At constant temperatures between 780°C and 850°C subsequent diffraction patterns were recorded to study the dissolution of precursor phases, the development of texture of both the Bi-2212 and Bi-2223 phases, the formation of the Bi-2223 phase and the behaviour of the ceramic during cooling. Kinetic analyses were performed revealing a change in the formation mechanism at a critical annealing temperature of the conductors. Additionally, the influence of the tape geometry on the texture evolution will be discussed. This work has been performed in cooperation with the Siemens AG and supported by the German BMBF under contract No. 13N6481/A6.

12–68

Magneto Optical and Electromagnetic Investigations of Multifilamentary Ag/BSCCO-2223 Tapes.

A. Polyanskii[1], *D.M. Feldmann*[1], *X.Y. Cai*[1], *L. Schwartzkopf*[1], *J. Jiang*[1], *D. Apodaca*[1], *Y. Wu*[1], *S. E. Babcock*[1], *D. C. Larbalestier*[1], *Q. Li*[2], *R.D. Parrella*[2], *M.W. Rupich*[2] and *G.N. Riley, Jr.*[2]. [1]University of Wisconsin, Applied Superconductivity Center, 1500 Engineering Dr., Madison, WI 53705 USA. [2]American Superconductor Corporation, Two Technology Dr., Westborough, MA 01581 USA.

The flux entry behavior in recent high-Jc multifilamentary Ag/BSCCO-2223 tapes was examined by magneto-optical and magnetic transport measurements, both at final size and through process. The influence of heat treatment on flux shielding is considerable. The defect density as observed by magneto-optical imaging is greatly increased by intermediate rolling and improved by subsequent heat treatment Ultrasonic fracture studies reveal that the fragment size is decreased significantly by intermediate rolling and is not greatly improved by subsequent heat treatment. However, Jc approximately triples to > 50kA/cm2 (77K, SF) after a second heat treatment. Tests on 100mm long sections of individual filaments show Jc (77K, SF) up to 80kA/cm2 but microstructure studies show that cracks, voids and other current-limiting obstacles are still plentiful on the 1-10mm length scale.

12–69

Reactivity of electrically isolating barrier layers in Bi(Pb)-2223/Ag tapes with coated filaments.

H. Caudevilla, *G.F. De la Fuente*, *L.A. Angurel* and *R. Navarro*. Instituto de Ciencia de Materiales de Aragón, CSIC-Universidad de Zaragoza, CPS, María de Luna 3, 50015 Zaragoza (Spain).

To reduce the ac losses due to currents between superconducting filaments of Bi(Pb)-2223/Ag tapes, electrically isolating barrier layers of different thickness have been used. In this way, the effective transverse resistivity between filaments at 77 K may be increased, reaching values one order of magnitude higher. A series of commercially available materials (Mg and Zr oxides and Ca, Sr and Ba zirconates), compatible with the common powder-in-tube and wire-in-tube fabrication process, has been studied. Tapes with 19, 31 and 37 filaments coated by dipping Bi(Pb)-2223/Ag hexagonal monocore wires on appropriated dispersions of submicron particles of these materials have been produced.The barrier layers chemically interact with the superconducting cores through intergrowths of the Bi-2223 phase and by contact points, which are always present and in a number higher than in uncoated tapes. Best results correspond to coating materials with a chemical stability higher than the oxides which may be produced during the reaction kinetics of Bi(Pb)-2223 precursor mixtures. Values of the current density at 77 K in the self-field up to 12 MAm-2 have been obtained on tapes with 31 filaments coated with Sr zirconate.

12–70

Efficiency of filament decoupling in Bi(Pb)-2223/Ag tapes with electrically isolating barrier layers.

H. Caudevilla, *J.A. Gómez*, *L.A. Angurel* and *R. Navarro*. Instituto de Ciencia de Materiales de Aragón, CSIC-Universidad de Zaragoza, CPS, María de Luna 3, 50015 Zaragoza (Spain).

The effective transverse resistivity of silver sheathed tapes should be increased to reduce the ac losses due to currents flowing between filaments though non- superconducting materials. An alternative is the introduction of thin electrically isolating barrier layers around each filament. The selected materials should undergo the full powder-in-tube (PIT) process with minimum transformations. However, the presence of barrier layers increases the fabrication problems. The coupling of the filaments has been found to be strongly dependent on the lack of uniformity along the barrier layers rather than the average thickness of the coating. These defects can introduce some connection points between the silver sheaths of neighbouring filaments. Magnetic ac determinations, in fields perpendicular to disc shaped samples obtained from multifilamentary Bi(Pb)-2223) tapes with isolate barrier layers, have been used to test, in a straightforward way, the coupling of the filaments. Silver sheathed tapes with 19 and 31 filaments coated with Sr and Ba zirconates and various

barrier thickness have been analysed. Ac susceptibility, in zero dc fields, and measurements of the turning branch of the dc magnetisation have been used in the quantification of the coupling.
Project supported by the European Community through Brite Euram Program.

12–71
Bi,Pb(2223) phase formation in Ag-sheathed tapes: direct in-situ observations by high-temperature neutron- and synchrotron X-ray diffraction.
E. Giannini, *E. Bellingeri*, *R. Passerini*, *F. Marti*, *M. Dhallé*, *M. Ivancevic* and *R. Flükiger*. Département de Physique de la Matière Condensée Université de Genève 24, quai Ernest-Ansermet CH-1211 Genève 4 Switzerland.

In-situ diffraction techniques proved to be very powerful for the understanding of the reactions occurring inside the Ag-sheathed Bi,Pb(2223) tapes. The mechanism leading to the transformation of Bi(2212) into Bi,Pb(2223) is now accepted to occur via nucleation and growth following a partial melting of Bi,Pb(2212). By means of in-situ high- temperature neutron diffraction, the first direct evidence of the formation of a transient liquid at the early stage of the Bi,Pb(2223) phase formation was found, and a quantitative analysis of secondary (Ca,Sr)-cuprates and a Ca-rich amorphous phase was performed. Moreover, the effect of the silver on the liquid phase and on the Bi,Pb(2223) growth was pointed out. In-situ high-energy synchrotron X-ray diffraction was used during the first heat treatment: the re-crystallisation of the Bi(2212) and the texture development were investigated and related to the behaviour of the other secondary phases. Cooling experiments showed how the still unreacted secondary phases can react, crystallise or precipitate on cooling. In-situ neutron diffraction showed that a re-crystallisation of the Bi(2212) phase upon slow cooling is not related to any decomposition of Bi,Pb(2223). A comparison with conventional ex-situ studies will be made. Transport measurements will complete this study and relate the observed phenomena to the superconducting properties of the final tapes.

12–72
Study of microstructure homogeneity in Bi2223 multifilamentary tapes.
Y. B. Huang, *D.M. Spiller*, *J. Jutson*, *S. Mills*, *I. Ferguson*, *R. Prowse*, *C. Groombridge* and *W.W. Blendl*. BICC Superconductors, Oak Road, Wrexham LL13 9XP, United Kingdom.

For Bi2223 multifilamentary tape made by the powder-in-tube (PIT) method, the filaments are generally thinner than 20 micron. Even so, observation of the microstructure inhomgeneity between filaments and within the filaments is still possible. The transport properties are also different for each filament. By means of SEM, we have shown that the 2223 phase grains were larger and better aligned when they were nearer the Ag/core interface, and the flatter filaments (usually in the centre part of the tape) contained better aligned 2223 phase grains and smaller secondary phase grains. Using a Micro-XRD system, for the first time, we have successfully analysed the phase content and grain alignment within each individual filament of many tapes. These tapes are produced using different deformation and heat treatment conditions, as well as different powders. We have found that within the tape cross-section, filaments can be divided into three groups according to their microstructure: filaments near the tape edges, those close to the wide surfaces of the tape and those in the central part of the tape. In these three groups, filaments have different 2223 phase formation rates and texture intensities, leading to different microstructure and superconducting transport properties. These differences are mainly due to the variation in filament shape and density. Reducing deformation inhomogeneity and optimising heat treatment conditions are very important in improving overall tape homogeneity and transport properties.

12–73
Critical current anisotropy in longitudinaly strained Bi(2223) tapes: probing the connectivity.
R. Passerini, *F. Marti*, *L. Porcar*, *M. Dhallé*, *G. Witz*, *B. Seeber* and *R. Flükiger*. Département de Physique de la Matière Condensée, Université de Genève, CH-1211 Genève 4, Switzerland.

We report on the critical current behaviour of strained mono- and multifilamentary Bi(2223) tapes at T = 4.2 K in moderate magnetic field (μ_0H < 7T), measured as a function of both the angle θ between field and tape and the level of applied longitudinal strain. In this range of temperature and field, the current is believed to be carried by a network of grain boundaries with a relatively wide distribution of coupling strengths. The in situ application of a longitudinal strain has been reported to provide an efficient way to destroy these links in a selective fashion. The anisotropy of the critical current density $J_c(H, \theta)$ is widely used as a probe of the "effective" texture the current paths. Combining these two experimental techniques to extract the angular distribution of current carrying grains at different strain levels enables us to make a detailed investigation of the relation between grain alignment and grain boundary coupling strength. A micro-structural SEM study shows the location and nature of the irreversible damage caused by the applied strain.

12–74
Flux penetration into the system of superconducting filaments in normal conducting matrix.
S. Takács and *F. Gömöry*. Institute of Electrical Engineering, Slovak Academy of Sciences, 842 39 Bratislava, Slovakia.

The measurements of complex AC susceptibility at different frequencies of the applied AC magnetic field were used to determine the character of the flux penetration into BSCCO superconducting filaments (with and without barriers) in silver matrix. For this reason, different shapes of the system were considered, namely coupled and uncoupled strips and ellipses, respectively. From the corresponding diffusion equation, the characteristic frequency (at given sample length, the thickness and the resistivity of the matrix) is determined below which the superconducting filaments are electromagnetically decoupled. By determining this characteristic frequency at given length, the effective resistivity between the filaments or the effective thickness between them can be determined, if the other parameter is known. The ratio of the diffusion length and the sample length gives

the character of the flux penetration, taking place from the sample ends (mainly through the matrix) and crossing the filaments, respectively.

12–75
Flat rolling of round and square superconducting multifilaments for HTS tapes.
M.Eriksen[1], *J.I.Bech*[1], *N.Bay*[1] and *P.Skov-Hansen*[2]. [1]Institut for Manufacturing Engineering, Technical University of Denmark, 2800 Lyngby, Denmark. [2]Nordic Superconductor Technologies A/S Priorparken 685, DK-2605 Brondby, Denmark.

In this work the influence of processing parameters in flat rolling of multifilament Ag/BSCCO tapes on the geometry and homogeneity of the individual filaments are investigated. 30 tapes have been processed with different parameters. The investigation is mainly based on experimental work supported by a few simple numerical simulations. The process parameters are four rolling diameters, three different rolling strategies, two material conditions and three different friction conditions. The final tape has been investigated in the transverse and longitudinal section from microscope pictures and by Jc measurements. For each cross section of the tape all the width/height ratios of the filaments are measured, and each tape is described by the average width/height ratio and the standard deviation of the width/height ratio. Numerical and experimental results show that tapes rolled from an initially square multifilament wire have far more homogeneous filaments than tapes rolled from round wire. The longitudinal and cross-sectional filament geometries as well as the width of the tapes depend very much on the roller diameter, while the other investigated parameters have minor influence on the tapes.

12–76
Influence of geometry and overpressure processing on Bi-2212/Ag multifilamentary tapes.
B. Lehndorff[1], *J. L. Reeves*[2], *A. Polyanskii*[2], *M. Rikel*[2], *E. E. Hellstrom*[2] and *D. C. Larbalestier*[2]. [1]Bergische Universität-GH Wuppertal, FB Physik, Institut für Materialwissenschaften, Gaußstr. 20, D-42097 Wuppertal, Germany. [2]Appl. Supercond. Center, University of Wisconsin-Madison, 1500 Engineering Dr., Madison, WI 53706, U.S.A.

Processing under elevated total pressure (up to 10 atm) and fixed p_{O2} of 1 atm has been shown to increase j_c in silver-sheathed Bi-2212 monocore tapes. The overpressure compresses the core during processing and may reduce porosity. In this experiment, overpressure processing was applied to multifilamentary Bi-2212/Ag tapes with various thickness. The goal was to study the influence of overpressure processing and geometry on microstructure and j_c. Overpressure was applied by compressing air to approximately 5 atm, thus obtaining an 1 atm partial pressure of oxygen in the total pressure of 5 atm. The critical current of the Bi-2212 tapes was determined at 4.2 K in self field. A thickness dependence of j_c was found. Magneto-optical imaging of the thinnest sample showed very high flux penetration, and SEM and X-ray analysis showed a fine-grained microstructure with many second phase particles. The sample with the highest j_c had intermediate thickness. Magneto-optical imaging showed less flux penetration; SEM and X-ray analysis exhibited a very compact microstructure with nearly no second phases. The thickest sample had lower j_c, probably due to the larger amount of porosity as shown by SEM. An interpretation for the differing second phase content and porosity will be proposed.

12–77
Intermediate mechanical deformation processes in the OPIT fabrication of HTS Bi-2223 tapes.
P. Skov-Hansen[1], *Z. Han*[1], *H. Wu*[1], *A. Polyanskii*[2], *D. M. Feldmann*[2], *X. Y. Cai*[2], *D. C. Larbalestier*[2], *P. Kovac*[3], *F. Marti*[4] and *R. Flükiger*[4]. [1]Nordic Superconductor Technologies A/S, Priorparken 685, DK-2605 Brondby, Denmark. [2]Applied Superconductivity Center, University of Wisconsin-Madison, 1500 Engineering drive, Madison, Wisconsin 53706, USA. [3] Institute of Electrical Engineering, Slovak Academy of Sciences, Dubravska cesta 9, 842 39 Bratislava, Slovakia. [4]University of Geneva, Dept. Phys. Mat. Cond., 24, quai Ernest Ansermet, 1211 Geneva, Switzerland.

Alternative methods for the plane-strain intermediate pressing process in the OPIT fabrication of high temperature superconducting Bi-2223 tapes have been an issue ever since tape-lengths increased from centimeter to meter scale. We address an important problem: how to introduce a continuous and more speedy process. In this work several new methods have been tested, among these continuous pressing, rolling with large diameters and rolling with large deformation zones. Results show that it is possible to reach better Ic and Jc values than through the traditional pressing method if process parameters such as deformation zone size, reduction ratio and friction parameters are known and controlled. Magneto-optical methods are used to obtain a full understanding of the electrical properties of the tapes.

12–78
AC-losses vs temperature and frequency in multifilamentary Ag-sheated bscco–2223.
R. Tebano[1], *F. Gömöry*[2], *R. Mele*[3] and *A. Melini*[3,4]. [1]Dipartimento di Scienza dei Materiali, Universita' degli Studi di Milano, via Cozzi, 53,Milano, 20126, Italy. [2]Institute of Electrical Engineering, Slovak Academy of Science, Dubravska 9, 842 39, Bratislava, Slovak Republic. [3]Pirelli Cavi & Sistemi S.p. A., v.le Sarca 222, Milano, 20126, Italy. [4]Dipartimento di Fisica, Universita' degli Studi di Milano, via Celoria, 16, Milano, 20133, Italy.

Losses in the AC-transport regime were measured in multifilamentary Ag-sheated BSCCO–2223 tapes. The measurements were performed in a temperature range of interest for the application to power transmission cables. The experimental results are in agreement with the critical state model developed by Norris. Therefore the hysteretic losses in the superconductor depend upon the temperature only through the critical current, which, as experimentally found, decreases linearly with rising temperature. Measurement in the frequency range $35 - 280$ Hz was also performed to confirm the hysteretic nature of losses. Experimental data show deviations from hysteretic behavior for values of current in the range $1 - 10$ A. The corresponding power losses vs frequencies fitting curves show a quadratic behavior indicating a typical eddy current contribution. A theoretical model

was developed, to calculate the eddy currents losses in the silver sheath, in agreement with the experimental data.

12–79

Phase formation in Bi2223 tapes at different cooling rates and oxygen partial pressure.

E. Young[1], *Y. Yang*[1], *C. Beduz*[1], *Y. Huang*[2] and *C.M. Friend*[2]. [1]Institute of Cryogenics, Unversity of Southampton, Southampton SO17 1BJ, UK. [2]BICC Superconductors, Oak Rd., Wrexham. LL13 9XP UK.

Appearance of 2212 phases during slow cooling from the sintering temperature has been found by many groups using standard XRD analysis. We have measured the amount of such 2212 as a function of sintering temperature, in order to compare with fast cooled samples of corresponding processing time. It was found that while the fast cooled samples maintained an apparent >90% 2223 phase by XRD, the slow cooled samples showed a gradual reduction of 2212 from >30% to <10% with increasing time. This indicated a difference in the microstructure between short and long sintering time before cooling, although XRD showed the same 90% 2223 phase in fast cooled samples. Field-cooled dc susceptibility of both fast and slow cooled samples was measured to provide independent information on the phase composition. The results suggested (1) no significant difference in phase composition between fast and slow cooled samples and (2) a gradual increase of 2223 phase with sintering time for both cooling rates. One possible reason is that XRD is not capable of distinguish finely dispersed 2212/2223 inter-growth, through which 2212 is gradually transformed into 2223 during the sintering stage. The inter-growth phase is segregated upon slow cooling but preserved by fast cooling.

Session Materials related to electronic applications

12–80

Comparison of structural and compositional properties of YBaCuO thin films for microwave applications.

A. Dégardin[1], *S. Bourg*[1], *X. Castel*[2], *C. Bodin*[1], *J. Berthon*[3], *C. Dolin*[4], *É. Caristan*[1], *F. Pontiggia*[1], *A. Perrin*[2] and *A. Kreisler*[1]. [1]LGEP - UMR 8507 CNRS - Universités Paris 6 & Paris 11 - Supélec, Plateau du Moulon, 91190 Gif-sur-Yvette, France. [2]LCSIM - UMR 6511 CNRS - Université Rennes 1 - Avenue du Général Leclerc, 35042 Rennes, France. [3]LCS - URA 446 CNRS - Université Paris 11 - Bâtiment 414, 91405 Orsay, France. [4]Unité Mixte de Physique CNRS - Thomson-CSF - Domaine de Corbeville, 91404 Orsay, France.

In order to develop microwave devices, YBaCuO thin films were sputtered on (100) single crystal MgO substrates, selected because of their good dielectric properties. Substrate preparation is a significant step for elaboration of YBaCuO films with good superconducting quality. In particular, the influence of substrate thermal annealing before superconducting material deposition has been studied from structural and physico-chemical properties of the YBaCuO film. Such a thermal treatment has been reported to allow the formation of steps on the MgO surface and hence to favour YBaCuO growth. Various characterization techniques have been used to discuss properties of the bare substrates and the films deposited on them. X-ray diffraction and phi-scan measurements have allowed to identify crystalline phases and determine film orientation in the growth plane. Secondary ion mass spectrometry analyses can show the impurity diffusion from substrate to film, that may be detrimental to the YBaCuO film. We have performed X-photoelectron spectroscopy analysis to study the formation of a passivation layer, previously detected by film surface observations with an original atomic force microscopy technique using conducting tips. All these characterization results will be discussed in conjunction with critical temperature measurements performed by ac susceptibility.

12–81

Non-destructive characterisation of HTSC wafer homogeneity by mm-wave surface resistance measurements.

R. Heidinger and *R. Schwab*. Forschungszentrum Karlsruhe, Institut für Materialforschung I Postfach 3640, D-76021 Karlsruhe, Germany.

The homogeneity of thin film properties is a major issue for the reliable use of high temperature superconductors in wireless and satellite communication. Among the materials parameters that are specific for the quality of superconducting materials in high frequency applications, the surface resistance R_s is the most direct one. A measurement facility based on the open resonator method is presented that allows the non-destructive and non-contacting mapping of superconducting large area wafers in terms of absolute R_s data at 145 GHz. The quantitative interpretation of the obtained two dimensional data sets is discussed with a particular attention given to small size defects. This case is experimentally demonstrated for a model wafer with artificial defects formed by 2 MeV α-radiation. A data evaluation procedure is proposed to parameterise the large scale R_s variation in terms of an accumulated probability function. The wafer qualification process is actually applied to sets of CeO_2 buffered YBCO films grown on sapphire substrates either by sputtering or by pulsed laser deposition. Three major classes are defined into which the characterised wafers can be grouped according to their homogeneity features. Temperature dependent Rs data were measured between 10 - 100 K at various selected locations of inhomogeneous wafers. They can be distinguished in terms of a (low temperature) residual resistance and a specific function of the reduced temperature.

12–82

Temporal response of high-temperature superconductor thin-film using femtosecond pulses.

V. Garces-Chavez[1], *A. De Luca*[2], *A. Gaugue*[2], *P. Georges*[1], *A. Kreisler*[2] and *A. Brun*[1]. [1]Laboratoire Charles Fabry de l'Institut d'Optique, Orsay, Essonne, 91403, France. [2]LGEP-SUPELEC, Gif sur Yvette, Essonne, 91192, France.

In order to develop fast infrared detectors we have studied some fundamental optical properties of thin $YBa_2Cu_3O_{7-\delta}$ (YBCO) films. The pump-probe femtosecond spectroscopy experiments have demonstrated the existence of an ultrafast (some picoseconds) optical response in high-temperature su-

perconductor (HTS) materials. Below critical temperature, time resolved optical reflectivity experiments have been employed to study the quasi-particle dynamics and to estimate the strength of both the carrier-carrier and carrier-phonon interactions in HTS materials. We have used the pump-probe technique to study the thermal properties of carriers and phonons in superconducting materials by taking the variations in intensity of the reflected probe beam as a function of time delay after the arrival of the pump pulse. We have used a Ti:sapphire femtosecond laser producing 100 fs pulses at 800 nm and 1 kHz repetition rate. We have obtained an optical fast response which contains a characteristic relaxation time about one picosecond in YBCO films of 2000 Å approximate thickness on MgO substrates. We will discuss the temporal responses as a function of temperature. The influence of YBCO film thickness will be also presented.

12–84

Growth and Superconducting Properties of $YBa_2Cu_3O_{7-\delta}$ / $Nd_{0.7}Sr_{0.3}MnO_3$ Multilayers.

L. M. Wang[1], *H. H. Sung*[1], *J. H. Chen*[2], *H. C. Yang*[2] and *H. E. Horng*[3]. [1]Department of Electronic Engineering, Da-Yeh University, Changhua 515, Taiwan, R. O. C. [2]Department of Physics, National Taiwan University, Taipei 106, Taiwan, R. O. C. [3]Department of Physics, National Taiwan Normal University, Taipei 106, Taiwan, R. O. C.

Superconducting/ferromagnetic(S/F) N × ($YBa_2Cu_3O_{7-\delta}$ / $Nd_{0.7}Sr_{0.3}MnO_3$) (YBCO/NSMO) multilayers with N = 10∼30 have been prepared by off axis magnetron sputtering onto (001) $SrTiO_3$. Patterned samples with different thickness of NSMO layers were measured in both the perpendicular and the parallel magnetic field orientations. Measurements on activation energies for flux motion in fields show a progressive increase of the coupling as the NSMO layers become thinner. The valves of activation energies for multilayers are about 2-order smaller than that for YBCO films. The results are discussed by taking account the proximity induced ferromagnetic pair breaking in strongly decoupled superconducting layers.

12–85

Ferromagnetic and superconducting oxide heterostructures for spin injection devices.

L. Fàbrega[1], *R. Rubí*[1], *J. Fontcuberta*[1], *V. Trtík*[2], *F. Sànchez*[2], *C. Ferrater*[2] and *M. Varela*[2]. [1]Institut de Ciència de Materials de Barcelona (C.S.I.C.), Campus de la U.A.B., 08193 Bellaterra (SPAIN). [2]Departament de Física Aplicada i Òptica, Universitat de Barcelona, Diagonal 648, 08028 Barcelona (SPAIN).

The mature stage of epitaxial growth of complex oxide thin films allows nowadays to conceive and obtain electronic devices made of monolithic oxide heterostructures. Among the most interesting ones are those combining high temperature superconductors (HTS) and ferromagnetic half-metallic manganites (FM), due to the remarkable properties of both types of materials. HTS/I/FM junctions, where I is an insulating oxide, constitute the basis of spin polarized quasiparticle injection devices: they are based on the reduction of the superconducting gap by the injection of a spin polarized electrical current coming from the ferromagnet, and could be used to build superconducting three terminal devices, as well as ultrafast, high resolution sensors. These devices are still in an early stage of development, due to the difficulty of synthezising homogeneous tunnel junctions in the required scale, and the lack of knowledge of their basic phenomenology. Here we report on the growth by pulsed laser ablation of such junctions, and discuss their microstructural and electrical properties as a function of their geometry and the procedure used to define it.

12–86

Effect of $YBa_2Cu_3O_{7-\delta}$ electrodes on the strain and lattice distortion in multilayered $SrTiO_3$ films.

P.K. Petrov[1], *S.S. Gevorgian*[1] and *Z.G. Ivanov*[2]. [1]Dept. of Microelectronics, Chalmers University of Technology, 412-96 Gothenburg, Sweden. [2]Dept. of Physics, Chalmers University of Technology and Gothenburg University, 412-96 Gothenburg, Sweden.

Properties of the thin films $YBa_2Cu_3O_{7-\delta}$ (YBCO)/ $SrTiO_3$ (STO) multilayer structures allow developing of low-loss varactors operating in wide band frequency range. The residual strain and lattice distortions in the layers strongly influence the electrical performance of these devices. In this report we present results of our X-ray investigations of different type YBCO/STO multilayers deposited on $LaAlO_3$ and MgO substrates. From the XRD patterns obtained using ω- and ϕ-scan, a, b, and c lattice parameters for the thin YBCO and STO films as well as the residual strain and lattice distortion values along these directions were evaluated. It was observed that when a YBCO thin film is used as an upper layer, the crystal cell of the STO film becomes orthorhombic. It is possible to reduce the residual strain as well as the difference between b and a parameters of STO crystal cell by using buffer layers. An attempt is made to correlate the strain and distortion with radio frequency (RF) and microwave properties of the varactors.

12–87

Raman Spectroscopy as a characterisation tool for FIB damage of HTS thin films.

N. Malde[1], *L. F. Cohen*[1] and *M. W. Denhoff*[2]. [1]Blackett Laboratory, Imperial College, Prince Consort Rd, London SW7 2BZ. [2]Institute for Microstructural Sciences, National Research Council, Canada.

The use of focused ion beams as a tool for patterning and junction definition in HTS thin films and heterostructures has grown in the last few years. A systematic investigation of the influence a focused beam of silicon ions at 200 keV and at various fluence levels.on the Raman spectra of YBCO thin films was carried out using a Renishaw Raman microprobe with a 1 micron spacial resolution The degree of damage was varied from zero to amorphisation of the film surface. It was found that the phonon modes were not strongly affected in terms of frequency shift, although there was a small downward trend of the mode associated with the O(4) ions suggesting oxygen loss or redistribution. However, the intensity of the phonon modes decreased as a function of damage in a manner which would allow for rapid characterisation of FIB processes. Simultaneously the background increased nonuniformly across the Raman spectra producing an extremely broad peak centred around 570 cm^{-1}. The

origin of this peak will be discussed.

12–88

Transport and High Frequency Behaviour of c-Axis $REBa_2Cu_3O_{7-x}$.

W. Schmitt, *R. Aidam*, *J. Geerk*, *G. Linker* and *R. Schneider*. Forschungszentrum Karlsruhe, INFP, P.O.B. 3640, D-76021 Karlsruhe, Germany.

We have deposited 100nm thick $REBa_2Cu_3O_{7-x}$ (RE=Gd,Y ,Yb) films on $LaAlO_3$ substrates by inverted cylinder sputtering in order to investigate the influence of the rare earth element with special respect to its ionic radius on the structural and transport properties of the films. The growth of the films was characterised by RBS, XRD and AFM. Measurements of the critical temperature T_c, the critical current density j_c, the specific resistance ρ and the surface resistance R_s at 19GHz were performed. We found increasing T_c and c-axis lattice constant values with ionic radius as measured previously in bulk samples while R_s was decreasing. The resistivity ρ, was increasing with ionic radius for Y and Gd like in bulk, but was higher as expected in $YbBa_2Cu_3O_{7-x}$ films, probably due to deposition problems with these films at sufficiently high substrate temperatures. We also observed decreasing R_s with increasing j_c-values irrespective of the ionic radius.

12–89

Nb_3Sn-films on sapphire for passive device applications.

M. Perpeet, *A. Cassinese*, *M.A. Hein*, *G. Müller* and *H. Piel*. Universität Wuppertal, Fachbereich Physik, Gaußstr. 20, D-42097 Wuppertal, Germany.

Nb_3Sn-films on sapphire can close the gap between Nb- and high temperature superconductor (HTS) films in terms of transition temperature T_c, surface impedance Z_s microwave power handling, and energy gap Δ. Phase-pure polycrystalline Nb_3Sn-films were prepared by Sn-vapor diffusion into differently thick Nb-films. The high T_c-value of 18K permits operation temperatures around 10K, which can easily be provided by cryocoolers. The BCS-like surface resistance R_s at 19GHz dropped at 4.2K below $15\mu\Omega$, which is about 10 times below typical R_s-values for HTS. The penetration depth of 70 nm is twice as low as that of HTS. The microwave field-dependence of R_s varied non-monotonically with film thickness. $1\mu m$ thick films yielded constant R_s up to $B_s^* = 25mT$, similar to epitaxial HTS films. Thinner films suffered from granularity, as concluded from the temperature induced change of the quadratic field dependence of R_s. Thicker films suffered from microwave heating at defects as concluded from the dependence of R_s on the film thickness and the thermal conductivity of different substrates. The reduced energy gap of phase-pure Nb_3Sn-films of 1.9 could be enhanced to 2.3 by Ti-doping. The achieved film performance appears attractive for passive microwave devices and radiation detectors.

Session SQUIDs, and SQUIDs applications

12–90

$YBa_2Cu_3O_7$ step-edge dc SQUID magnetometers.

I.S. Kim, *J.M. Kim*, *H.C. Kwon*, *Y.H. Lee* and *Y.K. Park*. Korea Research Institute of Standards and Science, Yusong PO Box 102, Taejon 305-600, Republic of Korea.

The fabrication of $YBa_2Cu_3O_7$ step-edge dc SQUID magnetometers have been studied. The devices have been fabricated using single layer deposition of $YBa_2Cu_3O_7$ thin film by a pulsed laser deposition technique on the stepped $SrTiO_3$ substrate. The formation of steps have been carried out by an Ar ion milling method, and controlled by changing the incident angle of Ar ion beam. Noise characteristics of the step-edge dc SQUID magnetometers have been analyzed.

12–91

Study of the magnetic recording media using a scanning dc SQUID microscope.

S.A. Gudoshnikov[1], *M.I. Koshelev*[2], *O.V. Snigirev*[2] and *A.M. Tishin*[2]. [1]Institute of Terrestrial Magnetism, Ionosphere and Radio Wave Propagation, Russian Academy of Sciences, (IZMIRAN), Troitsk, Moscow region 142092, Russia. [2]Department of Physics, Moscow State University, Moscow 119899 GSP, Russia.

A possibility to use a scanning SQUID microscope as a tool for imaging of the surface magnetic field produced by magnetic recording media has been investigated. A scanning high-Tc dc SQUID microscope with a sensitivity of 100 pT in unit of bandwidth and a spatial resolution close to 30 μm was applied to perform quantitative measurements of magnetic field produced by the fragments of standard 3.5 in. floppy disks at liquid nitrogen temperature. The images of fragments of unformatted, formatted and recorded floppy disks have been obtained. The distribution of magnetic fields produced by unformatted disk media had an irregular character with signal magnitude less than 0.5 μT for SQUID-sample space separation about 50 μm. The formatted disk images demonstrated a regular tracks with maximum signal amplitude close to 5 μT for the same space separation. Specific distribution of maxima and minima of magnetic field along the tracks have been detected for fragments of recorded disks. Influence of the perpendicular and parallel magnetic fields on recorded data were investigated. A read-out probe based on high-Tc dc SQUID for detecting an information from magnetic recording media are discussed.

12–92

Magnetic Detection of Mechanical Degradation of Low Alloy Steel by SQUID-NDE system.

N.K. Kasai[1], *S. Nakayama*[2], *Y. Hatsukade*[1,3] and *M. Uesaka*[4]. [1]Electrotechnical Laboratory, Tsukuba, Ibaraki, 305-8568, Japan. [2]Seiko Insturuments Inc., Matsudo, Chiba, 270-2222, Japan. [3]Waseda university, Shinjyuku, Tokyo, 169-0072, Japan. [4]University of Tokyo, Tokai, Ibaraki, 319-1106, Japan.

Nondestructive evaluation (NDE) is very important for structural safety of nuclear power plants. The low alloy steel A533B is a ferromagnetic and the typical material of light water reactor pressure vessels. We have measured the mag-

netic property changes in the A533B specimens caused by mechanical degradation using a SQUID-NDE system with a concentric second order gradiometer. The specimens for tensile test were applied tensile load of elastic region, 0.378 %, 0.43 % and 2.9 % residual strain respectively. Large changes were appeared in the map of SQUID output when Lueders band appeared on the surface of the specimen. The results are consistent with the SQUID-NDE results of carbon steel specimens reported before. The fatigue test specimens were subjected cyclic loading of 10 thousand cycles and 480 MPa, 50 cycles and 500 MPa, and 100 thousand cycles and 500 MPa, respectively. The map of SQUID output varied with the cycle number or the cyclic load. The results will be discussed in connection with the other measurements such as B-H curve, Barkhausen noise and residual stress distribution.

12–93
Design Aspects of the FHARMON Fetal Heart Monitor.
A.P. Rijpma, *H.J.M. ter Brake*, *J. Borgmann*, *H.J.G. Krooshoop* and *H. Rogalla*. Low Temperature Division, Department of Applied Physics, University of Twente, PO Box 217, 7500 AE Enschede, The Netherlands.

A promising application of SQUID magnetometers is the magnetic measurement of fetal heart activity. In this paper we will consider design aspects of a monitor for the measurement of such activity in a clinical environment. The monitor will make use of high-T_c SQUIDs, which can be cooled by means of a turnkey cryocooler, thus realizing a user-friendly system. This paper will focus on the design of the sensor head containing the SQUIDs, rather than on the cooling aspects. In order to operate outside a shielded environment, active compensation is applied to suppress the earth field. Additionally, a shield will be used against hf-disturbances. Next, to improve the signal-to-noise ratio, the output of three SQUID magnetometers is combined using the gradiometer principle. For the gradiometer, a baseline of 6 cm is chosen. This baseline is based on fetal magnetocardiograms that were recorded with a low-T_c system, of which the baseline could be varied. To improve the balance of the system, electronic noise cancellation of the orthogonal field components is planned with two additional SQUIDs. A single channel demonstrator with these characteristics is under construction for test purposes.

12–94
Direct coupled HTS magnetometers.
P.R.E. Petersen[1,2], *Y.Q. Shen*[1], *M.P. Sager*[1,2], *T. Holst*[1] and *J.B. Hansen*[2]. [1]NKT Research Center, Priorparken 878, DK-2605 Brøndby, Denmark. [2]Department of Physics, Technical University of Denmark, DK-2800 Lyngby, Denmark.

HTS magnetometers have been made on 10 * 10 mm^2 MgO substrates by directly coupling the magnetometer pick-up loop to the loop of a DC SQUID. The DC SQUIDs were made with $YBa_2Cu_3O_{7-\delta}$ step-edge Josephson junctions. The effective area of the magnetometer pick-up loop is ~35 mm^2. The inductance of the pick-up loop was estimated to be ~10 nH and the inductance of the SQUID loop was determined to be around 100 pH by applying a modulation current directly to the SQUID loop. The best magnetometer has a white noise level of 55 $fT/Hz^{1/2}$ and a 1/f-knee at 1 Hz (AC-biased). The typical sensitivity of the fabricated magnetometers was 3 - 5 nT/Φ_0 Noise measurements were made on a field-cooled magnetometer. When cooled inside a four layer m-metal shield the white noise level was 150 $fT/Hz^{1/2}$ with a 1/f-knee around 1 Hz. Cooling in magnetic fields of 50 mT and 100 mT did not increase the white noise level, but the position of the 1/f-knee changed to ~5 Hz and ~10 Hz, respectively. Based on the knowledge gained by making the magnetometer we have designed a 1st. order planar gradiometer that is now being fabricated.

12–95
Low Temperature Scanning SQUID.
B. C. Yao, *M. J. Wang*, *C. C. Hung*, *C. C. Chi* and *M. K. Wu*. Material Science Center & Department of Physics, Tsing Hua University, Hsinchu, Taiwan, R.O.C.

We have constructed a novel 2-D magnetic flux microscope using a Nb-base dc SQUID with a pickup loop ~10um inner hole side length. During imaging, the sample is moved past the SQUID at a separation of about 10 um for achieve high spatial resolution. The details of the design and operation of this system are described, and several illustrations of the capabilities of this microscope are presented. The system achieve a spacial resolution of about 10 um and a field resolution of about few $pTHz^{1/2}$

12–96
HTS Single Layer Gradiometers with a Large Baseline and Electronically Improved Balance.
A. Eulenburg, *E.J. Romans*, *C. Carr*, *A.J. Millar*, *C.M. Pegrum* and *G.B. Donaldson*. Dept of Physics and Applied Physics, University of Strathclyde, Glasgow, G4 0NG, UK.

Directly coupled first order HTS gradiometers reported to date have two main disadvantages. Firstly, the baseline is limited by the typical use of 10mm x 10mm substrates which results in a gradient sensitivity too small for some applications. Secondly, the presence of the SQUID in the centre of the structure represents a significant parasitic effective area and thus restricts the balance of the device to typically 1%. In order to achieve a larger baseline of ~14mm and thus a higher gradient sensitivity, we have fabricated directly coupled first order single layer gradiometers on 30mm x 10mm bicrystal substrates. The YBCO thin films are deposited by pulsed laser deposition which has been optimised for the growth on larger substrates. To reduce the parasitic effective area we have positioned two (nominally) identical SQUIDs in the centre of the structure that are coupled in opposite directions to the gradiometer loops. Each SQUID is operated independently using flux modulation via direct current injection to minimise cross-talk between the channels. With a linear combination of the two SQUID outputs we are able to operate the gradiometer whilst cancelling the response to uniform fields. We report the device behaviour in both shielded and unshielded environments, and discuss their use in non-destructive evaluation and biomagnetism.

12–97

Operation of integrated HTS dc-SQUID magnetometers in unshielded environment.

K.O. Subke, *C. Hinnrichs*, *S. Krey*, *H.-J. Barthelmeß*, *C. Pels* and *M. Schilling*. Institut für Angewandte Physik und Zentrum für Mikrostrukturforschung, Universität Hamburg, Jungiusstraße 11, D-20355 Hamburg, Germany.

Many applications of SQUIDs from high-temperature superconductors (HTS) require low noise sensors operating in unshielded environment. In addition to the electromagnetic ac-disturbances the magnetometers are operated in moderate static magnetic fields, like the earth's magnetic field. An increase of the low frequency noise can occur due to the motion of vortices in the superconducting films of the magnetometer, if it is cooled or moved in the field. A high epitaxial quality of the films is prerequisite to pin vortices in the films, especially for the top superconducting layer in multilayer devices. Additionally, the condensation of vortices during cooling to 77 K in a static field of 50 μT can be avoided by patterning the device with holes or slits such that the maximum linewidth is below 4 μm. We prepared dc-SQUID magnetometers with integrated multiloop pickup coil (IMPUC) and directly coupled magnetometers on 10x10 mm^2 24° $SrTiO_3$ bicrystal substrates. We analyze the noise properties of these magnetometers in shielded and in unshielded environment.

We acknowledge financial support by the Bundesministerium für Bildung, Wissenschaft, Forschung und Technologie, Federal Republic of Germany, under contract number 13N7323/8.

12–98

Technique for compensation of background magnetic field for HTS dc SQUID systems operating in unshielded environment.

S.A. Gudoshnikov[1], *L.V. Matveets*[1], *A.A. Khorev*[2], *O.V. Snigirev*[2], *L. Dörrer*[3], *R. Weidl*[3] and *P. Seidel*[3]. [1]Institute of Terrestrial Magnetism, Ionosphere and Radio Wave Propagation, Russian Academy of Sciences, (IZMIRAN), Troitsk, Moscow region 142092, Russia. [2]Moscow State University, Moscow, 119899, Russia. [3]Institut fur Festkorperphysik, Friedrich-Schiller-Universitat Jena, Germany.

A HTS dc SQUID with a direct readout electronics based on a liquid-nitrogen-cooled preamplifier was suggested as a reference magnetometer for compensation of the environment disturbances acting on the HTS dc SQUID measuring systems (gradiometers and magnetometers) operating in unshielded environment. To compensate the Earth's magnetic field the system was initially zero field cooled inside a mumetal shield, the reference channel feedback was locked and after that the shield was taken away. The feedback signal of the reference magnetometer was fed to a compensation coil which produce a compensating magnetic field (almost equal to the Earth's magnetic field) at the location of the signal-measuring sensor. A high slew rate of 10^6 $\hat{O}_0$/s and a high dynamic range of 150 dB of the reference magnetometer electronics allow the flux-locked-loop mode operation in unshielded environment without unlocking. The results of the system test will be presented in conference report.

12–99

Scanning SQUID Microscopy of Superconducting and Magnetic Films.

A.Tzalenchuk[1,2], *Z.G.Ivanov*[1], *A.Lõhmus*[3] and *T.Claeson*[1]. [1]Department of Physics, Chalmers University of Technology and University of Göteborg, S-412 96 Göteborg, Sweden. [2]Institute of crystallography RAS, 117333 Moscow, Russia. [3]Institute of Physics, University of Tartu, Riia 142, EE2400 Tartu, Estonia.

We have designed and fabricated a variable temperature scanning SQUID microscope (SSQM) with a spatial resolution of a few microns. The SSQM features non-magnetic temperature regulation and topographic imaging capabilities. The SQUID sensor is based on submicron step-edge YBCO Josephson junctions. The SSQM characteristics were determined by studying the flux coupling between a test HTS circuit and the sensor SQUID. The SSQM was used to study phase transitions in manganese tetroxide and other magnetic thin films in a temperature range 10-100 K. A flux distribution in HTS materials was measured in a wide temperature range below the temperature of the superconducting transition. This work has been supported in part by TFR, STINT, RFBR, and ESF.

12–100

Noise measurements in a dc SQUID based Cryogenic Current Comparator.

J. Sesé[1], *A. Camón*[1], *C. Rillo*[1], *E. Bartolomé*[2], *J. Flokstra*[2] and *G. Ritveld*[3]. [1]ICMA, CSIC-University of Zaragoza, 50009 Zaragoza, Spain. [2]University of Twente, P.O.Box 217, 7500 AE Enschede, The Netherlands. [3]NMi Van Swinden Laboratorium, P.O.Box 654, 2600 AR Delft, The Netherlands.

The Cryogenic Current Comparator is the most sensitive device for precision measurements (<0.01 ppm) of the ratio of very small dc currents (<1μA). It consits of windings of superconducting wire inside an open overlapped toroidal tube made with lead foil. As the Meissner effect is accomplished on the lead tube, two unbalanced magnetomotive forces produce a shielding current in the inner surface of the tube that returns redistributed through the external surface, thus circulating on the self-inductance of the toroidal tube. If the external surface current is zero the ratio of the two currents will be, ideally, the inverse ratio of the turn numbers of the used windings. This condition can be experimentally detected by a flux transformer that couples the toroidal tube to a SQUID. There are several uncertainty sources limiting the precision with which the current ratio can be determined. A study of the noise sources arising from low frequency thermo-mechannical effects on the coupling between the flux transformer and the toroidal tube does not exist in literature yet. In this paper we present a systematic analysis of all the noise sources of a complete CCC system in a helium bath at controlled temperature (T<4.2 K), and derive strategies for the construction of optima CCC´s.

12–101
Characteristics of High-T_c $YBa_2Cu_3O_{7-\delta}$ SQUIDs with Shunted Resistance.
J.H. Chen[1], *M.J. Chen*[1], *H.C. Yang*[1], *H.E. Horng*[2], *C.H. Chen*[2], *S.Y. Yang*[2] and *J.T. Jeng*[2]. [1]National Taiwan University Department of Physics One Section 4, Roosevelt Road Taipei,106-17 Taiwan. [2]National Taiwan Normal University Department of Physics 88 Section 4, Ting-Chou Road Taipei,117-18 Taiwan.

The normal state resistance and the peak-to-peak value V_{pp} of V-Φ curves of bicrystal SQUIDs were measured to study the effect of the shunt resistance on the SQUIDs characteristics. The shunted resistance was across the junction or the bank of SQUIDs. It was observed that the shunted resistance across the junction can improve the phase locking of junction arrays while the shunted resistance across the banks of SQUIDs can avoid the deterioration of the V_{pp} when the inductance of SQUIDs is high. The results are discussed.

12–102
Characterization of biepitaxial YBCO dc-SQUIDs based on c-axis misaligned grain boundary junctions.
E. Sarnelli[1], *G. Testa*[1,2], *F. Tafuri*[2,3], *F. Carillo*[2], *F. Lombardi*[2], *F. Miletto Granozio*[2] and *U. Scotti di Uccio*[2]. [1]Istituto di Cibernetica - CNR, Arco Felice, Napoli, 80072 Italy. [2]INFM- Dipartimento di Scienze Fisiche, Universita' di Napoli "Federico II", Napoli, 80125 Italy. [3]Dipartimento di Ingegneria dell'Informazione, Seconda Universita' di Napoli, Aversa, Italy.

Dc SQUIDs based on 45° a-axis tilt and twist biepitaxial grain boundary junctions have been fabricated and characterized. Junctions have been realized by growing superconducting $YBa_2Cu_3O_{7-x}$ films with a double orientations, (103) on the $SrTiO_3$ substrate and (001) on the MgO seed layer. A detailed characterization of the SQUID properties of washer and hole-like geometries has been carried out. SQUIDs work in the whole temperature range from 4.2 K up to 80 K. Values of the I_cR_N quality factor of the order of 2 mV at T= 4.2 K and 100 μV at T= 77 K and of the magnetic flux-to-voltage transfer parameter $h = \partial V/\partial\Phi \simeq 30\ \mu V/\Phi_o$ have been obtained respectively. Magnetic flux noise spectral density as low as 40 $\mu\Phi_o/\sqrt{Hz}$. The observed phenomenology confirms differences from the one typical of 45° c-axis tilt grain boundary junctions, commonly obtained by bicrystal and traditional biepitaxial techniques. An investigation on the nature of the current steps appearing at finite voltages in the current-voltage characteristics has been also undertaken.

12–103
The system to operate cryogenics calorimeters with superconducting phase transition thermometers.
V. Khanin[2], *V.Y. Slobodchikov*[2] and *S. Uchaikin*[1]. [1]Max Planck Institute fuer Physik, Munich, 80805, Germany. [2]Cryoton Ltd, Troizk, Moscow region, 142092, Russia.

The four-channel system to investigate cryogenics particle detectors based on superconducting phase transition thermometer is reported. In the system four DC SQUID are used to amplify the signal from the usual and position detectors operating at the temperature range of 5-200 mK. The bandwidth and slew rate are 180 kHz and 55 mA/s accordingly. The system parts influence on the performances limitation is discussed.

12–104
Measurement System for Magnetorelaxometry with Planar and Axial SQUID Gradiometer.
J. Schambach, *L. Warzemann* and *P. Weber*. Friedrich-Schiller-University Jena Max-Wien-Platz 1 D-07743 Jena Germany.

Magnetorelaxometry is the measurement of the relaxation of the magnetization of single domain ferro- or ferrimagnetic nanoparticles after switching off a magnetizing field H_{mag}. The relaxation of such particles (dispersed in a carrier liquid) is either due to the movement of whole particles (Brownian relaxation) or due to the rotation of the magnetization vector inside the particle (Néel relaxation). In this paper a system for the detection of the relaxation of magnetic nanoparticles in spatially expanded objects (e.g. for in vivo investigations) in a disturbed environment is presented. The entire system, which includes a nonmagnetic x-y stage and a Helmholtz coil of 80 cm diameter (magnetization up to 7 mT), is controlled by PC. For measuring the relaxation signals either a planar or an axial LTS SQUID gradiometer system was used. The principle differences of both types of measurement configuration are specified and the characteristic features of the measuring signals are compared. The two different gradiometer systems were used for measurements of the spatial distribution of magnetic nanoparticles within various samples.

12–105
A SQUID Switch for Non Invasive Measurements in a Macroscopic Quantum Coherence experiment.
C. Cosmelli[1,2], *P. Carelli*[3,2], *M.G. Castellano*[4,2], *F. Chiarello*[1,2], *R. Leoni*[4,2] and *G. Torrioli*[4,2]. [1]Dipartimento di Fisica, Universita' La Sapienza, Roma, 00185, Italy. [2]Istituto Nazionale di Fisica Nucleare, Roma, 00185, Italy. [3]Dip. Di Energia Elettrica, Fac. di Ingegneria, Monteluco di Roio, L'Aquila, 67040, Italy. [4]Istituto di Elettronica dello Stato Solido - CNR, 00156, Italy.

In view of realizing a Macrocopic Quantum Coherence experiment to test Quantum Mechanics with a system of SQUIDs, we have realized a SQUID "switch" to perform a Non Invasive Measurement (NIM) of the flux of an rf SQUID. The SQUID switch (a dc SQUID with no shunt resistance across the Josephson junctions) is infact a non linear device that can perform a NIM when biased by a proper external field. We will present the measurements performed at 4.2K of the escape rate of the SQUID from the superconducting to the normal state, showing its behavior in the thermal regime. We will show that the present device can perform the desired measurements when cooled to the final temperature of 10mK.

12–106
16-channel operation of high Tc SQUID magnetometers for magnetocardiogram.
H.C. Kwon, *I.S. Kim*, *Y.H. Lee*, *J.M. Kim* and *Y.K. Park*. Korea Research Institute of Standards and Science Taejon 305-600 Korea.

A 16-channel high temperature superconducting quantum interference device(SQUID) system was developed for magnetocardiogram(MCG). The SQUID sensors are directly-coupled YBCO magnetometers on STO bicrystal substrates and have a noise level of typically 170 $fT/Hz^{0.5}$ down to 4 Hz. The 16-channel magnetometer probes are modular and each probe can be easily replaced. To minimize the vibration-induced noise, each probe was tightly held against the insert body by the Be-Cu spring. For the data acquisition, processing and field map, a software was written in the graphical language LabVIEW that allows modifications to be made easily by the non-specialist. The performance of the SQUID system was demonstrated by recording of 16-channel MCGs and by presentation of field distributions.

12–107

A new general purpose low-T_c multiloop SQUID family.

D. Drung, *S. Knappe*, *C. Aßmann*, *M. Peters*, *K. Wenzel* and *Th. Schurig*. Physikalisch-Technische Bundesanstalt, D-10587 Berlin, Germany.

Low-T_c multiloop SQUIDs have been used successfully during the last years in biomagnetic multichannel systems, picovoltmeter applications, NMR experiments and others. In order to improve the performance of the former PTB-type W7 and W8 SQUID series we have developed a new series W9. The theoretical basis for the design of this SQUID family was a new mathematical description for magnetic coupling, effective area, and inductance of SQUID sensors. Our new SQUID family consists of SQUIDs with outer pickup coil dimensions of 1.5 mm to 7 mm, effective areas of 0.2 mm^2 to 4.5 mm^2, and SQUID inductances of 100 pH to 420 pH, respectively. Each SQUID contains additional components as e.g. integrated feedback coils, various damping resistors, filter capacitors.Two of the devices have an integrated 0.47 μH or 1.1 μH input coil on chip which is wound around the pickup coil in order to minimize the capacitance between input coil and SQUID. At T = 4.2 K, white noise levels down to 9 $ft/\sqrt{Hz}$, 3 $ft/\sqrt{Hz}$, and 1 $ft/\sqrt{Hz}$ have been achieved for 1.6 mm, 3.4 mm, and 7 mm pickup coils, respectively, including electronic noise. Using a new shunt technology, we are able to operate the SQUIDs down to the mK temperature range.

12–108

Read-out electronics for a 9-channel High-T_c dc SQUID system.

S. Bechstein, *D. Drung*, *M. Scheiner*, *F. Ludwig* and *Th. Schurig*. Physikalisch-Technische Bundesanstalt, D-10587 Berlin, Germany.

A read-out electronics for operating a 9-channel high-T_c dc SQUID system has been developed. This system electronics consists of two parts - the flux locked loop (FLL) electronics mounted on top of the liquid nitrogen dewar containing the SQUIDs and the control unit (CU). The FLL is connected to the CU by a special cable the length of which can be chosen arbitrarily. The system consists of 3 triple modules each containing 3 direct-coupled FLL electronic boards with bias reversal. The preamplifier voltage noise is 0.4 $nV/\sqrt{Hz}$ with a 1/f corner at about 0.3 Hz. Each module is equipped with a voltage-controlled oscillator for providing the bias reversal clock and a circuit for driving the thick-film heaters implemented in each SQUID package for releasing trapped flux. The working points of the SQUIDs are adjusted using analogue voltages between -10 V and +10 V produced in the CU.In order to minimise the number of wires between FLL and CU, a serial two- line bidirectional (I^2C) bus is used to transfer the control signals. An in-system programmable micro-controller is used to control the main features of the CU. In order to avoid interference from the controller clock, the micro-controller is switched into the sleep mode during SQUID measurements. The CU is compatible with all of our FLL electronics versions including our 15 MHz bandwidth low-T_c SQUID read-out electronics. This work was supported by the German BMBF under grant number 13N7326.

12–109

Noise Characteristics of Asymmetric Multi-Junction HTSC rf-SQUID Magnetometer and Gradiometer on Bi-crystal Substrates.

M. Fardmanesh, *K. Barthel*, *J. Schubert*, *H. Bousack* and *A. Braginski*. Institute of Thin Film and Ion Technology, Research Center Juelich, Germany.

Asymmetric multi-junction YBCO rf-SQUID magnetometers and gradiometers have been made using 200 nm thick patterned (standard photolithography) PLD YBCO films on the symmetric Bi-Crystal SrTiO substrates. Low 1/f noise performance has been obtained for the rf-SQUIDs (magnetometers and gradiometers) on the bi-crystal substrates by implementing a design principle avoiding large area films on the bi-crystal grain boundary of the substrates. Washer rf-SQUID magnetometers are made with a design principle same as for a dc-SQUID on bi-crystal substrates using different slit structure and asymmetric junctions with width ratios of 1/2, 1/3, and 1/4. The 1/f noise behavior of the above devices while is lower compared to that of the conventional designs, show a dependence on the width of the larger junction, increasing with the increase of the junction width. A new multi-junction design for gradiometers is also presented implementing the same principle using asymmetric junctions while avoiding any large YBCO film weak links on the substrate grain boundaries

12–110

Step-Edge Structure Dependence of 1/f Noise in rf-SQUIDs and The Effect of IBE Parameters.

M. Fardmanesh, *J. Schubert*, *Y. Zhang*, *H. Bousack* and *A. Braginski*. Institute of Thin Film and Ion Technology, Research Center Juelich, Germany.

Step-edge junction rf-SQUID gradiometers and magnetometers are made using PLD YBCO films on $LaAlO_3$ and $SrTiO_3$ substrates. Effects of the step-edge structure, prepared by different IBE parameters, on the1/f noise and signal of the SQUIDs have been investigated. For the normal incident ion beam etched steps, a hard layer of re-deposited material is found to form on the side-walls of the steps standing up to e.g. a few hundred nm height above the step-edge for 300 nm deep steps on $LaAlO_3$. This is found to be much less for the steps on $SrTiO_3$ substrates. The re-deposited layer is found to strongly reduce the yield of the SQUIDs on $LaAlO_3$ substrates and drastically increase the 1/f noise for the working devices. The SQUIDs' signal on $SrTiO_3$

substrates are found to be less sensitive to the re-deposited material at the edge of the steps. SQUIDs made on $LaAlO_3$ substrate with steps etched using different angled incident ion beam, have shown a higher reproducibility and lower 1/f noise behavior avoiding re-deposition of the material at the steps. The detailed effects of the step etching parameters on the noise and signal of the devices are presented in this work

PLENARY SESSION 13

Thursday Morning, September 16th, 8:30-10:00

8:30 13–1

Progress in the applications of bulk high temperature superconductors.

M. Murakami. ISTEC, Superconductivity Research Laboratory 1-16-25, Shibaura, Minato-ku, Tokyo, 105-0023 Japan.

Recent progress in melt processing enabled us to grow large single-grain bulk superconductor RE-Ba-Cu-O (RE: rare earth elements) materials with large critical current density (Jc) values. Such bulk superconductors can exhibit a large electromagnetic force through the interaction with magnetic fields. A heavy object can be suspended without contact, which can only be realized in bulk superconductors. Thus, many practical applications have been proposed and some prototype devices have already been developed. Those are magnetic bearings, flywheel energy storage system, load transport system, hysteresis motors. Large magnetic fields over several teslas can also be trapped by such high Jc bulk superconductors. Trapped field magnets will be used in many novel devices, since the magnetic field is much higher than those of conventional permanent magnets. In this paper, I will summarize the present status of such bulk applications.

9:15 13–2

Challenges in the Realization of SFQ Digital Circuits.

T. Van Duzer Department of Electrical Engineering and the Electronics Research Laboratory, University of California, Berkeley, CA 94720-1770, USA.

Single-flux-quantum digital circuits offer the possibility of operation at speeds significantly exceeding those of semiconductors. This paper focuses on work needed for implementation of large Rapid Single Flux Quantum (RSFQ) circuits in LTS technology. There are several serious challenges. First, most available process lines for niobium integrated circuits are not capable of making complex circuits for ultra-high speeds. Another hurdle in realizing a large logic circuit at several tens of gigahertz and higher is in the distribution of the clock; several approaches have been studied but they have not yet been widely demonstrated. It also is necessary to prove the correct digital operation of circuits operating far above 10 GHz, which is the approximate limit for testing with external equipment. Bit-error-rate testing is essential and must be done on-chip for very high frequencies. Additionally, the long-standing memory problem in superconductor technology is worsened for RSFQ circuits by their ultra-high speeds and extremely small signal energy. Finally, it will be necessary to develop circuits to interface from chip to chip or from logic to memory.

ORAL SESSION 14A+15A: Wires and Tapes II

Thursday Morning, September 16th, 10:30-12:45

10:30 *14A–1

Current Limiting Mechanisms in BSCCO-2223 Tapes.

D. C. Larbalestier. Applied Superconductivity Center, University of Wisconsin, Madison University of Wisconsin, Madison, WI USA.

The real current limits to BSCCO tapes still remain unclear. In recent times we have been studying the barriers to current flow by combined study of whole multifilament tapes and of individual filaments extracted from such tapes. From such studies we deduce that the key flux pinning and connectivity current limiting mechanisms lie on scales of about 0.1-100 microns. Cracking induced by porosity in the tapes is a major issue that is being studied by through process studies. The results of our recent studies with composites made at UW and in other groups will be described. It seems clear that local Jc values significantly exceed 100 kA/cm2.

11:00 14A–2

Enhanced Critical Current Density in Overdoped $YBa_2Cu_3O_{7-\delta}$ - Grain Boundaries.

R.R. Schulz, *H. Bielefeldt*, *B. Goetz*, *H. Hilgenkamp*, *A. Schmehl*, *C.W. Schneider* and *J. Mannhart*. Experimentalphysik VI, Center for Electronic Correlations an Magnetism, Institute of Physics, Augsburg University, D-86135 Augsburg, Germany.

The physics of interfaces in high-T_c superconductors and in semiconductors are surprisingly closely related. Based on this, we have developed a model to describe the electronic behavior of grain boundaries in high-T_c superconductors. Guided by this model we have found that appropriate doping significanty improves their critical current density and reduces their normal state resistivity. This is demonstrated for the examplary case of grain boundary junctions in bicrystalline Ca-doped $YBa_2Cu_3O_{7-\delta}$ films.

11:15 14A–3

Preparation of (100) and (110) textured Ag tapes for superconducting biaxially aligned coated tapes.

H. Suo[1,2], *J.-Y. Genoud*[1], *E. Walker*[1], *G. Triscone*[1], *M. Schindl*[1], *E. Koller*[1], *Ø. Fischer*[1] and *R. Flükiger*[1]. [1]DPMC, University of Geneva, 24 quai E.-Ansermet, 1211 Geneva 4, Switzerland. [2]Beijing Polytechnic University, 100022 Beijing, China.

The texturing mechanisms in pure Ag were studied in details. The deformation and recrystallization parameters were optimised in order to obtain the two (100)<001> cube texture and (110) texture that are known to be of high interest for in-plane aligned superconducting coated tapes preparation. A pure cube texture is obtained when a fine grains Ag ingot is pre-heated at 100°C before cold rolling and annealed in a primary vacuum at 700°C for 30 min. The FWHMs of the three X-ray pole figures are with no more than 10° the smallest ever reported for cube textured Ag. Oriented Distribution Function (ODF) was used to carefully control and understand the texture transformations from

the deformation texture to the final recrystallization texture. The (110)<uvw> texture was obtained after a high level of standard cold rolling deformation followed by an annealing at 800°C in a primary vacuum. The ODF data showed that if the (110) orientation is of high quality, several <uvw> directions are found along the same Ag tape. In a small length scale, those (110) tapes are suitable for Re-123 (Re=Nd) epitaxial growth: $NdBa_2Cu_3O_{7-\delta}$ sputtering on those (110) tapes gave a unique biaxial orientation with a FWHM as small as 6° in the X-ray pole figures. This proves that those Ag tapes are suitable for biaxially aligned coated tapes preparation.

11:30 14A–4
Microstructure and properties of Bi2212/Ag tapes grown in high magnetic fields.
W.P. Chen[1,2], *H. Maeda*[1,2], *K. Kakimoto*[1], *P.X. Zhang*[1], *K. Watanabe*[1,2], *M. Motokawa*[1,2], *H. Kitaguchi*[3] and *H. Kumakura*[3]. [1]Institute for Materials Research, Tohoku University, Sendai 980-8577, Japan. [2]CREST, Japan Science and Technology Corporation, Tsukuba 305-0047, Japan. [3]National Research Institute for Metals, Tsukuba 305-0047, Japan.

Textured crystal growth in high magnetic fields was applied to prepare well-textured Bi2212/Ag tapes over 20 mm in thickness. Dip-coated Bi2212/Ag tapes were set horizontally and vertically for partial melting-solidification in vertically applied 2.5, 5, 7.5 and 10 T magnetic fields. The microstructure of the tapes was examined by SEM and the critical current was measured by four-probe method. For the tapes prepared in 2.5, 5 and 7.5 T magnetic fields, the horizontally set tapes were quite different from the vertically set tapes both in microstructure and in critical current density. In the horizontally set tapes the grains were aligned nearly parallel to each other and very high Jc values were obtained; in those vertically set tapes the grains were randomly oriented and the Jc values were much lower. For those tapes prepared in 10 T magnetic field, however, the difference between the horizontally and the vertically set tapes can not be observed. Interaction between the magnetic field and the Ag-Bi2212 interface in the texture development is discussed and the magnetic field is found to have the dominant effect.

11:45 15A–1
Processing of Tl-1223(F) thick films for HTS power applications.
J.C. Moore[1], *T.A. Gladstone*[1], *X. Zhou*[1], *M.D. McCulloch*[2] and *C.R.M. Grovenor*[1]. [1]Dept. of Materials, University of Oxford, Oxford, U.K. [2]Dept. of Engineering, University of Oxford, Oxford, U.K.

Tl-1223 offers an alternative superconducting material to YBCO for use in power applications operating at 77K in moderate magnetic fields. We are therefore investigating the fabrication of Tl-1223 thick films for use in two applications; resistive fault curr ent limiters and current-carrying conductors. We are studying the feasibility of using untextured Tl-1223 thick films as a fault current limiting device and have fabricated precursor films on polycrystalline alumina, zirconia and magnesia using powder/binder slurries. The processing parameters affecting porosity, grain size and cracking of the precursor film have been identified. Superconducting films have been fabricated using two thalliation methods, non-contact thallium diffusion using a Tl-2212/TlF sour ce and a contact method based on the Tachikawa diffusion composite process. We will compare the phase purity, microstructure and properties achieved using the two methods. For current carrying conductor applications, biaxial texture is essential to achieve high Jc's in magnetic field. The development of scaleable, low-cost thick film deposition techniques is needed if biaxially textured tape is to be commercially viable. We are investigating the processing parameters which affect texture formation in 2-10 m icron thick Tl-1223 films on textured Ag using spray pyrolysis and will report on the effects of fluorine substitutions, precursor film quality and heat treatment conditions.

12:00 15A–2
Progress on Fabrication and Procesing of $(Hg,X)_1Ba_2Ca_2Cu_3O_y$ Superconductor on Ceramic and Metallic Substrates.
J. Schwartz[1,2] and *P.V.P.S.S. Sastry*[1]. [1]National High Magnetic Field Laboratory, Florida State University, Tallahassee, Florida, 32310, USA. [2]Department of Mechanical Engineering, Florida State University, Tallahassee, Florida, 32310, USA.

The $Hg_1Ba_2Ca_2Cu_3O_y$ (Hg1223) superconductor has the highest T_c (135K) among all the high temperature superconducting cuprates, as well as a significant irreversibility field above 100 K. Significant progress has been made in understanding the synthesis process and phase stability of HgX1223 superconductors (X=Bi, Pb, and Re). The use of $CaHgO_2$ as the external mercury source allows the formation of HgX1223 phase at $T < 800$ °C. Both Bi- and Pb-doping allows the formation of significant amount of liquid phase during the reaction and yields very dense superconducting phase with some degree of texture among the grains. We have undertaken a detailed study on HgX1223 materials to evaluate the relative merits of various dopants and their suitability for using them in bulk form as well as thick and thin films. HgX1223 films were deposited on a variety of ceramic and metallic substrates to study the role of oxide-metal interface on the formation and microstructure of HgX1223. Thick BaCaCuO films were dip-coated on silver and gold foils whereas, thin BaCaCuO films were deposited by laser ablation or electro-deposition on ceramic substrates. The precursor films were sealed in evacuated quartz tubes and reacted using $CaHgO_2$ as the external mercury source. Both silver and gold were found to promote texture of HgX1223 by altering the mercury partial pressure in the vicinity of the interface. Samples were characterized for phase purity, microstructure and interfacial reactions using XRD, SEM, and magnetization measurements. Details of the measurements and the optimized processing conditions are discussed.

12:15 15A–3
Improved Critical Current Density of Rapidly Heated/Quenched Processed $Nb_3(Al,Mg)$ and $Nb_3(Al,Ge)$ Multifilamentary Wires.
A. Kikuchi, *Y. Iijima* and *K. Inoue*. National Research Institute for Metals.

We have been successful to enhance the critical current density J_c of $Nb_3(Al,Mg)$ and $Nb_3(Al,Ge)$ multifilamen-

tary wires by reducing the Al alloy core size. By using Al-5at%Mg and Al-20at%Ge alloys for the core materials, and pure Nb for the matrix materials, we have fabricated many kinds of multifilamentary Nb/Al-alloy composite wires through rod-in-tube method. The composite wires were applied to rapidly-heated/quenched process, and additionally annealed at 750-850 °C in order to improve the long-range order of $Nb_3(Al,Ge)$ crystal structure or to deposit A15 phase $Nb_3(Al,Mg)$. The maximum values of Tc and H_c2(4.2 K) for the $Nb_3(Al,Ge)$ multifilamentaly wires are 19.4 K and 39 T, respectively. J_c (4.2 K, 23 T) of 0.3 μm-core $Nb_3(Al,Ge)$ multifilamentary wire has reached to a 20,000 A/cm^2, which is about two times larger than that of 1.5 μm-core $Nb_3(Al,Ge)$ multifilamentary wire. The reduction of Al-Ge alloy diameter may enhance the volume fraction of the ordered A15-$Nb_3(Al,Ge)$ phases through increasing of diffusion pairs density in the composite. Much more improvements of J_c were obtained for the $Nb_3(Al,Mg)$ wires by reducing the Al-Mg alloy core size.

12:30 15A–4

Effect of Uranium Doping and Neutron Irradiation on the Properties of Bi-2223/Ag Superconducting Tapes.

Y.C. Guo[1], *J. Horvat*[1], *J.W. Boldeman*[1], *S.X. Dou*[1], *A. Gandini*[2], *Y. Ren*[2], *R. Sawh*[2], *R. Weinstein*[2], *S. Tönies*[3], *C. Klein*[3] and *H.W. Weber*[3]. [1]Institute for Superconducting and Electronic Materials, University of Wollongong, Northfields Av., Wollongong, New South Wales 2522, Australia. [2]Institute for Beam Particle Dynamics, University of Houston, Houston, TX 77204-5506, USA. [3]Atomic Institute of the Austrian Universities, Stadionallee 2, A-1020 Vienna, Austria.

Bi-2223/Ag tapes were doped with uranium oxide and the influence of U-doping on phase formation, microstructure, Tc and Jc was investigated. Heat-treated tapes were irradiated with thermal neutrons. Jc, anisotropy of Jc and Jc dependence on magnetic field were compared between the doped and undoped tapes in the irradiated state. The U-doping was found to decrease the sintering temperature of the tapes by lowering the melting temperature. XRD and magnetic measurements showed that the doping did not affect the Bi-2223 formation and Tc. However, the doping degraded the Jc slightly, e.g. Jc dropped by ~10 percent at the level of 0.6 wt percent of uranium oxide. AC susceptibility measurements indicates that grain connectivity was slightly improved in all the doped tapes. After irradiation, Jc of the doped tapes was significantly improved in magnetic fields compared to the undoped tapes. In particular, the anisotropy of Jc was substantially reduced. For example, Jc for 0.6 wt percent uranium oxide doped tapes is 27 times that for the undoped tape in 500mT (H//c). TEM observations show that the tracks produced by the fission of 235U due to irradiation are randomly distributed in low level doped tapes, while some star-like tracks are observed in high level doped tapes. These tracks serve as flux pinning centres and consequently improve the Jc behaviour in magnetic fields.

ORAL SESSION 14B+15B: Fault Current Limiters and Related Materials

Thursday Morning, September 16th, 10:30-12:45

10:30 *14B–1

Development of resistive current limiters with YBCO films.

B. Gromoll[1], *H.-P. Krämer*[1], *G. Ries*[1], *W. Schmidt*[1], *B. Heismann*[1], *H.-W. Neumüller*[1], *R. R. Volkmar*[2] and *S. Fischer*[2]. [1]Siemens AG, Corporate Technology, 91050 Erlangen, Germany. [2]Siemens AG, Power Transmission and Distribution, 13623 Berlin, Germany.

After the successful test of a 100kVA functional model the thin film approach has to demonstrate its applicability to a 1 MVA class model. According to the modular concept each phase can be built of up to eight switching modules, each module containing up to four switching elements connected in parallel. The switching elements consist of YBaCuO films with a thickness of 250 nm and a critical current density above $2 \cdot 10^6$ A/cm^2. The films are deposited on 4" sapphire wafers by thermal coevaporation. To prevent the formation of hot spots the superconducting film is covered with a 100 nm thick gold layer. The current path is etched in the form of a 7 mm wide and 80 cm long spiral. The desired nominal voltage and current values of one element are 600 V_{rms} and 33 A_{rms} resp., yielding a switching power of 20 kVA per element.

The three phases of the limiter are assembled in one cryostat and are bath cooled by liquid nitrogen. The cryostat is equipped with a coldhead and a compressor ensuring the operating temperature of 77 K by recondensation of the evaporated nitrogen on the coldhead.

This work has bee supported by the German Federal Ministry for Education, Science, Research and Technology BMBF under contract no. 13N6842A. Part of the work is done within the joint collaboration between Hydro Quebec, Canada and Siemens, Germany.

11:00 *14B–2

European project on a self-limiting superconducting power link.

T. Verhaege[1], *P.F. Herrmann*[1], *J. Bock*[2], *L. Cowey*[2], *G. Moulaert*[3], *H.C. Freyhardt*[4,5], *A. Usoskin*[4] and *J. Paasi*[6]. [1]Alcatel CIT, F-91460 Marcoussis, France. [2]Aventis, D-50351 Hürth, Germany. [3]Laborelec, B-1630 Linkebeek, Belgium. [4]ZFW gGmbH, D-37073 Göttingen, Germany. [5]Universität Göttingen, D-37073 Germany. [6]TUT, FI-33101 Tampere, Finland.

Superconducting Power Links (SUPERPOLI) will offer the opportunity for low-loss power transmission of high nominal currents and fault current limitation (FCL) simultaneously in one single device. They will find their applications as generator out-lines or in the medium voltage power distribution grid. The total room temperature losses amount to only 1/7 of the Joule losses in classical three phases bar systems, and the cross-section is approximately 4 times smaller. The link will be assembled from superconducting tubular modules with flexible interconnections. Liquid nitrogen will flow around the conductors, inside a double stainless steel envelope ensuring the thermal vacuum insula-

tion. As a significant step towards the GVA-class 3-phases application, the first aim of the project is the demonstration of a one phase functional model of length 2 m for 20 kVrms, 2 kArms/5kArms operation; it will include the development of two alternative low-ac-loss conductor designs suitable for current limitation: a low-cost composite tubular Bi-2212 conductor with moderate Jc; and a coated tubular Y-123 conductor, presenting a very high Jc. During current limitation, the dissipated power in the model will approach 1 MW.
This work is supported in part by EU Brite/EuRam No BE97 4738

11:30 *14B–3
Quench in bulk HTS materials: Application to the Fault Current Limiter.
P. Tixador[1], *X. Obradors*[2], *R. Tournier*[1], *T. Puig*[2], *D. Bourgault*[1], *X. Granados*[2], *X. Chaud*[1], *E. Mendoza*[2], *E. Beaugnon*[1], *D. Isfort*[1], *J.M. Duval*[1] and *E. Varesi*[2]. [1]CNRS, CRETA, 38000 Grenoble , France. [2]ICMAB, CSIC , Campus UAB, 08193 Bellaterra, Spain.

The fault current limiter is a very attractive and promising application for electrical networks. This device may be either resistive nor inductive or hybrid. The requirements and stresses on the material are different but all three are based on the quench of a superconducting element from its superconducting state to its resistive state. We will review different high T_c bulk materials for fault current limiters. Polycrystalline elements are easy to elaborate but show low performances in terms of critical current density and electrical field hence large amounts of material are required. The texturation enhances both J_c and the electrical field. YBCO single domains obtained either by Bridgman or by top seeding growth lead to very high Jc and electrical fields. For these reasons they are very good candidates for current limitation. Nevertheless contrary to polycrystalline materials they are very sensitive to hot spots which are unavoidable for a fault current limiter. We will show that by adapting the operating temperature or the material in terms of critical current, normal state resistivity and critical temperature, hot spots do not lead to damages. It will be illustrated by limitations measurements at different temperatures on several centimetre long samples.
Work financied partially by E.U. under contract B.E. 97-4829 (BYFAULT).

12:00 15B–1
Quenching in BSCCO hollow cylinders employed in an inductive fault current limiter.
V. Meerovich, *V. Sokolovsky*, *G. Jung* and *S. Goren*. Ben-Gurion University, Beer-Sheva, 84105, Israel.

We present the results of a study of quenching in BSCCO cylinders used as active elements of an inductive fault current limiter (FCL). The operation principle of the FCL is the increase of the impedance under fault conditions resulting from building up the voltage drop across the cylinder. It is shown that there are two ways leading to the appearance of this voltage drop. First, the voltage drop increases slowly according to the voltage-current characteristic. This process is associated with the vorte x motion. The dissipation occurs practically uniformly in all the volume of the BSCCO cylinder without marked heating. The second way is the formation of a local normal zone (overheating domain). It was shown experimentally that the appearance of the domain is due to cracks in the cylinder. In the case of smooth inhomogeneties, the domain was not formed during all the limitation time of about 0.1s. The experimental data illustrating the different types of the behavior of a FCL are presented. Using the mathe matical model of an inductive FCL, the analysis of the operation of a large-scale device is carried out. The estimation shows that, in large-scale FCLs, the domain created on cracks cannot lead to the voltage drop sufficient for fault current limitation, but the local overheating can cause destruction of a superconducting element.

12:15 15B–2
One DC Reactor Type Fault Current Limiter for Three-phase Power System.
M. Yamaguchi, *S. Fukui*, *K. Usui*, *T. Horikawa* and *T. Satoh*. Graduate School of Science and Technology, Niigata University, Niigata 8050, Japan .

A simulation and test results of a proposed one dc reactor type fault current limiter(FCL) for three-phase power system, using a high temperature superconducting(HTS) coil, are described. This type of FCLs feature almost no power loss during normal operation as well as a current limitation, an automatic insertion of necessary impedance under fault condition and accordingly quick appearance of impedance at an occurrence of fault, fast recovery to normal state after the fault removal, etc. A fault current could be automatically interrupted by a proposed modified half controlled bridge, not using a circuit breaker. A conceptual design of an HTS coil of one reactor type FCL required for 6.6 kV-2000 A power system is made and compared with a design of three reactors type FCLs. The required inductance of one reactor type FCL is 94.7 mH and a stored energy is 3.4 MJ, which is about seven-eighths of three-reactors type FCL. The most obvious advantage of one reactor type FCL is that it requires only one HTS coil.

12:30 15B–3
Operation of an HTS Fault Current Limiter in an Asymmetrical Three Phase System.
V. Sokolvsky[1], *V. Meerovich*[1], *I. Vajda*[2], *T. Porjesz*[3] and *A. Szalay*[4]. [1]Physics Dept, Ben Gurion University, Beer Sheva, Israel. [2]Dept. of Electrical Machines and Drives, TU Budapest, Budapest, Hungary. [3]Dept. of General Physics, Eotvos University, Budapest, Hungary. [4]S-Metalltech ltd, Budapest, Hungary.

Usually the operation of fault current limiters (FCL) based on high-temperature superconductors is analyzed in one-phase electrical systems (networks). In this paper the influence of an inductive HTS FCL on the electromagnetic processes in a three-phase system under a one-phase fault has been investigated. In this case the currents in the faultless phases may increase and can achieve a value several times higher than the nominal current. This may lead to a non-correct operation of the automatic protection elements even in the faultless phases. For the numerical calculation of the processes in a three-phase system with an inductive HTS FCL, the inductive coupling between the phases has been taken into account. The equivalent circuit of the in-

ductive FCL contains a non-linear element representing the superconductor. The thermal processes in the superconductor have also been considered. To investigate the real physical processes, an experimental setup with an HTS FCL has been designed and constructed to carry out measurements on the effects of the asymmetric overload of a three phase system and the operation of the HTS device.

ORAL SESSION 14C+15C: SQUIDS and SQUIDS Applications II

Thursday Morning, September 16th, 10:30-12:45

10:30 *14C–1

SQUID-NDE of semiconductor samples with high spatial resolution.

J.Beyer[1], *Th.Schurig*[1], *A.Luedge*[2] and *H.Riemann*[2]. [1]Physikalisch-Technische Bundesanstalt Berlin, D-10587 Berlin, Germany . [2]Institut fuer Kristallzuechtung Berlin, D-12489 Berlin, Germany.

We developed a SQUID-based, noninvasive method for the investigation of doping inhomogeneities in semiconductor samples. It is based on the detection of photocurrents exited in the sample by a focused laser beam. A highly sensitive SQUID system is used to detect these photocurrents via their magnetic field. Our method is capable of visualizing small, growth related fluctuations of the doping level (striations) of the semiconductor with a spatial resolution of a few tens of micrometers determined by the excitation spot size. The dynamics of the magnetic signal caused by the pulse excitation of photocurrents is related to characteristic charge carrier life times and can be measured with our high bandwidth SQUID system. Numerical simulations of photocurrent distributions in samples with special doping profiles have been performed and used for forward calculations of the magnetic signal. The results will be discussed in comparison with experimental data. The instrumentation of a PC-controlled laboratory setup for semiconductor wafer inspection will be presented.

11:00 *14C–2

Superconducting sensors for weak magnetic signals in combination with BiCMOS electronics at 77 K.

P. Seidel[1], *L. Dörrer*[1], *F. Schmidl*[1], *N. Ukhansky*[1,2], *R. Neubert*[1], *D. Hieronymus*[1], *S. Wunderlich*[1], *R. Gross*[3], *F. Nitsche*[3] and *S. Linzen*[1]. [1]Institut für Festkörperphysik, Friedrich-Schiller-Universität Jena, Jena, D-07743, Germany. [2]Institute of Terrestrial Magnetism, Ionosphere and Radio Wave Propagation, Troitsk, 142092, Russia. [3]MAZeT GmbH, Erfurt, D-99099 Erfurt.

Different sensors for weak magnetic signals were realized using thin high temperature superconducting films on different substrates including buffered silicon. Superconducting quantum interference devices (SQUIDs), magnetometers and planar gradiometers based on them as well as a new type of a Hall effect sensor with a superconducting antenna were tested with respect to signal resolution, band width and spatial resolution. To realize adapted measuring systems e.g. for biomagnetism or non-destructive evaluation common room temperature electronics offers some disadvantages. Thus we tested discrete semiconducting devices as well as special adapted integrated BiCMOS circuits (ASIC's) placed near the sensors at 77 K. We demonstrate performance of such electronics as well as of the whole magnetic sensor systems.

11:30 14C–3
Practical Low Noise dc SQUIDs for a Cryogenic Current Comparator.
E. Bartolomé, *J. Flokstra* and *H. Rogalla*. University of Twente, P.O.Box 217, 7500 AE Enschede, The Netherlands.

Washer type Nb-Al/AlO_x/Al-Nb dc SQUIDs with an energy resolution near the Quantum Limit and direct coupling to the inductive loop of a Cryogenic Current Comparator for the measurement of very small currents are being developed. In order to improve the sensitivity, the McCumber parameter tends to one. This approach requires the accurate determination of the capacitance per unit area of the junctions: it was found as 0.03 pF/μm^2 at 4.2 K and 0.034 pF/μm^2 at 1.6 K. Series of SQUIDs with $\beta_c \rightarrow 1$, diminishing junction areas and a single input turn were fabricated. The high value shunt resistors were made in PdAu (sheet resistance: R_{box}(66nm)=9 ωm/m). V - Φ curves with a large $\partial V/\partial\Phi$ transfer funcion were recorded. Good coupling is achieved thanks to the relatively large size of the washer hole. SQUIDs with β_c=0.5, 5×5 μm^2 junctions and increasing number of turns were measured to study the appearence of resonances and the possible damping methods. The resonant SQUID characteristics could be simulated with the help of the computer program JSIM. Noise measurements were performed in a recently developed Two Stage configuration using a DROS as second stage. The white and low frequency noise at the resonances were investigated.

11:45 14C–4
High-T_c SQUID magnetometers in $YBa_2Cu_3O_{7-\delta}$ thin films with resistively shunted inductances.
F. Kahlmann[1], *W.E. Booij*[1], *M.G. Blamire*[1], *P.F. McBrien*[1], *N.H. Peng*[2], *C. Jeynes*[2] and *E.J. Tarte*[1]. [1]IRC in Superconductivity, University of Cambridge, Madingley Road, Cambridge CB3 0HE, United Kingdom. [2]urrey Centre for Research into Ion Beam Applications, School of Electronic Engineering, Information Technology and Mathematics University of Surrey, Guildford GU2 5XH, United Kingdom.

We present a systematic study of the performance of high-T_c dc SQUID magnetometers with resistively shunted inductances. The magnetometers are based on a single layer of $YBa_2Cu_3O_{7-\delta}$ deposited onto 10 mm x 10 mm $SrTiO_3$ bicrystal substrates with 24^o misorientation angle. The shunt resistors were fabricated by ion implantation combined with conventional photolithography using standard AZ photoresist. The square pick-up loop of the SQUID magnetometer design used during the course of this work has an outer dimension of 9 mm and a linewidth of 3.1 mm. The SQUID loop itself is located in the middle of the pick-up loop and has a linewidth of 4 μm. The size of the inner area of the SQUID loop has been varied in order to get different inductance values. The width was kept constant at 5 μm whereas the length has been increased from 80 μm over 125 μm to 168 μm, resulting in total inductance values of 100 pH, 150 pH and 200 pH, respectively. We will report the magnetic flux noise spectra of these devices and compare the experimentally determined results to theoretical predictions made by Enpuku et al. Finally, we try to answer the question which optimisation rules apply for the fabrication of SQUID magnetometers on bicrystal substrates to get the best performance in terms of magnetic field sensitivity.

12:00 15C–1
HTS SQUIDs and cryogenically operated magnetoresistive sensors - an open competition?.
C. Dolabdjian[1], *S. Saez*[1], *D. Robbes*[1], *C. Bettner*[2], *U. Loreit*[2], *F. Dettmann*[2], *G. Kaiser*[3] and *A. Binneberg*[3]. [1]GREYC-CNRS, UPRES-A 6072,ISMRA et Université de Caen 6, Bd. du Maréchal Juin 14050 Caen Cedex, France. [2]Institut fuer Mikrostrukturtechnologie und Optoelektronik Im Amtmann 6 D-35578, Wetzlar, Germany. [3]Institut fuer Luft- und Kaeltetechnik Bertolt-Brecht-Allee 20 D-01309, Dresden, Germany.

In this contribution a comparison between an HTS dc SQUID (NKT company, 1 cm2 pick-up loop) and a magnetoresistive (MR) sensor with an additionally magnetic focuser is given. The latter device consists of an amorphous soft ferromagnetic strip with width of 3 mm and a length of 18 mm, with a barber pole structured MR detector placed in its middle and operated in a simple half Wheatstone bridge configuration. The field amplification structure areas of both sensors have nearly the same size. The directly coupled SQUID has a normal resistance of 2 Ohm. We measured a direct white noise level of 100 fT/Hz-1/2 in the frequency range above 1 kHz. We have measured the resistance as a function of the applied magnetic field of one single half bridge resistor at a temperature of 86 K. Thus, we have found a maximum value of 46 Ohm, with a maximum transfer coefficient of 51.8 kOhm/T in a range of +/- 25 microT. Direct measurements performed using a single MR half bridge resistor at a bias voltage of 8.6 V, lead to a voltage sensitivity of 2575 V/T and a noise level of 326 fT/Hz-1/2 at frequencies above 10 kHz. This noise level corresponds to the resistors Johnson noise expected for this temperature. All these measurements were made in a shielded environment. A reference magnetometer was operated simultaneously for comparison. For operation of the MR sensor at best conditions in a shielded environment, with a half bridge bias voltage of 10 V and assuming the Johnson noise limitation, a transfer coefficient as high as 11260V/T and a white noise of 30fT/Hz-1/2 can be expected.

12:15 15C–2
The spatial distribution of flux lines in YBCO dc SQUIDs and the correlation with their low-frequency noise properties.
R. Straub[1], *S. Keil*[1], *D. Koelle*[2], *K. Barthel*[3], *R. Gross*[2] and *R.P. Huebener*[1]. [1]Physikalisches Institut, Lehrstuhl für Experimentalphysik II, Universität Tübingen, 72076, Germany. [2]II. Physikalisches Institut, Lehrstuhl für Angewandte Physik, Universität zu Köln, 50937, Germany. [3]Institut für Schicht- und Ionentechnik (ISI), Forschungszentrum Jülich, 52428, Germany.

We report on the direct imaging of Abrikosov- and Josephson-Vortices trapped in bicrystalline YBCO washer dc SQUIDs and on the correlation of the local distribution of vortices at variable magnetic field with low-frequency noise measurements. The vortex imaging and noise measurements are performed with the SQUIDs mounted on a liquid nitrogen cooled cryostage of a scanning electron microscope, which allows investigation of the SQUIDs at variable tem-

perature (77 K < T < T $_c$) and in controllable magnetic fields up to several hundred μT, while the SQUIDs are operated in a standard flux locked loop. Our imaging technique, which yields a spatial resolution of about 1 μm, is based on the electron-beam-induced local displacement Δr of vortices, which is detected as a flux change $\Delta\Phi = \Delta r(\partial\Phi / \partial r)$ in the SQUID loop. Hence, the signal height provides direct information on the coupling strength $\partial\Phi/\partial$r. Since $\partial\Phi/\partial$r determines the amount of flux noise which a fluctuating vortex induces in the SQUID, we obtain valuable information on possible low-frequency noise sources in the SQUIDs. We investigated washer SQUIDs with regular arrays of micron-sized holes (antidots) to image the competing formation of multiquanta trapped in antidots vs. the formation of interstitial vortices and their impact on low fequency noise in different magnetic fields. Furthermore, we can correlate the perferred pinning sites with the surface morphology of the films close to the SQUID hole, where $\partial\Phi$ / ∂r is largest.

12:30 15C–3
High T_C dc SQUIDs operated in the presence of large thermal fluctuations.
K. Barthel[1], *D. Koelle*[1,2], *R. Kleiner*[3], *R. Gross*[2] and *A. Braginski*[1]. [1]Institut für Schicht und Ionentechnik, Forschungszentrum Jülich, D-52425 Jülich, Germany. [2]II. Physikalisches Institut, Lehrstuhl für Angewandte Physik, Universität zu Köln, D-50937 Köln, Germany. [3]Physikalisches Institut III, Universität Erlangen-Nürnberg, D-91058 Erlangen, Germany.

Thermal fluctuations have a strong impact on the ultimate performance of high-T_c dc SQUIDs when the thermal energy approaches either the Josephson coupling energy $E_J \equiv I_0\Phi_0/2\pi$ or the magnetic energy $\sim \Phi_0^2/2L$ in the SQUID loop of inductance L. These conditions are eqivalent to the noise parameter $\Gamma \equiv k_BT/E_J$ or the normalized inductance L/L_{th} approaching values close to unity ($L_{th} \equiv \Phi_0^2/4\pi k_BT$). We present a comparison between theoretical predictions and systematic measurements of transfer function V_Φ and white noise energy ϵ for $YBa_2Cu_3O_{7-\delta}$ dc SQUIDs within a wide range of Γ and L/L_{th} up to values above one (large fluctuation limit). %the limit of large thermal fluctuations i.e. up to $\Gamma \geq 1$ and $L \geq L_F$. Good agreement between theory and experiment is observed for V_Φ and ϵ vs Γ, however with an increasing discrepancy for higher inductances. This hinders optimization of practical devices for applications in magnetometry, where large L are desirable. Resistively shunting the SQUID inductance has been predicted to increase V_Φ and decrease the thermal noise [Enpuku and Doi, Jpn. J. Phys.**33**, 1856 (1994)]. We investigated SQUIDs of varying L with and without well defined PdAu shunt resistors. An improvement in V_Φ and thermal noise is observed for SQUIDs with shunted inductances as high as 300pH (i.e. $L/L_{th} \approx 1$ at $T = 77$K) with reasonably good $\epsilon \approx 9 \times 10^{-30} J/Hz$.

ORAL SESSION 14D: AC Losses I

Thursday Morning, September 16th, 10:30-11:45

10:30 *14D–1
Transport AC losses in Bi-2223 multifilamentary tapes - conductor materials aspect.

B.A.Glowacki[1,2] and *M.Majoros*[1,3]. [1] IRC in Superconductivity, University of Cambridge, Madingley Road, Cambridge CB3 OHE,U.K. [2]Department of Materials Science and Metallurgy University of Cambridge, Pembroke Street, Cambridge CB2 3QZ, U. K. [3]Institute of Electrical Engineering, SAS, Bratislava, Slovak Republic.

Transport ac losses in technical superconductors based on Bi-2223 tape material are influenced by many parameters. The major factors that define the ac performance of such conductors are the following: the size and number of filaments, their geometrical arrangement in the cross-section of the conductor, the twist pitch length, the resistivity of the matrix, the presence of oxide barriers around the filaments and deformation procedures such as sequential pressing or rolling followed by appropriate thermal treatment. In the present paper the above aspects are addressed from the viewpoint of the materials science of technical conductor design. Transport ac losses at power frequencies in different types of Bi-2223 conductor are presented and analysed. The results of conductor design analysis with respect to the coexistence of the superconductor with other materials in the conductor structure are presented. New concepts for minimisation of the transport ac losses are discussed in detail.

11:00 14D–2
The self-field ac losses of twisted Bi-2223 conductors.
C.M. Friend, *Y.B. Huang* and *D.M. Spiller*. BICC Supercondcutors, Oak Road, Wrexham LL13 9XP, UK.

The self-field losses of Bi-2223 round wires and tapes with twisted filaments have been studied. Twist pitches varied from 3.3-20 mm. Losses are calculated using both the 1st and 3rd harmonics of the measured sample voltage and are compared to those for untwisted conductors. As expected from classical theory, it is found that twisting the filaments of the tape-in-tube round wires has little effect on the self-field loss behaviour. However, significant differences from untwisted samples are observed for the twisted 37-filament AgAu(10wt%) clad tapes. At currents below 0.5I_C the hysteretic losses are much lower whilst the 1st harmonic measurements indicate the appearance of an additional loss in the silver matrix (though the total loss is still less than that for an untwisted sample). At higher currents there is an upward inflexion in the loss curve and the magnitude of the loss approaches that for an untwisted tape. This behaviour can be explained in terms of the geometry of the filaments and the self-field flux profile within the tape.

11:15 14D–3
Aspect Ratio Modified Effective Transverse Matrix Resistivity in Multifilamentary HTSC/Ag Strands.
E.W. Collings and *M.D. Sumption*. Materials Science and Engineering, the Ohio State University.

Magnetization has been measured vs. magnetic field strength on short samples of superconducting strand with various strand and filament aspect ratios. Bi:2223 strands with strand aspect ratios varying from round to 20:1 have been measured, as well NbTi/CuMn composites for reference. Measurements were made at 4.2K, with H directed parallel and perpendicular to the broad face of the tape. While dH/dt dependence of M(H) was influenced by logarithmic and exponential filamentary-magnetization decays and ex ponential strand-magnetization decays due to eddy currents, the latter component was extracted, and from it the effective matrix transverse resistivity. The apparent or effective resistivities were much larger than expected based on the usual filling-factor corrected resistivity of the Ag matrix. This unexpected result is explicable in terms of the flattened filamentary array geometry combined with the sample geometry.

11:30 14D–4
Critical current densities and magnetic losses in Bi-2223 tapes determined from experiments in perpendicular AC magnetic field.
F. Gömöry, *F. Strycek*, *E. Seiler*, *P. Kovac* and *S. Takács*. Institute of Electrical Engineering, Slovak Academy of Sciences, Bratislava, 842 39, Slovak Republic.

Behavior of BiSCCO-2223/Ag mono- and multi-core tapes in AC magnetic field oriented in perpendicular to the tape wide face was studied experimentally by AC magnetic susceptibility and AC magnetization loop recording. In the perpendicular arrangement, the induced currents use the path similar to that followed by transport current, and e.g. the AC losses and critical current densities can be confronted with those determined in transport experiments. We found that the critical state model for a superconducting strip or disk describes well our experiments. This agreement was excellent in the case of mono-core tapes. We present how the temperature dependence of wide-band AC susceptibility can be used to deduce the temperature dependence of critical current density. For multi-core tapes the model works only in the interval just before the saturation, again the susceptibility data can be used for critical current and magnetic loss determination. Measurements at different frequencies revealed the role of eddy currents in Ag matrix and interfilament coupling currents. Taking these mechanisms into account, we succeeded to explain the observed deviations.

ORAL SESSION 15D: Digital Applications

Thursday Morning, September 16th, 11:45-12:45

11:45 *15D–1
Applications of Josephson electronics to digital systems.
J.X. Przybysz. Northrop Grumman Science & Technology Center Linthicum, MD, 21090 USA.

Opportunities exist for the insertion of Josephson junctions into communication satellites, infrared focal plane arrays, Doppler radars, and telecommunication data switches. The high speed of Josephson analog to digital converters and the low power consumption of Josephson digital logic may be combined to enable on-board routing of data packets in communication satellites. The low power consumption of lobe counting analog to digital converters makes it possible to digitize the output of cooled infrared sensors directly on the focal plane, something that is not possible with any other technology. The unmatched high dynamic range of Josephson analog to digital converters makes it possible for Doppler radars to distinguish smaller moving targets from larger stationary objects. The high speed of Josephson digital logic makes it possible to switch gigabits per second data on-the-fly and to minimize the number of logic gates by handling the data in bit-serial format. The remarkable progress of Josephson electronics in each of these areas will be reviewed. Remaining challenges will be described. Particular emphasis will be given to the common problem of data input/output interfaces.

12:15 15D–2
Digital-to-Analog Converter Concept with RSFQ Circuits.
R. Koch, *P. Ostertag* and *W. Jutzi*. Institut fuer Elektrotechnische Grundlagen der Informatik, University of Karlsruhe, Hertzstr. 16, D-76187 Karlsruhe, Germany.

Digital-to-analog converters (DAC) are needed at the output of digital systems or at the front end as part of an analog-to-digtal converter (ADC). Several concepts are discussed.The output voltages are built up by a string of dc SQUIDs for each binary digit. With proper control circuits the output voltage does not return to zero between two voltage levels yielding a smooth staircase after filtering. Distortions owing to glitches are almost eliminated in spite of an ordinary binary input format. Simulation results of a 3 bit DAC with the Nb-Al_2O_3-Nb technology for 1 kA/qcm and RI$\sim$ 0.25 mV are presented at microwave clock frequencies.

12:30 15D–3
Hybrid Analog-to-Digital Converter based on a Delta Sigma Modulator in HTS Technology.
B. Ruck, *R. Dittmann* and *M. Siegel*. Institut fuer Schicht- und Ionentechnik, Forschungszentrum Juelich GmbH, 52425 Juelich, Germany.

e will present a complex design of an Analog-to-Digital Converter consisting of a high speed superconducting first-order delta-sigma modulator and a decimation filter based on semiconducting devices. The estimated resolution of the hybrid ADC converter is 18 bit at 10 MHz. The delta-sigma modulator is operating with an oversampling frequency of

40 GHz. The data stream of the modultor is reduced using a serial/parallel shift register. The bit rate of the RSFQ output data stream is 5 GHz. The output signal is amplified using semiconducting amplifiers and the frequency is devided by 4. The following decimation filter is based on standard CMOS circuits operated at 1.25 GHz. We have fabricated and successfully tested the first-order delta-sigma modulator using a high-temperature superconducting multilayer technology with bicrystal Josephson junctions. The circuit has been fabricated on a $SrTiO_{7-\delta}$ bicrystal substrate. The $YBa_2Cu_3O_{7-\delta}$ /$SrTiO_{7-\delta}$/$YBa_2Cu_3O_{7-\delta}$ trilayer was fabricated by laser deposition. The bottom layer served as the superconducting groundplane. The Josephson junctions were formed at the bicrystal line in the upper layer. The integrator resistance has been made from a Pd/Au thin film. The circuit consists of a dc/SFQ converter, a Josephson transmission line, a comparator, a L/R integrator and an output stage. The correct operation of the modulator has been tested using dc measurements. The linearity of the modulator was studied by measuring the harmonic distortions of a 19.5 kHz sine wave input signal. From the recorded spectrum, a minimum resolution of 5 at least bit can be estimated. This accuracy was limited by the noise of the preamplifier. The correct operation of the c rrent feedback loop was demonstrated by cutting the feedback inductance

POSTER SESSION 16

Thursday Afternoon, September 16th, 15:30-17:30

Session Bulk materials and materials aspects

16–1

Dependency of physical properties on F content in $Tl_{0.8}Pb_{0.2}Bi_{0.2}Sr_{1.8}Ba_{0.2}Ca_{2.2}Cu_3O_{(9+\delta)}F_x$ ($0 \leq x \leq 2$) polycrystalline bulk.

J. H. Lee[1], *B. J. Kim*[1], *Y. C. Kim*[1], *D. Y. Jeong*[2], *H. K. Kim*[2] and *H. Y. Lee*[2]. [1]Pusan National University, Pusan 609-735, Korea. [2]Korea Electrotechnology Research Institute, Changwon 641-120, Korea.

Dependency of T_c, phase evolution and microstructure on F content and heat-treatment time was studied in high-T_c superconducting $Tl_0.8Pb_0.2Bi_0.2Sr_1.8Ba_0.2Ca_2.2Cu_3O_{9+\delta}F_x$ ($0 \leq x \leq 2$) polycrystalline bulks prepared using a two-step reaction method. CuF_2 was used as a source of F. T_c increased with increasing F content up to 0.5 and then gradually decreased with increasing F content up to 2.2. T_c higher than 120 K was achieved in a specimen with x=0.5. Results of ac susceptibility measurements and microstructural investigation through scanning electron microscopy in all the specimens indicated that F dopping retards formation and growth of Tl-1223 phase, but enhances densification. Specimens with x=0.5 and x=1.0 reveals plate-like grains which tend to aligned in preferred orientations. The microstructure and the high T_c indicate a great potential of the present materials in practical applications. The role of dopped F on T_c and morphology will be discussed.

16–2

Hg and Tl HTS thin films by high gas pressure treatment with DTA controlled process.

A.Morawski[1], *A.Paszewin*[1], *T.Łada*[1], *A.Presz*[1], *H.Marciniak*[1], *R.Gatt*[2], *L.-G.Johansson*[3], *M. Valkeapää*[3] and *K.Przybylski*[4]. [1]High Pressure Research Centre, Polish Academy of Sciences, ul. Sokolowska 29/37, 01-142 Warsaw,Poland. [2]Physics Department, University of Wisconsin, 1150 University Avenue, Madison, WI 53706, U.S.A. [3]Department of Inorganic Chemistry, University of Göteborg, 41296, Göteborg, Sweden. [4]Department of Solid State Chemistry, University of Mining and Metallurgy, Al. Mickiewicza 30, 30-059 Cracow, Poland.

High gas pressure treatment of specimens initially obtained by the laser ablation method results in very good quality thin films. On the other hand, films made by LPE (Liquid Phase Epitaxy) method have single crystalline mirror-like Hg-1223 layer with the highest T_c (135 K) among HT_c cuprates. Assuming the heat treatment of thin films made by laser ablation method needs short time (less than half an hour) and requires applying very rapid temperature rise (up to 100 °C/min) and rapid cooling after the heat treatment run in aim to avoid possibility of $CaHgO_2$ phase precipitation on the film surface, it is possible to perform the DTA control. The in-situ DTA control is very promising for tuning the starting level of the crystallization process temperature. The knowledge of the DTA curve from the crystallization run, performed previously as a pattern, make possible to crystallize single-phase films. Additionally, the DTA allows to choose the proper temperature of crystalliza-

tion at various oxygen pressure for predicted oxidation state of the thin layer in one run of high pressure high temperature treatment applied after crystallization. Typical DTA runs for some Hg and Tl phases are shown. The XRD, EDX and transport parameters are presented.

16–3

Optimal Tc in the mercury double layer system Hg-2212 by Pb doping.

P. Toulemonde[1], *P. Bordet*[1], *J.J. Capponi*[1], *P. Odier*[1] and *J.L. Tholence*[2]. [1]Laboratoire de Cristallographie - CNRS Grenoble. [2]LEPES - CNRS Grenoble.

The superconductor with the highest T_c (135 K) is the well known compound $HgBa_2Ca_2Cu_3O_{8+\delta}$. Its T_c is 20 K above the thallium equivalent Tl-1223. The Tl bilayer compound Tl-2223 has also a high T_c (125 K), but higher than that of the corresponding Tl monolayer. Is it possible to reach the same increase of T_c in the Hg-bilayer system compared to the Hg-monolayer family ? We investigate this idea on the first member discovered in 1994 : $Hg_2Ba_2(Y,Ca)Cu_2O_{8-\delta}$. The first underdoped Ca-substituted samples $Hg_2Ba_2(Y_{1-x}Ca_x)Cu_2O_{8-\delta}$, synthesized by high-pressure – high temperature process, have shown superconducting transitions between 40 K and 70 K, depending on the Ca content (x = 0.15, 0.40 respectively). Due to limited solubility of Ca (x = 0.4), it was not possible to rise Tc further more in pure mercury samples. The Ca solubility is related to the stability of the $Hg_2O_{2-\delta}$ bilayer which can be increased by Pb^{4+} substitution in the mercury bilayer. A series of samples $(Hg_{1-y}Pb_y)_2Ba_2(Y_{1-x}Ca_x)Cu_2O_{8-\delta}$ (with $0 < y < 0.25$ and $0 < x < 1$) has been synthesized by HP-HT treatment with the purpose to reach the optimal T_c. They are nearly monophasic, except for Ca or Pb rich samples ($CaHgO_2$ and/or $BaPbO_3$ impurities). The variation of lattice parameters shows the continuous substitution of Pb^{4+}, up to y = 0.25, and of Ca^{2+}, up to x = 1. From a.c. susceptibility measurements, the optimal T_c is close to 84 K. Identical results are obtained for Tl^{3+} doping in (Hg,Tl)-2212. This optimal T_c appears relatively low as compared to that of Hg-1212 (~127 K) possibly due to the large "buckling" of CuO_2 planes in (Hg,Pb)-2212 compounds which is similar to that of (Hg,Tl)-2212 : 173°. Similar studies are underway for (Hg,A)-2223 reaching $T_c = 120$ K for A = Tl.

16–4

Toward new low anisotropy materials in superconducting artificial multilayers $(BaCuO_2)_2/(CaCuO_2)_n$.

V. Braccini[1], *D. Marré*[2], *M. Putti*[1] and *A.S. Siri*[1]. [1]University of Genoa, Physics Department, Via Dodecaneso 33, 16146 Genoa - Italy. [2]I.N.F.M., Research Unity of Genoa, Physics Department, Via Dodecaneso 33, 16146 Genoa - Italy.

Superconducting superlattices whose growth and structure is determined by the deposition kinetic instead of by thermodynamics, provide us a powerful tool to study HTSC properties and to fit them to possible applications. As example, it is in principle possible to reduce their anisotropy by simplifying the block layer structure or by increasing the number of CuO_2 planes in a unit cell. By Pulsed Laser Deposition, we grew such kind of materials using infinite layer phases both pure and doped to supply CuO_2 planes and charge reservoir blocks. We found out that using CR obtained by substituting high concentrations of Ag and Sc on the copper site in infinite layer compounds leads to a semiconducting behaviour. Oxygen doping, on the contrary, seems to be much more effective. Indeed, the $BaCuO_2$ phase, grown in high oxygen pressure, brings about charge transfer mechanisms and thus a superconducting behaviour. We deposited $BaCuO_2/CaCuO_2$ superconducting superlattices with different periodicity and studied their transport and structural properties. These compounds are very unstable and have the tendency to dissociate into secondary semiconducting phases. Various attempts to balance charge and increase the stability of the phase have been made and the experimental results obtained are presented and compared.

16–5

Copper Oxides Superconductors of Composite $Y_{1-x}Ca_xBa_2Cu_4O_8$.

A. Diaz[1], *A. Bustamante*[1], *D. Sanchez*[2] and *D. Tellez*[3]. [1]Laboratorio de Superconductividad, Facultad de Ciencias Fisicas, Universidad Nacional Mayor de San Marcos, Apartado Postal 14-0149, Lima 14 - Peru. [2]Centro Brasileiro de Pesquisas Fisicas, Rua Xavier Sigaud 150, CEP 22290-180, Rio de Janeiro, Brazil. [3]Departamento de Fisica, Universidad Federal de Pernambuco, 50670-901 Recife PE, Brazil.

The structures of the new high temperature superconductors are related to that of perovskite, $CaTiO_3$, which can be represented by the general formulae ABO_3. The structure of superconducting, orthorhombic system Y:124 are interconnected by double layer of Cu-O chains between the copper-oxygen sheets. The double strings of the 124 superconductors are formed from CuO_4 units that share edges and corners along the b axis. Yttrium can be replaced by a variety of rare earth cations. The variable oxygen stoichiometry of the single Cu-O chains in the 123 materials is not observed in the double chains of the 124 compounds. A important characteristic of the system Y:124 is that have a good stability gravimetric about of 800°C. If the system is doped with calcium (Ca), the compound $(Y_{1-x}Ca_x)Ba_2Cu_4O_8$ remains orthorhombic and changes T_c; the inconvenient has been the need of high p_{O_2} ($\geq$ 100 atm =10 MPa) in solid state reaction. However with other techniques (sol-gel or nitrate pirolisis method) they can be prepared at ordinary oxygen pressure. Nevertheless these solution based methods are complicates and require delicate techniques. In this work we have prepared 124 superconductors using CuI instead of CuO as starting precursor.

16–6

Processing and superconducting properties of $Hg_{1-x}Re_xBa_2Ca_2Cu_3O_{8+\delta}$.

A.Sin[1], *S.Piñol*[2], *A.G.Cunha*[3], *M.T.D.Orlando*[3] and *P.Odier*[1]. [1]Laboratoire de Cristallographie-CNRS, 25 Av. Des Martyrs, Bp166, F38042 Grenoble CEDEX09, France. [2]Institut de Ciència de Materials de Barcelona (CSIC), Campus de la UAB, Bellaterra E-08193, Barcelona, Spain. [3]Departamento de Física, Universidade Federal do Espírito Santo, 29060-900 Vitória-ES, Brazil.

The superconductor family $HgBa_2Ca_{n-1}Cu_nO_y$ (n=1,2,3,...) has been intensively studied since its discovery in 1993. The n=3 member of this Hg-superconductor series has the record of T_c of 135 K at ambient pressure and under high pressures around 30GPa can reach 160 K. It presents current densities as high as 10^6 A/cm^2 at 90 K and 1T. Irreversibility fields above 0.5 T at 100 K can be also achieved. These characteristics demonstrate the high potential that these superconductors have. Their processing is however difficult due to the volatility of Hg. In the sealed quartz tube technique, the chemical reaction is of the gas-solid type. The synthesis involves two steps: i) synthesis of the precursor phase, and ii) mercuration in a sealed quartz tube. In this work the importance of the synthesis of the precursor phase is emphasised. It has a dominant influence in the total pressure achieved during the synthesis. It has important consequences on the superconducting volume fraction. Moreover, the control of the oxygen content in the precursor phase is crucial to obtain the highest Tc. However, overdoped materials having a smaller Tc (126K), have an increased irreversibility line and a reduced magnetic anisotropy. Then, it is interesting to search for an optimum between Tc reduction and increase of the irreversibility line. Another important aspect is the reversibility of the annealing process for processing the superconducting phase. This fact is shown owing to the inside pressure measurement made possible by the TBA technique. This is an important feature for mastering the densification processes of Hg-1223 powders and could apply in the powder-in-tube technology.

16–7

In-situ pressure measurements and synthesis parameters in Hg-cuprate superconductors.

A.Sin[1], *A.G.Cunha*[2], *M.T.D.Orlando*[2], *S.Piñol*[3] and *P.Odier*[1]. [1]Laboratoire de Cristallographie-CNRS, 25 Av. des Martyrs, Bp166, F38042 Grenoble Cedex09, France. [2]Departamento de Física, Universidade Federal do Espírito Santo, 29060-900 Vitória-ES, Brazil. [3]Institut de Ciència de Materials de Barcelona (CSIC), Campus de la UAB, Bellaterra E-08193, Barcelona, Spain.

$HgBa_2Ca_{n-1}Cu_nO_{2n+2+\delta}$ (n=1 , 2, 3, ...) superconductors have been extensively studied since their discovery in 1993. The most interesting compound of the series is the n=3 member, which shows the highest T_c so far reported at ambient pressure (135 K). The synthesis of the unsubstituted compound poses serious problems at pressures < 50 bar due mainly to HgO_δ instability. That is the reason why most authors studied the doping of high-valency cations in $Hg_{1-x}M_xBa_2Ca_2Cu_3O_{8+\delta}$ where M = Pb, Bi, W or Re in our case. The chemical reactions involved in the synthesis of mercury based cuprates combine gas phases (Hg, O_2) and solid phases ("$M_xBa_2Ca_2Cu_3O_y$"). Sealed quartz tube is absolutely necessary. Then, one of the most important parameter to form the superconductor phase is the total pressure inside the tube. The analysis of the reacting phases shows that the pressure influences the ratio between the desired phase Hg-1223 and HgCaO2 an intermediate phase. This last binary oxide constitutes the most difficult impurity to eliminate, it remains frequently in the final product. For the first time, we have developed a measurement of the pressure directly in side the quartz tube, instantaneous and non-destructive by the so-called thermobaric analyser (TBA) apparatus. It allows to understand the reaction mechanisms occurring and to adjust the main synthesis parameters such as filling factor, heating and cooling ramps in order to avoid the formation of $HgCaO_2$.

16–8

Pressure effects in $Hg_{0.82}Re_{0.18}Ba_{(2-y)}Sr_yCa_2Cu_3O_{8+\delta}$.

A.Sin[1], *M.T.D.Orlando*[2], *M.Nunez-Regueiro*[3], *A.G.Cunha*[2] and *P.Odier*[1]. [1]Laboratoire de Cristallographie-CNRS, 25 Av. des Martyrs, Bp166, F38042 Grenoble Cedex09, France. [2]Departamento de Física, Universidade Federal do Espírito Santo, 29060-900 Vitória-ES, Brazil. [3]Centre de Reserche sur les Tres Basses Temperatures-CNRS, 25 Av. des Martyrs, Bp166, F38042 Grenoble Cedex09, France.

$HgBa_2Ca_{n-1}Cu_nO_{2n+2+\delta}$ (n=1, 2, 3...) superconductors have been extensively studied since their discovery in 1993. As a general result, application of pressure on these superconducting cuprates increases their Tc for underdoped and optimally doped compounds. For example the T_c of $HgBa_2Ca_2Cu_3O_{8+\delta}$ (n=3 135K at ambient pressure), which is the highest T_c of any superconductors, increases up to 164K at 30 GPa. The respective contributions from reservoir block and superconducting block to this effect are not so well established. The influence of substitution in the reservoir, i.e. Hg by Re in the composition $Hg_{0.82}Re_{0.18}Ba_{(2-y)}Sr_yCa_2Cu_3O_{8+\delta}$ is thus very interesting and discussed. On the other hand, chemical pressure is very attractive to simulate this mechanical pressure effect on superconductivity. One of the ways to do this is to substitute Ba by a smaller cation such as Sr. However, the general trend of a partial Sr substitution by Ba in cuprate superconductors is to decrease their Tc values (except for La-Sr-Cu-O system). We have prepared Sr substituted $Hg_{0.82}Re_{0.18}Ba_{(2-y)}Sr_yCa_2Cu_3O_{8+\delta}$ compounds by the quartz tube technique, controlled by an in-situ measurement of the total pressure (TBA). The T_c decreases linearly with Sr substitution. This might be due to underdoping provoked by the incapacity of Sr substituted compounds to incorporate enough oxygen to reach the optimal doping.

16–9

Bi-epitaxial YBaCuO films grown on eutetic substrates.

J. Santiso[1], *L.A. Angurel*[2], *V. Laukhin*[1,3], *R.I. Merino*[2], *M. Doudkowsky*[1], *G. García*[1], *J.I. Peña*[2], *M.L. Sanjuán*[2], *A. Figueras*[1] and *V. M. Orera*[2]. [1]Institut de Ciència de Materials de Barcelona (C.S.I.C.), Campus de la Universitat Autònoma de Barcelona, 08193 Bellaterra (Spain). [2]Instituto de Ciencia de Materiales de Aragón (C.S.I.C.-Universidad de Zaragoza), Facultad de Ciencias, Pza San Francisco, 50009 Zaragoza (Spain). [3]Permanent address:Institute of Problems of Chemical Physics, RAS, Chernogolovka, MD 142432 Russia.

YBaCuO thin films, grown by Metal-Organic Chemical Vapor Deposition, have been deposited on ceramic substrates: $CaZrO_3$ or eutetics of Ca-stabilised zircona-$CaZrO_3$. Epitaxial growth has been obtained on both phases. Different configurations of the superconducting film can be induced by modifying the eutectic microstructure of the substrate

or by selecting its adequate crystallographic orientation. In particular, lamellar- structured films with alternating parallel c-axis and (103)-oriented strips, or alternating c-axis oriented strips with two different in-plane orientations have been fabricated. The samples composition was analysed by EPMA and micro-Raman. The influence of the different microstructures of the films on the physical properties has been analysed. The temperature dependence of the ac susceptibility, for different dc magnetic fields, has been used to obtain information about the granularity of the samples and to estimate the critical current values (values up to 10^5 A/cm^2 at 77 K have been obtained). For the lamellar films, this characterisation has been also carried out by transport measurements in order to get information about the anisotropy of the superconducting and normal state properties of the films.

16–10

The Influence of Preparative Sequence on the Intergrain Coupling of Tl-1223 HTS-Ceramics.

Chr. L. Teske. Institut f. Anorganische Chemie CAU Kiel, D-24098, Germany.

The nature of the intergranular pinning was studied by investigating the AC susceptibility χ' (T,H_{ac}) and χ''(T,H_{ac}) at field amplitudes in the range of 80 < H_{ac} < 800 [A/m]. We achieved a clear improvement of intergranular coupling by changing the preparative sequence. The properties of HTS-material in the Tl(Bi/Pb)-Ba(Sr)-Ca-Cu-O system depend on both the chemical composition and strongly on the nature of the granular microstructure. Reground powder samples of optimised Tl-1223-type ceramics have a low reactivity causing weak-links during the PIT tape preparation. To overcome this without forming additional secondary phases by further doping, we tested new preparative methods. At first a set of optimised Tl-1223-type ceramics were prepared, each having different nominal composition, either with Pb *or* Bi partially substituting for Tl or with variant ratio Sr/Ba. Phase purity was checked by Rietveld technique. Then reground mixtures each of two of these different Tl-1223 samples were reacted again, forming solid solutions either containing Bi *and* Pb partially substituting for Tl or having a changed ratio Sr/Ba. These samples in each case have the lowest gradient in the linear plots of the peaks in χ''(T,) in terms of magnetic field amplitude dependency.

16–11

DTA High Pressure System for in-situ Identification of Phase Transformation during Hg and Tl HTS Crystallization Process.

T. Lada[1], *A.Paszewin*[1], *A.Morawski*[1], *A.Presz*[1], *S.Gierlotka*[1], *K.Przybylski*[2] and *R.Gatt*[3]. [1]High Pressure Research Centre, Polish Academy of Sciences, ul. Sokolowska 29/37, 01-142 Warszawa, Poland. [2]Department of Solid State Chemistry, University of Mining and Metallurgy, Al. Mickiewicza 30, 30-059 Cracow, Poland. [3]Physics Department, University of Wisconsin, 1150 University Avenue, Madison, WI 53706, U.S.A.

Although the high pressure technology for obtaining HTS superconducting crystals is known for some time, there is a reasonable lack in thermodynamical data describing the crystallization process. Sufficient information may be collected via an elementary differential thermal analysis (DTA) run under conditions corresponding with the crystallization process. Mercury and thallium-based HTS crystals should to be grown at high pressure and high temperature regime with a strict time program. To fulfill these demands a special equipment is required. Based on results of the previous investigations, we have modified the high pressure system used to crystallization. These modifications allow to perform DTA experiment with following parameters: maximum temperature 1200 °C, maximum temperature rate 1000 °C/min, temperature resolution 0.1 °C, time resolution 0.1 s, sample volume up to 5 cm ^{3}, working pressure up to 1.5 GPa, inner environment - inert gas with up to 25% oxygen. The reducing and oxygenating atmospheres within that range may be applied as well. The described DTA High Pressure System allows to identify critical temperatures for phases that appear one after another as a reaction product. Here we present results obtained with that system for some mercury and thallium-based HTS compounds crystallization.

16–12

Percolation effects of the $YBa_2Cu_3O_x$ phase in the Y_2BaCuO_5 green phase.

G.A.Costa[1,2], *P.Mele*[1,2] and *A.Ubaldini*[1,2]. [1]INFM, Via Dodecaneso 33, I-16146 Genova, Italy. [2]Dipartimento di Chimica e Chimica Industriale, Universita' di Genova, Via Dodecaneso 31, I-16146 Genova, Italy.

The presence of Y_2BaCuO_5 phase (Y-211) in $YBa_2Cu_3O_x$ (Y-123) matrix is highly positive for the grain growth and alignment in the bulk superconductor [1, 2]. With the purpose to check if a continuous path of Y-123 in Y-211 exists, we gradually increased the Y-211 excess until 99 wt.%. We found that the Y-123 phase continued to cover the Y-211 grains. Experiments performed on bar-shaped samples allowed to conclude that the percolation threshold value is near (but lower than) 1 wt. % Y-123 in Y-211 phase. The Y-211 rich bars were placed on two Y-211 100 wt. % pellets to avoid the contact with the crucible, and then alloyed by the Melt-Texture-Growth technique [1]: occasionally, the growth of needle-like crystals in the space between the sample and the alumina boat was observed by optical microscopy. The SEM-EDAX analysis revealed two kind of crystals: black needles, with squared section, were biphasic crystals in which the core is the Y-211 insulating phase and the skin is the Y-123 phase, and green needles, with hexagonal section, only constitued of Y-211 phase. The results were confirmed by Raman analysis performed to test the oxygen content of Y-123 phase. References [1] M. Murakami, Melt-processed high-temperature superconductors, M. Murakami Ed., Singapore, World Scientific (1993) 21. [2] K. Salama and S. Sathyamurty, IEEE Trans. on Appl. Superc. (1998), in press.

16–13

Dynamic Compaction for the Fabrication of HTS Ceramic Components.

A. G. Mamalis[1], *A. Szalay*[2], *B. Raveau*[3], *G. Desgardin*[3], *L. Chubraeva*[4], *I. Vajda*[5], *N. Gobl*[2], *T. Porjesz*[6] and *I. Kotsis*[7]. [1]NTUA, Athens, Greece. [2]S-Metalltech ltd, Budapest, Hungary. [3]CRISMAT-ISMRA, Caen, France. [4]VNII El. Mach, St-Petersburg, Russia. [5]TU Budapest, Budapest, Hungary. [6]Eotvos University, Budapest, Hungary. [7]University of Veszprem, Veszprem, Hungary.

Dynamic compaction techniques like explosive and electromagnetic compactions may be considered as tools to produce ceramics with unique properties. The above techniques have been theoretically and experimentally investigated for the case of HTS ceramics with a special view of their applications for levitating devices. The density of the pinning centers can be affected by the processing technology for the reasons that new grain boundaries are formed due to fracturing of the initial grains, on the one hand, and the shock induced dislocations form pinning centers, on the other, so that the final result is the enhancement of the respective superconducting parameters. The properties of the HTS ceramic compacts like grain size distribution, morphology as well as the influence of the compaction velocity which are important for levitation force improvement have been analyzed. The superconducting compacts of YBCO are further processed by rolling, extrusion and machining. The plastic deformation during the above processes will be characterized and modelled for each manufacturing stage to obtain the optimum parameters from the point of view of the projected applications.

Session Wires tapes and coated conductors

16–14

Development of ion assisted sputter deposition of biaxially aligned YSZ layers.

G. De Winter[1], *J. Denul*[2] and *R. De Gryse*[1]. [1]University of Gent, Gent, B-9000, Belgium. [2]Centre for Vacuum and Materials Sciences, Gent, B-9000, Belgium.

Biaxially textured Yttria Stabilized Zirconia layers have been deposited on different substrate materials using a modified sputter source. This modified sputter source generates a beam of energetic ions directed towards the substrate. An experimental set up was realised in which the incidence of energetic particles on a growing film under a controlled angle is achieved. Most layers were deposited with an angle of 55° between the ion flux and the substrate normal. From X-Ray Diffraction pole figures it is clear that bi-axial texturing is achieved on both metallic and glass substrates. The best FWHM values achieved until now are psi = 11° (characteristic for out of plane orientation) and phi = 22° (characteristic for in plane orientation). This process is being optimised further in order to increase the degree of texturing. This research was supported in part by the Brite-EuRam project MUST (Multi-functional flexible high temperature superconducting tape) (contract BRPR-CT97-0331) and in part by the Special Research Fund of the Unversity of Gent as part of the project : Studie van de microstructuur van deklagen gegroeid door middel van ionen bundel geassisteerde depositie.

16–15

Electrical, magnetic and AC loss properties of Bi-2223/Ag(alloy) tapes subjected to bending strain.

L. Bigoni[1], *F. Barberis*[1], *E. Cereda*[1], *F. Curcio*[1], *P. La Cascia*[2], *L. Martini*[1] and *V. Ottoboni*[1]. [1]ENEL-SRI, Segrate, Milan, 20090, Italy. [2]Univerity of Bologna, 40126, Italy.

The degradation of electrical properties of Bi-2223/Ag(alloy) tapes due to bending strain represents an important parameter in designing superconducting coils and predicting their behaviour in terms of critical current, V-I characteristic and AC loss. At this purpose, V-I characteristic of Bi-2223/Ag(alloy) tapes subjected to progressive bending processes, as a function of magnetic field applied both parallel and perpendicular to the tape surface, have been deeply investigated. The dependence on magnetic field and bending strain of the critical current and the power law index of the V-I curve, n, has been determined. The analysis of transport properties degradation due to bending strain has been completed by measuring the AC loss evolution of the tapes and correlating it to the V-I dependence on the magnetic field.

16–16

Preparation of Tl-based superconducting tapes by electrochemical deposition.

E. Bellingeri, *H. Suo*, *J.-Y. Genoud*, *M. Schindl*, *E. Walker* and *R. Flükiger*. DPMC, Université de Genève 24, Quai Ernest Ansermet CH-1211 Genève 4, Switzerland.

An alternative preparation method of Tl based superconducting tapes, in particular the Tl(1223) phase, was developed. This method is based on the co-deposition of the metals by an electrochemical process followed by a high temperature thermal treatment in order to form the superconducting phase. Nitrates of the metals are dissolved in DMSO and the depositions on metallic substrates are performed in a standard three electrodes cell. The thermal treatment is performed in a high isostatic pressure furnace (1 bar Oxygen / 50 bar Helium) in order to prevent Tl evaporation. The main advantage of this technique is that it is very fast, cheap and can be easily scaled up to produce long length tapes in a continuos process. The desired stoichiometry is obtained by varying iteratively the concentration of nitrates in the starting solution. To guarantee the scalability of the process Ag was chosen as substrate material and experiments were performed on standard foils, textured ribbons and single crystals. Preliminary results reagarding deposition of Tl(1223) are presented and the role of the different kinds of Ag substrates is discussed.

16–17

Optimum geometry of ceramic cores in multifilamentary Ag/BSCCO tapes.

J.I. Bech[1], *M. Eriksen*[1], *B. Seifi*[1], *N. Bay*[1], *P. Skov-Hansen*[2] and *B. Kindl*[3]. [1]Department of Manufacturing Engineering (IPT), Technical University of Denmark (DTU), Lyngby, 2800, Denmark. [2]Nordic Superconductor Technologies A/S(NST)Brøndby, 2605, Denmark. [3]Materials Research Department, Risø, Roskilde, 4000, Danmaark.

The Ag/BSCCO-2223 composite tapes are widely used for high temperature superconducting (HTS) tapes. It is well known that the ceramic cores within the same tape have very different quality regarding superconducting properties. It is also well known that that the BSCCO layer within a few micrometers from the BSCCO/Ag interface has very high texture, density and Jc. One of the challenges in developing the new generations of Ag/BSCCO tapes with improved Ic is to design and process the tapes in a way so that the entire BSCCO cross section has the best possible quality in order to utilise the full potential of the BSCCO material. In this work multifilament tapes are produced by the PIT process using rectangular singlefilaments packed in rectangular outer sheaths. Rectangular multifilament wires with 2 different width/height ratios have been flat-rolled using 3 different roller diameters, 2 reduction strategies and 2 annealing strategies. The tapes generally have very wide and thin, homogenous filaments and a high Interface-Layer Fraction (ILF, the fraction of the BSCCO cross-section within the high quality interface-layer). Results show that rolling parameters have a large influence on the geometry of tapes and filaments. Especially the geometry of the wire before rolling is important.

16–18

Step Sintering and Jc Behavior in Multifilamentary Bi-2223 Tapes.

D.A. Esparza and *M.T.Malachevsky*. Centro Atomico Bariloche - Comision Nacional de Energia Atomica - 8400 S.C. de Bariloche - Argentina.

19-filament silver sheathed tapes were prepared by the "powder in tube" method. The starting partially reacted commercial precursor consisted of an 80 % of Bi-2221 as the main phase. The filaments were evenly distributed in the silver matrix as was revealed by optical and scanning microscopy observations. The critical current density Jc at 77 K and 0 T was measured after each 12-hour heat treatment and its dependence upon the cumulative sintering time was studied. The existence of an initial plateau was observed that could be related with the retarding effect of the silver in the formation of the 2223 phase. After 108 hours a maximum is reached and beyond that time the critical current density begins to decay. Samples subjected to 10% reduction in thickness by lamination after each 12 hour annealing reached similar Jc values after 36 hours. These samples were again step annealed without further deformation and the Jc growth rate was found to be higher. The different behaviors were interpreted as being a consequence of the 2221-2223 phase transformation, as followed by X-ray powder diffraction.

16–19

Manufacturing and Characterisation of a Novel Geometry for (Pb,Bi)2223 Superconducting wires.

D.M. Spiller, *C.M. Friend*, *Y.B. Huang*, *I.G. Ferguson* and *W.W. Blendl*. BICC Superconductors, Oak Road, Wrexham LL13 9XP. UK.

An important parameter for original equipment manufacturers to adopt HTS conductor technology into their existing manufacturing processes is the ease with which they can adapt existing equipment. Therefore an HTS conductor with round cross section is preferred. The ideal geometry for an HTS conductor would offer an isotropic behaviour in the presence of an applied field. This would enable current application designs to be used and production methods utilised, simplifying the design. We present a novel superconducting wire with round cross section. The geometrical configuration of the wire results in a negligible angular dependence of I_C with field with a ΔI_C with different field orientation $<$ 5%. Self field a.c. loss measurements have been carried out with the results being less than that of a traditional elliptical tape. This may be explained by the filament geometry of this novel design. The results of twisted wires with an isotropic filament geometry will also be discussed.

16–20

Temperature dependence of filament coupling in multyfilament Bi-2223 tapes: Magneto-optical study.

T. H. Johansen[1], *Y. M. Galperin*[1,2], *M. Bazilievich*[1], *A. V. Bobyl*[2] and *D. V. Shantsev*[1,2]. [1]Department of Physics, University of Oslo, P. O. Box 1048, Blindern, 0316 Oslo, Norway. [2]A. F. Ioffe Physico-Technical Institute, Polytechnicheskaya 26, St.Petersburg 194021, Russia.

Temperature dependence of coupling between filaments in multyfilament Ag-sheathed Bi-2223 tape was investigated using magneto-optical method for temperatures from 20 K to T_c. Magnetic flux distributions above the tape were measured in the remanent state after applying large magnetic field 105 mT. The total flux distribution can be separated into two contributions. The first one (i) is that expected for a uniform superconductor of the same shape. It results from the presence of coupling between superconducting filaments. The second one (ii) is a fine structure of flux distribution which results from persistent currents inside individual filaments. We separate contributions (i) and (ii) using information about peculiar arrangement of filaments in the tape that can seen from optical image. Using theoretical results for the Bean model in perpendicular geometry we determine critical current densities, J_{c1}, and J_{c2} corresponding to both contributions. For contribution (i) J_{c1} is the critical current density of interconnections between filaments, for contribution (ii) J_{c2} is intrafilament critical current density. It is shown that J_{c1} and J_{c2} have qualitatively different temperature dependences. Temperature dependence for J_{c1} is typical for weak links, while that for J_{c2} is typical for depinning critical current. Thus, as temperature increases, coupling between filaments becomes more important.

16–21

Magneto-optical study of multyfilament Bi-2223 tapes in current-carrying state: Visualisation of individual filaments.

T. H. Johansen[1], *Y. M. Galperin*[1,2], *M. Bazilievich*[1], *A. V. Bobyl*[2], *D. V. Shantsev*[1,2] and *M. E. Gaevski*[2,3]. [1]Department of Physics, University of Oslo, P. O. Box 1048, Blindern, 0316 Oslo, Norway. [2]A. F. Ioffe Physico-Technical Institute, Polytechnicheskaya 26, St.Petersburg 194021, Russia. [3]Department of Materials Science, Uppsala University, P O Box 534, SE-751 21 Uppsala, Sweden.

The aim of the present work is to study the current-carrying state and the remanent state after transport current of Ag-

sheathed multyfilament Bi-2223 tape with different magnetic history. Magneto-optical technique was used to measure magnetic flux distributions on the tape surface with 3 micron resolution at temperature 20 K. Fine structure of flux distributions associated with distribution of filaments in the tape was investigated in detail. A correlation is observed between flux distributions measured on tape in different magnetic states. The experimental results are in a qualitative agreement with the Bean model predictions for an array of strips. Evolution of flux distribution during the current pulse is also investigated. For currents below 13 A (which is much less than the critical current), the flux distribution is stable during 200 ms pulse. For larger currents, a relaxation of flux distribution is observed implying a redistribution of current in the tape during 200 ms pulse.

16–22

Ageing effect on ac losses of BSCCO−2223 tapes with different geometrical structures.

P. Caracino[1], *G. Grasso*[2], *P. Guasconi*[2] and *D. Uglietti*[3]. [1]Pirelli Cavi e Sistemi - Viale Sarca, 222 20126 Milano Italy. [2]INFM UdR di Genova - Via Dodecaneso, 33 146 Genova Italy. [3]INFM UdR di Milano - Via Cozzi, 53 20126 Milano Italy.

At present widespread applications in the field of superconductivity are using BSCCO−2223 tapes as conductor elements. One of the main tape requirements is represented by the mechanical strength that must be higher enough to sustain all the stresses applied during the manufacturing process. The aim of this study is to compare the transport AC losses measured on BSCCO−2223 tapes with different geometrical distribution of filaments and sheath materials. Moreover the impact of mechanical ageing on critical current and transport AC losses for those different geometries has been evaluated. Mechanical ageing was realised by double bending tapes on different diameters at room temperature. AC losses were measured electrically by means of a lock-in technique. We discussed the obtained results as function of contributions to AC losses due to different transport mechanisms.

16–23

Performance Characteristics of Bi-2212 Multifilament Round Wire and Cable Designs.

L. R. Motowidlo[1], *R. S. Sokolowski*[1], *T. Hasegawa*[2], *D. R. Dietderich*[3] and *R. M. Scanlan*[3]. [1]IGC Advanced Superconductors, Waterbury, CT 06704, USA. [2]Showa Electric Wire & Cable, 2-1-1, Kawasaki, Kanagawa 210,Japan. [3]SC Magnet Group,Lawrence Berkeley National Lab.,Berkeley,CA 94707,USA.

Long lengths of multifilamentary Bi-2212/Ag wires have been successfully fabricated for utilization in various high magnetic field applications. The performance characteristics of round strand designs having outer diameters ranging from 1 mm to 0.5 mm will be presented. The critical current density is shown to increase to over 300,000 A/cm^2 at 4.2K in self field with decreasing the filament diameter to about 13 microns. Measurements are performed on long helical samples having voltage taps 50 cm apart. The n-values of these wires are analyzed and found to be as high as 15 to 20 in applied magnetic fields out to 15 Tesla. However, in the case of badly suasaged filaments due to improper thermal-mechanical processing the n-value may be as low as 4. The dependence of Jc on temperature and magnetic field of Bi-2212 strands will be presented as well as performance charactistics of Rutherford type cables having 18 to 20 stands.

16–24

Single source MOCVD systems for YBCO deposition onto moved tapes.

O. Stadel[1], *J. Schmidt*[1], *G. Wahl*[1], *C. Jimenez*[2], *F. Weiss*[2], *M. Krellmann*[3], *D. Selbmann*[3], *S.V. Samoilenkov*[4], *O.Yu. Gorbenko*[4] and *A.R. Kaul*[4]. [1]Institut für Oberflächentechnik und Plasmatechnische Werkstoffentwicklung (IOPW), Technische Universität Braunschweig, Bienroder Weg 53, 38108 Braunschweig, Germany. [2]Laboratoire des Materiaux et du GeniePhysique (LMGP), ENSPG, Rue de La Houille Blanche, Domaine Universitaire BP46, F-38402 Saint Martin D'Heres Cedex, France. [3]Institut für Festkörper und Werkstofforschung Dresden (IFW), Postfach 270016, D-01171 Dresden, Germany. [4]Department of Chemistry, Moscow State University, 119899 Moscow, Russia.

YBCO thin films were continuously deposited onto moved substrates in a liquid single source MOCVD system with a hot wall reactor, which had two slits for the moved substrate. The precursors were solved in an organic solvent and dosed as solution by a mass flow controller. The band evaporator divided the solvent from the precursors and fed only the precursor vapour into the deposition chamber in a continuous process. XRD study of YBCO films obtained showed a strong preferential c-axis orientation with a narrow rocking curve of (005)YBCO: FWHM = 0.1°(on SrTiO3), and good in plane orientation: measured by (102)YBCO phiscans FWHM = 0.6°. The critical current density over 1 MAcm^{-2} (77 K) was achieved on single crystal substrates. Based on these results a new MOCVD-system was designed, in which the buffer layers and YBCO on long metal tapes shall be deposited. This system was enhanced in respect to long time deposition and deposition velocity.

The authors acknowledge the financial support of EU (Brite-EuRam Project BRPR-CT98-0676) and Volkswagen Foundation (I/73 628).

16–25

Evidence for anisotropic texturing in silver sheathed Bi(2223) tapes through magnetic measurements.

C. Ferdeghini[1], *M.R. Cimberle*[2], *G. Grasso*[1] and *I. Pallecchi*[3]. [1]INFM-Research Unit of Genoa, Via Dodecaneso 33, 16146 Genoa, Italy. [2]CNR-CFSBT, Via Dodecaneso 33, 16146 Genoa, Italy. [3]Università di Genova, Dipartimento di Fisica, Via Dodecaneso 33, 16146 Genoa, Italy.

To improve the current carrying capability in composite superconductors as Bi(2223)/Ag tapes, the phase texturing undoubtedly represents a key factor. So far, the analysis of the grain orientation inside tapes was performed by X-ray and neutron diffraction techniques. Here we propose an innovative method to study the grain texturing in Bi(2223)/Ag tapes during the different steps of the mechanical deformation process. This method is based on the fact that in the BSCCO system, a very strong anisotropy be-

tween the in-plane and out-of-plane critical current densities is present. As a consequence, regardless to the orientation of an external magnetic field applied to the tape, the measured magnetic moment is always dominated by the currents flowing in the a-b planes of the grains. Therefore, by comparing measurements performed with different field orientations with respect to the tape, it is possible to evaluate the mean orientation angle for the grains, and to follow its evolution within a series of subsequent rolling steps before the final thermal treatment. These results indicate that the longitudinal orientation of the grains is generally different from the transversal one. During the rolling process, both orientations monotonically decrease, reaching about 21° and 19° after the final step, respectively.

16–26

YSZ buffer layers on large metallic and ceramic substrates.

J. Dzick[1,3], *J. Hoffmann*[1], *S. Sievers*[1,3], *K. Thiele*[1], *J. Wiesmann*[1], *F. García-Moreno*[1,2], *A. Usoskin*[2], *C. Jooss*[1] and *H. C. Freyhardt*[1,2]. [1]Institut fuer Materialphysik, Universitaet Goettingen, Windausweg 2, 37073 Goettingen, Germany. [2]Zentrum fuer Funktionswerkstoffe, Windausweg 2, 37073 Goettingen, Germany. [3]kabelmetal electro GmbH, Kabelkamp 20, 30179 Hannover, Germany.

Biaxially-textured yttria-stabilized zirconia (YSZ) films are prepared on technical substrates such as metallic tapes or ceramic plates to serve as templates for high-current carrying YBCO films. These YSZ films are deposited by an ion-beam-assisted deposition process (IBAD). A deposition chamber with two 11 cm Kaufman ion sources and a deposition chamber with two 11 cm ion sources and one 21 cm Kaufman ion source are applied. On Ni tapes YSZ films with a high quality in-plane texture characterized by a FWHM of smaller than 20 degrees could be produced. In this contribution results will be presented on the upscaling of this process to 2 m long and 70 mm wide metallic tapes. Furthermore, the IBAD systems are now developed to an extend to allow the homogeneous coverage of ceramic substrates of a size up to 20 cm * 50 cm with biaxially textured YSZ films. The quality of the texture is followed by investigating the growth and superconducting properties of YBCO films on these large-area substrates. Part of this work was supported by the German BMBF and kabelmetal electro GmbH under grant number 13 N 6924/6. Further investigations were performed within a development project of the Siemens AG which is also supported by the German BMBF (Project No. 13 N 6482)

16–27

How important is the precursor powder quality for bringing Bi-tapes to market ?.

M. Gerards[1] and *R. Riddle*[2]. [1]Merck KGaA, Darmstadt Werk Gernsheim D-64579 Gernsheim Germany. [2]Merck Ltd. Poole BH15 1TD England.

For many years a lot of effort was put into optimization of HTS precursor powder quality which is one of the key factors for high performance Bi-tapes. Recent developments impressively demonstrated success on improving Jc in such superconducting tapes for power applications. Now the next step forward is the consequent development of efficient, low cost and quality maintaining way of tape manufacture. On this way powder manufacturer have to face with new problems resulting from upscaling of fabrication process which has dramatic influence on powder quality. In this presentation we like to start a discussion on how can we deal with subjects like local impurities in powders? Can we manage reproducibility and homogenity of powders? What are the up-scale effects?

16–28

Large-area HTS conductors obtained by novel PLD technique on metallic substrates.

A. Usoskin[1], *F. García-Moreno*[1,2], *S. Sievers*[2,3], *J. Knoke*[1], *H. C. Freyhardt*[1,2], *J. Dzick*[2,3] and *J. Wiesmann*[2]. [1]Zentrum fuer Funktionswerkstoffe gGmbH Goettingen, Windausweg 2, D-37073 Goettingen, Germany. [2]Institut fuer Materialphysik, Windausweg 2, D-37073 Goettingen, Germany. [3]kabelmetal electro GmbH, Kabelkamp 20, D-30179 Hannover, Germany.

Recent achievements in the technology of large-area film-based high-Tc superconductors reveal attractive applications in e.g. HF and power engineering. In the present study further steps are reported in developing HTS coated conductors. YBCO films with high-quality in-plane texture have been grown on YSZ-IBAD buffered polycrystalline Ni and stainless steel (SS) substrates using a modified pulsed laser deposition technique based on (i) a variable-azimuth-ablation method, (ii) a quasi-equilibrium substrate heating, and (iii) a „soft" substrate translation including the rotation and linear motion of long substrates. The installation developed for this aim is capable of HTS film deposition on long tubular substrates with a diameter up to 70 mm and on long flexible ribbons with a width up to 200 mm. For the short YBCO coated Ni and SS substrates (10 x 10 mm^2) critical current densities J_c up to 2 MA/cm^2 and 1.2 MA/cm^2, respectively, were observed at 77K and 0T. J_c values of more than 1 MA/cm^2 were reached for $\sim$ 100 mm-long SS tapes. Long YBCO coated Ni and SS tapes and tubes were manufactured with lengths up to 0.5 m.
This work is supported by the German BMBF, kabelmetal electro GmbH (Project No 13N6924/6), and EU Brite/EuRam No BE97 4738.

16–29

Magneto-optic investigation of bent Bi-2223 multifilamentary tapes.

M.R. Koblischka[1], *T. H. Johansen*[1] and *P. Vase*[2]. [1]University of oslo, Department of Physics, Oslo, N-0316, Norway. [2]NST A/S, Brondby, DK-2605, Denmark.

Following earlier work on monofilamentary Bi-2223 tapes, we investigate the effect of bending applying bending strains between 0.5% and 9% to multifilamentary Bi-2223 tapes with 19 filaments. Flux patterns are visualized using an intact tape, i.e. the visualization is done while keeping the silver sheath intact after removing the bending strain. The images clearly reveal the superior performance of the multifilamentary tapes, although high-resolution flux patterns show a similar cracking effect.

16–30

Slow cooling effect on transport and structural properties of Ag-sheathed Bi(2223) tapes.

G. Grasso, *F. Grilli* and *P. Guasconi*. INFM-Research Unit of Genoa, Via Dodecaneso 33, 16146 Genoa, Italy.

The high temperature treatment of Ag-sheathed Bi(2223) tapes manufactured by the Powder-In-Tube method has been suitably modified with the aim of improving the transport properties of these superconducting materials in presence of an external magnetic field. The effect of a slow cooling process and/or of a final low temperature treatment stage on the magnetic field dependence of the critical current density as well as of other structural and superconducting properties of Bi(2223) tapes is presented. Preliminary results show that an improvement of the transport properties in magnetic field, at the liquid nitrogen temperature, can be effectively achieved by the slow cooling process. At a field of 0.3 T applied perpendicular to the tape, the improvement is quantified in a factor of about 3. However, its origin appears to be more likely correlated with an increase of Tc of about 2.5°C than to an improvement of the intrinsic pinning properties of the Bi(2223) phase.

16–31

Deformation-induced defects in a ceramic core and their healing with thermal processing the Ag/BiSCCO superconducting tapes.

V. Beilin[1], *A. Goldgirsh*[1], *E. Yashchin*[1], *M. Roth*[1] and *A. Verdyan*[2]. [1] School of Applied Science, the Hebrew University of Jerusalem, Jerusalem, 91904 Israel. [2]Center for Technological Education Holon, affiliated with Tel-Aviv University, P.O.B. 305, Holon, 5812, Israel.

Effects of rolling and pressing on transport ctritical current density, J_c its magnetic field dependence $J_c(H)$ and the magnetic susceptibility of Ag/BiSCCO tapes were studied at various steps of tape processing by the oxide powder in tube method. Intermediate deformation (ID) has been shown to result in narrowing of current carring percolative channel inside inside ceramic ceramic core and in the enchancement of channel granularity in as-deformed state. Analysis of J_c vs. H dependenceis, bending tests and magneto-optical studies reveald that channel narrowing was due to the generation of ID-indused mickrocracks which were fast healed during the very early stages of the next sintering step.Reduced core granularity has been set up in a very short sintering period after ID being followed by the appropriate J_c enhancement. This process has been studied over the wide range of sintering temperatures.The locations of healed microcracks can behave like additional weak links through which magnetic flow goes into the ceramic core. Significant facilitation of 2212 to 2223 phase transformation by ID was also observed at the early sintering stage.

16–32

Phase decomposition and transformation during final process of Ag/Bi-2223 tapes.

H.K. Liu, *R. Zeng*, *X.K. Fu* and *S.X. Dou*. Institute for Superconducting and Electronic Materials University of Wollongong, Wollongong, NSW 2522 Australia.

Bi-2223 phase decomposition and residual liquid phase transformation at temperature between 700 and 845 degree Centigrade during final process of Ag/Bi-2223 powder in tube tapes and the effect on critical current density have been investigated. In order to determine the fraction of Bi-2223 phase decomposition and residual liquid phase transformation, the two-step procedure and quenching technique at different temperature have been used. It was found that at the temperature region of 823 - 845 degree Centigrade Bi-2223 phase co-existed with liquid and other secondary phases. The Bi-2223 phase was stable in the range of 823 - 832 degree Centigrade and the liquid phase can be effectively converted to Bi-2223 phase if the second step annealing in the two-step process were set to this range. Below this temperature region liquid phase was mainly transformed into Bi-2212. At temperatures below 810 degree Centigrade, Bi-2223 phase decomposed mainly into Bi-3221 phase. The critical current density showed a clear correlation with the fraction of Bi-2223 in the tape.

16–33

Mechanical properties of superconducting Bi-2223/Ag composite tapes.

Z. Han, *H. Wu*, *P. Skov-Hansen* and *P. Vase*. Nordic Superconductor Technologies A/S, Priorparken 685, DK-2605 Brondby, Denmark

The mechanical properties of Bi-2223/Ag composite tapes are very important parameters for many practical applications. The strength and critical strain of the tapes are studied by tensile and bending tests. Tapes with different sheath materials, including pure Ag, Ag-Mg-Ni alloy and enforced Ag-Au alloy, have been used in this study. Results show that choosing strong sheath materials can increase the strength and critical strain of the tapes significantly. The residual compressive stress due to the difference in thermal expansion coefficients between the metallic sheath and the ceramic core has a strong influence on the strength and the critical strain of the tapes. The maximum residual strain of the Bi-2223 tapes is about 0.2%, which does not really depend on the sheath materials. To further increase the critical strain, the mechanical properties of the Bi-2223 core need to be improved.

16–34

Measurements on long Silver/BSCCO tapes by a contact-less method.

M.D. Bentzon and *P. Vase*. Nordic Superconductor Technologies A/S Priorparken 685 DK-2605 Broendby Denmark.

We present an experimental set-up capable of measuring Ic of superconducting tapes with a spatial resolution in the order of 1 cm and with a through put of 150 m per hour. Measurements are performed on silver alloy sheat/Bi-2223 tapes and the set-up is operating by applying an external magnetic field to the tape and measuring the shielding and remanent fields created by the tape by using Hall probes. The measured remanent field is used to estimate Ic. The correlation between Ic and the remanent field is performed by calibration. The main goal of this paper is to study the potentials of the method when applied in the production of superconducting tapes. The studies include reproducibility, non-destructiveness, response to defects, corre-

lation to current-voltage measurements performed on long length tapes and to filaments coupling. The results show that the reproducibility and the signal to noise ratio are so high that the method can be used to identify individual tapes by their signal pattern. The non-destructiveness is generally good. The first measurement of a tape decreases the critical current by less than 2%, and each following cycle is observed to have an effect of less than 0.5%. The spatial resolution depends on the tape speed and is typically 1 cm. Comparing the data with current-voltage measurements is performed and the results show that the contactless method also can be applied to evaluate Ic measured over long lengths. Another example of the usefulness of the contact-free set-up is demonstrated by determination of the degree of filament coupling performed at different external field frequencies. These results show that the filaments have coupled completely at 10 Hz. Due to a superior spatial resolution the method offers the tape manufactu er a detailed picture of the superconductive properties of the tape and is therefore a very good tool for product development and for quality control.

16–35

Mono and multifilamentary Bi(Pb)-2223 tapes with Ag-Cu-Ti alloyed sheaths.

M. Artigas, *J.A. Gómez*, *J.M. Pérez* and *R. Navarro*. Instituto de Ciencia de Materiales de Aragón, CSIC-Universidad de Zaragoza Centro Politécnico Superior, María de Luna 3, 50015 Zaragoza, SPAIN.

Some of the materials more deeply studied on Bi(Pb)-2223 composite tapes are Ag-Cu alloys. Economic raw materials and a wide range of solubility of Cu in Ag were the main advantages. However, in spite of the relatively high critical current density values reported for these tapes, their technological application is limited by several problems associated to the diffusion of Cu through the sheaths and its reactivity against the core. A way to overcome these problems implies the use of a third alloying element. In this paper, the results of a series of systematic studies on sheathed mono and multifilamentary Bi(Pb)-2223 tapes fabricated from Ag-Cu-Ti alloys with different Ti concentrations are presented. These tapes have been prepared by the powder-in-tube and wire-in-tube methods, and information concerning their microstructure, hardness and critical current density has been obtained. The results allow to propose some explanations for the hardening mechanism operating in these alloys. In addition, some aspects of the reactivity of alloy sheathed mono and multifilamentary tapes are reported.
Project supported by the European Community through Brite Euram Program.

16–36

Critical Currents of Bi-2223 tapes in extremely non-uniform local magnetic fields perpendicular to the axis of grain alignment.

F.A.Darmann, *G.D.McCaughey*, *M.H.Apperley* and *T.P.Beales*. Australian Superconductors, Australian Technology Park, Eveleigh NSW 1430.

The magnetic field pattern of pancake windings of Bi 2223 tape is investigated. The analysis revealed a very non-uniform field distribution across the radial extent and width of the pancake. A model is proposed for the sheet current density across the width of the tape valid for low frequency applied currents. The effect of this non-uniform field is discussed in terms of Eddy current and hysteretic AC losses at levels of current approaching the DC critical current

Session Flux pinning and ac losses

16–37

Total AC loss of BSCCO/Ag tape in different orientations of the external AC magnetic field.

J. J. Rabbers, *B. ten Haken*, *O. A. Shevchenko* and *H. H. J. ten Kate*. University of Twente, Low Temperature Division, P.O. Box 217, 7500 AE Enschede, The Netherlands.

In practical applications, BSCCO/Ag tapes are exposed to an AC magnetic field and fed with an AC transport current. The total AC loss, measured on a short sample, can be separated in two components, which has to be summed to obtain the total AC loss. First the transport current loss influenced by an external AC magnetic field. The second contribution is the magnetisation loss, which depends also on the transport current running through the conductor. In this paper the total AC loss of a short BSCCO/Ag sample is considered, especially the loss as a function of the angle between magnetic field and the wide side of the tape is investigated. Based on the critical state model for a slab in parallel field, angle dependent loss relations are deduced. The loss as a function of the angle between magnetic field and the conductor is described with a magnetic field and angle dependent critical current and the dimension of the conductor perpendicular to the magnetic field. This description works reasonably well for magnetic fields both below and above the penetration field and transport current amplitudes up to the critical current.

16–38

Development of Bi,Pb(2223) multifilamentary tapes with oxide barriers.

G. Witz[1], *Y.B. Huang*[1,2], *R. Passerini*[1], *F. Marti*[1], *M. Dhallé*[1], *L. Porcar*[1], *E. Giannini*[1], *M. Leghissa*[3], *K. Kwasnitza*[4] and *R. Flükiger*[1]. [1]DPMC, Université de Genève, Geneva, CH-1211, Switzerland. [2]Presently at BICC Superconductors, Great Britain. [3]Siemens AG, Erlangen, Germany. [4]PSI, Villigen, Switzerland.

A significant reduction of AC losses in Bi,Pb(2223) tapes has been achieved by using oxide ($BaZrO_3$ and $SrZrO_3$) barriers between filaments. These barriers increase the transverse resistivity between filaments which suppresses induced coupling currents. Presently, the AC loss level of barrier tapes (0.33mW/Am in a 0.1T, 50Hz parallel field) approaches the requirements for their application in devices such as transformers. However, their J_c values are still relatively low. In order to obtain low AC losses, the barrier continuity has to be preserved, which necessitates modifications of the standard PIT process. The influence of precursor powder composition, deformation procedure and annealing conditions on the critical current density and barrier quality are discussed. The field dependence of J_c and its anisotropy in barrier tapes are compared with those of standard tapes. Current transfer length measurements are presented, and

the barrier resistivity which can be deduced from this type of analysis is compared to the one which is calculated from AC loss measurements.

16–39
On 50 Hz magnetic field losses of superconducting High-T_c multifilament Bi(2223)/Ag tapes with high-resistive barriers.
K.Kwasnitza and *S.Clerc*. Paul Scherrer Institute, CH-5232 Villigen, Switzerland.

A short review is given on our numerous experimental investigations concerning the ac loss reduction efficiency of high-resistive $BaZrO_3$ or $SrZrO_3$ barriers around the Bi(2223) filaments. The decay time constant of the coupling currents could be reduced from 45 ms to 0.9 ms due to the ρ_c-enhancement by the individual barriers or a barrier network, together with the use of a small twist length. Depending on the amplitude of the perpendicular magnetic field a significant loss reduction was found at 25 Hz and a marked loss reduction at 50 Hz. We measured also the influence of tape geometry and of some Mg-addition to the Ag matrix on the loss behavior. The role of the number of tapes in a stack, used for the magnetization measurements was systematically investigated. The necessary final efforts to get acceptably low 50 Hz losses in perpendicular $\Delta B \approx 0.2T$,especially for superconducting transformer applications, are outlined. The investigated tape conductors are from the University of Geneva.

16–40
AC Losses in HTS multilayer cable conductor.
S. Redaelli[1,2], *F. Gömöry*[3] and *R. Mele*[1]. [1]Pirelli Cavi & Sistemi, Viale Sarca 222, MIlano, 20126, Italy. [2]Dipartimento di Fisica, Universita' degli studi di Milano, Milano, 20133, Italy. [3]Institute of Electrical Engineering, Slovak Academy of Science, Dubravska 9, 842 39 Bratislava, Slovak Republik.

It is very well known that in a HTS multilayer cable conductor a uniform current distribution among the layers allows to reduce AC losses, compared to a conductor with current penetrating from the external surface. This reduction is effective in the large AC amplitude current regime and a suitable analysis is required to calculate the ac loss in this regime in multilayer cable conductors. In this view, a theoretical description of the AC losses in a multilayer cable conductor with uniform current distribution is developed. The cable conductor is modelled as consisting of n superconducting concentric tubes, neglecting the winding angle of the tapes. In the framework of the critical state model, the profile and the flux of magnetic field is calculated. The total loss is then obtained by summing the losses of each shell. In the limit of a large number of layers with small thickness compared to the radius of the conductor, this model gives losses 1/2n times the monoblock model loss. In the following the results will be discussed and compared with the experimental data for 2−layers and multilayers cable conductors.

16–41
Global Properties of HTS Tape Model using Field-Dependent Power-Law in Finite Element Calculations.
N. Nibbio, *M. Sjöström* and *B. Dutoit*. EPFL-CIRC, 1015 Lausanne, Switzerland.

DC measurements of superconductors are often interpreted with a power-law between voltage and current where the critical current and exponent are both dependent on the externally applied field. Such a global relation is then translated into local properties of the superconductor given a corresponding relation between electric field and current density. We have introduced these local properties in calculations using the finite element method in a commercial software. The global properties were computed from the simulations and compared with those of the given hypothesis, in order to check a self-consistency of the model, which gave a good agreement. Furthermore, the model was validated in comparing modelled and measured AC losses under the critical current.

16–42
Losses in HTS Tapes due to External AC Magnetic Field and AC Transport Current.
N. Nibbio, *M. Sjöström* and *B. Dutoit*. EPFL-CIRC, 1015 Lausanne, Switzerland.

The E-J power law as electric characterisation of the HTS material in finite element computations has shown good agreement with measurements of field-dependent critical current and losses due to transport current. We use this technique to investigate the loss caused by AC transport current in self-field and in applied AC magnetic field in both elliptical monocore and multicore tapes, where the current is generated by means of a voltage source. The current density is first kept constant and then varied with local magnetic field. Furthermore, the simulations show that the transfer current decreases due to the screening currents induced by the external field.

16–43
Field distribution evolution on Bi(2223) tapes by dynamic Hall probe array measurements.
B. Dutoit, *M. Sjöström* and *N. Nibbio*. Swiss Federal Institute of Technology, Lausanne, 1015, Switzerland.

Fields on the top of Bi(2223) tapes are measured dynamically with Hall probe array connected to a high speed multiple channel data acquisition system. High accuracy is achieved using an eight channels digital lock-in amplifier. Measurement of field distribution evolution is made for a sinusoidal current pulsed through the sample, and for the penetration of a DC applied field. Monofilamentary and multifilamentary samples are processed. Results are compared to finite elements method calculations using a field dependent power law relation between electric field and current density.

16–45

Angle Dependency of AC losses in a BSCCO/Ag Tape – Simulation and Experiment: a Comparison.

O. A. Shevchenko, *J. J. Rabbers*, *H. J. G. Krooshoop*, *B. ten Haken* and *H. H. J. ten Kate*. Faculty of Applied Physics, University of Twente, P.O. Box 217, 7500AE Enschede, The Netherlands.

The magnetic field of an AC coil varies in amplitude, direction and time. In order to estimate the AC loss of such a coil, a numerical model is developed that can describe a single tape with untwisted filaments carrying a given transport current and placed in a given transverse exter-nal magnetic field. In the network model the true current distribution is replaced with a number of line currents and Kirchhoff equations are used instead of integrating Maxwell equations. A precisely measured V-I curve of a short sample is used as input. The model calculates both the current distribution and the ac loss for an arbitrary combination of the current and magnetic field amplitude and direction. Both the current and the magnetic field may vary with time. The model is verified with experimental data obtained at 77 Kelvin. It allows calculating the ac loss at 64 Kelvin and at any intermediate temperature as well. The model is suitable to predict and evaluate the ac loss of HTS superconducting coils at typical operating parameters.

Work supported by the Netherlands Technology Foundation STW, Utrecht, The Netherlands

16–46

Measurements of losses in bulk Bi-2223 plate carrying dc transport currents exposed to an alternating field.

T. Hardono[1], *C.D. Cook*[1], *X.K. Fu*[2], *J.X. Jin*[2], *S.X. Dou*[2], *F. Darmann*[3] and *M.H. Apperley*[3]. [1]School of Electrical, Computer & Telecommunications Engineering, University of Wollongong, NSW 2522 Australia;. [2]Institute for Superconducting and Electronic Materials, University of Wollongong, NSW 2522 Australia;. [3]Australian Superconductors, Eveleigh NSW 1430 Australia;.

A bulk Bi-2223 superconducting plate has been successfully manufactured with a high critical current. Prospective candidates of such materials are current leads for various superconducting devices in which the materials offer high current density and zero resistances. However, there are some losses incorporated in these materials when applied to ac environments. This paper discusses the hysteresis losses arising in the sample exposed to an ac field of 50 Hz with dc transport currents flowing in the sample. The loss components of the sample have been derived using the V-I curves of the sample that has a total dimension of 4.0 mm × 10.3 mm × 54.0 mm and has a maximum value of critical current as high as 119 A in self field. Approximations for the losses have also been made based on the BCS model. It is shown that the losses of the sample due to the ac field exposed parallel to the sample is in the same order as the estimations for $I \ll I_{co}$ and for $H \gg H_p$. It is also investigated that a field applied perpendicularly to the sample causes about one order higher losses than that applied parallel to the sample.

16–47

Shielding currents in orthorhombic superconductors.

A. Sanchez and *C. Navau*. Departament de Fisica, Universitat Autonoma de Barcelona, 08193 Bellaterra, Barcelona, Spain.

The problem of finding the magnetic response of diamagnetic samples, such as superconductors, has a strong interest for many applications. The magnetic response of samples that are infinitely long in the direction of the applied field is known since long time ago, because the direction of the shielding currents is easily obtained from the problem symmetry. However, in the realistic case of finite samples, theoretical results have appeared only recently. These solutions have been worked out for systems that are mathematically two-dimensional such as infinite strips and cylinders, for which the current trajectories are known. In this work, we apply a method based on magnetic energy minimization to calculate the magnetic response of a perfectly diamagnetic sample of orthorhombic shape. Results on the obtained shielding currents and the magnetic fields created by them are presented and discussed.

16–48

Voltage noise of $YBa_2Cu_3O_{7-\delta}$ thin films in the vortex glass phase.

A. Taoufik[1], *A. Tirbiyine*[1], *S. Senoussi*[2], *E. Aassif*[3] and *A. Ramzi*[1]. [1]Equipe des Matériaux Supraconducteurs à Haute Température Critique, Département de Physique, Faculté des Sciences, Université Ibn Zohr, B. P:28/S, 80000 Agadir, Morocco. [2]Laboratoire de Physique des Solides (associé au CNRS. URA. 0002), Université Paris Sud, 91405 Orsay Cedex, France. [3]Laboratoire d'Instrumentation et de Mesure, Département de Physique, Faculté des Sciences, Université Ibn Zohr, B. P:28/S, 80000 Agadir.

The voltage noise of a high quality $YBa_2Cu_3O_{7-\delta}$ thin films is measured in the vortex glass transition region as a function of magnetic field (0-140 Kg), angle between the c-axis and the direction of applied field, temperature (25-90 K), and current density, we compare the results of voltage noise in the superconducting vortex-glass phase to the characteristics J-E analyzed in the picture of the vortex glass theory which proposed a second-order phase transition from vortex liquid to vortex glass in disordered superconductors having random pinning centers and predicts that the E(J) functional follows a power law at the vortex glass transition, our findings show clearly the change of the voltage noise behavior and the excess voltage-noise V_b is found to vanish at the vortex glass transition temperature T_g.

16–49

Modelling current distribution in granular superconductors: transport, inductive and simultaneous measurements on YBCO samples.

J.L. Giordano[1], *L.A. Angurel*[1], *F. Lera*[1], *A. Badía*[1] and *C. López*[2]. [1]Instituto de Ciencia de Materiales de Aragón (C.S.I.C.–Universidad de Zaragoza), CPS, María de Luna 3, Zaragoza, E - 50 015, Spain. [2]Departamento de Matemática, CPS, María de Luna 3, Zaragoza, E - 50 015, Spain.

The interplay of electric transport and magnetic shielding

currents within a type-II superconducting wire is an interesting technological problem deeply related to the current distribution capable of both tasks simultaneously: to shield an external applied magnetic field carrying a given transport current. This problem has been experimentally studied on $YBa_2Cu_3O_{7-x}$ policrystalline ceramic cylinders under longitudinal transport DC currents and parallel magnetic fields at temperatures up to $\cong 0.9 \times T_c$, by using pulsed currents under DC fields, and AC-susceptibility and magnetization techniques with simultaneous transport measurements (from 0 to I_c). A theoretical approach has been made in the framework of the Critical State Model. The measurements were analyzed and compared with the predictions obtained with a minimum magnetic energy model. In this current distribution model low field penetration is obtained for a given transport current I, and low sensitivity of the AC-susceptibility for currents up to $\cong 0.25 \times I_c$ takes place in agreement with the experimental observations.

16–50

The 1/f noise of high-temperature superconductor$YBa_2Cu_3O_{7-\delta}$ thin films.

A. Tirbiyine[1], *A. Taoufik*[1], *S. Senoussi*[2], *E. Aassif*[2,3] and *A. Ramzi*[1]. [1]Equipe des Matériaux Supraconducteurs à Haute Température Critique, Département de Physique, Faculté des Sciences, Université Ibn Zohr, B. P:28/S, 80000 Agadir, Morocco. [2]Laboratoire de Physique des Solides (associé au CNRS. URA. 0002), Université Paris Sud, 91405 Orsay Cedex, France [3]Laboratoire d'Instrumentation et de Mesure, Département de Physique, Faculté des Sciences, Université Ibn Zohr, B. P:28/S, 80000 Agadir.

We have investigated the noise spectral density at a constant current 1nA and 3nA (1nA in this report) in the presence of the applied magnetic field and various temperature to study the origin of the noise in high T_c superconducting $YBa_2Cu_3O_{7-\delta}$ thin films in the mixed state. The range of the measuring temperature T was from 80 to 90 K. It is demonstrated that processes of vortex pinning and depinning, as well as motion of vortex disturbed by both of thermal fluctuation and random impurities contribute to the noise spectra. We discuss the relationship between the voltage noise properties and the vortex motion. In particular, our findings also show that the power spectral density of our samples exhibits 1/f frequency dependence.

Session Fusion, SMES, detectors and accelerators

16–51

Laboratory-Scale SMES Device with Liquid Nitrogen Cooled HTS Coil.

A. Friedman[1], *N. Shaked*[1], *E. Perel*[1], *M. Sinvani*[1], *Y. Wolfus*[1], *E. Yogev*[2], *O.Kugel*[2], *G. Meiron*[2] and *Y. Yeshurun*[1]. [1]Institute for Superconductivity, Department of Physics, Bar-Ilan University, Ramat-Gan, 52900, Israel,. [2]Israel Electric Company, Haifa, PB10, 31000, Israel.

We have designed, built and tested two prototypes of SMES operating in the temperature range between 64 K to 77 K using liquid nitrogen cooling. This feature is of particular value for SMES and current limiter devices where some energy release exists in the coil during the operation. To increase the stored energy we have used a ferromagnetic core surrounding the HTS coil. The coils made of BSSCO/silver tape were purchased from American Superconductor Corp. On the first stage of the project we have built the SMES device, which stores 60 J at temperature 77 K and 130 J at 64 K. Maximal energy stored in the coil without core was 4.5 J. To decrease the losses in DC-DC converter its elements carrying high current were placed into liquid nitrogen. The present SMES device is designed for operation as a small model of the power conditioning system. Commercially available UPS was used for AC-DC and DC-AC conversion system. The maximal stored energy in the coil without ferromagnetic core is of 50 J at operating current 50A at 77K. By introducing the core we can increase the stored energy up to 600 J. The stored energy of about 2000 J can be achieved at 64K.

16–52

RF magnetron sputtering target for Nb_3Al made by powder metallurgy.

K. Agatsuma[1], *H. Tateishi*[1], *K. Arai*[1], *T. Saitoh*[2] and *N. Futaki*[2]. [1]Electrotechnical Laboratory, Tsukuba, Ibaraki, 305-8568 Japan. [2]Fujikura Ltd., Koutou-ku, Tokyo, 135-8512 Japan.

We have studied a high field pulsed superconductor with high elastic modulus fiber reinforcement. We call the conductor Fiber Reinforced Superconductor (FRS). Nb_3Al superconductor is a potential candidate superconductor for fusion reactors because of good properties of mechanical stress and irradiation toughness instead of the difficulty of fabrication into wire. As the fiber reinforced superconducting film will be performed by magnetron sputtering techniques on the reinforced fibers by two opposed planar targets in future, the difficulty of fabrication of Nb_3Al superconductor might be overcome. In this process a single sputtering target for the Nb_3Al compound would be desired to be developed to shorten the deposition process. We have made a single sputtering target of Nb_3Al compound by powder metallurgy. We have attempted to make a single target out of the mixed powder of Nb and stable Nb-Al compound powder in order to avoid difference in stoichiometry. We use a stable Nb-Al compound which consists of the pressed powder of Nb and $NbAl_3$, or Nb_2Al mixture. Also we made a single phase Nb_3Al target. Thin Nb_3Al films on MgO and Al_2O_3 substrate were made using these targets. The experimental results for Nb_3Al films on the substrate are presented in this paper.

16–53

Studies of decay and snapback effects on LHC dipole magnets.

L. Bottura[1], *M. Haverkamp*[2] and *M. Schneider*[3]. [1]Cern, division LHC-MTA, CH-1211 Geneva 23, Switzerland. [2]University of Twente, The Netherlands. [3]TU, Technische Universität, Vienna, Austria.

The goal of CERN's new Large Hadron Collider (LHC) is to reach a high particle collision energy together with a high luminosity. Thus, the quality of the magnetic field in the dipole magnets of the LHC has to be accurately controlled, especially during the injection and initial acceleration phase. Superconducting LHC model magnets show a rich spectrum

of so-called "dynamic'' field imperfections, which have to be compensated in order to reach the desired homogeneity. Two effects of particular importance are field component decay during injection, and "snapback''during the first few seconds of acceleration. At the nominal LHC ramp rate the snapback happens over typically 15 to 20 mT, with a time scale of a few seconds. The knowledge of the decay and snapback phase is essential for compensation. The dynamic behaviour of several LHC dipole model magnets was measured as a function of various parameters in the operation cycle and powering history. We show how the systematic variation of only one single operation cycle parameter can affect the behaviour of the sextupole component.

16–54

Direct Measurements of Temperature and Electric Field Distribution Inside the LHD Helical Conductor.

V.S. Vysotsky[1,3], *Y.A. Ilyin*[1,3], *N. Yanagi*[2], *M. Takeo*[1], *S. Sato*[1], *A.V. Gavrilin*[2], *S. Imagawa*[2], *A. Iwamoto*[2], *S. Hamaguchi*[2], *T. Mito*[2], *T.Satow*[2], *S.Satoh*[2] and *O.Motojima*[2]. [1]Kyushu University, Fukuoka, 812-8582, Japan. [2]National Institute for Fusion Sciences, Toki, Gifu, 509-5292, Japan. [3]Visiting scientist from Kurchatov Institute, 123182, Moscow, Russia.

The KISO-32 superconductor used for the helical coils of LHD consists of 15 NbTi/Cu superconducting strands and a pure aluminum stabilizer with a CuNi clad, both embedded in a copper housing. The outer surface of the cable is covered by a Cu-oxide layer. In such complicated structure, sufficient temperature gradient may exist between the outer and inner parts of the superconductor during a quench development. Current diffusion from the superconducting strands to the stabilizer may have different time constants in different elements. The parasitic "Hall currents" may reduce the stability of the superconductor. Direct measurements of temperature distribution and electric field, INSIDE the conductor, would be of great importance for better understanding of its behavior. A special sample coil from KISO-32 conductor was prepared in Kyushu University, and tested in NIFS. Tiny thermocouples and electrodes were imbedded into conductor's body in several cross-sections. A normal zone was initiated by resistive heaters, and internal temperature distribution as well as electric fields were measured DIRECTLY. We observed a considerable temperature difference between the inner and outer parts of the superconductor. The inner electric field distribution was recorded also. Oscillating phenomena were observed with an appearance and disappearance of a normal zone in some areas of the conductor. In the paper, experimental details and some results are presented.

16–56

Electromagnetic analysis of current distribution in multistrand superconducting cables.

L.Bottura[2], *M. Breschi*[1], *F. Negrini*[1] and *P.L. Ribani*[1]. [1]Department of Electrical Engineering - University of Bologna - Bologna - 40136 - Italy. [2]LHC Division - CERN - 1211 Geneva 23 - Switzerland.

Non uniform current distribution in multistrand superconducting cables is one of the most important sources of reduction of quench currents at transient conditions. In this paper we present a new electro- magnetic model for the simulation of current or field ramps in superconducting coils, taking into account non linear longitudinal resistances, joint resistances and interstrand resistances. Starting from Maxwell equations, a system of partial differential equations is obtained; the unknowns of the problem are the differences between strands currents and strands currents in the uniform distribution case. A general method of computation of self and mutual inductances is used to calculate induced voltages between strands due to currents circulating in the strands of the same multistrand cable and in neighboring coils. The system is numerically solved by means of the finite element method. The dependence of current redistribution rate on joint resistance, interstrand resistance and magnetic parameters is studied, in order to evaluate optimum parameters for stable operation. Comparison of characteristic current redistribution times and lengths, with experimental and previously analytically determined data, is shown.

16–57

Design and Fabrication of a Superconducting Trim Quadrupole for the LHC.

F. Toral[1], *L. García-Tabarés*[2], *A. Ijspeert*[3], *J. Salminen*[3], *J. Etxeandia*[4] and *F. López-Mantaras*[1]. [1]CIEMAT, Madrid, 28040, Spain. [2]CEDEX, Madrid, 28014, Spain. [3]CERN, Geneva, 1211, Switzerland. [4]ANTEC, Portugalete, Vizcaya, 48920, Spain.

This paper describes the calculation, design and manufacturing of a 550 A superconducting trim quadrupole (MQTL) prototype for the future Large Hadron Collider (LHC) of CERN. The project is part of a collaboration agreement between CERN and CIEMAT. A compact magnet has been developed (bore diameter of 56 mm, outer diameter of 194 mm) with a considerable strength (110 T/m at 1.9K) and a length of 1.2m. The development included the required facilities for its fabrication like the special winding machine, the tooling, etc. The first part of the paper deals with the magnetic and mechanical design, which includes some innovative aspects such as the magnetic iron circuit using elliptical holes to minimise magnetic saturation effects on the field quality, or the pre-stressing device based on the so called "scissors laminations principle". All these calculations are aiming to achieve a low cost magnet design by using techniques such as the double layer - double pancake winding procedure or the above mentioned scissors laminations to reach the required pre-compression. The second part describes the fabrication of the prototype including the design and manufacturing of a special winding machine, the impregnation mould and the winding and assembly tooling, as well as the manufacturing of the complete magnet which will soon be tested at CERN's facilities.

16–58

The Design, Construction and Test of a Gradient Solenoid for the High Powered RF Cavity Experiment for the Muon Collider.

M. A. Green[1] and *S. T. Wang*[2]. [1]Lawrence Berkeley National Laboratory, Berkeley CA 94720, USA. [2]Wang NMR, Livermore CA 94550, USA.

his report describes the construction and test of a split solenoid that has a warm bore of 440 mm and a cryostat length of 900 mm. (A 650 mm section contains the magnetic field.) When the coils are hooked so the fields are additive, the central induction is 5.0 T at its design current. When the coils are hooked so that the fields are in opposition, the induction at the center of the solenoid is zero and the peak induction on the solenoid axis is I3.7 T. The on-axis induction gradient is 35 T per meter when the coils are hooked in opposition. The magnet is used as part of a two cell 805 MHz high power RF cavity test system for the cooling system for a muon collider. The high power RF cavity will be tested at a gradient up to 40 MV per meter in a nearly uniform magnetic field and in a field with an on axis gradient of up to 35 T per meter. The superconducting coils are wound with an MRI superconductor that has dimensions of 1.0 by 1.65 mm. This conductor has a copper to superconductor ratio 4 to 1 and a superconducting filament diameter of 87 microns. When the coils are operated at their design currents in opposition, the force pushing the two coils apart is about 3 MN. The force pushing the coils apart is carried by the aluminum coil mandrel and a solid aluminum sheath outside of the superconducting winding. The coil was wound as a wet lay-up coil using alumina filled epoxy (Stycast). A layer of hard aluminum wire wound on the outside of the superconducting coil carries some of the hoop forces and limits the strain so that training does not occur. At its design current, the peak induction in the windings is about 7 T. This report describes the construction of the coils and th results of a preliminary test of the magnet before it was shipped to Fermi National Laboratory.

16–59

A Design for a Combined Function Superconducting Dipole for a Muon Collider FFAG Accelerator.

M. A. Green. Lawrence Berkeley National Laboratory, Berkeley CA 94720, USA.

The acceleration stages for a muon collider require that the muons be accelerated in a given ring for twenty turns of fewer. One type of accelerator that appears to be attractive for a synchrotron that accelerates the muon a factor of four in energy in a few turns if the Fixed Field Alternating Gradient (FFAG) type of accelerator. As the energy of the muon beam increases, the muons move toward a higher field region of a DC combined function dipole. The following dipole and quadrupole magnet characteristics are required for a muon FFAG machine to be successful: 1) The dipole will be a fixed field dipole with a impressed quadrupole and sextupole field. There may or may not be separate quadrupoles that may or may not have added sextupole windings. 2) The horizontal aperture of the required good field region is wider than the vertical aperture of the required good field region. 3) The magnet is relatively short, so that the conventional SSC type of superconducting dipole or quadrupole ends can not be used. The field at the end of the magnet must fall off abruptly within the distance of less than one vertical aperture. For a magnet that is 400 mm long, the end region can be no more than 40 mm long. 4) The structure of the integrated filed within the end region must be the same as the structure of the two-dimensional filed at the center of the magnet. To demonstrate the type of magnet needed for superconducting FFAG machine for a muon collider accelerator, the preliminary design for a magnet with the following characteristics is presented: 1) The magnet vertical aperture is 80 mm; the magnet horizontal aperture is 160 mm. 2) The combined function dipole magnetic field length is 362 mm. 3) The magnet produces a dipole 1.217 T and quadrupole with a gradient of 45.7 T m-1, and a sextupole of 461.2 T m-2. This magnet will produce a peak field in the superconductor that is of the order of 8.2 T. Since the muon will decay within the bore of this magnet, the decay electrons will deposit about 8 W per mete into a room temperature vacuum chamber within the bore of the magnet.

16–60

Stability and quench propagation in a long length NbTi CICC.

E. Balsamo, A. Catitti, S. Chiarelli, M. Ciotti, A. Della Corte, E. Di Ferdinando, P. Gislon, C. Mastacchini, M.V. Ricci and *M. Spadoni*. Associazione EURATOM-ENEA sulla Fusione, C.E. Frascati Frascati (Rome), 00044, Italy.

A crucial issue for a superconducting coil in order to be safely used in the magnetic system of a fusion reactor is stability against all foreseen disturbances. Up to now very few experiments have supported the development of the design criteria and analysis models. In particular a gap exists for the stability of long length conductors under magnetically induced disturbances. In these conditions the study of the quench and its propagation characteristics have to be known in order to understand if stability is decreased because of the decreased heat transfer coefficient due to the lack of induced flow effects. The experiment consists of an instrumented NbTi test module into a couple of co-axial copper pulsed coils. A background 3 Tesla magnetic field is obtained by a 0.6 m bore superconducting coil. A plus/minus 25 V, 1 kA power supply has been used for the test module to follow for a longer time the quench propagation. A parametric study of all the main physical quantities has been performed and the obtained results interpreted with a finite element code for the analysis of the stability and quenching transients in force flow cooled superconducting coils.

16–61

Transient Behaviour of a Resistive Joint in the ATLAS Toroids during the Magnet Ramp-up and Discharge.

G. Volpini[1] and *E. Acerbi*[1,2]. [1]INFN sez. di Milano, lab. LASA, via f.lli Cervi 201, 20090 Segrate (MI) Italy. [2]Universita' degli Studi di Milano, dipartimento di Fisica, lab. LASA, via f.lli Cervi 201, 20090 Segrate (MI) Italy.

Several resistive joints are foreseen inside ATLAS air-core Toroids windings. The maximum temperature rise, due to steady-state Joule dissipation, permissible at such joints sets an upper limit on the joint resistance, which must be lower than $10^{-9}\Omega$. On the other hand this resistance can not be arbitrarily small, since during the magnet ramp-up and discharge there appear inside these joints large eddy-currents, whose value is inversely proportional to the joint resistance; these currents may even exceed the Rutherford's I_c and furthermore their resistive decay generates an heat dissipation that can be significantly larger than the steady-state value.

In order to estimate the amount of these eddy-currents we have developed an electrical model of a joint, based on a continuous network of inductors and resistances; this model has been later confirmed experimentally by means of tests on sample joints. This model allowed us to compute the time evolution of the current distribution inside the joints under different conditions; in particular we show that for the layer-to-layer joint the optimum trade-off between steady-state and transient dissipation is obtained when the joint is about 2.5m long. This value has been adopted for B0, a smaller size model of one Barrel Toroid coil.

16–62

Progress in the Construction of the B0 Model of the ATLAS Barrel Toroid Magnet.

E. Acerbi[1,2], *F. Alessandria*[1], *G. Ambrosio*[1], *G. Baccaglioni*[1], *F. Broggi*[1], *L. Rossi*[1], *M. Sorbi*[1] and *G. Volpini*[1]. [1]INFN, sez. di Milano, LASA lab., via f.lli Cervi 201, 20090 SEGRATE Italy. [2]Universita' degli studi di Milano, dip. di Fisica, LASA lab., via f.lli Cervi 201, 20090 SEGRATE Italy.

The ATLAS Barrel Toroid air-core magnet (BT) will be composed by eight superconducting coils each 25 m long and 5 m wide. In order to validate the technologies and manufacturing processes involved in this project, a smaller model of one BT coil, named B0, is now under construction. This model is shorter (9 m long instead of 25 m) but it retains all the major features of the BT coils; several European firms are presently developing and constructing its main components. This paper presents a general overview of the B0 project status, with special emphasis to a) the aluminium-clad NbTi conductor production and qualification and b) to the double coils winding and impregnation, both already completed.

Session System aspects and high fields

16–63

Confocal Open Resonators Based on Superconducting Film Structures.

A.B. Kazarov. Institute of Radio Engineering and Electronics of the Russia.

In this paper, confocal open resonators with dielectric mirrors double-side covered by superconducting films are discussed. For solving the boundary value problem equivalent boundary conditions for superconducting multilayer structures are used. Using of such conditions allows one to simplify significantly the mathematical model of the problem and at the same time to take into account physical effects in multilayer superconducting mirrors. Surface roughness of the films is also taken into account. With the help of methods developed in previous works of the author for open resonators analytical expressions for disperse characteristics and Q-factor of the resonator are obtained. The results of computer modeling the characteristics of open resonators for low- and high-temperature superconductors as well as for normally conducting materials are presented for multilayer superconducting film mirrors as well as for bulk superconducting mirrors of the resonator. As it can be seen from the results obtained, by selecting the thickness of superconducting films and substrates the Q-factor can be increased as much as one order. In this connection, use of multilayer superconducting film structures instead of bulk superconductors seems to be very perspective way of improving the characteristics of open resonators in millimeter and submillimeter wave regions.

16–64

Stressed state of conductors in solenoidal windings.

E.A. Deviatkin. Institute of Problems in Mechanics of Russian Academy of Sciences, Moscow 117526, Russia.

Stresses in conductors of superconducting solenoids, namely, in round wires made of a composite superconductor and square cables-in-conduit conductors are studied. It was shown, in particular, that significant stresses (of the same order of magnitude as yield limit of many metals used in cryogenics) can be present in conductors before solenoids are cooled and energized. Changes in the stressed state of conductors when the solenoid is energized are analyzed with the assumption of their elastic perfect pasticity. Some problems of approximate analytical calculation of "smeared" elastic Lorentz force-induced stresses in a central section of long solenoids are considered. Training problem connected with the heat generation induced by a plastic deformation of conductors having a work hardening is discussed. This work is supported by the INTAS, Contract No.96-2306.

16–66

Induced currents and AC losses in superconducting cables due to changing fields at the and portions of magnets.

S. Takács. Institute of Electrical Engineering, Slovak Academy of Sciences, 842 39 Bratislava, Slovakia.

The diffusion equation for the magnetic field penetration into flat cables is derived and used to find the solutions for the induced currents in the strands. For magnetic fields changing at the ends of the magnet winding, some general results are given for the additional AC losses and the currents in the strands. These results are compared with the properties of cables in homogeneous applied magnetic field. The additional losses in the homogeneous field region are negligible, the losses in the inhomogeneous field region are nearly the same as if the homogeneous field acted on the whole cable length L. The current distribution in the individual strands is strongly influenced by the length a, on which the applied field is changing at the cable ends. The enhancement of the induced currents, decreasing generally the critical current of the cable, is important for the stability of some magnets. This enhancement is smallest for $a = 0$, when the strand current is increased twice compared with the infinite cables in homogeneous applied fields. One can minimize the additional currents in the strand by choosing appropriate values of L and a, but for the central part of the cable only.

16–67

Sensitive usage of proton-MR in forensic medicine.

U. Onbasli[3], *T.O. Eruygun*[1] and *A. Dincer*[2]. [1]University of Istanbul Institute of forensic medicine, Istanbul,Uskudar, 81130, Turkey. [2]Radyomar MR imaging center, Istanbul, Bakirkoy, Turkey. [3]University of Marmara, dept. of phys., Ridvanpasa cad., 2.SOK., 85/12, Göztepe, Istanbul, 81080, Turkey.

The product of superconducting technology provided by a homogenous magnetic field strengths of 1.5 Tesla and higher has recently been employed in MR-equipment. Our research concerned possible mild head injuries detected by Proton Magnetic Resonance Spectroscopy, P-MRS. Thus, the sport of boxing was used as the basis for "invivo" investigation. Measurement of Frontal White Lobe and Corpus Callosum Splenium localisation by MRI and P-MRS was also made. Before and after a minor trauma, no meaningful difference was registered in MRI data. However, with P-MRS sensitive tool, both qualitative and quantitative significant differences were observed. P-MRS investigation has been carried out using Automised Single Voxel Proton Spectroscopy Software. Peak levels of metabolites were observed in the Spectrum Press Pulse Sequence, N-acetylaspartate (NAA), Creatine (Cr) and Choline (Cho). Before trauma, a spectrum was taken as a base. Post trauma, the NAA metabolism marker of nerve cells decreased. Despite this, Cho increased a characteristic indicator of the replenishment of membrane. This technique has been suggested as the most reliable tool for sensitive detection of neuron deficiency. Thus, in Forensic Medicine this would provide a criteria of concrete proof of regarding very mild head injuries.

16–68

Development of cryocooled Bi-2212/Ag solenoid magnet system generating 8T in 50mm room temperature bore.

H. Kitaguchi[1], *H. Kumakura*[1], *K. Togano*[1], *M. Okada*[2] and *J. Sato*[3]. [1]National Research Institute for Metals. [2]Hitachi Ltd. [3]Hitachi Cable Ltd.

Magnet systems using the combination of Bi-2212/Ag conductors and cryocooler are closer to reality because of the rapid progress in conductor fabrication and cryocooler engineering. We are performing a development project of cryocooled Bi-2212 magnet system generating 8T in 50mm room temperature bore. In this project, the system is designed to be composed of two magnets of solenoid winding by using ROSAT (Rotation-Symmetric Arranged Tape-in-tube) wires and operated at 10K with 30W refrigeration capacity (two cryocoolers of 15W@10K). Inner and outer magnets are designed to generate 3.8T and 4.2T at 10K with operating coil current density of 80 and 100 A/mm ^{2}, respectively. The dimensions of the inner and the outer magnets are 80mm (bore) x 169mm (outer diameter) x 178mm (height) (total conductor length, 1km) and 187mm x 295mm x 187mm (total conductor length, 3km), respectively. We finish the fabrication and a preliminary test of the inner magnet in April 1999. The whole system and a full operation test will be completed in March 2000. In this paper, we report the details of system design, the performance of ROSAT wires for coil winding, and the test results of the inner magnet.

16–69

Scaling for the Quench Development in HTSC Devices - Theory.

A.L. Rakhmanov[1], *V.S. Vysotsky*[2,3], *Y.A. Ilyin*[2,3], *T. Kiss*[2] and *M. Takeo*[2]. [1]SCAPE, Russian Academy of Sciences, Moscow, Russia. [2]Kyushu University, Fukuoka, 812-8581, Japan. [3]Visiting scientist from Kurchatov Institute, 123182, Moscow, Russia.

Full size HTSC magnets and other HTSC devices are becoming a reality. Current density in the HTSC tapes and wires is increasing, especially at the temperature range ~20K. On the other hand, smooth voltage-current characteristics, relatively high operation temperature and low resistive Ag-matrix used in HTSC superconductors make it difficult to distinguish clearly its normal and superconducting parts. This demands the new approaches for HTSC devices design to be developed. In many cases, quench in different superconducting devices develops as quasi-stationary overheating if the Joule heat exceeds the heat removal to ambient. For the relatively uniform samples the quenching current and the quenching temperature at which quench occurs may be derived just from heat balance equations without any use of idea of superconductivity and normal zone propagation. We developed such approach and showed that near the quench current the time dependencies of the temperature and the electric field obeys the universal scaling laws different for the cases less and more than the quench current. The scaling parameters are quench temperature and current, parameters of voltage-current characteristics and cooling. The simple scaling law may be used as a first step approach to HTSC devices design. In this paper scaling theory is presented. In the next paper the comparison of scaling law with the experiments is presented.

16–70

Scaling For The Quench Development In HTSC Devices - Comparison With The Experiment.

V.S. Vysotsky[1,2], *Y.A. Ilyin*[1,2], *T. Kiss*[1], *M. Takeo*[1] and *A.L. Rakhmanov*[3]. [1]Kyushu University, Fukuoka, 812-8581, Japan. [2]Visiting scientist from Kurchatov Institute, 123182, Moscow, Russia. [3]SCAPE, Russian Academy of Sciences, Moscow, Russia.

Because of the smooth voltage-current characteristics, relatively high operation temperature and low resistive Ag-matrix used in HTSC superconductors, it is difficult to distinguish clearly its normal and superconducting parts. This demands the new approaches for describing HTSC quench development. Such approach was developed and it was shown that near the quench current the time dependencies of the temperature and the electric field obeys the universal scaling laws different for the cases less and more than the quench current. The scaling parameters are quench temperature and current, parameters of voltage-current characteristics and cooling. In this paper we present the comparison of different experiments on quench development with the scaling law suggested. The data about temperature and voltage traces at different conditions were received from testing of different kind of HTSC superconducting devices. Namely, short tape samples, small pancake coil, superconducting HTSC films. The feasibility to use this simple scaling law as a first step approach to HTSC devices design is

discussed.

16–71
An influence of the number of Bi(2223)Ag pancake coils on the critical currents of the assembled magnet systems and the energy stored.
J. Pitel[1], *P. Kovac*[1], *T. Melisek*[1], *H. Kirchmayr*[2] and *A. Katzler*[2]. [1]Institute of Electrical Engineering Slovak Academy of Sciences Dúbravská 9 842 39 Bratislava Slovakia. [2]Institut fur Experimentalphysik Technische Universität Wien Wiedner Hauptstrasse 8 1040 Wien Austria.

Theoretical study of an influence of the number of pancake coils made of the anisotropic Bi(2223)Ag multifilamentary tapes on the critical currents of individual coils as well as of them assembled magnets was made. Simultaneously, the energy of the magnetic field stored in the magnets was evaluated. The goal of the study has been to investigate the factors which limit the energy stored in the HTS magnets with respect to the tape Ic(B) anisotropy. It is shown that the radial component of the magnetic field close to the magnet flanges is the main factor influencing the critical current of the cylindrical magnets. The results of numerical calculations of the set of model magnets, utilizing the data measured for 55 filament Bi(2223)Ag tape of Vacuumschmelze GmbH production, are presented. Extrapolation of the results for micro-SMES magnets based on high temperature superconducting tapes, is discussed.

16–72
High Magnetic Field Critical Behavior in Dy Substituted YBCO.
I. Nedkov[1], *T. Koutzarova*[1], *V. Lovchinov*[2] and *T. Mydlarz*[3]. [1]Institute of Electronics, Bulg.Acad.Sci., Sofia, 1784, Bulgaria. [2]Institute Solid State Physics, Bulg.Acad.Sci., Sofia, 1784, Bulgaria. [3]International Laboratory of High Magnetic Fields and Low Temperatures, Wroclaw, 53-529, Poland.

A systematic study is presented on the superconductivity and magnetic ordering of Dy ions in Dy-substituted YBCO with general formula $Y_{1-x}Dy_xBa_2Cu_3O_{7-y}$. Dy substituted YBCO bulk materials have been proved to be suitable for applications in external magnetic fields. The substitution can be considered as a chemical doping which provokes the appearance of a second magnetic phase in the perovskite structure. The present investigations are focused on the influence of a high magnetic field (up to 15 kOe)in the 4.2 - 300 K temperature range on a large number of samples with different Dy substitutions. The temperature dependence of the magnetic moment connected with the Dy antiferromagnetic ordering is discussed. A field-induced phase transition and a field dependence of the Dy ordering were observed. In samples with Dy-substitution x>0.4, an increase of the magnetic field led to the destruction of the superconducting phase and to the appearance of a field-induced antiferromagnetic phase.

16–73
Anomalies of Homological row of a Superconductings metaloxides.
V.A.Demchenko. Institute of Thermoelectricity, General Post Chernovtsy 274000, Box 86, Ukraine.

Correlation dependence between the temperature of superconducting transition (Tc) and thermodynamical equilibrum meaning of thermoelectric power coefficent, measured at room temperature (ar) is found as a result of mathematical-statistical processing of a large number of the empirical data. All compounds are placed in six zones of 22K wide, it appears from this, which are divided by sites of about 3K width. Tc changes close to 1/ar inside each zone depends on oxygen's concentration. The top five zones ar are limited from both sides by bending lines, which are crossed in a point with Tc = 148K, that corresponds to initial height of a Heops pyramid (148,2 m). In the most lower zone is limited only on the left. When Tc = 60Š, that corresponds to transition temperature from Orto-1 in the Orto-2 a phase and changes of influence of pressure on Tc , right bending line has a point of an excess. Received results can be used for diagnostics Tc of synthesis materials stage. The presence of the forbidden sites on an axis Tc means quantization of temperature. The observable effect is similar to quantization of a magnetic flow in superconductors.

16–74
Quench protection of 13 kA HTS prototype leads for the LHC.
A.Ballarino, *F.Rodriguez-Mateos* and *O.Wendling*. CERN,CH-1211 Geneve 23, Switzerland.

Prototype 13 kA HTS current leads, supplied by several manufacturers, have been tested and characterised at CERN. These prototypes incorporate different HTS materials, both in the bulk and in the metal-stabilised form. To show the viability of HTS components in high-current leads, measurements have been performed to study the behaviour of the leads in case of resistive transition of the HTS element. This paper reports on the results and interpretation of the quench measurements performed on different leads brought to critical temperature causing them to quench.

16–75
Development of Current Leads Using Electrolycally Deposited BSCCO 2212 Tapes. Manufacturing and Testing of Prototype Leads.
J. Le Bars and *T. Dechambre*. CEA/SACLAY DSM/DAPNIA/STCM Bât 123 91191 GIF-SUR-YVETTE CEDEX.

Current leads of BSCCO 2212 up to 150 A at 77 K have been industrially produced and tested. The superconducting part is made of parallel short strips produced using a continuous industrial process. We report on the way to make such a current lead, giving details of the different parts of the apparatus and the results of the electrical tests at 4.2 K and 77 K.

16–76

A Variable Temperature Test Facility with Variable Field Orientation.

D. Ryan[1], *M.N. Wilson*[1], *J. van Beersum*[2], *P.F. Herrmann*[4] and *K. Marken*[3]. [1]Oxford Instruments, Tubney Woods, Abingdon, OX13 5QX, UK. [2]University of Twente, Faculty of Physics (Low temperature division), PO Box 217, 7500 Enschede Netherlands. [3]Oxford Superconducting Technology, 600 Milik St, PO Box 429, Carteret NJ07008-0429 USA. [4] Alcatel, Route de Nozay, F-91460 MARCOUSSIS, France.

A facility for testing HTS conductors has been constructed and used to measure several B2212 tapes. The samples, in the form of a 5 turn helix, are immersed in the field of a split solenoid in which the coils may be powered independently to rotate the field vector on the sample. Sample temperature may be varied from 4K upwards and current supplied up to 1000A. Using pulsed currents, the samples may be stressed via Lorentz force. Measurements will be presented for the critical currents of different B2212 conductors as a function of temperature and field orientation. This work forms part of the SHIFT project, supported by EC Brite Euram contract BE 96 3638.

16–77

Characterization of Bi-2223 conductor for high field insert coils.

H.W. Weijers[1], *Y.Viouchkov*[1], *M.D. Bentzon*[2] and *J. Schwartz*[1]. [1]National High Magnetic Field laboratory, Tallahassee, Florida, 32310, USA. [2]Nordic Superconductor technologies A/S, Brondy, DK-2605, Denmark.

A study is presented on Bi-2223 conductor regarding its potential for use in high field insert coils. Mechanical characterization consists of stress-strain curves obtained at 300 K and 77 K using a linear tensile tester. At 77 K critical current measurements were performed during the stress-strain measurement, showing an onset of significant degradation at 0.4 % strain. From 0 to 0.4% strain, Ic decreased with a small slope of about 6% in Ic per % strain. The critical current of a short sample was measured at 4.2 K in applied fields from 0 to 30 T, oriented parallel to the a-b plane. A React-and-Wind double pancake was wound, instrumented with several voltage taps and a strain gauge, and tested in a background of up to 19 T. The coil results are compared with the expectations based on the short sample measurements as well as the properties of other insert coils that are reported in literature.

16–78

Current distribution in a 1T cryocooler-cooled pulse coil wound with a Bi2223 interlayer-transposed 4-strand parallel conductor.

M.Iwakuma[1], *K.Funaki*[1], *H.Tanaka*[1], *K.Kajikawa*[1], *H.Hayashi*[2], *K.Tsutsumi*[2], *A.Tomioka*[3], *M.Konno*[3] and *S.Nose*[3]. [1]Research Inst. of Supercond., Kyushu University, Fukuoka 812-8581, Japan. [2]Kyushu Electric Power Co.,Inc., Fukuoka 815-8520, Japan. [3]Fuji Electric Co.,Ltd., Kawasaki 210-8530, Japan.

We fabricated and tested a small 1T cryocooler-cooled pulse coil operating at 40K to develop an oxide superconducting coil for SMES. We adopted a new type of winding configuration. A 4-strand parallel conductor composed of Bi2223 rectangular cross-sectional multifilamentary wires were wound into a 16-layer solenoidal coil with an inner diameter of 52mm, an outer diameter of 112mm and a height of 120mm. The strands were insulated and transposed between layers, that is only at the upper and lower ends of layers, so as to be inductively equivalent with each other. The AlN plates with a thickness of 0.6mm and a width of 6mm were arranged between layers as a heat drain for the sake of high thermal conductivity inside the winding. The coil could be successfully operated in a continuous triangular-waveform mode with an amplitude of 1T at 1Hz. In this paper, we discuss the current-distribution properties in the 4-strand interlayer transposed parallel conductor. We investigated the current distribution among strands with Rogowski coils by applying ac transport current with a small amplitude at 50Hz. As a result, it was confirmed that the transport current flowed almost uniformly with a difference of less than 10%.

16–79

Preliminary design of 5 T - Bi2223/Ag - magnet at 30 K.

G. Masullo[1], *A. Matrone*[1], *R. Quarantiello*[1], *L. Bigoni*[2], *L. Martini*[2], *G. Grasso*[3] and *A.S. Siri*[3]. [1] CRIS - Consorzio Ricerche Innovative per il Sud via Nuova delle Brecce n. 260 80147 Napoli - Italy. [2] ENEL/SRI - Nucleo Materiali e Rivestimenti Innovativi Via R. Emilia 39, 20090 Segrate (MI) , Italy. [3] INFM - Unità di Genova, Via Dodecaneso 33, 16146 Genova , Italy.

A preliminary design of 5T-50mm bore magnet by using Bi-2223/Ag tapes has been made. The optimization of magnetic design to reduce the orthogonal field has been discussed. Some aspects of constructional design have been investigated. In particular the manufacture of a double pancake by co-winding two Bi-2223/Ag tapes has been discussed. A list of possible wire suppliers has been screened and preliminary critical current measurements have been done. The critical aspects inherent the realisation of windings with Bi-2223/Ag tapes have been evaluated by controlling the real degradation of the electrical properties of the tapes produced when subjected to the fabrication process of a coil.

16–79P1

Cryostatic stabilization of a large supercoducting coil in pressurized superfluid helium.

H. Kobayshi, *J. Osakabe*, *T. Tanifuji* and *M. Tomita*. Nihon University, 1-8 Kanda Surugadai Chiyodaku, Tokyo.

The heat transfer to the pressurized superfluid helium confined in cooling channels is different from that of the normal boiling helium. By taking the specific heat transfer characteristcs into account, the cryostatic stabilization of a large superconducting coil such as LHD (Large Helical Device) for intensification of the generating magnetic field has been studied. In the present paper the mechanism of the heat transfer in the superfluid helium has been clarified by thermometry for the parallel channel which simulate the cooling path in large superconducting winding. The temperature gradient along the simulated channel length produces the

subcooled normal helium so that the rapid temperature rise is prevented. we can expect the highly stabilized operation.

Session Materials related to electronic applications

16–80
Significant Improvements in the Surface Smoothness of dc Magnetron-sputtered $YBa_2Cu_3O_{7-\delta}$ Films on r-cut Sapphire Substrates With rf Magnetron-sputtered CeO_2 Buffer Layers.
J.H. Lee[1], *V.A. Komashko*[2], *W.I. Yang*[1], *H.J. Kwon*[1] and *S.Y. Lee*[1]. [1] Department of Physics and Center for Advanced Materials and Devices, Konkuk University, Seoul, 143-701, Korea. [2]Institute for Metal Physics of Ukranian Academy of Sciences, Kiev, 252680, Ukraine.

Epitaxial CeO_2 buffer layers were grown on r-cut sapphire substrates by an rf magnetron sputtering method. Decrease in the deposition rate as well as employment of a post-annealing process at 1000 °C made it possible for the buffer layers of 45 nm thickness to have very smooth surfaces without any structure-like cracks and outgrowths. From the AFM data, the R_t-factor, the vertical distance between the deepest and the highest point of the surface profile, appeared to be 0.6 nm. YBCO films prepared on CeO_2-buffered sapphire substrate at 730 °C also appeared to have smooth surfaces with $R_t \sim 1.9$ nm and 3.8 nm for the films with 0.14 and 0.28 μm thicknesses, respectively. Only (00ℓ) peaks were observed in the XRD data with the FWHM of the (005) reflex of $\Delta(\theta - 2\theta) = 0.16$ °. The rocking curve revealed that the FWHM $(\Delta\omega) = 0.55$ °. The YBCO films have the zero-resistance temperatures more than 87 K, the transition width less than 1 K and ρ (300 K)/ ρ(100 K) more than 3 with ρ denoting the resistivity.

16–81
Thin film deposition of superconducting borocarbides: a preliminary study for in situ realization of devices.
G. Grassano, *M.R. Cimberle*, *C. Ferdeghini*, *I. Pallecchi*, *M. Putti* and *A.S. Siri*. INFM/CNR Dipartimento di Fisica, Via Dodecanneso 33, 16146 Genova, Italia.

The borocarbides are compounds in which superconducting and/or magnetic ordering are present in the same temperature region. The recent availability of thin film deposition technique for these materials makes possible the realization of devices such as planar Josephson junctions, tunnel junctions etc. With this goal, we realized a system to perform multitarget laser ablation deposition using shadow maskes in UHV conditions to obtain an in situ growth of the complete device. We chose as borocarbide the Lu-based compound that we deposited on MgO in form of thin film, for the first time. Deposition on MgO with metallic buffer layers was also realized. In general a device needs the presence of insulating layer, for which we used MgO. The choice is due to the fact that the MgO layer provides a suitable substrate for the subsequent borocarbide deposition. No significant differences are detected from electrical and morphological characterization between the films lying above and under the MgO film. With this technique we tried to realize S-I-S junctions; the width of the pattern was nearly 200 microns. Various tri-layers (borocarbide-oxide-borocarbide) on MgO substrates were deposited at various temperatures and with various oxide thicknesses. The preliminary characterization of the devices will be presented.

16–82
Development of a radiation heater for large-area double-sided HTS deposition by high-pressure DC-sputtering.
M. Getta[1,2], *G. Müller*[1], *J. Pouryamout*[1,2] and *R. Wagner*[1,2]. [1]Bergische Universität Wuppertal, Wuppertal, NRW, 42097, Germany. [2]Cryoelectra GmbH, Wuppertal, NRW, 42287, Germany.

The planar high-pressure DC-sputtering requires substrate temperatures up to 790°C for the deposition of high-quality $YBa_2Cu_3O_{7-\delta}$ films. Contact heaters can achieve this with inner temperatures up to 930°C, for double-sided deposition with a thin quartz-glass plate between substrate and heating plate it is necessary to reach up to 1000°C. With contact heaters these high temperatures can homogeneously not be reached over large areas without enormous technical problems. Therefore, we built up and tested a radiation heater, which contains a Si/SiC-meander with an effective diameter of 100 mm in a radiation shield system, that is open to the substrate side. Si doped SiC shows a unusual high electrical and thermal conductivity for ceramic materials, so temperatures up to 1200°C can be reached in the middle of the meander. The complete heater was designed for wafers up to Ø 4 inch. Pyrometric measurements of the meander and substrate temperature were as well done as in-situ measurements of the film-growth temperature. With this knowledge we were able to determine compensation functions, which result in constant growth conditions during the film deposition despite of the changing thermal coupling. The first double-sided Ø 1 inch HTS films yielded for both sides $T_c \geq 89$ K, $j_c(77\,K) \geq 4\,MA/cm^2$ and $R_s(77\,K) = 1m\Omega$ at 19 GHz.

16–83
Microwave properties of $DyBa_2Cu_3O_7$ films on AO–,LAO–,YAO–substrates and measurements in dielectric resonators.
K. Irgmaier, *S. Drexl*, *R. Semerad* and *H. Kinder*. Technische Universitaet Muenchen, Physik–Department E10, James–Frank–Str. 1, 85748 Garching, Germany.

We have compared the microwave properties of YBCO and RE-BaCuO films on three different substrate materials, namley sapphire, LaAO and YAO. We characterized the films by measuring R_s as function of power and temperature using the dielectric resonator technique. On sapphire, the crack formation caused by the differential heat expansion is limiting the film thickness. The critical thickness varies when the Yttrium is replaced by rare earth elements. When using Dy-BaCuO, the critical thickness decreased, but R_s decreased even more, so that an overall reduction to 70% of YBCO was achieved. The power handling properties (B_{max} = 15 mT) were the same for YBCO and Dy-BaCuO. On LaAO, film thickness were 600 nm. Because of this larger thickness, the power handling properties at 77 K were the same as on sapphire. We will also report on first results for $YAlO_3$ substrates. Measurements at temperatures below 77 K revealed that the slope of the R_s(T)–curve was steeper

with Y than with Dy, so that there was a crossover around 60 K again.

16–84

Nd/Ba substitutions in $NdBa_2Cu_3O_y$ thin films.

P.B. Mozhaev[1,2], *P. Larsen*[1], *G.A. Ovsyannikov*[2], *Z.G. Ivanov*[1] and *T. Claeson*[1]. [1]Department of Physics, Chalmers University of Technology, Göteborg, S-41296, Sweden. [2]Institute of Radio Engineering and Electronics RAS, Moscow, 103907, Russia.

Thin $Nd_{1+x}Ba_{2-x}Cu_3O_y$ (NBCO) films were deposited using simultaneous pulsed laser ablation of two targets with different element compositions. Films with excess Nd and Ba (x=-0.15...0.15) were prepared and studied. Smooth surface and decreasing T_c of the films with excess Nd suppose substitution of Ba with Nd in the film lattice. Excess Ba, in contrast, introduced no changes in T_c compared with stoichiometric film, but resulted in formation of particles on the film surface with density up to 10^8 cm^{-2}. Such behaviour can be explained as suppressed Nd substitution with Ba, leading to formation of a NBCO film with composition close to stoichiometric and extraction of excess Ba into $(BaCu)O_z$ particles on the film surface. Strong effect of deposition parameters and oxygenation sequence on the film properties was observed.

16–85

$YBa_2Cu_3O_x$ superconducting thin films on (130) $NdGaO_3$ substrate.

A.D. Mashtakov[1], *I.K. Bdikin*[2], *I.M. Kotelyanskii*[1], *P.B. Mozhaev*[1], *G.A. Ovsyannikov*[1] and *E.I. Raksha*[1]. [1]Institute of Radio Engineering and Electronics RAS, Moscow, 103907, Russia. [2]Institute of Solid State Physics, Chernogolovka, Moscow dist. 142432, Russia.

Thin $YBa_2Cu_3O_x$ (YBCO) films were deposited on (110)- and (130)-oriented $NdGaO_3$ (NGO) substrates using DC sputtering at high oxygen pressure technique. CeO_2 buffer layers were prepared on some substrates using RF magnetron sputtering of a Ce cathode in Ar/O_2 atmosphere. T_c of all films was 89-90 K. The obtained films and heterostructures were studied using X-ray diffractional techniques. Misorientation of (001)YBCO direction from the normal of the NGO(110) substrate was observed. Orientational relations of YBCO film on NGO(130) substrate, NGO(110) substrate and NGO(110) substrate with CeO_2 buffer layer were: (001)YBCO//(110)NGO, [110]YBCO//<111>NGO. CeO_2 buffer layer on NGO(110) substrate grows (001)CeO_2//(110)NGO, <010>CeO_2// <111>NGO in contrast with buffer layer growth on the NGO(130) substrate: (110)CeO_2//(110)NGO, [001]CeO_2//[110]NGO. The resulting CeO_2 film (111) direction is close to the normal on the NGO(130) substrate. YBCO film on the CeO_2 buffer layer consisted of two domains: (001)YBCO//(100)CeO_2 and (001)YBCO//(010)CeO_2. The third possible domain - (001)YBCO//(001)CeO_2 - was not observed, probably due to deposition conditions favoring domains with c axis close to substrate normal.

16–86

Phase relations in thin RBCO (R=Lu,Ho,Gd,Nd) epitaxial films prepared by MOCVD.

S.V. Samoilenkov[1], *O.Yu. Gorbenko*[1], *S.V. Papucha*[1], *N.A. Mirin*[1], *I.E.Graboy*[1], *A.R.Kaul*[1], *O. Stadel*[2], *G. Wahl*[2] and *H.W. Zandbergen*[3]. [1]Chemistry Department, Moscow State University, 119899 Moscow, Russia. [2]IOPW, TU Braunschweig, Bienroder Weg 53, 38108 Braunschweig, Germany. [3]National Centre for HREM, Delft TU, Rotterdamseweg 137, 2628 AL Delft, The Netherlands.

Thin epitaxial films of $RBa_2Cu_3O_7$ (RBCO, R=Lu,Ho,Gd,Nd) have been prepared by MOCVD technique on perovskite substrates. The appearance of secondary phase inclusions in slightly off-stoichiometric films was systematically studied by means of XRD, SEM and TEM/HREM. The phase relations found differed considerably from those of corresponding R-Ba-Cu-O bulk ceramics. No evidence was observed for the presence of R_2BaCuO_5 or $BaCuO_2$, which are the equilibrium secondary phases with bulk RBCO. In contrast, well oriented growth of R_2CuO_4 (R=Nd and Gd), R_2O_3 (R = Lu,Ho,Y), $Lu_2Cu_2O_5$, Ba_2CuO_3 and $BaCu_3O_4$ was found, depending on the films' stoichiometry. The remarkable change of the phase relations with the change of rare earth cation should be stressed. Because of the thermodynamic reason, the formation of coherent or semi-coherent interfaces between embedded inclusions and the matrix is critical for a stabilization of otherwise non-equilibrium oxide phases in epitaxial films. The crystal structure of unstable-in-bulk cuprate $BaCu_3O_4$ was determined using electron nano-diffraction of the films' cross-sections. The conditions for its thermodinamic stability are characterized. The influence of the phase composition and content on the properties of RBCO thin films is outlined. The evolution of the superconducting properties of the epitaxial films as a function of R is discussed.

16–87

The effect of laser beam intensity homogenisation on the smoothness of YBCO films obtained by laser ablation.

R.A.Chakalov[1,2], *F.Wellhofer*[1,3], *S.Corner*[2], *M.Allsworth*[2] and *C.M.Muirhead*[2]. [1]Interdisciplinary Laser Deposition Facility, The University of Birmingham, Edgbaston, Birmingham B15 2TT, United Kingdom. [2]School of Physics and Astronomy, The University of Birmingham, Edgbaston, Birmingham B15 2TT, United Kingdom. [3]School of Metallurgy and Materials, The University of Birmingham, Edgbaston, Birmingham B15 2TT, United Kingdom.

The excellent electrical properties of the obtained films and the high deposition rate have made the laser ablation a preferred technique for fabrication of thin films of HTS and other related oxides. Despite the significant improvement of the method during the last several years the resulting films still suffer from poor surface morphology. This feature prevents them from including in multilayer structures, which are nowadays considered as the next necessary step in HTS materials application. Boulders and grains of off-stoichiometric phases are among the considerable sources of increased film roughness. The mechanisms of their formation could be very different but one of the reasons is low

laser fluence on the target material, insufficient for the initiation of proper laser ablation process. Usually, the energy density in the spot is controlled in order to exceed a certain threshold value. However, due to the beam intensity spatial inhomogeneity, there can be areas within the spot with quite different laser fluence. To overcome this problem we use a beam intensity optical homogeniser. By means of crossed cylindrical lenses the raw beam of the excimer laser is cut into 24 segments and overlayed at a plane of integration. We present evidences that the uniform and homogeneous spot on the target improves several times the overall smoothness of the deposited YBCO films.

16–88
Ag/YBCO thin film growth by single resistive evaporation.
A. Verdyan, *I. Lapsker* and *J. Azoulay*. Center for Technological Education Holon affiliated with Tel-Aviv University.

It commonly accepted that thin film formation of YBCO on conducting substrate is one of the keys to further development of advanced devices in the microelectronic and high field applications. In this work we report on a preparation of superconducting YBCO thin film deposited on unbuffered silver substrate using a simple conventional vacuum system equipped with only single resistive heated evaporation source. A thick Ag film (1000 nm) was first deposited on a polished clean MgO substrate. A pulverized mixture of Y, Cu, and BaF_2 was then inserted in to resistive evaporation boat. The evaporation process lasted 15 minutes thus coating the Ag film on the substrate with a 500 nm thickness of amorphous film. Subsequently heat process under low oxygen partial pressure was carried out. The results of the film evaluation are presented and discussed.

16–89
Importance of the interface effects in Au-$YBa_2Cu_3O_{7-\delta}$ sintered composites at low temperature.
C. Lambert-Mauriat, *J.M. Debierre* and *J. Marfaing*. Lab. MATOP-CNRS, case 151,Fac. des Sc. et Techn. de Saint-Jérôme, Avenue Normandie-Niemens,F-13397 Marseille cedex 20.

Development of innovative and performant systems for electronic devices can be attempted with sintered composites. We combine experimental and numerical studies to investigate the behaviour of the resistivity of Au-$YBa_2Cu_3O_{7-\delta}$ composites as a function of the gold volume fraction, ϕ, in the temperature range 50 K - 300 K. Below the superconducting critical temperature T = 92 K, a systematic shift of the metal-superconductor transition threshold is observed as T varies. More, below 220 K, the resistivity curves present an unexpected maximum whose amplitude and position change with T. Our experimental results are well described within a random conductor network model which incorporates porosity and interface resistances. The importance of the interfacial effect is great at low temperature and the numerical data show that porosity alone cannot account for the maximum of the resistivity. Conversely, a peak is observed in the simulations when a substancial interface resistivity is imposed. A very good agreement between experimental and numerical results is found and a possible interpretation of the temperature dependence of this interfacial resistivity is discussed.

16–89P1
Gas sensitivity of the cuprate oxides.
O.J. Bomk, *V.V. Il'chenko*, *G.V. Kuznetsov*, *A.M. Pinshuk*, *V.V. Skursky* and *A.I. Tsiganova*. Kiev University, Kiev, Volodimirska, 64, 252033, Ukraine.

The physical properties high-temperature superconducting ceramics on the basis of the cuprate oxides are much influenced by the gas environment. In this work materials as YBaCuO and related non-superconducting phase were investigated which at the moment have the best opportunities for practical application. Oxide cuprate ceramics are characterized by open system pores. The results of experimental researches of the gas sensitivity find an explanation within the framework of the electronic theory catalytic, establishing connection between sorption and catalytic properties of the surface and electrical characteristics of ceramics.The majority cuprate oxides is characterized by the n-type of conductivity, that causes its reduction at the chemosorption of donor molecules such as (aceton, ethanol, diethyl ether, oxid of carbon CO). Adsorption of the acceptor molecules (oxygen, chlorine, oxid of nitrogen NO2) causes increase of the conductivity such ceramics. The selectivity depends on activation energy (Ea) of the chemosorption gas, as the concentration of the adsorption molecules is n=exp (Ea/kT) determines concentration additional electrons in the crystal lattice. The Fermi energy position determines correlation between the influence of the external factors (electrical field, illumination, implantation) and speed catalytic of reactions on a surface cuprate oxides.

Session System Aspects related to electronic applications

16–90
On-orbit status of the high temperature superconductivity space experiment (htsse-ii).
M. Nisenoff. US Naval Research Laboratory Code 6850.1 4555 Overlook Avenue SW Washington DC 20375-5347 USA.

The High Temperature Superconductivity Space Experiment (HTSSE-II) was successfully placed into orbit on 23 February 1999 when the Advanced Research and Global Observation Satellite (ARGOS) was launched on a Delta-II rocket into a circular polar orbit. The HTSSE-II experiment contains eight HTS components and subsystems, which were developed by various industrial and government laboratories in the 1992 to 1994 time frame and then integrated with a closed cycle refrigerator into the HTSSE-II payload during 1995. (For details about HTSSE-II components and payload, see IEEE Trans. Microwave Theory and Techniques, vol. 44, no. 7, part II, July 1996.) After numerous delays due to problems associated with the ARGOS satellite, ARGOS was finally launched on 23 February 1999, about three years after the original launch date. The cryogenic refrigerators on the HTSSE-II payload were scheduled to be started about 1 May 1999 and the monitoring of the status of the HTS devices was scheduled to begin shortly thereafter. In

this talk, after a brief review of the HTS components on HTSSE-II, the status of these devices will be reviewed and changes, if any, observed over the past five years, both during ground storage and in space after launch, will be presented.

16–91

Transformation of Heat Energy to Electric Energy in a System of Mesoscopic Superconducting Rings.

A.V.Nikulov. Institute of Microelectronics Technology and High Purity Materials, Russian Academy of Sciences.

Zero velocity of superconducting electrons is forbidden in a superconducting ring if a magnetic flux inside it is not divisible by the flux quantum. Therefore a system of mesoscopic superconducting rings can be used as a thermo-electric generator. A change of the superconducting electron density causes a voltage in a consequence of the electromagnetic induction law, if the velocity of superconducting electrons is not equal zero. The most interesting case is an induction of a direct voltage in an inhomogeneous ring. A voltage with a direct component appears if a ring section with lowest critical temperature is switched iteratively from normal to superconducting state and backwards. The thermal fluctuation can induce a direct voltage at an unaltered temperature. This is possible because a preferential direction of superconducting electron motion exists in a ring if a magnetic flux inside it is not divisible by the flux quantum. A system of the inhomogeneous superconducting rings can be used as a power source. The power of a ring is proportional to T_c^2 and is very small. In order to obtained the power 1 Wt a system with no less than 10^8 HTSC rings should be used. But because a ring size is small, such system can be made by methods of microelectronics technology on a substrate with area 1 cm^2.

16–92

RF Magnetic Shielding Effect of an HTS Cylinder.

M. Itoh[1], *K. Mori*[2], *K. Itoh*[1] and *Y. Horikawa*[1]. [1]Deptartment of Electronic Engineering, Kinki University, Japan. [2]Division of System Science, Kobe University, Japan.

Radio frequency (RF) magnetic shielding is required in many applications to reduce the influence of environmental electromagnetic waves, and to protect the environment from the leakage of any generated electromagnetic field. The high-critical temperature superconductor (HTS) is an ideal material for use as a magnetic shielding vessel which employs perfect diamagnetism. In general, however, the detailed characteristics of RF shielding effect for HTS vessel are unknown. In the present research, it is measured the RF shielding effect, the ratio of the output voltages of the receiving antenna with and without the shielding vessel, on three Bi-Pb-Sr-Ca-Cu-O (BPSCCO) bulk cylinders which are different l/r (7.3, 10.0, 15.3), where l and r are the length and inner radius for BPSCCO cylinder, respectively. In the present research, it is found that the RF shielding effects of three BPSCCO cylinders decrease with an increase in frequency range from 1 MHz to 1 GHz of the applied electromagnetic wave, and obtain the similar results. Also discussed are RF shielding effect of double-cylinder, constructed by superimposing a BPSCCO cylinder (l/r=15.3) over a BPSCCO cylinder (l/r=7.3).

16–93

Estimation of Magnetic Field within High Effective Magnetic Shielding Vessel.

M. Itoh[1], *K. Mori*[2], *Y. Horikawa*[1] and *T. Minemôto*[2]. [1]Deptartment of Electronic Engineering, Kinki University, Japan. [2]Division of System Science, Kobe University, Japan.

The value of the maximum shielded magnetic flux density Bs of a high-critical temperature superconductor (HTS) vessel, in general, do not satisfy the criteria required for practical use. The present authors have improved the magnetic shielding effects associated with the superposition of single or multi-layered ferromagnetic cylinders over a Bi-Pb-Sr-Ca-Cu-O (BPSCCO) bulk cylinder; termed the high effective magnetic shielding vessel. Little is known, however, of the characteristics and evaluation procedures used to determine the behavior of the magnetic flux density Bin within the shielded vessel when exposed to an external magnetic flux density Bex of less than the value of Bs. The value of Bin to an applied Bex is measured by an HTS dc-SQUID magnetometer, although it takes a lot of time to measure the flux density in the superconducting BPSCCO cylinder. Therewith, it is estimated the value of Bin from the Bin-Bex characteristics for the BPSCCO cylinder and single or multi-layered soft-iron cylinder, where the characteristics of soft-iron cylinder measured by use of a gaussmeter. The estimated values agreed well with the experimental values. The present paper examines the estimation method and optimum shielding conditions for constructing an ideal magnetic shielding vessel.

16–94

Low noise hybrid TlBaCaCuO / GaAs 5.4 GHz transponders.

K.C.Huang[1], *A.Jenkins*[1], *D.J.Edwards*[1] and *D.Dew-Hughes*[1]. [1] Department of Engineering Science, University of Oxford, Parks Road, Oxford, OX1 3PJ, UK.

Low noise satellites play critical roles in space communications. This paper presents the combination of high temperature superconducting (HTS) passive circuits with GaAs FETs to implement a low noise and small size RF repeater at cryogenic temperatures of around 77 K. A novel HTS preselector interdigital filter, a three-stage low-noise amplifier, a mixer, and a self-feedback local oscillator with a novel two-dimensional HTS resonator were designed, fabricated and interconnected to form a low-noise hybrid superconductor / semiconductor microwave transponders. All HTS devices were fabricated from TlBaCaCuO thin films deposited on MgO and $LaAlO_3$ substrates. The centre RF frequency was 5.4 GHz with an IF frequency of 2.4 GHz. Downconversion was achieved by means of the 3 GHz local oscillator plus mixer. The measured performance is demonstrated for each of the components and for the entire system. In addition to a reduced noise figure, the advantages of small size and low power consumption are observed because of the utilization of thin film HTS materials on high dielectric constant substrates.

16–95

HTS filters and cooled electronics for communications - system performance and cooling needs.

R.B.Greed[1] and *J.Tilsley*[2]. [1]1 Marconi Research Centre, Great Baddow, Chelmsford, Essex, CM2 8HN, England. [2]2 Marconi Infra-Red, Southampton, Hampshire, SO15 0EG, England.

Future Third-Generation communications systems using both TDMA and W-CDMA air interface standards to support the growth in multi-media services demand improved sensitivity and selectivity at the base transceiver station (BTS). Increased sensitivity provides extended coverage, higher capacity CDMA systems, longer 'hand-set' talk time, while better selectivity reduces interference, improves bandwidth utilisation. A transceiver to meet the higher performance requirements in which key components are fabricated using thin-film High Temperature Superconductor (HTS) technologies is described. For HTS techniques to be commercially viable a high performance cryo-packaging comprising a r.f. module, an enclosing vacuum dewar and a compact, maintenance 'free' and reliable cryo-cooler is essential. The paper emphasises the necessary design approaches to meet the thermal and mechanical conditions of the cryo-package over the temperature range 55K to 345K. The materials for the r.f. module are selected to thermally match the HTS substrates to the housing. In-situ tuning methods allow the HTS filters to be optimised at the operating temperature, 60K, and in vacuum. The dewar design features novel microwave and thermal interconnects across the vacuum space. The cryo-packaging includes an integrated small Stirling cycle cooling engine designed for a 5 watt heat lift at 60K. The r.f. performance of a six channel filter and LNA module for tower mounted amplifier for mobile communications is also presented.

16–96

Jena Superconductive Electronics Foundry (JeSEF).

H.-G. Meyer, L. Fritzsch, R.P.J. Ijsselsteijn, J. Ramos, H. Elsner, W. Morgenroth, J. Kunert, G.Wende, M. Schubert and *R. Stolz*. Institute for Physical High Technology Dept. of Cryoelectronics P.O.Box 100239 D-07702 Jena Germany.

In 1993 JeSEF, a superconductive electronics foundry was founded in the IPHT Jena, dealing with electronic circuits for companies and institutes. The complete infrastructure for a competitive Josephson technology established in the past few years encloses a CAD system for circuit design, the deposition of films, lithographic processes down to the submicrometer region, and the electrical characterization including a microwave measuring technique up to 110 GHz. We offer the following services: photomasks for institues dealing with cryoelectronics, microfabrication processes such as photolithography (contact and projection exposure), electron beam lithography, wet chemical and dry etching (ion beam etching and reactive ion etching). The standard processes for SFQ circuits in niobium technology are available for customers. The following superconductive circuits can be purchased: microwave circuits for the Josephson voltage standard (1 Volt) including chip carrier and cryoprobe, field-sensitive integrated LTS gradiometer and magnetometer SQUIDs, single-layer HTS SQUIDs based on bicrystal junctions, flux transformers and multiturn input coils for HTS SQUIDs, SQUID electronics operating at 77 K. Furthermore complete SQUID systems adapted to customer's applications are offered. Especially, for Transient Electromagnetic Prospection (TEM), a geomagnetic prospection method, SQUID systems are available.

16–97

Thermoelectric Generator with the Passive Superconducting branch.

V.A.Demchenko. Institute of Thermoelectricity, General Post Chernovtsy 274000, Box 86, Ukraine.

The semiconductors used in thermoelectric converters of energy do not allow essentially to increase effectiveness work of these devices, that forces to search for new materials and the approaches in designing. Wide temperature and technological range of High- temperature superconductors makes them attractive for useing in thermoelectricity. The replacement of one of active branch of thermoelectrical refrigerator into the passive superconducting one has allowed to lower the record depth of cooling of cold thermojunction for this class of devices. The similar application of a superconductor is offered in the thermoelectric generator. The thermodynamic analysis of work of thermogenerator with the passive superconducting branch has allowed to receive, formula for calculations of efficiency, similarly received earlier by A.F.Ioffe. Significant increase of effectiveness of work of thermogenerator with the passive superconducting branch at low temperatures, as estimations show, quite justifies the charges on their cooling by cryogenic liquids. The using of such thermogenerators is especially effective in space, where there is no need in artificial cooling. The most suitable material for passive superconducting branch of thermotransformer of energy are thread like monocrystals with a critical current not less than 10000 A/sq.ce.

16–98

Numerical analyses of superconductive electronic structures at high frequencies.

H.Toepfer, T.Lingel and *F.H.Uhlmann*. Technical University of Ilmenau Department of Fundamentals and Theory of Electrical Engineering P.O.Box 100565 D-98684 Ilmenau Germany.

The high-fequency properties of passive superconducting structures were investigated numerically by means of the finite-difference time-domain method. Special emphasis has been put on the propagation of narrow voltage pulses in interconnecting structures. In the contribution, the analysis technique is described and results of its application are presented. Conclusions for the layout of signal paths and interfacing components in Rapid Single Flux Quantum logic circuits are drawn.

Session Digital Applications

16–99

SQUID Applications for SFQ Logic Circuits.

Y.Harada. Kokushikan University, Faculty of Engineering 4-28-1 Setaga.

This article describes a simulation study on SQUID appli-

cations for Single-Flux- Quantum(SFQ) Logic Circuits. It includes two topics such as detection of a SFQ pulse and transmission-control of a SFQ pulse in a Josephson transmission line(JTL). Because one of current sources of a JTL is removed, a current void in which no current exists in a Josephson junction is formed. This current void is moved by applied SFQ pulses. Focusing on a circulating current at the current void, SFQ-pulse transmission is non-destructively detected by the SQUID. A SFQ up-down shift register which supplies the circulating current to the SQUID is proposed. A SQUID inserted in a JTL operates as a gate which controls SFQ-pulse transmission through it. A SFQ-pulse storage loop which is composed of a JTL loop and a SQUID. An injected SFQ-pulse runs around the storage loop permanently. Multiple SFQ-pulses can be injected at the loop. This storage loop is a main part of a SFQ oscillator. The SQUID can eliminate the SFQ-pulse transmission in the loop.

16–100

Digital Superconducting Gauges of Temperature.

V.A.Demchenko. Institute of Thermoelectricity, General Post Chernovtsy 274000, Box 86, Ukraine.

Now indication of temperature and its processing in the means of automatics is more often made by digital devices, and all gauges of temperature remain practically analogs. Exception make precision methods of measurement of temperature on to basis of SQID, but it is faster exotic. Urgent order of time are the digital gauges of temperature. It will considerably simplify the procedure of measurement also will raise its accuracy and reliability. The digital gauge of temperature allows to exclude from the circuit of measurement two element - amplifier and analog-digital converter. Superconducting materials allow the realize this idea. The description of a design of digital superconducting gauge of temperature is given. The gauge of temperature working in a parallel code is a little bit inconvenient because of a plenty of making wires, that will bring significant indignations in the process of measurement. More acceptable are frequency - depended gauges and gauges working in consecutive code. The essential lack of digital superconducting of temperature is the limited range of measur temperatures, but in some time, probably, this idea will manage to be distributed on semiconductors or other materials.

16–101

Basic RSFQ circuits and digital SQUIDs realised in standard Nb/Al-Al_2O_3/Nb technology.

M. Khabipov[1,2], *L. Fritzsch*[1], *S. Lange*[3], *R. Stolz*[1], *H.Uhlmann*[3] and *H.-G. Meyer*[1]. [1]Institute for Physical High Technology, Department of Cryoelectronics, Jena, P.O. Box 100239, D-07702, Germany. [2]Permanent address: IREE Russian Academy of Sciences, Mokhovaya St. 11, Moscow, 103907 Russia. [3]Technical University of Ilmenau, Ilmenau,P.O. Box 100565, D-98684, Germany.

Basic RSFQ circuits and digital SQUIDs with different designs were fabricated using a Nb/Al-Al_2O_3/Nb technology and were experimentally tested. The critical current density of the Josephson junctions is 500 A/cm^2. The sheet resistance of the Mo resistor layer is set to 1 Ω. The proper operation of the basic RSFQ circuits including dc/SFQ-converters, switching elements, T-flipflops, and SFQ/dc-converters is experimentally proved. Operation margins of bias currents up to 20% have been measured. The correct performance of the switching circuit was experimentally proven up to about 100 GHz. We realised a digital SQUID circuit with feedback loop integrated on the same chip. It consists of a comparator circuit generating voltage pulses of both polarity depending on the flux in the pickup loop. The feedback loop is compensating the input flux and stabilises the working point of the comparator circuit via a write gate in the pickup loop. The proper response of the feedback circuit for clock frequencies of the comparator circuit up to 100 MHz was experimentally verified.

16–102

Ramp Edge Junctions on a Ground Plane for RSFQ Applications.

A.H. Sonnenberg, *G.J. Gerritsma* and *H. Rogalla*. Low Temperature Division, Faculty of Applied Physics, University of Twente P.O. box 217, 7500 AE, Enschede, The Netherlands.

Application of ramp edge junctions in RSFQ circuits requires junctions connected by low inductances. Ungrounded striplines give rise to large stray fields and undesired inductances such as junction leads. In order to minimize these inductances we have fabricated the junctions on top of a buried ground plane. We have chosen for a buried ground plane in stead of a ground plane on top of the junction in order to minimize thermal cycling and oxygenation problems of the junctions. Direct injection SQUIDs have been fabricated for inductance measurement. The inductance values have been measured both on and off the ground plane as a function of temperature and microstrip length. In order to test the junctions in an RSFQ environment a balanced comparator has been fabricated. Measurements on high speed testing will be presented. This work has been sponsored by the EC, under project number 23429

16–103

RSFQ-Based D/A Converter for Precise-Measurement Applications.

F. Hirayama, *H. Sasaki*, *S. Kiryu*, *M. Maezawa*, *T. Kikuchi* and *A. Shoji*. Electrotechnical Laboratory, Tsukuba, Ibaraki, 305-8568 Japan.

We are proposing a digital to analog (D/A) converter based on RSFQ (Rapid Single Flux Quantum) logic circuits, which is expected to synthesize a wave-form with metrological accuracy. It is an advantage that the D/A converter does not require complicated and expensive semiconductor microwave electronics. The converter consists of three functional blocks, i.e. , a pulse-number multiplier (PNM), a pulse distributor (PD), and a number of voltage multipliers (VMs). A pulse synchronized with an external precise oscillator (frequency f, ~10MHz) is converted to a train of a definite number (m, ~1000) of SFQ pulses by PNM, split and gated to VMs corresponding to bits of digital code by PD. The n-th VM generates 2^n of h/(2e) "voltage quanta" per one input pulse and output of VMs are connected in series, thus the total output voltage will be exactly equal to f*m*h/(2e)*(digital-code). These components were designed and fabricated at our laboratory utilizing ETL standard process (ESP) technology, which features Nb/AlOx/Nb

junction, SiO_2 insulation, and Pd resistor. The critical current density of the junction and the sheet resistance are 1.4 kA/cm^2 and 1.2 Ohm, respectively. We confirmed correct operation of the components by low frequency functional tests.

16–104
Measurements of a High Tc RSFQ 4-Stage Shift Register and the Inductance of the Shift Register Cell.
Y. H. Kim[1], *J. H. Park*[1], *J. H. Kang*[2], *T. S. Hahn*[1], *C. H. Kim*[1], *J. M. Lee*[1] and *S. S. Choi*[1]. [1]Korea Institute of Science and Technology, Seoul 130-650, Korea. [2]University of Inchon, Inchon 402-749, Korea.

For a future high speed and low power device, superconducting single flux quantum(SFQ) circuit is a good candidate. We have fabricated high temperature superconductor RSFQ shift register circuits using YBCO grain-boundary junctions and ramp-edge Josephson junctions. Each circuit is composed of a four stage shift register and two inductively coupled read SQUIDs, positioned on each side of the shift register to measure the correct operation of the circuit. Data shifts from one stage to the next were controlled by the current pulses injected to the junction bias lines. Our new homemade probe equipped with high speed coax lines were used in this experiment to reduce the interference of the two read SQUIDs. The inductance of the data storage cell was measured upon the size of cell to investigate the optimum size for the correct operation of the shift register. To control the inductance of the data storage cell in an easier fashion and to build more complicated circuits, we also fabricated shift register circuits using HTS ramp edge junctions.

16–105
Comparators for HTS ADCs based on the tri-crystal Josephson junctions.
A.Yu. Kidiyarova-Shevchenko[1,2], *F. Komissinsky*[3], *E.A. Stepancov*[4], *Z.G. Ivanov*[1], *D.E. Kirichenko*[5], *M.M. Khapaev, Jr.*[6], *M. Jacobson*[1] and *T. Claeson*[1]. [1]Chalmers University of Technology, Gothenburg, Sweden. [2]Nuclear Physics Institute, Moscow State University, Moscow, Russia. [3]Institute of Radio Engineering and Electronic RAS, Moscow, Russia. [4]Institute of Crystallography RAS, Moscow, Russia. [5]Physics Dep., Moscow State University, Moscow, Russia. [6]Computer Science Dep., Moscow State University, Moscow, Russia.

We have investigated different comparators for S-D and Flash type high temperature superconducting analog-to-digital converters (ADC). The circuits were optimized in order to achieve maximum performance of the related ADCs in terms of input bandwidth, resolution and operating margins. The comparators were designed and fabricated on (Y)ZrO_2 tri-crystal substrates with three parallel 24^o grain boundaries placed $10\mu m$ apart. The circuits were implemented by using an integrated circuit technology, including deposition of the YBCO layer, insulator and gold resistors. Circuit elements with the smallest size of $0.6\mu m$ were patterned by using e-beam lithography and Ar ion beam milling. The quality of the Josephson junctions were tested on the three chips with 32 junctions on each and a spread of less than 10% in junction critical current was determined. A novel design method for inductance calculation with 3D magnetic field distribution and extraction of the inductance matrix of the equivalent circuit for multilayer superconducting circuits was developed. The method allows the inductance calculation with accuracy greater then 5% for circuits with complicated topology and without superconducting groundplane. At the meeting we will present layouts and results of experimental testing of the comparators.

16–106
Universal NAND Gate Based on Single Flux Quantum Logic.
H. Myoren, *S. Ono* and *S. Takada*. Faculty of Engineering, Saitama University, 255 Shimo-Okubo, Urawa, Saitama 338-8570, Japan.

Single flux quantum (SFQ) logic circuits have been reported that they have the ability to operate at high frequency and at ultra-low power. To construct logic circuit, AND gate, OR gate and NOT gate have been reported so far. Universal gate such as NAND gate is attractive since any logic circuits can be constructed using one kind of the logic gate. Constructing NAND (or NOR) gate using SFQ circuit, we could construct any logic function using SFQ logic circuits. From this reason, NAND gate is very important for constructing integrated SFQ circuits. In this study, we propose an universal gate of NAND logic based on SFQ logic. In the proposed gate, three superconducting loops share two Josephson junctions (JJs) in common. The critical currents of JJs were designed to allow two loops among them to keep SFQ at the same time. We simulated dynamic operation of this NAND gate using JSIM program. The results show that the NAND gate can operate at frequency up to ~25GHz, and the power consumption of this circuit is close to $0.06\mu W$/gate, using Nb/AlO_x/Nb JJs with the critical current density of $0.8kA/cm^2$.

16–107
HTS implementation of Analogue to Digital Converters.
J. S. Satchell and *I. L. Atkin*. DERA (Malvern), Malvern, Worcs, WR14 3PS, United Kingdom.

Low Tc implementations of analogue to digital converters (ADCs) have demonstrated extremely impressive performance, and further improvements are expected shortly. For example sigma-delta converters containing the complete decimation filter have been made. Superconducting ADCs would be more widely deployed if comparable performance was obtainable using high temperature superconductors (HTS). However any HTS implementation must face increased noise, higher inductance values and at present a much less reproducible junction technology. Complete ADCs may be too complex for HTS in the foreseeable future, and a hybrid design, with some of the complex digital filtering implemented in semiconductor technology, appears more practical. Engineering choices must be made to decide how much of the circuit should be made in HTS. Calculations will be presented of the performance and production yield tradeoffs for this class of design.

16–108

Matching of Rapid Single Flux Quantum Digital Circuits and Superconductive Microstrip Lines.

N.A. Joukov[1], *A.Yu. Kidiyarova-Shevchenko*[2,3], *D.E. Kirichenko*[1], *A.B. Pavolotskij*[3] and *M.Y. Kuprianov*[3]. [1]Department of Physics, Moscow State University, 119899 Moscow, Russia. [2]Department of Physics and Engineering Physics, Chalmers University of Technology, S-41296 Gothenburg, Sweden. [3]Nuclear Physics Institute, Moscow State University, 199899 Moscow, Russia.

The problem of transmission of the information in the form of Single Flux Quantum (SFQ) pulses in complex Rapid Single Flux Quantum (RSFQ) digital circuits has attracted a considerable interest in the last few years. Two possible solutions of this problem had been proposed, i.e. transmission of the pulses using the Josephson Transmission Lines (JTL) and the superconductive microstrip transmission lines. We have analyzed these solutions in application to digital RSFQ correlator. It was shown that the solution based on microstrip lines allows to reduce the number of Josephson junctions and to rise up the integration scale of the device. We essentially modified the previously proposed method for matching RSFQ digital circuits by superconducting microstrip lines. This modification allows to avoide the using of capacitors of large geometric sizes as matching components and to reduce significantly the geometrical area occupied on a chip by RSFQ drivers and receivers. We have designed, simulated and fabricated these circuits using standard niobium technology. A theoretical analysis has been compared with experimental results.

Session Oscillators and Volt standards

16–110

High Temperature Superconducting Low Noise Oscillator.

T.A. Koetser[1] and *R.B. Greed*[2]. [1]T.A. Koetser Marconi Research Centre West Hanningfield Road Great Baddow Chelmsford Essex CM2 8HN. [2]R.B. Greed Marconi Research Centre West Hanningfield Road Great Baddow Chelmsford Essex CM2 8HN.

Work is ongoing at present to produce a very low noise oscillator at 1.8GHz. Low noise is achieved by the incorporation of a high temperature superconducting (HTS) planar disk resonator. The HTS resonator, which is etched YBCO on a $LaAlO_3$ substrate, is excited in the TM_{010} mode only, in which the current density carries only a radial component. Hence any slight edge defects do not introduce radiative loss. Combined with a low surface resistance, this enables the realisation of a very high Q resonator. Excitation is performed with microstrip feed and output lines which are capacitively coupled to the disk. The planar resonator will be implemented into a microstrip feedback loop, together with a low noise amplifier, a phase setting component and a coupler. To date, the planar disk resonator has been manufactured and successfully tested at 60 Kelvin. Unloaded Q has been measured at 175,000. The noise figure of the amplifier has been measured to be less than 0.2dB at 60 Kelvin. Future work includes implementing the designed components into the oscillator package. The paper will present detail on the research and fabrication techniques carried out, and the noise measurements obtained. Support for this work is provided by Marconi Electronic Systems and the European Commission (ACTS Program)

16–111

Subharmonic Gap Structures in Josephson Flux Flow Oscillators.

M.A. Nordahn[1], *M.H. Manscher*[1], *J. Mygind*[1] and *L.V. Filippenko*[2]. [1]Department of Physics, Technical University of Denmark, B309, DK-2800 Lyngby, Denmar. [2]Institute of Radio Engineering and Electronics RAS, Mokhovaya 11, Moscow 103907, Russia.

Subharmonic gap structures in very long overlap $Nb - AlO_x - Nb$ Josephson tunnel junctions have been investigated. The experimental results show peaks in the dynamic conductance at both odd and even integer fractions of the gap voltage. At high magnetic fields, the I-V curves become insensitive to variations of the magnetic field while retaining the conductance peaks. Variation of temperature does not noticeably change the peak position relative to the gap voltage. Investigation were done on long samples with similar geometry, and the results are qualitatively the same for all samples. The presence of the odd subharmonics can be explained by the Josephson self-coupling effect originally predicted by Werthamer, whereas the even subharmonics may be due to Multiple Andreev Reflections. The results are important for the development of the flux flow oscillator used as local oscillator in the integrated all-superconducting 200-800 GHz receiver.

16–112

Josephson-Junction Arrays with Lumped and Distributed Coupling Circuits.

V.K. Kornev, *A. V. Arzumanov* and *N. A. Shcherbakov*. Physics Department, Moscow State University, Moscow, 119899, Russia Department of Physics, Moscow State University, Moscow, 119899, Russia;

Josephson-junction arrays with lumped and distributed coupling circuits have been studied by means of numerical simulation technique. It has been shown that the finite coupling radius results in a "saturation" of the phase-locked oscillation line-width reduction with number N of Josephson junctions for the case of lumped circuits. Therefore the maximum factor of the reduction is about 100 for the arrays with the lumped coupling circuits. It has been found that an additional reduction in phase-locked oscillation line width can be provided by the impact of the standing electromagnetic waves that are excited in the distributed coupling circuits. The distributed circuits, have been analysed, constitute the pieces of either microstrip or slit superconducting lines. Despite the fact that Josephson junctions can be also connected into dc superconducting loops, the phase-locked oscillation state in-phase may be provided by strong interaction between the junctions and electromagnetic standing waves. The interaction neutralises the phase shifts caused by external magnetic field. The crucial role of high frequency losses has been also studied. Different ways of Josephson junction connection to the distributed circuits have been analysed, and the possible designs of both low-Tc and high-Tc Josephson multi-junction structures are discussed.

16–113
Linewidth Measurement of Josephson Array Oscillators with Microstrip Resonators.
A. Kawakami, *Y. Uzawa* and *Z. Wang*. Kansai Advanced Research Center, Communications Research Laboratory, 588-2 Iwaoka, Iwaoka-cho, Nishi-ku, Kobe, Hyogo, 651-2401, Japan.

The linewidth of the Josephson array oscillator was measured using integrated receiver consisting of two Josephson array oscillators and a SIS mixer. The oscillators were formed with 30 Josephson junctions and Nb microstrip resonators. In the I-V characteristics of the oscillator, a current step which we call fundamental steps resulting from the resonance of the microstrip resonators was observed around 1.17 mV which corresponds to designed frequency (566 GHz). When the oscillators were biased at the fundamental step, if-power spectrum was observed and the composite linewidth of the oscillator was measured about 8 MHz at 4.2 K. At this biased point, the dynamic resistance per a shunted junction of the oscillators were about 0.39 and 0.23 ohm respectively. By assuming that, the linewidth was mainly dominated by the dynamic resistance 0.39 ohm, the linewidth was estimated to be about 87 MHz. These suggest that the array was in the Phase-locking status in the fundamental step and the status caused the linewidth to be narrow compared to the linewidth of single junction.

16–114
Microwave properties of SINIS Josephson junction series arrays.
H. Schulze[1], *R. Behr*[1], *J. Kohlmann*[1], *F. Mueller*[1], *I.Ya. Krasnopolin*[2] and *J. Niemeyer*[1]. [1]Physikalisch-Technische Bundesanstalt, 38116 Braunschweig, Germany. [2]Russian Research Institute for Metrological Service, Moscow, 117965 GSP-1, Russia.

We have fabricated series arrays of several thousands of overdamped SINIS junctions integrated into a superconducting microstripline. The SINIS junctions, intrinsically shunted Josephson junctions with a superconductor-insulator-normal conductor-insulator-superconductor structure, have been fabricated in Nb-Al-AlO_x-technology. In large series arrays, the junctions are mutually synchronized by the microwave power which they emit into the microstripline. When the stripline parameters are suitably chosen, the series array can be operated as a microwave oscillator. In addition, the array can be operated as Josephson voltage standard with internal microwave generator. Very low external microwave power is required in this case, as a major part of the microwave needed is generated by the Josephson array itself. An important condition for an integration of the microwave supply into the Josephson voltage standard chip is, therefore, met. Measurements performed to determine the mutual synchronization and the microwave distribution in large SINIS series arrays are presented. This work was supported in part by the BMBF (ref. no. 13N6835) and the EU (ref. no. SMT4-CT98-2239)

16–115
Influence of the phase-whirling states on the fluxon motion in two inductively coupled long Josephson junctions.
E. Goldobin[1], *A. Wallraff*[2] and *A.V. Ustinov*[2]. [1]Institute of Thin Film and Ion technology, Research Center Juelich GmbH, 52425, Juelich, Germany. [2]Physics Institute III, University of Erlangen-Nuernberg, 91054, Erlangen, Germany.

In a system of inductively coupled long Josephson junctions it is expected that phase dynamics in one junction affects the phase dynamics in the other and vise versa. We study experimentally and theoretically the influence of phase-whirling state in one junction of the 2-fold stack on the single fluxon dynamics in the other junction. We show analytically that the interaction with the fast phase-whirling state averages to an increase of the effective damping for the moving fluxon. Experimentally we measure the difference in zero-field step voltage of one junction while the other one in Meissner and in phase-whirling state. Obtained data are in good agreement with the theoretical results.

16–116
Two-stacks of parallel arrays of long Josephson junctions.
G. Carapella[1,2], *G. Costabile*[1,2], *G. Filatrella*[2,3] and *R. Latempa*[1,2]. [1]Dipartimento di Fisica, Baronissi 84081, Italy. [2]UdR INFM dell'Universita' di Salerno, Baronissi 84081, Italy. [3]Universita' del Sannio, Benevento 82100, Italy.

We have fabricated and tested devices consisting of two parallel arrays of long Josephson junctions vertically stacked. Both the external electrodes and the middle electrode are made of Nb, the junction barrier consist of Al oxide. The intermediate electrode, thinner than the London penetration depth λ_L in Nb, provides the access to bias the arrays independently, and to measure the static and the dynamic properties of eache array. Due to the attractive interaction between the flux quanta in the junctions of each array, and the fluxon coherence between the the arrays, we observe phenomena that can be explained in terms of the occurrence of locked fluxon states.

16–117
Optical functions of cuprate superconductors.
N.P.Netesova. M.V.Lomonosov Moscow State University.Department of Physics.Lab.Cryoelectronics,C60a Moscow.119899 Russia.

Calculation and experimental data for the optical functions of cuprate superconductors extending to 40 eV are discussed in terms of three fundamental physical processes: free-electron effects, interband transitions, and collective oscillations. Dispersion theory is used to obtain an accurate estimate of the average optical parameters the free-electron behavior over the entire range below the onset of interband transitions. The interband transitions to 11 eV are identified using polyoscillator model. Plasma resonances involving both the conduction band and d electrons are identified as 25 eV.

16–118

Programmable Josephson voltage standards using SINIS junctions.

J. Kohlmann, *H. Schulze*, *R. Behr*, *F. Mueller* and *J. Niemeyer*. PTB, Bundesallee 100, D-38116 Braunschweig, Germany.

Josephson junctions with non-hysteretic current-voltage characteristic are required for some electronic applications such as programmable voltage standards. These overdamped junctions are realized by shunted Josephson junctions. We have fabricated arrays of several thousands of intrinsically shunted junctions based on a superconductor-isolator-normal metal-isolator-superconductor (SINIS) sandwich using the established Nb/Al-Al-oxide technology. Due to their high characteristic voltage in the range from 0.1 mV to 0.2 mV, SINIS junctions can be operated at microwave frequencies of about 70 GHz. The same microwave setup applied for conventional SIS voltage standards can therefore be used, as the frequency range is the same. We present results of 1 V arrays with up to 8192 SINIS junctions, which can be used for metrological applications. For programmable voltage standards these arrays are divided into a binary sequence. The potentials and limitations of these arrays are discussed. The SINIS junctions are compared with other kinds of junctions such as superconductor-normal metal-superconductor (SNS) junctions. This work was supported in part by the BMBF (ref. no. 13N6835 and 13N7259) and the EU (ref. no. SMT4-CT98-2239).

ORAL SESSION 17A: AC Losses II

Thursday Afternoon, September 16th, 17:30-19:00

17:30 17A–1

AC loss of YBCO tape in AC back ground field.

O.Tsukamoto[1], *M.Ciszek*[1], *D.Miyagi*[1], *J.Ogawa*[1], *O.Kasuu*[2], *H.Ii*[2], *K.Takeda*[2] and *M.Shibuya*[2]. [1]Yokohama National University. Japan. [2]Engineering Research Association for Superconductive Generation Equipment and Materials (Super-GM), Japan.

We developed a method to measure AC loss of HTS tape-carring transport current in AC back ground field. The AC loss is supplied by a power supply for the transport current and by the back ground field. The transport current loss which is supplied by the power supply is measured by measuring the potential difference between potential taps attached on the tape. In our method, the lead wires from the potential taps were wound spirally on a cylindrical surface enclosing the tape, which much decreased the inductive voltage. The inductive voltage was also canceled using cancellation coils coupled to the transport current and the current of a electric magnet supplying the back ground field. With this arrangement, measurement error of the AC loss caused by the phase error between the AC transport current and the back ground field becomes practically negligible. The magnetization loss which was supplied by the back ground field was measured by a conventional method using a pick-up coil attached on the tape. Using our method, we measured the AC losses of YBCO tape. In the paper, the AC loss characteristics of the YBCO tape are discussed comparing with those of Bi/Ag sheathed tapes.

17:45 17A–2

The Calorimetric Measurement of AC Losses in HTS Conductors in Combinations of Applied Magnetic Fields and Transport Currents.

S.P.Ashworth and *M.Suenaga*. Materials Science Division Brookhaven National Laboratory PO Box 5000 Upton New York NY -11973 USA.

The ac losses in isolated HTS superconductors can be measured by electrical methods in two classes of experimental condition; (1) when one of field or current is constant and the other has a simple sinusoidal variation and (2) when both have in-phase sinusoidal variation. In any other class of condition it is more straightforward to use calorimetric techniques. For assemblies containing multiple conductors the calorimetric techniques is easier to interpret in all classes of field and current conditions. We present details of our simple, original calorimetric technique which may be utilised in a wide range of experimental conditions to provide data on AC losses. We then give results of measurements of the AC losses in HTS conductors in a variety of conditions of applied magnetic field and transport current. These conditions are designed to reproduce the applied fields and currents which will be experienced by the conductors in power applications and include; (a) sinusoidal fields and dc currents (b) sinusoidal currents and fields with phase variation and (c) dc currents and dc fields with 'ripple' components.

18:00 17A–3
AC losses of multifilamentary Bi(2223) tapes in external magnetic field with different internal resistive barrier structures between the filaments.
H. Eckelmann, *J. Krelaus*, *R. Nast* and *W. Goldacker*. Forschungszentrum Karlsruhe, Institut für Technische Physik, Karlsruhe, D-76021, Germany.

AC losses in external magnetic fields in multifilamentary Bi2223 tapes are mainly dominated by hysteresis losses in the filaments and coupling current losses in the normal conducting matrix. The most promising way to reduce these losses is to enhance the matrix resistivity by inserting resistive barriers and to twist the filaments. The effective matrix resistivity depends strongly on the barrier geometry and quality and on the direction of the external magnetic field. For practical application the tapes need to carry high critical currents thus the application of a twist to the filaments should not significantly reduce the critical current compared to untwisted tapes. We have developed different concepts to apply resistive $SrCO_3$ barriers in the matrix between the filaments of multifilamentary Bi(2223) tapes. The effectiveness of the different barrier structures with respect to the reduction of the AC losses was investigated and will be discussed regarding theoretical aspects. Especially, intention is paid to the optimisation aim of the overall critical current as well as on the twist behaviour of the different tapes. Overall properties of the different barrier structures are compared to select the structure most suitable for low AC loss.

18:15 17A–4
AC losses of twisted multifilamentary Bi-2223 tapes under AC perpendicular fields.
E. Martínez[1], *Y. Yang*[1], *C. Beduz*[1], *Y. Huang*[2] and *C.M. Friend*[2]. [1]Institute of Cryogenics, University of Southampton, Southampton, United Kingdom. [2]BICC Cables Ltd. Technology Center, Wrexham LL13 9XP, United Kingdom.

We present experimental results of AC losses of twisted and untwisted multifilamentary PbBi2223 tapes, under perpendicular AC magnetic fields. The different contributions to the AC losses, such as hysteretic, eddy current and coupling current losses, are analysed by measuring the 3rd and 1st harmonic of the induced voltage in the pick-up coil. This study has been performed on Ag and AgAu(10%) alloy sheathed tapes. Our results show that for pure silver matrix, the filaments are coupled in all range of measured fields, even for tapes of 10 mm twist pitch, and the losses are mainly due to the hysteretic contribution of the superconducting core. On the contrary, twisting of the filaments of Ag-Au alloy sheathed tapes results in uncoupling of the filaments at fields lower than the coupling field, beween 2-10 mT depending on the twist pitch. In this case, a strong decrease of the hysteretic losses with respect to the coupled-filament regime has been observed. The overall losses taking into account of coupling loss are still lower (up to 30-50% at power frequencies) than for coupled filaments.

18:30 17A–5
Measurements of Losses in a High-Temperature Superconductor Exposed to Both AC and DC Magnetic Fields and Transport Currents.
N. Schönborg[1], *N. Magnusson*[2] and *S. Hörnfeldt*[3]. [1]Royal Institute of Technology, Department of Electric Power Engineering SE-100 44 Stockholm Sweden. [2]Royal Institute of Technology, Department of Electric Power Engineering SE-100 44 Stockholm Sweden. [3]ABB Corporate ResearchSE-721 78 Västerås Sweden.

In certain prospective applications of high-temperature superconductors, e.g. the winding of a magnetostrictive actuator, the conductor will be exposed to DC bias magnetic fields and transport currents. It is therefore interesting to develop semi-empirical models, based on measurements, for the losses under these conditions. In this paper we present an experimental study of the AC losses in a Bi-2223 high-temperature superconducting tape carrying transport currents in externally applied magnetic fields. Both the current and the magnetic field consist of an AC and a DC component. The losses were measured calorimetrically, at a fixed temperature, for different combinations of currents and magnetic fields. In every single measurement, the magnetic field is directly proportional to the current, which is the normal case in practical applications.

18:45 17A–6
A simple HTS-cable model to study the effect of the geometrical arrangement of the tapes on AC losses.
R. Tebano[1], *D. Uglietti*[2], *G. Coletta*[3], *L. Gherardi*[3], *F. Gömöry*[4] and *R. Mele*[3]. [1]Dipartimento di Scienza dei Materiali, Universita' degli Studi di Milano, Via Cozzi 53, Milano, 20126, Italy. [2]INFM, UdR di Milano, Dipartimento di Scienza dei Materiali, Universita' degli Studi di Milano, Via Cozzi 53, Milano, 20126, Italy. [3]Pirelli Cavi & Sistemi S. p. A. , Viale Sarca 222, Milano, 20126, Italy. [4]Institute of Electrical Engineering, Slovak Academy of Science, Dubravska 9, 842 39 Bratislava, Slovak Republik.

There are different mechanisms that contribute to the actual losses in a HTS-cable in the transport regime. A simplified cable model was developed in order to single out some of the various mechanisms that influence the losses. It consists of a single layer of tapes with zero pitch angle, each tape being fixed along the thickness of a rectangular slab of fiberglass. The slabs are mounted around a fiberglass cylindrical support, and can be moved along the radial direction by means of a couple of screws. Sliding the slabs along the screws sets the gap between the tapes. It is then possible to easily change the geometry of the system by changing the diameter and/or the number of tapes involved and to study how this affects the ac losses. The current was forced to distribute equally among all the tapes exploiting two different arrangements. Firstly, the tapes were connected in series. Secondly, the tapes, each of them being in series with a resistor, were connected in parallel. Experimental data, obtained in the various configurations, were discussed and compared with different theoretical models.

ORAL SESSION 17B: Fusion, SMES, detectors, accelerators

Thursday Afternoon, September 16th, 17:30-19:00

17:30 *17B–1

The superconducting magnet system for the WENDELSTEIN 7-X Stellarator.

J. Sapper and W7-X team. Max-Planck -Institut für Plasmaphysik, EURATOM Association, D-85748 Garching, Germany.

The superconducting magnet system of the new stellarator WENDELSTEIN 7-X to be placed in Greifswald, Germany consists of 50 non-planar and 20 planar large magnet coils. The conductor used is a cable-in-conduit type, composed from copper stabilized NbTi strands (CICC). The workability and long length fabrication of the conductor have been essential conditions for its lay-out. The helium tight jacket is made from hardenable Aluminium alloy by co-extrusion. The operation will be at supercritical He conditions. The nominal performance of the 350 ton weighing magnet system is at 6 Tesla and a coil current of 1.75 MA. The stored energy will be 620 MWs.
The paper describes the lay-out of the magnet system as well as the already done prototype work and the current activities in European industry for manufacturing of the coils in the next years.
Detailed results from the prototype coil tests in the facilities at Forschungszentrum Karlsruhe will be reported.
The planned routine tests for the magnet coils before the assembly on site at CEA Saclay will be presented.

18:00 17B–2

AC loss measurements of the 100kWh SMES model coil.

N. Hirano[1], *K. Shinoda*[1], *S. Hanai*[2], *T. Hamajima*[2], *M. Kyoto*[2], *N. Martovetsky*[3], *J. Zbasnik*[3], *M. Yamamoto*[4], *T. Himeno*[4] and *T. Satow*[5]. [1]Chubu Electric Power Co., Inc., 20-1 Ohdaka-cho, Midori-ku, Nagoya, 459-8522, Japan. [2]Toshiba Corporation, 2-4 Suehiro-cho, Tsurumi-ku, Yokohama 230-0045, JAPAN. [3]Lawrence Livermore National Laboratory, L-641, 7000 East Ave., Livermore, CA 94550, USA. [4]International Superconductivity Technology Center, 5-34-3 Shinbashi, Minato-ku, Tokyo 105-0004, JAPAN. [5]National Institute for Fusion Science, 322-6 Oroshi, Toki, Gifu 509-5292, JAPAN.

A SMES model coil was designed and fabricated to establish component technologies needed for a small-scale 100kWh SMES. Performance tests were carried out at Japan Atomic Energy Research Institute in 1996. The coil has been tested also at Lawrence Livermore National Laboratory in 1998 in collaboration with Japan and the United States of America. In AC loss tests, the coupling losses in the coil were about 15 times larger than those measured in the CICC short sample. It was confirmed from the analysis of the AC loss measurements that the coupling loss of the coil consists of two components with a short (about 220ms) and a long (about 30s) time constants. Since increase of the contact resistance between the superconducting strands reduces AC loss, we made a small size CIC conductor with CuNi coated strands and fabricated a small solenoid coil. Measured AC loss of the small coil was reduced to be about 1/6. We calculated the temperature rise of the improved conductor under the condition of cyclic operation at the designed field change rate of the 100kWh SMES plant. Since calculated temperature is less than the current sharing temperature, the SMES pilot plant will be stable in operation.

18:15 17B–3

High Field Solenoids for Muon Cooling.

M. A. Green[1], *Y. Eyssa*[2], *S. Kenny*[2], *J. R. Miller*[2] and *S. Prestemon*[2]. [1]Lawrence Berkeley National Laboratory, Berkeley CA 94720, USA. [2]National High Magnetic Field Laboratory, Tallahassee FL 32310, USA.

The proposed cooling system for the muon collider will consist of a 200 meter long line of alternating field straight solenoids interspersed with bent solenoids. The muons are cooled in all directions using a 400 mm long section liquid hydrogen at high field. The muons are accelerated in the forward direction by 900 mm long, 805 MHz RF cavities in a gradient field that goes from 6 T to -6 T in about 300 mm. The high field section in the channel starts out at an induction of about 2 T in the hydrogen. As the muons proceed down the cooling channel, the induction in the liquid hydrogen section increases to inductions as high as 30 T. The diameter of the liquid hydrogen section starts at 750 mm when the induction is 2 T. As the induction in the cooling section goes up, the diameter of the liquid hydrogen section decreases as the induction in the cooling section increases. When the high field induction is 30 T, the diameter of the liquid hydrogen section is about 80 mm. When the high field solenoid induction is below 8.5 T or 9T, niobium titanium coils are proposed for generating the magnetic field. Above 8.5 T or 9 T to about 20 T, graded niobium tin and niobium titanium coils would be used at temperatures from 4.2 K down to 1.8 K. Above 20 T, a graded hybrid magnet system is proposed, where the high field magnet section (above 20 T) is either a conventional water cooled coil section or a water cooled Bitter type coil. This report presents the results of a study of a muon cooling solenoid system. Three types of superconducting coils have been studied. They include; epoxy impregnated intrinsically stable coils, ventilated cryogenically stable coils, and cable in conduit conductor (CICC) coils with helium in the conduit. A preliminary design of the bent solenoid u ed for momentum cooling is also described.

18:30 17B–4

Test Results of Compensation for Load Fluctuation by Using 1kWh/1MW Module-Type SMES.

H. Hayashi[1], *T. Sannomiya*[1], *K. Tsutsumi*[1], *F. Irie*[1], *T. Ishii*[2] and *R. Ikeda*[3]. [1]Kyushu Electric Power Co.,Inc..2-1-45,Shiobaru,Minami-ku,Fukuoka,815-8520,Japan. [2]West Japan Engineering Consultants,Inc.1-7-11,Chuo-ku,Fukuoka,810-0003,Japan. [3]Fukuoka Denki Keiki Co.,Inc.4-18-15,Minami-ku,Fukuoka,815-0031,Japan.

We have completed a 1kWh/1MW module-type SMES named "ESK"(Experimental SMES of Kyushu Electric Power Co., Inc.) which is thought to be the first step for the realization of the practical SMES system for power line control. Some preliminary tests of compensation for load fluctuation in the 6kV and 66kV commercial power line have also been taken place at the site in Fukuoka City. The re-

sults showed remarkable reduction of short period fluctuation. This suggests the availability of large SMES for the stabilization in the large power line.

18:45 17B–5
Comparison of HTS and LTS μ-SMES Concepts.
R. Mikkonen, *J. Lehtonen* and *J. Paasi*. Tampere University of Technology, Laboratory of Electromagnetics, P.O. Box 692, FIN-33101 Tampere, Finland.

The growth of electronics and electronically-controlled devices has caused commercial and industrial customers to be increasingly concerned with power quality issues. Voltage sags and short-duration power outages can cause significant financial burdens on certain customers. Thus the main interest of SMES concept is currently focused on power quality considerations. Related to these viewpoints a conduction cooled 5 kJ HTS SMES system operating at 20 K has been constructed and demonstrated to compensate a short term loss of power. In addition a cryogen free 0.2 MJ Nb_3Sn SMES concept operating at 10 K has been designed. The technical comparison of these two SMES coils has been evaluated. The questions under discussion are related to stability and quench event. The slanted electric field-current density characteristics and a wide margin between the operating and critical temperature of a HTS coil result in a transition which differs quite drastically from its LTS counterpart. Higher operating temperature with increased specific heat make HTS windings less sensitive to mechanical or thermal disturbances which are crucial for LTS magnets.

ORAL SESSION 17C: Materials Related to Electronic Applications

Thursday Afternoon, September 16th, 17:30-19:00

17:30 *17C–1
Series production of large area YBCO - films for microwave and electrical power applications.
W. Prusseit, *S. Furtner* and *R. Nemetschek*. THEVA Thin Film Technology, 85386 Eching, Germany.

Large area YBCO - films are series produced by thermal co-evaporation using a deposition scheme known as Garching process, which allows intermittent oxygen supply in a high vacuum ambient by an oxygen cup spaced closely underneath the moving substrates. The deposition area of 9" diameter is capable to handle very large wafers up to 8" diam. or numerous smaller wafers. The large distance between substrates and boat sources and an elaborate heater design guarantee excellent film uniformity over the entire deposition area. YBCO - films deposited by this technique are commercially fabricated for a variety of applications - the most prominent are resistive fault current limiters and microwave filters for mobile or satellite communications. IMUX and OMUX - filters are currently space qualified by Robert Bosch GmbH and are expected to be launched and installed on an experimental platform of the international space station ALPHA in 2001. Both of the above applications require quite different film specifications on the one hand, but at the same time extremely high uniformity and reproducibility on the other hand, since hundreds of YBCO - films are combined to large systems or have to be approved for manned space missions. The success of such projects is direct evidence that the technique of thermal evaporation is readily capable to meet these high demands and will become the major deposition technique to support the emerging HTS market.

18:00 17C–2
Epitaxial (101) YBa2Cu3O7 thin-fims on (103) NdGaO3 substrates.
Y.Y. Divin[1], *U. Poppe*[1], *C.L. Jia*[1], *J.W. Seo*[2,3] and *V. Glyantsev*[4]. [1]Institut für Festkoerperforschung, Forschungszentrum Juelich GmbH, D-52425 Juelich, Germany. [2]Institute de Physique Universite de Neuchatel,CH-2000, Switzerland. [3]IBM -Zuerich Research Laboratory, CH-8803 Rueschlikon, Switzerland. [4]Conductus Inc., Sunnyvale, CA 94086, USA.

High-Tc thin films with tilted c-axis orientation are promising candidates for the fabrication of planar-type Josephson junctions. We have fabricated epitaxial (101) oriented YBa2Cu3O7 thin-fims by high-pressure dc sputtering on 18.6-degree tilted vincinal NdGaO3 substrates, which corresponds to a (103) orientation in pseudo cubic notation. The microstructure and electrical transport of these tilted c-axis films have been studied in comparison with c-axis oriented films and films with different tilt angles. It is shown by HREM that these films got a single-domain microstructure with a-b planes tilted for about 18-degree with respect to the normal of the film surface. The films show a high anisotropy of the specific resistance at 100 K and of the critical current density at 77 K, which was around two orders of magni-

tude. This quasi a-axis growth of YBa2Cu3O7 thin films was confirmed by sputtering on the stepped surface of NdGaO3 substrates, obtained by argon milling. The fabricated step-edge junctions contained, two additional grain-boundaries due to a (101) domain around the 18-degree tilted part of the substrate surface in the vincinity of the lower region of the slightly rounded step edge. The exceptional growth behavior at the special tilt of the(103) substrate orientation will be explained by a growth model which minimizes the strain of the growing film.

18:15 17C–3

Electrostatic modulation of superconductivity in ultrathin epitaxial $GdBa_2Cu_3O_{7-x}$ films.

C.H. Ahn, S. Gariglio, P. Paruch, T. Tybell, L. Antognazza and *J.-M. Triscone*. Département de Physique de la Matière Condensée, Université de Genève, 24 quai Ernest-Ansermet, 1211 Genève 4, Switzerland

We have used the polarization field of the ferroelectric oxide $Pb(Zr_xTi_{1-x})O_3$ to modulate in a reversible and non-volatile fashion the critical temperature of the high temperature superconductor $GdBa_2Cu_3O_{7-x}$ in ferroelectric / ultrathin high T_c oxide heterostructures. For slightly underdoped samples, a change of the normal state resistivity of up to 50up to 7 K being observed. In more underdoped samples, an insulating state was induced. The transition from superconducting to insulating behavior, which does not involve chemical or crystalline modification of the material, occurs at a resistivity of $\sim$2 mΩ cm, in agreement with the value predicted for a material possessing poor screening and large phase fluctuations.

C. Ahn et al. Science 284, 1152 (1999).

18:30 17C–4

Spatial variation of the non-linear surface impedance of HTS films.

L. Hao and *J.C. Gallop*. National Physical Laboratory, Teddington, TW11 0LW, UK.

Spatially resolved measurements of HTS microwave surface impedance represent an important requirement for the assessment of large area HTS thin films which are of considerable importance to the development of microwave applications of the cuprate superconductors. We describe further development of a novel technique for the characterisation of microwave properties of HTS films which allows the spatial variation of this important physical parameter to be measured . The method employs a dielectric puck system which can be moved over the surface of a large HTS wafer, sampling the surface impedance at a number of discrete frequencies between 5 and 15 GHz. The surface impedance can also be rapidly measured as a function of microwave magnetic field strength. Spatial resolution for the prototype system is as small as 1-2 mm. We have recently developed an alternative, and much faster, method by using a loop oscillator which can be interrupted by a fast microwave switch. The surface resistance and the shift in surface reactance can be measured by using this method. The decay of microwave power in the resonator is then monitored as a function of time to determine the power dependent surface impedance parameters. This process is extremely fast and straightforward and the loop oscillator configuration permits only relatively inexpensive components to be used. We describe measurements made at 11.5GHz of the spatial variation of the non-linear surface impedance of a number of HTS films at 77K.

18:45 17C–5

Optimization of Microwave Losses of Ferromagnetic Perovskite Thin Films for Magnetically Tunable Microwave Superconducting Filters.

J. Wosik[1], *M. Strikovski*[1], *L.-M. Xie*[1], *P. Przyslupski*[2], *M. Kamel*[1] and *S. A. Long*[1]. [1]Electrical and Computer Engineering Department and Texas Center for Superconductivity, University of Houston, 4800 Calhoun Rd., Houston, TX 77204-5932, USA. [2]Institute of Physics, Polish Academy of Sciences, Al. Lotnikow 32/36, PL-02 668 Warszawa, Polan.

Low-loss ferrite materials used in superconducting microwave electronics are not crystallographically compatible with HTS materials and can only be used in hybrid microwave structures. There is a need for an alternative magnetic material, which would be compatible with monolithic HTS thin film technology. Excellent candidates for such compatibility are perovskite oxides exhibiting ferromagnetic properties. We have investigated, below Curie temperature, magnetic properties and microwave losses of $Nd_xSr_(1-x)MnO_3$ (NSMO) and $La_xCa_(1-x)MnO_3$ thin films deposited by both high-pressure dc sputtering and laser ablation methods. Several films with different doping, Curie temperatures Tf ranging from 60 K to 220 K, saturation magnetization from 1000 G to 3000 G, and coercitivity fields from 100 to 400 G, were tested. Both a 13 GHz sapphire dielectric resonator and a 3 GHz S-shaped microstripline resonator, coupled in a flip chip configuration to such a NSMO film, were used. The correlation between the microwave losses and magnetic properties of NSMO and LCMO films as well as optimization of the film properties, regarding minimum microwave losses, will be discussed. In addition, evaluation of magnetic tunability controlled by the $\mu(H_dc)$ dependence for a 3 GHz monolithic microstrip with a YBCO microstrip line patterned on the top layer of the YBCO/NSMO/ LAO structure will be also presented.

ORAL SESSION 17D: Josephson Junctions II

Thursday Afternoon, September 16th, 17:30-19:00

17:30 *17D–1

Investigation of microstructure of ramp-type $YBa_2Cu_3O_{7-d}$ structures.

H. Sato, *F.J.G. Roesthuis*, *A.H. Sonnenberg*, *A.J.H.M. Rijnders*, *D.H.A. Blank* and *H. Rogalla*. University of Twente, 7500 AE, Enschede, Netherland.

The electrical properties of ramp-type junctions strongly depend on the quality of the interface of the barrier layer deposited on the etched ramp. We studied the morphology of ramps in $YBa_2Cu_3O_{7-d}$ films and subsequently the barrier layer by Scanning Electron Microscopy (SEM) and Atomic Force Microscopy (AFM). The ramps have been fabricated by Ar ion beam etching using standard photoresist masks. SEM and AFM showed the formation of tracks along the slope of the ramp, originating from the irregular shape of the edge of the photoresist mask. These tracks, with typical dimensions of 200 nm, enlarge the risk of non-uniform deposition of barrier layer. Fabricated ramp-type junctions with a 20 nm $PrBa_2Cu_3O_{7-d'}$ barrier, using $SrTiO_3$ as insulating layer, show RSJ-like I-V behavior at high temperatures with I_c of 50 μA and Rn of 1 Ωat 81.2 K. At lower temperatures, however, the junctions show a flux flow type behavior with large I_c. Preliminary experiments with modified reflowed resist edges show a smoother ramp surface with possible improvements of the junction characteristics. The relation between the microstructure of the ramp surface and the junction properties will be presented.

18:00 17D–2

Josephson phenomenology and microstructure in $YBa_2Cu_3O_{7-\delta}$ artificial grain boundaries characterized by misalignment of the c-axes.

F. Tafuri[1,2], *F. Miletto Granozio*[2], *F. Carillo*[2], *F. Lombardi*[2], *U. Scotti di Uccio*[2], *K. Verbist*[3] and *G. Van Tendeloo*[3]. [1] Dipartimento di Ingegneria, Seconda Università di Napoli, Aversa (CE) , Italy. [2]INFM-Dipartimento di Scienze Fisiche- Università di Napoli "Federico II",Napoli, Italy. [3]EMAT, University of Antwerp (RUCA), Groenenborgerlaan 171, B-2020 Antwerp, Belgium.

$YBa_2Cu_3O_{7-\delta}$ artificial grain boundary Josephson junctions have been fabricated, employing a recently implemented biepitaxial technique. The grain boundaries are characterized by a misalignment of the c-axes (45° c-axis tilt or 45° c-axis twist) and are still mostly unexplored. Different substrates and seed layers have been investigated. We carried out a complete characterization of their transport properties and microstructure. Junctions associated with these grain boundaries exhibit an excellent Josephson phenomenology, high values of the IcRn product and a Fraunhofer-like dependence of critical current on the magnetic field, differently from traditional biepitaxial junctions. Remarkable differences in the transport parameters of tilt and twist junctions have been observed, which can be of interest for several applications. Moreover, the possibility to employ these junctions to explore the symmetry of the order parameter is presented, by taking advantage of the anisotropic and easily tunable properties of the proposed structure. High resolution electron microscopy showed the presence of perfect basal plane faced boundaries in the cross sections of tilt boundaries. It is shown that clean basal plane boundaries exhibiting uniform Josephson properties could be obtained by employin vicinal substrates.

18:15 17D–3

Interval deposition: growth manipulation for use in fabrication of planar $ReBa_2Cu_3O_{7-\delta}$ junctions.

A.J.H.M. Rijnders, *G. Koster*, *D. H.A. Blank* and *H. Rogalla*. Univ. of Twente, Dept. of Applied Physics, Low Temperature Division, P.O.Box 217, 7500 AE, Enschede, The Netherlands.

In complex high-T_c superconducting electronic circuits and devices which include several Josephson junctions a planar technology is desirable. Despite research efforts on a-axis junctions and planar microbridges these technologies have not (yet) been proven to be viable for complex circuits. Planar c-axis junctions with an artificial barrier are expected to yield better results, provided that the junction interfaces can be controlled on an atomic level. Starting with an atomically smooth substrate, i.e., TiO_2 terminated $SrTiO_3$, we studied the growth, using the interval deposition technique, of $REBa_2Cu_3O_{7-\delta}$. In this technique, material, needed for completion of just one unit-cell layer, is deposited in a short period followed by an interval where this material is allowed to form the right crystalline structure. A high supersaturation during the deposition period leads to the formation of small islands, which reduce the nucleation-probability on these islands. Using this technique, the layer-by-layer growth mode is enhanced, as shown by RHEED. In this contribution we present the studies on the growth using interval deposition and surface morphology of both the electrodes and barrier, using RHEED and scanning probe microscopy.

18:30 17D–4

Microwave responses of $Bi_2Sr_2Ca_1Cu_2O_{8+y}$ Intrinsic Josephson junctions.

K. Nakajima[1,3], *Y. Aruga*[1], *H.B. Wang*[3], *T. Tachiki*[1], *Y. Mizugaki*[1,3], *J. Chen*[1,3], *T. Yamashita*[2,3] and *P.H. Wu*[4]. [1]Research Institute of Electrical Communication, Tohoku University, Sendai, Japan. [2]New Industry Creation Hatchery Center, Tohoku University, Sendai, Japan. [3]CREST, Japan Science & Technology Cooporation, Japan. [4]Department of Electronic Science & Engneering, University of Nanjing, Nanjing 210093, China.

Microwave responses of $Bi_2Sr_2Ca_1Cu_2O_{8+y}$ intrinsic Josephson junctions have been studied. Variable size mesa junctions were fabricated by Ar ion milling on the ab-planes of BSCCO single crystals grown by TSFZ method. The mesas involve about 40 junctions along the c-axes. Microwave application at a certain frequency for the BSCCO junctions induces current steps at even voltage intervals on the I-V curves. The higher order steps are produced with increasing microwave power but the step voltages are not affected by the power nor temperature variation. The voltage interval is much larger than that of Shapiro steps expected from a phase-locking of 40 junctions stacked along the c-axes of BSCCO mesas. It may be possible that the current steps is induced by higher frequency electromagnetic waves

excited in the BSCCO mesas. Possible explanations of the higher frequency excitation are disscussed.

18:45 17D–5

Experiments on Energy Level Quantization in Underdamped Josephson Junctions.

E.Esposito[1,2], *C.Granata*[1,3], *M. Russo*[1,2], *B.Ruggiero*[1,2] and *P.Silvestrini*[1,2]. [1] Istituto di Cibernetica del CNR, I-80072, Arco Felice (Napoli), Italy. [2] Macroscopic Quantum Coherence Group, Istituto Nazionale Fisica Nucleare, I-80126 Napoli, Italy. [3]AtB, Advanced Technologies Biomagnetics, I-66013 Chieti Scalo, Italy.

Macroscopic quantum effects in Josephson systems have attracted great interest in the scientific community both for the physics involved and in view of applications. We present experiments on the presence of energy level quantization at temperatures above the classical-quantum crossover one in underdamped Josephson junctions. This has been possible having a great care in insulating the sample from its electromagnetic envoirment, and by extending the measurements of the escape rate out of the zero-voltage state at high sweeping bias rate (dI/dt up to 100 A/sec). The effect of the presence of the discret energy levels monotonically decreases with decreasing the bias sweeping rate dI/dt. We propose a technique to control the effective dissipation by integrating molybdenum resistors wiring with the junction. The meander shaped resistive lines also provide an "in-situ" filtering stage, which strongly reduce the external noise coming into the junction. The extremely low value of dissipation obtained is also encouraging in view of experiments of Macroscopic Quantum Coherence, basic ingredient of quantum computing.

PLENARY SESSION 18

Friday Morning, September 17th, 8:30-10:30

8:30 18–1

Strategies for Tailoring New High T_c Superconductors.

M. Marezio and *F. Licci*. Istituto MASPEC-CNR, Fontanini-PARMA, 43010, Italy.

Since the discovery of superconductivity in 1911, most of the tailoring of new superconducting materials have been based on empirical criteria such as educated substitutions inspired by the periodic table. This task has become very complicated with the advent of high T_c oxide superconductors. In particular, it would be difficult to envisage new superconducting systems different from cuprates and bismuthates. By analysing as to how some superconducting materials were discovered, four strategies may be proposed. These are based on: i) band structure calculations, which may lead to systems different from known ones; ii) high resolution electron microscopy studies, which may lead to different structural arrangements within the same systems; iii) systematic studies of phase diagrams; iv in-situ high pressure studies of the critical temperature of known systems, which may lead to cation or anion substitutions simulating at ambient the structure stable under pressure and responsible for the higher T_c .

9:00 18–2

Roadmap of Superconducting Elecronics.

C.E.Gough. Superconductivity Research Group, University of Birmingham, School of Physics and Astronmy, B15 2TT, UK.

We will present an overview and update of the SCENET report on Superconducting Electronics: a Roadmap for Europe available on the SCENET web site or at http://www.cm.ph.bham.ac.uk/reports/roadmap98/roadmap.html. The report considers the principal areas of superconducting applications, both conventional and HTS, including SQUIDs, wireless and communications, digital, sensors and detectors, and the refrigeration and materials issues underlying their development. A number of recommendations are made to ensure that Europe remains competitive in the field.

9:30 18–3

Research and Developments of High-Tc Superconductivity in Japan.

S. Tanaka. Superconductivity Research Laboratory / ISTEC, 1-10-13 Shinonome Koto-ku, Tokyo, JAPAN

After the discovery of high temperature superconductivity, we have done mainly fundamental research intensively for about ten years, and we thought that we have gotten acquainted with these peculiar materials fairly well, even though the detailed mechanism of high temperature superconductivity is not clarified yet. Thus the developments of future applications are becoming dominantly important.
The main subjects of applications are as follows;
1) Developments of superconducting tapes, which must be operated at liquid nitrogen temperature under strong magnetic field beyond 5T.
2) Developments of SQUID applications, including single flux quantum device of very fast operation beyond 50GHz.
3) Developments of bulk superconductors, having high remnant magnetic field beyond 5T at liquid nitrogen temperature.
4) Research of fundamental properties of high-Tc superconductors, in order to develop new device physics.
The possible future expansion of these research and developments to the future applications will be discussed in more details.

10:00 18–4

Superconductivity in the US.

H. Weinstock. Air Force Office of Scientific Research Arlington, VA 22203-1977 USA.

A profile will be provided of the primary areas of superconductivity research and development (R&D) in the United States, as well as the sources and trends in funding. This will include a discussion of the major superconductivity programs of the Department of Energy (DoE), the Department of Defense (DoD), the National Science Foundation (NSF), the National Institute of Standards and Technology (NIST), and the National Aeronautics and Space Administration (NASA). The presentation will describe in some detail the DoE's Superconductivity Program for Electric Systems, currently with an annual budget of about $30,000,000, the largest single superconductivity program in the US. The role of private companies (both large and small), universities and national laboratories will be considered, along with how they interact. The history and R&D activities of some of the companies will be featured, as well as their perceptions of their futures. The unique role in the US of both venture capital and government support for small businesses – companies with 500 or fewer employees – will be discussed, and specific examples relating to superconductivity applications will be presented. Finally, some personal observations will be offered on the future direction and growth of applied superconductivity in the US.

PLENARY SESSION 19

Friday Morning, September 17th, 11:00-13:15

11:00 19–1

Status of superconducting power applications.

H.-W. Neumüller. Siemens AG Corporate Technology D-91050 Erlangen, P.O.Box 3220.

High-Tc superconductivity (HTS) has successfully enhanced the prospect of its application in power engineering, and market studies predict that commercial use thereof is coming ever closer. The considerable market potential for HTS constitutes a long-term driving force (5 to 10 years) in worldwide development of that kind of new product which either cannot be produced at all by means of conventional technology or, if so, which does not have the same performance levels. Significant projects using low-Tc superconductors center on magnetic energy storage (SMES) and generators. Most of the world-wide activities are concentrating on HTS power transmission cables. Successful tests of demonstrators and functional models of up to 50m in length and up to several thousands of Amperes (designed for future 400 MVA cables) have already been performed in a laboratory

environment. Typical of the present development stage are pilot installations under real power station conditions. HTS stationary transformers have already proved themselves in the power range 630-800 kVA, even on test sites, and the next prototypes under construction will have ratings of 10 MVA. Highly convincing advantages and short-term amortisation indicate that HTS transformers are promising for railway transportation systems. Superconductivity furthermore creates scope for totally innovative equipment, such as fault current limiters. Magnetic and mechanical storage devices such as SMES and flywheels with HTSC bearings improve the energy management and power quality in customer networks, for sensitive production lines, for power line stabilisation and for public transportation. Despite all the remarkable progress, we still have to overcome a number of bottlenecks like materials and refrigeration system costs. The action taken for HTSC is always determined by competing conventional solutions, which means that HTSC applications have to be economical and cost-effective.

11:45 19–2
AC Losses in multilayer HTS Prototype of Power Transmission Cables
R. Mele, *G. Coletta*, *L. Gherardi* and *M. Nassi*. Pirelli Cavi & Sistemi, Milano, Italy.

AC loss study in HTS cable conductor represents a major issue in the design of the High Temperature Superconducting (HTS) cable for power transmission line. In this view AC losses are investigated in a set of short-length samples, hand-wound HTS prototype multi-strand conductors (PMCs) and factory made multilayer HTS conductor. These are samples of the prototype manufactured in the framework of an EPRI-DOE contract, as the first phase of the development of an HTS 'pipe' type 50-m prototype cable, made by Pirelli in a continuous length using industrial equipment. All the conductors consist of several layers of helically-wound Bi-2223/Ag sheathed HTS tape with critical currents Ic ranging from 1300 A to 3300 A.
To investigate into the AC behaviour of these conductors, AC loss measurements are carried out mainly based on an electrical, "transport", method, with ac currents up to 1400 A rms. The measurements are performed at different frequencies, for checking the hysteretic nature of the main component of the ac losses. Results of calorimetric measurements on the same short samples are also analysed, showing a very good consistency with the electrical ones.
Finally the full size 50 m long HTS Cable carrying 2000 A rms at 115 kV, designed and developed by Pirelli in the frame of the EPRI-DOE contract, was characterised. The AC losses were measured with an electrical method on the prototype installation, complete of cryostat, electrical insulation and refrigeration system, at 50 Hz. The results of these measurements are discussed and compared with the ac loss measured on the short length cable conductors and with the ac loss models.

12:15 19–3
Status for business development of HTS SQUID applications.
T. Freltoft and *Y.Q. Shen*. NKT Research Center A/S Priorparken 878 DK-2605 Brøndby Denmark.

One of the most obvious applications of superconductivity is the unsurpassed sensitivity of SQUIDs for low frequency magnetic field detection. However, large scale applications of LTS SQUIDs are said to be limited by the necessity of He cooling. After the demonstration of low noise HTS SQUID magnetometers in 1994/95 the road should be paved towards the development of a number of commercial applications, but where are they? In this paper, a review is given of some of the current demonstration projects and of the technical and other challenges yet to be overcome towards the future large scale exploitation of SQUID systems.

12:45 19–4
Superconductors and Cryogenics for Future Communication Technology.
M. Klauda[1], *T. Kässer*[1], *B. Mayer*[1], *C. Schrempp*[1], *C. Neumann*[2], *N. Klein*[3] and *H. Chaloupka*[4]. [1]Bosch Telecom GmbH; Space Communication Systems; D-71520 Backnang; Germany. [2]Robert Bosch GmbH; Corporate Research and Development; D-70049 Stuttgart; Germany. [3]Forschungszentrum Jülich; D-52425 Jülich; Germany. [4]Universität Wuppertal; Fachbereich Elektrotechnik; D-42097 Wuppertal; Germany.

More than ten years after the discovery of High Temperature Superconductivity (HTSC), one major application internationally discussed are passive RF components for communication technology. Since the early beginning of the research on HTSC, miniaturisation of communication systems and better performance with respect to losses and noise figures have been considered as the main benefits of these materials. In the following years as well the complicated material properties and the difficult preparation of optimum quality thin films as - in especial - the very challenging cooling issue turned out to be major obstacles in the way to a commercial application of these new compounds. Within the last five years significant progress has been achieved all over the world in manufacturing high performance RF-subsystems and systems as demonstrators. Nevertheless, the commercial success so far has not met the optimistic forecasts being given throughout the last decade, especially within the field of cellular communication. The main reason for this are the precautions of the customers with respect to costs and reliability of the cryogenic cooling. In the ongoing German program "Superconductors and Ceramics for Future Communication Technology", funded by the German Ministry of Education and Research, parallel to the development and testing of superconducting systems, major efforts with respect to the development of a reliable, efficient and cost-effective cooling technology will be undertaken. The talk will give examples of the above mentioned BMBF-program and of other international activities in the fields of satellite communication, cellular communication, and cryotechnology. Rentability considerations for the use of HTSC and cryotechnology in various fields of application will be given and we try to give some forecast over the technology trends within the next five years in some areas of cryogenic communication technology.

Author's Index

A

B

C

D

E

F

G

H

I

J

K

L

M

N

O

P

Q

R

S

T

U

V

W

X

Y

Z